

AD-781 804

IMPROVED REPRODUCIBILITY OF SOLID
ROCKET PROPELLANTS

D. A. Flanigan, et al

Thiokol Corporation

Prepared for:

Air Force Rocket Propulsion Laboratory

15 December 1973

DISTRIBUTED BY:

NTIS

National Technical Information Service
U. S. DEPARTMENT OF COMMERCE
5285 Port Royal Road, Springfield Va. 22151

UNCLASSIFIED

SECURITY CLASSIFICATION OF THIS PAGE (When Data Entered)

AD 781 804

| REPORT DOCUMENTATION PAGE | | READ INSTRUCTIONS BEFORE COMPLETING FORM |
|--|--|---|
| 1. REPORT NUMBER AFRPL-TR-73-111 | 2. GOVT ACCESSION NO. | 3. RECIPIENT'S CATALOG NUMBER |
| 4. TITLE (and Subtitle) Final Report - Improved Reproducibility of Solid Rocket Propellants | 5. TYPE OF REPORT & PERIOD COVERED Final Report | |
| | 6. PERFORMING ORG. REPORT NUMBER 38-73 | |
| 7. AUTHOR(s) D. A. Flanigan and E. L. Vance R. E. Askins | 8. CONTRACT OR GRANT NUMBER(s) Contract Number F04611-72-C-0067 | |
| 9. PERFORMING ORGANIZATION NAME AND ADDRESS Thiokol Chemical Corporation Huntsville Division Huntsville, Alabama 35809 | 10. PROGRAM ELEMENT, PROJECT, TASK AREA & WORK UNIT NUMBERS Prog. Structure No. 31488 BPSN 623.48 Project No. 3148 | |
| 11. CONTROLLING OFFICE NAME AND ADDRESS Air Force Systems Command Air Force Rocket Propulsion Laboratory Edwards Air Force Base, California 93523 | 12. REPORT DATE 15 December 1973 | |
| 14. MONITORING AGENCY NAME & ADDRESS (if different from Controlling Office) Wayne E. Roe AFRPL/MKPB Edwards Air Force Base, California 93523 | 13. NUMBER OF PAGES | |
| | 15. SECURITY CLASS. (of this report) Unclassified | |
| 16. DISTRIBUTION STATEMENT (of this Report) APPROVED FOR PUBLIC RELEASE; DISTRIBUTION UNLIMITED | | |
| 17. DISTRIBUTION STATEMENT (of the abstract entered in Block 20, if different from Report) DDC DECLASSIFIED 15 JUL 1974 D | | |
| 18. SUPPLEMENTARY NOTES | | |
| 19. KEY WORDS (Continue on reverse side if necessary and identify by block number) Ammonium perchlorate, CTPB propellant, HTPB propellant, ingredient characterization, ballistic evaluation, mechanical property characterization, fractionations | | |
| 20. ABSTRACT (Continue on reverse side if necessary and identify by block number) How variations in propellant ingredients affect mix-to-mix propellant burn rate and mechanical properties is defined. Source, size, shape, and particle size distribution of ammonium perchlorate are variations studied. Techniques were developed through which any lot of ammonium perchlorate can be characterized in such a way that an exact definition of oxidizer blend is available for meeting precisely the burn rate and physical property | | |

DD FORM 1 JAN 73 1473 EDITION OF 1 NOV 65 IS OBSOLETE

UNCLASSIFIED

426

SECURITY CLASSIFICATION OF THIS PAGE (When Data Entered)

Reproduced by
NATIONAL TECHNICAL
INFORMATION SERVICE
U S Department of Commerce
Springfield VA 22151

UNCLASSIFIED

SECURITY CLASSIFICATION OF THIS PAGE(When Data Entered)

requirements in processible CTPB and HTPB propellants. The techniques were confirmed in demonstration (five-gallon) mixes. Mechanical property and ballistic assessment of the technique's validity was accomplished.

ii

UNCLASSIFIED

SECURITY CLASSIFICATION OF THIS PAGE(When Data Entered)

| | | |
|---------------|----------------------------------|-------------------------------------|
| ACCESSION for | NTIS | <input checked="" type="checkbox"/> |
| | DDC | <input type="checkbox"/> |
| | UNANNOUNCED | <input type="checkbox"/> |
| | JUSTIFICATION | |
| BY | DISTRIBUTION/AVAILABILITY GROUPS | |
| | Dist. AVAIL. and/or SPECIAL | |
| | A | |

When U.S. Government drawings, specifications, or other data are used for any purpose other than a definitely related Government procurement operation, the Government thereby incurs no responsibility nor any obligation whatsoever, and the fact that the Government may have formulated, furnished, or in any way supplied the said drawings, specifications, or other data, is not to be regarded by implication or otherwise, or in any manner licensing the holder or any other person or corporation, or conveying any rights or permission to manufacture, use, or sell any patented invention that may in any way be related thereto.

FOREWORD

This report documents work performed under Contract F04611-72-C-0067, Improved Reproducibility of Solid Propellant Rocket Motors. This program was conducted by Thiokol Chemical Corporation for Air Force Systems Command's Air Force Rocket Propulsion Laboratory, Edwards, California 93523.

| | |
|-----------------------|-------------------------|
| Program Structure No. | 31488 |
| BPSN | 623148 |
| Project No. | 3148 |
| Program Monitor | Wayne Roe AFRPL/MKPA |

Thiokol internal report number 38-73 (Control No. U-73-38A) has been assigned to this report. This report contains no classified information.

Mr. G. F. Mangum served as Project Director, Dr. M. Miller as Program Manager and Dr. D. A. Flanigan and Mr. S. L. Vance as Principal Investigators.

This report has been reviewed and is approved.

FOR THE COMMANDER

CHARLES R. COOKE, Chief
Solid Rocket Division

CONTENTS

| | <u>Page No.</u> |
|--|-----------------|
| SUMMARY | 1 |
| OBJECTIVE AND SCOPE | 1 |
| TECHNICAL ACCOMPLISHMENTS | |
| Phase I - Ingredient Characterization | 2 |
| Task 1 - AP Characterization | 2 |
| Task 2 - Binder Characterization | 9 |
| Task 3 - Aluminum Characterization | 9 |
| Phase II - AP Blend Characterization | 9 |
| Task 1 - Select CTPB Control Formulation | 18 |
| Task 2 - Define Optimum Oxidizer Blends | 19 |
| Phase III - AP/CTPB Propellant Characterization | 78 |
| Ballistic Evaluation of the Optimum Blends in TP-H7036 | |
| Analysis of Soft Cure in CTPB Propellants | 179 |
| Evaluation of AP Obtained from Donaldson Classifier | 187 |
| 90 Micron AP Runs | 191 |
| 50 Micron AP Runs | 195 |
| High Speed Grind AP Runs | 195 |
| Fluid Energy Milled AP Runs | 201 |
| SWECO Mill Ground AP Runs | 210 |
| Freeze-Dried UFAP Runs | 210 |
| Aluminum Powder Runs | 212 |
| CONCLUSIONS | 218 |
| RECOMMENDED PROCEDURE FOR CHARACTERIZING AP | 224 |
| GLOSSARY | 226 |
| APPENDICES | |

APPENDICES

- A. M-S-A Analysis on 200 and 400 Micron AP
- B. M-S-A Distribution Curves on Kerr-McGee and PEPCON Oxidizer Lots
- C. Friability Test Method
- D. Classification of Propellant Ingredients
 - 1. Equipment Description and Operation
 - 2. Procedure for Donaldson Classifier
 - 3. Classification of AP - Procedure
 - 4. Classification of Aluminum Powder - Procedure
 - 5. Evaluation of Classification Results
 - 6. Particle Size Classification of Plastic Powders, Shaller, R. E. and Lapple, C. E., 1971
- E. Tabulated Data from Donaldson Classifier Runs and Particle Size Distribution and Grade Efficiency Curves for Classifier Runs

TABLES

| | <u>Page No.</u> |
|---|-----------------|
| 1. Ammonium Perchlorate Assay | 3 |
| 2. Specification for Ammonium Perchlorate with Tricalcium Phosphate Conditioner | 5 |
| 3. Ratios and Exotherm Peak Temperatures of AP | 7 |
| 4. AP Physical Characteristics | 8 |
| 5. Analysis of HC-434 | 10 |
| 6. Analysis of MAPO | 11 |
| 7. Analysis of ERL 0510 | 12 |
| 8. Analysis of Iron Linoleate | 12 |
| 9. Analysis of Dioctyl Adipate (DOA) | 13 |
| 10. Analysis of HTPT (R45M) | 14 |
| 11. Analysis of DDI | 15 |
| 12. Analysis of HX-752 | 16 |
| 13. Analysis of Aluminum, Spherical, Class 4 | 17 |
| 14. Oxidizer Grind Ratios | 32 |
| 15. Strand Burn Rate Measurement Data | 34 |
| 16. Burning Rate Data | 35 |
| 17. Rotap Screen Analyses on Kerr-McGee and PEPCON Blends | 35 |
| 18. Surface Areas of Kerr-McGee and PEPCON Blends | 36 |
| 19. Reproducibility Factors | 37 |
| 20. Burning Rate Reproducibility Factor Correlation | 62 |
| 21. Constant WMD Mixes (210 micron Kerr-McGee) | 66 |
| 22. Constant WMD Mixes (254 micron PEPCON) | 66 |

TABLES (continued)

| | <u>Page No.</u> |
|--|-----------------|
| 23. Selected Optimum Blends | 79 |
| 24. Optimum Blends in CTPB | 80 |
| 25. Optimum Blends in HTPB | 81 |
| 26. Effect of Humidity Exposure on Ballistics | 86 |
| 27. TX-3 vs Strands (small mix) Selected Optimum Blend | 87 |
| 28. TX-3 vs Strand (5-gal Mix) | 88 |
| 29. Mechanical Properties, T-260 & T-261 | 90 |
| 30. Mechanical Properties, T-269 & T-270 | 91 |
| 31. Mechanical Properties, T-267 & T-268 | 92 |
| 32. Mechanical Properties, T-264 | 93 |
| 33. Mechanical Properties, T-265 | 94 |
| 34. Mechanical Properties, T-266 | 95 |
| 35. Mechanical Properties, T-271 & T-272 | 96 |
| 36. Mechanical Properties, T-273 & T-277 | 97 |
| 37. Mechanical Properties, T-278 & T-285 | 98 |
| 38. Mechanical Properties, T-274 | 99 |
| 39. Mechanical Properties, T-276 | 100 |
| 40. Mechanical Properties, T-275 | 101 |
| 41. Mechanical Properties, T-260 | 102 |
| 42. Mechanical Properties, T-268 | 103 |
| 43. Mechanical Properties, T-270 | 104 |
| 44. Mechanical Properties, T-271 | 105 |
| 45. Mechanical Properties, T-273 | 106 |
| 46. Mechanical Properties, T-278 | 107 |

TABLES (continued)

| | <u>Page No.</u> |
|---|-----------------|
| 47. Biaxial Test Data (T-260) KM/KM in CTPB | 166 |
| 48. Cumulative Damage Tests (T-260) KM/KM in CTPB | 167 |
| 49. Cumulative Damage Tests (T-270) P/P in CTPB | 168 |
| 50. Cumulative Damage Tests (T-268) KM/P in CTPB | 169 |
| 51. Cumulative Damage Tests (T-264) KM/KM in CTPB (Humidified) | 170 |
| 52. Cumulative Damage Tests (T-265) P/P in CTPB (Humidified) | 171 |
| 53. Cumulative Damage Tests (T-266) KM/P in CTPB (Humidified) | 172 |
| 54. Cumulative Damage Tests (T-271) KM/KM in HTPB | 173 |
| 55. Cumulative Damage Tests (T-273) P/P in HTPB | 174 |
| 56. Cumulative Damage Tests (T-278) KM/P in HTPB | 175 |
| 57. Cumulative Damage Tests (T-274) KM/KM in HTPB (Humidified) | 176 |
| 58. Cumulative Damage Tests (T-276) P/P in HTPB (Humidified) | 177 |
| 59. Cumulative Damage Tests (T-275) KM/P in HTPB (Humidified) | 178 |
| 60. Oxidizer Fraction in Optimum Blends | 182 |
| 61. Mechanical Properties for Kerr-McGee Blends in TP-H7036 | 183 |
| 62. Mechanical Properties for PEPCON Blends in TP-H7036 | 184 |
| 63. Mixer Comparison for Kerr-McGee Blends in TP-H7036 | 185 |
| 64. Mixer Comparison for PEPCON Blends in TP-H7036 | 186 |
| 65. Theory Test Data for Various Size Fractions of Oxidizer | 188 |
| 66. Propellant Formulation | 189 |
| 67. Summary of Work with Nominal 90 Micron AP | 194 |

TABLES (continued)

| | <u>Page No.</u> |
|---|-----------------|
| 68. Summary of Work with Nominal 50 Micron AP | 196 |
| 69. Summary of Work with High Speed Grind AP | 202 |
| 70. Summary of Work with Fluid Energy Milled AP | 203 |
| 71. Summary of Work with SWECO Ground Dry Powder | 211 |
| 72. Summary of Work with Aluminum Powder | 213 |
| 73. Recommended Procedure for Characterizing a New Lot of Ammonium Perchlorate | 225 |

FIGURES

| | <u>Page No.</u> |
|--|-----------------|
| 1. Burn Rate-Pressure Relationship for Mixture of 400, 200, and 3 micron AP | 21 |
| 2. Graphical Representation of Blend Composition Points for Wet Packing Fraction and Viscosity Measurement | 22 |
| 3. Wet Packing Fraction Data - Beaker Premixed followed by Centrifugation | 23 |
| 4. Wet Packing Fraction Data - Premixed in Centrifuge Tube followed by Centrifugation | 24 |
| 5. Composition-Viscosity Matrix for TP-H7036 (less curative) (400, 200, and 3 micron AP) | 26 |
| 6. Composition-Viscosity Matrix for TP-H7036 (less curative) (400, 200, and 16 micron AP) | 27 |
| 7. Viscosity Response Plot for a Mixture of 400, 200 and 16 micron AP in TP-H7036 | 28 |
| 8. Viscosity Response Plot for a Mixture of 400, 200, and 3 micron AP in TP-H7036 | 29 |
| 9. Burn Rate-Pressure Relationship for Kerr McGee Blends in TP-H7036 Propellant | 30 |
| 10. Burn Rate-Pressure Relationship for PEPCON Blends in TP-H7036 Propellant | 31 |
| 11. AP Particle Size Distribution (Modified MSA) | 38 |
| 12. AP Particle Size Distribution (Modified MSA) | 39 |
| 13. AP Particle Size Distribution (Modified MSA) | 40 |
| 14. AP Particle Size Distribution (Modified MSA) | 41 |
| 15. AP Particle Size Distribution (Modified MSA) | 42 |
| 16. AP Particle Size Distribution (Modified MSA) | 43 |
| 17. AP Particle Size Distribution (Modified MSA) | 44 |

Figures (continued)

| | <u>Page No.</u> |
|---|-----------------|
| 18. AP Particle Size Distribution (Modified MSA) | 45 |
| 19. AP Particle Size Distribution (Modified MSA) | 46 |
| 20. AP Particle Size Distribution (Modified MSA) | 47 |
| 21. AP Particle Size Distribution (Modified MSA) | 48 |
| 22. AP Particle Size Distribution (Modified MSA) | 49 |
| 23. AP Particle Size Distribution (Modified MSA) | 50 |
| 24. AP Particle Size Distribution (Modified MSA) | 51 |
| 25. AP Particle Size Distribution (Modified MSA) | 52 |
| 26. AP Particle Size Distribution (Modified MSA) | 53 |
| 27. Plot of "Distribution Describing Parameters" as Burn Rate for Kerr-McGee Oxidizer | 55 |
| 28. Plot of "Distribution Describing Parameters" as Burn Rate for Kerr-McGee Oxidizer | 56 |
| 29. Plot of "Distribution Describing Parameters" as Burn Rate for Kerr-McGee Oxidizer | 57 |
| 30. Plot of "Distribution Describing Parameters" as Burn Rate for Kerr-McGee Oxidizer | 58 |
| 31. Plot of "Distribution Describing Parameters" as Burn Rate for Pacific Engineering Oxidizer | 59 |
| 32. Plot of "Distribution Describing Parameters" as Burn Rate for Pacific Engineering Oxidizer | 60 |
| 33. Plot of "Distribution Describing Parameters" as Burn Rate for Pacific Engineering Oxidizer | 61 |
| 34. Plot of "Distribution Describing Parameters" as Burn Rate for Pacific Engineering Oxidizer | 62 |
| 35. Compositions Exhibiting Constant WMD for Kerr-McGee AP | 64 |

Figures (continued)

| | <u>Page No.</u> |
|---|-----------------|
| 36. Compositions Exhibiting Constant WMD for Pacific Engineering AP | 65 |
| 37. Composition - Constant Burn Rate Relationship for Kerr-McGee Blends | 68 |
| 38. Composition - Viscosity Plot for Kerr-McGee Blends | 69 |
| 39. Composition - Constant Burn Rate Relationship for PEPCON Blends | 70 |
| 40. Composition - Viscosity Plot for PEPCON Blends | 71 |
| 41. Lines of Constant Burn Rate versus Composition for all Kerr-McGee and all PEPCON Blends | 73 |
| 42. Composition - Constant Burn Rate Relationship for Mixtures of 400 Micron Kerr-McGee, 200 Micron PEPCON, and a Kerr-McGee 20 Micron Fraction | 74 |
| 43. Composition - Viscosity Plot for Blends of 400 Micron Kerr-McGee, 200 Micron PEPCON, and a Kerr-McGee 20 Micron Fraction | 75 |
| 44. Composition - Constant Burn Rate Relationship for Mixtures of 400 Micron PEPCON, 200 Micron Kerr-McGee and a Kerr-McGee 20 Micron Fraction | 76 |
| 45. Composition - Viscosity Plot for Blends of 400 Micron PEPCON, 200 Micron Kerr-McGee, and a 20 Micron Kerr-McGee Fraction | 77 |
| 46. Burn Rate - Pressure Data for Optimum Blends in CTPB Propellant | 83 |
| 47. Burn Rate - Pressure Data for Optimum Blends in HTPB Propellant | 84 |
| 48. Burn Rate - Pressure Relationships for the Humidified Optimum Blends in CTPB and HTPB Propellants | 85 |
| 49. Failure Boundary - (T-260) KM/KM in CTPB | 113 |
| 50. Failure Boundary - (T-261) KM/KM in CTPB | 114 |

Figures (continued)

| | <u>Page No.</u> |
|--|-----------------|
| 51. Failure Boundary (T-269) P/P in CTPB | 115 |
| 52. Failure Boundary (T-270) P/P in CTPB | 116 |
| 53. Failure Boundary (T-267) KM/P in CTPB | 117 |
| 54. Failure Boundary (T-268) KM/P in CTPB | 118 |
| 55. Failure Boundary (T-264) KM/KM in CTPB (Humidified) | 119 |
| 56. Failure Boundary (T-265) P/P in CTPB (Humidified) | 120 |
| 57. Failure Boundary (T-266) KM/P in CTPB (Humidified) | 121 |
| 58. Failure Boundary (T-271) KM/KM in HTPB | 122 |
| 59. Failure Boundary (T-272) KM/KM in HTPB | 123 |
| 60. Failure Boundary (T-273) P/P in HTPB | 124 |
| 61. Failure Boundary (T-277) P/P in HTPB | 125 |
| 62. Failure Boundary (T-278) KM/P in HTPB | 126 |
| 63. Failure Boundary (T-285) KM/P in HTPB | 127 |
| 64. Failure Boundary (T-274) KM/KM in HTPB (Humidified) | 128 |
| 65. Failure Boundary (T-276) P/P in HTPB (Humidified) | 129 |
| 66. Failure Boundary (T-275) KM/P in HTPB (Humidified) | 130 |
| 67. Comparison of Uniaxial and Biaxial Failure Behavior (T-260) KM/KM in CTPB | 131 |
| 68. Comparison of Uniaxial and Biaxial Failure Behavior (T-270) P/P in CTPB | 132 |

Figures (continued)

| | <u>Page No.</u> |
|--|-----------------|
| 69. Comparison of Uniaxial and Biaxial Failure Behavior (T-268) KM/P in CTPB | 133 |
| 70. Comparison of Uniaxial and Biaxial Failure Behavior (T-264) KM/KM in CTPB (Humidified) | 134 |
| 71. Comparison of Uniaxial and Biaxial Failure Behavior (T-265) P/P in CTPB (Humidified) | 135 |
| 72. Comparison of Uniaxial and Biaxial Failure Behavior (T-266) KM/P in CTPB (Humidified) | 136 |
| 73. Comparison of Uniaxial and Biaxial Failure Behavior (T-271) KM/KM in HTPB | 137 |
| 74. Comparison of Uniaxial and Biaxial Failure Behavior (T-273) P/P in HTPB | 138 |
| 75. Comparison of Uniaxial and Biaxial Failure Behavior (T-278) KM/P in HTPB | 139 |
| 76. Comparison of Uniaxial and Biaxial Failure Behavior (T-274) KM/KM in HTPB (Humidified) | 140 |
| 77. Comparison of Uniaxial and Biaxial Failure Behavior (T-276) P/P in HTPB (Humidified) | 141 |
| 78. Relaxation Modulus (T-260) KM/KM in CTPB | 142 |
| 79. Relaxation Modulus (T-261) KM/KM in CTPB | 143 |
| 80. Relaxation Modulus (T-269) P/P in CTPB | 144 |
| 81. Relaxation Modulus (T-270) P/P in CTPB | 145 |
| 82. Relaxation Modulus (T-267) KM/P in CTPB | 146 |
| 83. Relaxation Modulus (T-268) KM/P in CTPB | 147 |
| 84. Relaxation Modulus (T-264) KM/KM in CTPB | 148 |
| 85. Relaxation Modulus (T-265) P/P in CTPB | 149 |
| 86. Relaxation Modulus (T-266) KM/P in CTPB (Humidified) | 150 |

Figures (continued)

| | <u>Page No.</u> |
|---|-----------------|
| 87. Relaxation Modulus (T-271) KM/KM in HTPB | 151 |
| 88. Relaxation Modulus (T-272) KM/KM in HTPB | 152 |
| 89. Relaxation Modulus (T-273) P/P in HTPB | 153 |
| 90. Relaxation Modulus (T-277) P/P in HTPB | 154 |
| 91. Relaxation Modulus (T-278) KM/P in HTPB | 155 |
| 92. Relaxation Modulus (T-285) KM/P in HTPB | 156 |
| 93. Relaxation Modulus (T-274) KM/KM in HTPB (Humidified) | 157 |
| 94. Relaxation Modulus (T-276) P/P in HTPB (Humidified) | 158 |
| 95. Relaxation Modulus (T-275) KM/P in HTPB (Humidified) | 159 |
| 96. Thermal Expansion Data (T-260) KM/KM in CTPB | 160 |
| 97. Thermal Expansion Data (T-270) P/P in CTPB | 161 |
| 98. Thermal Expansion Data (T-268) KM/P in CTPB | 162 |
| 99. Thermal Expansion Data (T-271) KM/KM in HTPB | 163 |
| 100. Thermal Expansion Data (T-273) P/P in HTPB | 164 |
| 101. Thermal Expansion Data (T-278) KM/P in HTPB | 165 |
| 102. Lot 4087 90 Micron AP Particle Size | 192 |
| 103. Effect of Feed Rate on 90 Micron AP Run | 193 |
| 104. Composite of Runs DC-19 and DC-20 | 197 |
| 105. Composite of Runs DC-21 through DC-30 | 198 |
| 106. Composite of Runs DC-39 through DC-41 and DC-63 through DC-65 | 199 |

Figures (continued)

| | <u>Page No.</u> |
|--|-----------------|
| 107. Effect of Feed Rate on 50 Micron AP Runs | 200 |
| 108. Composite of Runs DC-54 through DC-59, DC-60 and DC-61 | 205 |
| 109. Composite of Runs DC-54 through DC-59 and DC-62 | 206 |
| 110. Effect of Feed Rate on HSG AP Runs | 207 |
| 111. Effect of Feed Rate on HSG AP Runs | 208 |
| 112. Composite of Runs DC-72 and DC-73 | 214 |
| 113. Composite of Runs DC-75 and DC-76 | 216 |

BACKGROUND AND SUMMARY

Current, typical raw material acceptance procedures (e.g., particle size measurements, chemical assay, "standardization" mixes using 5-gallon or 20-gallon size mixes of propellant) are expensive and time consuming. The oxidizer blends and curing agent concentration for the standardization mixes are selected based on previous experience with other lots of raw materials. If the required ballistic and mechanical property goals are not achieved, then additional standardization mixes are made using variations in oxidizer blends and/or polymer-curing agent concentrations. This program was designed to provide some technically responsible means of accepting new lots of ingredients for production programs without resorting to "use" types of acceptance tests. Major emphasis was placed on defining how variations in the ingredients, especially the source, size, shape, and particle size distribution of the AP, affect mix-to-mix propellant burn rate and mechanical properties. Consequently, all ingredients were thoroughly characterized, chemically and physically where pertinent, and incorporated into well characterized, in-production carboxyl terminated polybutadiene and hydroxy terminated polybutadiene propellants.

Variations were made in the AP, in a known and controlled manner, to define and develop techniques through which any lot of AP can be characterized in such a way that an exact definition of oxidizer blend is available for meeting precisely the burn rate and physical property requirements in processible CTPB and HTPB propellants. The weight median diameter of the oxidizer was shown to be the best "distribution describing parameter" for controlling burning rate. Triangular plots, based on particle size distribution, were developed to define lines of constant burn rates. Overlays, showing counterpart information on process and properties, were developed so that an optimum AP particle size blend could be selected using oxidizer supplied by a single vendor or by different vendors since AP from different vendors exhibited different stabilities, burn rates and particle size distributions. A reduction in end-of-mix viscosity of about 30% (compared to production lots of propellants) was realized through optimization of AP blend while maintaining burn rate. The validity of these techniques and propellant reproducibility were confirmed in demonstration (five-gallon size) mixes. Mechanical property and ballistic assessment of technique validity was accomplished. These techniques, when applied to marginally processible propellants, should permit the utilization of high solids, higher surface area propellant formulations.

Evaluation of the Donaldson Particle Classifier confirmed that the unit was capable of providing AP fractions in the 0.5 - 50 micron particle size range. Feed (input) problems were encountered with AP having a WMD (MSA) in the 0.5 - 2.0 micron size range with the coated feed-stock exhibiting the better characteristics.

OBJECTIVE AND SCOPE

The over-all objective of this program was to demonstrate improved reproducibility of solid propellant properties by complete characterization and control of the ammonium perchlorate (AP) and processing variables. This program was initiated to demonstrate improved reproducibility of solid propellant ballistic and mechanical properties, with emphasis on the determination of the effects of AP size distribution, AP surface area and ingredient source.

TABLE 1

AMMONIUM PERCHLORATE ASSAY

| Lot No. | Vendor | pH | | Acid Insoluble | | Chloride | | Sulfated Ash | | Bromate | |
|---------|--------------------|-------------|------|----------------|-------|-------------|-------|--------------|-------|-------------|---------|
| | | Analysis, % | Avg. | Analysis, % | Avg. | Analysis, % | Avg. | Analysis, % | Avg. | Analysis, % | Avg. |
| 4089 | KM ¹ | 6.2 | 6.2 | 0.003 | 0.004 | 0.008 | 0.008 | 0.208 | 0.196 | 0.00016 | 0.00016 |
| | | 6.2 | | 0.004 | | 0.007 | | 0.184 | | 0.00016 | |
| 4090 | KM | 6.2 | 6.2 | 0.002 | 0.002 | 0.005 | 0.005 | 0.248 | 0.250 | 0.00017 | 0.00017 |
| | | 6.1 | | 0.003 | | 0.005 | | 0.251 | | 0.00017 | |
| 4093 | KM | 6.2 | 6.2 | 0.003 | 0.004 | 0.013 | 0.013 | 0.223 | 0.220 | 0.00023 | 0.00026 |
| | | 6.2 | | 0.004 | | 0.013 | | 0.217 | | 0.00028 | |
| 4094 | KM | 6.3 | 6.3 | 0.003 | 0.004 | 0.021 | 0.021 | 0.194 | 0.192 | 0.00027 | 0.00028 |
| | | 6.3 | | 0.004 | | 0.021 | | 0.189 | | 0.00030 | |
| 4102 | PEPCO ² | 6.1 | 6.2 | 0.003 | 0.002 | 0.094 | 0.094 | 0.368 | 0.364 | 0.00027 | 0.00027 |
| | | 6.2 | | 0.002 | | 0.094 | | 0.360 | | 0.00027 | |
| 4103 | PEPCO | 5.9 | 5.9 | 0.004 | 0.004 | 0.104 | 0.104 | 0.366 | 0.367 | 0.00026 | 0.00026 |
| | | 5.9 | | 0.005 | | 0.104 | | 0.368 | | 0.00026 | |
| 4104 | PEPCO | 6.0 | 6.0 | 0.001 | 0.002 | 0.132 | 0.132 | 0.359 | 0.353 | 0.00036 | 0.00035 |
| | | 6.0 | | 0.002 | | 0.134 | | 0.347 | | 0.00034 | |
| 4105 | PEPCO | 6.0 | 6.0 | 0.001 | 0.001 | 0.126 | 0.126 | 0.334 | 0.330 | 0.00030 | 0.00030 |
| | | 6.0 | | 0.001 | | 0.126 | | 0.326 | | 0.00031 | |

1. Kerr - McGee
2. Pacific Engineering Company

TABLE 1 (CONT'D)
AMMONIUM PERCHLORATE ASSAY

| Lot No. | Vendor | Chlorate | | Iron | | Perchlorate | | Phosphate | | Water | | |
|---------|--------------------|------------------|--------|------------------|--------|----------------|-------|----------------|-------|----------|-------------|-------------|
| | | Analysis, % | Avg. | Analysis, % | Avg. | Analysis, % | Avg. | Analysis, % | Avg. | Total, % | Internal, % | External, % |
| 4089 | KM ¹ | 0.0049 0.0049 | 0.0049 | 0.0012 0.0015 | 0.0014 | 99.87 99.59 | 99.73 | 0.072 0.074 | 0.073 | .032 | .015 | .017 |
| 4090 | KM | 0.0049 0.0049 | 0.0049 | 0.0017 0.0013 | 0.0015 | 99.90 99.70 | 99.80 | 0.079 0.084 | 0.082 | .032 | .016 | .016 |
| 4093 | KM | 0.0048 0.0048 | 0.0048 | 0.0012 0.0009 | 0.0010 | 99.77 99.43 | 99.60 | 0.069 0.064 | 0.066 | .064 | .049 | .015 |
| 4094 | KM | 0.0098 0.0098 | 0.0098 | 0.0007 0.0006 | 0.0006 | 99.70 99.71 | 99.70 | 0.062 0.059 | 0.060 | .033 | .025 | .013 |
| 4102 | PEPCO ² | 0.0198 0.0198 | 0.0198 | 0.0007 0.0007 | 0.0007 | 99.60 99.75 | 99.68 | 0.074 0.073 | 0.074 | .044 | .033 | .012 |
| 4103 | PEPCO | 0.0198 0.0148 | 0.0173 | 0.0010 0.0008 | 0.0009 | 99.77 99.89 | 99.83 | 0.084 0.083 | 0.084 | .037 | .025 | .012 |
| 4104 | PEPCO | 0.0198 0.0198 | 0.0198 | 0.0005 0.0007 | 0.0006 | 99.95 99.82 | 99.88 | 0.078 0.090 | 0.084 | .070 | .060 | .010 |
| 4105 | PEPCO | 0.0148 0.0198 | 0.0173 | 0.0006 0.0006 | 0.0006 | 99.71 99.84 | 99.78 | 0.073 0.070 | 0.072 | .070 | .060 | .010 |

1. Kerr - McGee
2. Pacific Engineering Company

TABLE 2

Specification for Ammonium Perchlorate with Tricalcium Phosphate Conditioner

Chemical and Physical Properties

| <u>Property</u> | <u>Class 1</u> | | <u>Class 3</u> | |
|---|----------------|------------|----------------|------------|
| | <u>Min</u> | <u>Max</u> | <u>Min</u> | <u>Max</u> |
| External Moisture, % | --- | 0.02 | --- | 0.02 |
| Internal Moisture, % | --- | 0.04 | --- | 0.07 |
| Acid Insoluble, % | --- | 0.04 | --- | 0.04 |
| pH of Water Solution | 5.0 | 6.5 | 5.0 | 6.5 |
| Chloride, as NH_4Cl , % | --- | 0.155 | --- | 0.155 |
| Sulfated Ash, as NaClO_4 , % | --- | 0.9 | --- | 0.9 |
| Bromate, as NH_4BrO_3 , % | --- | 0.004 | --- | 0.004 |
| Chlorate, as NH_4ClO_3 , % | --- | 0.020 | --- | 0.020 |
| Iron, as Fe_2O_3 , % | --- | 0.0036 | --- | 0.0036 |
| Perchlorate, as NH_4ClO_4 , % | 98.3 | --- | 98.3 | --- |
| Phosphate, as P_2O_5 , % | 0.06 | 0.10 | 0.06 | 0.10 |
| Particle Size Distribution | | | | |
| Cumulative % Retained | | | | |
| No. 30 Sieve | --- | --- | --- | 3.0 |
| No. 40 Sieve | 6.0 | 4.0 | 35.0 | 55.0 |
| No. 50 Sieve | 3.0 | 11.0 | 90.0 | 100.0 |
| No. 70 Sieve | 13.0 | 43.0 | 98.0 | 100.0 |
| No. 100 Sieve | 50.0 | 86.0 | --- | --- |
| No. 140 Sieve | 85.0 | 98.0 | --- | --- |
| No. 200 Sieve | 97.0 | 100.0 | --- | --- |

Differential scanning calorimeter (DSC) scans were performed on each of these eight lots of AP. The areas under the exotherm in the DSC scans are proportional to the extent of decomposition. If the areas of these exotherms are then divided by the area of the AP phase change for a particular sample, values are obtained which quantitatively show the amount of decomposition at each exotherm. The ratios for these eight lots of AP, along with the exotherm temperatures are shown in Table 3. The data do not include the major exotherm which begins at approximately 400°C. In other words, these data only represent what might be described as preliminary decomposition. Three times more preliminary decomposition occurs for PEPCON AP than is noted with Kerr-McGee AP. Also, the temperature at which this preliminary exotherm occurs is lower for the PEPCON AP. Both of these observations would indicate projected thermal instability with PEPCON AP. These data are in agreement with projections drawn from examination of the chemical assay data as a result of the high chlorate content.

Thermogravimetric analysis (isothermal TGA) were performed on each lot of AP at 190°C (350°F). The TGA data are also shown on Table 3, depicting the time to 1% weight loss. Note the shorter times for 1% weight loss with the PEPCON AP. Both the DSC and TGA data point out the greater thermal stability of Kerr-McGee AP compared to that of PEPCON AP.

The physical characterization of the 200 micron and 400 micron AP consisted of particle size measurement by two techniques, surface area determination, and a measure of the ease of friability of the AP.

The particle size distribution of each lot was determined by the standard ROTAP technique. The values of weight median diameter (WMD) are shown in Table 4. The distribution was also determined by the Mine Safety Appliance Co. (MSA) technique. This technique had to be modified so that sufficient settling times could be obtained for meaningful analysis. This was accomplished by using diethyl phthalate as the settling liquid. A summary of the technique developed, as well as the settling schedule, is shown in Appendix A. The MSA values for WMD are shown in Table 4. The technique appears to be most satisfactory for both 200 and 400 micron AP. The MSA determined distribution curves are shown in Appendix B.

The surface areas of the eight lots of Kerr-McGee and PEPCON AP have been measured by a krypton absorption (BET) technique. The results are shown in Table 4. Of significant interest is the fact that not much difference exists in the surface areas of 400 micron and 200 micron AP. This must be attributed to either a more spherical particle in the 400 micron fraction or more surface imperfections in the 200 micron fraction. As a general rule, the PEPCON AP exhibits a slightly higher surface area than

TABLE 3

Ratios and Exotherm Peak Temperatures of AP

| <u>Manufacturer</u> | <u>Lot No.</u> | <u>Exotherm Area</u> <u>Endotherm Area</u> | <u>Exotherm Peak</u> <u>Temp., °C</u> | <u>TGA Data</u> <u>Time (hrs)</u> <u>to 1% Wt. Loss (190°C)</u> |
|---------------------|----------------|---|--|---|
| Kerr-McGee | 4089 | 1.05 | 322 | 5.92 |
| Kerr-McGee | 4090 | 1.03 | 331 | 7.55 |
| Kerr-McGee | 4093 | 1.32 | 324 | 6.05 |
| Kerr-McGee | 4094 | 1.75 | 319 | 6.67 |
| PEPCON | 4102 | 4.25 | 302 | 4.17 |
| PEPCON | 4103 | 4.00 | 302 | 3.12 |
| PEPCON | 4104 | 4.08 | 298 | 3.42 |
| PEPCON | 4105 | 3.63 | 300 | 3.53 |

TABLE 4

AP PHYSICAL CHARACTERISTICS

| Lot No. | Type | Vençor | Particle Size MSA (WMD) | Particle Size ROTAP (WMD) | Surface Area m ² /g | Friability % |
|---------|-------|--------|----------------------------|------------------------------|---|-----------------|
| 4089 | 200 µ | KM | 180 | 190 | 0.0443 0.0693 (0.0598, 0.0624, 0.0614) | 2.0 |
| 4090 | 200 µ | KM | --- | 187 | 0.0781 0.0827 | 4.2 |
| 4093 | 400 µ | KM | 378 | 422 | 0.0682 0.0704 | 0.04 |
| 4094 | 400 µ | KM | --- | 428 | 0.0448 0.0441 | 0.04 |
| 4102 | 200 µ | PEPCON | 175 | 174 | 0.0835 0.0909 | 2.0 |
| 4103 | 200 µ | PEPCON | --- | 173 | 0.1003 0.1035 | 5.0 |
| 4104 | 400 µ | PEPCON | 395 | 410 | 0.0905 0.0839 | 0.2 |
| 4105 | 400 µ | PEPCON | --- | 418 | 0.0791 0.0764 | 0.2 |

do similar size fractions obtained from Kerr-McGee. Extraordinarily poor reproducibility was obtained on Kerr-McGee Lot 4089 (200 micron). To determine whether this irreproducibility is a result of poor sampling, three individual samples were taken from different locations in a single drum of this lot and submitted for surface area measurement. The results of this analysis are also shown in Table 4. The improved reproducibility of results indicates analytical error in the first replicate test.

Friability tests were performed on each of the eight lots of AP. The results are shown in Table 4. No meaningful trend can be determined. The friability test (Appendix C) is crude at best and little significance should be attached to these data.

Task 2 - Binder Characterization

A rather comprehensive characterization of HC-434 polymer was completed. The data collected appear in Table 5. Enough of this lot of polymer was reserved to complete the CTPB portion of this program. Note that in those analyses required for acceptance, none are out of specification.

The curatives, cure catalyst, and plasticizer for a typical 88% total solids CTPB propellant have likewise been assayed and are within specification. These data are shown in Tables 6 through 9.

A similar comprehensive characterization has been completed on Lot 3921 HTPB (R-45M) polymer. These data appear in Table 10.

The cure and bonding agents for the HTPB system have been assayed and the results are shown in Tables 11 and 12. Note that no specification limits have been set on HX-752 bonding agent. This results from not having assayed sufficient lots of material to determine sound requirements. It should be pointed out that this lot of HX-752 bonding agent has been utilized in most of the HTPB effort of TCC/Huntsville with satisfactory results.

Task 3 - Aluminum Characterization

The aluminum selected for utilization in this program has been assayed and found to be within specification. The assay results are shown in Table 13.

Phase II - AP Blend Characterization

The objective of this phase was to characterize several blends of AP in a selected CTPB formulation and to select a blend of Kerr-McGee AP, a blend of PEPCON AP, and a mixed blend which would meet burn rate requirements and be optimized for improved mechanical properties. This process for selecting the "optimum blends" should be applicable to any set of AP lots.

TABLE 5
ANALYSIS OF HC-434

MATERIAL: HC-434

TCC LOT NO: 3960

VENDOR: Thiokol Chemical Corp.

ANALYSIS RESULTS

| <u>Required Analyses</u> | <u>Limits</u> | | <u>TCC Acceptance</u> |
|--------------------------|---------------|-------------|-----------------------|
| | <u>Min.</u> | <u>Max.</u> | |
| Acid Equiv/100 g | 0.050 | 0.057 | 0.0510 |
| Moisture, % | --- | 0.05 | 0.042 |
| PBNA, % | 1.3 | 2.5 | 1.90 |
| Total Cl, % | --- | --- | 0.034 |
| Total Unsat n, % | --- | --- | 89.4 |
| Free Acid, % | --- | --- | 25.24 |
| Cis, % | --- | --- | 11.51 |
| Trans, % | --- | --- | 65.96 |
| Vinyl, % | --- | --- | 22.52 |
| Spec. Grav., 25°/25°C | 0.903 | 0.915 | 0.909 |
| Viscosity, poises | 200 | 275 | 219 |
| Intr. Viscosity | --- | --- | 0.118 |
| Molecular Weight | --- | --- | 4017 |
| Refractive Index | --- | --- | 1.515 |
| Functionality | --- | --- | 2.048 |

TABLE 6

ANALYSIS OF MAPO

MATERIAL: MAPOTCC LOT NO: 4021VENDOR: ArsyncoANALYSIS RESULTS

| <u>Required Analyses</u> | <u>Limits</u> | | <u>TCC Acceptance</u> |
|----------------------------|---------------|-------------|-----------------------|
| | <u>Min.</u> | <u>Max.</u> | |
| Assay, Imine, % | 95.5 | --- | 99.40 |
| Hydrolyzable Cl, % | --- | 0.5 | 0.012 |
| Total Cl, % | --- | 1.0 | 0.19 |
| Moisture, % | --- | 0.6 | 0.42 |
| Specific Gravity, 25°/25°C | 1.070 | 1.090 | 1.0787 |

TABLE 7
ANALYSIS OF ERL 0510

MATERIAL: ERL 0510
TCC LOT NO: 3856
VENDOR: Union Carbide

ANALYSIS RESULTS

| <u>Required Analyses</u> | <u>Limits</u> | | <u>TCC Acceptance</u> |
|----------------------------|---------------|-------------|-----------------------|
| | <u>Min.</u> | <u>Max.</u> | |
| Epoxy Equiv, g/ge | 107 | 95 | 99.30 |
| Equiv/100 g | 0.935 | 1.053 | 1.0070 |
| Nitrogen, % | 4.5 | 5.0 | 4.78 |
| Moisture, % | --- | 0.35 | .047 |
| Hydrolyzable Cl, % | --- | 0.6 | 0.25 |
| Specific Gravity, 25°/25°C | 1.206 | 1.225 | 1.2130 |
| Viscosity, cps | 550 | 850 | 779.8 |

TABLE 8
ANALYSIS OF IRON LINOLEATE

MATERIAL: Iron Linoleate
TCC LOT NO: 3643
VENDOR: Harshaw Chem. Co.

ANALYSIS RESULTS

| <u>Required Analyses</u> | <u>Limits</u> | | <u>TCC Acceptance</u> |
|--------------------------|---------------|-------------|-----------------------|
| | <u>Min.</u> | <u>Max.</u> | |
| Moisture, % | --- | 0.3 | 0.27 |
| Fe, % | 6.9 | 7.1 | 7.10 |
| Spec. Grav., 25°/25°C | 0.98 | 1.02 | 1.0016 |

TABLE 9
ANALYSIS OF DIOCTYL ADIFATE (DOA)

MATERIAL: Dioctyl Adipate (DOA)

TCC LOT NO: 4026

VENDOR: Harchem Div.

ANALYSIS RESULTS

| <u>Required Analyses</u> | <u>Limits</u> | | <u>TCC Acceptance</u> |
|--------------------------|---------------|-------------|-----------------------|
| | <u>Min.</u> | <u>Max.</u> | |
| Moisture, % | --- | 0.10 | 0.044 |
| Assay, % | 99.00 | --- | 99.22 |
| Acidity, % Acetic Acid | --- | 0.010 | 0.0029 |
| Spec. Grav., 25°/25°C | 0.921 | 0.927 | 0.9240 |

TABLE 10
ANALYSIS OF HTPB (R45M)

MATERIAL: HTPB (R-45M)

TCC LOT NO: 3921

VENDOR: ARCO

ANALYSIS RESULTS

| <u>Required Analyses</u> | <u>Limits</u> | | <u>TCC Acceptance</u> |
|--------------------------|---------------|-------------|-----------------------|
| | <u>Min.</u> | <u>Max.</u> | |
| Moisture, % | --- | 0.1 | 0.038 |
| Hydroxyl Equiv/100 g | 0.070 | 0.079 | 0.0748 |
| Peroxide, % | --- | 0.10 | 0.064 |
| Fe, % | --- | 0.01 | < 0.01 |
| Spec, Grav, 25°/25°C | 0.87 | 0.92 | 0.902 |
| Viscosity, p, 25°C | 40 | 70 | 61.0 |
| Cis, % | --- | --- | 19.00 |
| Trans. % | --- | --- | 58.12 |
| Vinyl, % | --- | --- | 22.88 |
| Molecular Weight | --- | --- | 3274 |
| Functionality | --- | --- | 2.45 |

TABLE 11
ANALYSIS OF DDI

MATERIAL: DDI
TCC LOT NO: 4009
VENDOR: General Mills

ANALYSIS RESULTS

| <u>Required Analyses</u> | <u>Limits</u> | | <u>TCC Acceptance</u> |
|----------------------------|---------------|-------------|-----------------------|
| | <u>Min.</u> | <u>Max.</u> | |
| NCO, % | 13.7 | 14.3 | 14.18 |
| Moisture, % | --- | 0.02 | 0.014 |
| Iron, % | --- | 0.01 | < 0.01 |
| Specific Gravity, 25°/25°C | 0.915 | 0.925 | 0.924 |
| Viscosity, cps, 25°C | 100 | 150 | 105.4 |
| Molecular Weight | --- | --- | 596 |
| Functionality | --- | --- | 2.01 |

TABLE 12
ANALYSIS OF HX-752

MATERIAL: HX-752
TCC LOT NO: 3966
VENDOR: 3M

ANALYSIS RESULTS

| <u>Required Analyses</u> | <u>Limits</u> | | <u>TCC Acceptance</u> |
|------------------------------|---------------|-------------|-----------------------|
| | <u>Min.</u> | <u>Max.</u> | |
| Equiv. Wt/Ring, g/g Equiv | --- | --- | 156.0 |
| H ₂ O, % | --- | --- | 0.110 |
| Specific Gravity, 25°/25°C | --- | --- | 1.1420 |
| Free Acid, Equiv/100 g | --- | --- | 0.00037 |
| Total Reactivity, g/g Equiv. | --- | --- | 137.74 |

TABLE 13
ANALYSIS OF ALUMINUM SPHERICAL, CLASS 4

MATERIAL: Aluminum Spherical Class 4

TCC LOT NO: 3941

VENDOR: Alcoa

ANALYSIS RESULTS

| <u>Required Analyses</u> | <u>Limits</u> | | <u>TCC Acceptance</u> |
|---------------------------|---------------|-------------|-----------------------|
| | <u>Min.</u> | <u>Max.</u> | |
| Aluminum Assay, % | 98.0 | --- | 99.50 |
| Volatiles, % | --- | 0.10 | 0.017 |
| Fe, % | --- | 0.40 | 0.19 |
| APD, microns | 17 | 32 | 17.6 |
| WMD micromerograph, μ | 22 | 37 | 25.2 |
| WMD, MSA, μ | --- | --- | 19.8 |
| Apparent Density, g/cc | 0.94 | 1.50 | 1.08 |
| Paste Viscosity, Kps | --- | 8.0 | 4.6 |

Task 1 - Select CTPB Control Formulation

A requirement for this program was the selection of a high total solids CTPB formulation, in production at the contractor's facility, which would serve as a baseline from which mechanical property improvements and improved reproducibility could be judged.

The propellant selected for this application was TP-H7036. This propellant, utilized in the Castor II series of motors, consists of 88% total solids (68% AP, 20% Al) and 12% binder. This propellant has been in production since mid-1966 and approximately 660 large mixes have been manufactured and used to load some 3.2 million pounds of propellant in the Castor II motors. The burn rate of TP-H7036 is quite easy to control. The mechanical properties have been adequate to meet the performance requirements; however, unpredicted and unexpected variations have been encountered on propellants from various mixes and when raw material lots were changed. The Castor II propellant was developed with the major emphasis on the low burning rate required and the propellant tensile properties, which were not optimized, were adjusted to provide the necessary performance.

The tensile properties tabulated for various material sets shown below imply that for some of the material sets the demonstrated production level for the elongation parameter would not be sufficiently high to tolerate the normal mix to mix and motor to motor variation encountered. That is, application of statistical analysis to the 0.251 in/in mean and ± 0.057 variation (three standard deviations) of raw material set 3a would indicate that some percentage of the mixes could be expected to fall below the 0.20 in/in minimum requirement; however, this condition has not been experienced in production.

Variations in the tensile properties of TP-H7036 are also shown below. It is evident from an examination of the tabulated numbers that the variations in the tensile properties of this propellant is a result of different capability levels of the various raw material sets. The variation in any given parameter from one set to another does not change significantly, but the level of the various properties shifts when major raw material changes have to be made. The tensile shifts are ordinarily attributed to variations in the CTPB polymer, and effort is not expended to adjust each parameter for each material set to some "optimum" level since performance requirements have been met. The target levels are arrived at by adding an overall variation, such as 0.06 in/in for TP-H7036 elongation, to the minimum specification requirements.

TP-H7036 TENSILE PROPERTY REPRODUCIBILITY

| Mat'l Set | No. of Mixes | P/CA ratio | Modulus (psi) | | | Strain @ Max. Stress (in/in) | | | Max. Stress (psi) | | | Strain Endurance (%) |
|--------------|--------------------|---------------|---------------|-----------|----------|------------------------------|-----------|----------|-------------------|-----------|----------|----------------------|
| | | | \bar{X} | Std. Dev. | C.V. (%) | \bar{X} | Std. Dev. | C.V. (%) | \bar{X} | Std. Dev. | C.V. (%) | |
| 1a | 10 | 1/.78 | 479 | 168 | 35.1 | 0.269 | 0.019 | 6.9 | 89 | 22 | 25.1 | -- |
| 1b | 70 | 1/.79 | 847 | 141 | 16.7 | 0.297 | 0.016 | 5.3 | 150 | 25 | 15.8 | 25.2 |
| 2 | 79 | 1/.79 | 884 | 109 | 12.3 | 0.253 | 0.017 | 6.9 | 144 | 15 | 10.7 | 23.9 |
| 3a | 20 | 1/.79 | 832 | 149 | 17.9 | 0.251 | 0.019 | 7.7 | 127 | 14 | 10.8 | 24.8 |
| 3b | 57 | 1/.79 | 635 | 140 | 22.1 | 0.301 | 0.018 | 6.0 | 119 | 24 | 20.2 | 27.8 |
| 4 | 78 | 1/.79 | 599 | 96 | 16.1 | 0.295 | 0.019 | 6.4 | 116 | 15 | 13.0 | 27.7 |
| 5 | 95 | 1/.79 | 817 | 105 | 12.8 | 0.299 | 0.016 | 5.3 | 158 | 15 | 9.5 | 27.1 |
| 6 | 113 | 1/.83 | 1028 | 141 | 13.7 | 0.274 | 0.015 | 5.5 | 162 | 17 | 10.5 | 24.4 |
| 7a | 30 | 1/.83 | 962 | 162 | 16.9 | 0.287 | 0.011 | 3.8 | 153 | 17 | 11.3 | 24.4 |
| 7b | 56 | 1/.82 | 947 | 87 | 9.2 | 0.283 | 0.013 | 4.6 | 156 | 12 | 7.6 | 24.5 |
| 8a | 25 | 1/.82 | 696 | 78 | 11.1 | 0.250 | 0.012 | 4.8 | 112 | 9.8 | 8.7 | 23.2 |
| 8b | 11 | 1/.82 | 724 | 40 | 5.5 | 0.266 | 0.017 | 6.3 | 120 | 6.1 | 5.1 | 25.1 |
| 8c | 8 | 1/.82 | 831 | 37 | 4.5 | 0.285 | 0.010 | 3.7 | 140 | 2.7 | 1.9 | 24.0 |
| 8d | 10 | 1/.82 | 992 | 132 | 13.4 | 0.266 | 0.015 | 5.7 | 142 | 11.8 | 7.4 | 20.4 |

NOTE: 77°F Test Temperature

Considering these things, the TP-H7036 formulation was selected as the CTPB production control formulation for evaluation in this task for the following reasons:

- 1) It has a long history of production which has provided much data for comparison.
- 2) It has an unexcelled flight history.
- 3) It contains no burn rate catalyst to cloud the issue of determining what oxidizer parameter controls burn rate.
- 4) It exhibits a high total solids loading.
- 5) It would serve as an excellent baseline from which mechanical property improvements and improved reproducibility could be judged since extensive mechanical properties characterization data are available.

Task 2 - Define Optimum Kerr-McGee Blend

This task was directed toward determining that blend of Kerr-McGee oxidizer which would provide the desired burn rate for TP-H7036 propellant, would result in the lowest possible end-of-mix viscosity, and would improve mechanical properties. The normal oxidizer distribution for TP-H7036 is 45% 400 micron AP, 27% 200 micron AP, and 28% 16 micron AP. Preliminary

observations suggest that lower end-of-mix viscosities might be achieved if the 16 micron fraction AP was replaced with a smaller size fraction. Therefore, the first item in this task was to determine whether the desired burn rate could be achieved by replacing the 16 micron fraction AP with a smaller size fraction AP. A three micron fraction AP was selected for evaluation. Calculations directed at providing the same WMD were performed and three blends of 400, 200, and 3 micron AP were selected for mix manufacture. Three one-pound mixes were manufactured and burning rate was determined. The resulting data are shown in Figure 1. Note that slightly lower than desirable burn rates were obtained when compared with the standard TP-H7036 blend (highest burn rate line). However, it is apparent that the desired burn rate could be achieved by replacing the 16 micron fraction AP with a similar fraction. Of further interest is the fact that, as the percentage of 400 micron AP decreases, the pressure exponent increases slightly.

With the knowledge that the 16 micron fraction AP could be replaced by a smaller fraction and still maintain the desired burn rate, the next work item was to determine if lower end-of-mix viscosities could be achieved with these similar size fractions. To accomplish this goal, wet packing fraction measurements were made with both the standard TP-H7036 oxidizer blend and oxidizer/aluminum ratio and with the smaller 3 micron fraction AP replacing the 16 micron fraction AP. Seven determinations were made at points illustrated in Figure 2. The aluminum size fraction (maintained constant at 20%) was 25 microns. The wet packing fractions were performed two ways. The first technique was to stir mixtures of oxidizer size fractions and aluminum in a beaker with hexane and wetting agent (Twitchell Base) to achieve complete dispersion with the solids. The sample was then transferred to the centrifuge tube and centrifuged at 2900 rpm's until constant bulk density was achieved. The resulting data are shown in Figure 3.

The second technique used was similar to the first except that ingredients were mixed in the centrifuge tube and no transfer was involved. The data resulting from this series of wet packing fraction measurements are shown in Figure 4. Note that major differences occur between the two techniques at the 50/50 mixture of 400 micron AP and the small fraction, whether it be the 3 or 16 micron AP.

The disappointing results from these two measurement techniques are primarily attributable to the fact that segregation of the very large and very small AP size fractions occurred in the centrifugation process.

It was felt that a more realistic approach toward obtaining the desired information as to which blend would obtain minimum viscosity would involve manufacturing propellant mixes, measuring viscosity, and then computing the viscosity versus composition maps for both the 400, 200, and 16 micron AP formulation and the 400, 200, and 3 micron AP formulation.

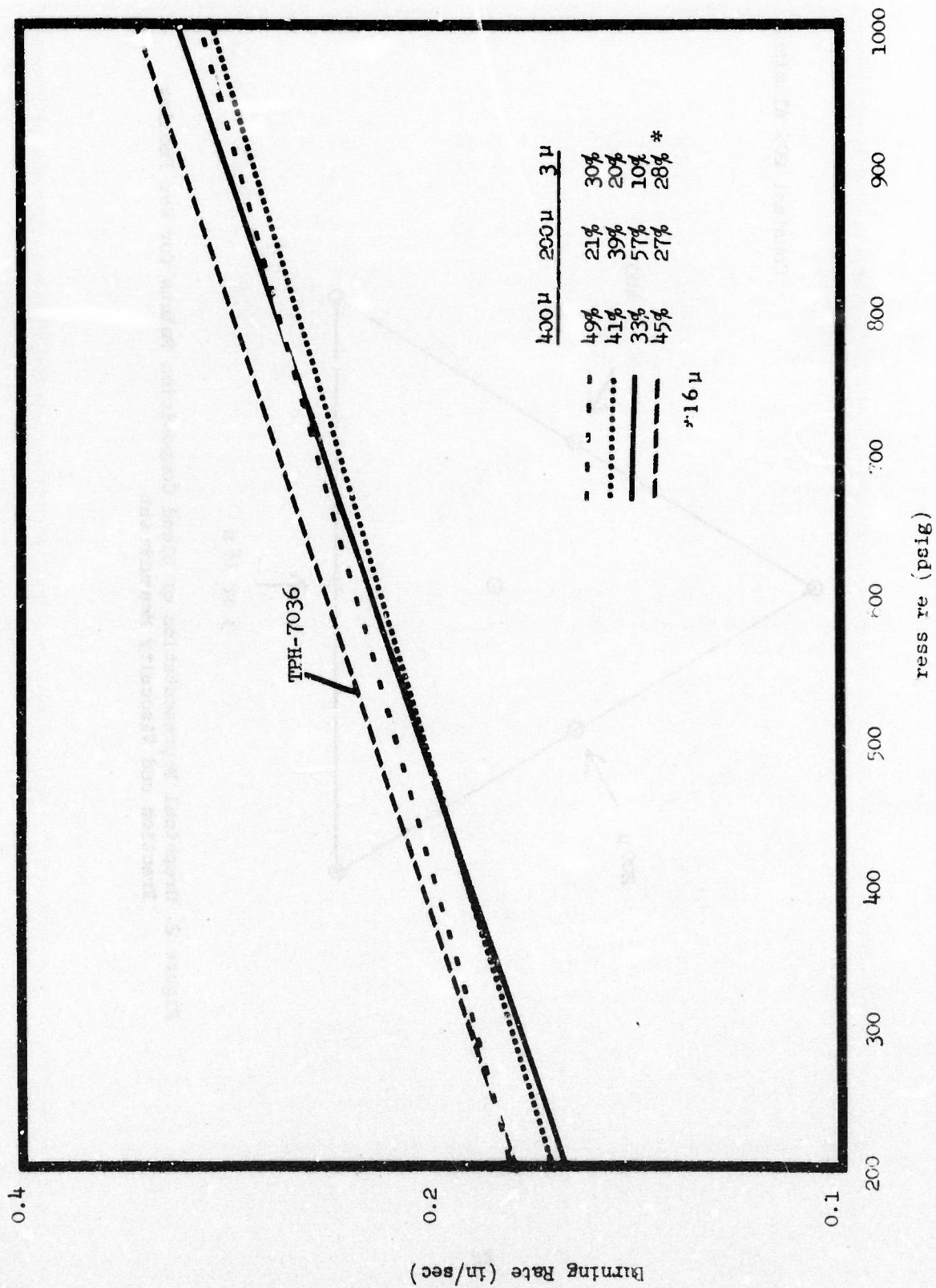


Figure 1. Burn Rate-Pressure Relationship for Mixture of 400, 200, and 3μ, AP

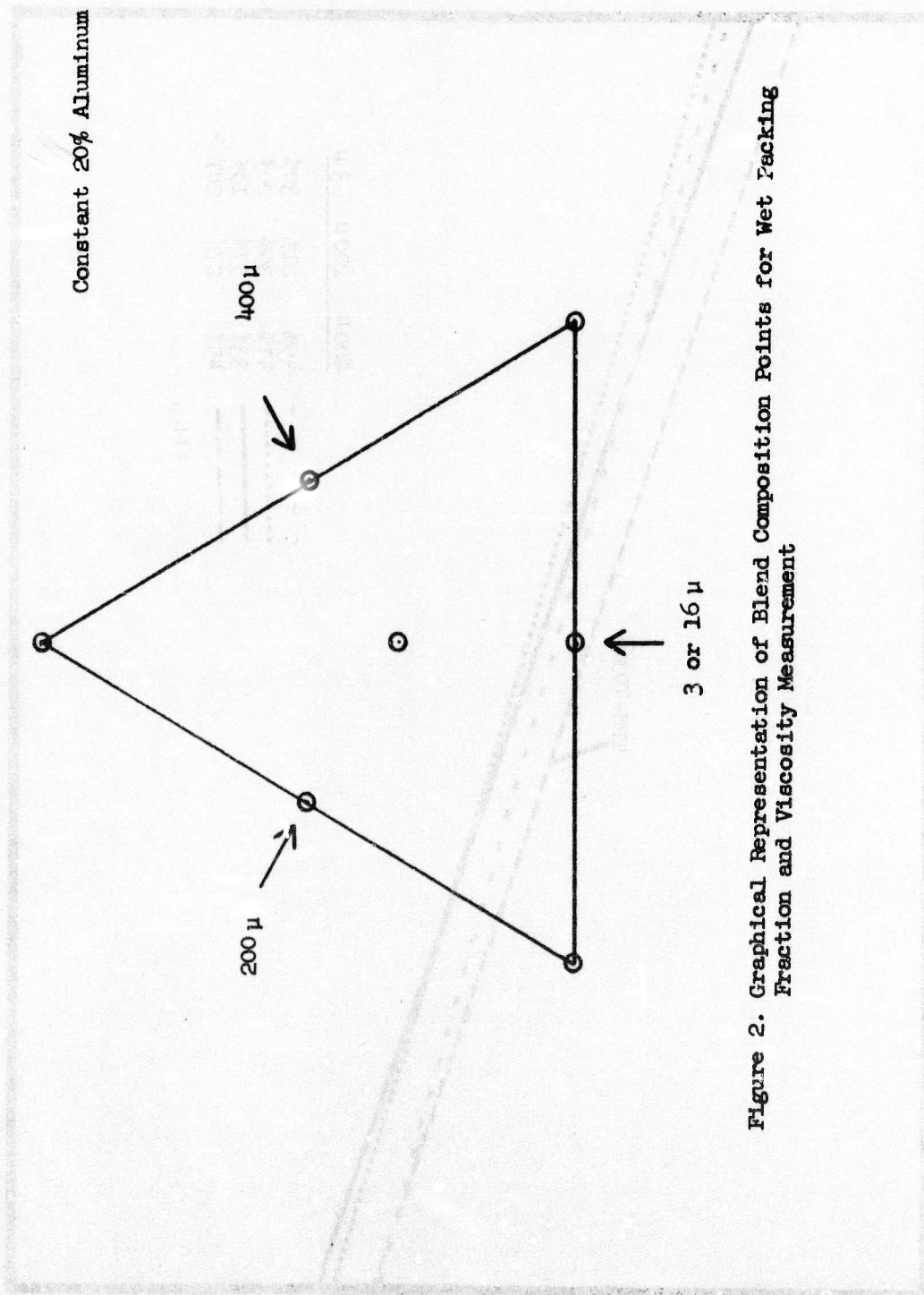


Figure 2. Graphical Representation of Blend Composition Points for Wet Packing Fraction and Viscosity Measurement

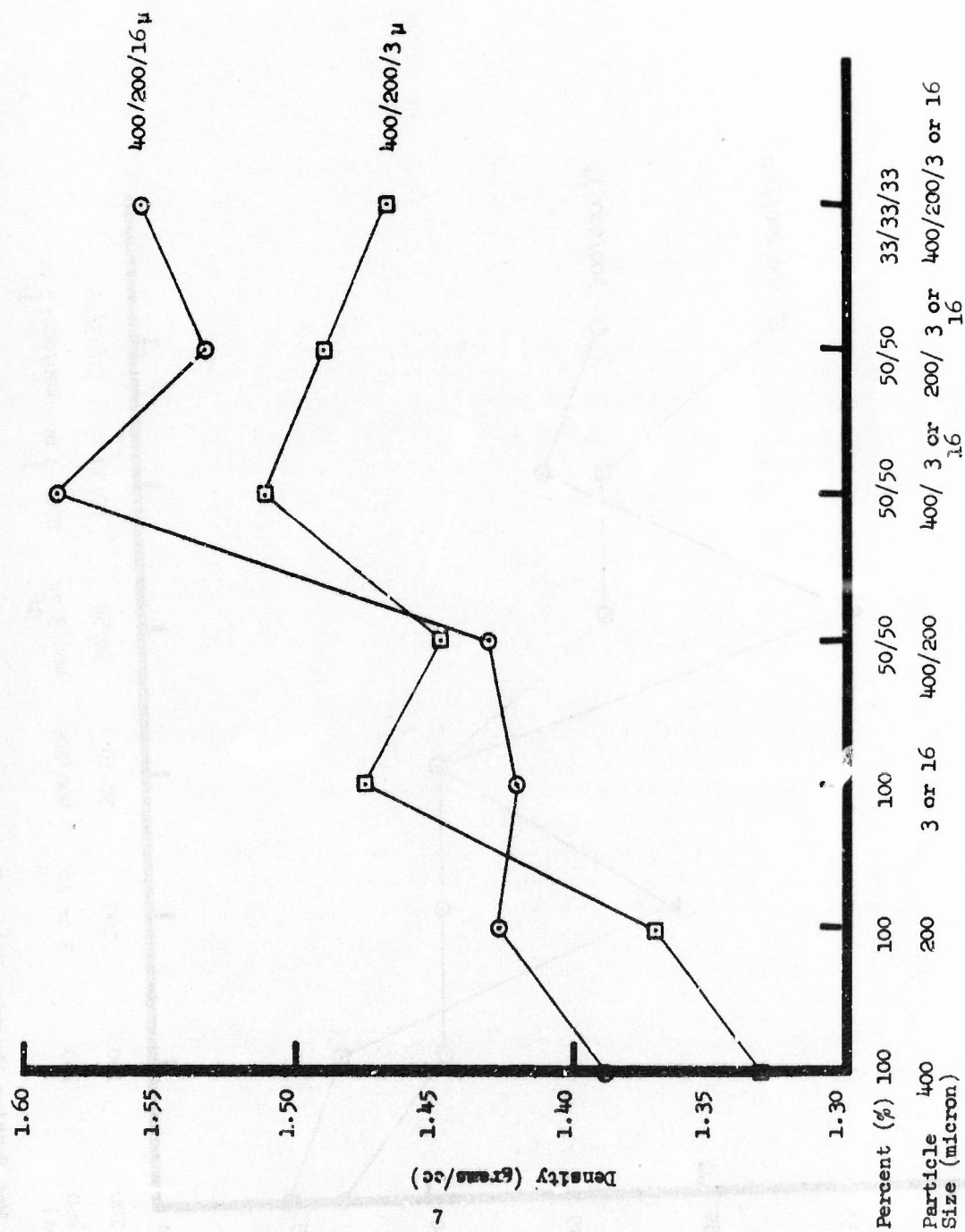


Figure 3. Wet Packing Fraction Data - Beaker Premixed Followed by Centrifugation

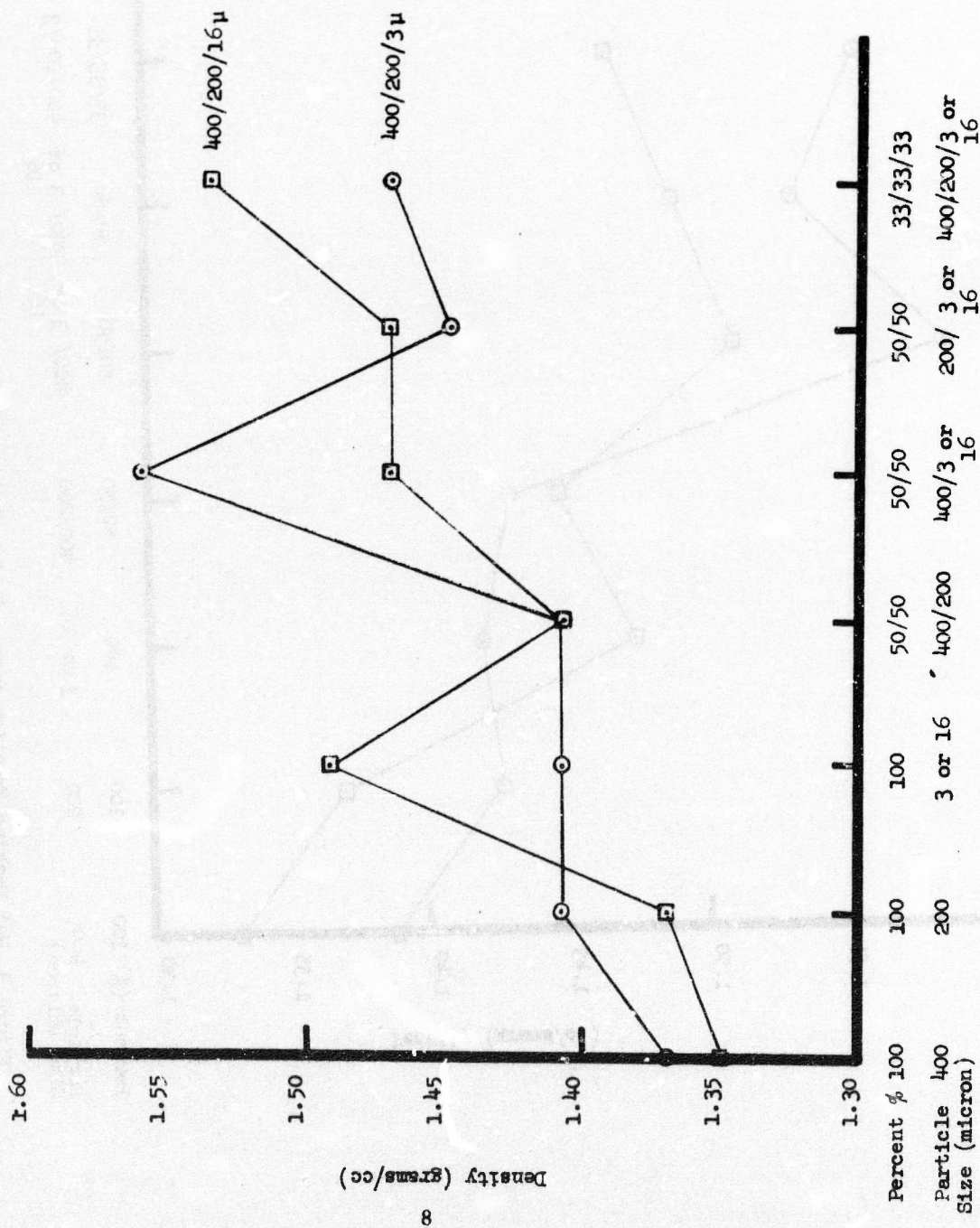


Figure 4. Wet Packing Fraction Data - Premixed in Centrifuge Tube Followed by Centrifugation

No curing agent is added to the mix so that the end-of-mix viscosities measured do not reflect actual propellant end-of-mix viscosities. However, the constancy of the mixing procedure should provide meaningful results.

Mixes were manufactured at the designated matrix points (Figures 5 and 6). The viscosities were measured on a HAAKE viscometer. Note that on some formulations numerical values for viscosity were not achieved.

To obtain measurable viscosities, a new triangular matrix was formed within the major matrix (Figures 5 and 6). Mixes were manufactured at these points and viscosities measured. The formulation containing the largest amount of the small size fraction again exhibited a viscosity higher than the apparatus could measure. Nevertheless, viscosity response plots were prepared for each of these trimodals. The composition-viscosity response plots are shown in Figures 7 and 8. Note that, although there is a larger area for a minimum viscosity for the 400, 200 and 3 micron AP trimodal, the opportunity to obtain lower viscosity for that trimodal is not apparent. In view of this judgement and the realization that 16 micron AP is less susceptible to particle growth than is the 3 micron AP, a decision was made to use the 400, 200, and 16 micron AP trimodal throughout the remainder of the program. Of significant importance is the observation that much lower viscosities can be obtained with the 400, 200, and 16 micron AP trimodal than are presently realized in the TP-H7036 propellant (see Figure 7). A single lot of oxidizer (Kerr-McGee) was used to prepare all 16 micron AP for this program.

The next work item was to determine a single blend of Kerr-McGee AP and a single blend of all-PEPCON AP which would match the desired TP-H7036 burn rate. To accomplish this, three one-gallon mixes were manufactured in which the percentage of the 16 micron fraction AP was varied 3% around a nominal. The burn rates were determined in a Crawford strand burner and the results are shown in Figures 9 and 10. The normal trimodal distribution of TP-H7036 is 45% 400 micron, 27% 200 micron, and 28% 16 micron. The variations performed, therefore, include composition change in the ground fraction between 25 and 31%. The 16 micron AP was swapped in each case for 400 micron material. Note, in comparing Figures 9 and 10, that to match burn rate with Kerr-McGee oxidizer, approximately 2.6% more ground material will be required than that which is considered normal. In contrast, to match burn rate with PEPCON oxidizer, approximately 2.2% less ground material will be required.

Having ascertained that blend of Kerr-McGee oxidizer and that blend of PEPCON oxidizer which is required to meet the TP-H7036 burn rate, it was now important to determine what physical characteristics of the oxidizer blend can best be correlated with burn rate. To accomplish this goal, a series of eight 1000 gram mixes was manufactured for both Kerr-McGee and PEPCON AP in which the ratios of the 400, 200, and 16 micron AP were widely varied. The variation in percentages of the various AP size fractions for each of the eight mixes is shown in Table 14.

Constant: Aluminum 20%
Binder 12%

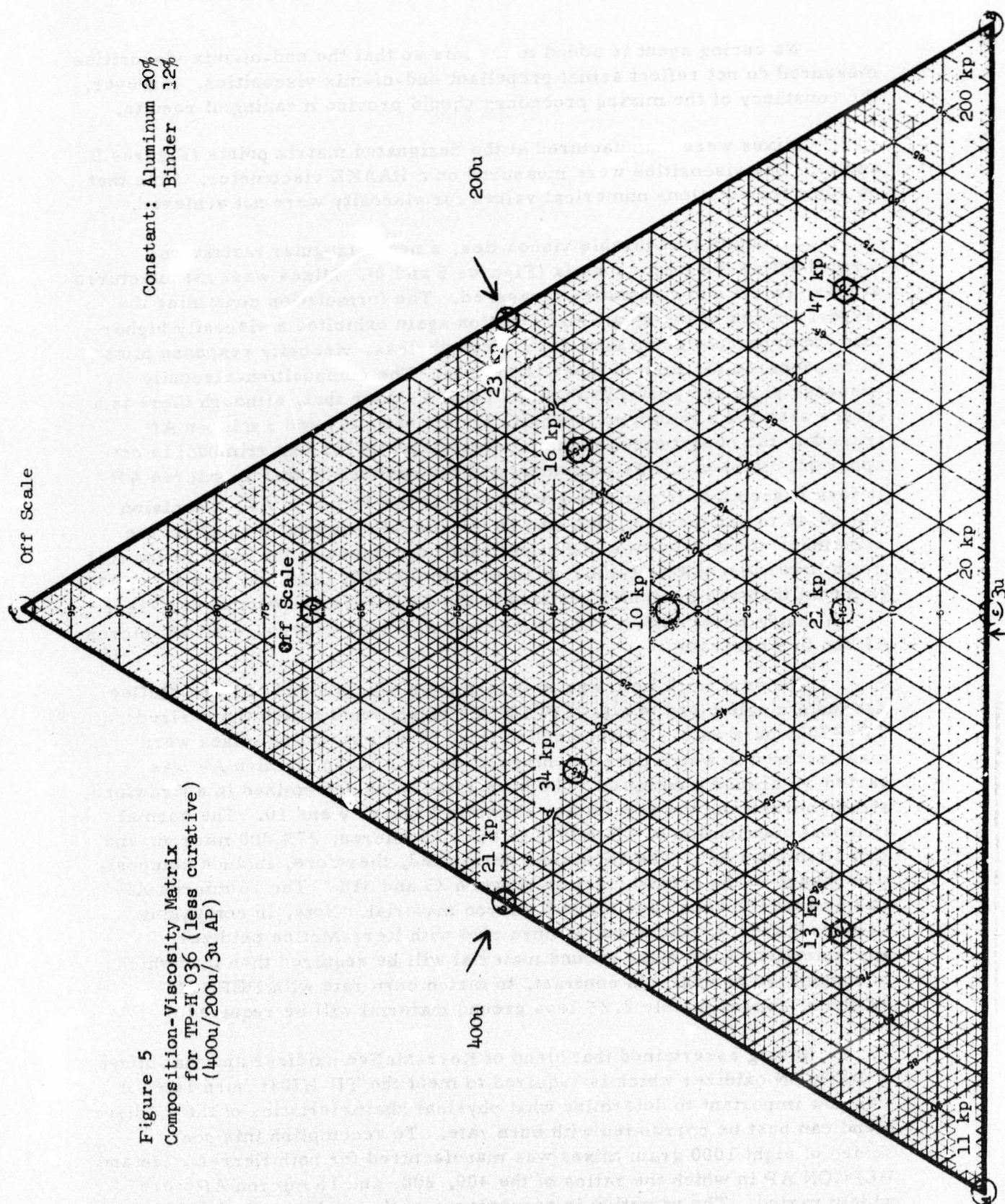
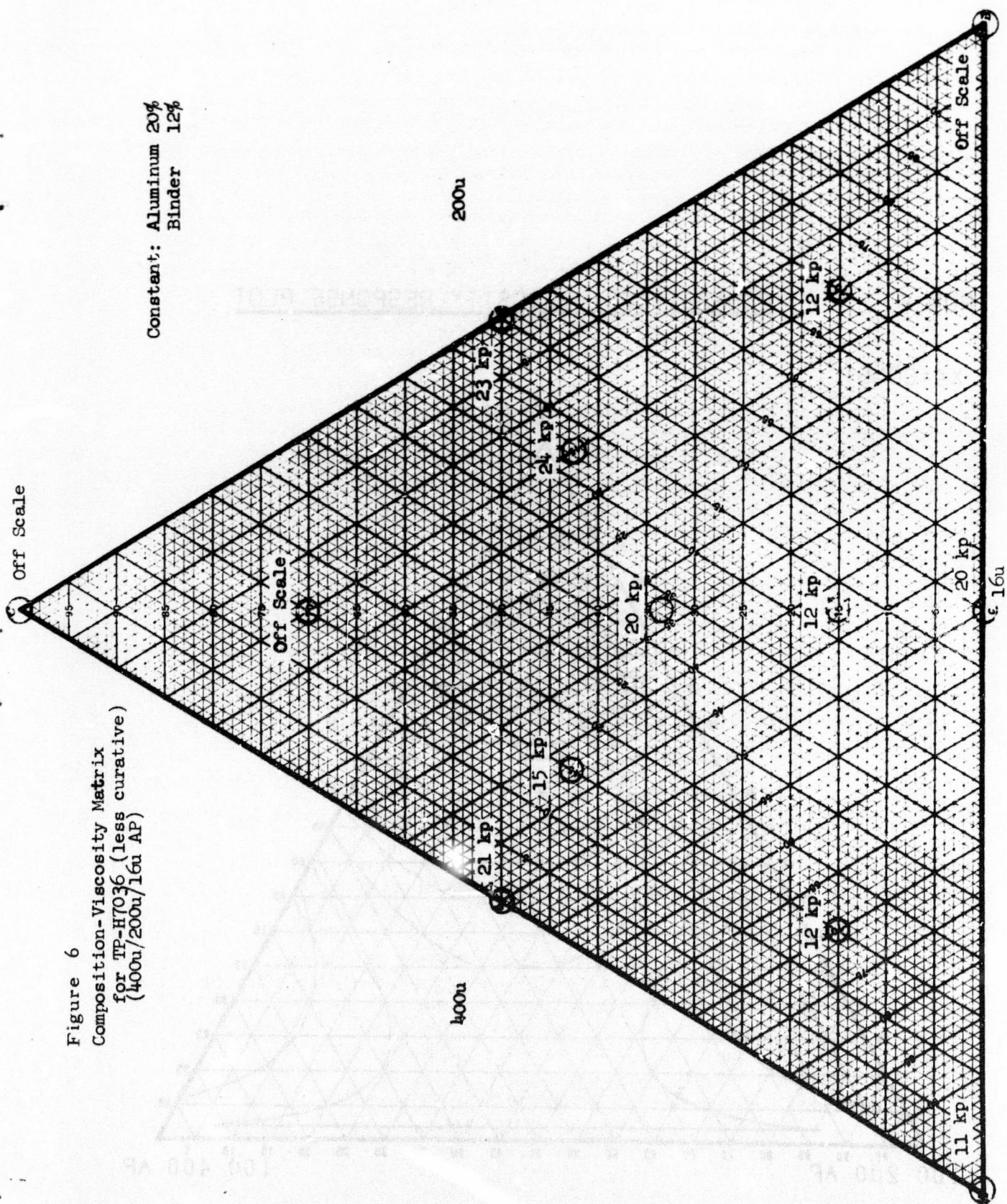


Figure 6
Composition-Viscosity Matrix
for TP-H7036 (less curative)
(400u/200u/16u AP)

Constant: Aluminum 20%
Binder 12%



RUN 6

COMPOSITION-VISCOSITY RESPONSE PLOT

X4=CONST

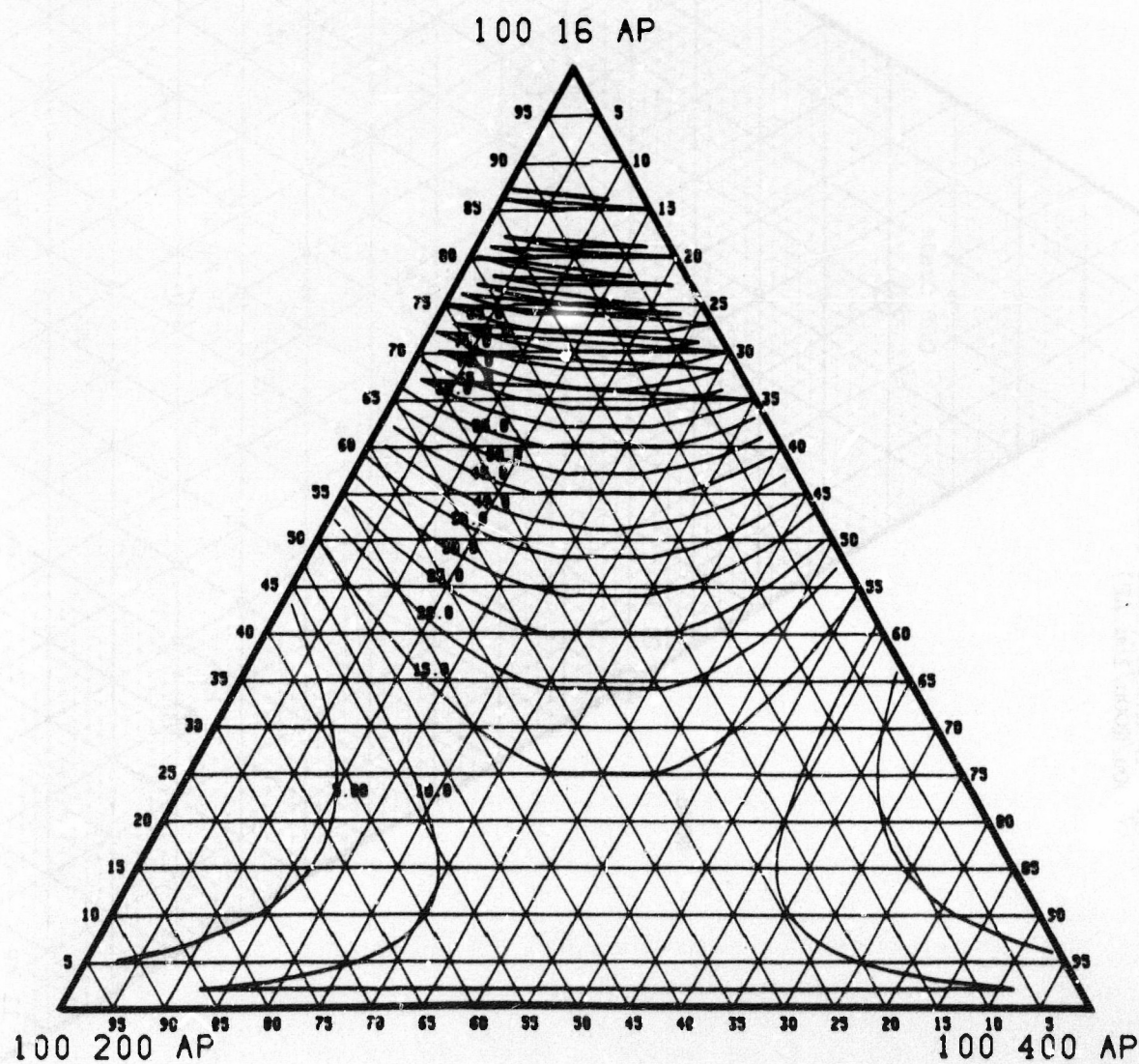


Figure 7. Viscosity Response Plot for a Mixture of 400, 200 and 16 micron AP in TP-H7036

F

RUN 5

COMPOSITION-VISCOSITY RESPONSE PLOT

X4=CONST.

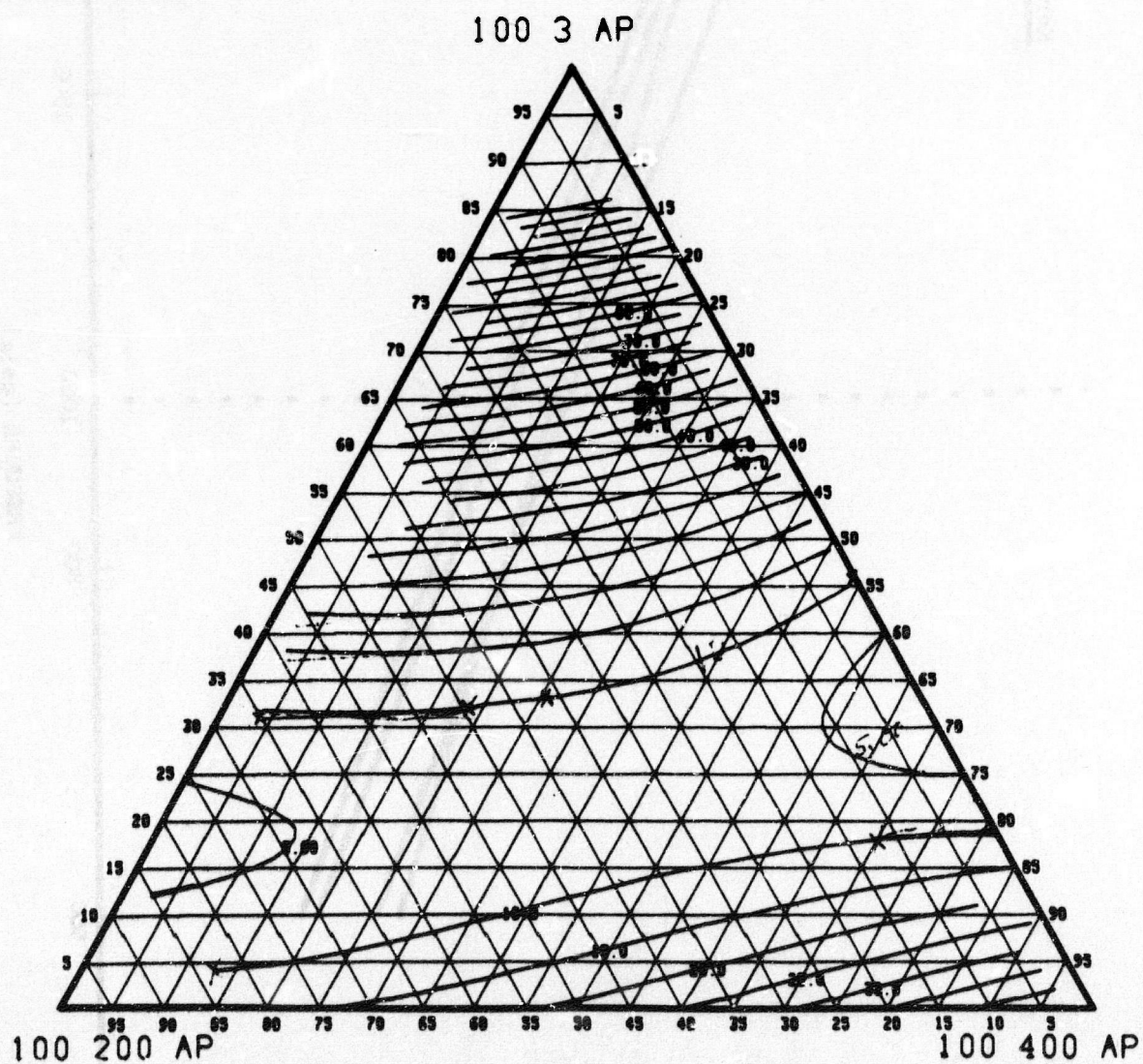


Figure 8. Viscosity Response Plot for a Mixture of 400, 200 and 3 micron AP in TP-H7036

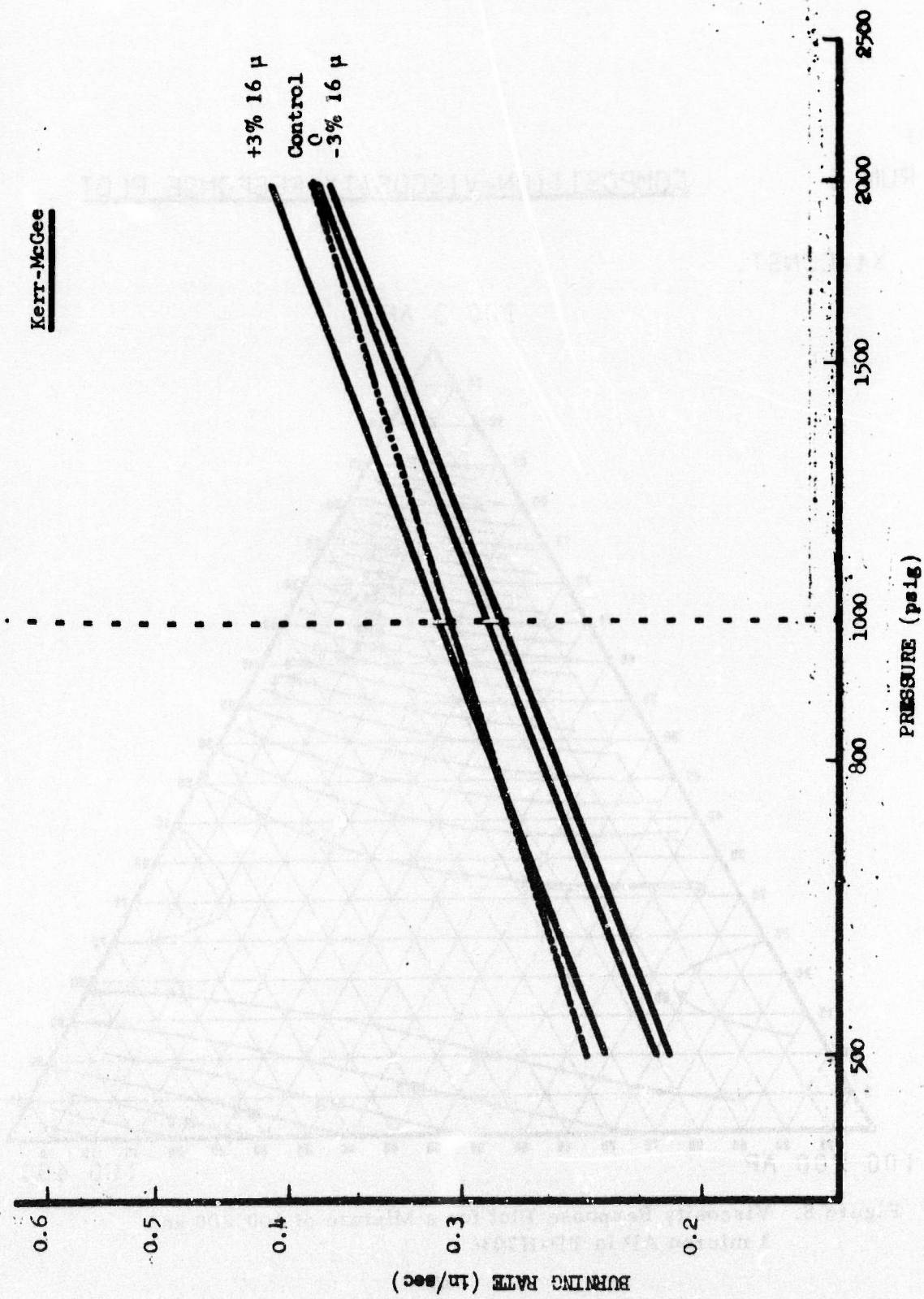


Figure 9. Burn Rate-Pressure Relationship for Kerr McGee Blends in TP-H7036 Propellant

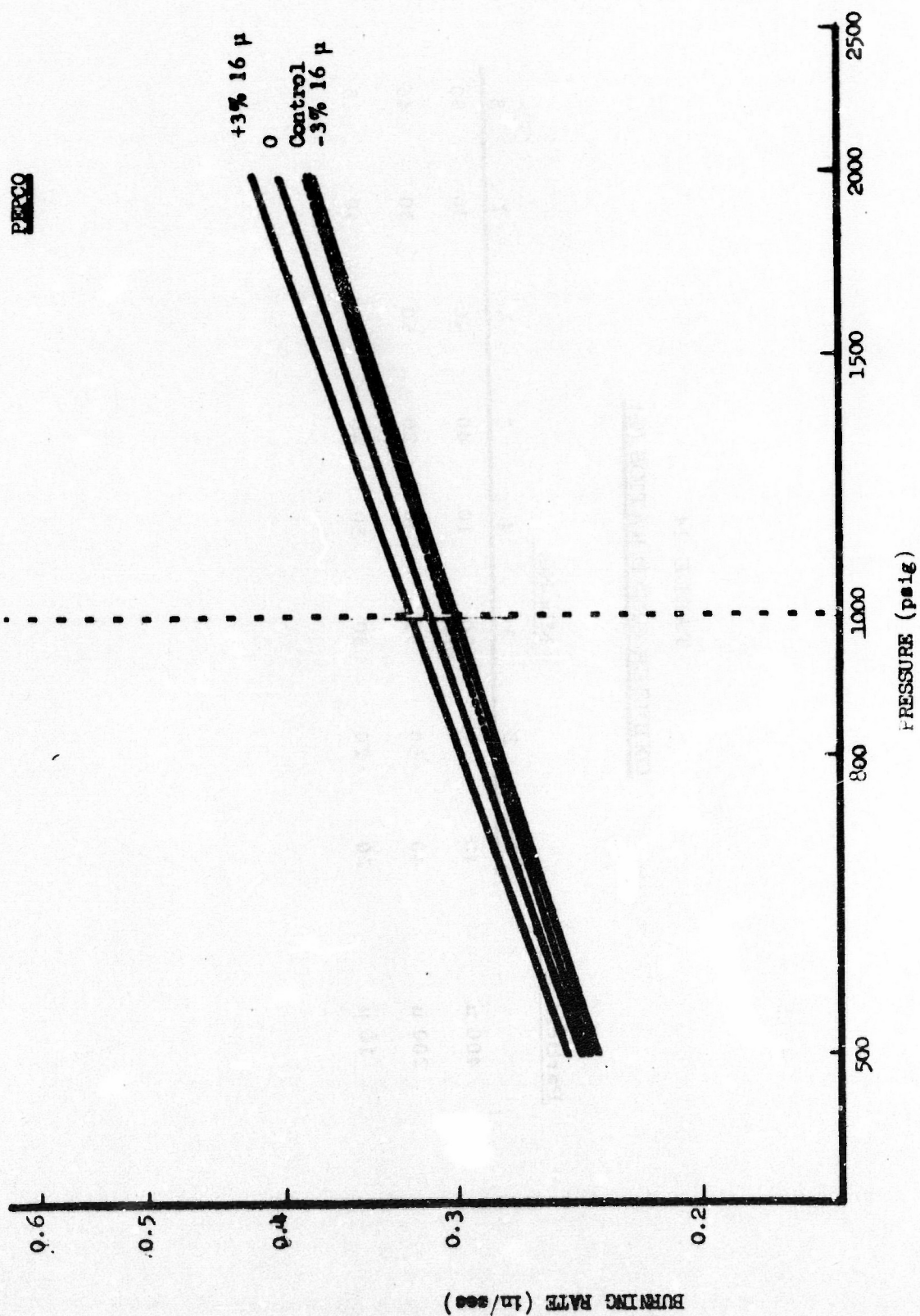


Figure 10. Burn Rate-Pressure Relationship for PEPCON Blends in TP-H7036 Propellant

TABLE 14
OXIDIZER GRIND RATIOS (%)

| Particle Size | Mix No. | | | | | | | |
|---------------|---------|----|----|----|----|----|----|----|
| | 1 | 2 | 3 | 4 | 5 | 6 | 7 | 8 |
| 400 μ | 40 | 20 | 20 | 10 | 40 | 40 | 30 | 50 |
| 200 μ | 40 | 60 | 50 | 40 | 20 | 50 | 30 | 45 |
| 16 μ | 20 | 20 | 30 | 50 | 40 | 10 | 40 | 5 |

Eight identical mixes of TP-H7036 propellant were manufactured for the eight Kerr-McGee blends and for the eight PEPCON blends. Burn rates for each of the propellants were determined in a Crawford strand burner at five separate pressures. Four strands were burned at each pressure. Typical results for the strand burn rate measurement are shown in Table 15. The burn rates determined for each of the 16 mixes are shown in Table 16.

To correlate these burn rates with some "distribution describing parameter", a complete physical characterization of the oxidizer blends was accomplished. This characterization included a ROTAP screen analysis, a modified MSA technique for determining AP size distribution, and a BET technique for surface area determination.

The values for the ROTAP screen analysis on each of the 16 blends (8 Kerr-McGee and 8 PEPCON) are shown in Table 17. The surface area of each blend was determined by the BET technique. These results are shown in Table 18.

The standard MSA technique for determining AP particle size distribution was modified in such a way that distributions on nominal 200 and 400 micron particles can be determined. The changes made in the technique involved utilizing dibutyl sebacate as the feed liquid and diethyl phthalate as the settling liquid. The use of these higher viscosity liquids increases the settling time for the larger AP particles. In addition, the capillary in the apparatus was increased in size to prevent clogging of the entrance by the larger AP particles in the 400 micron size fraction.

Having made these changes, MSA's were performed on the 8 separate Kerr-McGee blends and the 8 PEPCON blends. Figures 11-18 represent the distribution curves for the 8 Kerr-McGee blends listed in Table 16. Figures 19-26 show identical data to Figures 11-18 except that these data were obtained on exactly the same PEPCON blends.

The MSA values of WMD for the 200 micron and 400 micron ammonium perchlorate are lower than values of WMD determined on the same lots of AP by the ROTAP techniques. These differences (~ 20 microns) are not unexpected and the techniques are based upon different physical principles. The MSA technique is based upon Stokes law of settling and the ROTAP is a screen analysis. If the particles were perfectly spherical, the two techniques would give identical values of particle size. Imperfections in shape will show up as larger particles in a screen analysis than by a settling technique; therefore, the observed differences are expected.

From the MSA, ROTAP, and surface area data, a series of other distribution parameters was calculated. Among those parameters were the average mean diameter, mean surface diameter, linear mean diameter, harmonic mean diameter, mean volume diameter, surface mean diameter, and mean weight diameter. The values of each of these parameters for each of the 16 blends are shown in Table 19.

TABLE 15

STRAND BURN RATE MEASUREMENT DATA

| 14Q-158 | | |
|-----------------|-------------------|----------------------|
| <u>PRESSURE</u> | <u>TIME (SEC)</u> | <u>RATE (IN/SEC)</u> |
| 500 | 5.83 | .257 |
| | 5.85 | .256 |
| | 5.81 | .258 |
| | 5.85 | .256 |
| 700 | 5.40 | .278 |
| | 5.33 | .281 |
| | 5.28 | .284 |
| | 5.37 | .280 |
| 1000 | 5.10 | .294 |
| | 4.91 | .305 |
| | 4.96 | .302 |
| | 5.03 | .298 |
| 1400 | 4.33 | .346 |
| | 4.27 | .351 |
| | 4.32 | .347 |
| | 4.19 | .358 |
| 1800 | 3.51 | .427 |
| | 3.51 | .427 |
| | 3.45 | .435 |
| | 3.48 | .431 |

TABLE 16

BURNING RATE DATA

| <u>MIX NO.</u> | <u>Burn Rate at 1000 psi (in/sec)</u> | |
|----------------|---------------------------------------|---------------|
| | <u>KM</u> | <u>PEPCON</u> |
| 1 | .273 | .310 |
| 2 | .302 | .349 |
| 3 | .299 | .354 |
| 4 | .356 | .388 |
| 5 | .311 | .340 |
| 6 | .282 | .320 |
| 7 | .316 | .350 |
| 8 | .271 | .304 |

TABLE 17

ROTAP SCREEN ANALYSES ON KERR McGEE AND PEPCON BLENDS

APD

| <u>Blend No.</u> | <u>Kerr McGee</u> | <u>PEPCON</u> |
|------------------|-------------------|---------------|
| 1 | 240 | 216 |
| 2 | 202 | 175 |
| 3 | 200 | 161 |
| 4 | 99 | 66 |
| 5 | 218 | 170 |
| 6 | 270 | 221 |
| 7 | 165 | 159 |
| 8 | 310 | 300 |

TABLE 18

SURFACE AREAS OF KERR McGEE AND PEPCON BLENDSKrypton Absorption (BET)
m²/g

| <u>Blend No.</u> | <u>Kerr McGee</u> | <u>PEPCON</u> |
|------------------|-------------------|---------------|
| 1 | .070 | .073 |
| 2 | .072 | .075 |
| 3 | .101 | .107 |
| 4 | .158 | .167 |
| 5 | .127 | .133 |
| 6 | .042 | .046 |
| 7 | .128 | .134 |
| 8 | .028 | .027 |

TABLE 19

REPRODUCIBILITY FACTORS

| KM | SSA | WMD | AMD | MSD | LMD | HMD | MVD | SMD | MWD |
|----|---------|--------|-------|-------|--------|--------|-------|--------|---------|
| 1 | 0.07023 | 228.46 | 4.294 | 5.414 | 6.827 | 3.7371 | 17.30 | 43.85 | 10.8730 |
| 2 | 0.07229 | 189.62 | 4.302 | 5.492 | 7.012 | 3.7374 | 17.29 | 42.65 | 10.8764 |
| 3 | 0.10111 | 173.08 | 4.270 | 5.247 | 6.448 | 3.7294 | 14.02 | 30.49 | 9.4333 |
| 4 | 0.15797 | 120.70 | 4.268 | 5.102 | 6.100 | 3.7322 | 10.89 | 19.46 | 7.9714 |
| 5 | 0.12673 | 195.33 | 4.261 | 5.102 | 6.107 | 3.7305 | 12.14 | 24.13 | 8.5640 |
| 6 | 0.04229 | 244.99 | 4.329 | 5.940 | 8.149 | 3.7390 | 24.36 | 72.82 | 13.6960 |
| 7 | 0.12783 | 176.43 | 4.264 | 5.124 | 6.157 | 3.7305 | 12.18 | 24.09 | 8.5840 |
| 8 | 0.02792 | 272.14 | 4.331 | 6.598 | 10.051 | 3.7246 | 33.32 | 110.44 | 16.8772 |
| 1 | 0.07319 | 230.93 | 1.782 | 2.955 | 4.900 | 1.0283 | 14.35 | 42.04 | 7.1606 |
| 2 | 0.07527 | 188.45 | 1.785 | 2.997 | 5.032 | 1.0284 | 14.34 | 40.88 | 7.1605 |
| 3 | 0.10748 | 172.44 | 1.600 | 2.621 | 4.293 | 0.9780 | 11.10 | 28.71 | 5.8205 |
| 4 | 0.16747 | 119.51 | 1.661 | 2.640 | 4.197 | 0.9950 | 8.79 | 18.39 | 5.0419 |
| 5 | 0.13298 | 199.08 | 1.785 | 2.810 | 4.424 | 1.0316 | 10.12 | 23.14 | 5.6746 |
| 6 | 0.04568 | 246.00 | 1.376 | 2.520 | 4.614 | 0.9186 | 17.65 | 67.50 | 7.5396 |
| 7 | 0.13401 | 177.88 | 1.786 | 2.821 | 4.457 | 1.0316 | 10.12 | 22.96 | 5.6746 |
| 8 | 0.02722 | 275.77 | 4.277 | 6.573 | 10.101 | 3.6916 | 33.78 | 112.94 | 16.9608 |

1000

100

DIAMETER (μ)

10

Figure 11. AP Particle Size Distribution
(Modified MSA)

1

0

10

20

30

40

50

60

70

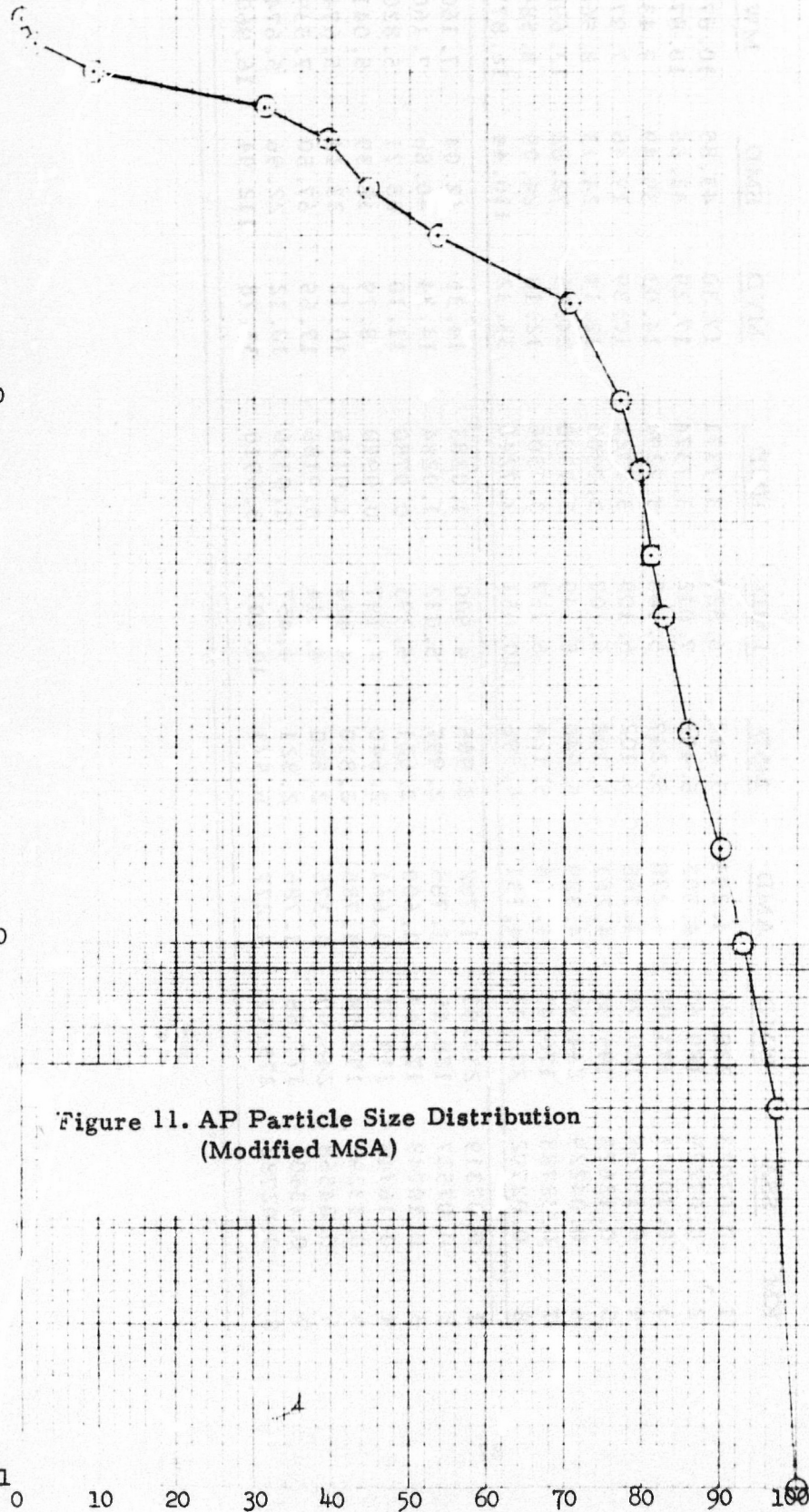
80

90

100

Percent (%)

38



1000

100

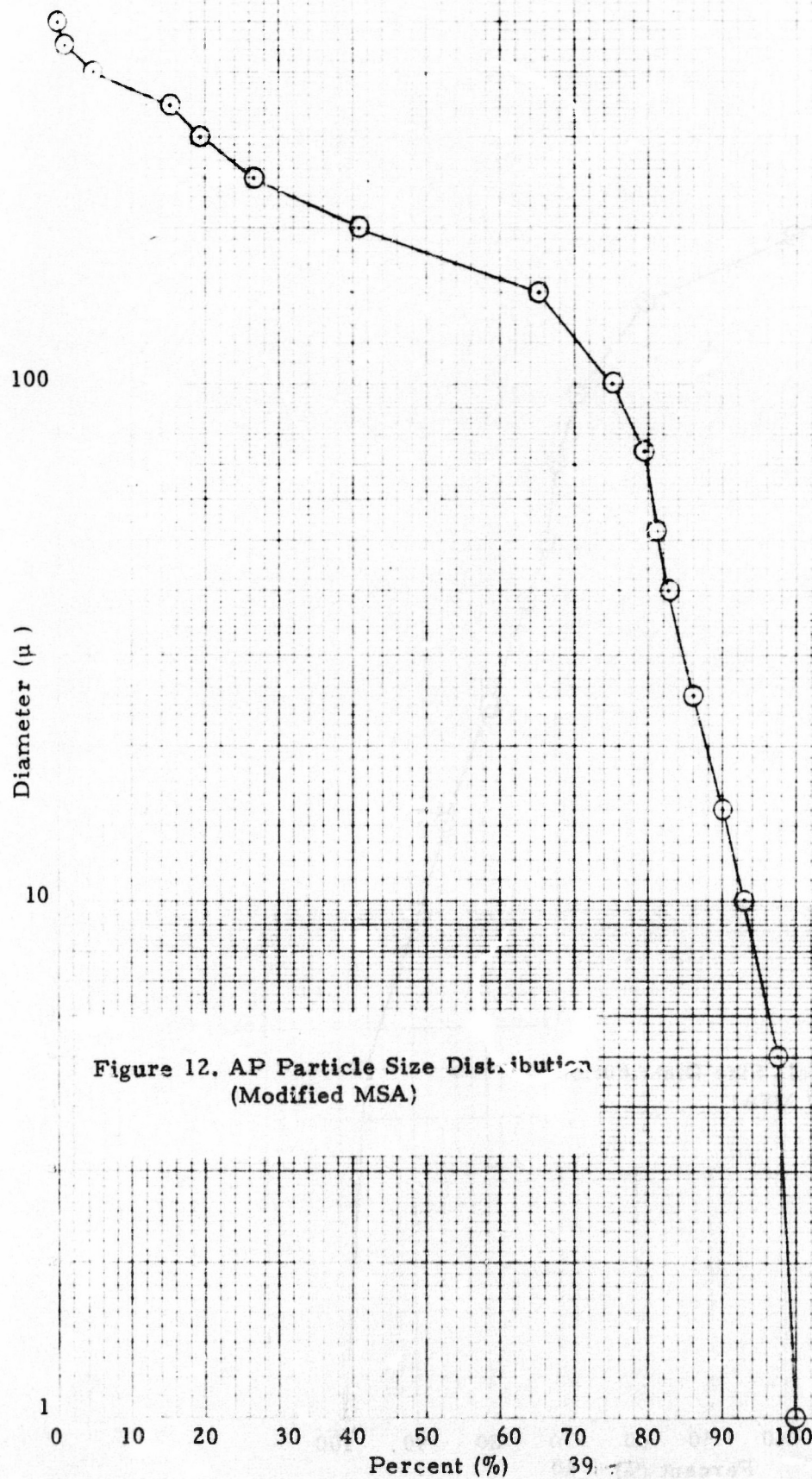
Diameter (μ)

10

1

Figure 12. AP Particle Size Distribution
(Modified MSA)

0 10 20 30 40 50 60 70 80 90 100
Percent (%)



1000

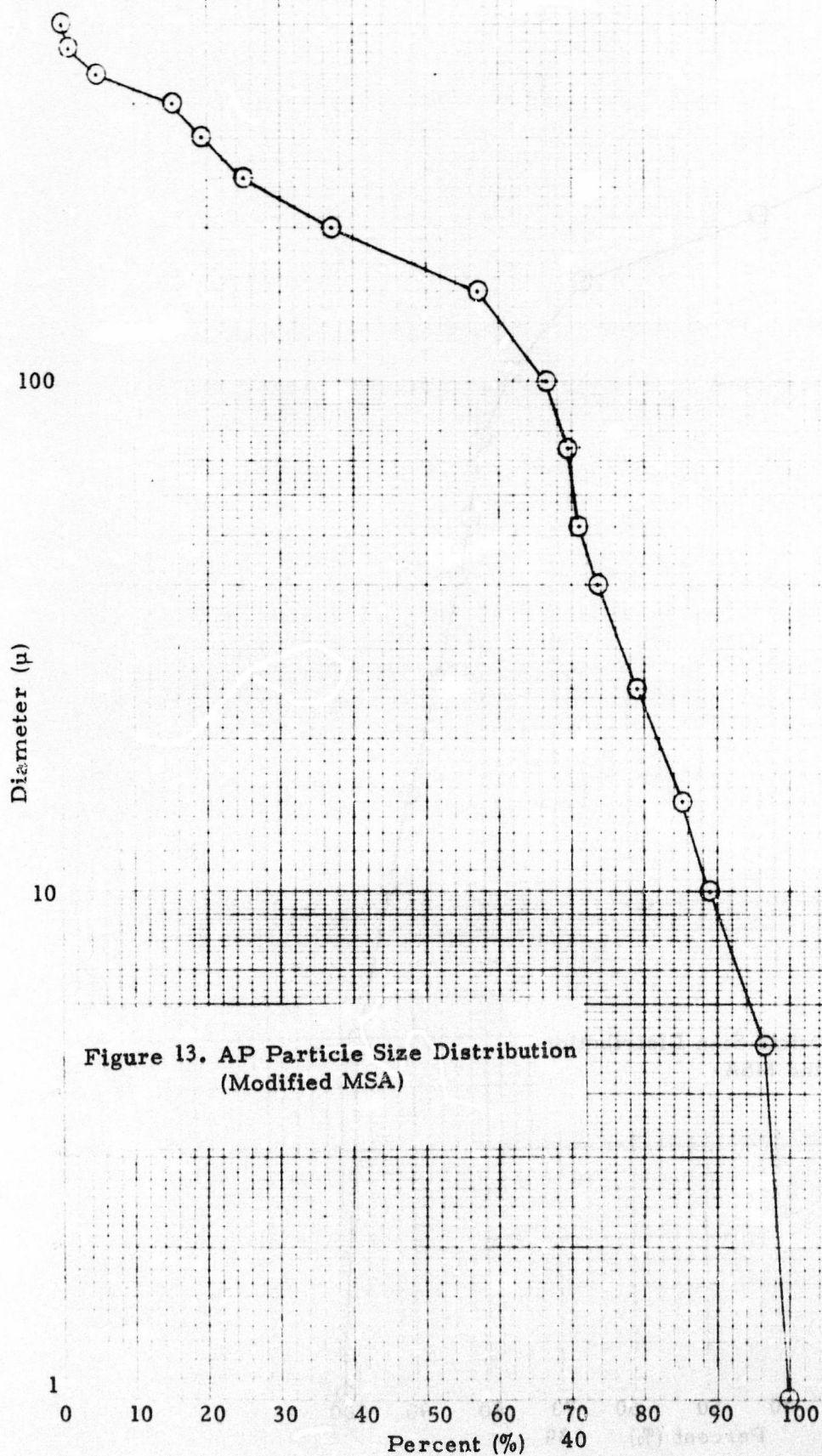


Figure 13. AP Particle Size Distribution
(Modified MSA)

1000

100

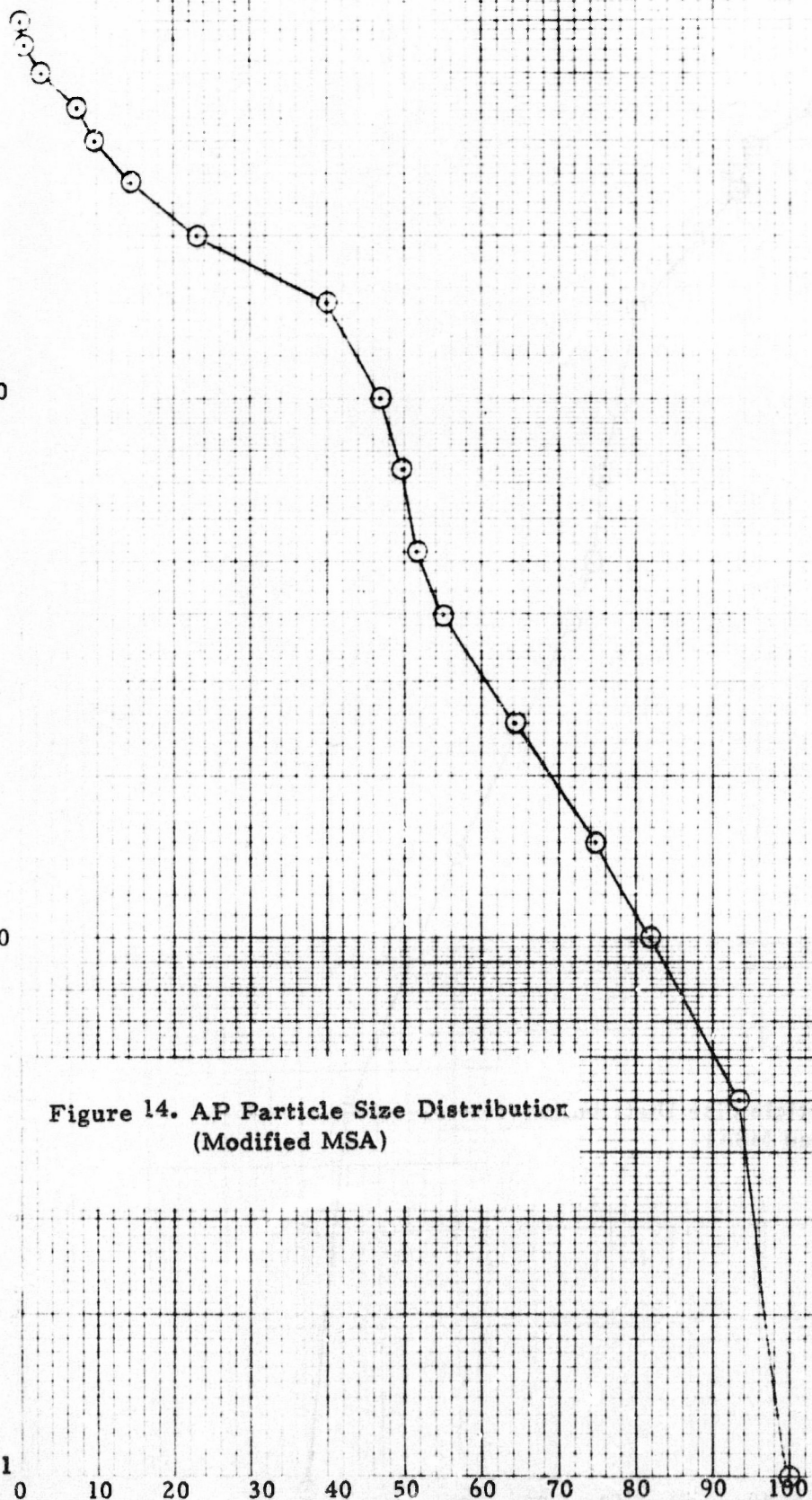
Diameter (μ)

10

1

Figure 14. AP Particle Size Distribution
(Modified MSA)

Percent (%) 41



1000

100

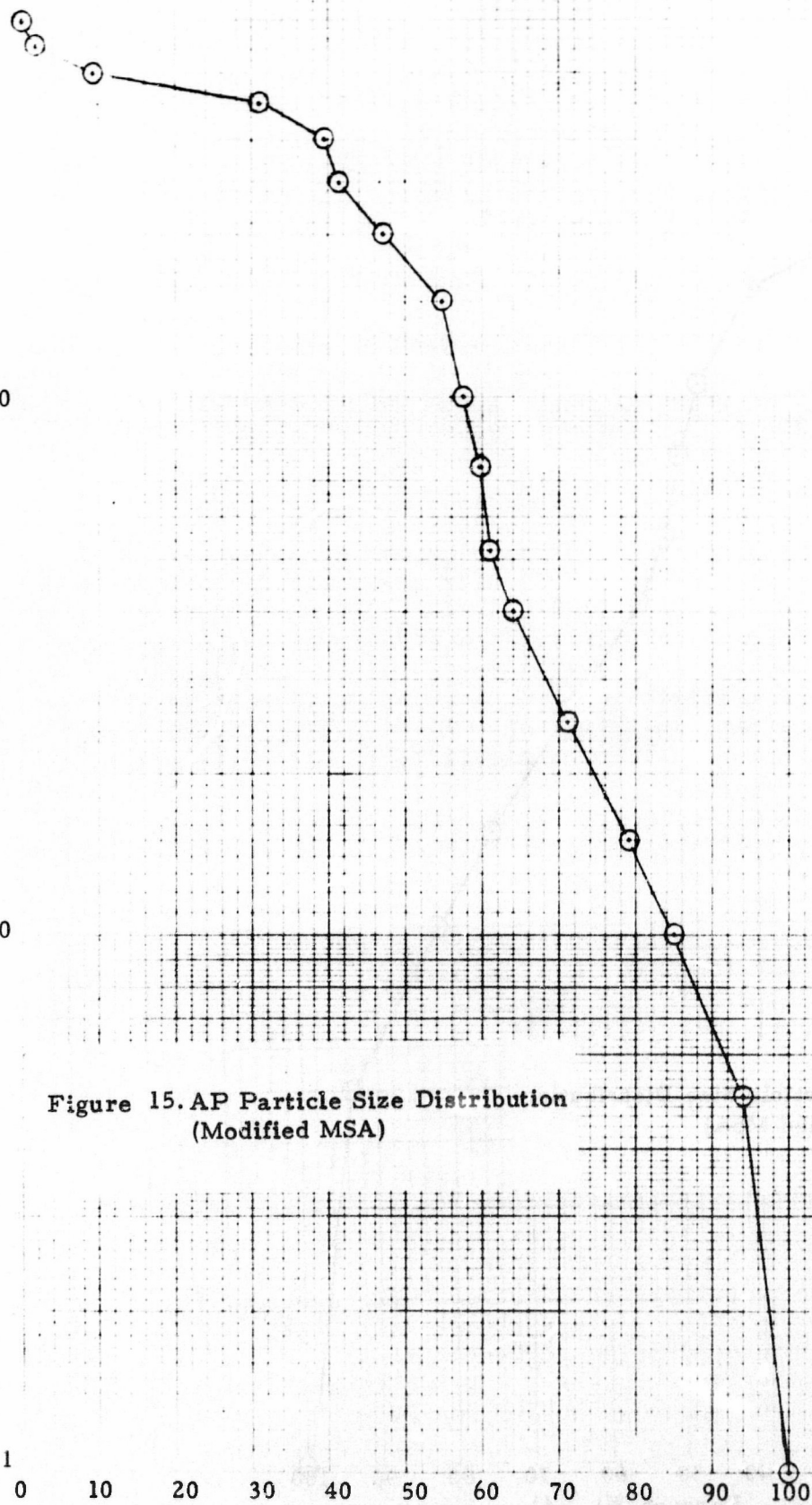
Diameter (μ)

10

Figure 15. AP Particle Size Distribution
(Modified MSA)

1

0 10 20 30 40 50 60 70 80 90 100
Percent (%) 42 !



1000

100

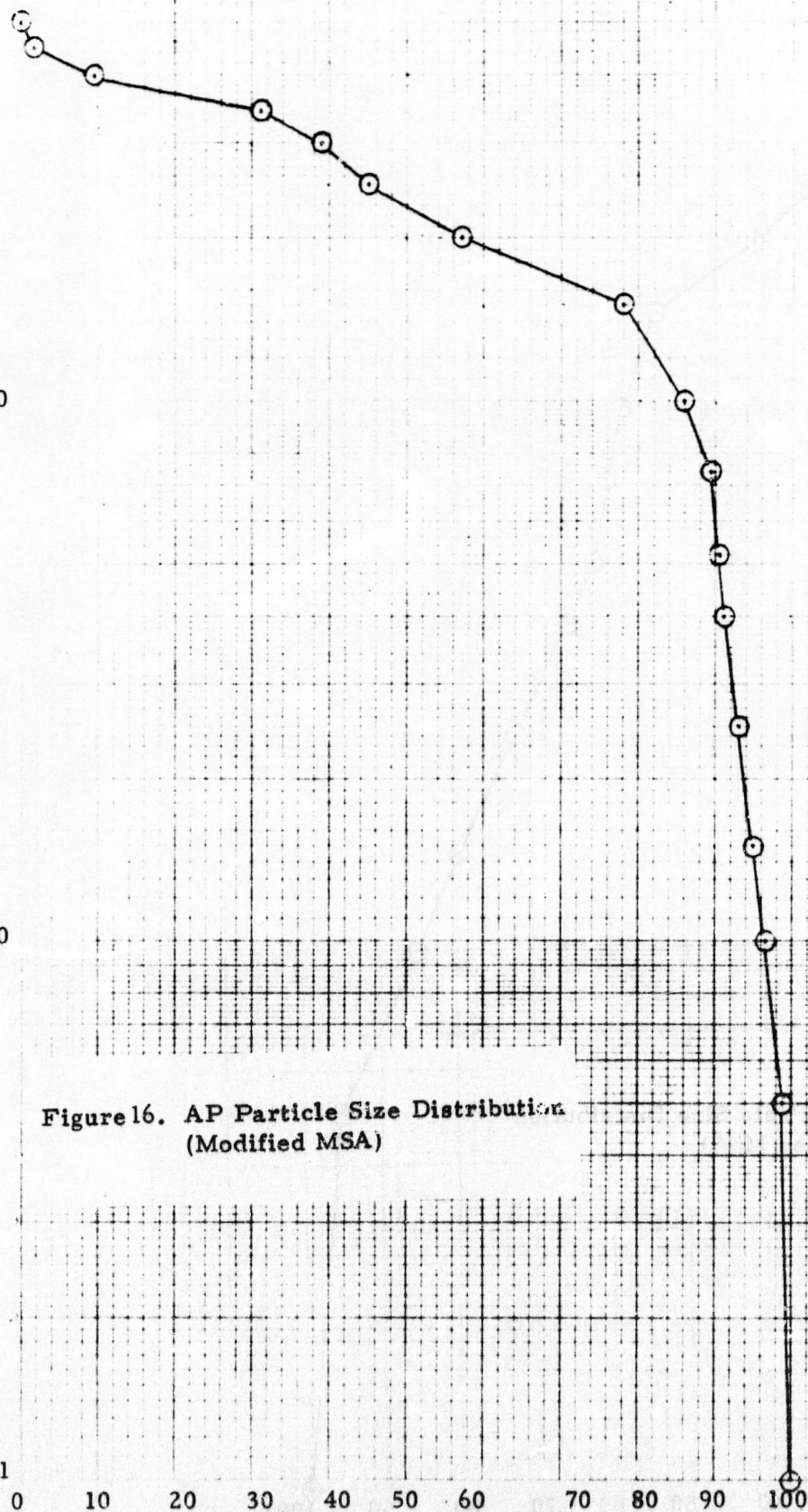
Diameter (μ)

10

1

Percent (%) 43

Figure 16. AP Particle Size Distribution
(Modified MSA)



1000

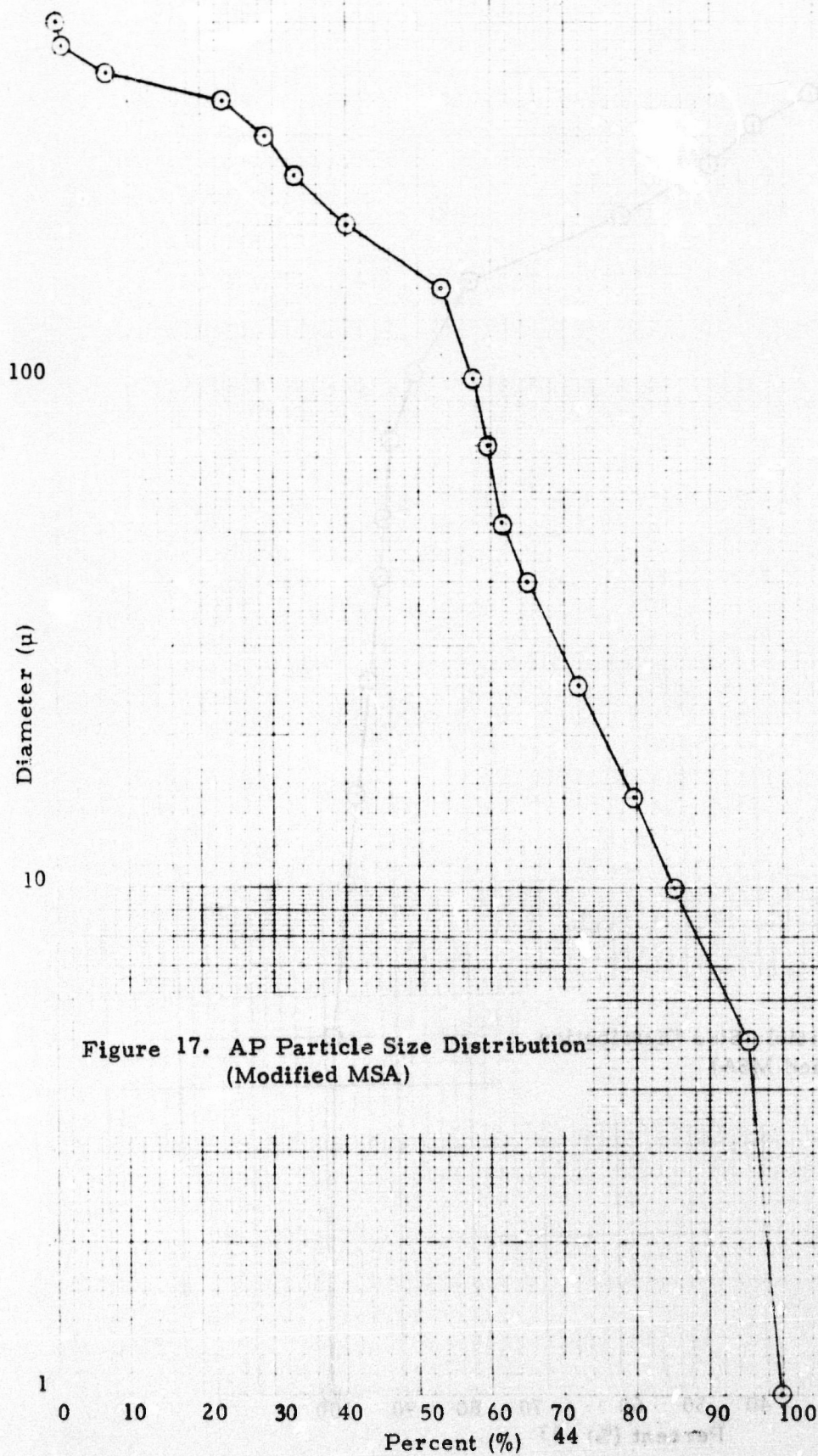


Figure 17. AP Particle Size Distribution
(Modified MSA)

1000

100

Diameter (μ)

10

1

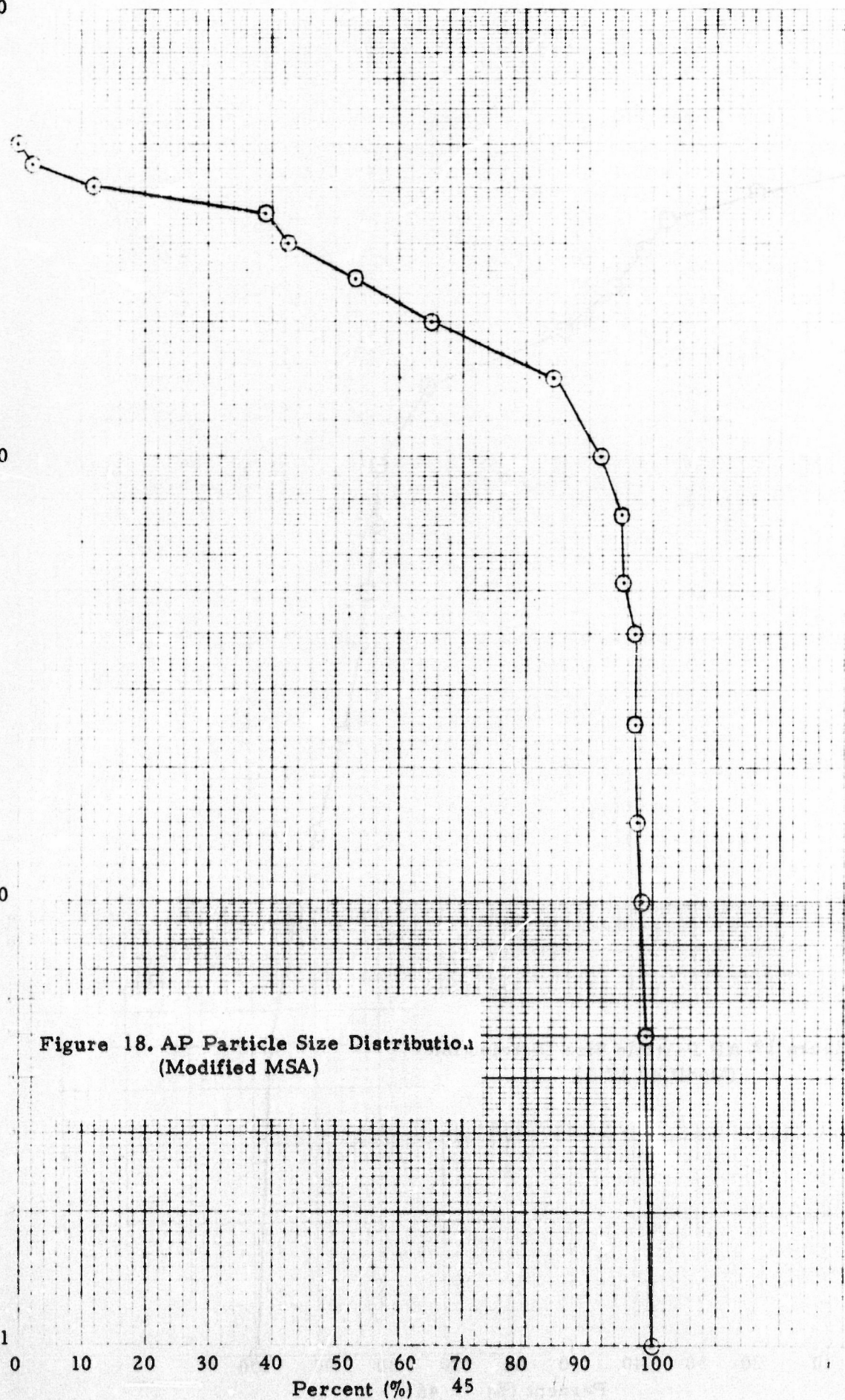


Figure 18. AP Particle Size Distribution
(Modified MSA)

Percent (%) 45

1000

100

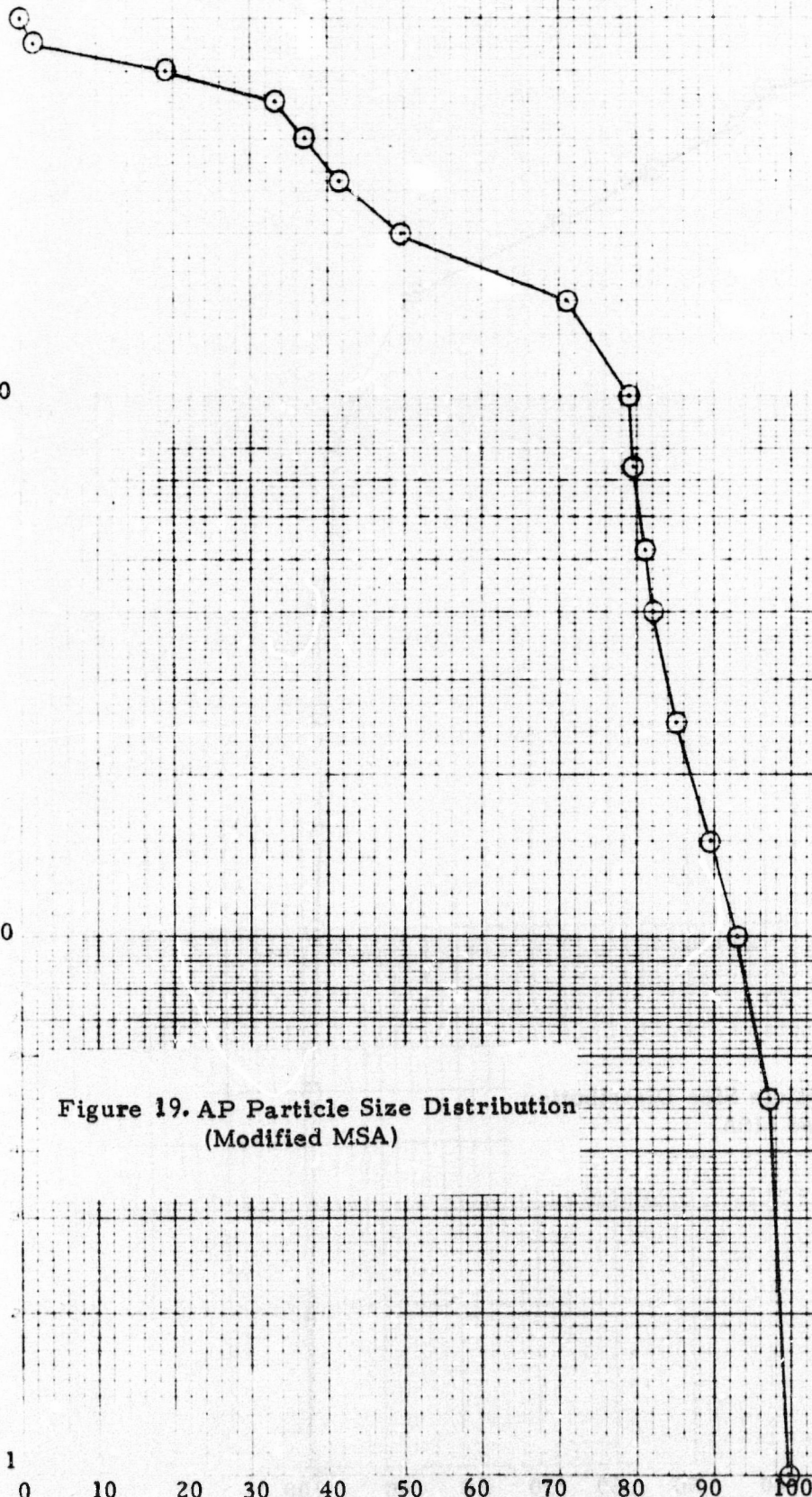
Diameter (μ)

10

1

Figure 19. AP Particle Size Distribution
(Modified MSA)

0 10 20 30 40 50 60 70 80 90 100
Percent (%) 46



1000

100

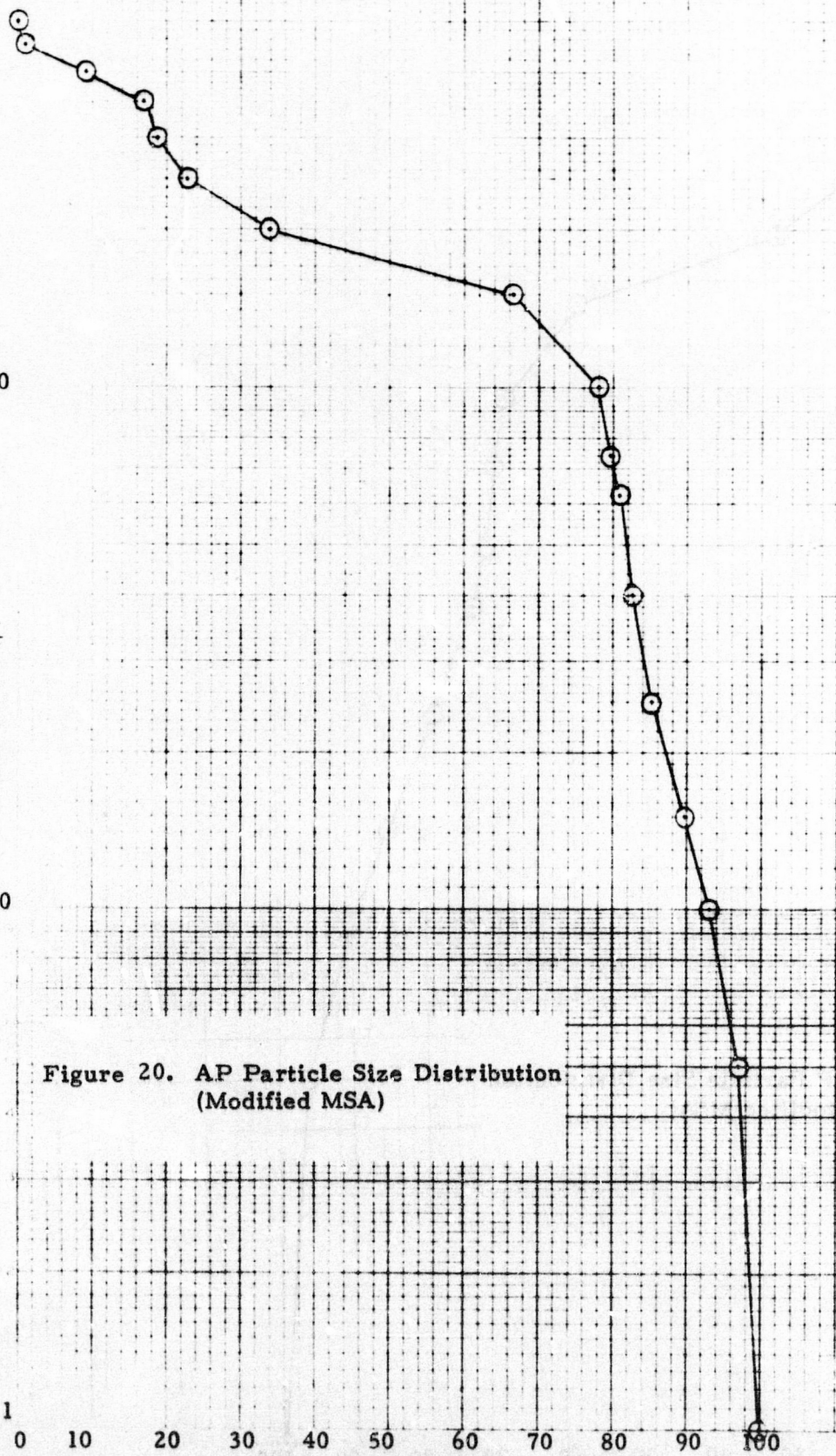
Diameter (μ)

10

1

Figure 20. AP Particle Size Distribution
(Modified MSA)

0 10 20 30 40 50 60 70 80 90 100
Percent (%)



1000

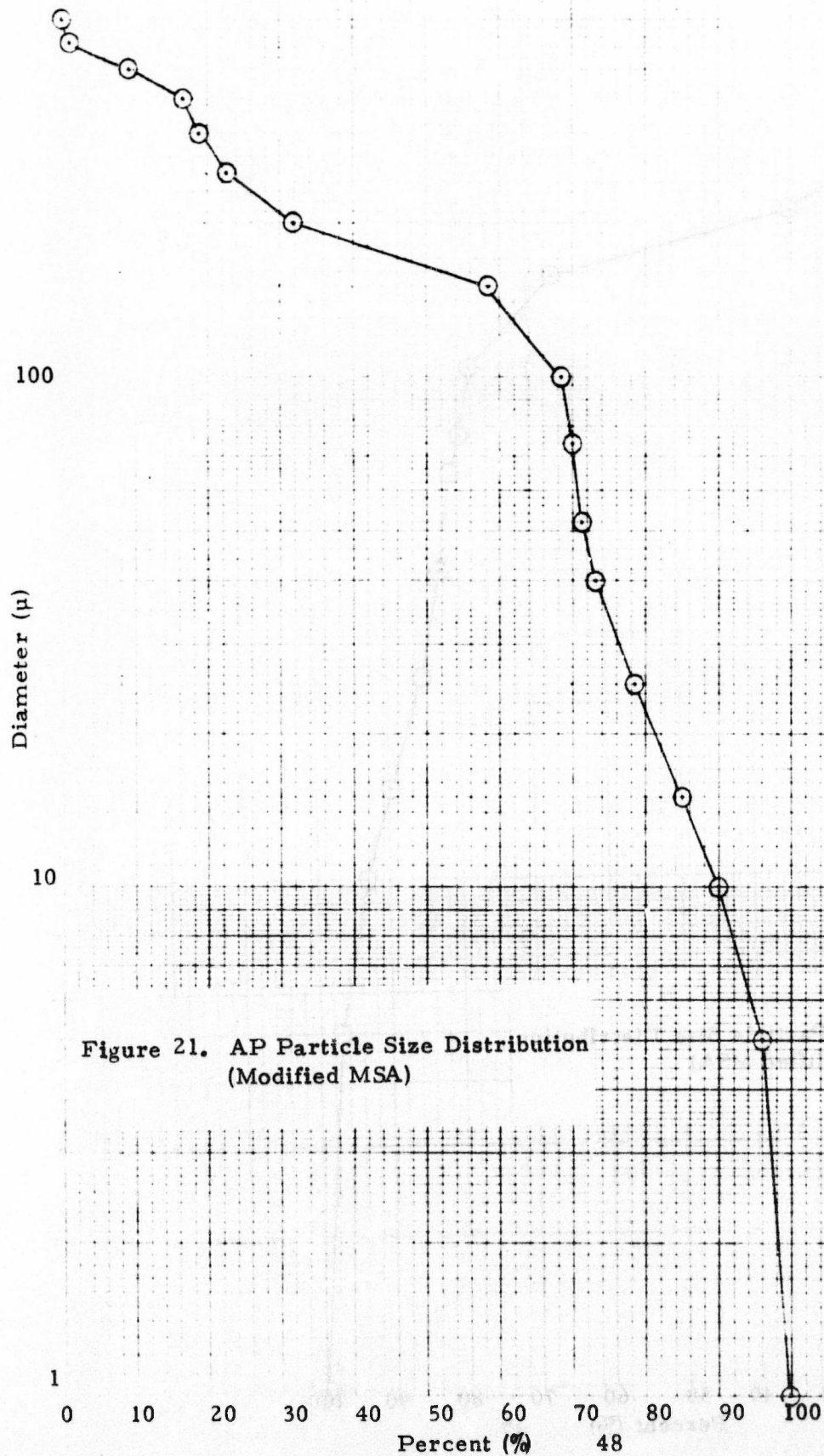


Figure 21. AP Particle Size Distribution
(Modified MSA)

1000

100

Diameter (μ)

10

Figure 22. AP Particle Size Distribution
(Modified MSA)

1

0

10

20

30

40

50

60

70

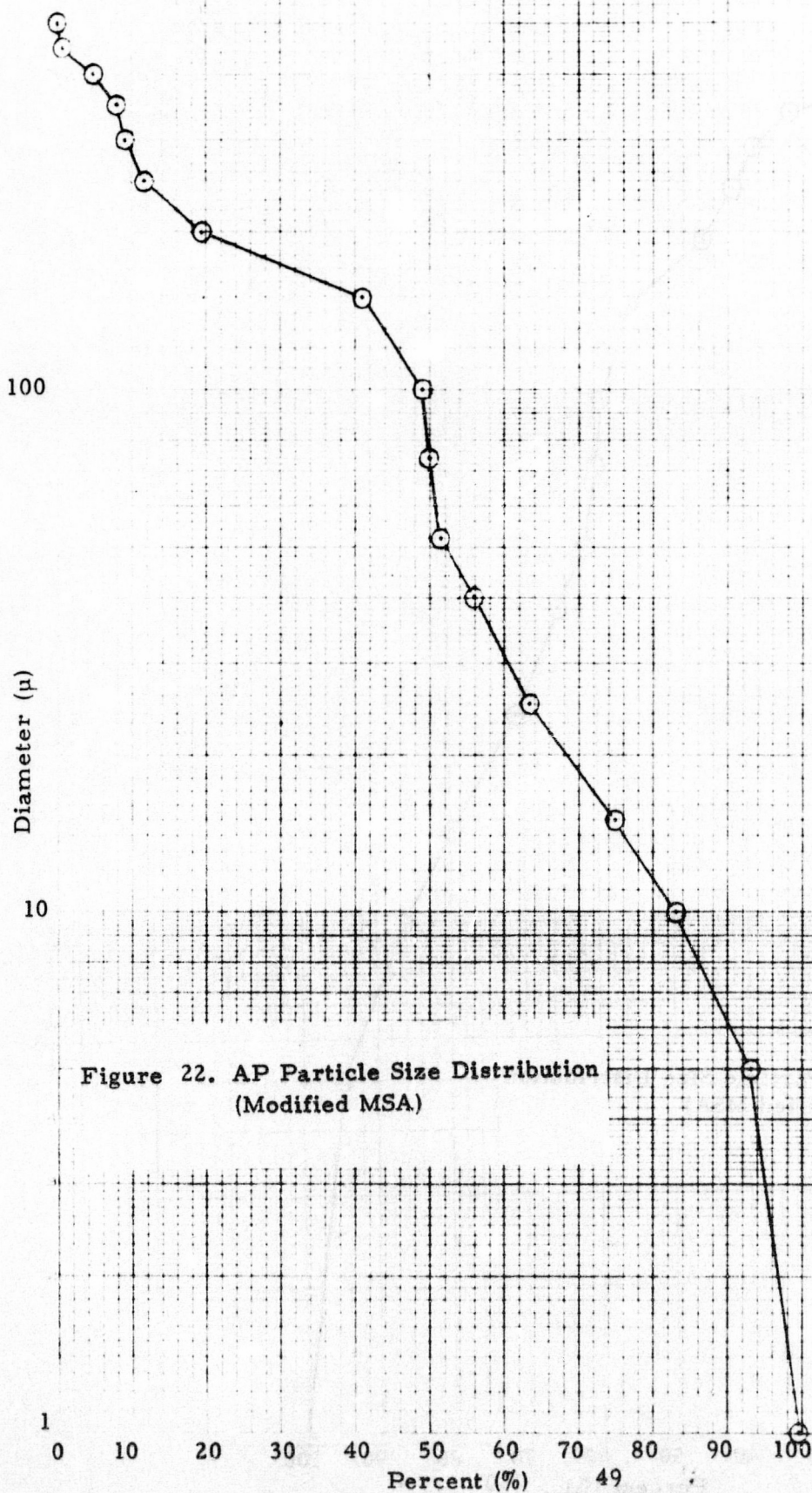
80

90

100

Percent (%)

49



1000

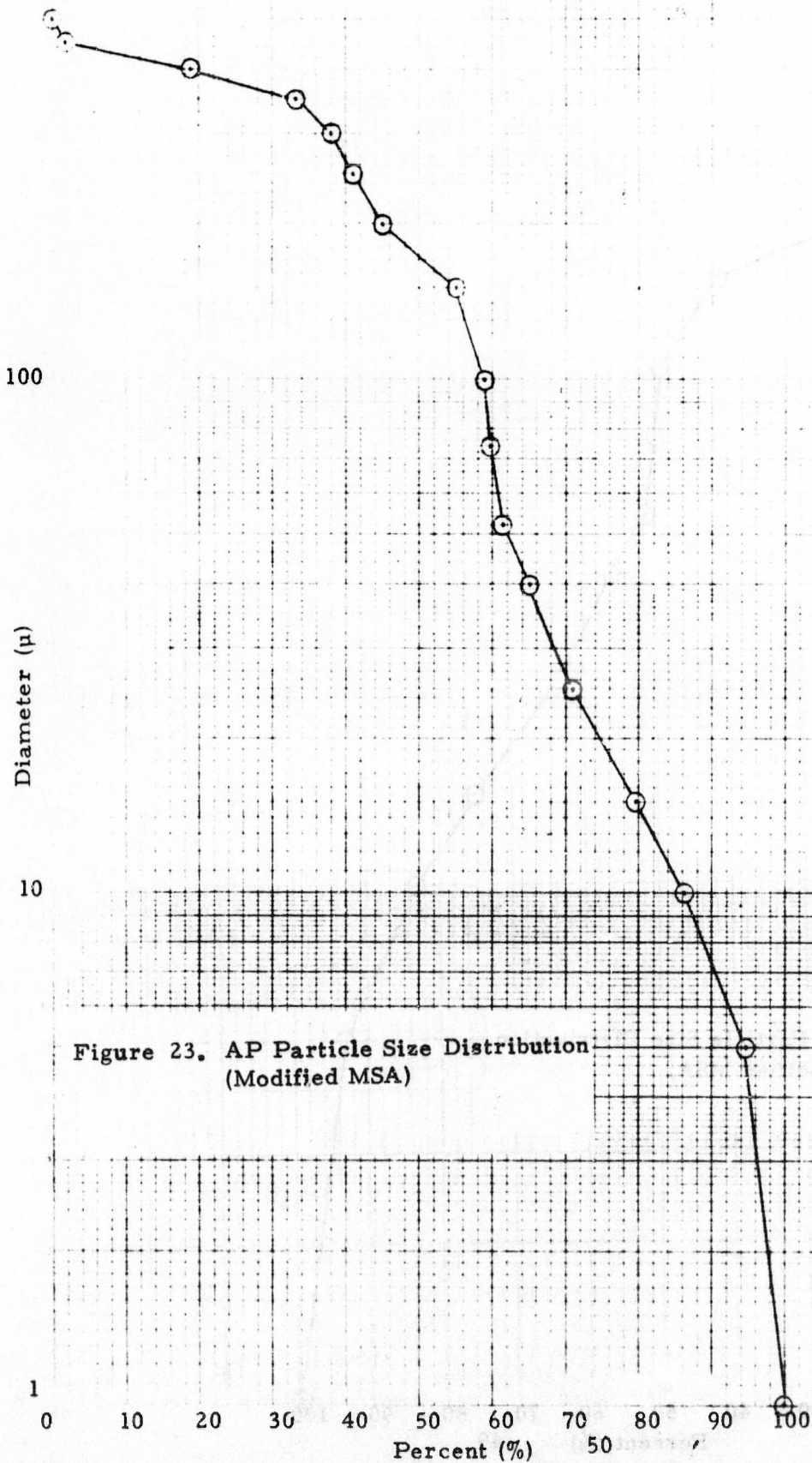


Figure 23. AP Particle Size Distribution
(Modified MSA)

1000

Diameter (μ)

100

10

1

Figure 24. AF Particle Size Distribution
(Modified MSA)

Percent (%)

51

0

10

20

30

40

50

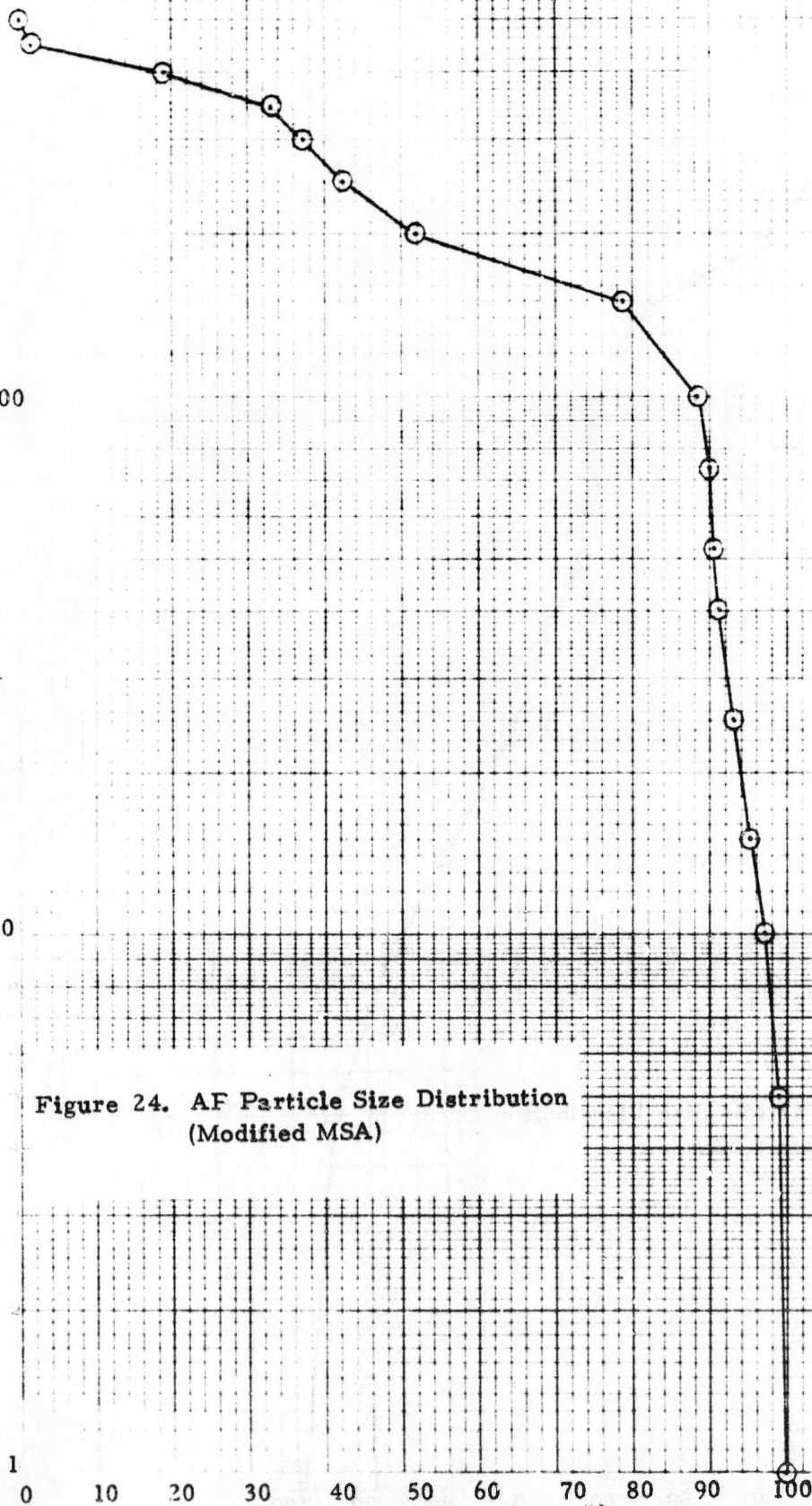
60

70

80

90

100



1000

100

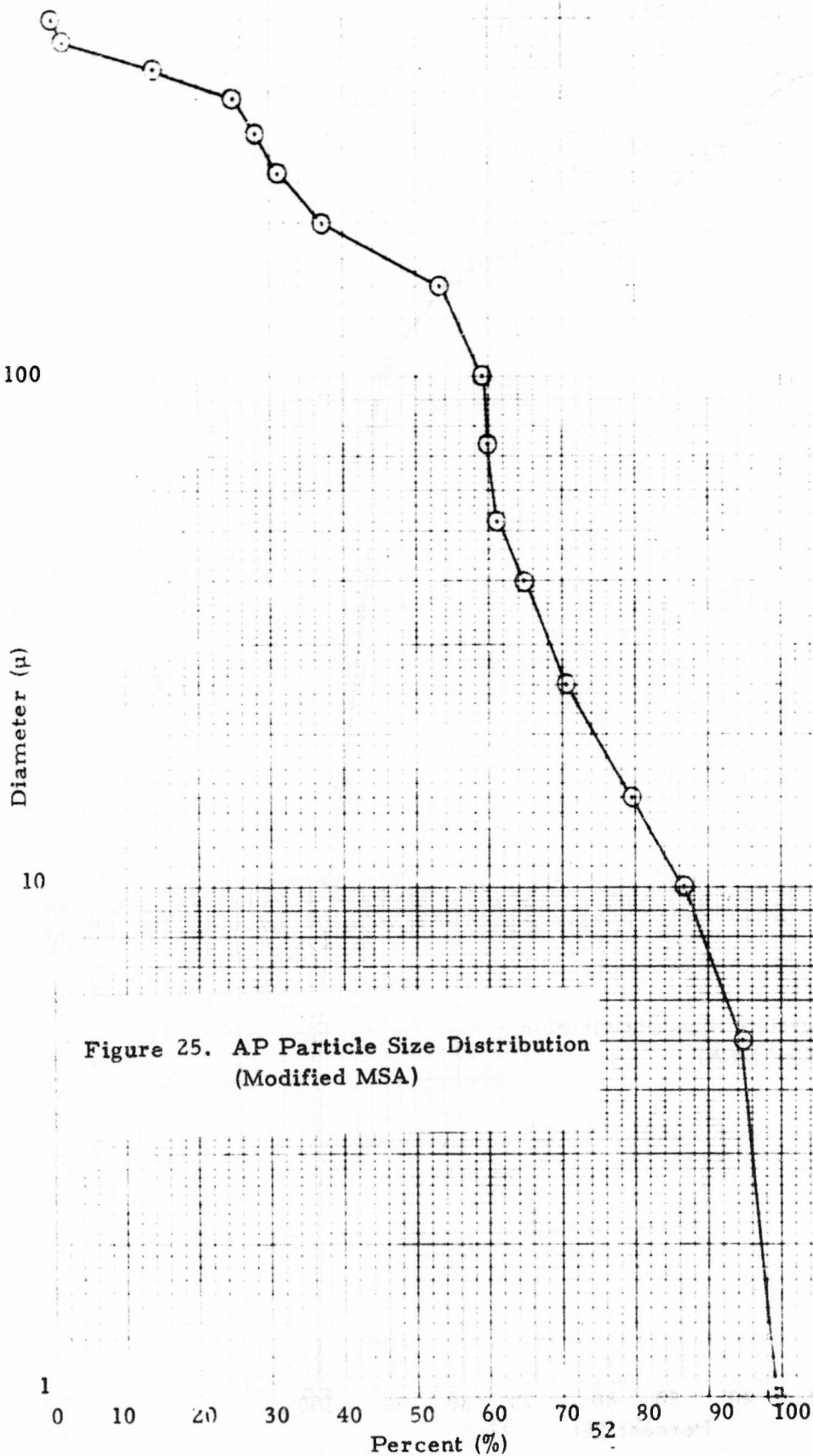
Diameter (μ)

10

1

Figure 25. AP Particle Size Distribution
(Modified MSA)

0 10 20 30 40 50 60 70 80 90 100
Percent (%)



1000

100

Diameter (μ)

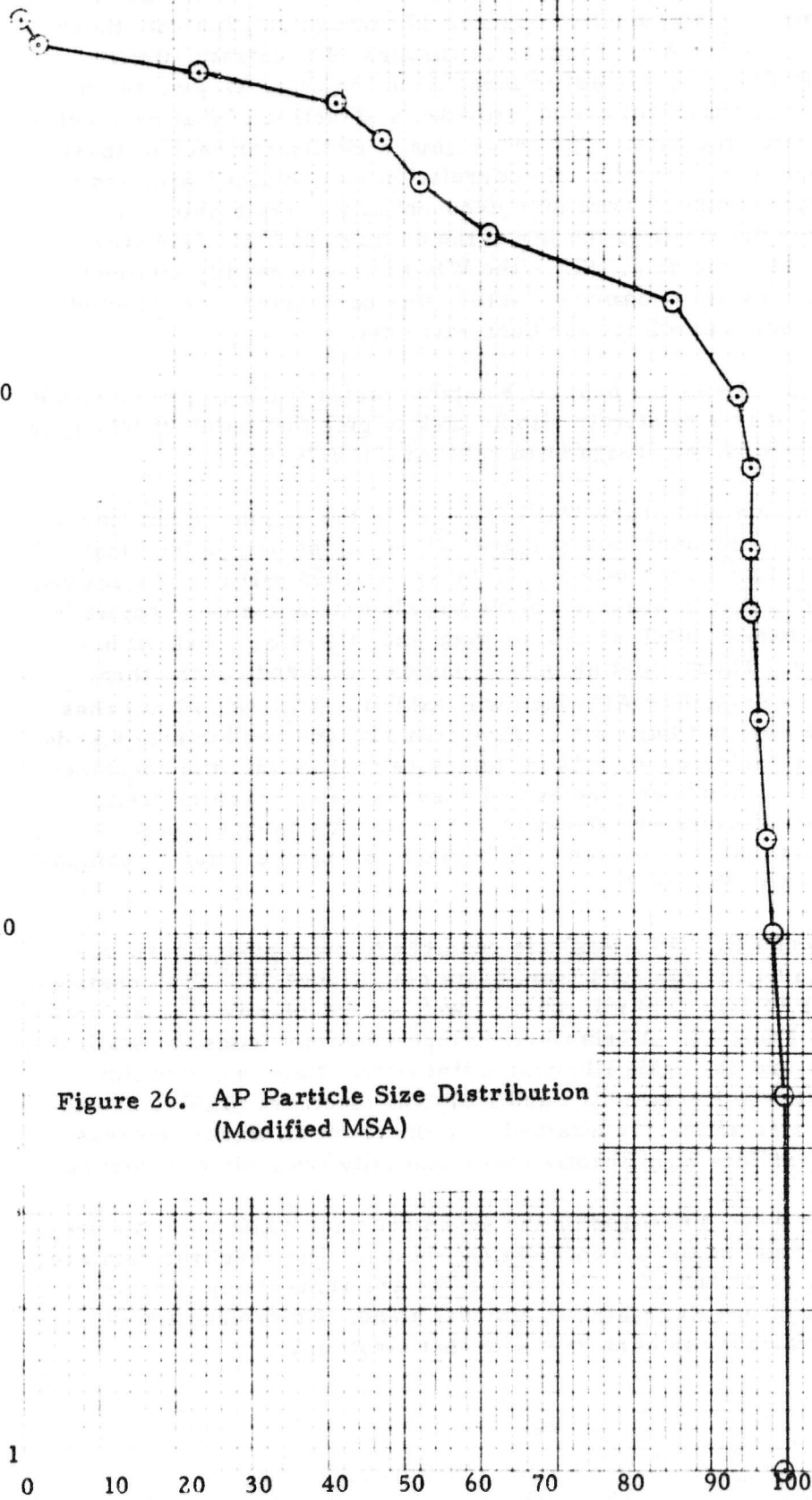
10

1

Figure 26. AP Particle Size Distribution
(Modified MSA)

0 10 20 30 40 50 60 70 80 90 100
Percent (%)

53



To ascertain which of these "distribution describing parameters" in Table 19 best correlate the burn rate of TP-H7036 propellant manufactured from Kerr-McGee and PEPCON AP, a plot of the burn rate for each of the propellants versus the values for each of these "distribution describing parameters" was made. Figures 27 through 30 illustrate these plots for the Kerr-McGee AP. Figures 31 through 34 illustrate similar plots for the PEPCON AP. A least squares fit of the data, as well as an assessment of the standard deviation, provided a selection of that parameter which best correlates the data. The one-sigma variation for each of these parameters is shown in Table 20. No correlation was obtained with some of the parameters and others were only exponentially correlatable. It appears that either the WMD or the log of the average particle diameter factor best correlates the data. Since the WMD is more readily attained than is the average particle diameter factor, this parameter was selected as that one which best correlates the burn rate data.

Since the WMD was the best correlatable factor for both Kerr-McGee and PEPCON AP, it is a relatively simple task to pick that value of WMD for each vendor which provides design burn rate for TP-H7036.

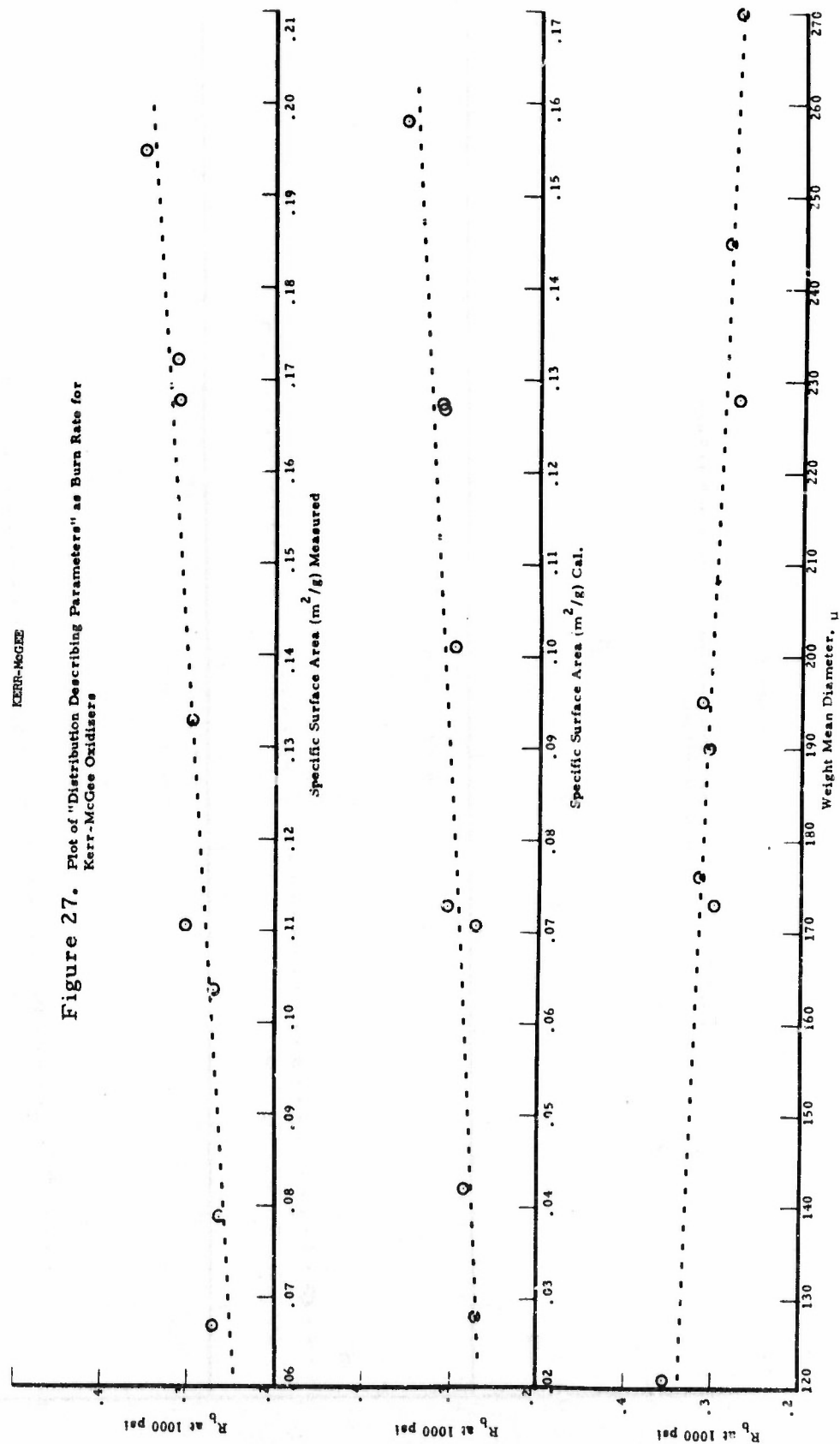
By examining a plot of the WMD for each of the original eight Kerr-McGee mixes versus the burn rate (Figure 27), it can be determined that the WMD at the designed burn rate (0.303 in/sec at 1000 psi) is 210 microns. With this definition, it is relatively simple to calculate a series of oxidizer blends which will exhibit WMD of 210 microns and, therefore, exhibit a constant burn rate. There exist an infinite number of blends of the three size fractions of Kerr-McGee AP which will exhibit a WMD of 210 microns and, therefore, a constant burn rate. Five trimodal and two bimodal blends (210 microns) were selected for mix manufacture to illustrate the constancy of burn rate. These blends and the end-of-mix viscosity resulting from TP-H7036 mix manufacture are shown in Table 21. A triangular plot illustrating the fact that the constant WMD mixes fall upon a straight composition line is shown in Figure 35.

The WMD of PEPCON AP blends required to meet design burn was determined to be 254 microns from examining Figure 31. The constant WMD blends for PEPCON (254 microns) as well as end-of-mix viscosities are illustrated in Table 22. A triangular composition plot (constant WMD of 254 microns), Figure 36, again illustrates linearity. Note in comparing the viscosities between Kerr-McGee and PEPCON oxidizers (Tables 21 and 22), that similar viscosities are attained with the trimodal mixes whereas the PEPCON AP exhibits significantly lower viscosity from binodal blends.

Burn rates were measured on the seven constant WMD Kerr-McGee mixes (TP-H7036) and on the seven PEPCON mixes. The resulting data are illustrated in Tables 21 and 22. The burn rates are remarkably constant with the exception of one Kerr-McGee bimodal blend. No explanation is available for the variance in burn rate with that single mix.

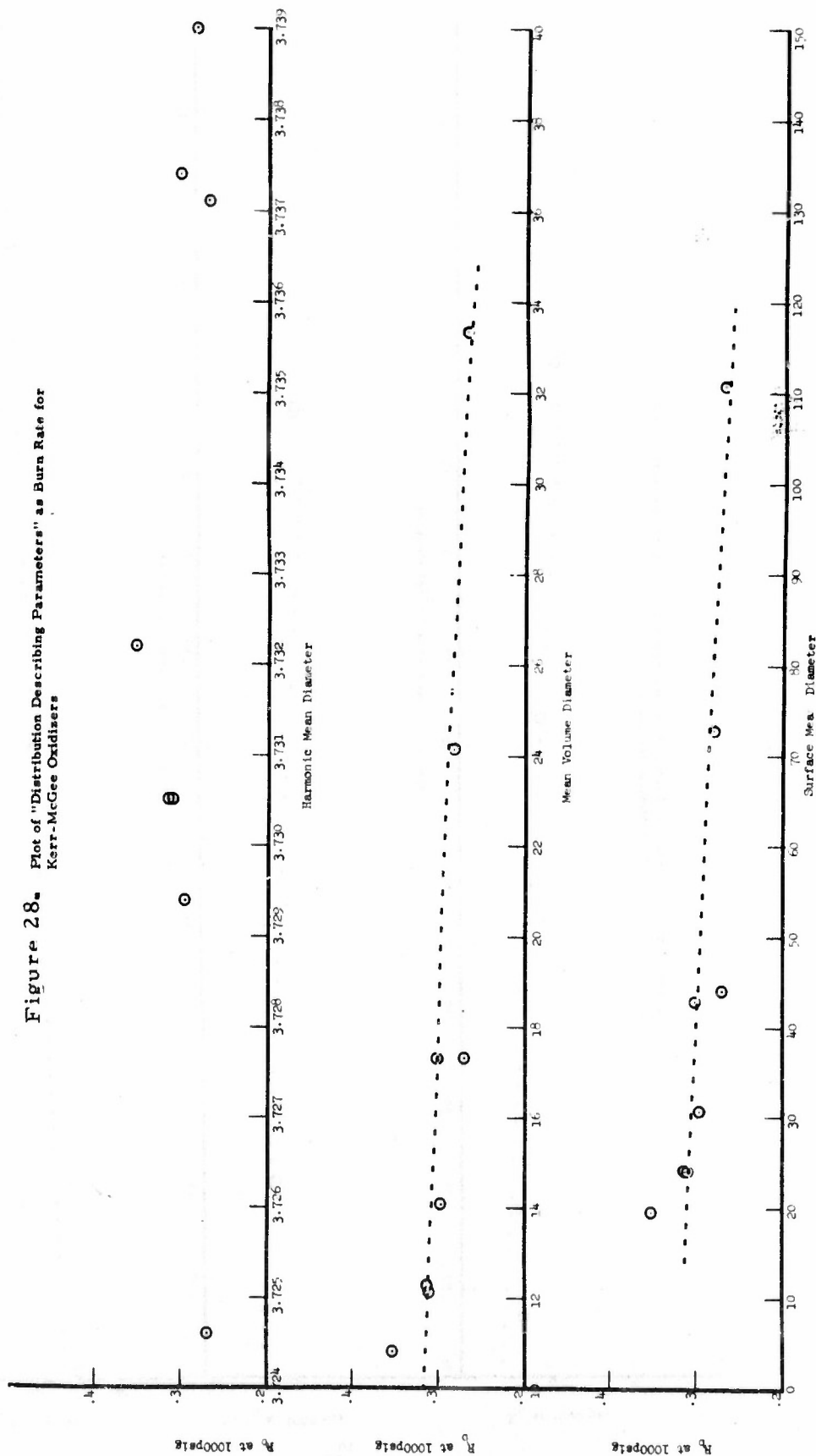
KERR-MCGEE

Figure 27. Plot of "Distribution Describing Parameters" as Burn Rate for Kerr-McGee Oxidizers

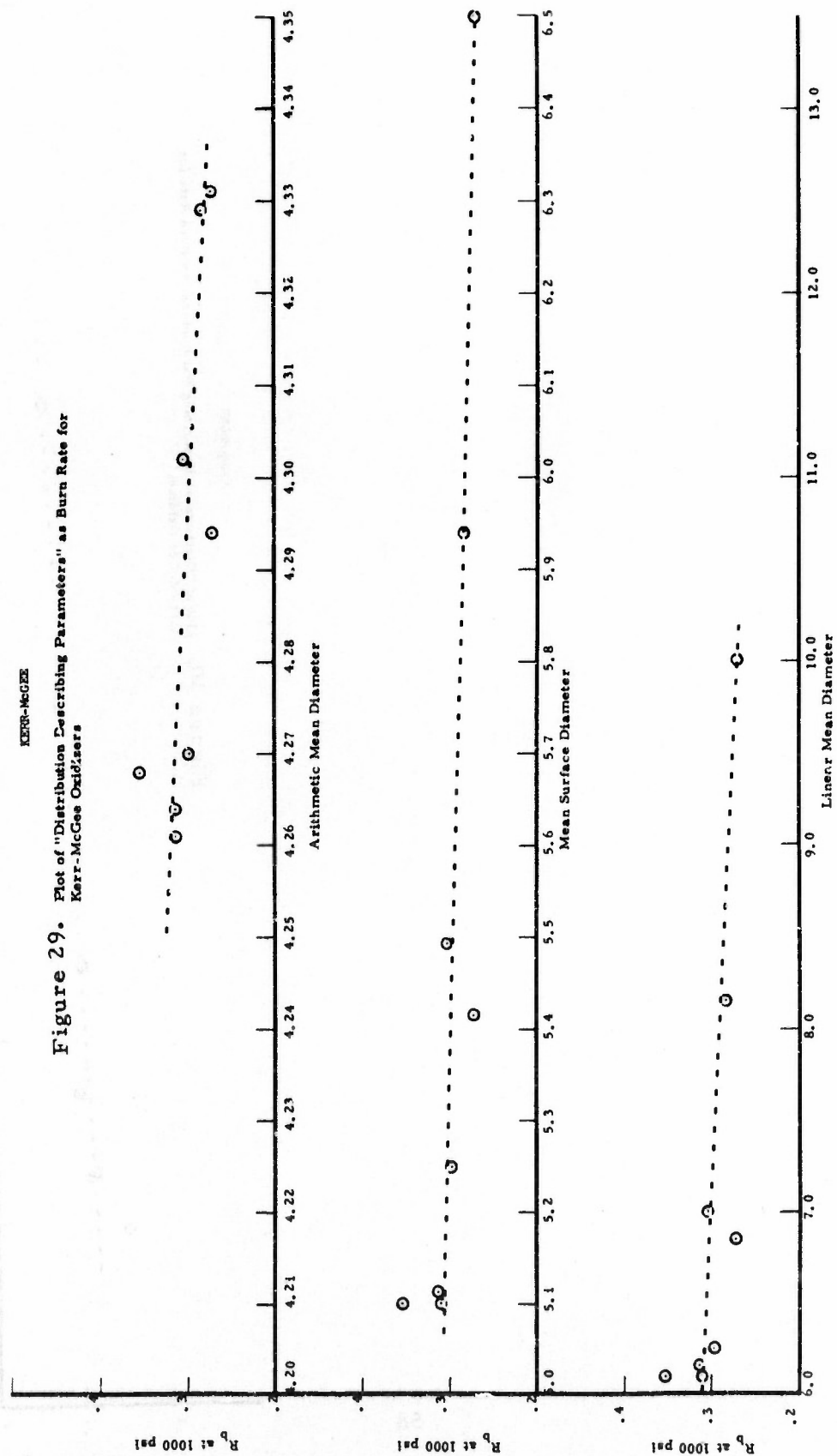


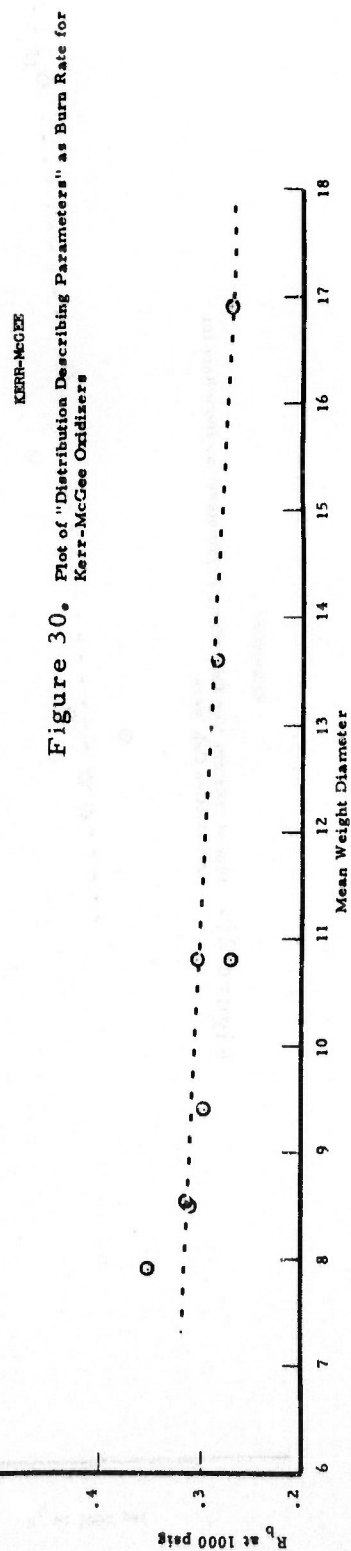
KERR-McGEE

Figure 28. Plot of "Distribution Describing Parameters" as Burn Rate for Kerr-McGee Oxidizers

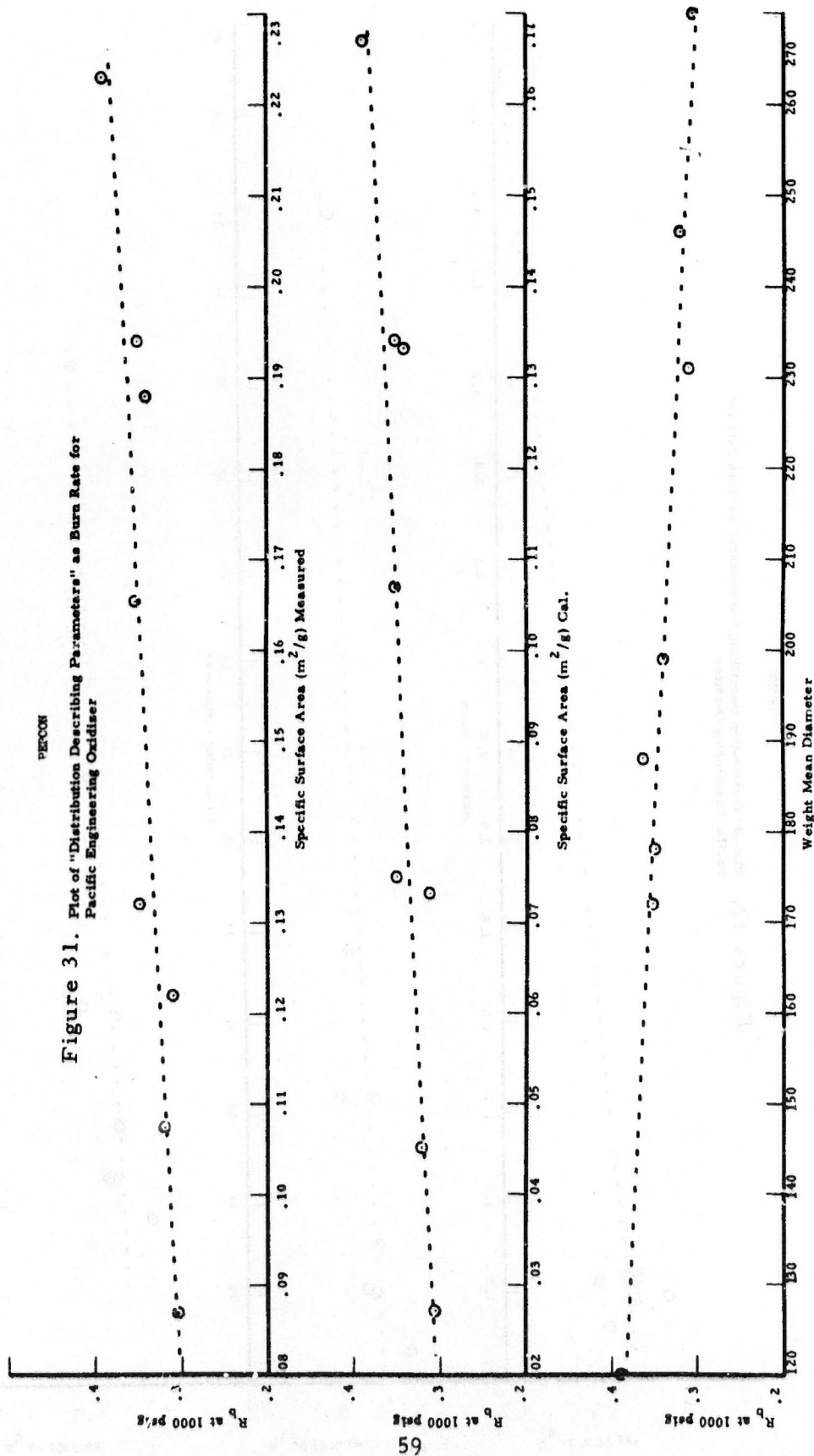


KERR-MCGEE
 Figure 29. Plot of "Distribution Describing Parameters" as Burn Rate for
 Kerr-McGee Oxidizers



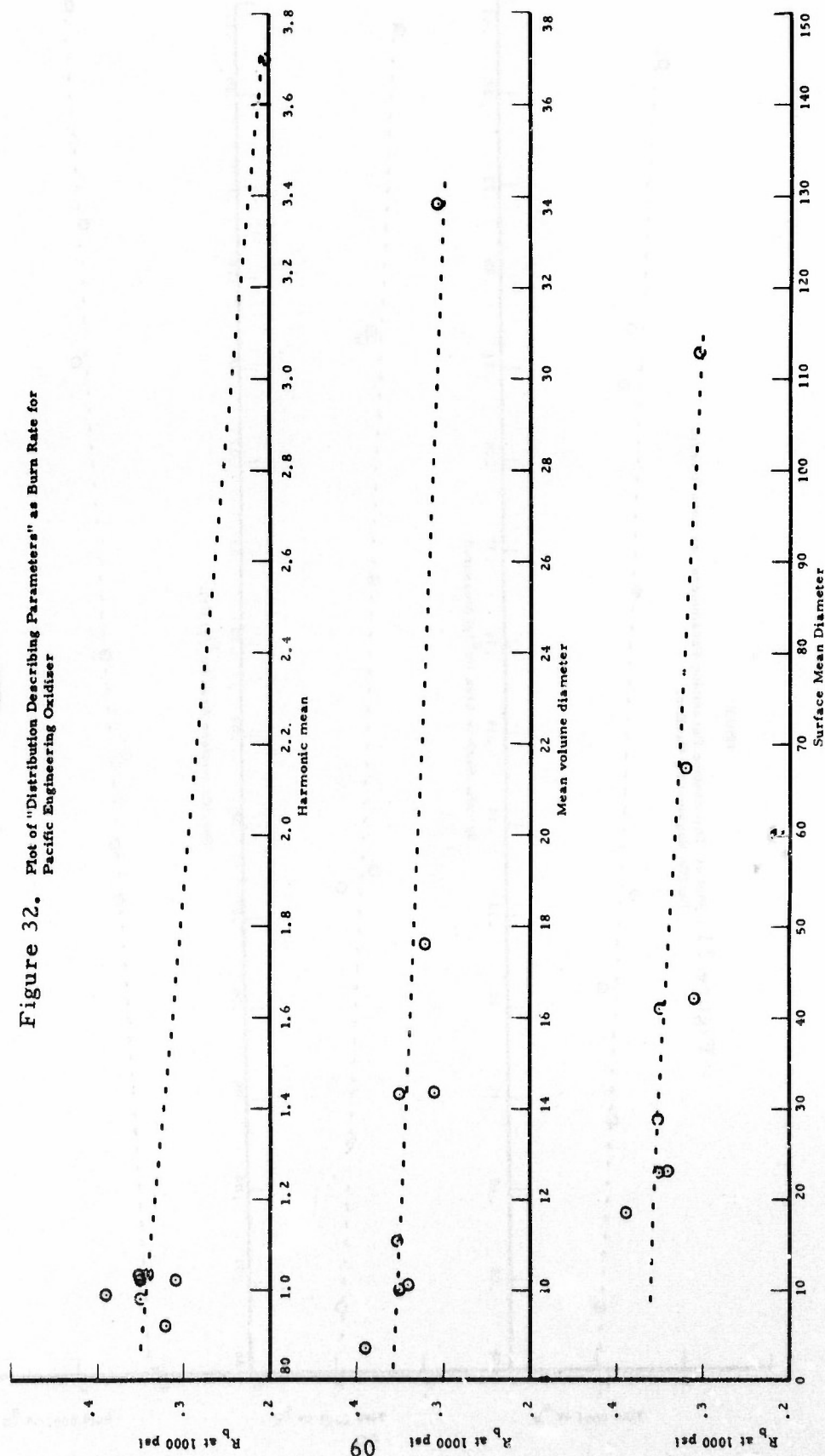


PEPCON
Figure 31. Plot of "Distribution Describing Parameters" as Burn Rate for
Pacific Engineering Oxidizer

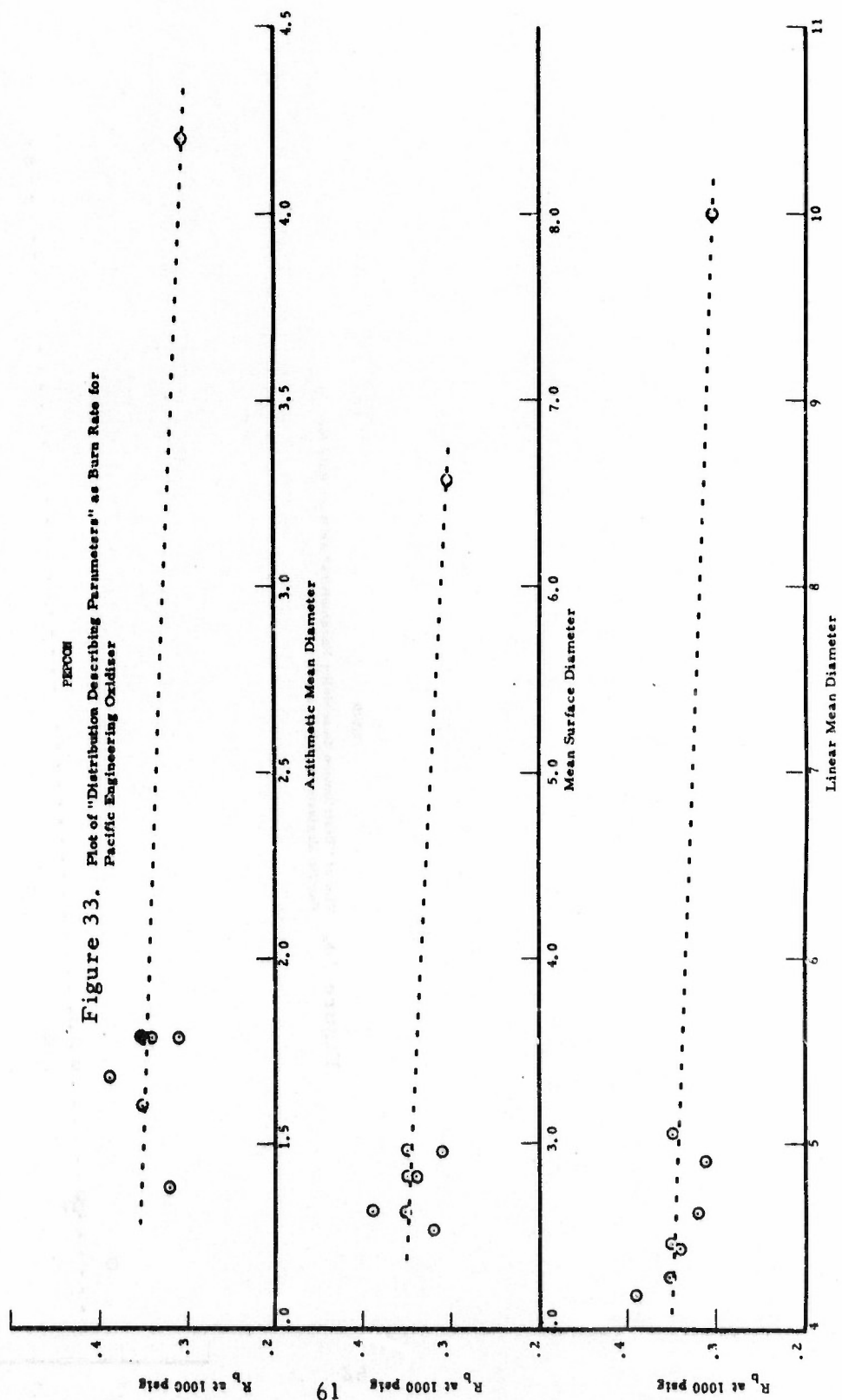


PEPCON

Figure 32. Plot of "Distribution Describing Parameters" as Burn Rate for Pacific Engineering Oxidizer



PERCON
Figure 33. Plot of "Distribution Describing Parameters" as Burn Rate for
Pacific Engineering Oxidiser



PEPCON
 Figure 34. Plot of "Distribution Describing Parameters" as Burn Rate for
 Pacific Engineering Oxidiser

62

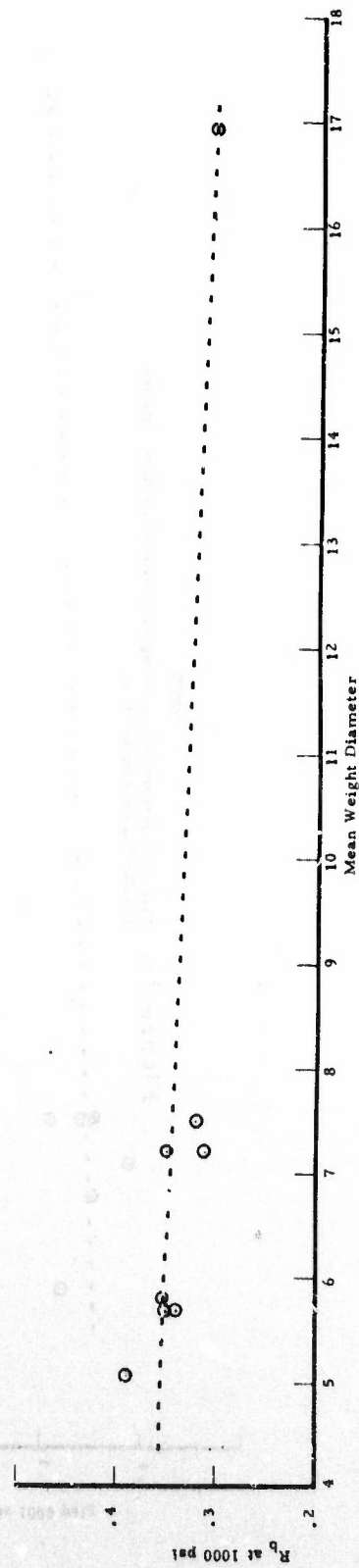


TABLE 20

BURNING RATE - REPRODUCIBILITY FACTOR CORRELATION

| | Kerr McGee <u>1σ</u> | PEPCON <u>1σ</u> |
|--------------------|---|---------------------------------------|
| SSA (calcd.) | .0402 | .0443 |
| WMD | .0353 | .0190 |
| LOG SSA (measured) | .0466 | .0427 |
| LOG APDF | .0327 | .0193 |
| MVD ^{.6} | .0610 | .0562 |
| LOG SMD | .0527 | .0482 |
| MWD | .0616 | .0637 |
| MSD ^{.3} | .0563 | .0756 |
| LMD ^{.3} | .0576 | .0729 |
| HMD | .1034 | .0764 |

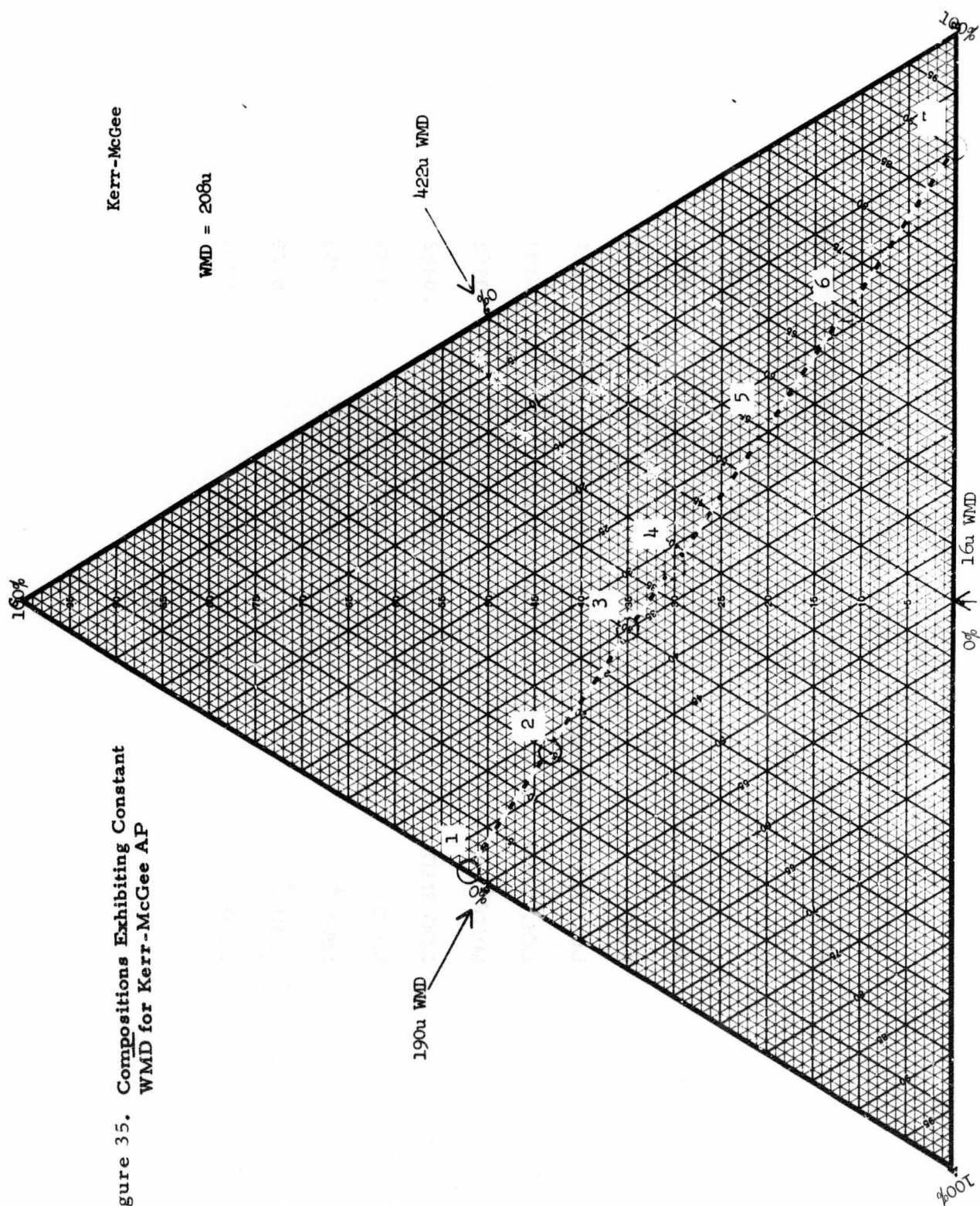


Figure 35. Compositions Exhibiting Constant WMD for Kerr-McGee AP

Figure 36. Compositions Exhibiting Constant WMD for Pacific Engineering AP

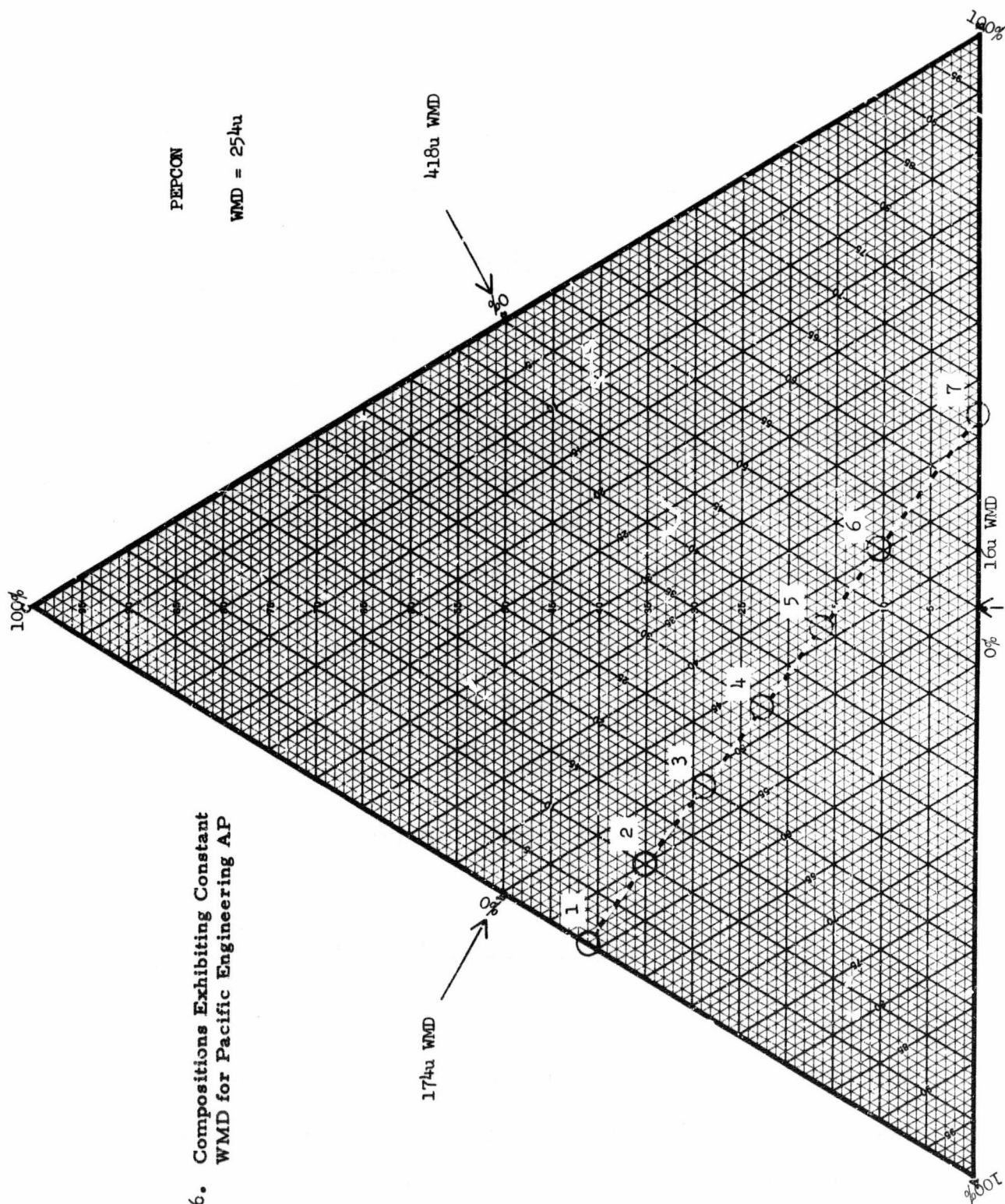


TABLE 21 /

CONSTANT \overline{WMD} MIXES \overline{WMD} = 210 MICRON (KERR-McGEE)

| MIX NUMBER | PERCENT AP | | | | | | |
|-----------------------|------------|------|------|------|------|------|------|
| | 1 | 2 | 3 | 4 | 5 | 6 | 7 |
| 422 MICRON | 48 | 42 | 35 | 32 | 25 | 18 | 10 |
| 187 MICRON | -- | 15 | 30 | 38 | 55 | 70 | 90 |
| 16 MICRON | 52 | 43 | 35 | 30 | 20 | 12 | -- |
| EOM VISCOSITY (Kp) | 56 | 40 | 28 | 18 | 28 | 28 | 64 |
| R_b @ 1000 psi | .368 | .316 | .299 | .302 | .296 | .301 | .304 |

TABLE 22

CONSTANT \overline{WMD} \overline{WMD} = 254 MICRON (PEPCON)

| MIX NUMBER | PERCENT AP | | | | | | |
|-----------------------|------------|------|------|------|------|------|------|
| | 1 | 2 | 3 | 4 | 5 | 6 | 7 |
| 418 MICRON | 59 | 55 | 51 | 47.5 | 43.5 | 40 | 33 |
| 174 MICRON | 0 | 10 | 20 | 30 | 40 | 50 | 67 |
| 16 MICRON | 41 | 35 | 29 | 22.5 | 16.5 | 10 | 0 |
| EOM VISCOSITY (Kp) | 26 | 26 | 18 | 20 | 20 | 18 | 32 |
| R_b @ 1000 psi | .305 | .305 | .313 | .301 | .319 | .299 | .298 |

Before selecting an optimum Kerr-McGee blend and an optimum PEPCON blend, it is important to review what has been done in order that the reasoning for selection of a given optimum blend is readily apparent. Basically, an optimum blend is defined as that blend of oxidizer which not only meets required burn rate but also exhibits the lowest viscosity of all possible blends which meet the burn rate. The technique for determining the optimum blend was initiated through determining a parameter associated with the physical aspects of AP which can be correlated with burn rate. As reported earlier, the best correlation factor for mixtures of 200, 400, and 20 micron AP was WMD. If one then picks a value of WMD which will provide the required burn rate, then all blends which exhibit this same WMD will provide a constant burn rate. Relatively simple calculations then provide a line of constant burn rate. The next step was to manufacture mixes along that line of constant burn rate, ascertain constancy of burn rate, and measure the viscosity for each mix. By plotting these viscosities versus composition, a point of minimum viscosity is defined and that is the optimum blend.

For mixtures of Kerr-McGee 400 micron AP, Kerr-McGee 200 micron AP, and a 20 micron AP ground fraction, the line of constant burn rate is shown in Figure 37. Mixes of TP-H7036 were manufactured at seven points along this line and the viscosities and burn rates determined. Note the constancy of burn rate at 1000 psi. The viscosities shown in Figure 37 are plotted versus composition in Figure 38. Note the strong dependence of viscosity upon oxidizer distribution. The optimum blend for mixtures of Kerr-McGee AP is then defined as the minimum in the curve plotted in Figure 38.

Identical studies were performed with mixtures of PEPCON AP. The line of constant burn rate (corresponds to a WMD of 254 microns) is shown in Figure 39. Mixes again were manufactured at seven compositions (five bimodal blends and two trimodal blends). As was the case with the Kerr-McGee AP, the burn rates are quite constant. The viscosities for each mix are listed in Figure 39 and plotted versus composition in Figure 40. Compared with the similar plot for Kerr-McGee AP blends, the response of viscosity to composition change is less sensitive (compare the shallowness of the two curves). Also, in this case, the optimum blend is defined as the minimum in the viscosity curve since all of these composition points meet the required burn rate.

Considerable difficulty was encountered in determining the optimum mixed blend of Kerr-McGee and PEPCON AP. An optimum mixed blend is defined as that mixture of Kerr-McGee (400 microns) and PEPCON (200 microns) AP, or vice versa, which meets TP-H7036 burn rate and exhibits a minimum viscosity.

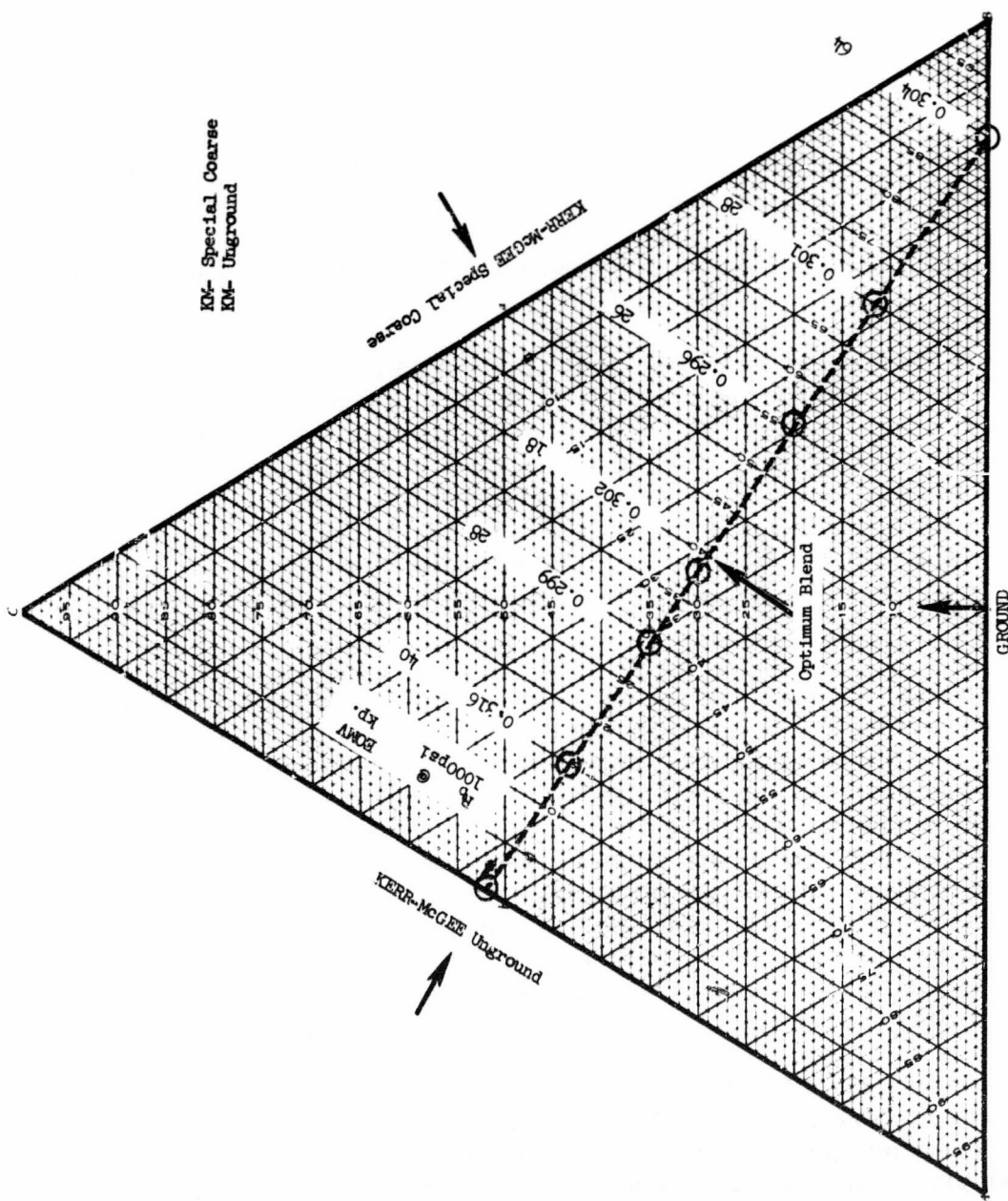


Figure 37. Composition-Constant Burn Rate Relationship for Kerr McGee Blends

Kerr-McGee Special Coarse / Kerr-McGee Unground

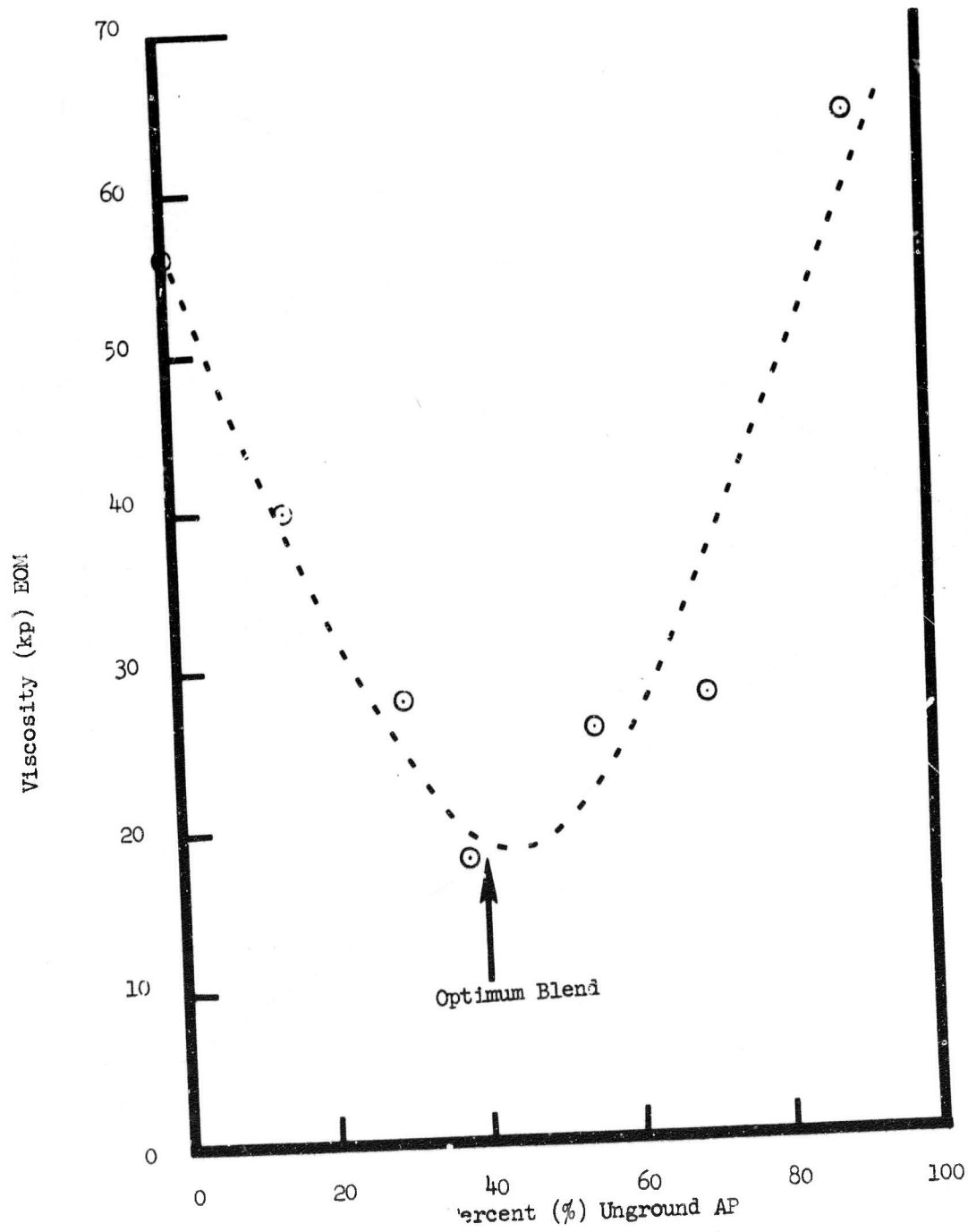


Figure 38. Composition Viscosity Plot for Kerr McGee Blends

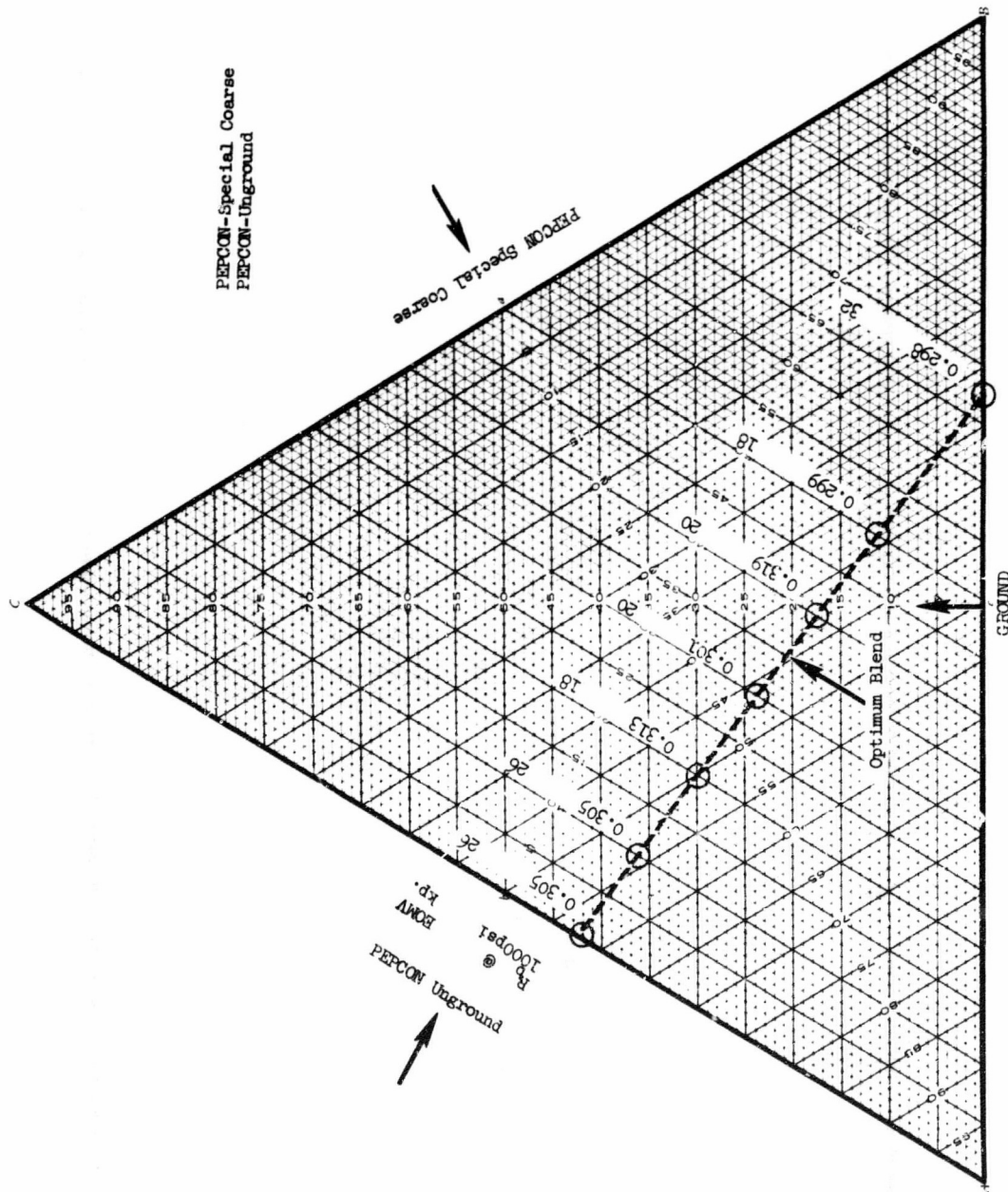


Figure 39. Composition-Constant Burn Rate Relationship for PEPCON Blends

PEPCON Special Coarse / PEPCON Unground

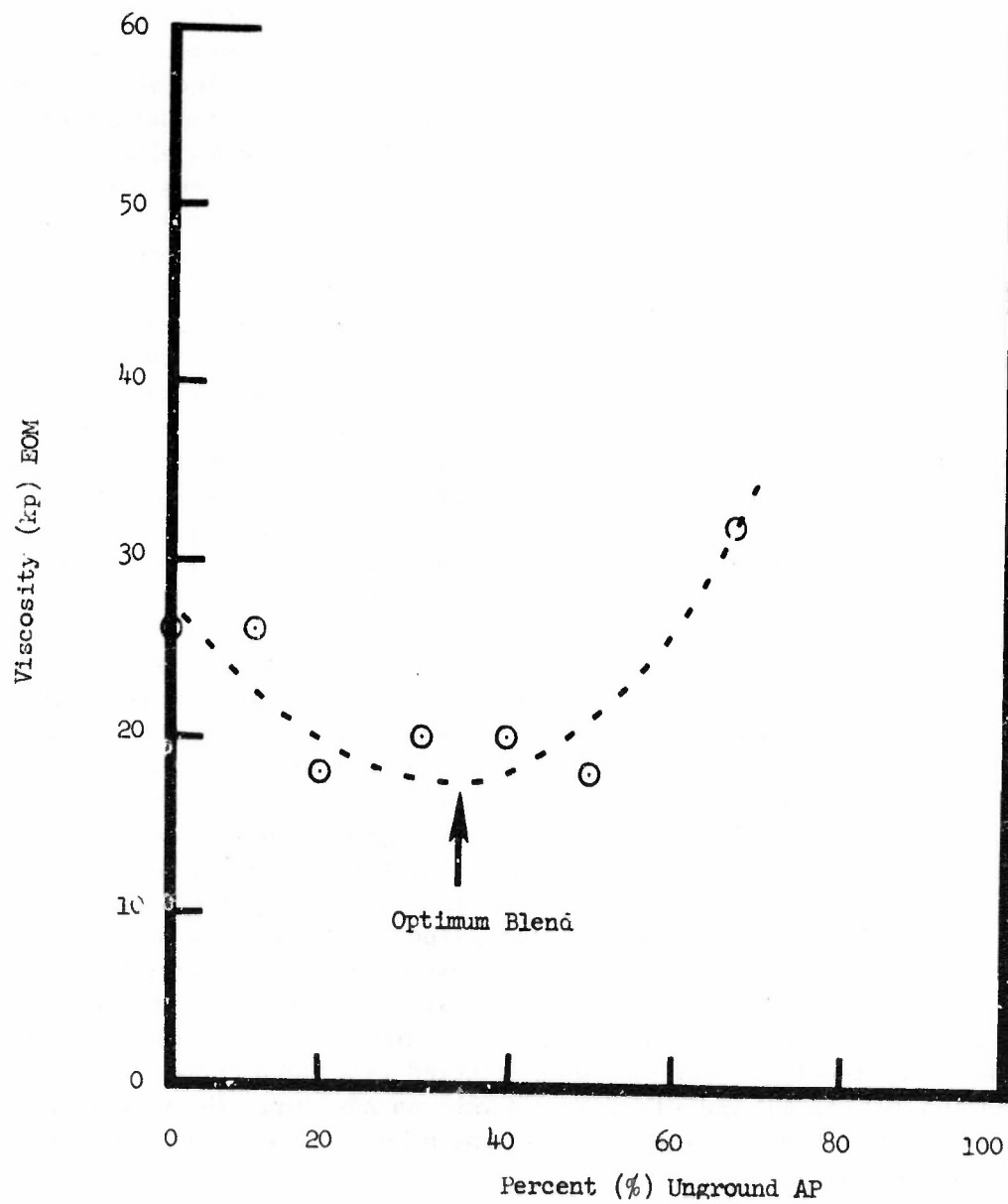


Figure 40. Composition-Viscosity Plot for PEPCON Blends

If one examines a plot of the lines of constant burn rate for all-Kerr-McGee AP blends and all-PEPCON AP blends (Figure 41), one notes an area between the two lines where any mixture of Kerr-McGee AP and PEPCON AP blend should fall. Attempts at mathematically calculating the WMD for mixed blends, three dimensional projections to define a constant burn rate line for mixed blends, and attempts at partitioning various quantities of all Kerr-McGee AP blends with all PEPCON AP blends met with no success as far as defining constant rate lines for mixed blends.

Analysis of the burn rate data obtained from examining each of the techniques for defining the optimum mixed blend indicated that the particular AP used as the 400 micron fraction exhibited the most influence on the burn rate. It was determined that the line of constant burn rate for a mixture of Kerr-McGee and PEPCON AP, where Kerr-McGee AP was the 400 micron AP and PEPCON AP was the 200 micron AP, fell on the line of constant burn rate for all Kerr-McGee blends. In other words, the line of constant burn rate for a mixed blend appeared to be controlled by a special coarse oxidizer. Figure 42 illustrates lines of constant burn rate for all-Kerr-McGee AP blends and all-PEPCON AP blends and further shows for a mixed blend of Kerr-McGee 400 micron AP and PEPCON 200 micron AP that constant burn rates are obtained when the compositions are identical to those with all-Kerr-McGee AP blends. Note the constancy of burn rate with these mixed blends. The viscosities listed in Figure 42 are plotted versus composition in Figure 43. The viscosity-composition curve shown in Figure 43 is similar in depth to an all-Kerr-McGee AP blend. It not only appears that the special coarse fraction controls burn rate but also controls the response of viscosity to composition. The optimum blend for mixes of Kerr-McGee 400 micron AP and PEPCON 200 micron AP was selected at the minimum of the viscosity-composition curve. Note also a lower viscosity for this particular mixed blend than was obtained for either the all Kerr-McGee AP blend or all-PEPCON AP blend.

A similar exercise was performed for a mixed blend of PEPCON 400 micron AP and Kerr-McGee 200 micron AP (see Figure 44). In this case, the line of constant burn rate corresponds to the line of constant burn rate for an all-PEPCON AP blend. As was the case with blends containing Kerr-McGee 400 micron AP, the burning rate is seemingly controlled by the 400 micron AP fraction. The burn rates again are quite constant and the viscosity is measured for each mix and are plotted versus composition in Figure 45. The shape of this curve is similar to that observed in an all-PEPCON AP blend. In other words, the response of viscosity to a composition is relatively small. The optimum mixed blend of mixtures of Kerr-McGee and PEPCON AP should be the one exhibiting the lowest viscosity since all of the burning rates are relatively constant. That optimum blend (compare Figures 43 and 45) was then selected as a blend containing Kerr-McGee 400 micron AP and PEPCON 200 micron AP, since the viscosity is at a lower value than that observed with any mixture of PEPCON 400 micron and Kerr-McGee 200 micron AP.

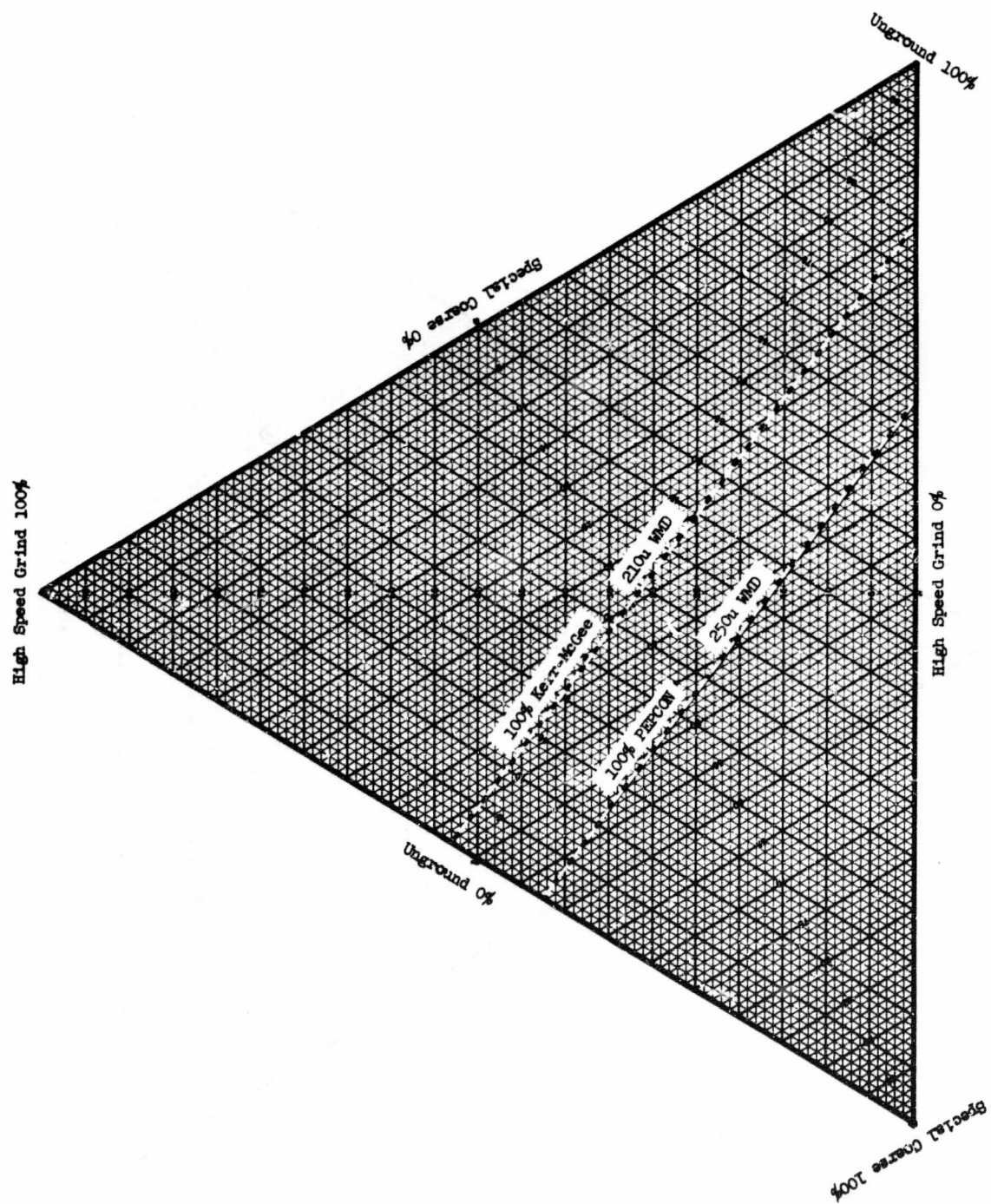


Figure 41. Lines of Constant Burn Rate vs Composition for All Kerr-McGee and All PEPCON Blends

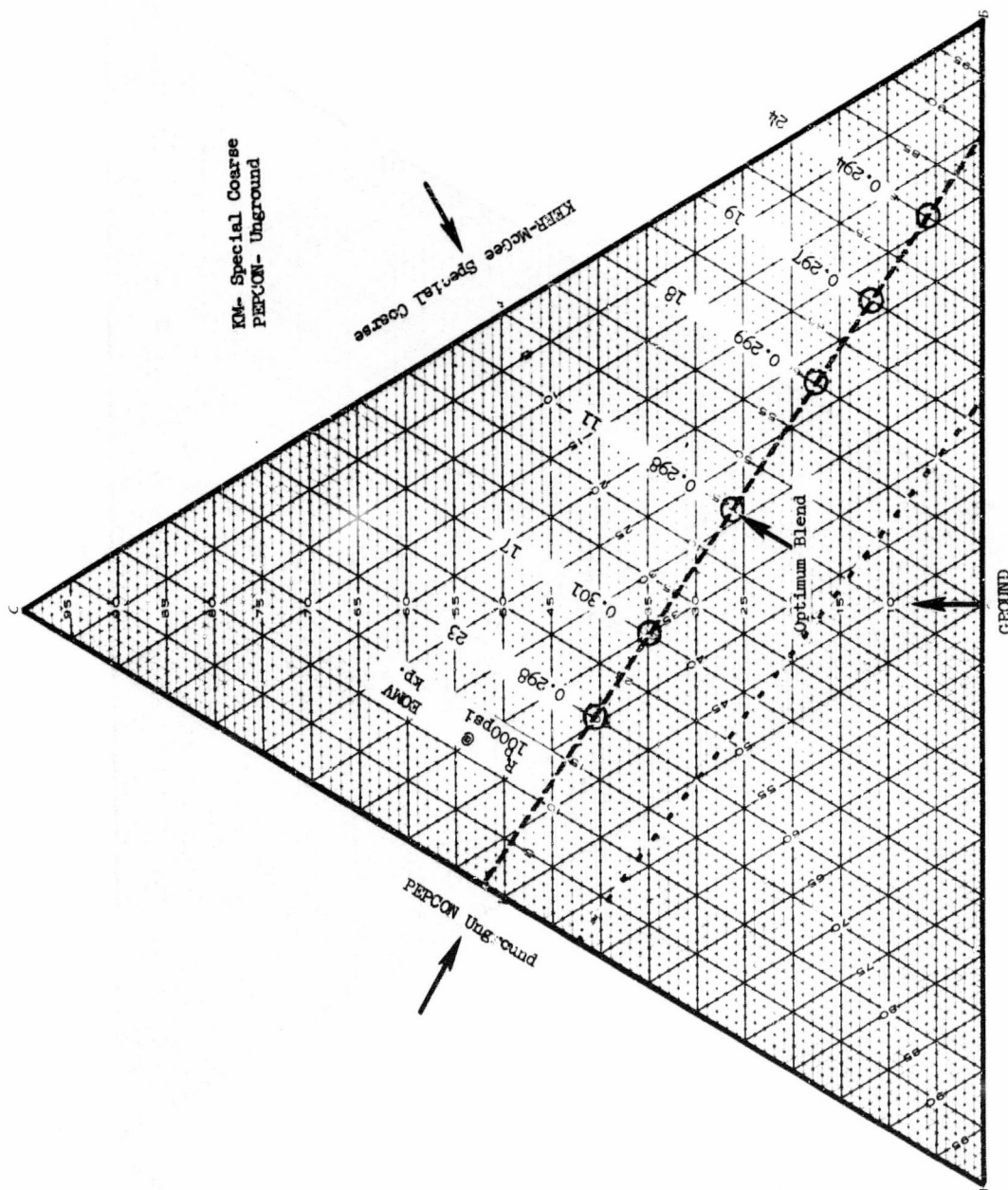


Figure 42. Composition-Constant Burn Rate Relationship for Mixtures of 400 Micron Kerr McGee, 200 Micron PEPCON and a Kerr McGee 20 Micron Fraction.

Kerr-McGee Special Coarse / PEPCON Unground

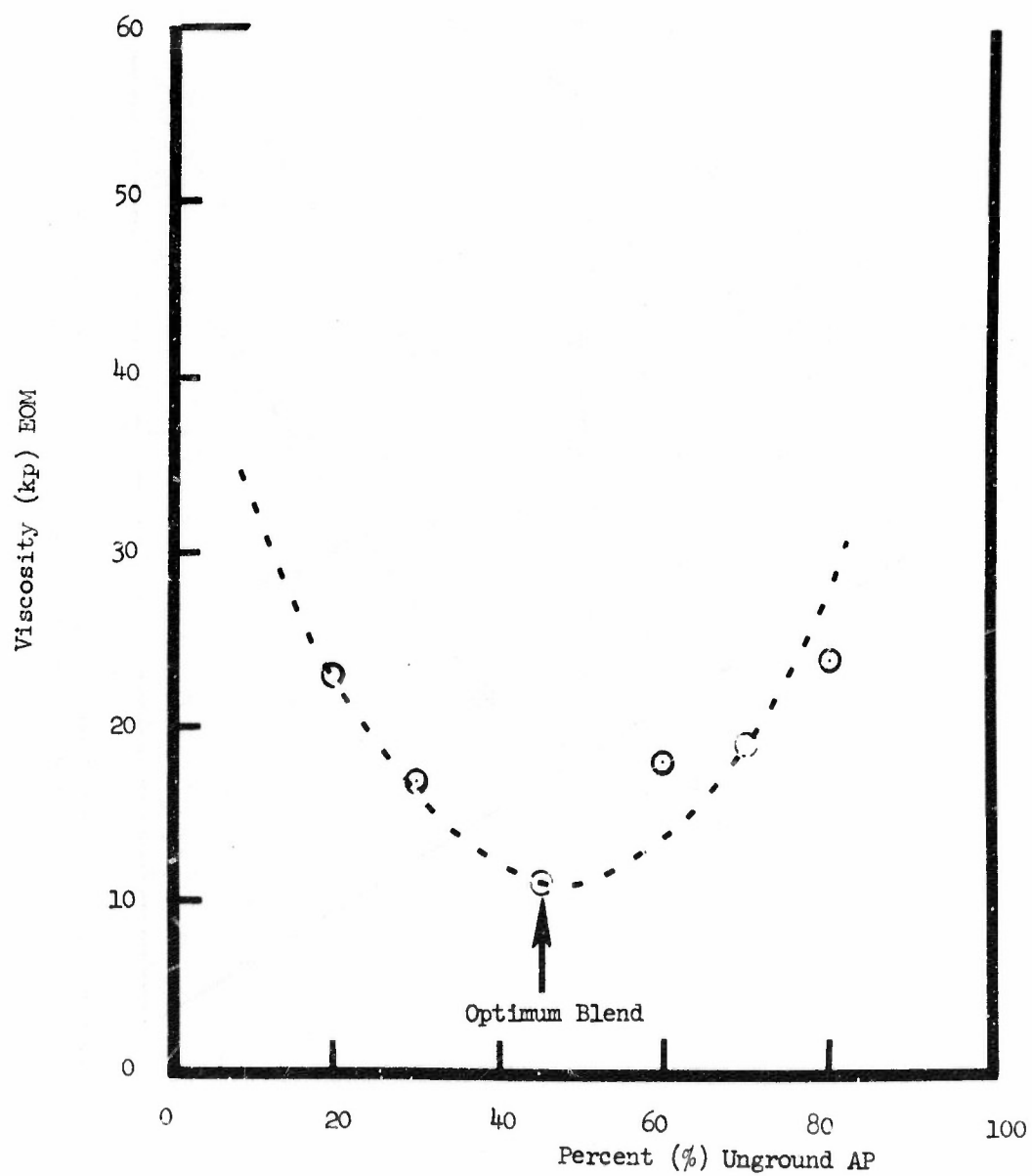


Figure 43. Composition-Viscosity Plot for Blends of 400 Micron Kerr McGee, 200 Micron PEPCON, and a 20 Micron Kerr McGee Fraction

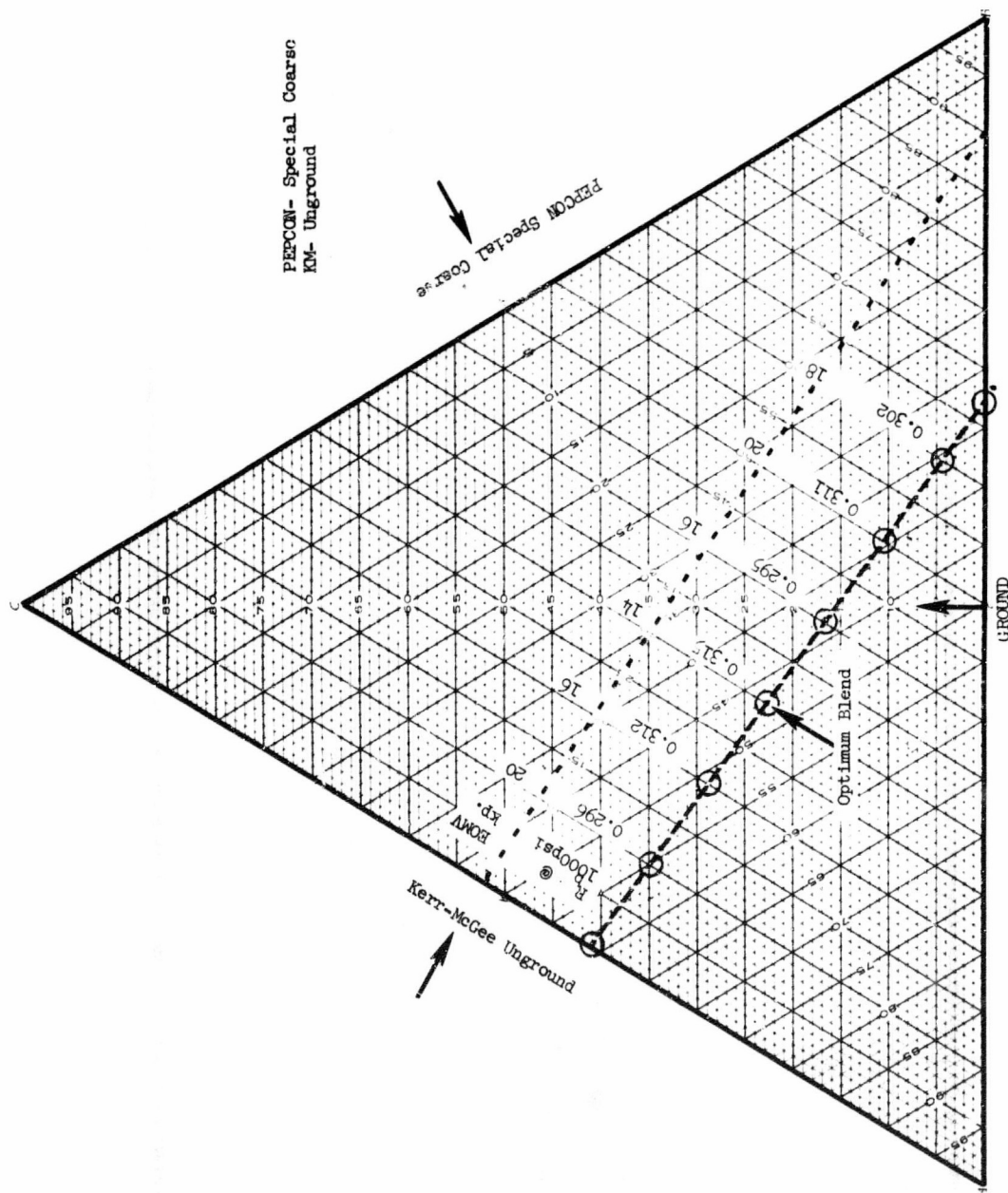


Figure 44. Composition-Constant Burn Rate Relationship for Mixtures of 400 Micron PEPCON, 200 Micron Kerr McGee and a Kerr McGee 20 Micron Fraction.

PEPCON Special Coarse / Kerr-McGee Unground

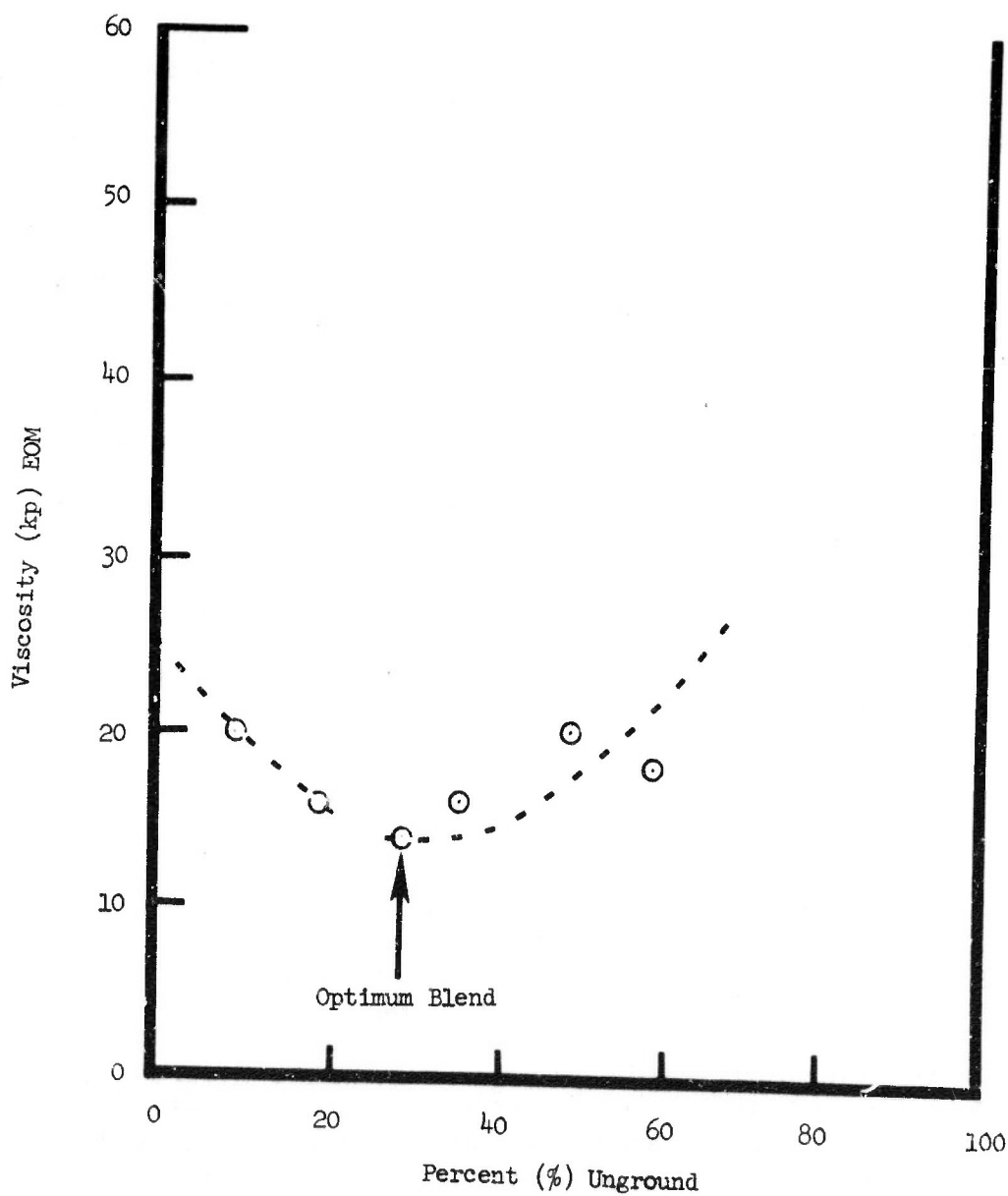


Figure 45. Composition-Viscosity Plot for Blends of 400 Micron PLPCON, 200 Micron Kerr McGee, and a 20 Micron Kerr McGee Fraction

The composition selected as the optimum blend for all-Kerr-McGee, all-PEPCON, and the mixed blend are shown in Table 23. Two-pound mixes of TP-H7036 were manufactured with each blend in both CTPB and HTPB polymer. The burn rates and viscosity for each of these mixes are shown in Table 23. The expected trend of lower viscosities and lower burn rates in the HTPB formulations are apparent. The constancy of burn rate in each system is excellent.

Phase III - AP/CTPB Propellant Characterization

Each of the optimum blends (Kerr-McGee AP, PEPCON AP, and mixed AP) was manufactured in replicate in the five-gallon vertical mixer. Before mix manufacture, each of the separate oxidizer size fractions were re-analyzed for moisture content and for any changes in size distribution that might have occurred during storage. The aluminum was prepared with polymer to eliminate dusting hazards and to provide reproducible dispersion within the propellant mix. The polymer-to-curing-agent ratio for mix manufacture was selected based upon the moisture content of the ingredients.

Two five-gallon mixes were manufactured for each optimum blend. Identical mix procedures and mix times were utilized. To prevent oxidizer agglomeration, the ground fraction of AP was added to the mixer first. This prevented any unnecessary storage time following weigh-up for the size fraction of AP which would be expected to agglomerate most severely.

From the first mix of each replicate, TX-3 motors were loaded as well as mechanical property samples for confirmation of mix-to-mix reproducibility. From a second mix, ice cream cartons and biaxial rails were loaded from which a comprehensive mechanical property characterization was to be accomplished.

To ascertain the effect of excess moisture upon the processibility and resulting ballistic and mechanical properties, each optimum blend (pre-mixed) was exposed to 50% relative humidity for one week. Following this exposure, a single five-gallon mix of TP-H7036 was manufactured with each humidified optimum blend.

Nine CTPB mixes were manufactured; replicates for each of the three optimum blends and a single mix for each humidified optimum blend.

The composition, as well as processing information, for each of the mixes are shown in Table 24. The propellant from each mix was cured for seven days at 145°F. The required number of motors and mechanical property samples were obtained from each mix.

An identical mix matrix, with the exception of a direct substitution of HTPB binder for CTPB binder, was manufactured with the selected optimum blends in an HTPB binder system. The compositions and processing data for these mixes are shown in Table 25. The expected lower viscosity of the HTPB propellants is apparent. All required motors and mechanical property samples were obtained from each mix.

TABLE 23

SELECTED OPTIMUM BLENDS

| | <u>Kerr McGee</u> | <u>Pepcon</u> | <u>Mixed Blend</u> |
|-------------------------------------|-------------------|---------------|--------------------|
| Birder | 12.00 | 12.00 | 12.00 |
| KM (400 μ) | 21.10 | --- | 19.70 |
| KM (200 μ) | 27.20 | --- | --- |
| P (400 μ) | --- | 30.94 | --- |
| P (200 μ) | --- | 23.80 | 30.60 |
| Ground AP | 19.70 | 13.26 | 17.70 |
| Al | 20.00 | 20.00 | 20.00 |
| <u>CTPB</u> | | | |
| EOM Viscosity (Kp/ $^{\circ}$ F) | 16/130 | 16/124 | 11/128 |
| r_b @ 1000 psi | .302 | .305 | .298 |
| <u>HTPB</u> | | | |
| EOM Viscosity (Kp/ $^{\circ}$ F) | 8/130 | 10/130 | 10/130 |
| r_b @ 1000 psi | .280 | .279 | .279 |

TABLE 24

OPTIMUM BLENDS IN CTPB

| Mix No. | Optimum Kerr McGee Blend | | Optimum PEPCON Blend | | Optimum Mixed Blend | | Humidified Optimum Blends | |
|------------------------------------|--------------------------|----------|----------------------|---------|---------------------|----------|---------------------------|--------------------------|
| | T-260 | T-261 | T-269 | T-270 | T-267 | T-268 | Kerr McGee T-264 | PEPCON T-265 Mixed T-266 |
| CTPB | 10.563 | 10.563 | 10.563 | 10.563 | 10.563 | 10.563 | 10.563 | 10.563 |
| NAPO | 0.266 | 0.266 | 0.266 | 0.266 | 0.266 | 0.266 | 0.266 | 0.266 |
| ERL-0510 | 0.071 | 0.071 | 0.071 | 0.071 | 0.071 | 0.071 | 0.071 | 0.071 |
| Iron Linoleate | 0.100 | 0.100 | 0.100 | 0.100 | 0.100 | 0.100 | 0.100 | 0.100 |
| DOA | 1.000 | 1.000 | 1.000 | 1.000 | 1.000 | 1.000 | 1.000 | 1.000 |
| Aluminum | 20.000 | 20.000 | 20.000 | 20.000 | 20.000 | 20.000 | 20.000 | 20.000 |
| AP (400 micron) | 21.100 | 21.100 | 30.540 | 30.540 | 19.700 | 19.700 | 21.100 | 19.700 |
| AP (200 micron) | 27.200 | 27.200 | 23.800 | 23.800 | 30.600 | 30.600 | 27.200 | 30.600 |
| AP (20 micron) | 19.700 | 19.700 | 13.260 | 13.260 | 17.700 | 17.700 | 19.700 | 17.700 |
| Bay Conditions | | | | | | | | |
| Relative Humidity | 20 | 18 | 18 | 14 | 20 | 17 | 20 | 28 |
| Temperature | 80 | 82 | 82 | 82 | 81 | 80 | 80 | 82 |
| Mixer Size | 5 gal | 5 gal | 5 gal | 5 gal | 5 gal | 5 gal | 5 gal | 5 gal |
| Mix Weight, lbs | 65 | 65 | 65 | 65 | 65 | 65 | 65 | 65 |
| End of Mix Viscosity, Kilopoise/°F | 11.2/146 | 10.0/146 | 8.4/145 | 8.4/145 | 10.0/145 | 10.0/145 | 11.2/145 | 8.8/145 |
| | | | | | | | | 10.0/145 |

*Exposed to 50% R. H. for 168 hours

**Optimum mixed blend contains Kerr McGee AP as the 400 micron fraction and PEPCON AP as the 200 micron fraction.

TABLE 25

OPTIMUM BLENDS IN HTPB

| | Optimum Kerr McGee | | Optimum PEPCON | | Optimum Mixed** | | Humidified Optimum Blends* | |
|----------------------|--------------------|-------|----------------|-------|-----------------|-------|----------------------------|-------|
| | T-271 | Blend | T-272 | Blend | T-273 | Blend | T-274 | Blend |
| HTPB (R-45) | 10.029 | | 10.029 | | 10.029 | | 10.029 | |
| PDI | 0.671 | | 0.671 | | 0.671 | | 0.671 | |
| DOA | 1.000 | | 1.000 | | 1.000 | | 1.000 | |
| HX-752 | 0.300 | | 0.300 | | 0.300 | | 0.300 | |
| Aluminum | 20.000 | | 20.000 | | 20.000 | | 20.000 | |
| AP (400 micron) | 21.100 | | 21.100 | | 21.100 | | 21.100 | |
| AP (200 micron) | 27.200 | | 27.200 | | 27.200 | | 27.200 | |
| AF (20 micron) | 19.700 | | 19.700 | | 19.700 | | 19.700 | |
| Pay Conditions | | | | | | | | |
| Relative Humidity | 20 | | 10 | | 22 | | 8 | |
| Temperature/° F | 82 | | 82 | | 79 | | 79 | |
| Mixer Size | 5 gal | | 5 gal | | 5 gal | | 5 gal | |
| Mix Weight, lbs | 65 | | 65 | | 65 | | 65 | |
| End of Mix Viscosity | | | | | | | | |
| Kilopoise/° F | 2.0/146 | | 2.0/145 | | 1.6/145 | | 1.6/145 | |
| | | | | | 2.0/148 | | 1.6/147 | |
| | | | | | 2.4/145 | | 1.6/145 | |
| | | | | | 5 gal | | 5 gal | |
| | | | | | 65 | | 65 | |
| | | | | | 22 | | 20 | |
| | | | | | 80 | | 79 | |
| | | | | | 5 gal | | 5 gal | |
| | | | | | 65 | | 65 | |
| | | | | | 2.4/145 | | 1.6/147 | |
| | | | | | 5 gal | | 5 gal | |
| | | | | | 65 | | 65 | |
| | | | | | 22 | | 22 | |
| | | | | | 80 | | 79 | |
| | | | | | 5 gal | | 5 gal | |
| | | | | | 65 | | 65 | |
| | | | | | 2.4/145 | | 1.6/145 | |
| | | | | | 5 gal | | 5 gal | |
| | | | | | 65 | | 65 | |
| | | | | | 22 | | 22 | |
| | | | | | 80 | | 79 | |
| | | | | | 5 gal | | 5 gal | |
| | | | | | 65 | | 65 | |
| | | | | | 2.4/145 | | 1.6/147 | |
| | | | | | 5 gal | | 5 gal | |
| | | | | | 65 | | 65 | |
| | | | | | 22 | | 22 | |
| | | | | | 80 | | 79 | |
| | | | | | 5 gal | | 5 gal | |
| | | | | | 65 | | 65 | |
| | | | | | 2.4/145 | | 1.6/147 | |
| | | | | | 5 gal | | 5 gal | |
| | | | | | 65 | | 65 | |
| | | | | | 22 | | 22 | |
| | | | | | 80 | | 79 | |
| | | | | | 5 gal | | 5 gal | |
| | | | | | 65 | | 65 | |
| | | | | | 2.4/145 | | 1.6/147 | |
| | | | | | 5 gal | | 5 gal | |
| | | | | | 65 | | 65 | |
| | | | | | 22 | | 22 | |
| | | | | | 80 | | 79 | |
| | | | | | 5 gal | | 5 gal | |
| | | | | | 65 | | 65 | |
| | | | | | 2.4/145 | | 1.6/147 | |
| | | | | | 5 gal | | 5 gal | |
| | | | | | 65 | | 65 | |
| | | | | | 22 | | 22 | |
| | | | | | 80 | | 79 | |
| | | | | | 5 gal | | 5 gal | |
| | | | | | 65 | | 65 | |
| | | | | | 2.4/145 | | 1.6/147 | |
| | | | | | 5 gal | | 5 gal | |
| | | | | | 65 | | 65 | |
| | | | | | 22 | | 22 | |
| | | | | | 80 | | 79 | |
| | | | | | 5 gal | | 5 gal | |
| | | | | | 65 | | 65 | |
| | | | | | 2.4/145 | | 1.6/147 | |
| | | | | | 5 gal | | 5 gal | |
| | | | | | 65 | | 65 | |
| | | | | | 22 | | 22 | |
| | | | | | 80 | | 79 | |
| | | | | | 5 gal | | 5 gal | |
| | | | | | 65 | | 65 | |
| | | | | | 2.4/145 | | 1.6/147 | |
| | | | | | 5 gal | | 5 gal | |
| | | | | | 65 | | 65 | |
| | | | | | 22 | | 22 | |
| | | | | | 80 | | 79 | |
| | | | | | 5 gal | | 5 gal | |
| | | | | | 65 | | 65 | |
| | | | | | 2.4/145 | | 1.6/147 | |
| | | | | | 5 gal | | 5 gal | |
| | | | | | 65 | | 65 | |
| | | | | | 22 | | 22 | |
| | | | | | 80 | | 79 | |
| | | | | | 5 gal | | 5 gal | |
| | | | | | 65 | | 65 | |
| | | | | | 2.4/145 | | 1.6/147 | |
| | | | | | 5 gal | | 5 gal | |
| | | | | | 65 | | 65 | |
| | | | | | 22 | | 22 | |
| | | | | | 80 | | 79 | |
| | | | | | 5 gal | | 5 gal | |
| | | | | | 65 | | 65 | |
| | | | | | 2.4/145 | | 1.6/147 | |
| | | | | | 5 gal | | 5 gal | |
| | | | | | 65 | | 65 | |
| | | | | | 22 | | 22 | |
| | | | | | 80 | | 79 | |
| | | | | | 5 gal | | 5 gal | |
| | | | | | 65 | | 65 | |
| | | | | | 2.4/145 | | 1.6/147 | |
| | | | | | 5 gal | | 5 gal | |
| | | | | | 65 | | 65 | |
| | | | | | 22 | | 22 | |
| | | | | | 80 | | 79 | |
| | | | | | 5 gal | | 5 gal | |
| | | | | | 65 | | 65 | |
| | | | | | 2.4/145 | | 1.6/147 | |
| | | | | | 5 gal | | 5 gal | |
| | | | | | 65 | | 65 | |
| | | | | | 22 | | 22 | |
| | | | | | 80 | | 79 | |
| | | | | | 5 gal | | 5 gal | |
| | | | | | 65 | | 65 | |
| | | | | | 2.4/145 | | 1.6/147 | |
| | | | | | 5 gal | | 5 gal | |
| | | | | | 65 | | 65 | |
| | | | | | 22 | | 22 | |
| | | | | | 80 | | 79 | |
| | | | | | 5 gal | | 5 gal | |
| | | | | | 65 | | 65 | |
| | | | | | 2.4/145 | | 1.6/147 | |
| | | | | | 5 gal | | 5 gal | |
| | | | | | 65 | | 65 | |
| | | | | | 22 | | 22 | |
| | | | | | 80 | | 79 | |
| | | | | | 5 gal | | 5 gal | |
| | | | | | 65 | | 65 | |
| | | | | | 2.4/145 | | 1.6/147 | |
| | | | | | 5 gal | | 5 gal | |
| | | | | | 65 | | 65 | |
| | | | | | 22 | | 22 | |
| | | | | | 80 | | 79 | |
| | | | | | 5 gal | | 5 gal | |
| | | | | | 65 | | 65 | |
| | | | | | 2.4/145 | | 1.6/147 | |
| | | | | | 5 gal | | 5 gal | |
| | | | | | 65 | | 65 | |
| | | | | | 22 | | 22 | |
| | | | | | 80 | | 79 | |
| | | | | | 5 gal | | 5 gal | |
| | | | | | 65 | | 65 | |
| | | | | | 2.4/145 | | 1.6/147 | |
| | | | | | 5 gal | | 5 gal | |
| | | | | | 65 | | 65 | |
| | | | | | 22 | | 22 | |
| | | | | | 80 | | 79 | |
| | | | | | 5 gal | | 5 gal | |
| | | | | | 65 | | 65 | |
| | | | | | 2.4/145 | | 1.6/147 | |
| | | | | | 5 gal | | 5 gal | |
| | | | | | 65 | | 65 | |
| | | | | | 22 | | 22 | |
| | | | | | 80 | | 79 | |
| | | | | | 5 gal | | 5 gal | |
| | | | | | 65 | | 65 | |
| | | | | | 2.4/145 | | 1.6/147 | |
| | | | | | 5 gal | | 5 gal | |
| | | | | | 65 | | 65 | |
| | | | | | 22 | | 22 | |
| | | | | | 80 | | 79 | |
| | | | | | 5 gal | | 5 gal | |
| | | | | | 65 | | 65 | |
| | | | | | 2.4/145 | | 1.6/147 | |
| | | | | | 5 gal | | 5 gal | |
| | | | | | 65 | | 65 | |
| | | | | | 22 | | 22 | |
| | | | | | 80 | | 79 | |
| | | | | | 5 gal | | 5 gal | |
| | | | | | 65 | | 65 | |
| | | | | | 2.4/145 | | 1.6/147 | |
| | | | | | 5 gal | | 5 gal | |
| | | | | | 65 | | 65 | |
| | | | | | 22 | | 22 | |
| | | | | | 80 | | 79 | |
| | | | | | 5 gal | | 5 gal | |
| | | | | | 65 | | 65 | |
| | | | | | 2.4/145 | | 1.6/147 | |
| | | | | | 5 gal | | 5 gal | |
| | | | | | 65 | | 65 | |
| | | | | | 22 | | 22 | |
| | | | | | 80 | | 79 | |
| | | | | | 5 gal | | 5 gal | |
| | | | | | 65 | | 65 | |
| | | | | | 2.4/145 | | 1.6/147 | |
| | | | | | 5 gal | | 5 gal | |
| | | | | | 65 | | 65 | |
| | | | | | 22 | | 22 | |
| | | | | | 80 | | 79 | |
| | | | | | 5 gal | | 5 gal | |
| | | | | | 65 | | 65 | |
| | | | | | 2.4/145 | | 1.6/147 | |
| | | | | | 5 gal | | 5 gal | |
| | | | | | 65 | | 65 | |
| | | | | | 22 | | 22 | |
| | | | | | 80 | | 79 | |
| | | | | | 5 gal | | 5 gal | |
| | | | | | 65 | | 65 | |
| | | | | | 2.4/145 | | 1.6/147 | |
| | | | | | 5 gal | | 5 gal | |
| | | | | | 65 | | 65 | |
| | | | | | 22 | | 22 | |
| | | | | | 80 | | 79 | |
| | | | | | 5 gal | | 5 gal | |
| | | | | | 65 | | 65 | |
| | | | | | 2.4/145 | | 1.6/147 | |
| | | | | | 5 gal | | 5 gal | |
| | | | | | 65 | | 65 | |
| | | | | | 22 | | 22 | |
| | | | | | 80 | | 79 | |
| | | | | | 5 gal | | 5 gal | |
| | | | | | 65 | | 65 | |
| | | | | | 2.4/145 | | 1.6/147 | |
| | | | | | 5 gal | | 5 gal | |
| | | | | | 65 | | 65 | |
| | | | | | 22 | | 22 | |
| | | | | | 80 | | 79 | |
| | | | | | 5 gal | | 5 gal | |
| | | | | | 65 | | 65 | |
| | | | | | 2.4/145 | | 1.6/147 | |
| | | | | | 5 gal | | 5 gal | |
| | | | | | 65 | | 65 | |
| | | | | | 22 | | 22 | |
| | | | | | 80 | | 79 | |
| | | | | | 5 gal | | 5 gal | |
| | | | | | 65 | | 65 | |
| | | | | | 2.4/145 | | 1.6/147 | |
| | | | | | 5 gal | | 5 gal | |
| | | | | | 65 | | 65 | |
| | | | | | 22 | | 22 | |
| | | | | | 80 | | 79 | |
| | | | | | 5 gal | | 5 gal | |

Ballistic Evaluation of the Optimum Blends in TP-H7036

From one of the replicate mixes for each optimum blend in both CTPB and HTPB propellants, six TX-3 motors (3 pound C. P.) were loaded. These motors, following cure, were tested over a pressure range of 400-1500 psia. The resulting burn rate data for each of the three CTPB optimum blend propellants is shown in Figure 46. These propellants were all formulated to exhibit identical burn rates (0.3 in/sec at 1000 psi in strands). The optimum Kerr McGee blend and the optimum mixed blend exhibited similar burn rates (.05 in/sec higher than in strands) whereas the optimum PEPCON blend demonstrated a 10% lower burn rate than the other blends. The burn rate of the PEPCON blend, however, is higher than was noted in strands. Figure 47. illustrates similar data for the optimum blend manufactured in HTPB. Again the optimum PEPCON blend exhibited a lower burn rate.

The ballistic data for the motors manufactured from the humidified optimum blends are shown in Figure 48. The trends exhibited in this data are the same as those noted for the non-humidified propellants. These data are tabulated in Table 26.

Before each of the five-gallon mixes was manufactured, a one-gallon vertical mix was manufactured for each formulation in order to ascertain burn rate response before scale-up to the five-gallon mix size. The burn rate in strands measured from each of these one-gallon mixes are compared with the TX-3 motor data from comparable five-gallon mixes. These data are illustrated in Table 27. Note that in each case the motor burn rate data is significantly higher and that the optimum PEPCON blend comes closer to matching strand and motor burn rate.

Contained in Table 28 is a comparison between the motor data and strand data obtained from the five-gallon mixes from which the motors were loaded. Note particularly that the comparison between strand and motor burning rate is much better. This would indicate that the burning rates obtained between the one-gallon vertical mix and the five-gallon vertical mix are significantly different.

CTPB

| | Mix no. | S.C. | Ung. |
|---|---------|------|------|
| ○ | T-261 | KM | KM |
| □ | T-267 | KM | P |
| ◇ | T-269 | P | P |

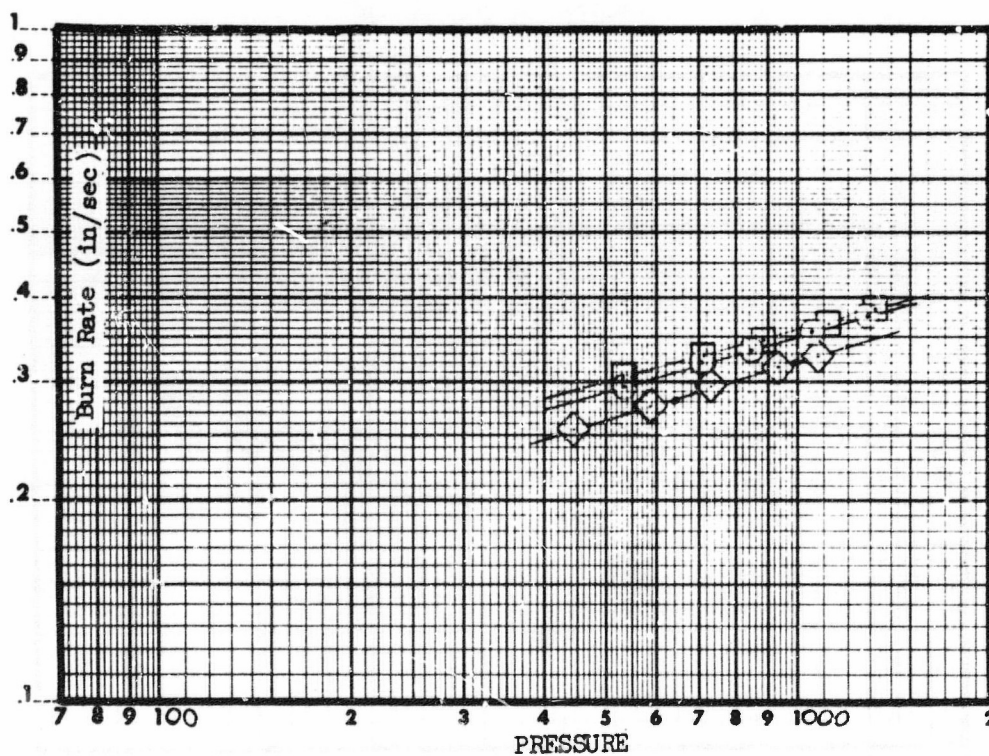


Figure 46. Burn Rate-Pressure Data for the Optimum Blends
in CTPB Propellant

HTPB

| Mix no. | S.C. | Ung. |
|---------|------|------|
| T-272 | KM | KM |
| T-285 | KM | P |
| T-277 | P | P |

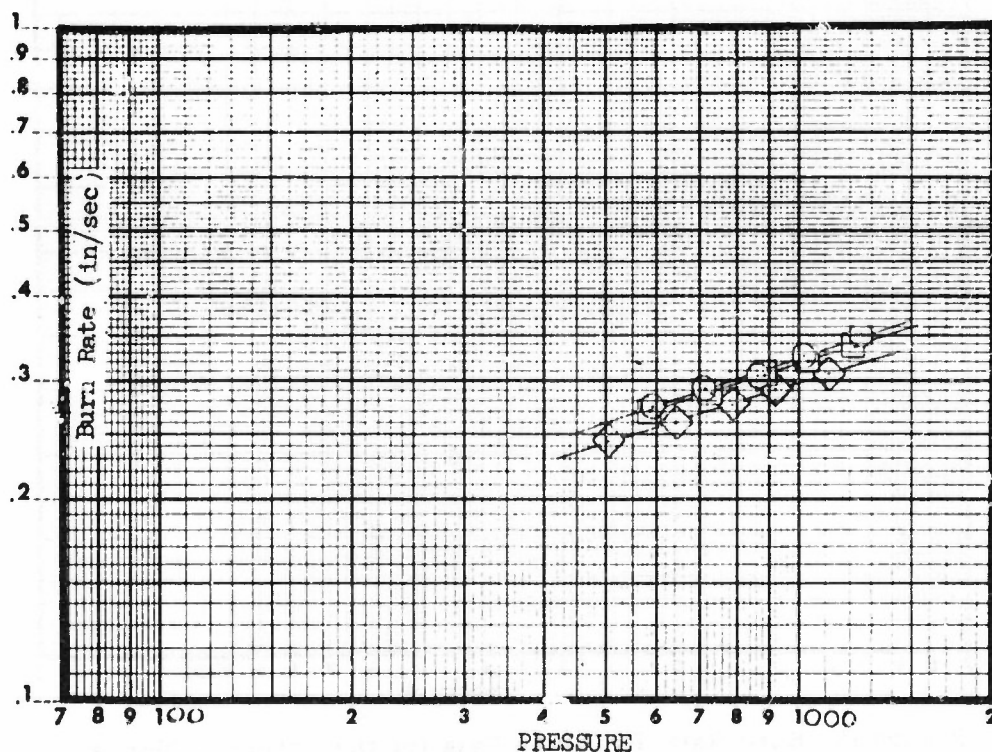


Figure 47. Burn Rate-Pressure Data for the Optimum Blends in HTPB Propellant

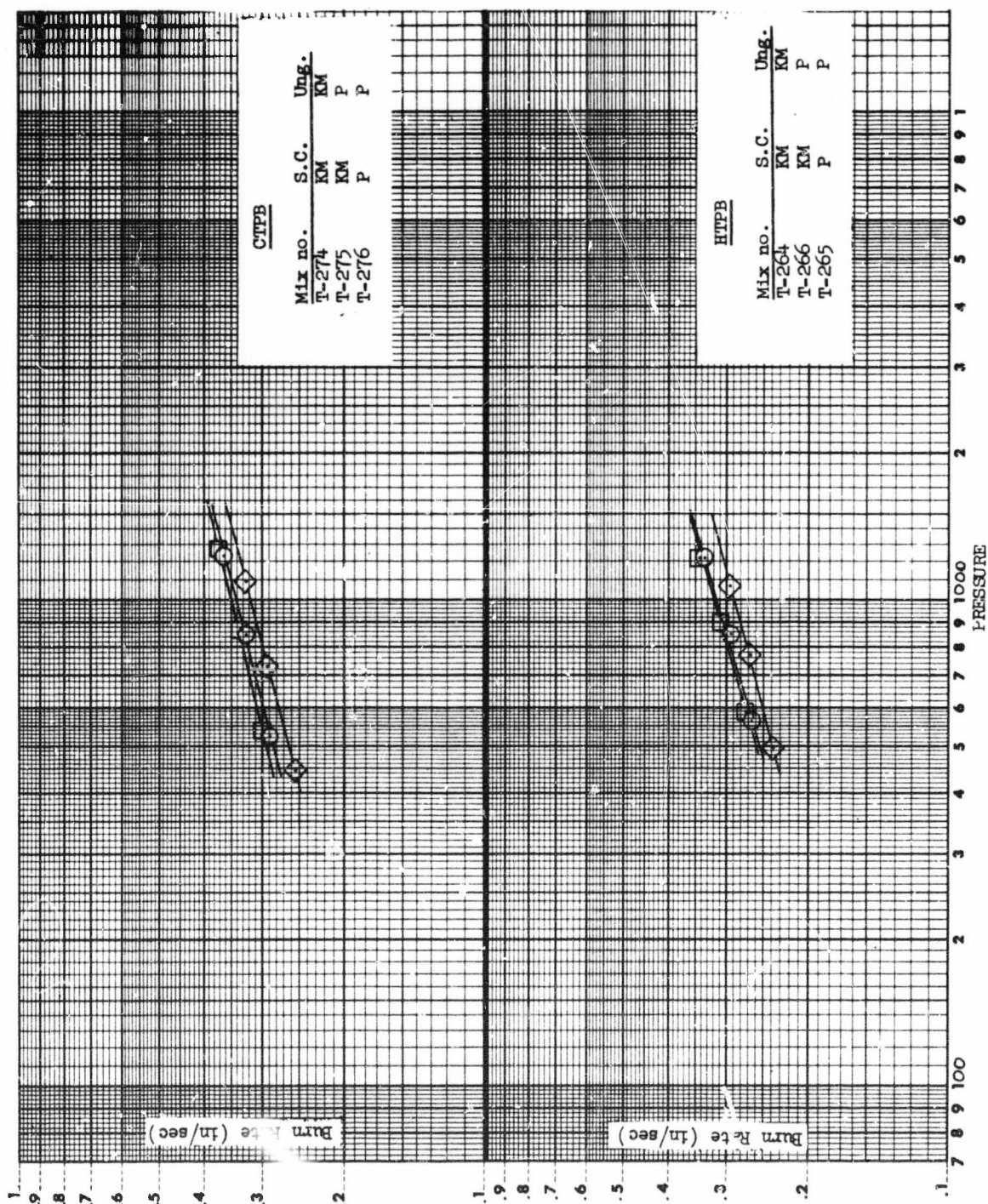


Figure 48. Burn Rate-Pressure Relationships for the Humidified Optimum Blends in CTPB and HTPB Propellants

TABLE 26

EFFECT OF HUMIDITY EXPOSURE ON BALLISTICSCTPB

| | | | | | |
|------------|-------------|-------|-------------|-------|-------------|
| Std. T-261 | .351 | T-267 | .356 | T-269 | .322 |
| RH T-264 | <u>.343</u> | T-266 | <u>.347</u> | T-265 | <u>.319</u> |
| | -2.3 % | | -2.5 % | | -0.9 % |

HTPB

| | | | | | |
|------------|-------------|-------|-------------|-------|-------------|
| Std. T-272 | .325 | T-285 | .316 | T-277 | .297 |
| RH T-274 | <u>.318</u> | T-275 | <u>.319</u> | T-276 | <u>.291</u> |
| | -2.2 % | | +6.9 % | | -1.0 % |

TABLE 27

TX-3 VS. STRANDS (Small Mix)
SELECTED OPTIMUM BLEND

| <u>CTPB</u> | | <u>HTPB</u> | |
|-------------|--------------|-----------------|-----------------|
| | Mix No. | | |
| | | $r_b @ 1000$ | $r_b @ 1000$ |
| | | in/sec | in/sec |
| K/K | Motor: T-261 | .351 | .325 |
| | Strand: | .302 | .280 |
| | | - 16.2 % | - 16.1 % |
| K/P | Motor: T-267 | .356 | .316 |
| | Strand: | .298 | .278 |
| | | - 19.5 % | - 13.7 % |
| P/P | Motor: T-269 | .322 | .297 |
| | Strand: | .305 | .279 |
| | | - 5.6 % | - 6.5 % |

TABLE 28

TX-3 VS. STRAND (5 Gal. Mix)

(r_b at 1000 psi)

| <u>CTPB</u> | | <u>HTPB</u> | |
|-------------|---------------|-------------|--------|
| K/K | Motor: T-261 | T-272 | .325 |
| | Strand: T-261 | T-272 | .301 |
| | | | -7.4% |
| K/P | Motor: T-267 | T-285 | .316 |
| | Strand: T-269 | T-285 | .309 |
| | | | -2.2 % |
| P/P | Motor: T-269 | T-277 | .297 |
| | Strand: T-269 | T-277 | .306 |
| | | | +3.6 % |

Mechanical Property Characterization

The optimum blends of Kerr-McGee, PEPCON, and mixtures of both have been incorporated in both CTPB and HTPB analogs of TP-H7036. Replicate five-gallon mixes were manufactured of the three optimum blends in CTPB. In addition, single CTPB mix was made with each optimum blend following exposure of each blend to 50% relative humidity for one week. The compositions of the selected optimum blends are shown below.

| <u>Composition</u> | <u>Kerr-McGee</u> | <u>PEPCON</u> | <u>Mixed Blend</u> |
|------------------------|-------------------|---------------|--------------------|
| Binder | 12.00 | 12.00 | 12.00 |
| KM (400 micron) | 21.10 | ----- | 19.70 |
| KM (200 micron) | 27.20 | ----- | ----- |
| P (400 micror) | ----- | 30.94 | ----- |
| P (200 micron) | ----- | 23.80 | 30.60 |
| Ground AP (Kerr-McGee) | 19.70 | 13.26 | 17.70 |
| Aluminum | 20.00 | 20.00 | 20.00 |

Following cure, mechanical properties were measured at temperatures ranging from 150°F down to -80°F. The tensile specimens were JANNAF Class A type. The mechanical properties* for the three optimum blends in CTPB are shown in Tables 29 through 31. The initial observation one gleans from these tables is that a satisfactory cure was not obtained. This is particularly true for the propellants exhibited in Tables 30 and 31. The result was initially surprising in that the same curing agent to polymer ratio utilized in production mixes was maintained throughout these mixes. In retrospect, it is possible, since the blends have been optimized for significantly lower viscosities, that a higher curing agent to polymer ratio would be required to achieve cure. A discussion of the experiments to be performed to elucidate the source of this soft cure are described in later sections. It is particularly interesting to note the excellent reproducibility in mechanical properties between the replicate mixes on Tables 29, 30 and 31.

The mechanical property data for those propellants manufactured from the optimum blends which had been exposed to humidity are shown in Tables 32 through 34. In comparing the data on Table 29 with 31, 30 with 33, and 31 with 34, one notes that the humidity exposure resulted in essentially no change in mechanical properties.

The mechanical property data for the HTPB analog of the same optimum blends are shown in Tables 35 through 40. The properties are judged to be excellent in all cases. As was the case with the CTPB propellants, excellent reproducibility between replicates is apparent and the lack of significant influence of moisture exposure upon the mechanical properties is likewise shown.

At least one set of tensile data at different strain rates (0.20 and 20.0 in/min.) was determined on at least one propellant formulation containing each optimum blend. These data were obtained in order that the time dependence of the propellant material properties be obtained. These data are exhibited in Tables 41 through 46.

*All mechanical property values corrected for change in cross section area of sample during elongation.

TABLE 29

MECHANICAL PROPERTIES

T-260 and T-261
 (Optimum Kerr-McGee Blend in CTPB)
 Strain Rate - 2.0 in/min

| | | <u>Modulus</u> <u>(psi)</u> | <u>Strain @ M.S.</u> <u>(in/in)</u> | <u>Ultimate Strain</u> <u>(in/in)</u> | <u>Max. Stress</u> <u>(psi)</u> |
|-------|-------|--------------------------------|--|--|------------------------------------|
| 150°F | T-260 | 381 | .286 | .301 | 75.6 |
| | T-261 | 365 | .275 | .290 | 69.1 |
| 100°F | T-260 | 525 | .276 | .293 | 87.4 |
| | T-261 | 507 | .268 | .282 | 81.2 |
| 77°F | T-260 | 751 | .267 | .308 | 101.5 |
| | T-261 | 708 | .264 | .290 | 93.2 |
| 40°F | T-260 | 1,314 | .259 | .307 | 127.2 |
| | T-261 | 1,269 | .258 | .291 | 116.9 |
| 0°F | T-260 | 2,520 | .255 | .326 | 166.1 |
| | T-261 | 2,240 | .252 | .321 | 155.5 |
| -40°F | T-260 | 10,578 | .266 | .416 | 297.9 |
| | T-261 | 10,209 | .225 | .400 | 283.3 |
| -70°F | T-260 | 25,141 | .074 | .209 | 611.6 |
| | T-261 | 21,876 | .078 | .228 | 598.3 |
| -80°F | T-260 | 26,877 | .064 | .099 | 758.7 |
| | T-261 | 27,166 | .067 | .115 | 759.2 |

TABLE 30
MECHANICAL PROPERTIES

T-269 and T-270
(Optimum PEPCON Blend in CTPB)
Strain Rate - 2.0 in/min

| | | <u>Modulus</u> <u>(psi)</u> | <u>Strain @ M.S.</u> <u>(in/in)</u> | <u>Ultimate Strain</u> <u>(in/in)</u> | <u>Max. Stress</u> <u>(psi)</u> |
|-------|-------|--------------------------------|--|--|------------------------------------|
| 150°F | T-269 | 202 | .281 | .317 | 40.1 |
| | T-270 | 185 | .286 | .321 | 38.2 |
| 100°F | T-269 | 270 | .271 | .316 | 45.4 |
| | T-270 | 256 | .270 | .318 | 45.1 |
| 77°F | T-269 | 410 | .255 | .324 | 55.0 |
| | T-270 | 397 | .263 | .326 | 55.6 |
| 40°F | T-269 | 829 | .233 | .311 | 72.5 |
| | T-270 | 771 | .236 | .300 | 71.8 |
| 0°F | T-269 | 1,462 | .219 | .325 | 99.6 |
| | T-270 | 1,553 | .214 | .328 | 99.7 |
| -40°F | T-269 | 7,507 | .160 | .338 | 205.9 |
| | T-270 | 7,596 | .152 | .333 | 207.1 |
| -70°F | T-269 | 16,437 | .083 | .384 | 457.9 |
| | T-270 | 16,423 | .089 | .368 | 412.1 |
| -80°F | T-269 | 22,195 | .073 | .141 | 666.5 |
| | T-270 | 24,955 | .071 | .148 | 665.6 |

TABLE 31

MECHANICAL PROPERTIES

T-267 and T-268
 (Optimum KM/PEPCON Blend in CTPB)
 Strain Rate - 2.0 in/min

| | | <u>Modulus</u> <u>(psi)</u> | <u>Strain @ M.S.</u> <u>(in/in)</u> | <u>Ultimate Strain</u> <u>(in/in)</u> | <u>Max. Stress</u> <u>(psi)</u> |
|-------|-------|--------------------------------|--|--|------------------------------------|
| 150°F | T-267 | 212 | .284 | .328 | 40.6 |
| | T-268 | 170 | .302 | .357 | 38.5 |
| 100°F | T-267 | 283 | .273 | .315 | 47.6 |
| | T-268 | 237 | .282 | .333 | 46.3 |
| 77°F | T-267 | 417 | .255 | .316 | 57.2 |
| | T-268 | 367 | .265 | .328 | 57.7 |
| 40°F | T-267 | 835 | .245 | .329 | 75.3 |
| | T-268 | 763 | .250 | .321 | 73.2 |
| 0°F | T-267 | 1,795 | .211 | .319 | 103.8 |
| | T-268 | 1,593 | .210 | .340 | 103.1 |
| -40°F | T-267 | 8,002 | .132 | .356 | 222.3 |
| | T-268 | 8,320 | .156 | .372 | 212.5 |
| -70°F | T-267 | 18,927 | .075 | .366 | 505.6 |
| | T-268 | 17,349 | .076 | .363 | 489.5 |
| -80°F | T-267 | 24,384 | .072 | .126 | 710.0 |
| | T-268 | 23,804 | .074 | .148 | 703.8 |

TABLE 32

MECHANICAL PROPERTIES

T-264
(Optimum Kerr-McGee Blend in CTPB)
Blend Exposed to 50% R.H. for One Week
Strain Rate - 2.0 in/min

| | | <u>Modulus</u> <u>(psi)</u> | <u>Strain @ M.S.</u> <u>(in/in)</u> | <u>Ultimate Strain</u> <u>(in/in)</u> | <u>Max. Stress</u> <u>(psi)</u> |
|-------|-------|--------------------------------|--|--|------------------------------------|
| 150°F | T-264 | 352 | .275 | .288 | 66.1 |
| 100°F | T-264 | 481 | .281 | .302 | 78.0 |
| 77°F | T-264 | 742 | .266 | .306 | 91.2 |
| 40°F | T-264 | 1,247 | .248 | .288 | 112.3 |
| 0°F | T-264 | 2,682 | .232 | .297 | 148.4 |
| -40°F | T-264 | 9,107 | .234 | .390 | 265.6 |
| -70°F | T-264 | 24,499 | .066 | .246 | 573.2 |
| -80°F | T-264 | 25,288 | .063 | .117 | 761.8 |

TABLE 33

MECHANICAL PROPERTIES

T-265
(Optimum PEPCON Blend in CTPB)
Blend Exposed to 50% R.H. for One Week
Strain Rate - 2.0 in/min

| | | <u>Modulus</u> <u>(psi)</u> | <u>Strain @ M.S.</u> <u>(in/in)</u> | <u>Ultimate Strain</u> <u>(in/in)</u> | <u>Max. Stress</u> <u>(psi)</u> |
|-------|-------|--------------------------------|--|--|------------------------------------|
| 150°F | T-265 | 173 | .294 | .324 | 36.8 |
| 100°F | T-265 | 250 | .285 | .344 | 42.5 |
| 77°F | T-265 | 386 | .269 | .352 | 51.1 |
| 40°F | T-265 | 737 | .243 | .333 | 66.4 |
| 0°F | T-265 | 1,559 | .225 | .357 | 96.0 |
| -40°F | T-265 | 6,828 | .136 | .402 | 202.8 |
| -70°F | T-265 | 19,601 | .073 | .365 | 489.1 |
| -80°F | T-265 | 21,139 | .072 | .149 | 664.5 |

TABLE 34

MECHANICAL PROPERTIES

T-266
(Optimum KM/PEPCON Blend in CTPB)
Blend Exposed to 50% R.H. for One Week
Strain Rate - 2.0 in/min

| | | <u>Modulus</u> <u>(psi)</u> | <u>Strain @ M.S.</u> <u>(in/in)</u> | <u>Ultimate Strain</u> <u>(in/in)</u> | <u>Max. Stress</u> <u>(psi)</u> |
|-------|-------|--------------------------------|--|--|------------------------------------|
| 150°F | T-266 | 181 | .297 | .330 | 37.0 |
| 100°F | T-266 | 252 | .280 | .334 | 42.8 |
| 77°F | T-266 | 394 | .264 | .338 | 52.5 |
| 40°F | T-266 | 646 | .237 | .331 | 69.2 |
| 0°F | T-266 | 1,850 | .198 | .325 | 98.0 |
| -40°F | T-266 | 8,462 | .117 | .361 | 218.6 |
| -70°F | T-266 | 18,172 | .069 | .373 | 494.6 |
| -80°F | T-266 | 22,643 | .071 | .145 | 690.1 |

TABLE 35

MECHANICAL PROPERTIES

T-271 and T-272
 (Optimum Kerr-McGee Blend in HTPB)
 Strain Rate - 2.0 in/min

| | | Modulus (psi) | Strain @ M.S. (in/in) | Ultimate Strain (in/in) | Max. Stress (psi) |
|-------|-------|------------------|--------------------------|----------------------------|----------------------|
| 150°F | T-271 | 448 | .419 | .443 | 110.9 |
| | T-272 | 480 | .423 | .436 | 122.8 |
| 100°F | T-271 | 618 | .453 | .477 | 126.5 |
| | T-272 | 722 | .448 | .466 | 141.4 |
| 77°F | T-271 | 1,150 | .421 | .443 | 147.9 |
| | T-272 | 1,187 | .459 | .477 | 169.7 |
| 40°F | T-271 | 2,343 | .463 | .493 | 192.5 |
| | T-272 | 2,518 | .484 | .521 | 213.3 |
| 0°F | T-271 | 5,743 | .521 | .593 | 281.5 |
| | T-272 | 4,817 | .524 | .568 | 299.9 |
| -40°F | T-271 | 16,266 | .363 | .403 | 552.5 |
| | T-272 | 15,195 | .315 | .362 | 520.1 |
| -70°F | T-271 | 29,616 | .070 | .100 | 801.3 |
| | T-272 | 25,127 | .078 | .113 | 788.5 |
| -80°F | T-271 | 40,205 | .051 | .062 | 918.5 |
| | T-272 | 41,859 | .048 | .060 | 894.6 |

TABLE 36

MECHANICAL PROPERTIES

T-273 and T-277
(Optimum PEPCON Blend in HTPB)
Strain Rate - 2.0 in/min

| | | <u>Modulus (psi)</u> | <u>Strain @ M.S. (in/in)</u> | <u>Ultimate Strain (in/in)</u> | <u>Max. Stress (psi)</u> |
|-------|-------|--------------------------|----------------------------------|------------------------------------|------------------------------|
| 150°F | T-273 | 472 | .409 | .419 | 108.8 |
| | T-277 | 434 | .430 | .443 | 109.6 |
| 100°F | T-273 | 706 | .444 | .460 | 130.1 |
| | T-277 | 661 | .445 | .461 | 125.8 |
| 77°F | T-273 | 1,218 | .436 | .451 | 153.4 |
| | T-277 | 1,166 | .474 | .499 | 153.3 |
| 40°F | T-273 | 2,449 | .489 | .512 | 200.8 |
| | T-277 | 2,417 | .498 | .528 | 197.6 |
| 0°F | T-273 | 5,463 | .518 | .555 | 286.3 |
| | T-277 | 6,423 | .509 | .535 | 310.4 |
| -40°F | T-273 | 16,518 | .349 | .381 | 481.0 |
| | T-277 | 16,003 | .400 | .424 | 522.6 |
| -70°F | T-273 | 26,123 | .068 | .106 | 718.2 |
| | T-277 | 28,064 | .062 | .083 | 772.9 |
| -80°F | T-273 | 34,613 | .044 | .050 | 831.4 |
| | T-277 | 36,118 | .046 | .052 | 852.5 |

TABLE 37

MECHANICAL PROPERTIES

T-278 and T-285
 (Optimum KM/PEPCON Blend in HTPB)
 Strain Rate - 2.0 in/min

| | | <u>Modulus</u> <u>(psi)</u> | <u>Strain @ M.S.</u> <u>(in/in)</u> | <u>Ultimate Strain</u> <u>(in/in)</u> | <u>Max. Stress</u> <u>(psi)</u> |
|-------|-------|--------------------------------|--|--|------------------------------------|
| 150°F | T-278 | 436 | .427 | .440 | 109.4 |
| | T-285 | 419 | .453 | .468 | 105.3 |
| 100°F | T-278 | 665 | .482 | .502 | 128.9 |
| | T-285 | 604 | .500 | .524 | 123.1 |
| 77°F | T-278 | 1,311 | .497 | .522 | 175.2 |
| | T-285 | 1,240 | .492 | .511 | 149.0 |
| 40°F | T-278 | 2,653 | .501 | .536 | 196.5 |
| | T-285 | 2,530 | .535 | .571 | 196.5 |
| 0°F | T-278 | 6,798 | .521 | .551 | 320.1 |
| | T-285 | 7,405 | .566 | .523 | 324.0 |
| -40°F | T-278 | 17,760 | .407 | .428 | 540.1 |
| | T-285 | 17,078 | .448 | .477 | 548.4 |
| -70°F | T-278 | 28,427 | .061 | .084 | 795.3 |
| | T-285 | 27,911 | .059 | .074 | 803.5 |
| -80°F | T-278 | 39,040 | .046 | .055 | 895.9 |
| | T-285 | 41,184 | .046 | .052 | 870.0 |

TABLE 38

MECHANICAL PROPERTIES

T-274
(Optimum Kerr-McGee Blend in HTPB)
Blend Exposed to 50% R. H. for One Week
Strain Rate - 2.0 in/min

| | | <u>Modulus</u> <u>(psi)</u> | <u>Strain @ M. S.</u> <u>(in/in)</u> | <u>Ultimate Strain</u> <u>(in/in)</u> | <u>Max. Stress</u> <u>(psi)</u> |
|-------|-------|--------------------------------|---|--|------------------------------------|
| 150°F | T-274 | 538 | .426 | .448 | 121.61 |
| 100°F | T-274 | 761 | .432 | .452 | 139.9 |
| 77°F | T-274 | 1,385 | .435 | .460 | 164.7 |
| 40°F | T-274 | 2,597 | .475 | .514 | 214.5 |
| 0°F | T-274 | 5,979 | .493 | .544 | 308.0 |
| -40°F | T-274 | 16,528 | .378 | .421 | 511.9 |
| -70°F | T-274 | 29,947 | .062 | .088 | 813.6 |
| -80°F | T-274 | 45,320 | .044 | .050 | 924.3 |

TABLE 39

MECHANICAL PROPERTIES

T-276

(Optimum PEPCON Blend in HTPB)

Blend Exposed to 50% R.H. for One Week

Strain Rate - 2.0 in/min

| | | Modulus (psi) | Strain @ M.S. (in/in) | Ultimate Strain (in/in) | Max. Stress (psi) |
|-------|-------|------------------|--------------------------|----------------------------|----------------------|
| 150°F | T-276 | 471 | .435 | .452 | 111.1 |
| 100°F | T-276 | 778 | .473 | .493 | 131.8 |
| 77°F | T-276 | 1,078 | .470 | .489 | 155.6 |
| 40°F | T-276 | 2,083 | .516 | .555 | 204.9 |
| 0°F | T-276 | 5,302 | .544 | .585 | 312.6 |
| -40°F | T-276 | 15,068 | .423 | .452 | 535.7 |
| -70°F | T-276 | 30,069 | .057 | .074 | 765.9 |
| -80°F | T-276 | 45,521 | .040 | .046 | 840.0 |

TABLE 40

MECHANICAL PROPERTIES

T-275
(Optimum KM/PEPCON Blend in HTPB)
Blend Exposed to 50% R.H. for One Week
Strain Rate - 2.0 in/min

| | | <u>Modulus</u> <u>(psi)</u> | <u>Strain @ M.S.</u> <u>(in/in)</u> | <u>Ultimate Strain</u> <u>(in/in)</u> | <u>Max. Stress</u> <u>(psi)</u> |
|-------|-------|--------------------------------|--|--|------------------------------------|
| 150°F | T-275 | 491 | .426 | .442 | 117.7 |
| 100°F | T-275 | 749 | .438 | .449 | 134.6 |
| 77°F | T-275 | 1,310 | .458 | .484 | 162.5 |
| 40°F | T-275 | 2,327 | .497 | .529 | 208.1 |
| 0°F | T-275 | 5,747 | .529 | .566 | 306.2 |
| -40°F | T-275 | 18,973 | .441 | .481 | 532.5 |
| -70°F | T-275 | 28,747 | .062 | .086 | 801.9 |
| -80°F | T-275 | 40,470 | .047 | .053 | 891.1 |

TABLE 41

MECHANICAL PROPERTIES

T-260

Strain Rate - 0.2 in/min & 20 in/min

| | | Modulus (psi) | Strain @ M.S. (in/in) | Ultimate Strain (in/in) | Max. Stress (psi) |
|-------|-----------|------------------|--------------------------|----------------------------|----------------------|
| 150°F | .2 in/min | 294 | .287 | .296 | 61.4 |
| | 20 in/min | 498 | .270 | .286 | 93.2 |
| 100°F | 20 in/min | 732 | .276 | .304 | 103.7 |
| 77°F | .2 in/min | 452 | .266 | .287 | 80.6 |
| | 20 in/min | 1,080 | .245 | .286 | 110.4 |
| 40°F | 20 in/min | 1,587 | .241 | .298 | 149.2 |
| 0°F | .2 in/min | 1,537 | .262 | .295 | 132.7 |
| | 20 in/min | 2,617 | .215 | .310 | 240.1 |
| -40°F | 20 in/min | 5,386 | .285 | .392 | 447.9 |
| -80°F | .2 in/min | 13,667 | .299 | .387 | 441.8 |

TABLE 42

MECHANICAL PROPERTIES

T-268

Strain Rate - 0.2 in/min & 20 in/min

| | | <u>Modulus</u> <u>(psi)</u> | <u>Strain @ M.S.</u> <u>(in/in)</u> | <u>Ultimate Strain</u> <u>(in/in)</u> | <u>Max. Stress</u> <u>(psi)</u> |
|-------|-----------|--------------------------------|--|--|------------------------------------|
| 150°F | .2 in/min | 124 | .323 | .344 | 30.6 |
| | 20 in/min | 243 | .298 | .354 | 50.1 |
| 100°F | 20 in/min | 390 | .275 | .359 | 61.3 |
| 77°F | .2 in/min | 212 | .269 | .304 | 42.3 |
| | 20 in/min | 720 | .235 | .331 | 72.5 |
| 40°F | 20 in/min | 1,304 | .218 | .317 | 105.3 |
| 0°F | .2 in/min | 827 | .244 | .332 | 76.7 |
| | 20 in/min | 2,355 | .179 | .327 | 181.6 |
| -40°F | 20 in/min | 5,231 | .134 | .416 | 347.9 |
| -80°F | .2 in/min | 13,667 | .297 | .387 | 441.8 |

TABLE 43MECHANICAL PROPERTIES

T-270

Strain Rate - 0.2 in/min & 20 in/min

| | | <u>Modulus</u> <u>(psi)</u> | <u>Strain @ M.S.</u> <u>(in/in)</u> | <u>Ultimate Strain</u> <u>(in/in)</u> | <u>Max. Stress</u> <u>(psi)</u> |
|-------|-----------|--------------------------------|--|--|------------------------------------|
| 150°F | .2 in/min | 133 | .299 | .320 | 29.2 |
| | 20 in/min | 267 | .276 | .324 | 48.4 |
| 100°F | 20 in/min | 387 | .275 | .338 | 60.2 |
| 77°F | .2 in/min | 222 | .264 | .311 | 42.2 |
| | 20 in/min | 796 | .242 | .334 | 70.7 |
| 40°F | 20 in/min | 1,191 | .222 | .330 | 99.5 |
| 0°F | .2 in/min | 852 | .245 | .300 | 75.5 |
| | 20 in/min | 2,209 | .170 | .334 | 171.6 |
| -40°F | 20 in/min | 5,124 | .137 | .415 | 340.9 |
| -80°F | .2 in/min | 14,336 | .279 | .328 | 419.0 |

TABLE 44

MECHANICAL PROPERTIES

T-271

Strain Rate - 0.2 in/min & 20 in/min

| | | <u>Modulus</u> <u>(psi)</u> | <u>Strain @ M.S.</u> <u>(in/in)</u> | <u>Ultimate Strain</u> <u>(in/in)</u> | <u>Max. Stress</u> <u>(psi)</u> |
|-------|-----------|--------------------------------|--|--|------------------------------------|
| 150°F | .2 in/min | 478 | .350 | .355 | 90.7 |
| | 20 in/min | 663 | .431 | .460 | 126.7 |
| 100°F | 20 in/min | 949 | .422 | .439 | 135.7 |
| 77°F | .2 in/min | 598 | .430 | .448 | 125.9 |
| | 20 in/min | 1,020 | .461 | .507 | 149.7 |
| 40°F | 20 in/min | 1,790 | .497 | .592 | 208.7 |
| 0°F | .2 in/min | 3,301 | .456 | .490 | 223.0 |
| | 20 in/min | 2,855 | .502 | .555 | 445.7 |
| -40°F | 20 in/min | 10,183 | .153 | .206 | 755.5 |
| -80°F | .2 in/min | 22,467 | .088 | .108 | 760.1 |

TABLE 45

MECHANICAL PROPERTIES

T-273

Strain Rate - 0.2 in/min & 20 in/min

| | | Modulus (psi) | Strain @ M.S. (in/in) | Ultimate Strain (in/in) | Max. Stress (psi) |
|-------|-----------|------------------|--------------------------|----------------------------|----------------------|
| 150°F | .2 in/min | 351 | .395 | .405 | 91.5 |
| | 20 in/min | 799 | .473 | .488 | 129.7 |
| 100°F | 20 in/min | 925 | .452 | .467 | 137.6 |
| 77°F | .2 in/min | 662 | .439 | .451 | 127.8 |
| | 20 in/min | 1,045 | .480 | .510 | 147.0 |
| 40°F | 20 in/min | 1,827 | .490 | .530 | 197.0 |
| 0°F | .2 in/min | 3,047 | .470 | .497 | 227.3 |
| | 20 in/min | 2,779 | .508 | .508 | 450.8 |
| -40°F | 20 in/min | 10,954 | .125 | .179 | 696.7 |
| -80°F | .2 in/min | 29,093 | .068 | .085 | 705.7 |

TABLE 46

MECHANICAL PROPERTIES

T-278

Strain Rate - 0.2 in/min & 20 in/min

| | | <u>Modulus</u> <u>(psi)</u> | <u>Strain @ M.S.</u> <u>(in/in)</u> | <u>Ultimate Strain</u> <u>(in/in)</u> | <u>Max. Stress</u> <u>(psi)</u> |
|-------|-----------|--------------------------------|--|--|------------------------------------|
| 150°F | .2 in/min | 434 | .316 | .326 | 87.6 |
| | 20 in/min | 644 | .474 | .490 | 127.2 |
| 100°F | 20 in/min | 954 | .465 | .492 | 133.8 |
| 77°F | .2 in/min | 595 | .446 | .459 | 124.5 |
| | 20 in/min | 1,132 | .500 | .550 | 146.9 |
| 40°F | 20 in/min | 2,078 | .514 | .598 | 192.3 |
| 0°F | .2 in/min | 2,803 | .487 | .506 | 227.4 |
| | 20 in/min | 2,773 | .552 | .601 | 460.0 |
| -40°F | 20 in/min | 11,245 | .153 | .215 | 732.8 |
| -80°F | .2 in/min | 28,643 | .077 | .089 | 764.2 |

Additional mechanical property data has been collected on the optimum Kerr McGee and PEPCON blends in both CTPB and HTPB binders. The failure boundaries constructed from the uniaxial data for each mix are shown in Figures 49 - 66.

The failure boundaries for the CTPB propellants tested are shown in Figures 49 - 57. The first feature of these failure boundaries which is immediately apparent is that their shape is different from that of the typical propellant failure boundary. Their shape is typical of the shapes of failure boundaries of under-cured propellant as would be expected from the very low modulus and stress levels obtained after cure of these mixes. What is not so readily apparent is that the failure boundaries shown for example in Figure 49 (Kerr McGee AP) and Figure 51 (PEPCON AP) are really quite similar. The only difference is that in the four to six hundred psi region a bulge exists in the Kerr McGee failure boundary that is not present in the PEPCON failure boundary. This region in which the transition from stress failures (at the upper portion of the failure boundary) and strain failures (at the right hand portion of the failure boundary) is occurring is a typical region of instability in propellant failure behavior and relatively small differences in formulation can result in apparently large differences in the failure boundary. It should be pointed out that these failure boundaries consist of plots of maximum stress versus strain at maximum stress. These are the parameters which are plotted when the failure boundary is used to represent propellant allowable stress conditions for rocket motor grain structural analysis. However, if stress at break had been plotted against strain at break for these propellants the failure boundaries would have had much more typical shapes. Failure strain for these propellants is considerably higher than strain at maximum stress. Again this condition is typical of the behavior of soft undercured propellants. This is also responsible for the relatively large scatter seen in many of these failure boundaries. Since soft propellants tend to have very long flat stress/strain curves, very minor changes in specimen treatment or conditioning can result in large changes in strain at maximum stress and hence a considerable spread along the X axis of the failure boundary. Figures 49 and 50 represent the failure boundaries of replicate propellants as do Figures 51, 52, 53, and 54. There is no significant difference in the shape of these pairs of failure boundaries indicating good mix to mix reproducibility. It is interesting to note on Figure 52 the failure points which lie at approximately 500 psi and 25 to 30% strain. These test results lie in the instability region and indicate how close mix T-270 was to exhibiting the type of bulge in this region which appears on the Kerr McGee failure boundaries. Again, if strain at break had been plotted instead of strain at maximum stress the failure boundary shape would have been more typical and these points would not have been outliers. Figures 55, 56, and 57 represent the failure boundaries obtained from Kerr McGee, PEPCON, and mixed AP propellants for which the ammonium perchlorate had been subjected to 50% relative humidity storage. The fact that this treatment of the oxidizer did not result in significant changes in the shape of the failure boundary is a further indication that the propellants shown in Figures 49 - 54 had been subjected to too high a level of relative humidity.

Figures 58 - 66 represent the failure boundaries obtained for Kerr McGee, PEPCON and mixed AP in HTPB propellant. It is immediately obvious that the shapes of these failure boundaries are much more typical than were obtained with CTPB propellant. The boundaries also show the excellent physical property potential offered by HTPB binders with very high strain capabilities being exhibited including strain endurance capabilities in the 34-36% range. Some outlying data is observed, particularly in Figures 58 and 62, but generally the data are reasonably well grouped and no large scatter is observed. Adverse moisture exposure during propellant mixing has obviously not effected the HTPB propellants at the same extent as it did the CTPB propellants, despite the fact that isocyanates used to cure HTPB are known to be quite moisture sensitive. Presumably, the reason for this is that the effect of moisture on HTPB would not be autocatalytic as is the case with moisture degradation of the FN bond in the CTPB propellants. Exposure of the AP used in these propellants to 50% relative humidity had in fact very little if any adverse effect on the physical properties. There is some slight reduction in the absolute strain level attainable in the case of the Kerr McGee blend and the slight decrease in strain endurance capability for both the Kerr McGee and PEPCON AP, but otherwise no adverse effects of moisture are apparent.

Data obtained from testing biaxial rail specimens on each propellant are shown in Table 47. Comparison of uniaxial and biaxial failure behavior can be obtained by plotting the biaxial data from Table 47 on the uniaxial failure boundary. Such has been done on Figures 67 - 77. In most cases, the biaxial data falls quite close to the uniaxial failure boundary indicating that the propellant fails by the same mechanism, maximum principal stress. More variance occurs between biaxial and uniaxial data in the softly cured CTPB propellants.

A comparison of biaxial versus uniaxial failure behavior permits deductions to be drawn regarding failure criterion applicable to propellant being investigated. In the case of the various ammonium perchlorate blends in CTPB propellant, however, any conclusions must be prefaced by the remark that the abnormal softness of the propellants and the consequent abnormal shapes of the failure boundaries render such conclusions tentative at best. Figures 67 - 77 show comparisons of biaxial with uniaxial data. The lines on these figures are the uniaxial failure boundaries. No uniaxial failure points as such are shown - only the biaxial failure points are shown for clarity.

Previous experiments with a wide variety of different propellants has shown that in a state of combined stress, such as biaxial tension, propellants may obey one of two different stress failure criteria - maximum principal stress or the sum of the principal stresses. In any case, all propellants tested in the past have shown failure behavior consistent with the maximum principal strain failure criteria. When a comparison of biaxial and uniaxial failure data is made on the failure boundary, these failure criteria manifest themselves as follows:

If the maximum principal stress theory applies, the biaxial data fall on the uniaxial failure boundary. The reason for this is that in the case of uniaxial tests, the maximum principal stress is the only stress present on the specimen. If the maximum principal stress theory applies, and only the maximum principal stress from the biaxial specimen (neglecting the induced stress along the width of the specimen which is one-half the magnitude of the applied stress) is plotted and in both cases the maximum principal strain is plotted, then the failure points will coincide.

If the sum of the principal stresses is the correct stress theory for failure, the uniaxial failure boundary is not changed (since, again, the maximum principal stress is the only stress present) but the biaxial failure data fall below the uniaxial failure boundary because more than one stress is present in the biaxial specimen and the second stress is not being taken into account. In this case, if the second stress is added to the maximum principal stress for the biaxial data, then the biaxial data will fall on the uniaxial failure boundary. In both cases, of course, the strain criterion would remain the same, maximum principal strain.

Taking the most straight-forward cases first, examination of figures 71, 72 and 73 (PEPCON AP, mixed AP, and PEPCON AP humidified, respectively) the uniaxial failure points clearly fall below the failure boundary. However, when the second (induced) stress is added to the maximum principal stress from the biaxial specimens, the new failure points agree very well with uniaxial failure boundaries. Clearly, in these cases, failure is occurring by the sum of the principal stresses. A mechanistic picture of what is happening here can be obtained if one realizes that this type of failure is characteristic of foams and unfilled sponge rubbers, whereas maximum principal stress failure is characteristic of gum rubbers containing no voids and containing either low amounts of filler or no filler at all. The mechanical picture for propellants which exhibit the type of behavior seen in Figures 71, 72 and 73 is that failure occurs by formation of voids around perchlorate particles, and propagation and interconnection of these voids to form cracks which eventually result in catastrophic failure of the specimen. Propellants which exhibit maximum principal stress failure, on the other hand, presumably experience failure in the binder itself before a large degree of void formation has taken place.

Figures 70 and 73 show a comparison of biaxial versus uniaxial failure behavior for Kerr McGee and humidified Kerr McGee oxidizer in CTPB. Here, the results are not as clear. The uniaxial failure points clearly seem to fall below the failure boundary, but when they are converted for the sum of the principal stresses, the degree of agreement between biaxial and uniaxial data seems only marginally improved. Closer examination of these figures will show that this is due to the "bulge" in the instability region of the failure boundary. If these curves had not exhibited that bulge but had instead exhibited shapes similar to those obtained with the PEPCON AP, the biaxial data plotted by the summed principal stress theory would agree much more closely with such a curve than did the uncorrected biaxial data. The biaxial stress field appears to be sufficient to remove the "bulge" from the failure boundary.

The one comparison of biaxial versus uniaxial failure data for CTPB propellants which cannot be satisfactorily resolved, is Figure 75. This figure shows a comparison of biaxial versus uniaxial failure data for the Kerr McGee PEPCON blend of oxidizer which had been subjected to 50% RH. Here, the maximum principal stress from the biaxial failure data falls on the uniaxial failure boundary. Correction of the biaxial data for the sum of the principal stresses would result in a biaxial failure boundary which would lay above the uniaxial failure boundary. Since this propellant is the only one of the CTPB propellants examined in this study which clearly fails by the maximum principal stress theory of failure rather than by the sum of the principal stresses, the reason why this one propellant should behave differently from all of the others remains unknown.

Figures 73 through 77 show similar comparisons of biaxial failure data with uniaxial failure boundaries for the various ammonium perchlorate blends in HTPB propellant while biaxial failure points are occasionally found beneath the uniaxial failure boundary, in no case does addition of the induced stress (as required by the sum of the principal stresses failure criterion) materially improve biaxial and uniaxial agreement. In the case of the HTPB propellant, the data indicate that regardless of the AP blends used, failure is occurring by the maximum principal stress theory and the disagreements sometimes seen between biaxial and uniaxial data are due to strain scatter which results from a combination of short special plastic strain gages which must be used for biaxial strain measurements and the high propellant strains exhibited by the HTPB propellants. Evidence for this can be seen in Figure 75 where most of the biaxial failure points lie outside and to the right of the uniaxial failure boundary. Failure by the maximum principal stress theory in HTPB propellant is consistent with what is believed to be known regarding the role of bonding agents in these propellants; that is, an oxidizer-binder bond is promoted which is sufficiently strong that failure takes place in the binder itself rather than by being initiated by a void formation around the perchlorate particles.

Cumulative damage test data obtained for each propellant are listed in Tables 48 through 59. The purpose of these tests was to determine whether the failure boundaries obtained for these propellants exhibited path dependence. The mechanism whereby the path dependency was tested was to interrupt a constant-strain-rate test roughly mid-way through the test and change the rate to a new strain rate at which the specimen was then taken to failure. Briefly, the results indicate no degree of path dependence for the propellants tested. Comparison of the data obtained at failure, when the strain rates were changed in the cumulative damage test, indicate that within the usual data scatter these failure points agreed with the failure boundary generated from simple constant strain rate tests. These results are not surprising in light of data currently being generated on other HTPB propellants at the Huntsville Division.

It should be pointed out that the failure boundary is not the only viable method of interpretation of cumulative damage data, however. The tests reported here are consistent with tests currently being conducted in that at the stress critical region of the failure boundary (that is at the top of the failure boundary for high strain rates or low temperatures) cumulative damage test data can adequately be interpreted by a stress cumulative damage theory of failure. In the strain-critical region of the failure boundary (below the instability point at lower strain rates or higher temperatures) the results can be interpreted satisfactorily by a strain cumulative damage theory of failure. However, the strain cumulative damage theory of failure will not adequately account for the results in the stress-critical region and vice versa; therefore, if the cumulative damage theory is used, it is necessary to change the theory when one passes through the instability region of the failure boundary. It is our view that this is an unnecessary complication in view of the simplicity and adequacy of interpreting cumulative damage data in terms of the failure boundary itself; that is, over the regime of rate changes measured, the failure boundary itself adequately predicts where failure will occur in cumulative damage tests).

The relaxation modulus data for both the CTPB and HTPB propellants is shown in Figures 78-95. In the CTPB propellants, the equilibrium modulus is low and is ascribed to the poor cure obtained in these propellants. The constancy of the value indicates the rate of relaxation does not change from CTPB to HTPB propellant.

The thermal expansion data obtained in replicate on each of the optimum blends in each binder are plotted in Figures 96-101. Note the reproducibility of the glass transition temperature and the difference between that temperature for CTPB and HTPB propellants. The low values for the linear coefficient of thermal expansion for Mix T-268 are attributable to the difficulty of performing this experiment with undercured propellant.

FAILURE BOUNDARY

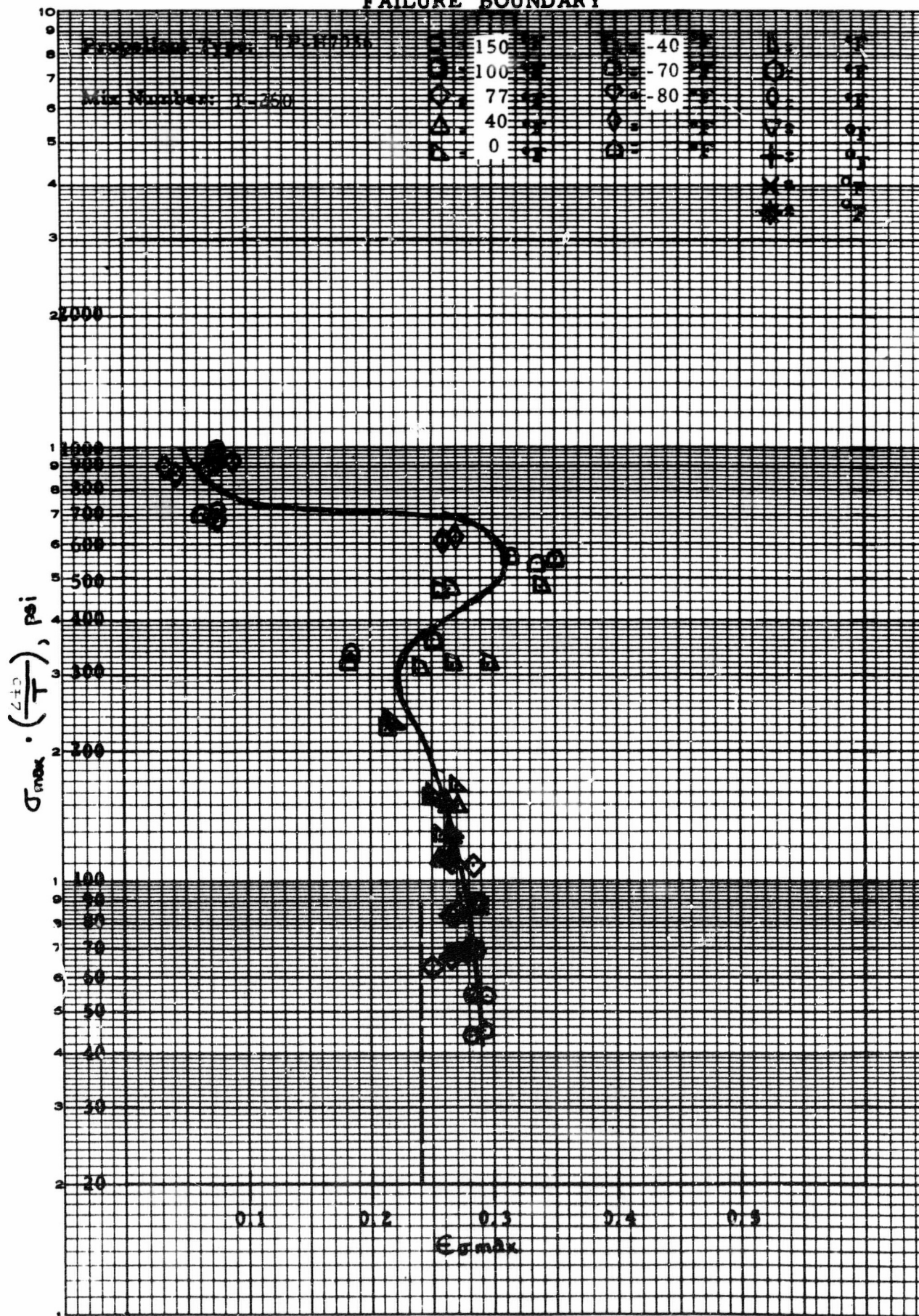


FIGURE 49. FAILURE BOUNDARY - T-260 - KM/KM in CTPB

FAILURE BOUNDARY

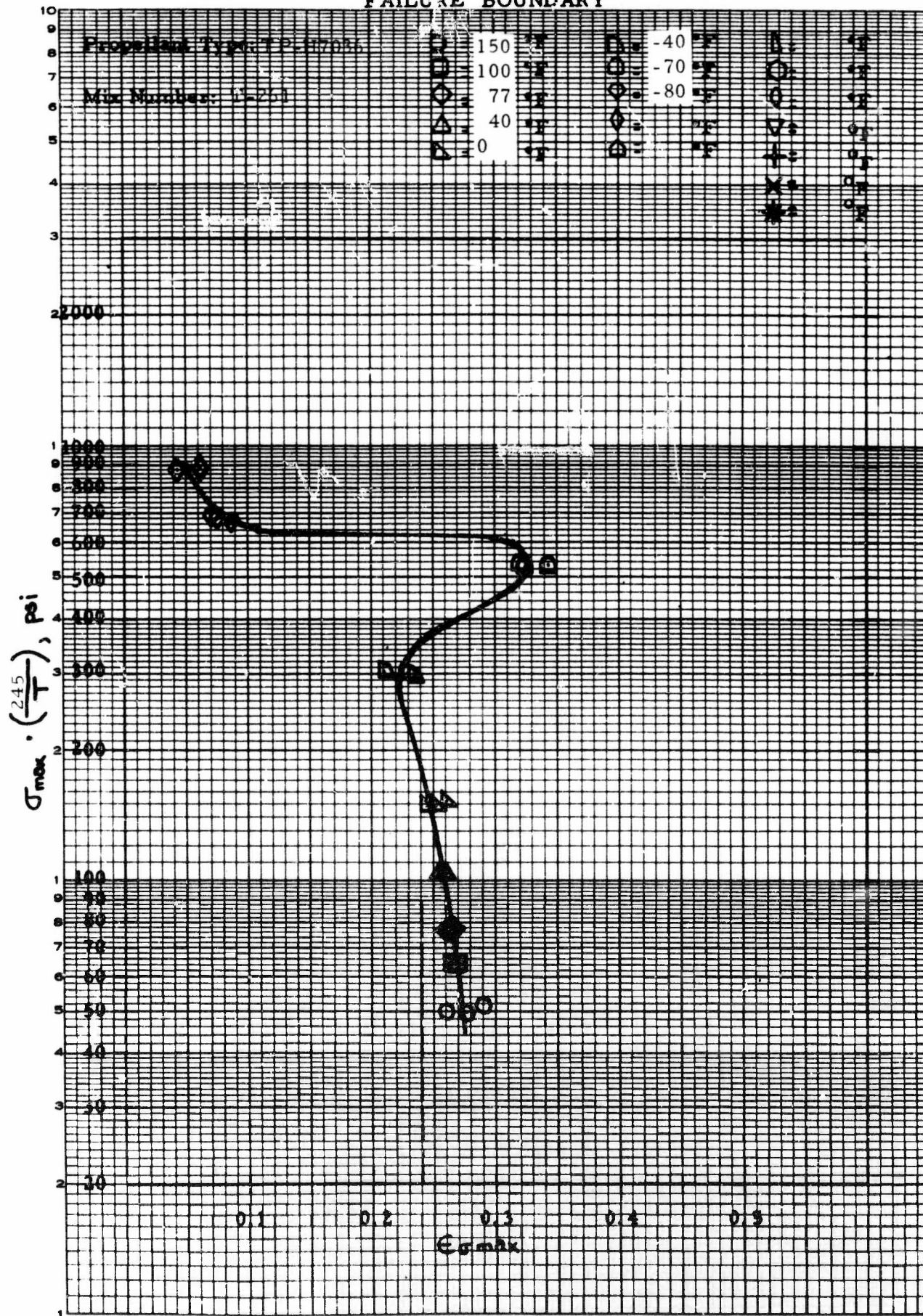


FIGURE 50. FAILURE BOUNDARY - T-261 - KM/KM in CTPB

FAILURE BOUNDARY

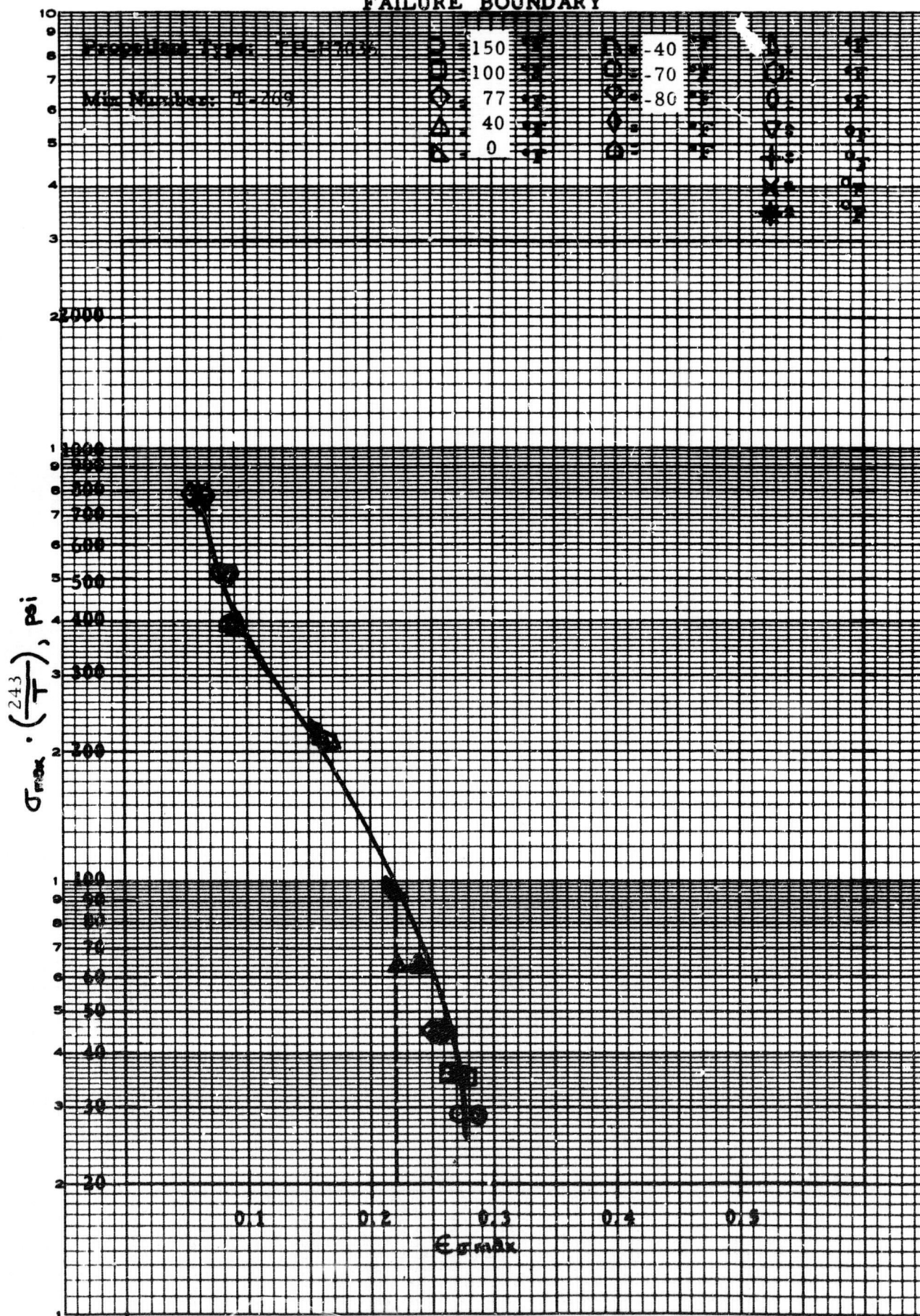


FIGURE 51. FAILURE BOUNDARY - T-269 - P/P in CTPB

FAILURE BOUNDARY

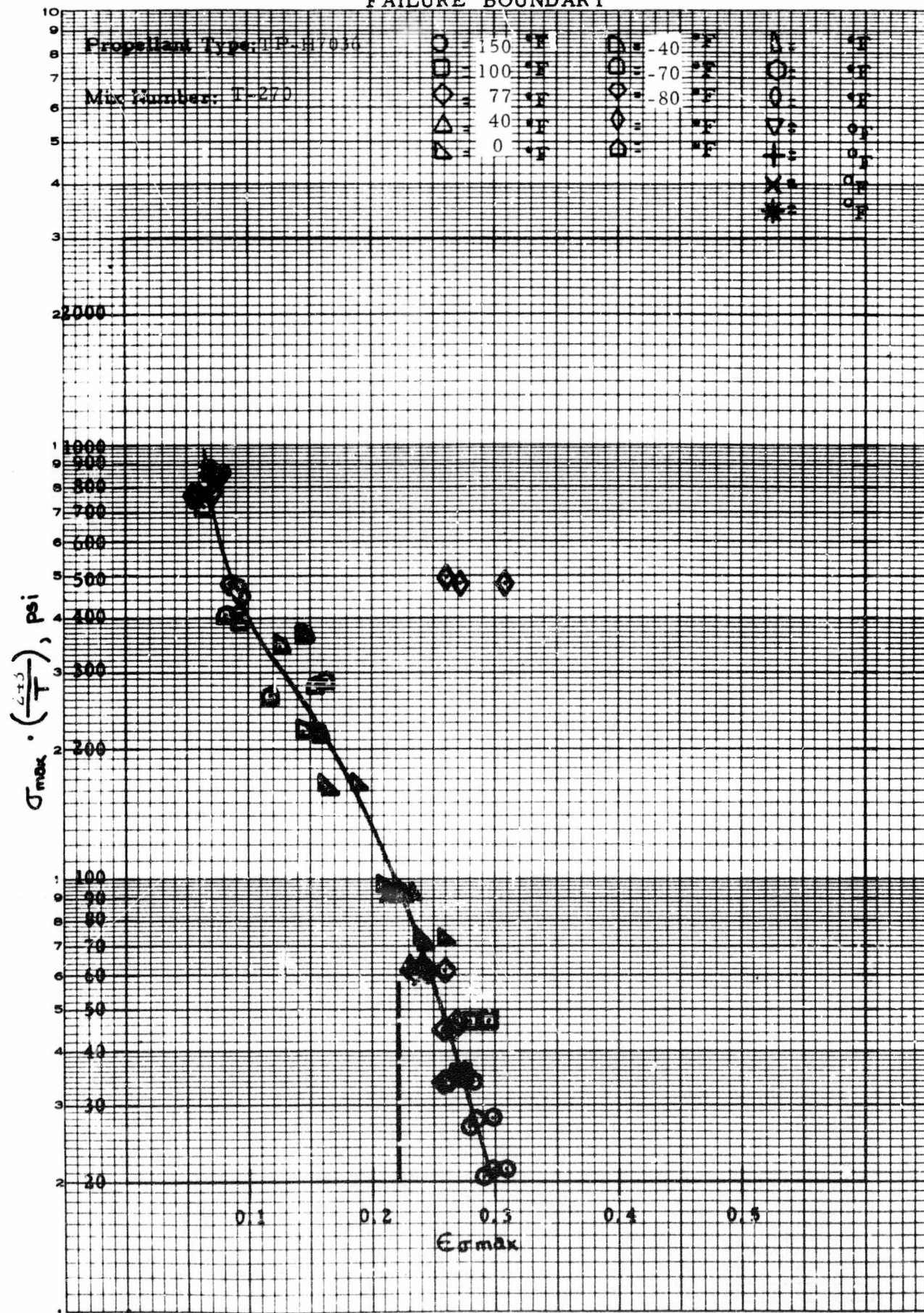


FIGURE 52. FAILURE BOUNDARY - T-270 - P/P in CTPB

FAILURE BOUNDARY

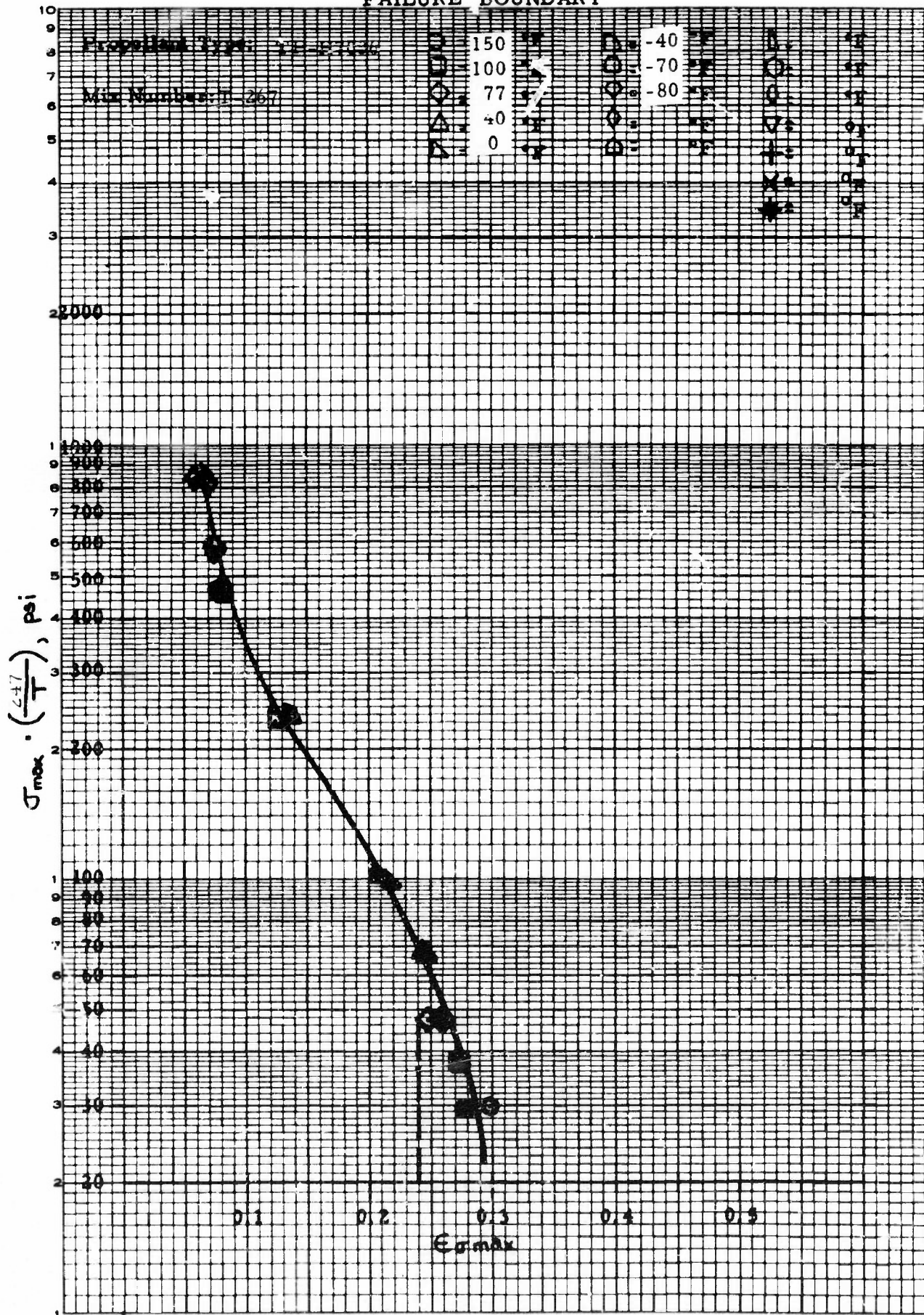


FIGURE 53. FAILURE BOUNDARY - T-267 - KM/P in CTPB

118

FAILURE BOUNDARY

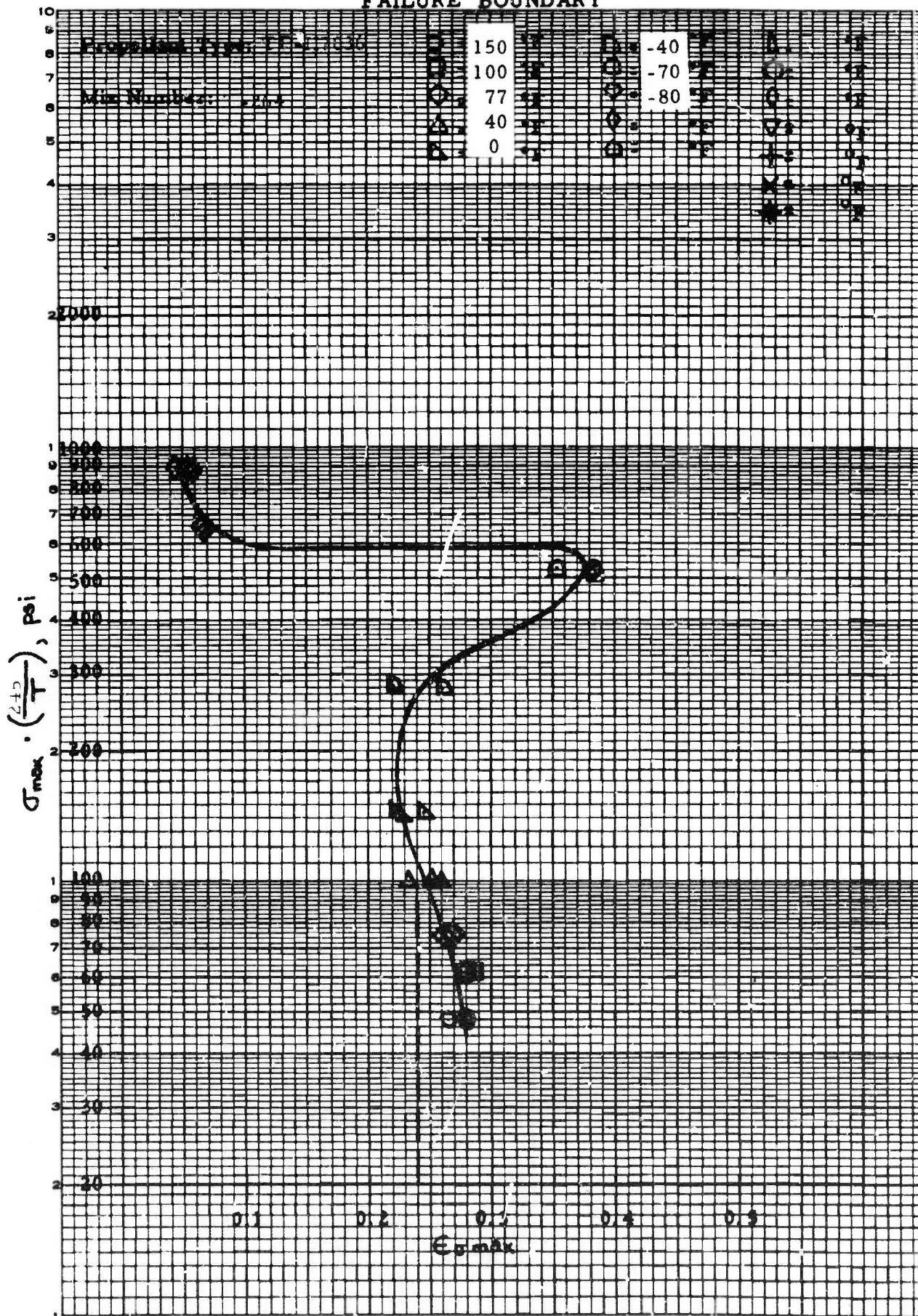


FIGURE 55. FAILURE BOUNDARY - T-264 - KM/KM in CTPB (humidified)

FAILURE BOUNDARY

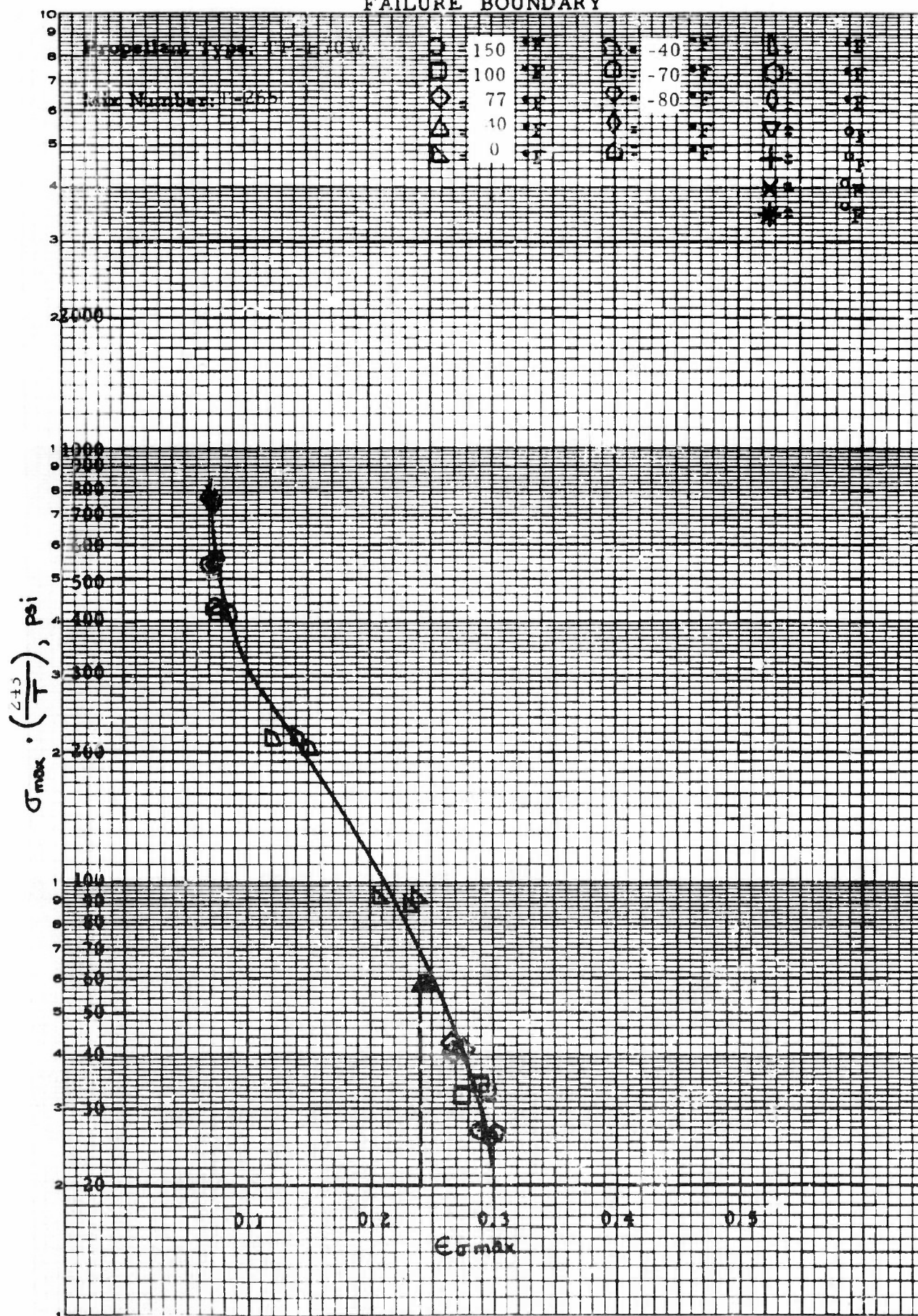


FIGURE 56. FAILURE BOUNDARY - T-265 - P/P in CTPB (humidified)

FAILURE BOUNDARY

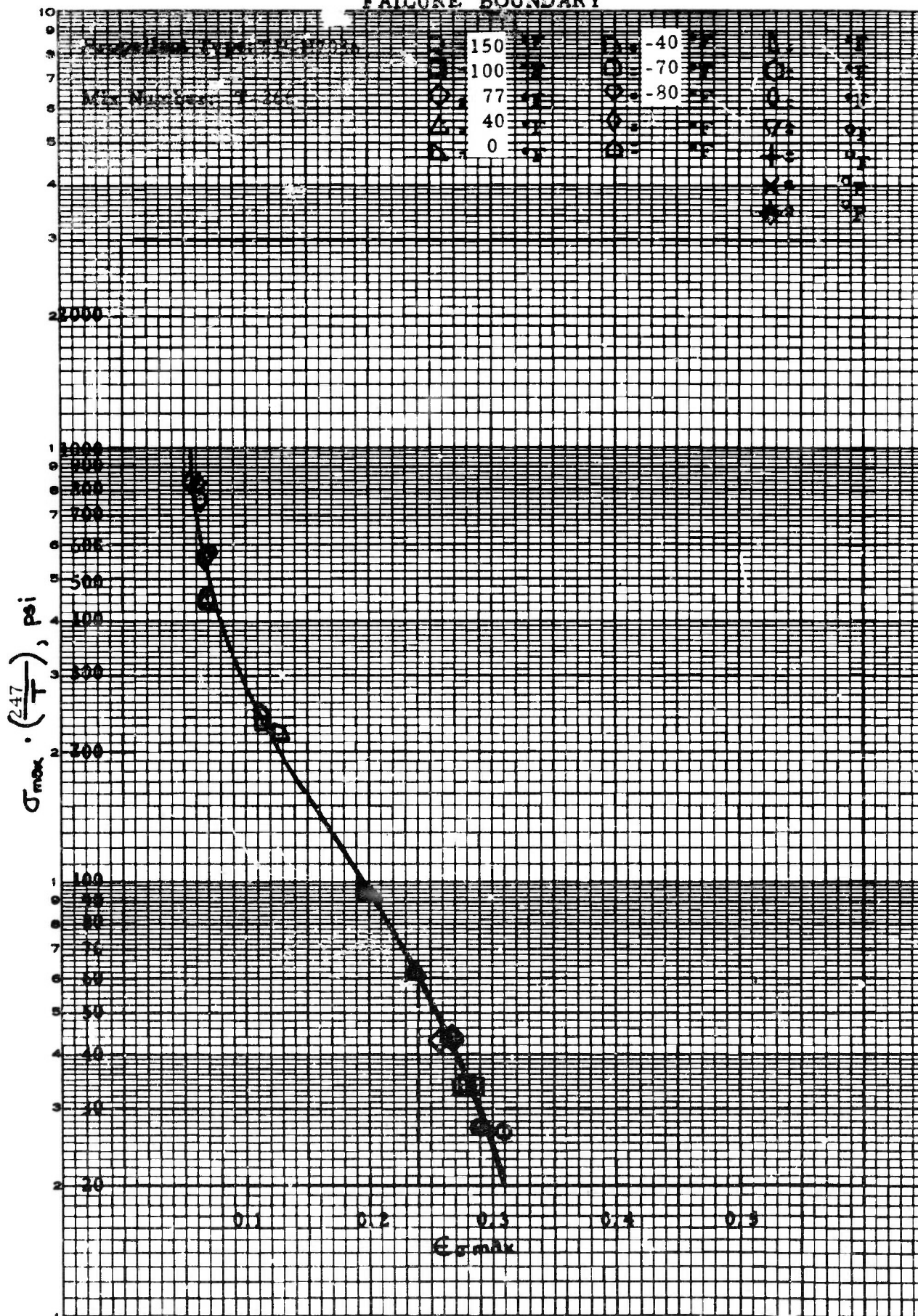


FIGURE 57. FAILURE BOUNDARY - T-266 . KM/P in CTPB (humidified)

FAILURE BOUNDARY

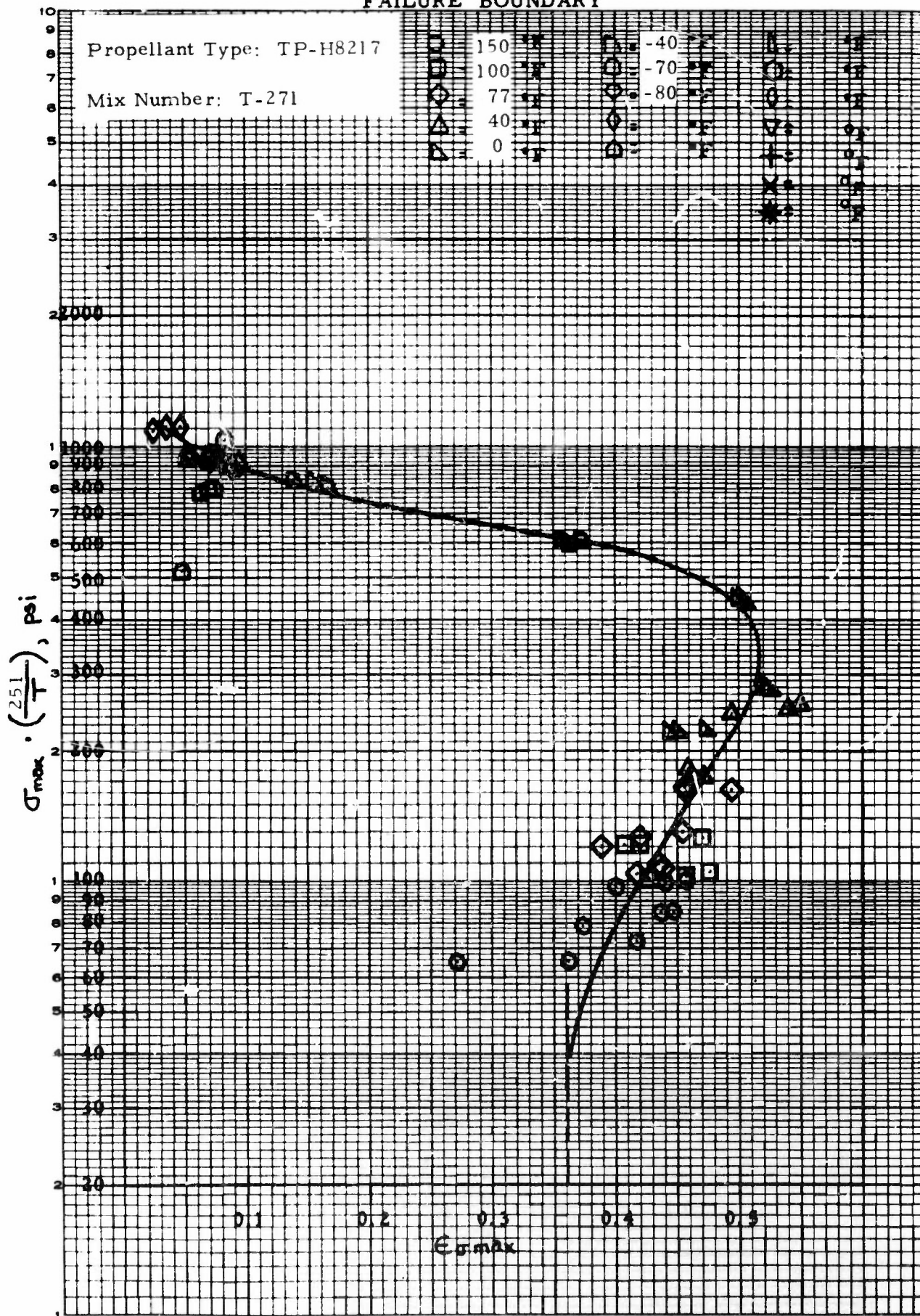


FIGURE 58. FAILURE BOUNDARY - T-271 - KM/KM in HTPB

FAILURE BOUNDARY

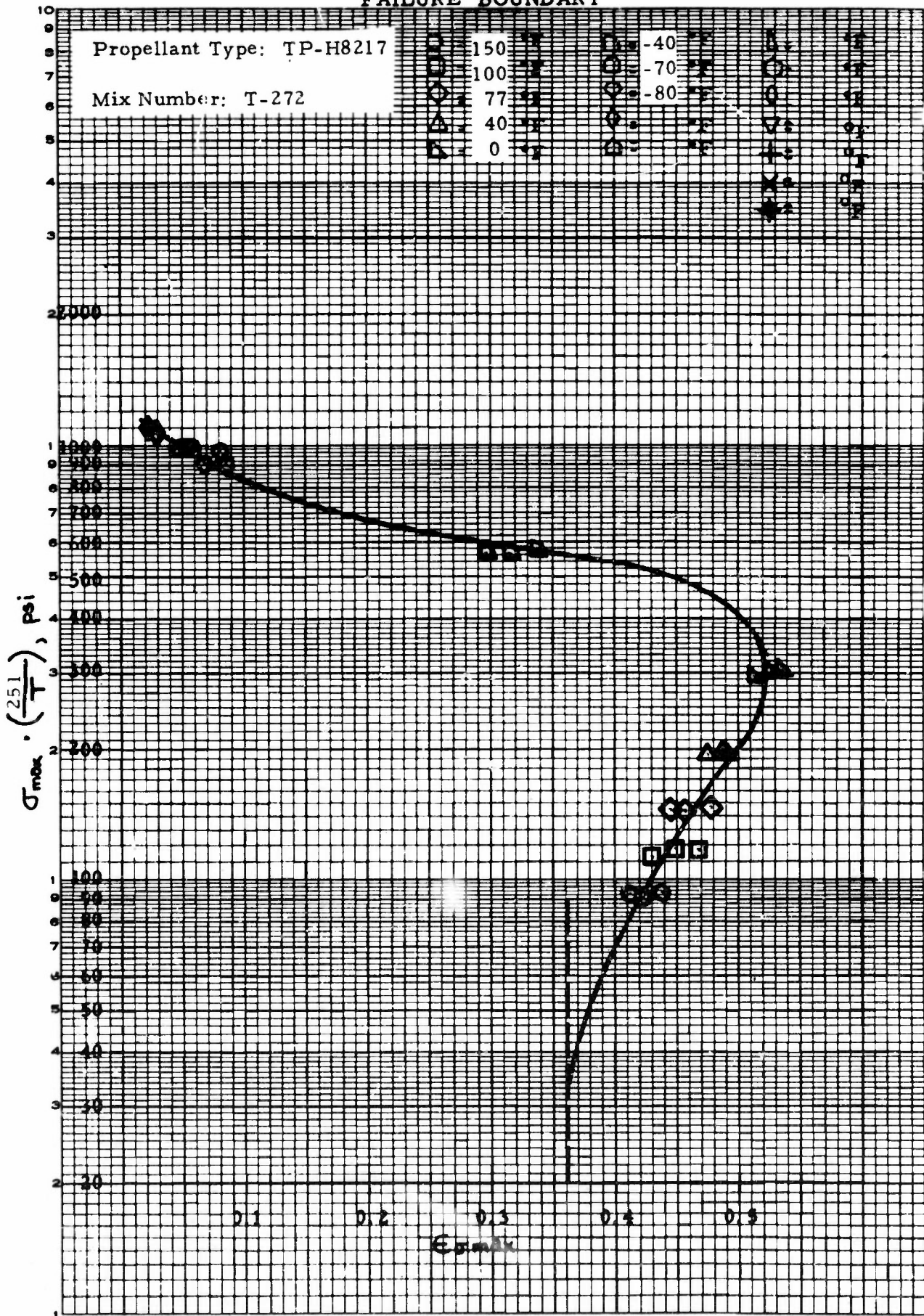


FIGURE 59. FAILURE BOUNDARY - T-272 - KM/KM in HTPB

FAILURE BOUNDARY

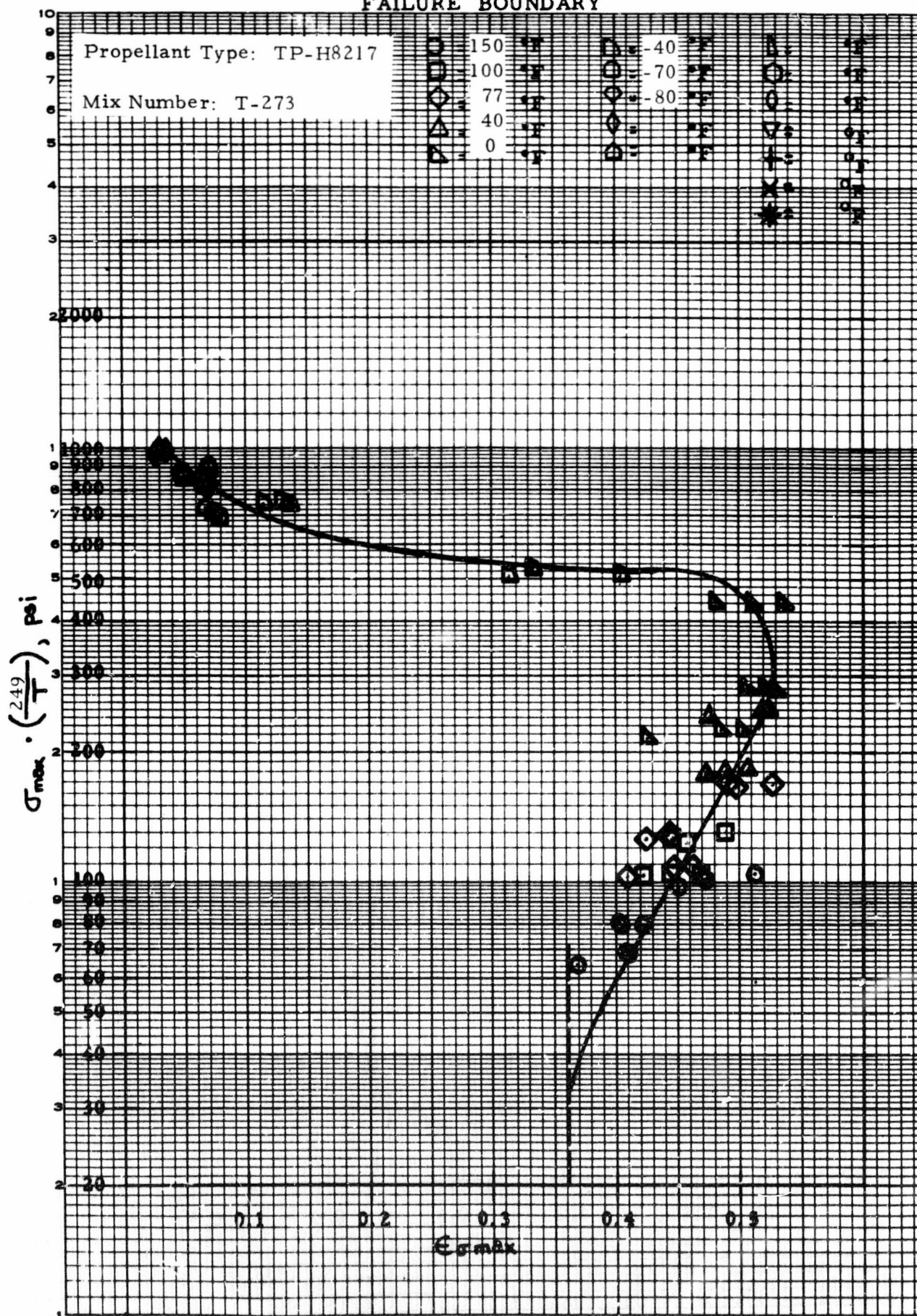


FIGURE 60. FAILURE BOUNDARY - T-273 - P/P in HTPB

FAILURE BOUNDARY

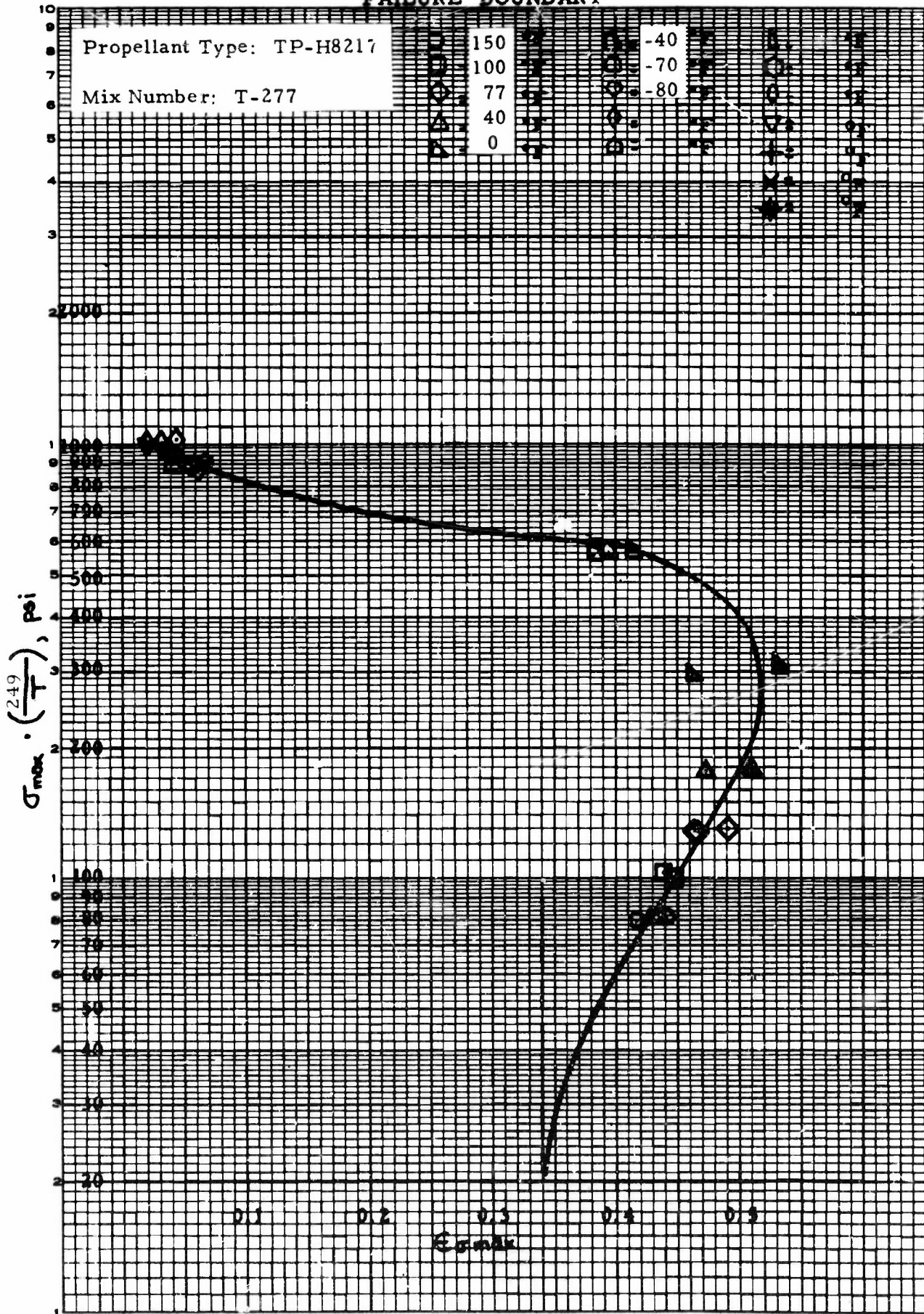


FIGURE 61. FAILURE BOUNDARY - T-277 - P/P in HTPB

FAILURE BOUNDARY

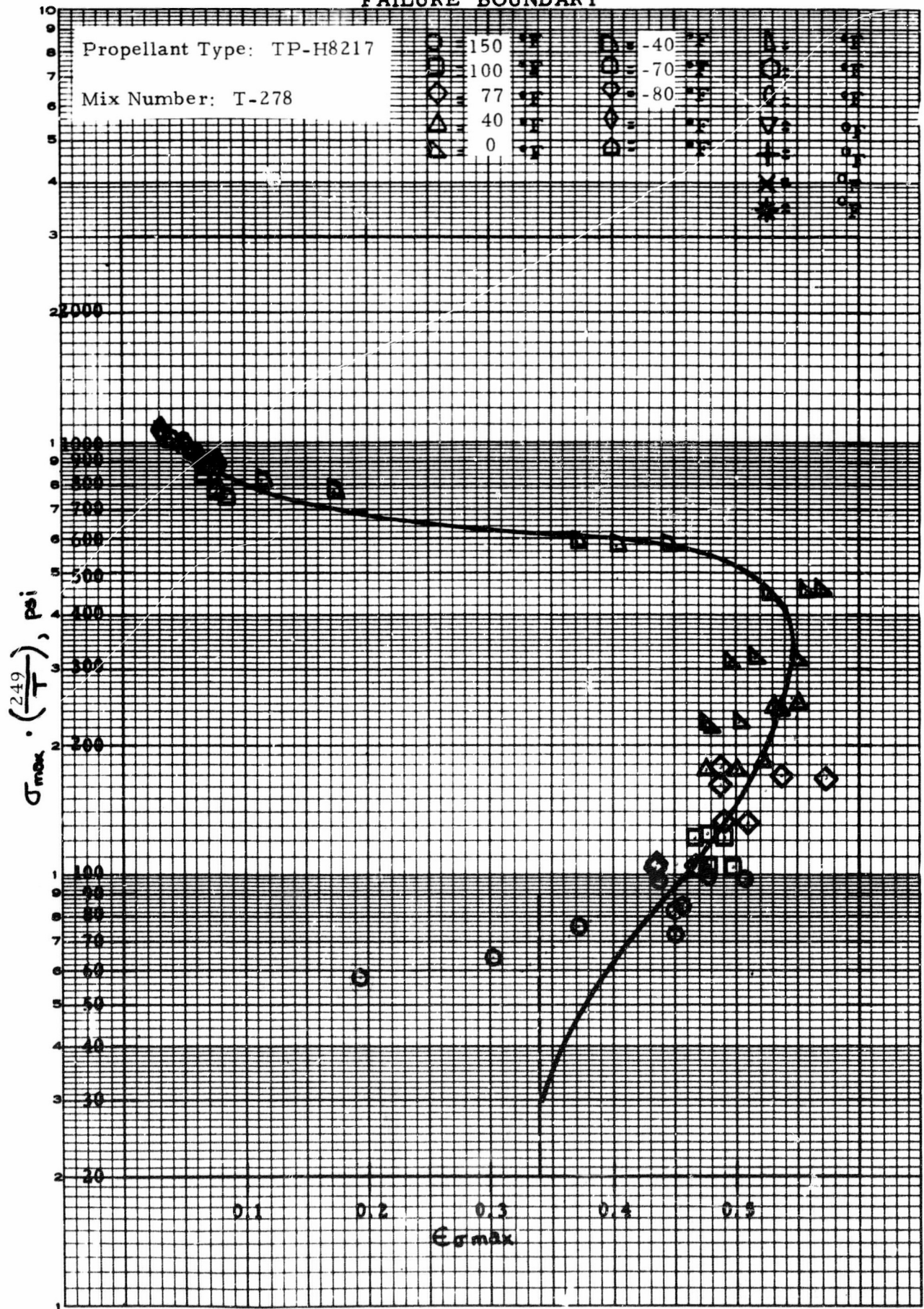


FIGURE 62. FAILURE BOUNDARY - T-278 - KM/P in HTPB

FAILURE BOUNDARY

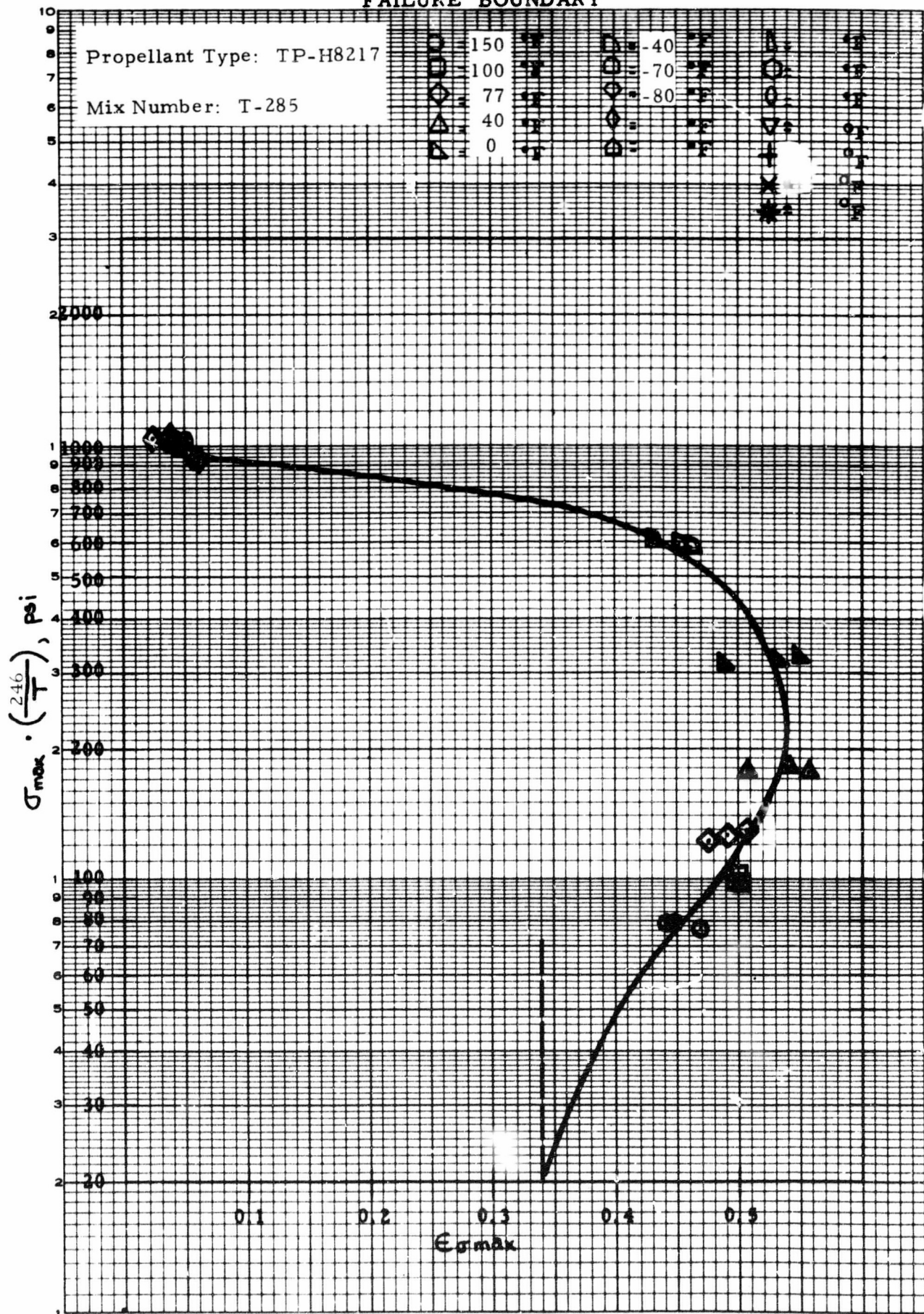


FIGURE 63. FAILURE BOUNDARY - T-285 - KM/P in HTPB

FAILURE BOUNDARY

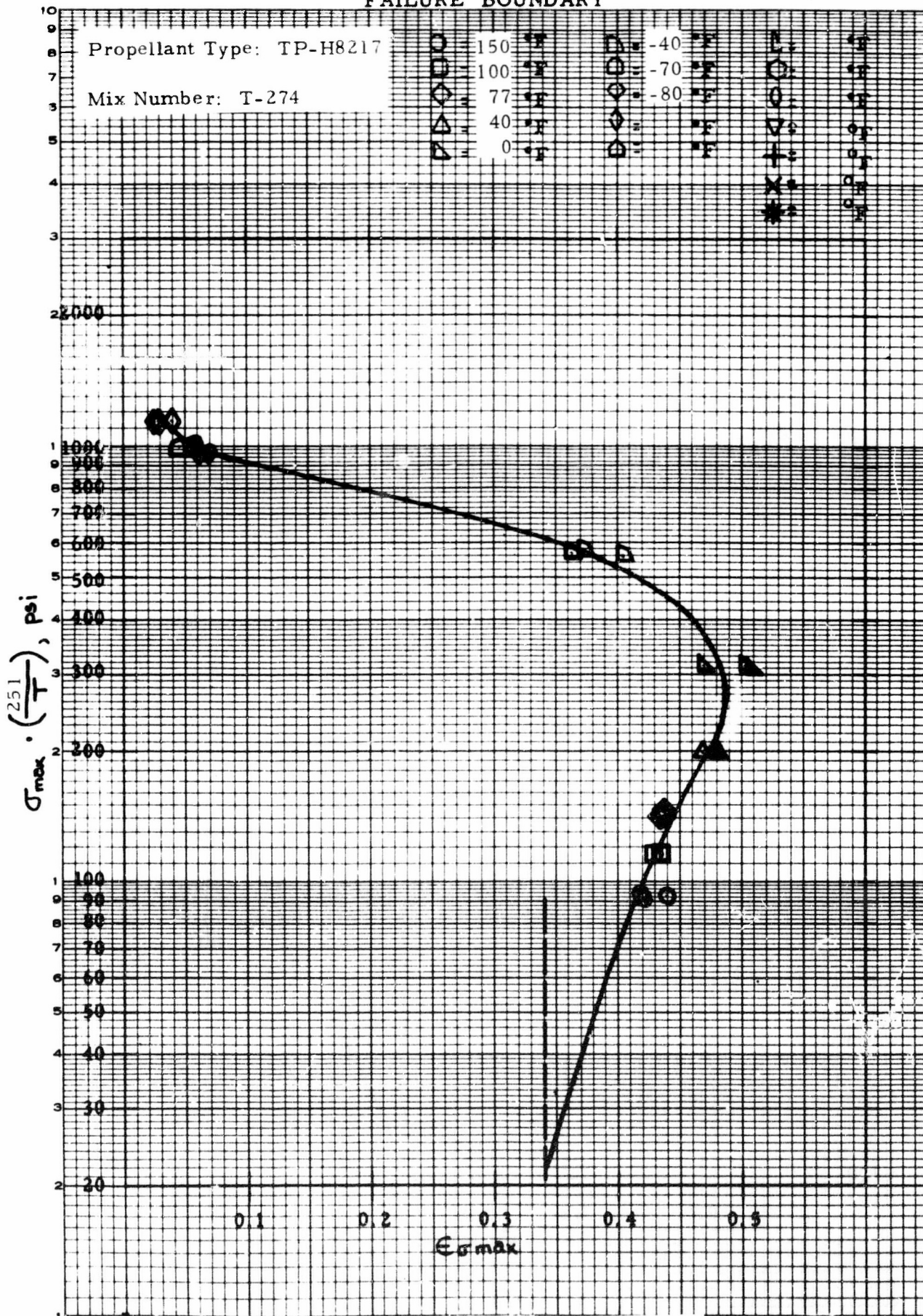


FIGURE 64. FAILURE BOUNDARY - T-274 - KM/KM in HTPB (humidified)

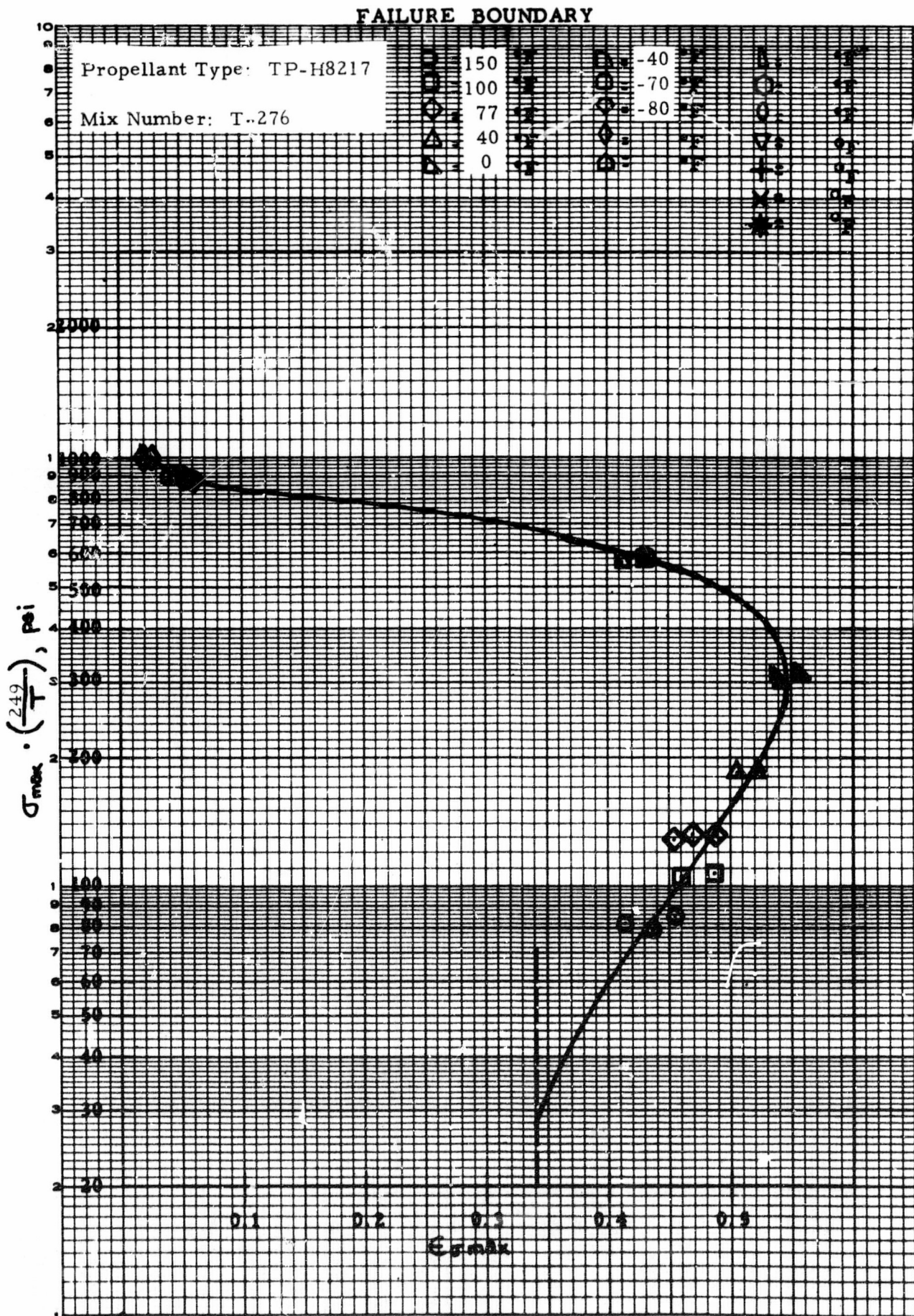


FIGURE 65. FAILURE BOUNDARY - T-276 - P/P in HTPB (humidified)

FAILURE BOUNDARY

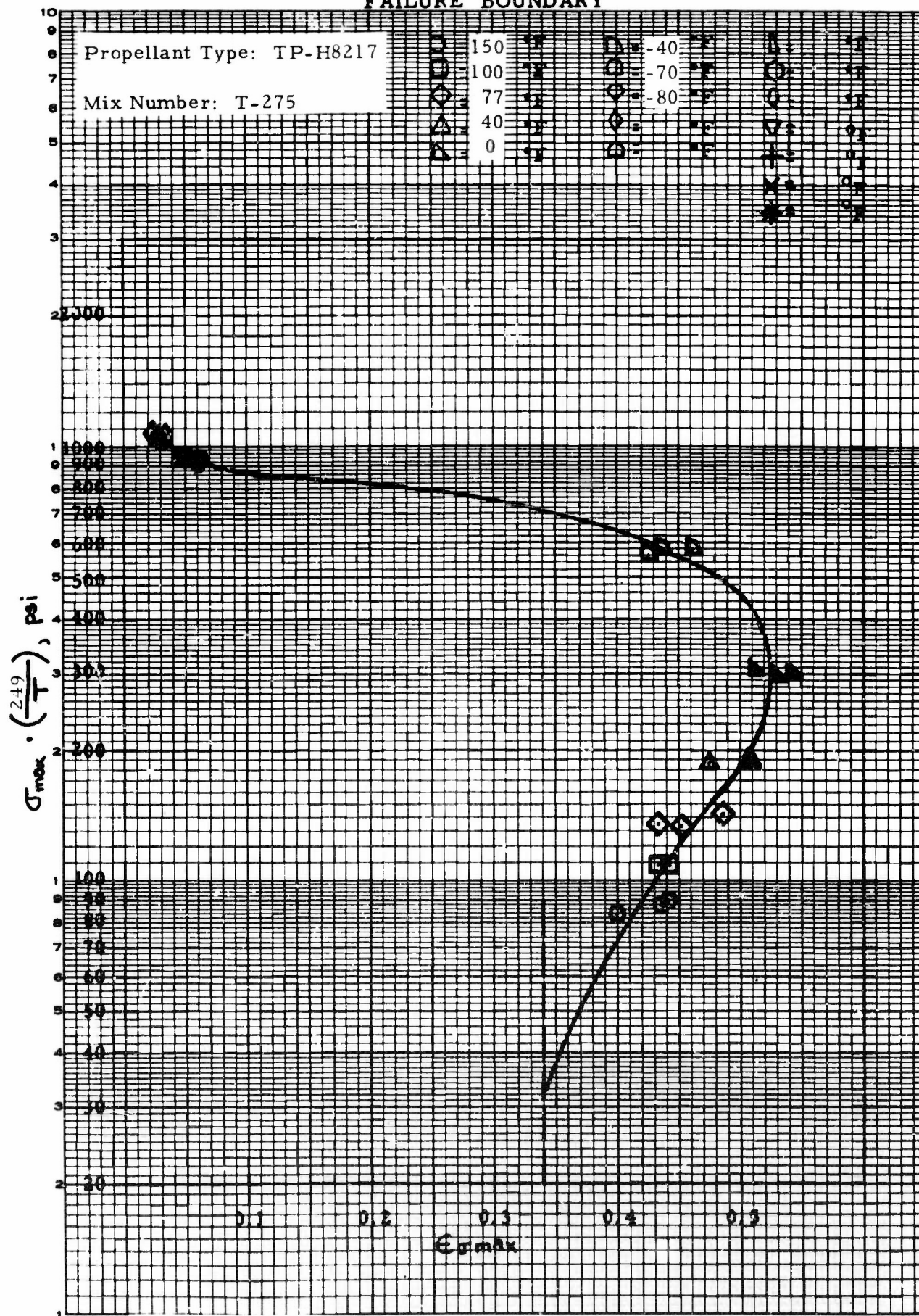


FIGURE 66. FAILURE BOUNDARY - T-275 - KM/P in HTPB (humidified)

FAILURE BOUNDARY

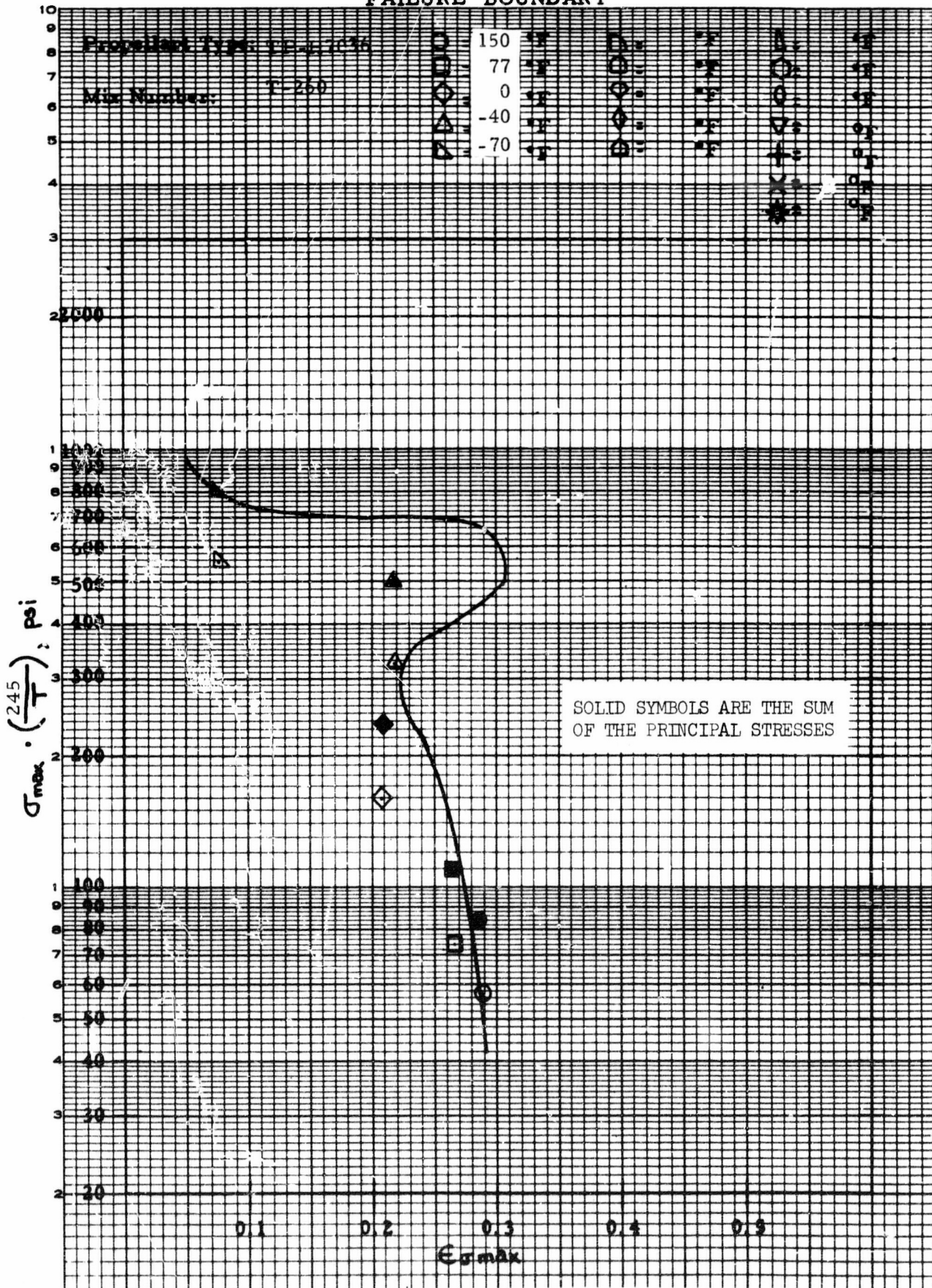


FIGURE 67. COMPARISON OF UNIAXIAL AND BIAxIAL FAILURE BEHAVIOR - T-260 - KM/KM in CTPB

[illegible]

132

FAILURE BOUNDARY

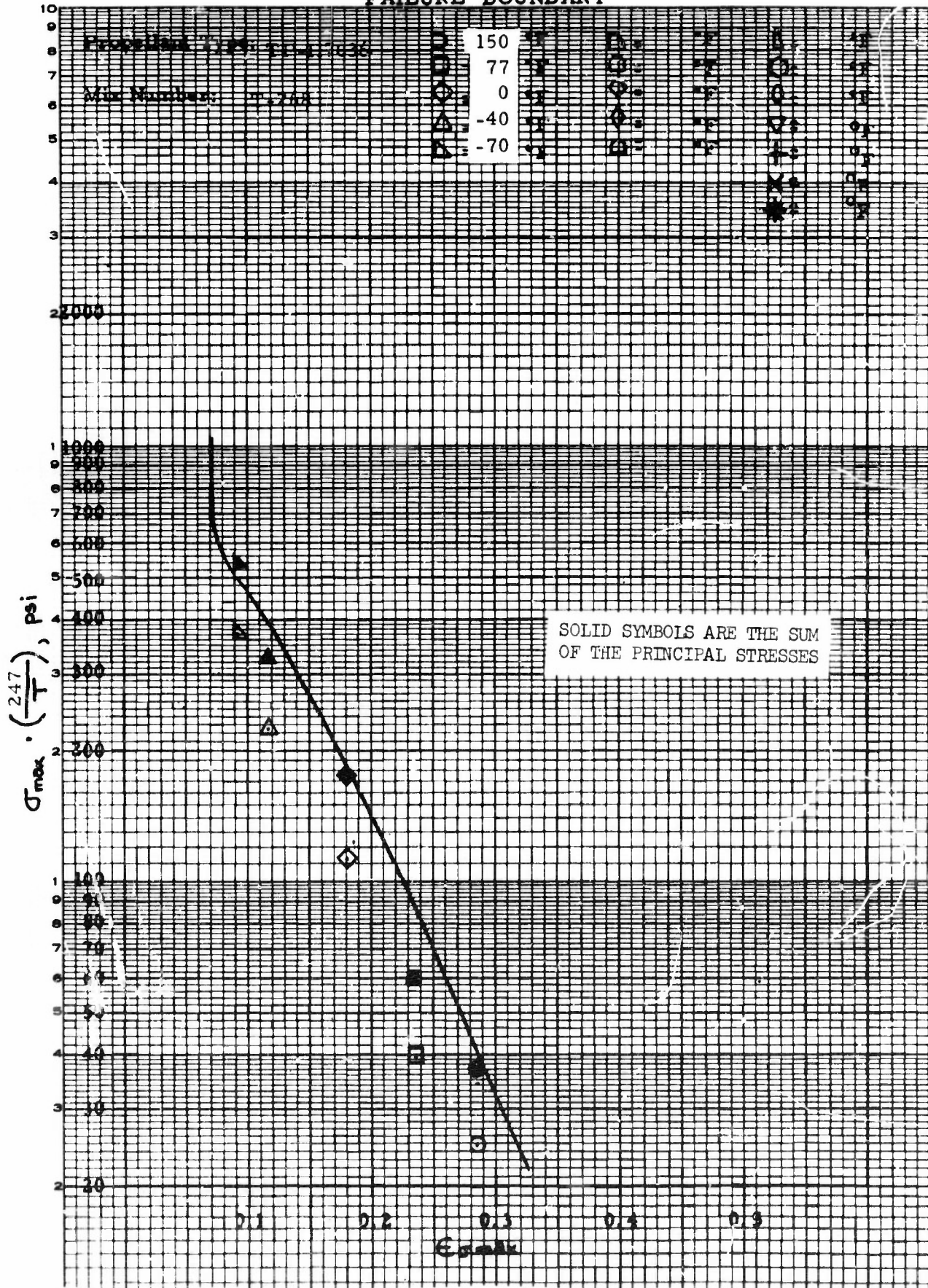


FIGURE 69. COMPARISON OF UNIAXIAL AND BIAXIAL FAILURE BEHAVIOR - T-268 - KM/P in CTPB

FAILURE BOUNDARY

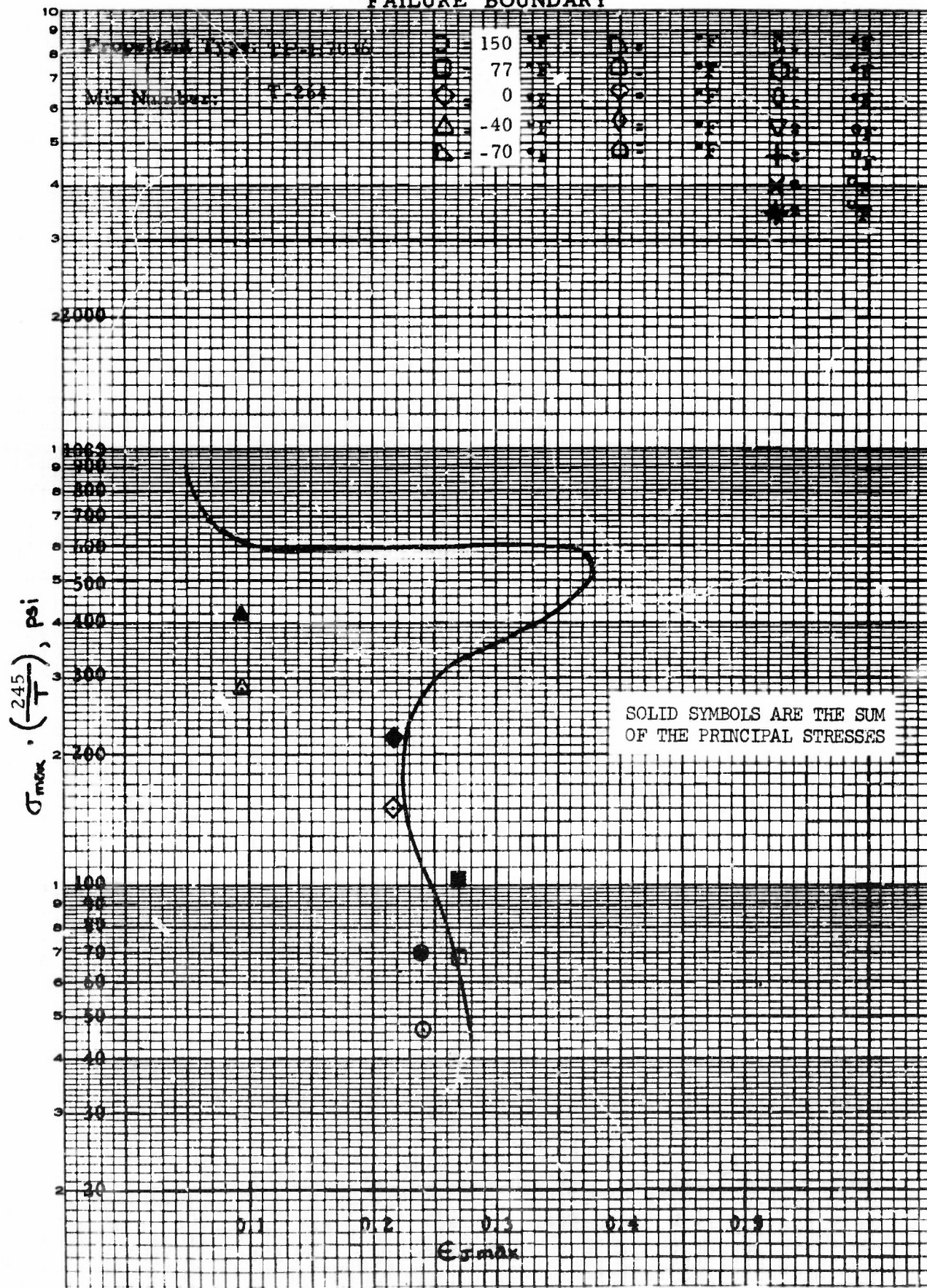


FIGURE 70. COMPARISON OF UNIAXIAL AND BIAxIAL FAILURE BEHAVIOR - T-264 - KM/KM in CTPB (humidified)

FAILURE BOUNDARY

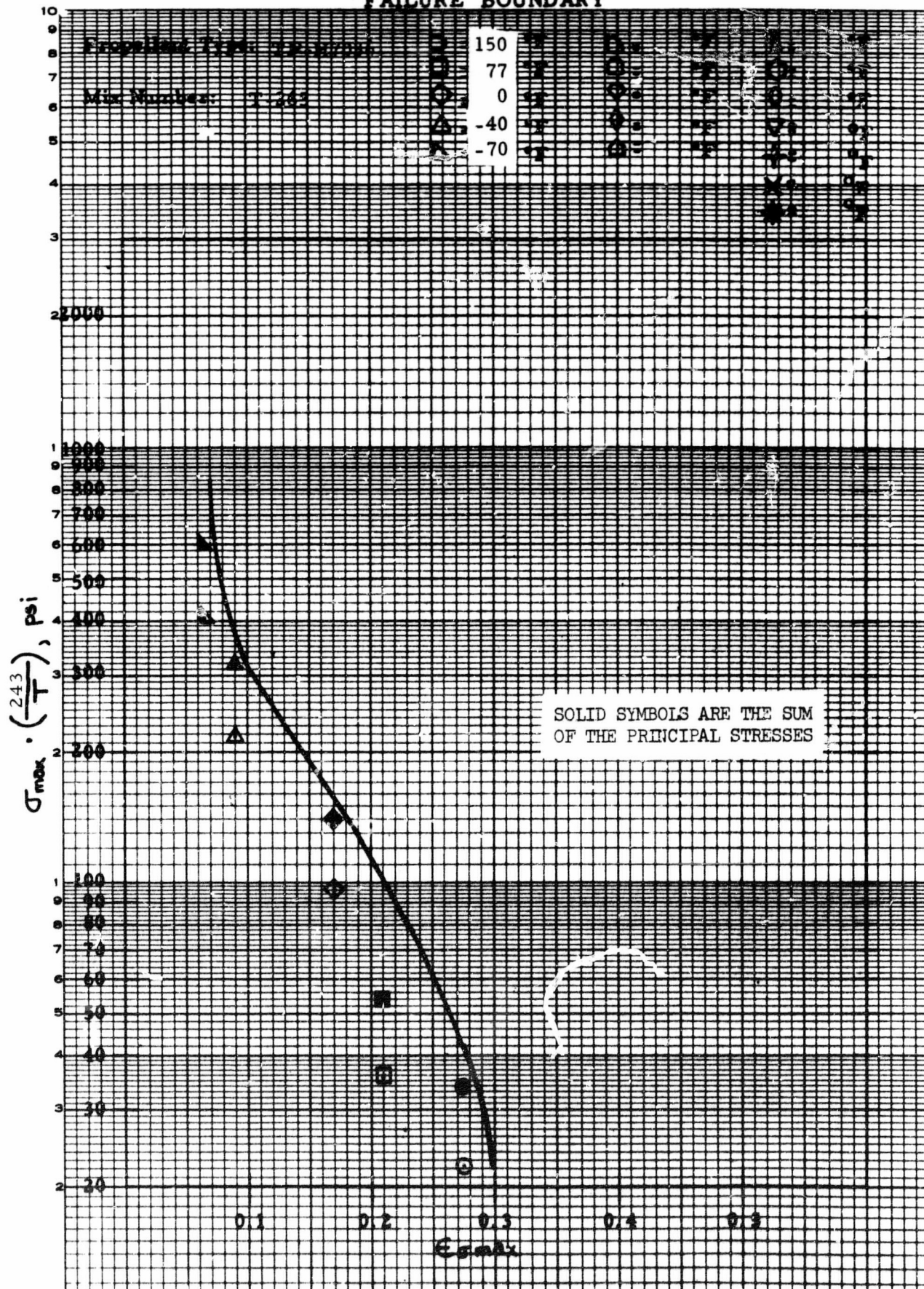


FIGURE 71. COMPARISON OF UNIAXIAL AND BIAxIAL FAILURE BEHAVIOR - T-265 - P/P in CTPB (humidified)

FAILURE BOUNDARY

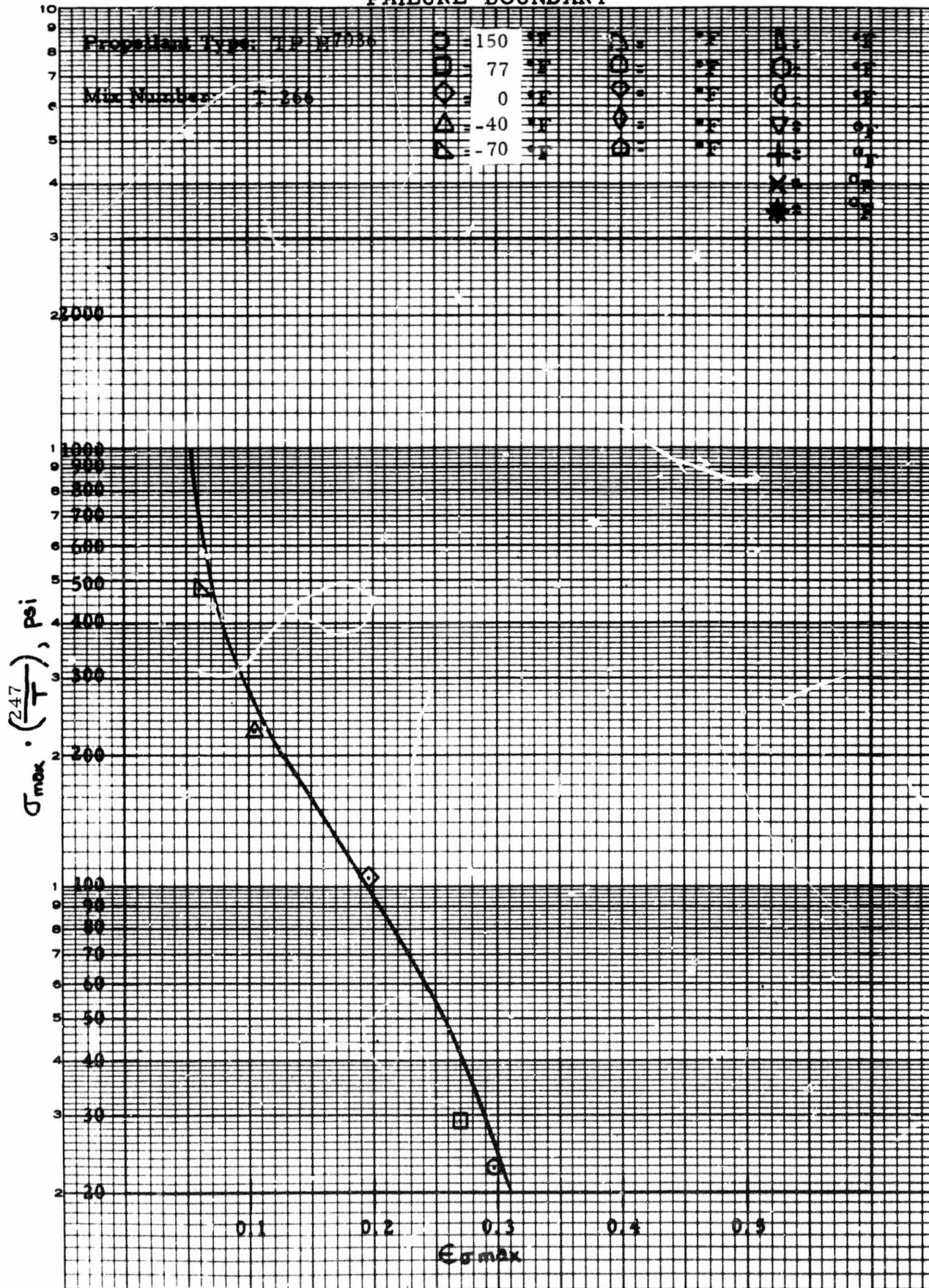


FIGURE 72. COMPARISON OF UNIAXIAL AND BIAxIAL FAILURE BEHAVIOR - T-266 - KM/P in CTPB (humidified)

FAILURE BOUNDARY

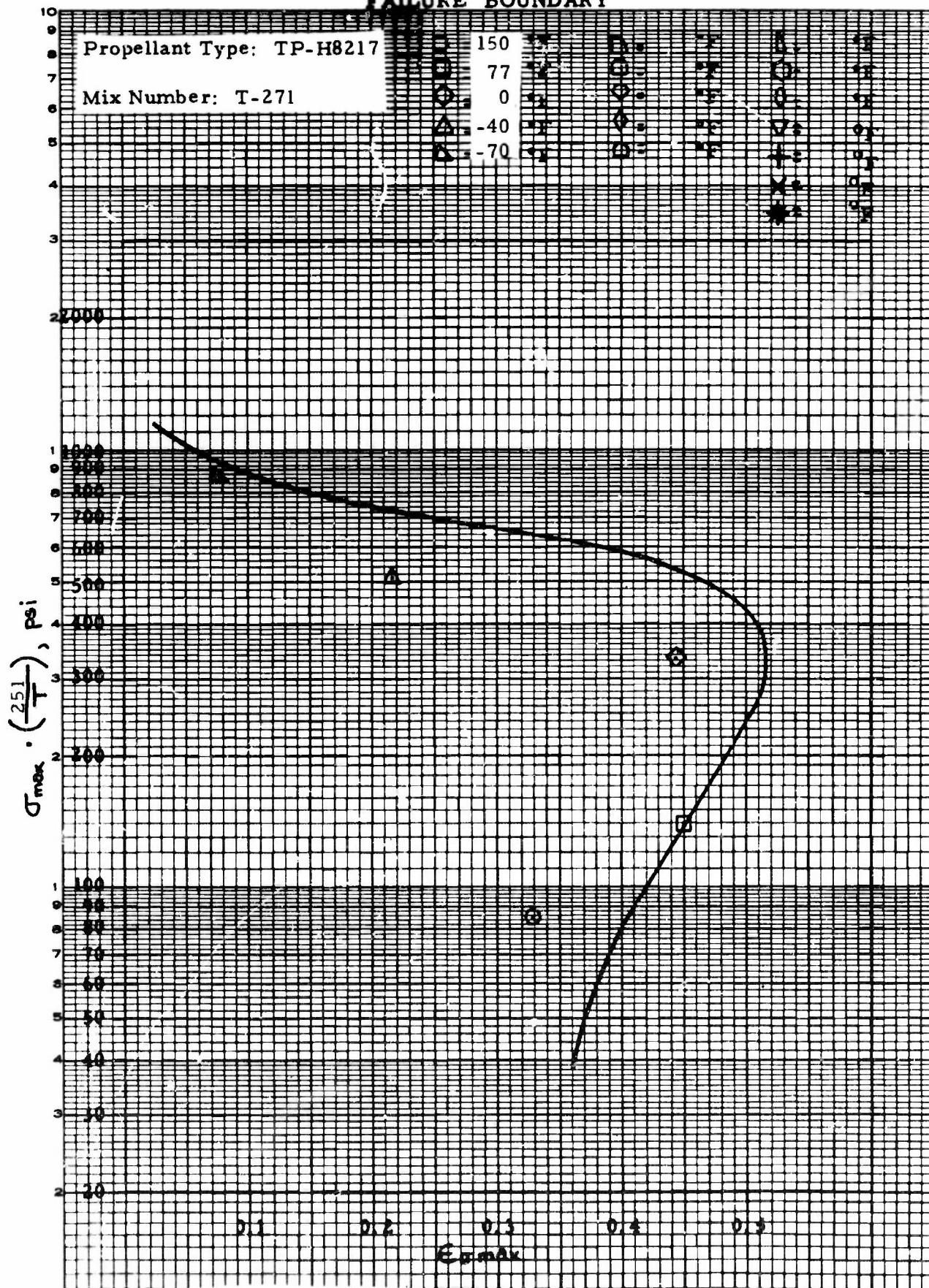


FIGURE 73. COMPARISON OF UNIAXIAL AND BIAxIAL FAILURE BEHAVIOR - T-271 - KM/KM in HTPB

FAILURE BOUNDARY

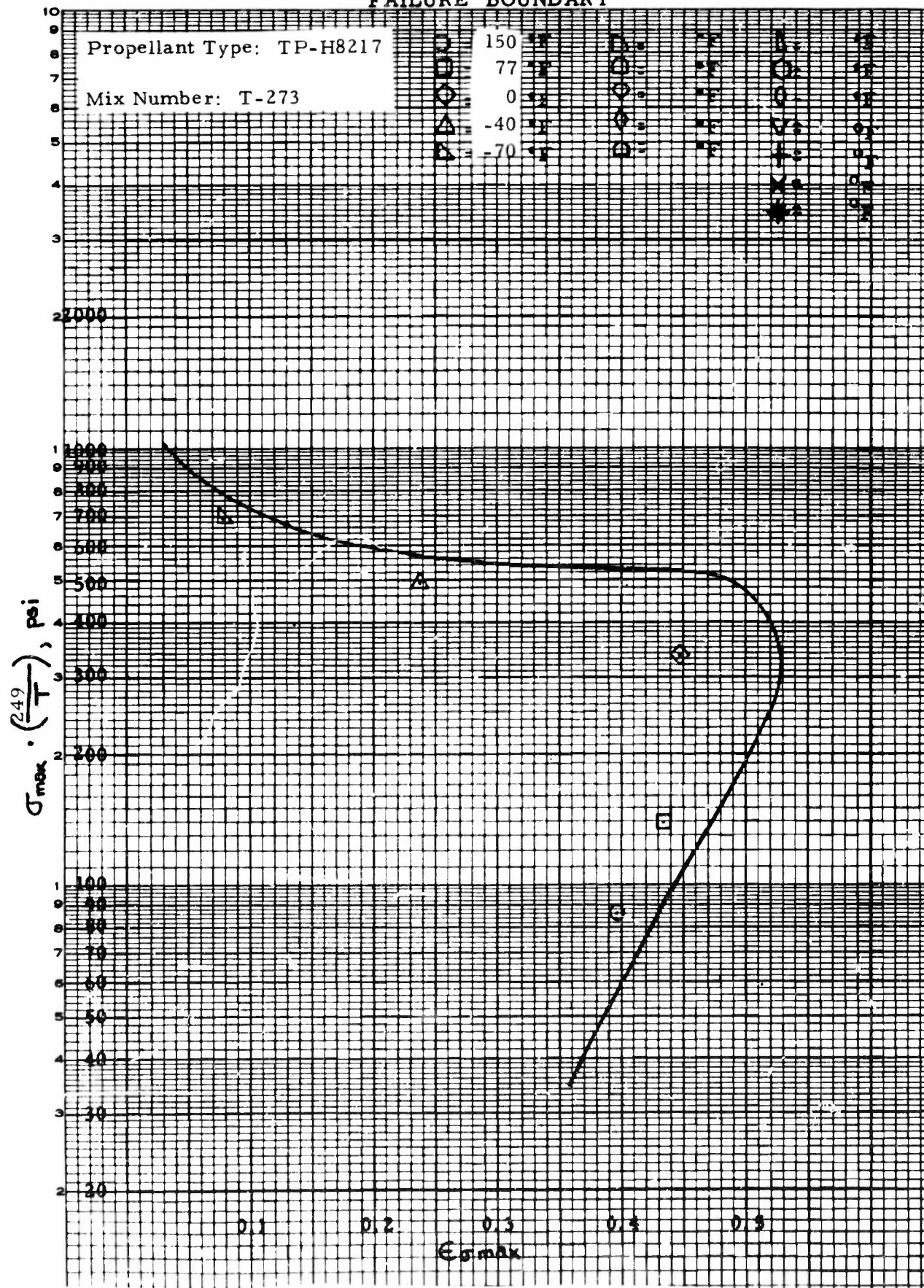


FIGURE 74. COMPARISON OF UNIAXIAL AND BIAXIAL FAILURE BEHAVIOR - T-273 - P/P in HTPB

FAILURE BOUNDARY

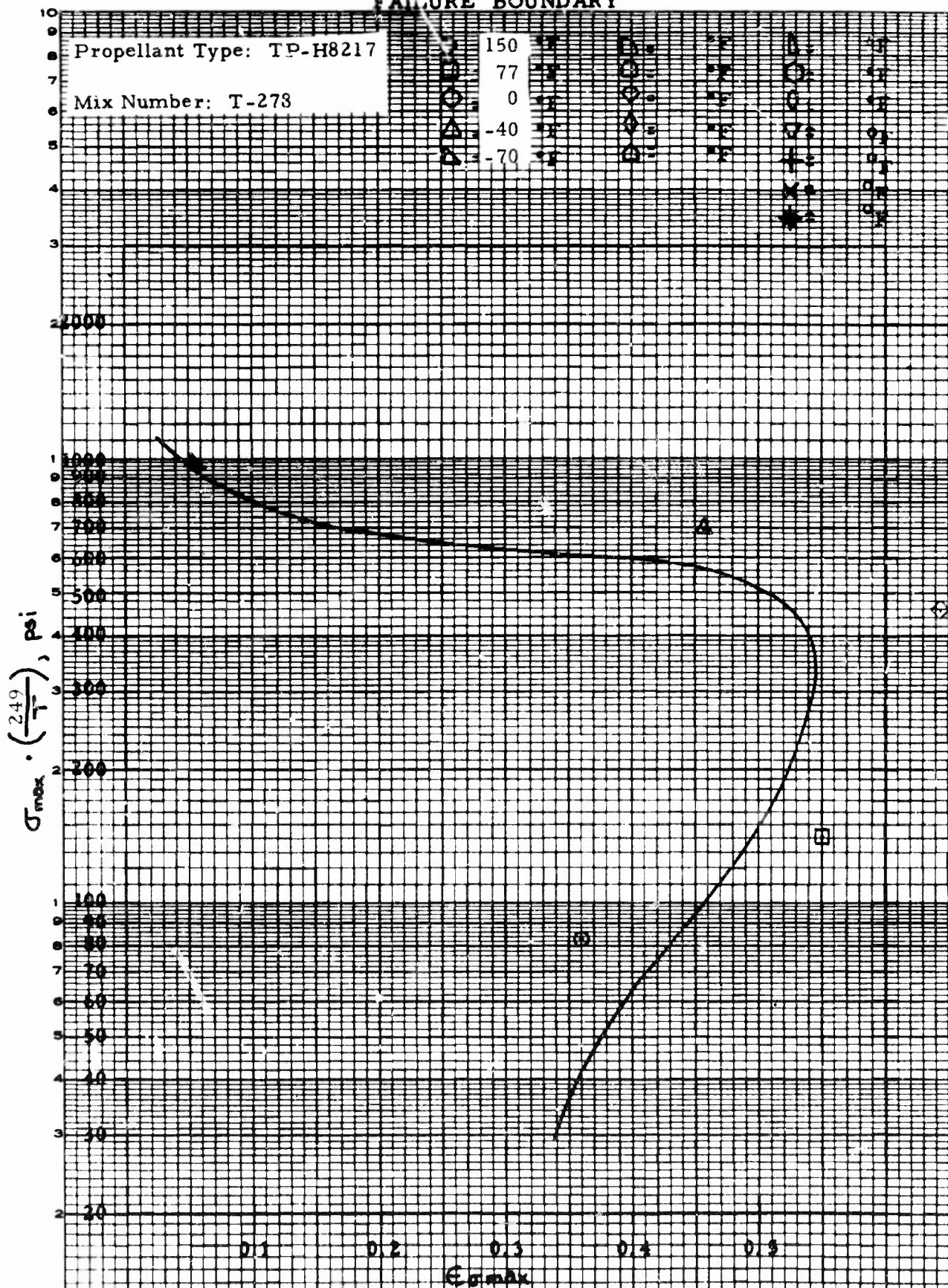


FIGURE 75. COMPARISON OF UNIAXIAL AND BIAxIAL FAILURE BEHAVIOR - T-278 - KM/P in HTPB

FAILURE BOUNDARY

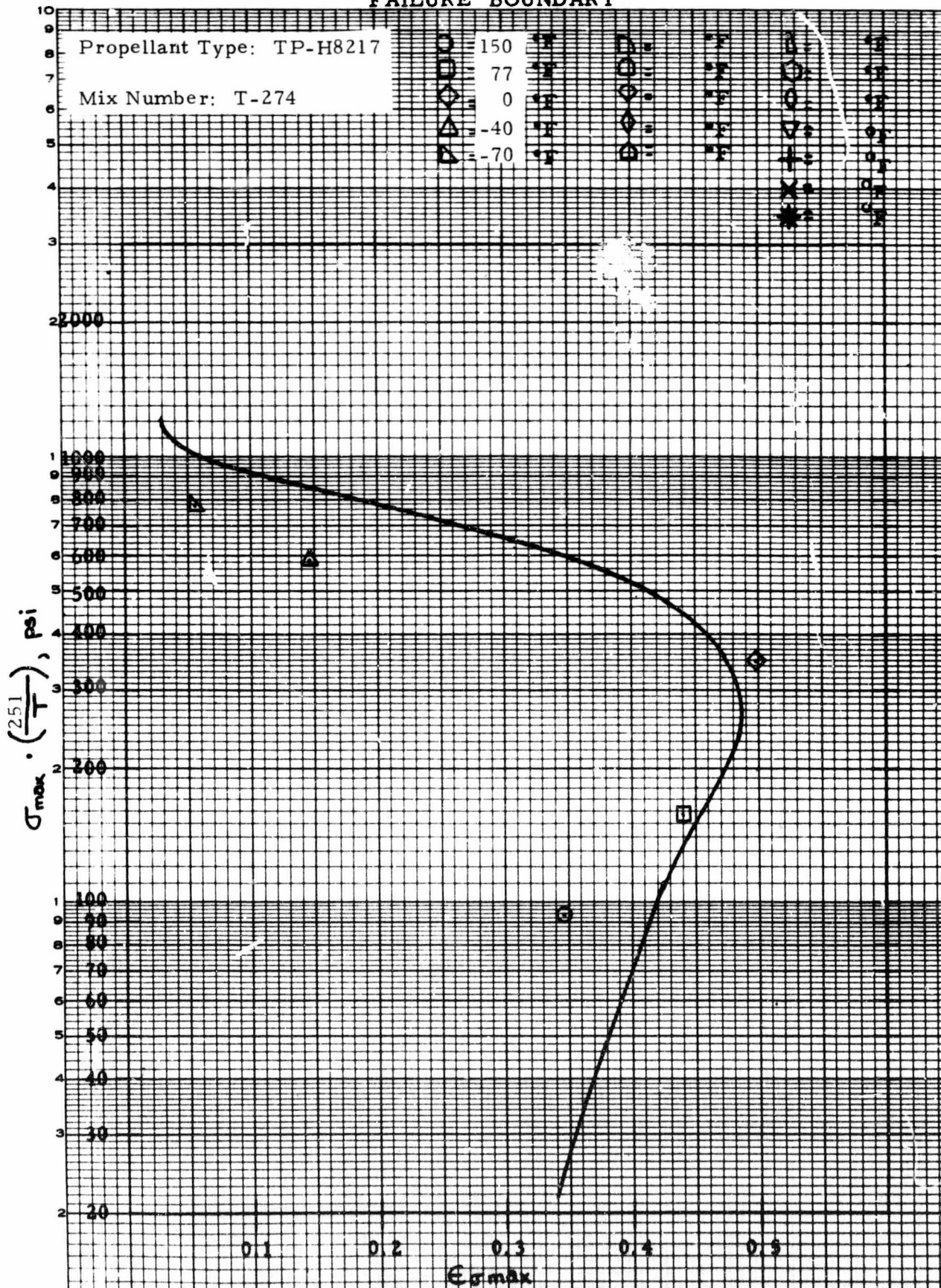


FIGURE 76. COMPARISON OF UNIAXIAL AND BIAxIAL FAILURE BEHAVIOR -
T-274 - KM/KM in HTPB (humidified)

FAILURE BOUNDARY

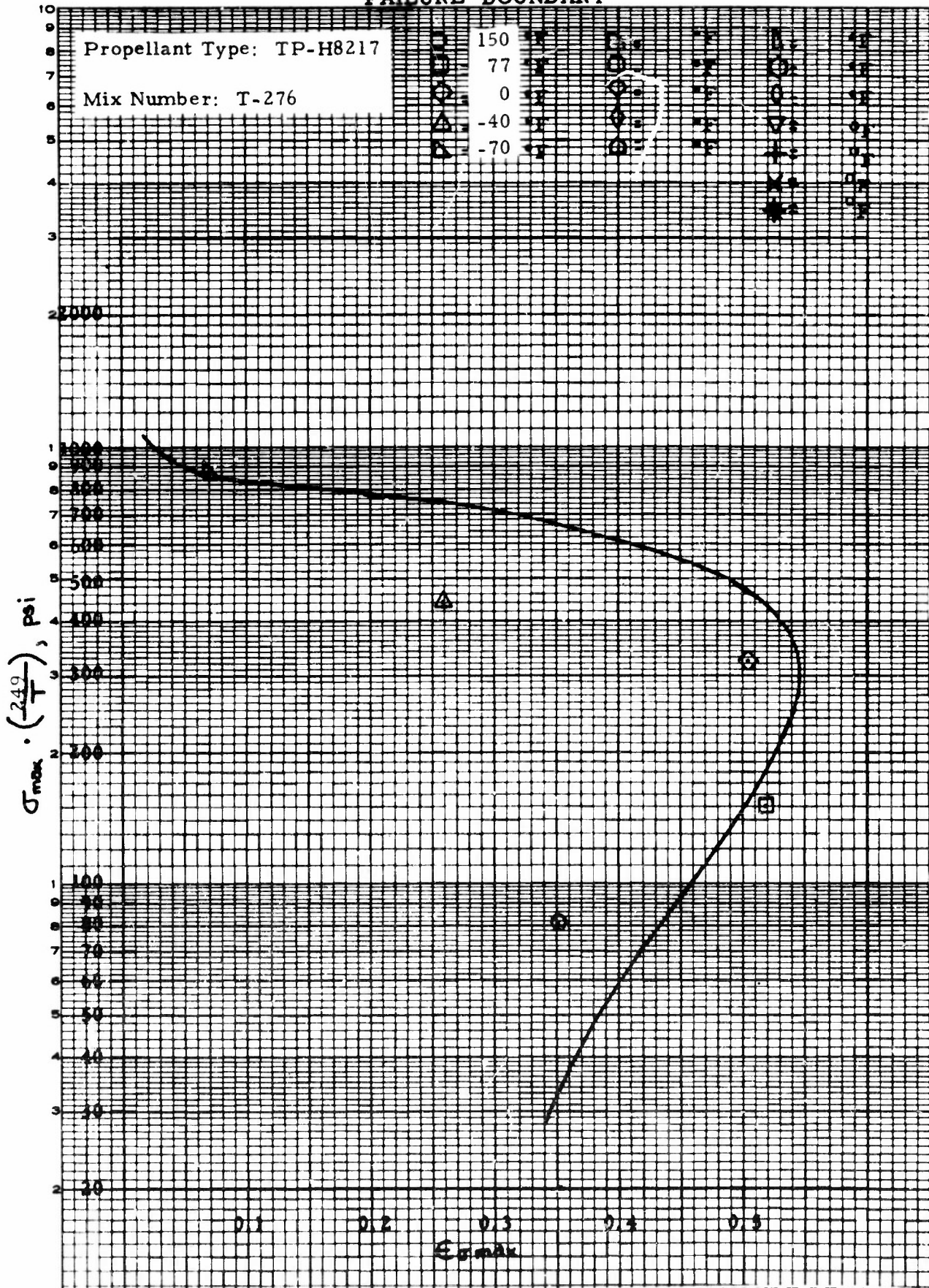
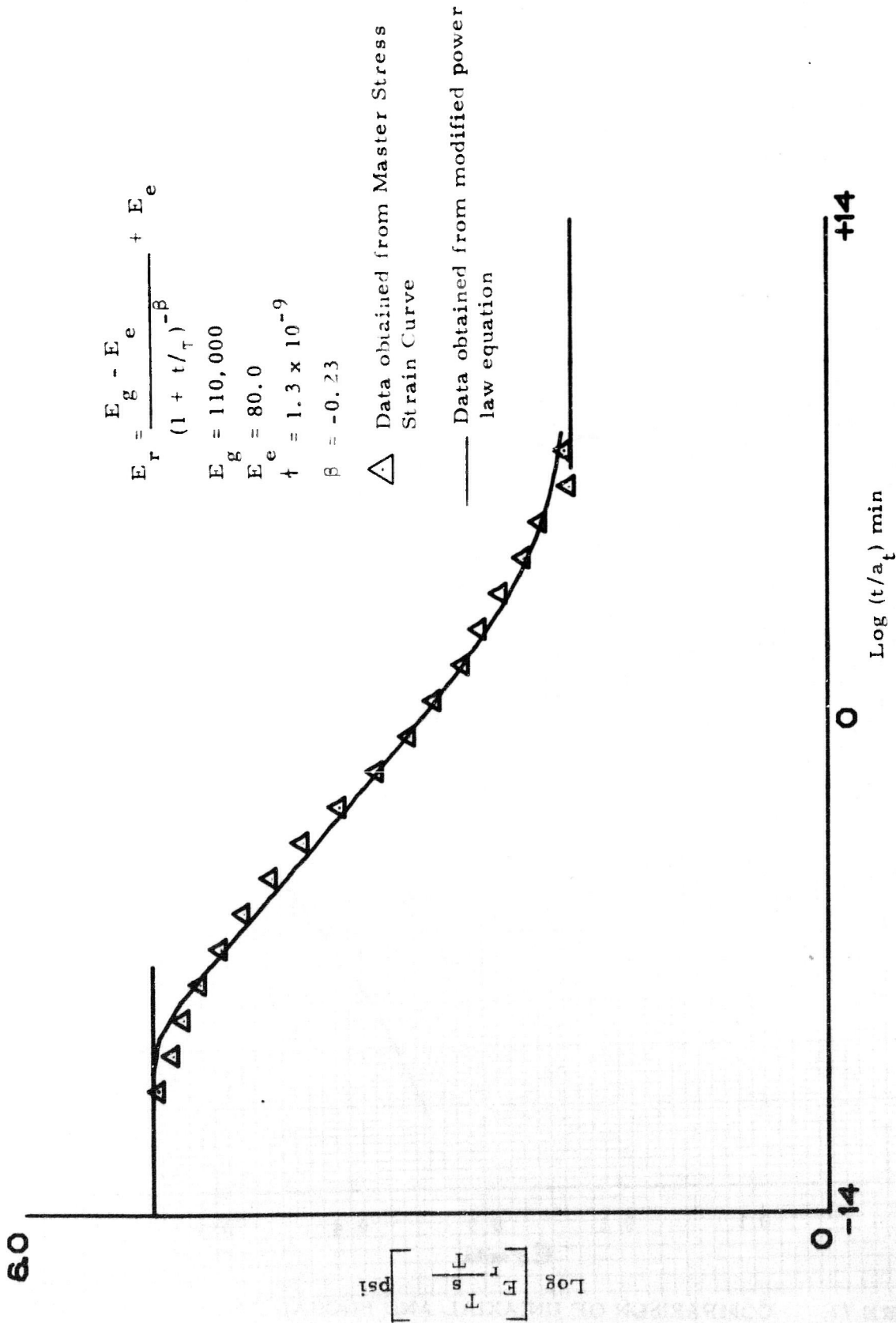
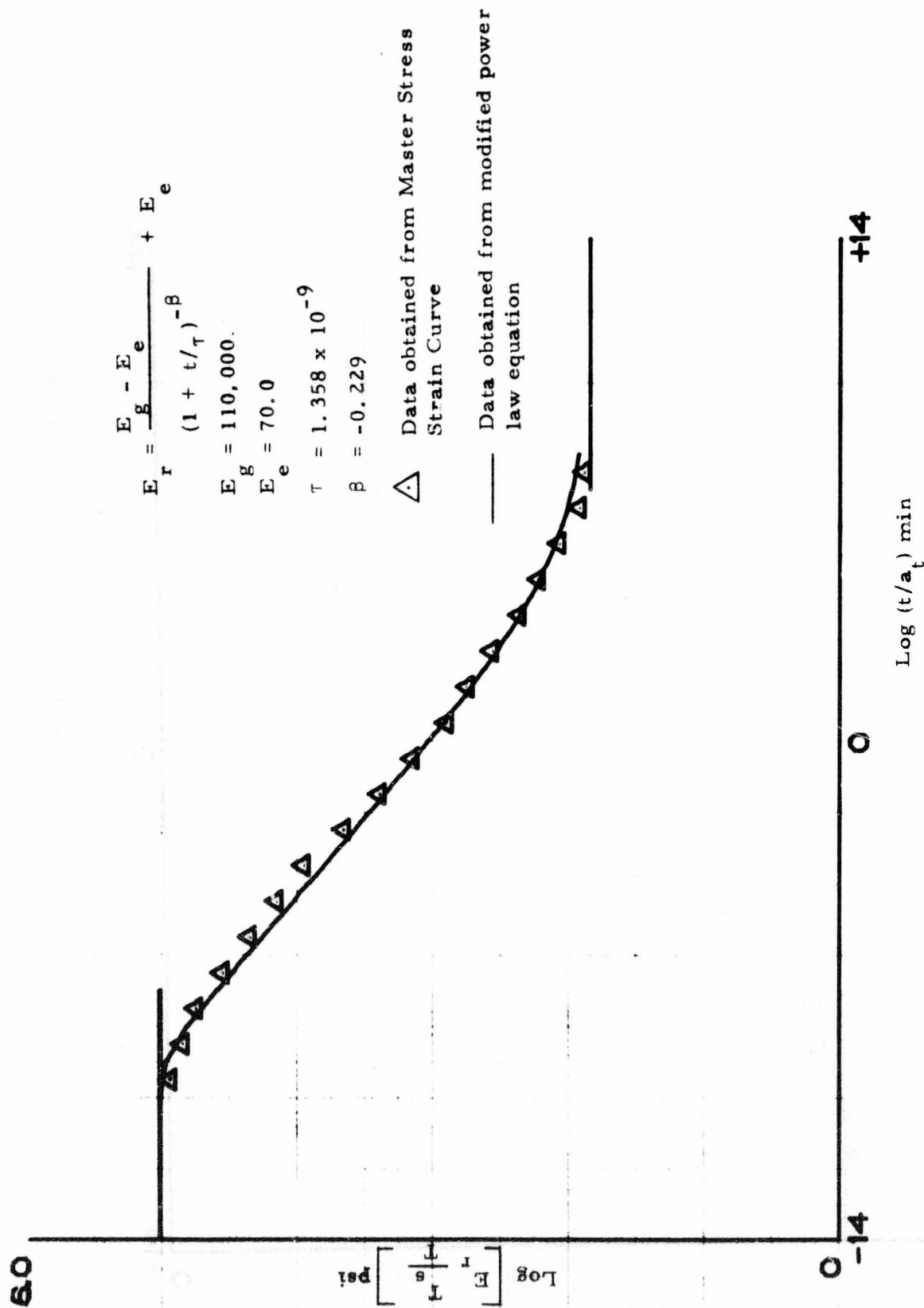


FIGURE 77. COMPARISON OF UNIAXIAL AND BIAXIAL FAILURE BEHAVIOR - T-276 - P/P in: HTPB (humidified)



Relaxation Modulus; TP-H7036, Mix T-260

FIGURE 78. RELAXATION MODULUS - T-260 - $\Delta M/\Delta M$ in CTPB



Relaxation Modulus; T P-H7036, Mix T-261

FIGURE 79. RELAXATION MODULUS - T-261 - KM/KM in CTPB

60

$\log \left[\frac{E_r}{T_s} \right]$
psi

0 -14

0

+14

$\log (t/a_t)$ min

Relaxation Modulus; TP-H7036, Mix T-269

FIGURE 80. RELAXATION MODULUS - T-269 - P/P in CTPB

$$E_r = \frac{E_g - E_e}{(1 + t/\tau)^{-\beta}} + E_e$$

$$E_g = 96,000$$

$$E_e = 35.0$$

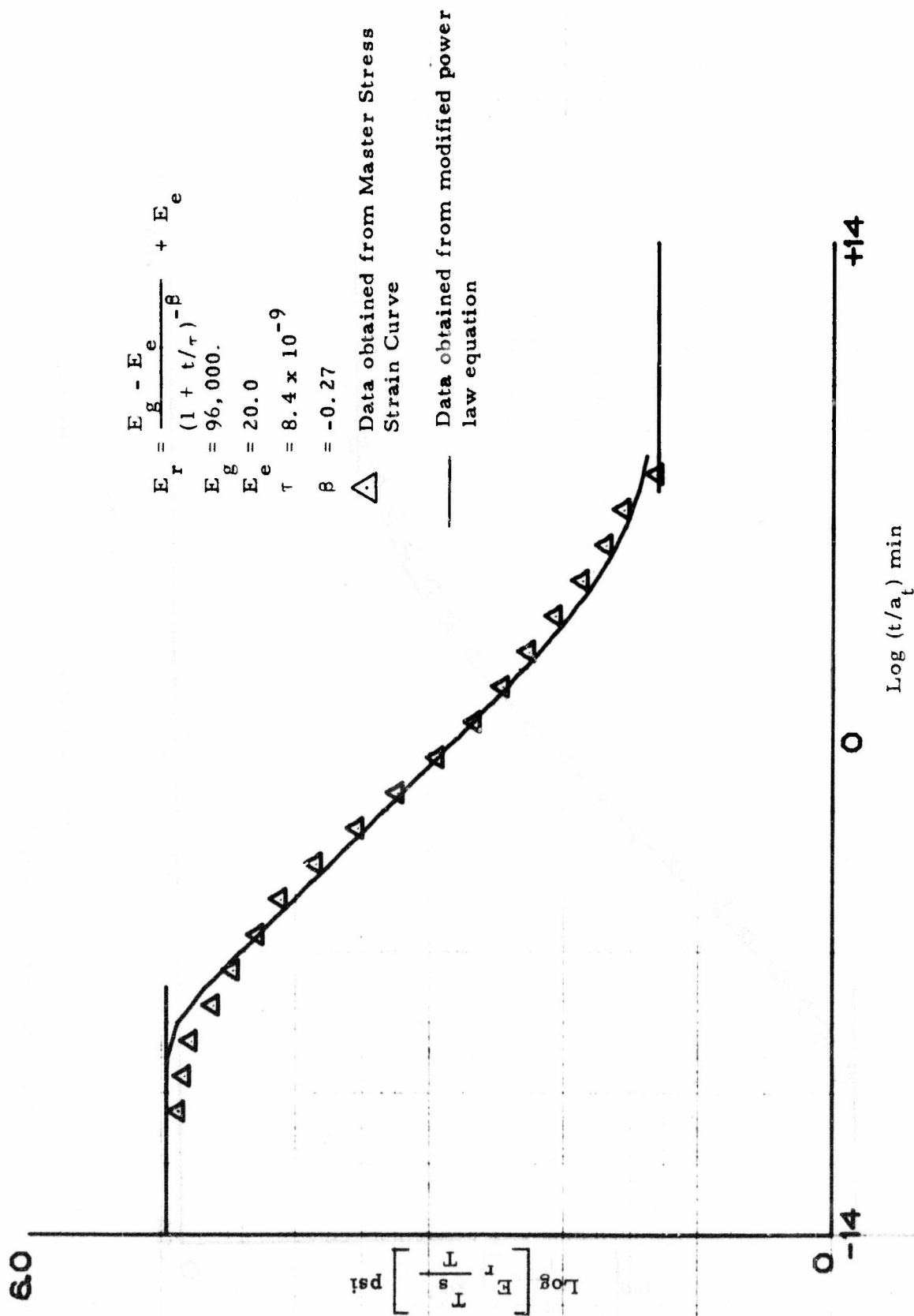
$$\tau = 1.75 \times 10^{-8}$$

$$\beta = -0.275$$

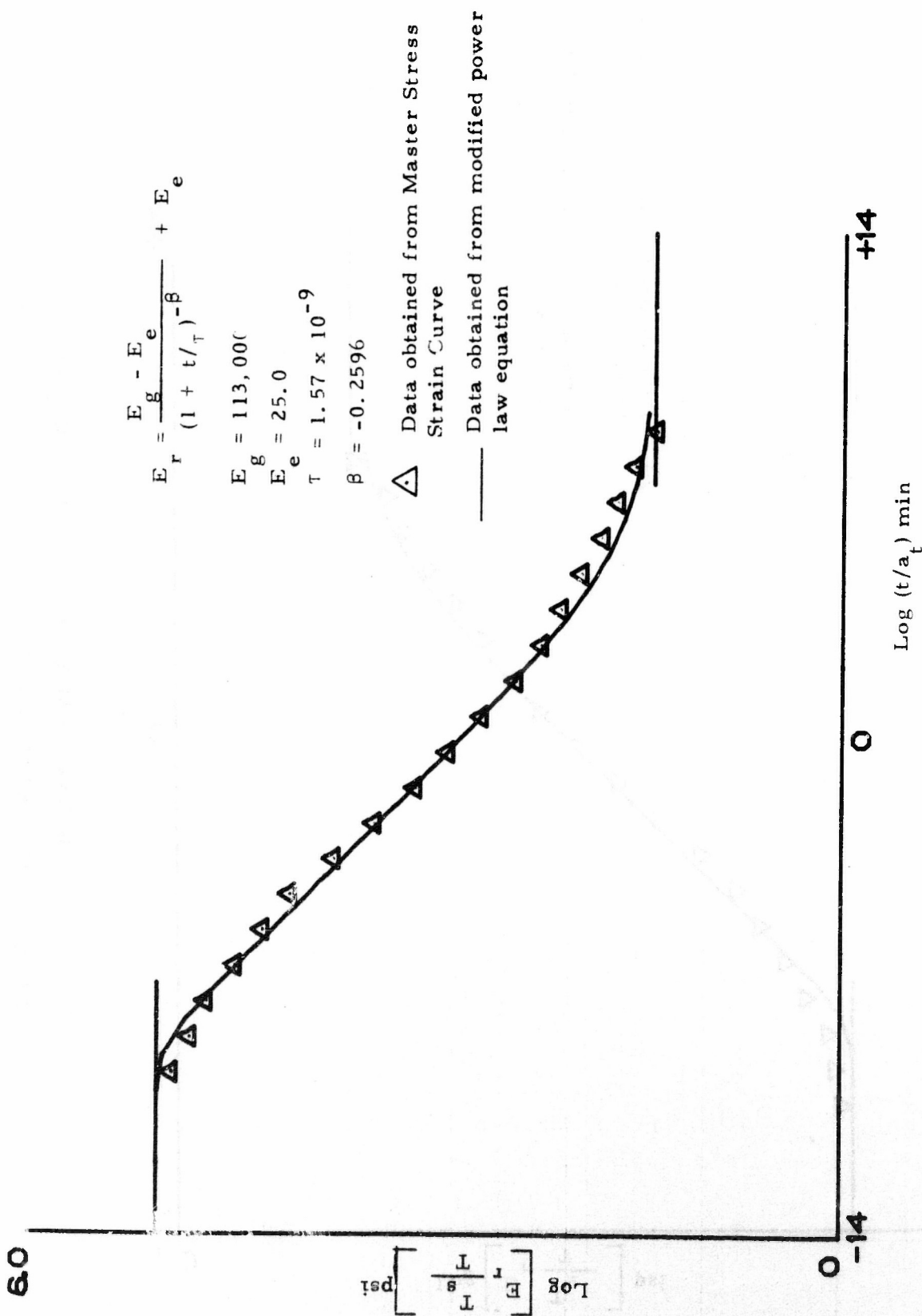


△ Data obtained from Master Stress Strain Curve

— Data obtained from modified power law equation



Relaxation Modulus; TP-H7036, Mix T-270
 FIGURE 81. RELAXATION MODULUS - T-270 - P/P in CTPB



Relaxation Modulus; TP-H7036, Mix T-267
 FIGURE 82. RELAXATION MODULUS - T-267 - KM/P in CTPB

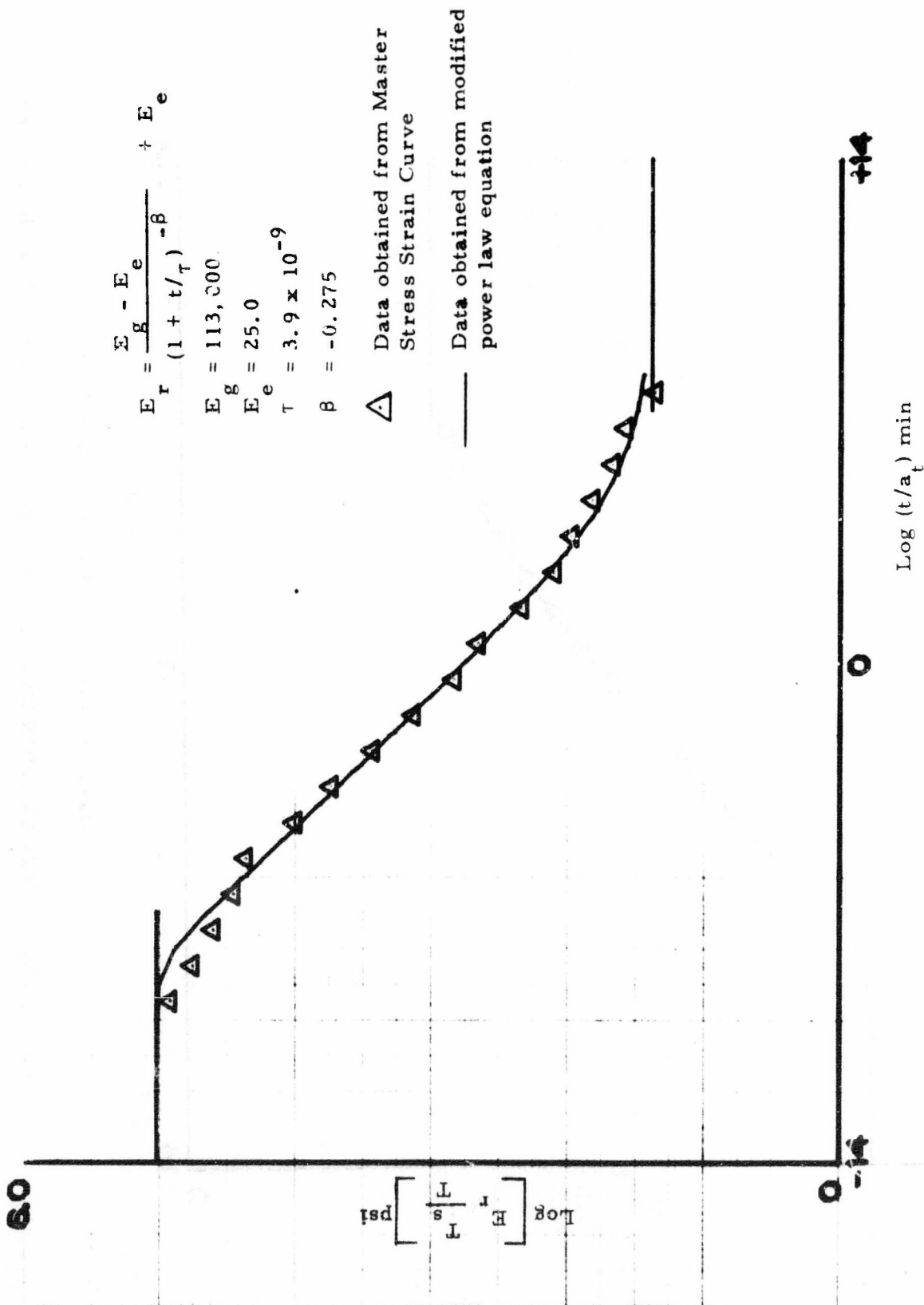
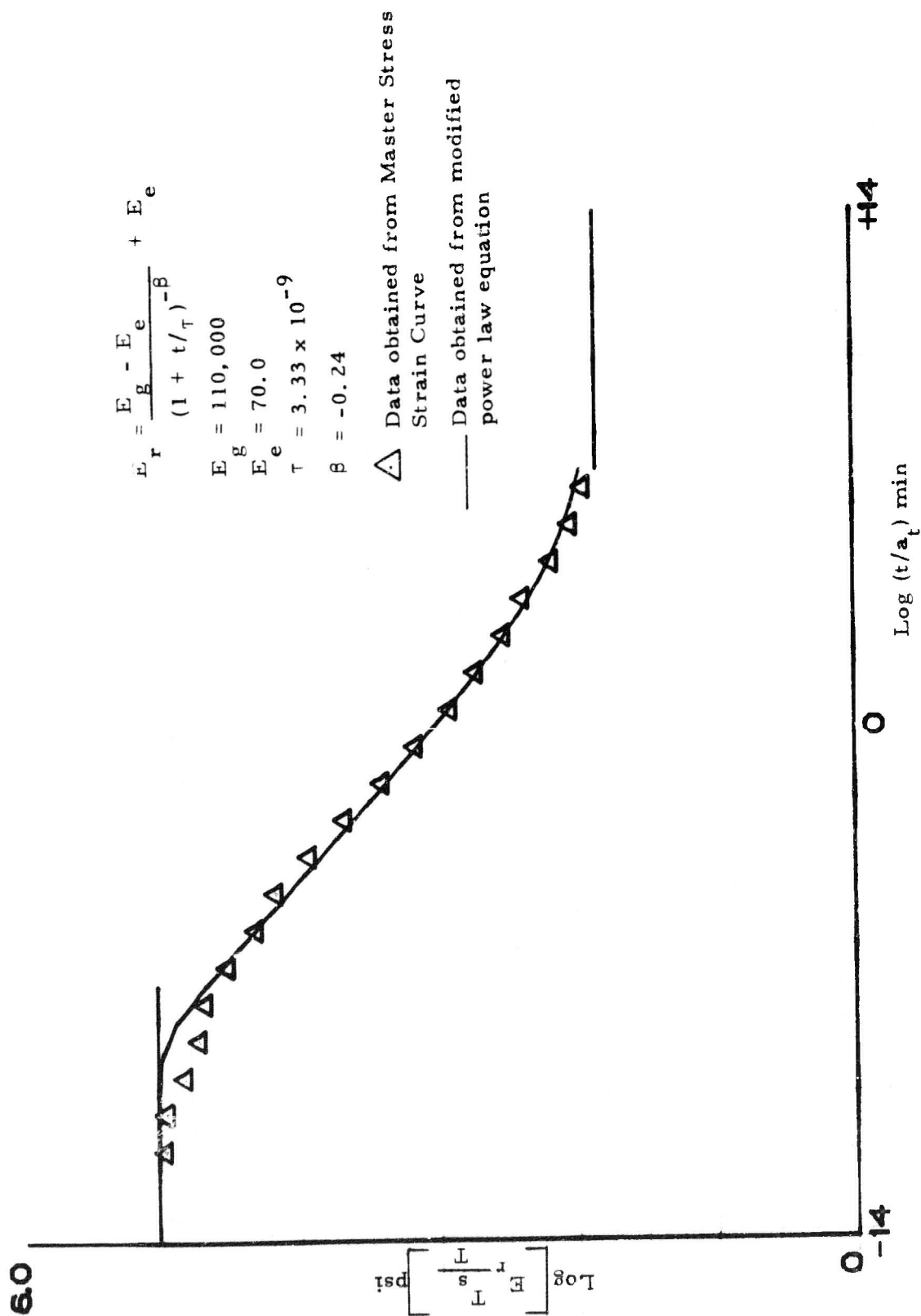


FIGURE 83. RELAXATION MODULUS - T-268 - KM/P in CTPB



Relaxation Modulus: TP-H7936, Mix T-264

FIGURE 84. RELAXATION MODULUS - T-264 - KM/KM in CTPB (humidified)

60

$$\log \left[\frac{E_t}{E_s} \right]$$
 psi

0 -14

0

+14

Log (t/a_t) min

Relaxation Modulus; TP-H7036, Mix T-265

$$E_r = \frac{E_g - E_e}{(1 + t/\tau)^{-\beta}} + E_e$$

$$E_g = 96,000$$

$$E_e = 25.0$$

$$\tau = 2.86 \times 10^{-8}$$

$$\beta = -0.287$$



△ Data obtained from Master Stress
Strain Curve

— Data obtained from modified power
law equation

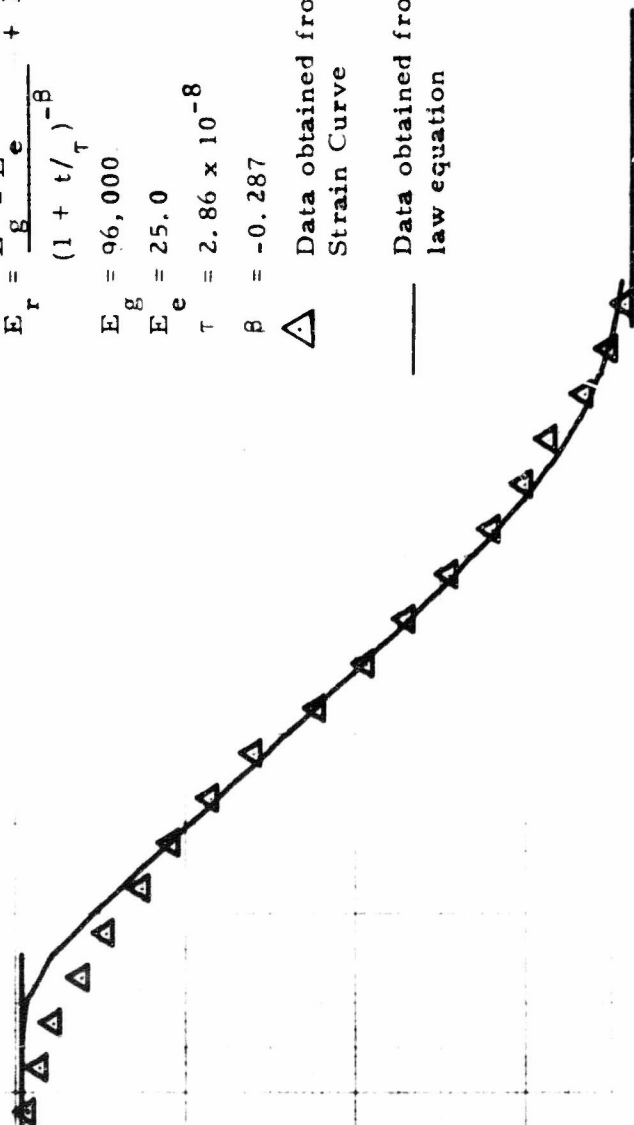
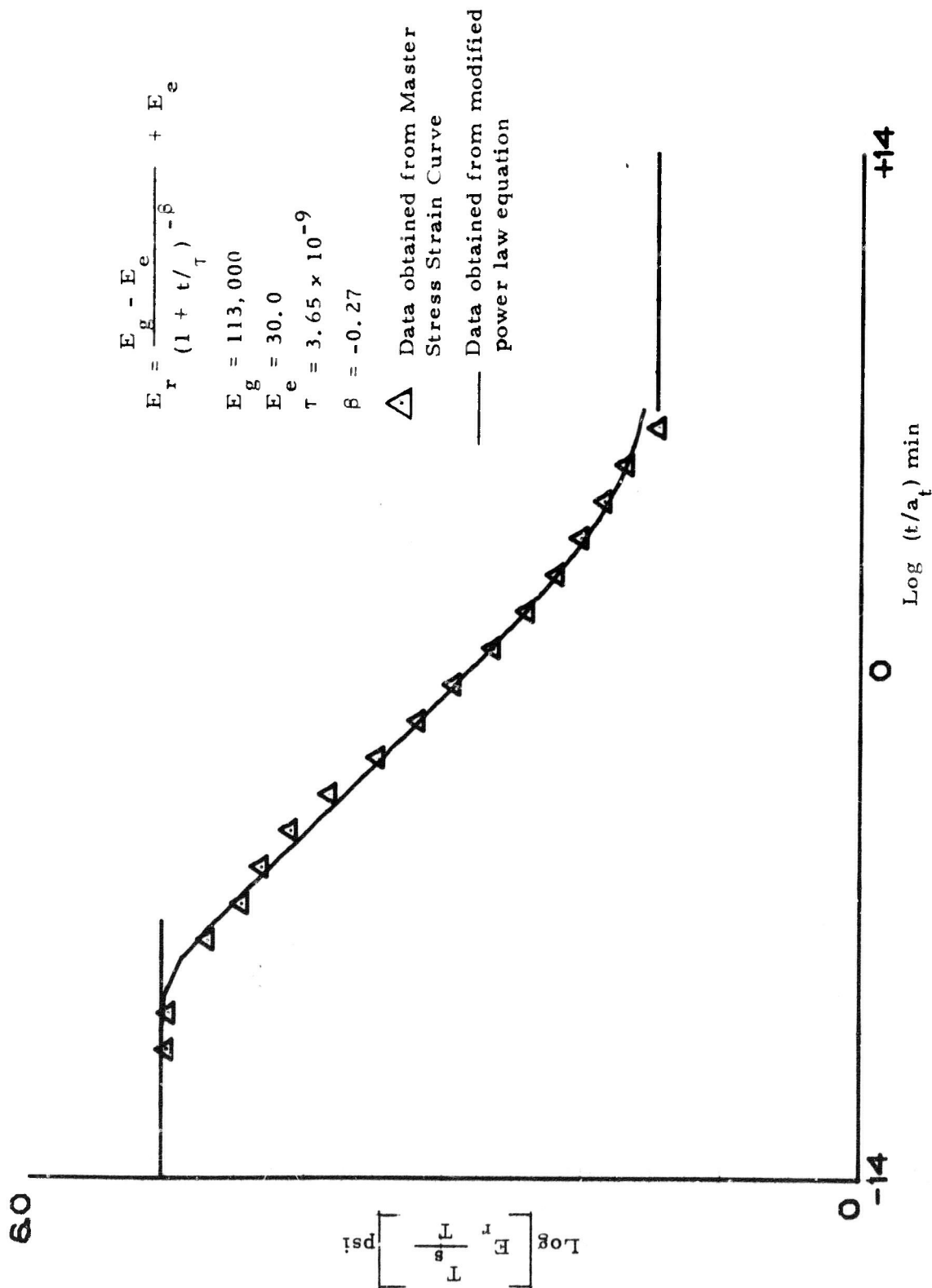
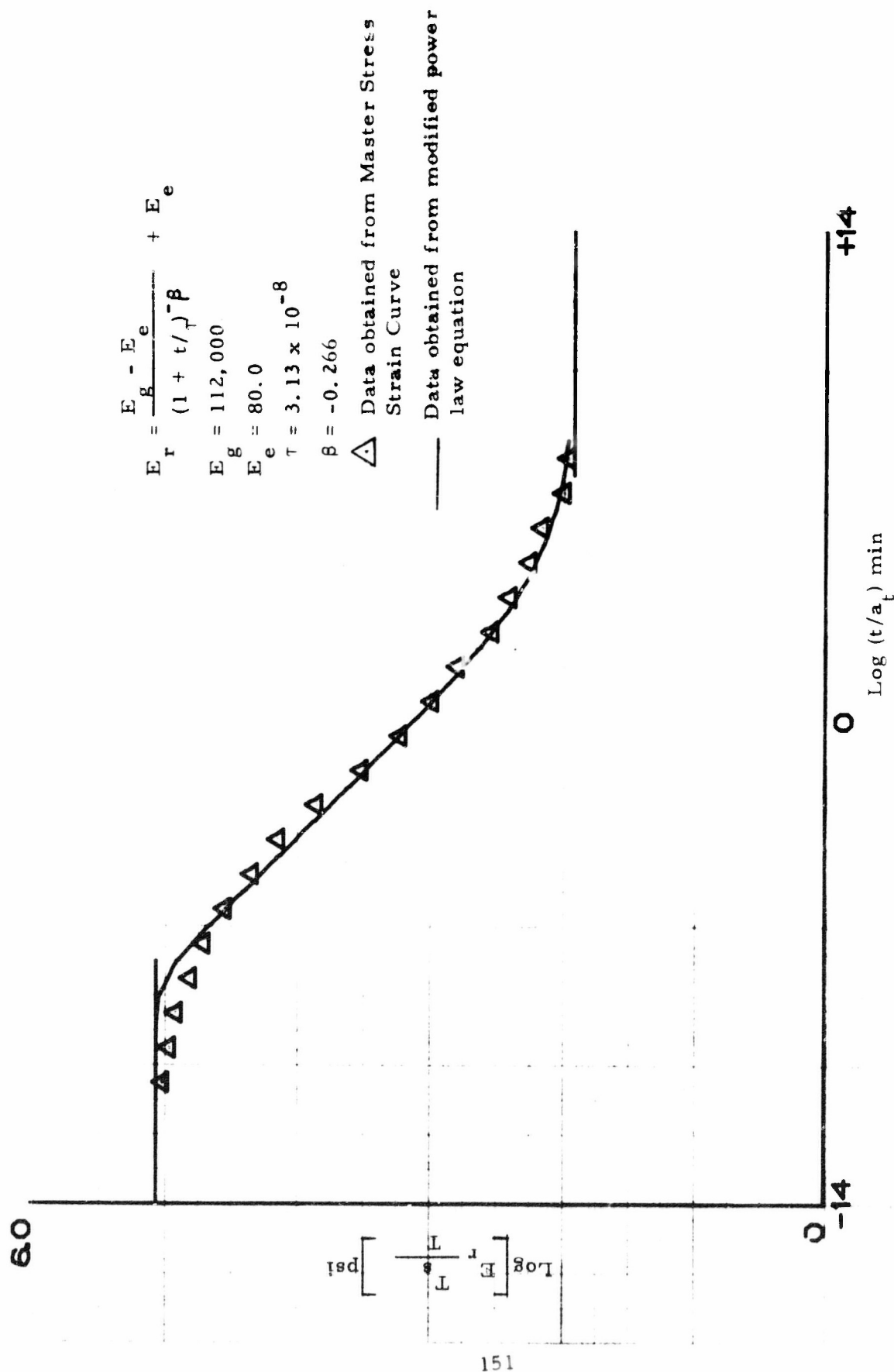


FIGURE 85. RELAXATION MODULUS - T-265 - P/P in CTPB (humidified)



Relaxation Modulus; TP-H7036, Mix T-266

FIGURE 86. RELAXATION MODULUS - T-266 - KM/P in CTPB (humidified)



Relaxation Modulus: TP-H8217, Mix T-271

FIGURE 87. RELAXATION MODULUS - T-271 - KM/KM in HTPB

60.

$$\log \left[\frac{E_r}{T_s} \right] \text{ psi}$$

0 -14

+14

 $\log (t/a_t) \text{ min}$

Relaxation Modulus; TP-H8217, Mix T-272

$$E_r = \frac{E_g - E_e}{(1 + t/\tau)^{-\beta}} + E_e$$

$$E_g = 112,000$$

$$E_e = 80.0$$

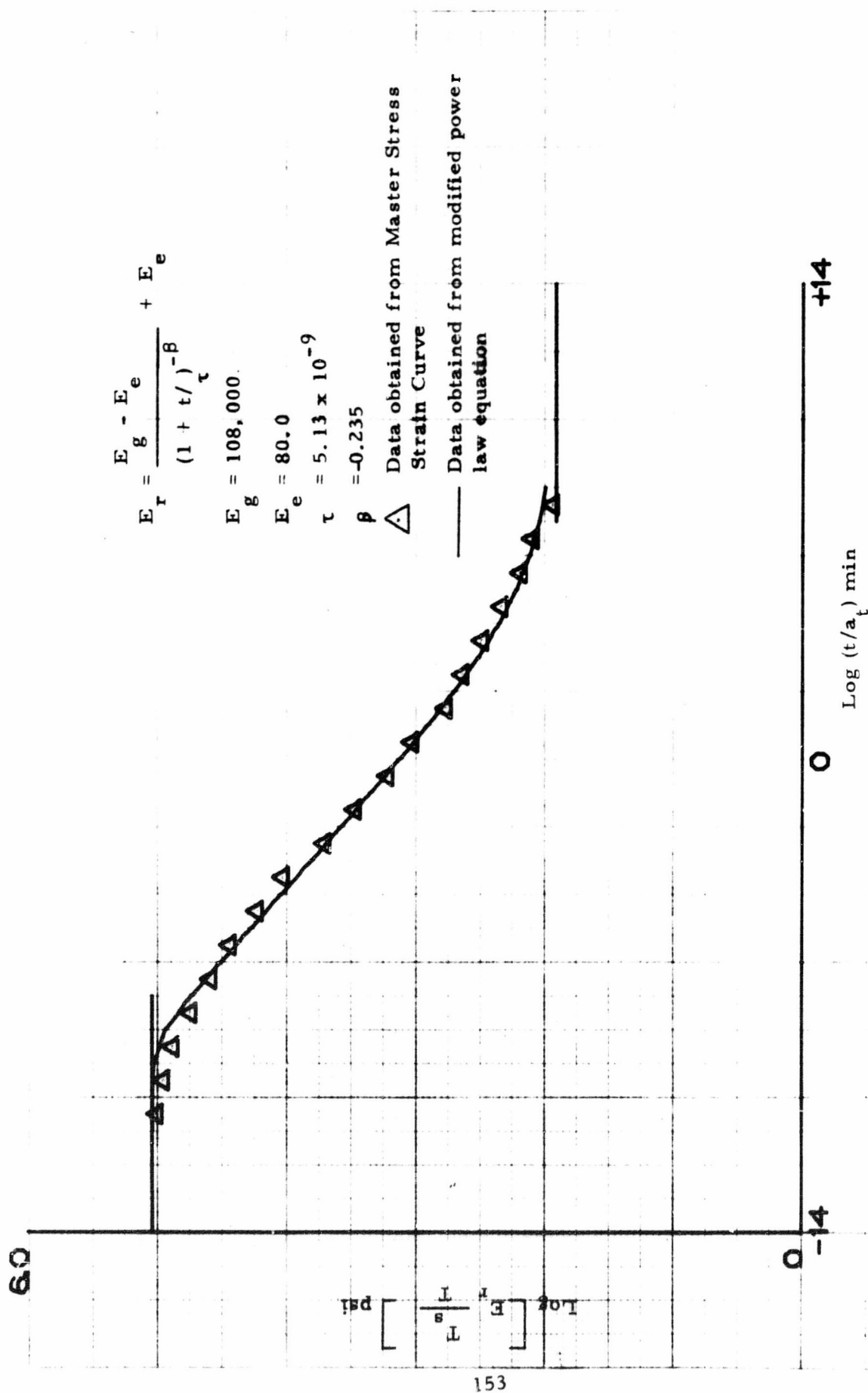
$$\tau = 3.87 \times 10^{-8}$$

$$\beta = -0.263$$

 \triangle Data obtained from Master Stress Strain Curve

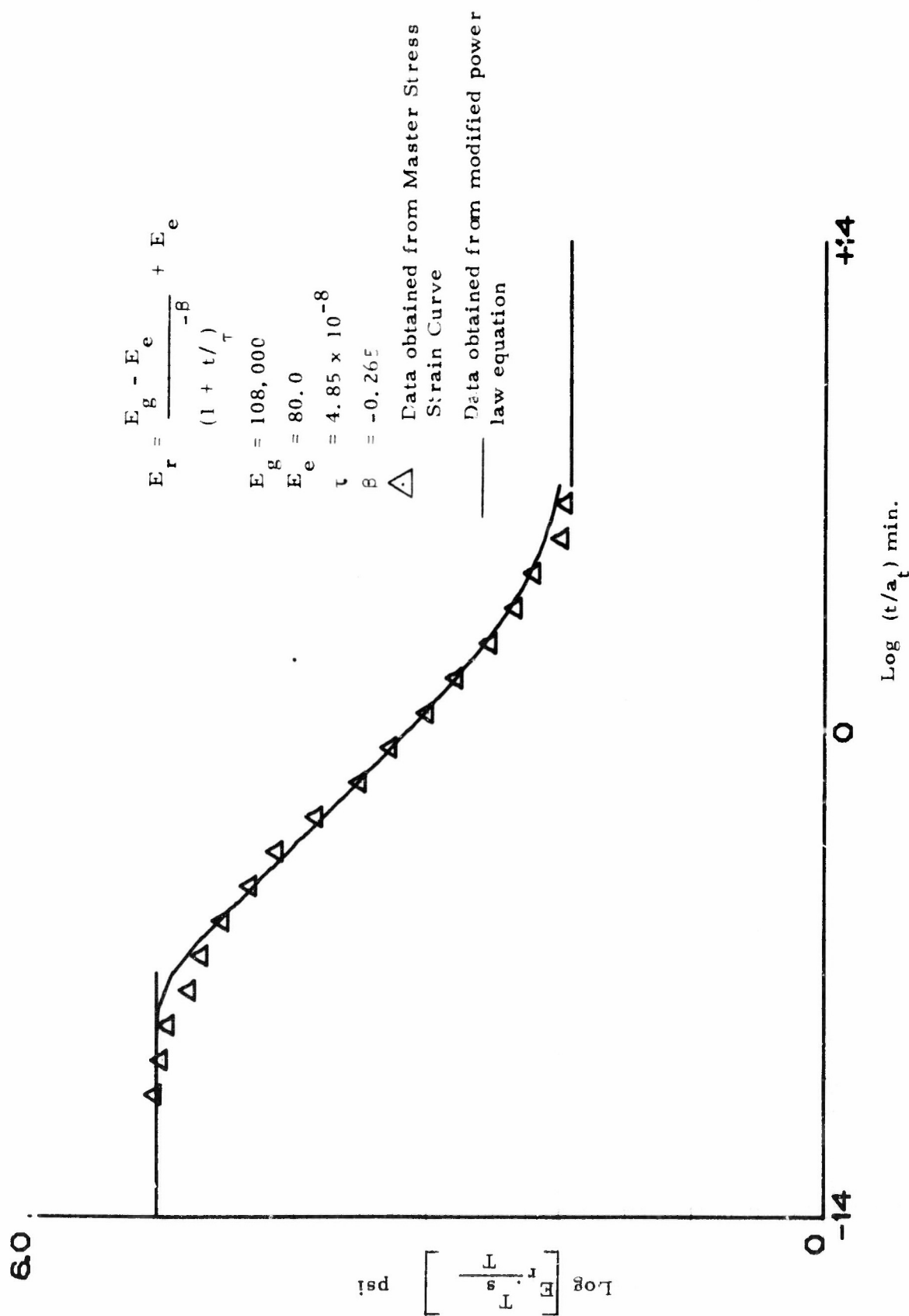
— Data obtained from modified power law equation

FIGURE 88. RELAXATION MODULUS - T-272 - KM/KM in HTPB

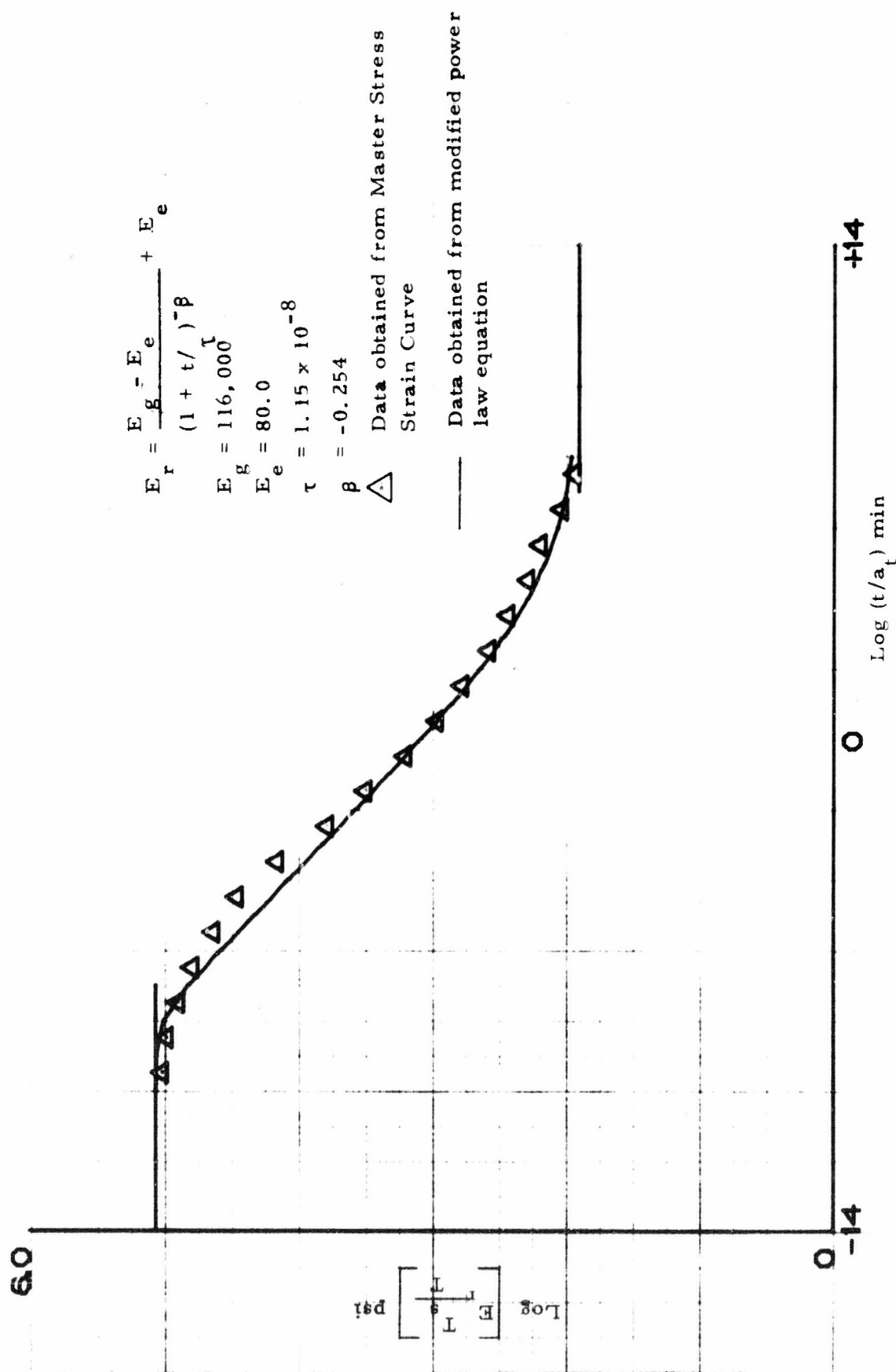


Relaxation Modulus; TP-H8217, Mix T-273

FIGURE 89. RELAXATION MODULUS - T-273 - P/P in HTPB



Relaxation Modulus; TP-H8217, Mix T-277
 FIGURE 90. RELAXATION MODULUS - T-277 - P/P in HTPB



Relaxation Modulus; TP-H8217, Mix T-278

FIGURE 91. RELAXATION MODULUS - T-278 - KM/P in HTPB

60

$$\text{Log} \left[\frac{E_r}{T_s} \right] \text{ psi}$$

156

0 -14

0

+14

Log (t/a_t) min

$$E_r = \frac{E_g - E_e}{(1 + t/\tau)^{-\beta}} + E_e$$

$$E_g = 116,000$$

$$E_e = 80.0$$

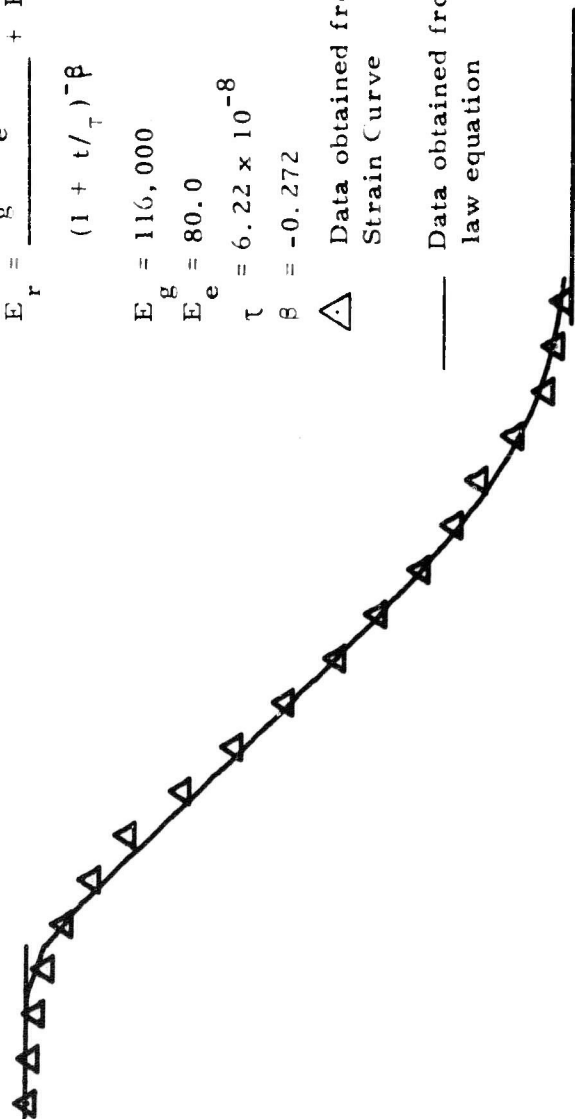
$$\tau = 6.22 \times 10^{-8}$$

$$\beta = -0.272$$



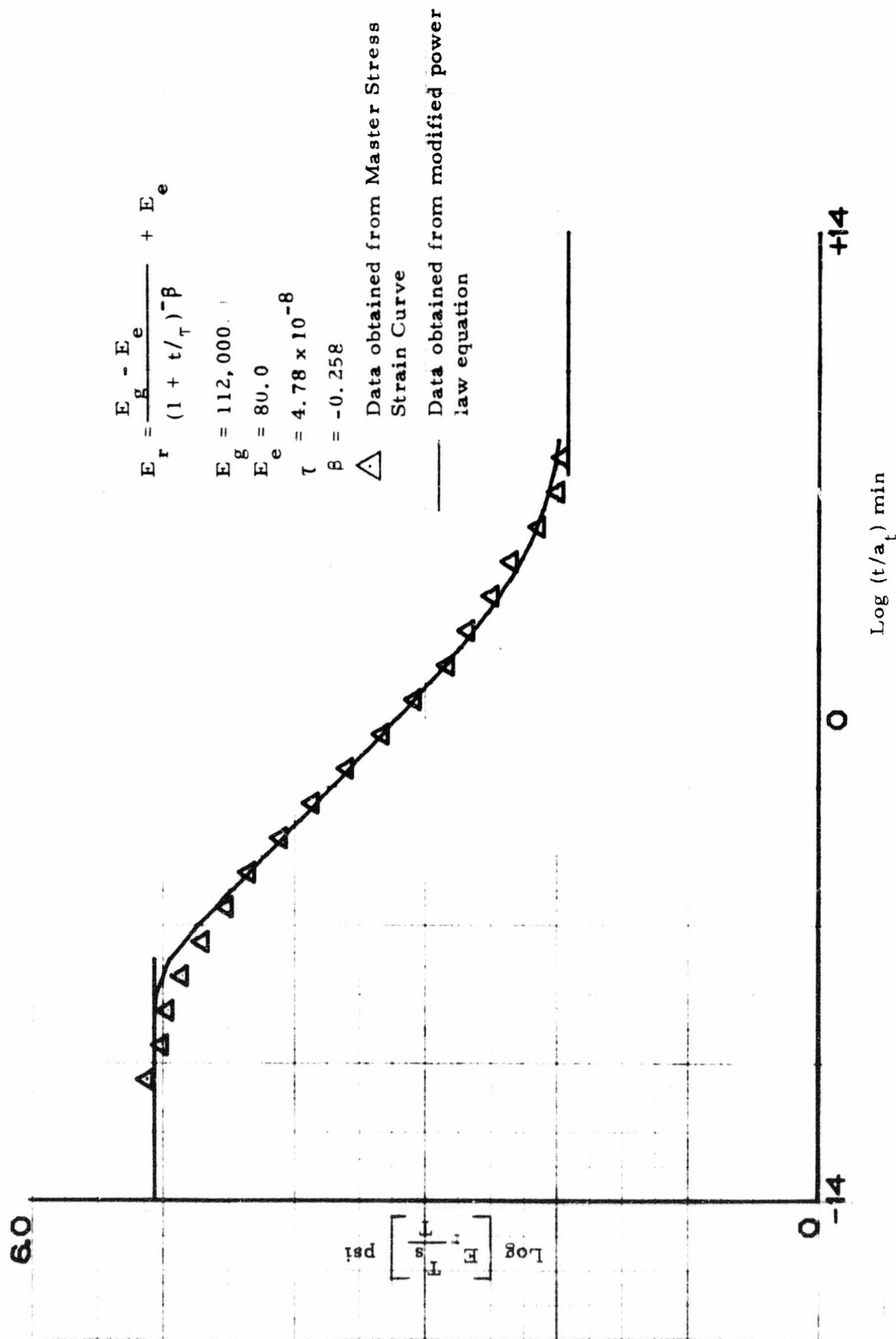
△ Data obtained from Master Stress Strain Curve

— Data obtained from modified power law equation



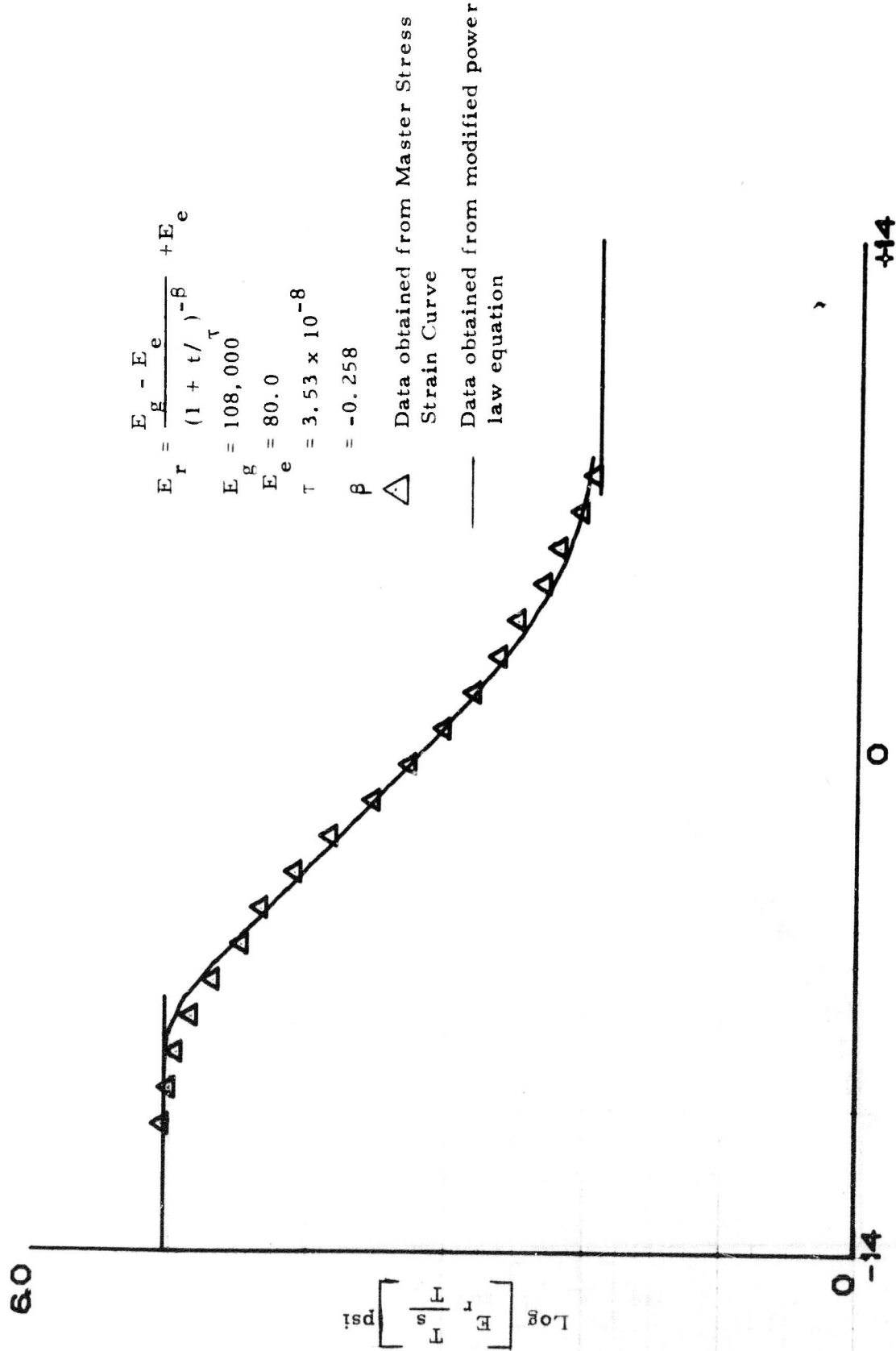
Relaxation Modulus; TP-H8217, Mix T-285

FIGURE 92. RELAXATION MODULUS - T-285 - KM/P in HTPB



Relaxation Modulus; TP-H8217, Mix T-274

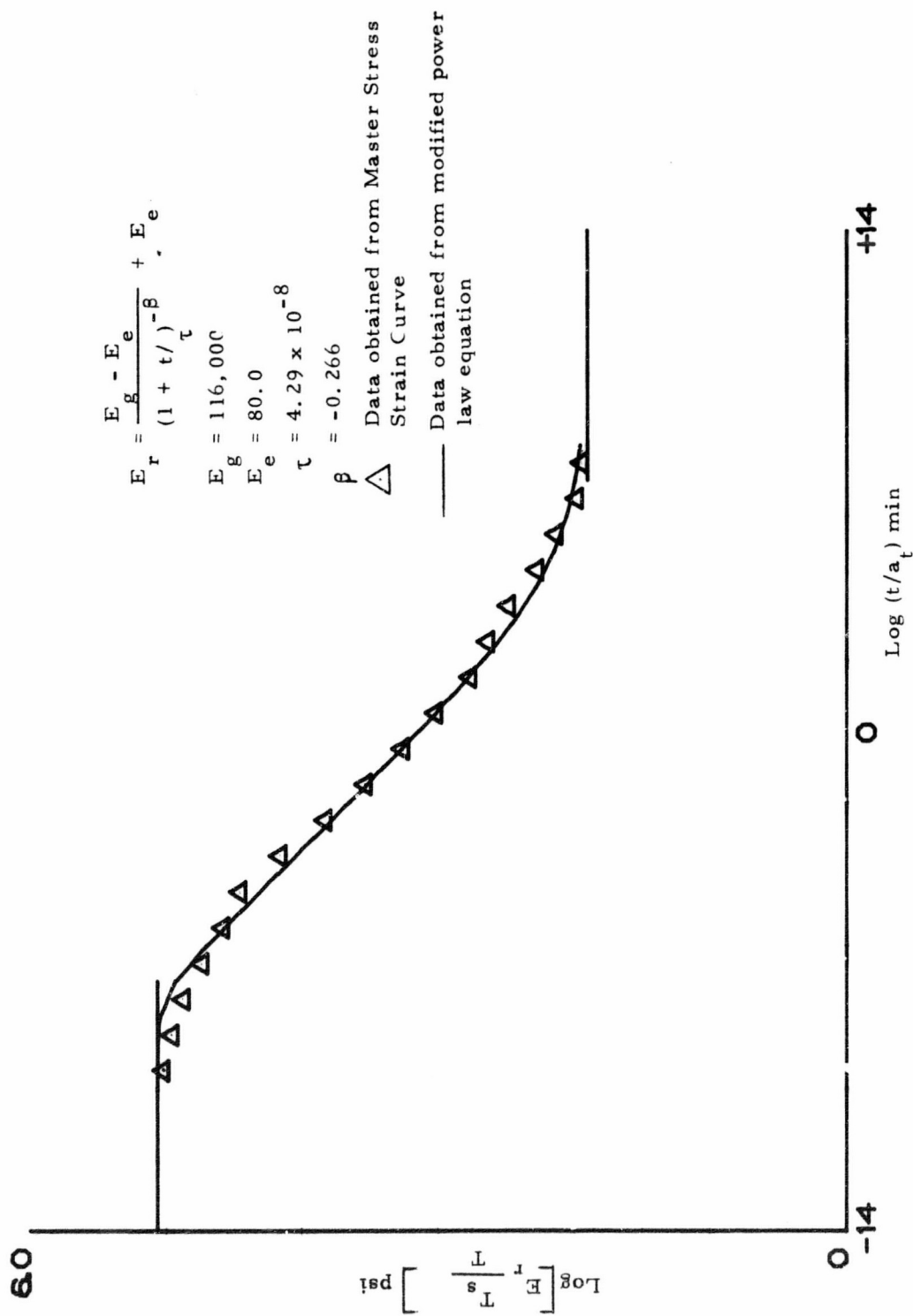
FIGURE 93. RELAXATION MODULUS - T-274 - KM/KM in HTPB (humidified)



Log (t/a_t) min

Relaxation Modulus; TP-H8217, Mix T-276

FIGURE 94. RELAXATION MODULUS - T-276 - P/P in HTPB (humidified)



Relaxation Modulus; TP-H8217, Mix T-275
 FIGURE 95. RELAXATION MODULUS - T-275 - KM/P in HTPB (humidified)

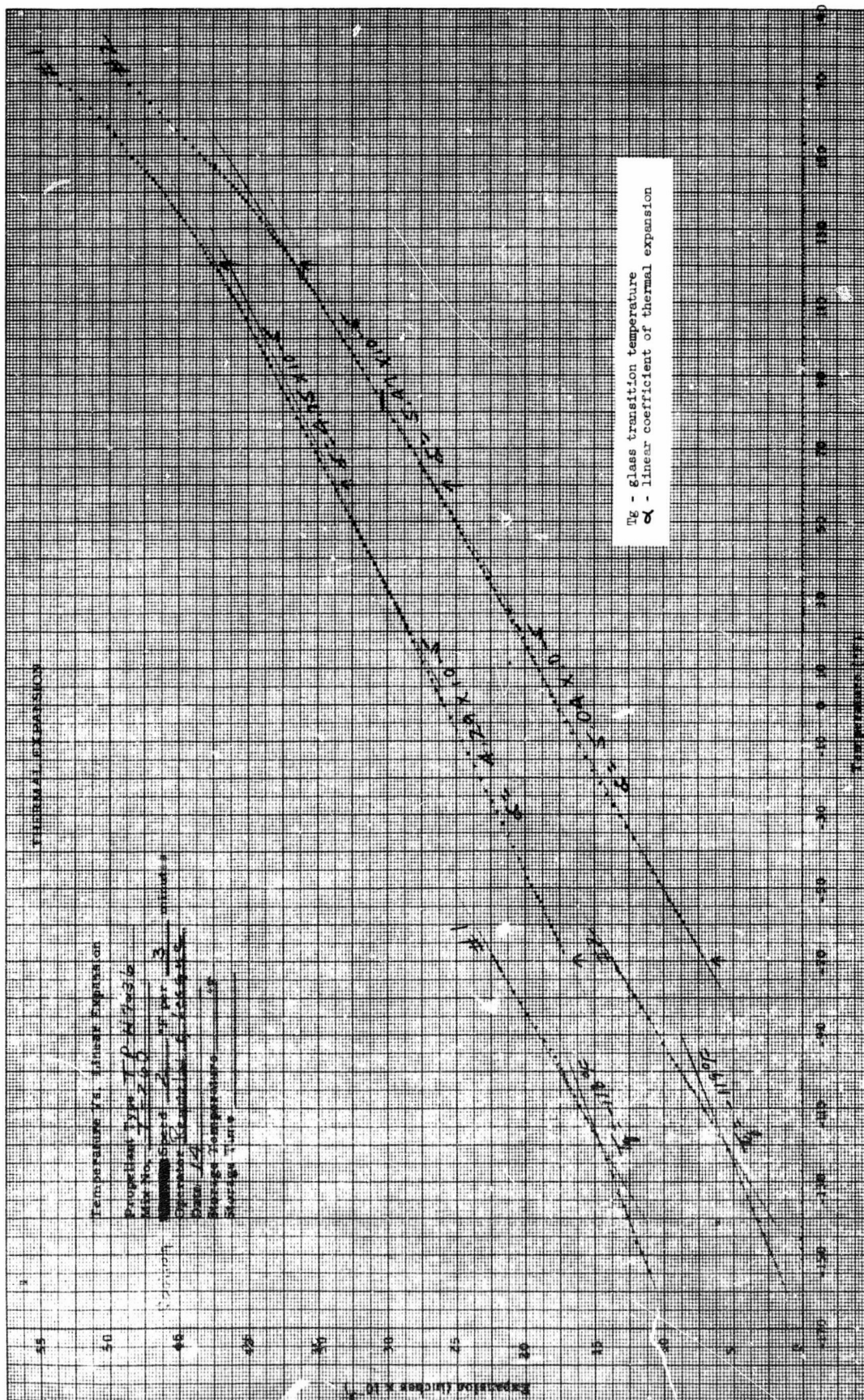


FIGURE 96. THERMAL EXPANSION DATA - T-260 - KM/KM in CTPB

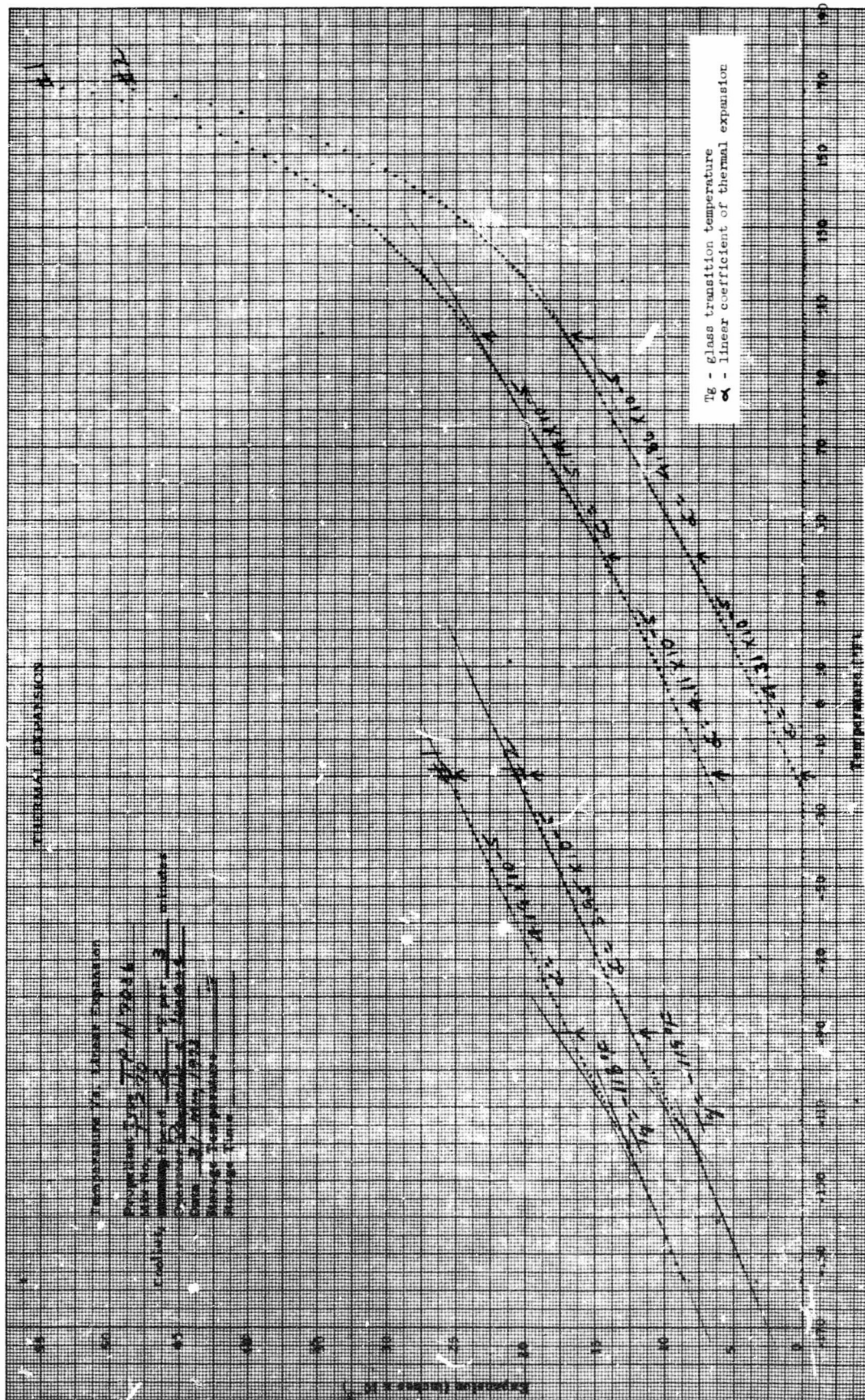


FIGURE 97. THERMAL EXPANSION DATA - T-270 - P/P in CTPB

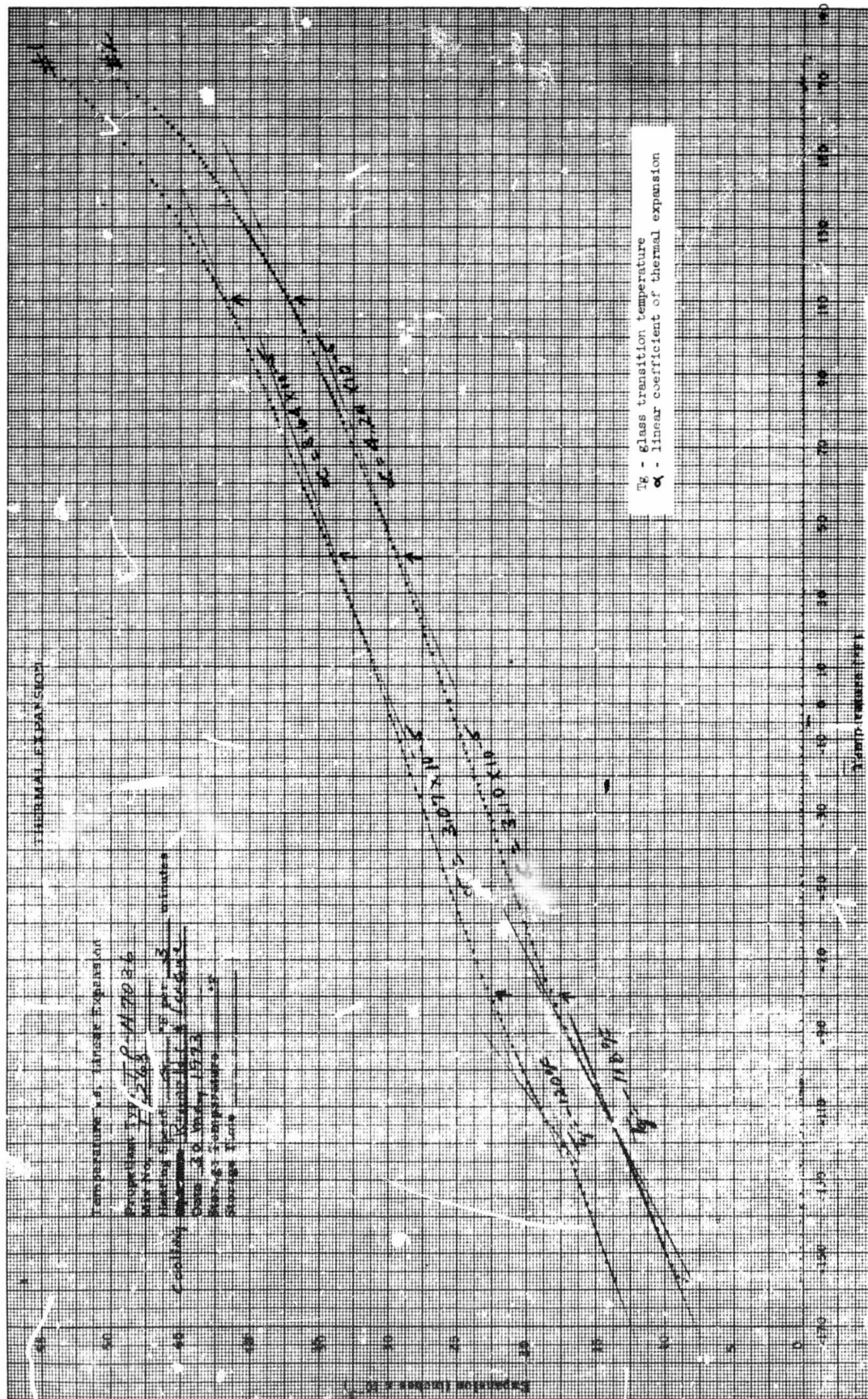


FIGURE 98. THERMAL EXPANSION DATA - T-268 - KM/P in CTPB

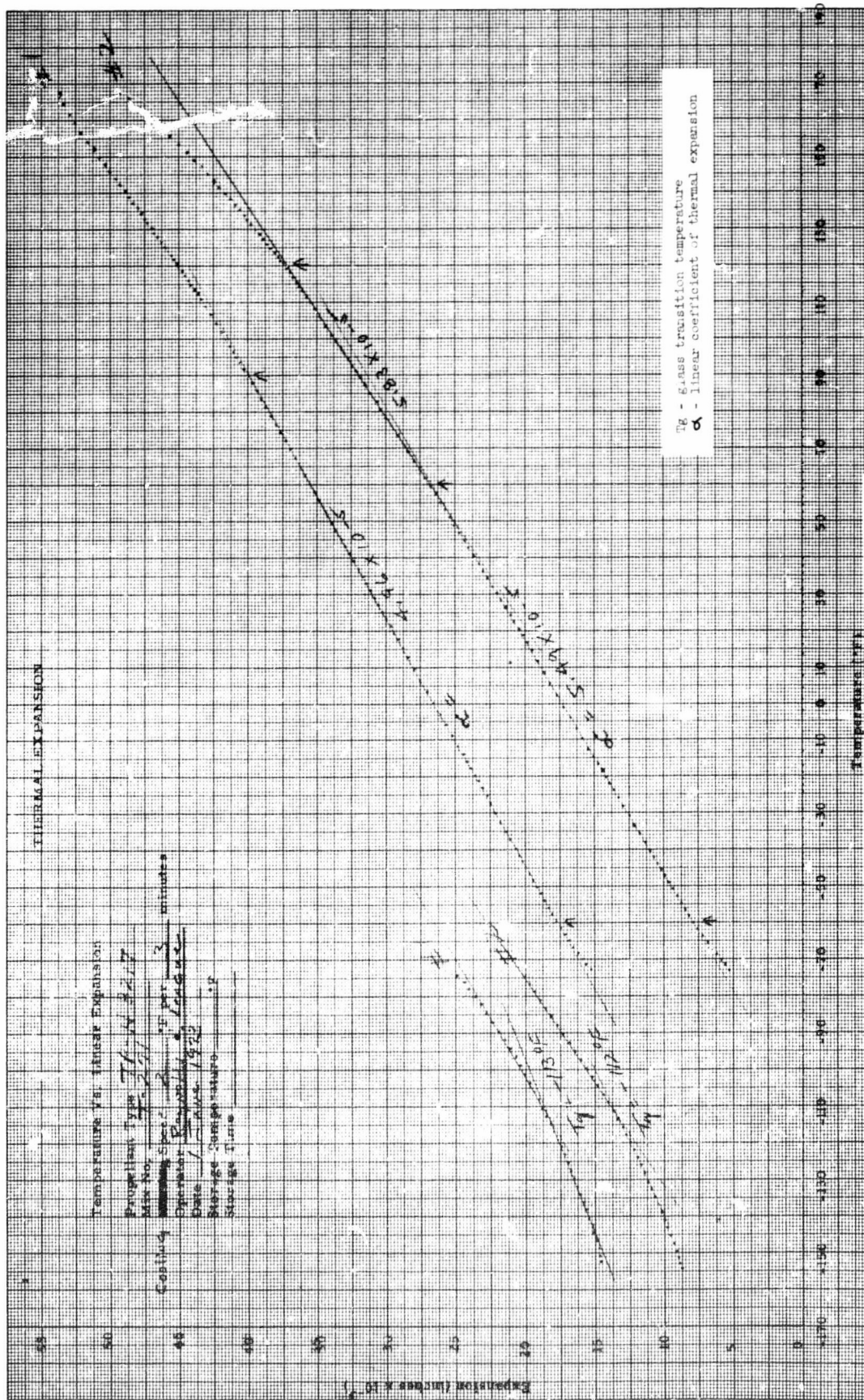


FIGURE 99. THERMAL EXPANSION DATA - T-271 - KM/KM in HTPB

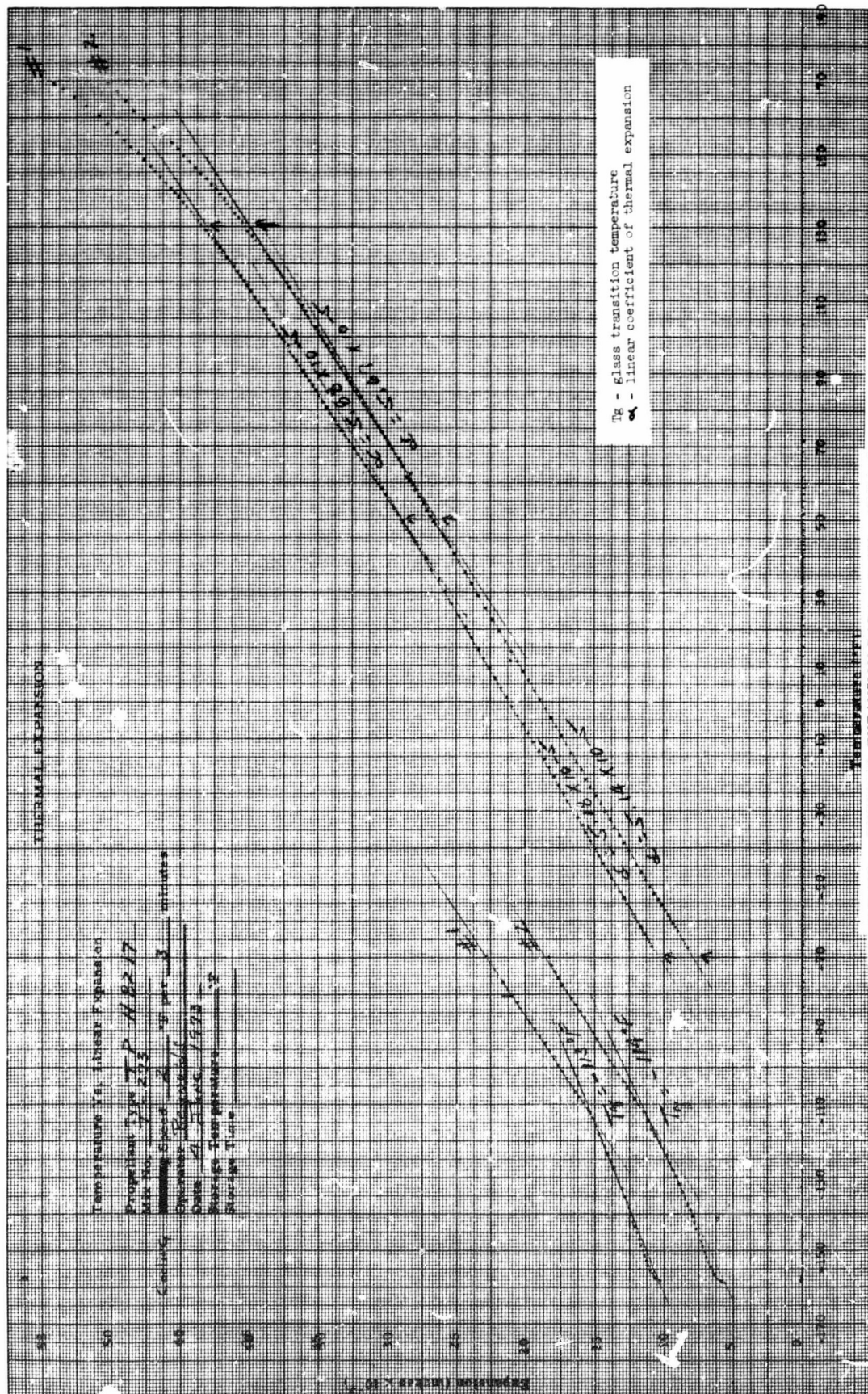


FIGURE 100. THERMAL EXPANSION DATA - T-273 - P/P in HTPB

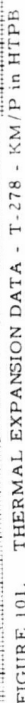


TABLE 47

| BIAXIAL TEST DATA | | |
|---|--|-------------|
| Temperature °F | Strain at Max. Stress T-260 (KM/KM in CTPB) | Max. Stress |
| 150 | .288 | 70 |
| 77 | .266 | 90 |
| 0 | .208 | 166 |
| -40 | .218 | 308 |
| -70 | .077 | 492 |
| <u>T-270 (P/P in CTPB)</u> | | |
| 150 | .282 | 37 |
| 77 | .168 | 47 |
| 0 | .193 | 109 |
| -40 | .083 | 235 |
| -70 | .077 | 380 |
| <u>T-268 (KM/P in CTPB)</u> | | |
| 150 | .285 | 34 |
| 77 | .236 | 48 |
| 0 | .181 | 117 |
| -40 | .117 | 212 |
| -70 | .092 | 324 |
| <u>T-264 (KM/KM in CTPB (humidified))</u> | | |
| 150 | .241 | 64 |
| 77 | .270 | 83 |
| 0 | .217 | 157 |
| -40 | .094 | 270 |
| -70 | - | - |
| <u>T-265 (P/P in CTPB (humidified))</u> | | |
| 150 | .275 | 31 |
| 77 | .210 | 44 |
| 0 | .170 | 101 |
| -40 | .091 | 208 |
| -70 | .065 | 362 |
| <u>T-266 (KM/P in CTPB (humidified))</u> | | |
| 150 | .297 | 34 |
| 77 | .270 | 35 |
| 0 | .196 | 108 |
| -40 | .103 | 215 |
| -70 | .060 | 416 |
| <u>T-271 (KM/KM in HTPB)</u> | | |
| 150 | .320 | 114 |
| 77 | .450 | 165 |
| 0 | .444 | 340 |
| -40 | .216 | 475 |
| -70 | .077 | 743 |
| <u>T-273 (P/P in HTPB)</u> | | |
| 150 | .396 | 117 |
| 77 | .434 | 166 |
| 0 | .448 | 343 |
| -40 | .238 | 465 |
| -70 | .079 | 604 |
| <u>T-278 (KM/P in HTPB)</u> | | |
| 150 | .360 | 113 |
| 77 | .550 | 169 |
| 0 | .643 | 358 |
| -40 | .457 | 651 |
| -70 | .057 | 850 |
| <u>T-274 (KM/KM in HTPB (humidified))</u> | | |
| 150 | .347 | 126 |
| 77 | .440 | 186 |
| 0 | .498 | 355 |
| -40 | .146 | 539 |
| -70 | .057 | 806 |
| <u>T-276 (P/P in HTPB (humidified))</u> | | |
| 150 | .352 | 110 |
| 77 | .519 | 180 |
| 0 | .504 | 331 |
| -40 | .259 | 414 |
| -70 | .069 | 760 |

TABLE 48
CUMULATIVE DAMAGE TESTS

T-260
KM/KM in CTPB

| Temp. °F | Head Speed in/min | σ @ Change | ϵ @ Change | σ Max. | ϵ @ σ Max. |
|-------------|----------------------|-------------------|---------------------|---------------|----------------------------|
| 150 | 0.2-2.0 | 7.6 | .135 | 13.9 | .271 |
| | | 8.4 | .146 | 76.8 | .256 |
| | 2.0-20.0 | 53 | .140 | 91 | .254 |
| | | 57 | .141 | 97 | .268 |
| | 20.0-2.0 | 66 | .126 | 70 | .284 |
| | | 64 | .116 | 70 | .256 |
| | 2.0-0.2 | Chart | Pen | Off | |
| | | 51 | .134 | 57 | .295 |
| | 0.2-2.0 | 58 | .131 | 100 | .269 |
| | | 59 | .135 | 102 | .259 |
| | 2.0-20.0 | 73 | .132 | 129 | .256 |
| | | 76 | .134 | 132 | .243 |
| 77 | 0.2-2.0 | 105 | .126 | 92 | .262 |
| | | 107 | .129 | 97 | .285 |
| | 2.0-20.0 | 74 | .134 | 75 | .280 |
| | | 71 | .134 | 74 | .276 |
| | 0.2-2.0 | 96 | .117 | 176 | .204 |
| | | 94 | .110 | 186 | .230 |
| | 2.0-20.0 | 140 | .106 | 278 | .195 |
| | | 134 | .103 | 267 | .187 |
| | 20.0-2.0 | 207 | .084 | 163 | .287 |
| | | 194 | .091 | 155 | .289 |
| | 2.0-0.2 | 155 | .103 | 131 | .298 |
| | | 141 | .101 | 129 | .285 |
| 0 | 0.2-2.0 | 96 | .117 | 176 | .204 |
| | | 94 | .110 | 186 | .230 |
| | 2.0-20.0 | 140 | .106 | 278 | .195 |
| | | 134 | .103 | 267 | .187 |
| | 20.0-2.0 | 207 | .084 | 163 | .287 |
| | | 194 | .091 | 155 | .289 |
| | 2.0-0.2 | 155 | .103 | 131 | .298 |
| | | 141 | .101 | 129 | .285 |
| | 0.2-2.0 | 96 | .117 | 176 | .204 |
| | | 94 | .110 | 186 | .230 |
| | 2.0-20.0 | 140 | .106 | 278 | .195 |
| | | 134 | .103 | 267 | .187 |

TABLE 49

CUMULATIVE DAMAGE TESTS

T-270
P/P in CTPB

| Temp. °F | Head Speed in/min | δ @ Change | ϵ @ Change | δ Max. | ϵ @ δ Max. |
|-------------|----------------------|-------------------|---------------------|---------------|----------------------------|
| 150 | 0.2 - 2.0 | 19 | .151 | 37 | .272 |
| | | 20 | .154 | 38 | .289 |
| | 2.0 - 20.0 | 24 | .136 | 49 | .282 |
| | | 23 | .130 | 49 | .245 |
| | 20.0 - 2.0 | 28 | .110 | 33 | .308 |
| | | 31 | .113 | 31 | .242 |
| | 2.0 - 0.2 | 22 | .130 | 25 | .287 |
| | | 24 | .134 | 21 | .196 |
| 77 | 0.2 - 2.0 | 29 | .136 | 55 | .247 |
| | | 28 | .134 | 53 | .232 |
| | 2.0 - 20.0 | 41 | .136 | 76 | .180 |
| | | 35 | .124 | 75 | .250 |
| | 20.0 - 2.0 | 57 | .114 | 51 | .298 |
| | | 58 | .111 | 48 | .264 |
| | 2.0 - 0.2 | 38 | .133 | 34 | .219 |
| | | 35 | .119 | 37 | .284 |
| 0 | 0.2 - 2.0 | 58 | .121 | 118 | .197 |
| | | 55 | .120 | 121 | .213 |
| | 2.0 - 20.0 | 87 | .098 | 185 | .157 |
| | | 93 | .104 | 191 | .170 |
| | 20.0 - 2.0 | 159 | .088 | 98 | .236 |
| | | 138 | .095 | 86 | .260 |
| | 2.0 - 0.2 | 84 | .099 | 69 | .294 |
| | | 82 | .103 | 66 | .266 |

TABLE 50
CUMULATIVE DAMAGE TESTS

T-268
KM/P in CTPB

| Temp. °F | Head Speed in/min | δ @ Change | ϵ @ Change | δ Max. | ϵ @ δ Max. |
|-------------|----------------------|-------------------|---------------------|---------------|----------------------------|
| 150 | 0.2-2.0 | 18 | .148 | 38 | .293 |
| | | 20 | .150 | 38 | .283 |
| | 2.0-20.0 | 23 | .130 | 50 | .278 |
| | | 24 | .133 | 51 | .266 |
| | 20.0-2.0 | 31 | .121 | 35 | .296 |
| | | 25 | .114 | 34 | .320 |
| | 2.0-0.2 | 19 | .133 | 28 | .304 |
| | | 20 | .129 | 27 | .328 |
| 77 | 0.2-2.0 | 29 | .142 | 49 | .192 |
| | | 27 | .135 | 56 | .274 |
| | 2.0-20.0 | 37 | .122 | 79 | .241 |
| | | 39 | .136 | 78 | .213 |
| | 20.0-2.0 | 58 | .114 | 49 | .318 |
| | | 60 | .111 | 48 | .170 |
| | 2.0-0.2 | 37 | .134 | 36 | .273 |
| | | 38 | .131 | 37 | .315 |
| 0 | 0.2-2.0 | 60 | .114 | 126 | .189 |
| | | 59 | .118 | 124 | .186 |
| | 2.0-20.0 | 109 | .116 | 229 | .196 |
| | | 96 | .105 | off scale | |
| | 20.0-2.0 | 151 | .091 | 92 | .254 |
| | | 149 | .091 | 96 | .250 |
| | 2.0-0.2 | 92 | .101 | 71 | .310 |
| | | 90 | .098 | 73 | .259 |

TABLE 51

CUMULATIVE DAMAGE TESTS

9-264

CTPB in CTPB(humidified)

| Temp. F | Head Speed in/min | σ @ Change | ϵ @ Change | σ Max. | ϵ @ Max. |
|------------|----------------------|-------------------|---------------------|---------------|-------------------|
| 150 | 0.2-2.0 | 39 | .149 | 66 | .276 |
| | | 38 | .144 | 65 | .258 |
| | 2.0-20.0 | 47 | .131 | 83 | .267 |
| | | 43 | .129 | 81 | .290 |
| | 20.0-2.0 | 56 | .129 | 59 | .284 |
| | | 56 | .129 | 60 | .306 |
| | 2.0-0.2 | 35 | .130 | 53 | .285 |
| | | 35 | .130 | 49 | .273 |
| | 0.2-2.0 | 52 | .138 | 89 | .264 |
| | | 52 | .119 | 90 | .225 |
| 177 | 2.0-20.0 | 65 | .139 | 117 | .250 |
| | | 64 | .134 | 114 | .215 |
| | 20.0-2.0 | 92 | .120 | 80 | .273 |
| | | 97 | .139 | 80 | .275 |
| | 2.0-0.2 | 63 | .128 | 64 | .301 |
| | | 64 | .133 | 63 | .288 |
| | 0.2-2.0 | 89 | .117 | 166 | .180 |
| | | 92 | .118 | 169 | .200 |
| | 2.0-20.0 | 123 | .108 | 246 | .184 |
| | | 119 | .103 | 238 | .152 |
| 0 | 20.0-2.0 | 191 | .084 | 140 | .309 |
| | | 197 | .088 | 140 | .286 |
| | 2.0-0.2 | 134 | .106 | 109 | .286 |
| | | 134 | .102 | 110 | .291 |

TABLE 52

CUMULATIVE DAMAGE TESTS

T-265

P/P in CTPB(humidified)

| Temp. °F | Head Speed in/min | σ @ Change | ϵ @ Change | σ Max. | ϵ @ σ Max. |
|-------------|----------------------|-------------------|---------------------|---------------|----------------------------|
| 150 | 0.2-2.0 | 15 | .144 | 29 | .275 |
| | | 16 | .148 | 32 | .286 |
| | 2.0-20.0 | 18 | .121 | 42 | .294 |
| | | 20 | .128 | 44 | .288 |
| | 20.0-2.0 | 28 | .139 | 27 | .319 |
| | | 27 | .125 | 28 | .298 |
| | 2.0-0.2 | 19 | .134 | 22 | .312 |
| | | 13 | .119 | 23 | .317 |
| | 0.2-2.0 | 23 | .133 | 48 | .250 |
| | | 23 | .134 | 46 | .288 |
| 77 | 2.0-20.0 | 31 | .126 | 64 | .219 |
| | | 25 | .138 | 67 | .244 |
| | 20.0-2.0 | 51 | .120 | 42 | .277 |
| | | 52 | .121 | 41 | .289 |
| | 2.0-0.2 | 32 | .138 | 30 | .307 |
| | | 31 | .132 | 32 | .304 |
| | 0.2-2.0 | 55 | .120 | 117 | .199 |
| | | 53 | .119 | 113 | .181 |
| | 2.0-20.0 | 75 | .100 | 165 | .183 |
| | | 76 | .106 | 170 | .209 |
| 0 | 20.0-2.0 | 141 | .095 | 84 | .284 |
| | | 136 | .091 | 83 | .285 |
| | 2.0-0.2 | 77 | .097 | 58 | .268 |
| | | 73 | .102 | 61 | .287 |

TABLE 53

CUMULATIVE DAMAGE TESTS

T-266
KM/P in CTPB(humidified)

| Temp. °F | Head Speed in/min | σ @ Change | ϵ @ Change | σ Max. | ϵ @ σ Max. |
|-------------|----------------------|-------------------|---------------------|---------------|----------------------------|
| 150 | 0.2-2.0 | 19 | .148 | 36 | .280 |
| | | 16 | .174 | 34 | .345 |
| | 2.0-20.0 | 21 | .131 | 46 | .302 |
| | | 22 | .132 | 47 | .264 |
| | 20.0-2.0 | 30 | .127 | 30 | .318 |
| | | 27 | .126 | 31 | .337 |
| | 2.0-0.2 | 21 | .135 | 24 | .349 |
| | | 18 | .129 | 22 | .377 |
| 77 | 0.2-2.0 | 26 | .136 | 52 | .272 |
| | | 28 | .134 | 54 | .255 |
| | 2.0-20.0 | 36 | .136 | 75 | .247 |
| | | 33 | .121 | 73 | .224 |
| | 20.0-2.0 | 59 | .114 | 46 | .266 |
| | | 62 | .126 | 47 | .173 |
| | 2.0-0.2 | 39 | .136 | 36 | .311 |
| | | 37 | .123 | 36 | .294 |
| 0 | 0.2-2.0 | 61 | .116 | 123 | .191 |
| | | 64 | .121 | 125 | .179 |
| | 2.0-20.0 | 100 | .103 | 191 | .172 |
| | | 99 | .104 | 203 | .186 |
| | 20.0-2.0 | 154 | .089 | 91 | .258 |
| | | 148 | .088 | 89 | .251 |
| | 2.0-0.2 | 96 | .105 | 69 | .299 |
| | | 98 | .103 | 70 | .318 |

TABLE 54

CUMULATIVE DAMAGE TESTS

T-271
 3M/KM in HTPB

| Temp. °F | Head Speed in/min | σ @ Change | ϵ @ Change | τ Max. | ϵ @ τ Max. |
|-------------|----------------------|-------------------|---------------------|-------------|--------------------------|
| -40 | 0.2 - 2.0 | 68 | .169 | 120 | .384 |
| | | 67 | .169 | 118 | .395 |
| | 2.0 - 20.0 | 89 | .195 | 147 | .406 |
| | | 88 | .209 | 136 | .343 |
| | 20.0 - 2.0 | 109 | .201 | 117 | .397 |
| | | 109 | .196 | 114 | .377 |
| | 2.0 - 0.2 | 84 | .214 | 96 | .427 |
| | | 85 | .204 | 95 | .406 |
| | 0.2 - 2.0 | 103 | .219 | 156 | .363 |
| | | 102 | .213 | 163 | .416 |
| -20 | 2.0 - 20.0 | 122 | .210 | 213 | .439 |
| | | 121 | .212 | 202 | .463 |
| | 20.0 - 2.0 | 159 | .197 | 163 | .478 |
| | | 157 | .183 | 157 | .474 |
| | 2.0 - 0.2 | 115 | .202 | 134 | .480 |
| | | 121 | .208 | 126 | .426 |
| 0 | 0.2 - 2.0 | 215 | .239 | 359 | .368 |
| | | 214 | .231 | 364 | .465 |
| | 2.0 - 20.0 | 268 | .241 | 460 | .328 |
| | | 276 | .251 | 480 | .387 |
| | 20.0 - 2.0 | 385 | .233 | 324 | .541 |
| | | 381 | .247 | 307 | .501 |
| | 2.0 - 0.2 | 279 | .251 | 224 | .491 |
| | | 252 | .251 | 230 | .476 |

TABLE 55

CUMULATIVE DAMAGE TESTS

T-273
P/P in HTPB

| Temp. °F | Head Speed in/min | σ @ Change | ϵ @ Change | σ Max. | ϵ @ σ Max. |
|-------------|----------------------|-------------------|---------------------|---------------|----------------------------|
| 150 | 0.2 - 2.0 | 51 | .192 | 74 | .245 |
| | | 53 | .198 | 78 | .253 |
| | 2.0 - 20.0 | 68 | .207 | 102 | .276 |
| | | 68 | .190 | 99 | .267 |
| | 20.0 - 2.0 | 85 | .221 | 67 | .225 |
| | | 85 | .217 | 62 | .247 |
| | 2.0 - 0.2 | 65 | .206 | 53 | .287 |
| | | 65 | .200 | 55 | .277 |
| 77 | 0.2 - 2.0 | 67 | .213 | 161 | .412 |
| | | 98 | .210 | 164 | .444 |
| | 2.0 - 20.0 | 121 | .209 | 209 | .466 |
| | | 116 | .209 | 206 | .473 |
| | 20.0 - 2.0 | 153 | .187 | 152 | .418 |
| | | 158 | .200 | 157 | .450 |
| | 2.0 - 0.2 | 115 | .209 | 121 | .433 |
| | | 98 | 0.21 | 118 | .364 |
| 0 | 0.2 - 2.0 | 199 | .235 | 337 | .438 |
| | | 192 | .234 | 326 | .355 |
| | 2.0 - 20.0 | 257 | .240 | 456 | .473 |
| | | 264 | .253 | 452 | .394 |
| | 20.0 - 2.0 | 366 | .258 | 300 | .507 |
| | | 357 | .229 | 289 | .459 |
| | 2.0 - 0.2 | 268 | .254 | 229 | .455 |
| | | 266 | .249 | 229 | .499 |

TABLE 56

CUMULATIVE DAMAGE TESTS

T-278
KM/P in HTPB

| Temp °F | Head Speed in/min | σ @ Change | ϵ @ Change | σ Max. | ϵ @ σ Max. |
|------------|----------------------|-------------------|---------------------|------------------------|----------------------------|
| 150 | 0.2 - 2.0 | 51 | .142 | 120 | .442 |
| | | 77 | .220 | 111 | .357 |
| | 2.0 - 20.0 | 85 | .198 | 146 | .463 |
| | | 85 | .201 | 148 | .450 |
| | 20.0 - 2.0 | 96 | .227 | (Spec. broke @ change) | |
| | | 109 | .222 | 96 | .227 |
| | 2.0 - 0.2 | 81 | .191 | 113 | .400 |
| | | 83 | .204 | 100 | .424 |
| | | | | 94 | .383 |
| | | | | | |
| 77 | 0.2 - 2.0 | 96 | .211 | 159 | .460 |
| | | 100 | .212 | 159 | .446 |
| | 2.0 - 20.0 | 116 | .210 | 191 | .381 |
| | | 116 | .218 | 209 | .514 |
| | 20.0 - 2.0 | 151 | .194 | 128 | .346 |
| | | 156 | .194 | 158 | .469 |
| | 2.0 - 0.2 | 118 | .210 | 128 | .491 |
| | | 118 | .208 | 126 | .472 |
| | | | | | |
| | | | | | |
| 0 | 0.2 - 2.0 | 191 | .236 | 318 | .399 |
| | | 189 | .233 | 319 | .327 |
| | 2.0 - 20.0 | 271 | .257 | 478 | .463 |
| | | 259 | .252 | 470 | .507 |
| | 20.0 - 2.0 | 362 | .256 | 301 | .533 |
| | | 363 | .254 | 304 | .564 |
| | 2.0 - 0.2 | 283 | .246 | 255 | .537 |
| | | 293 | .256 | 234 | .488 |
| | | | | | |
| | | | | | |

TABLE 57

CUMULATIVE DAMAGE TESTS

T-274

KM/KM in HTPB(humidified)

| Temp °F | Head Speed in/min | τ @ Change | ϵ @ Change | τ Max. | ϵ @ τ Max. |
|------------|----------------------|-----------------|---------------------|-------------|--------------------------|
| 150 | 0.2-2.0 | 67 | .148 | 129 | .392 |
| | | 77 | .173 | 127 | .372 |
| | 2.0-20.0 | 99 | .191 | 157 | .384 |
| | | 103 | .210 | 163 | .409 |
| | 20.0-2.0 | 125 | .221 | 119 | .367 |
| | | 124 | .214 | 116 | .334 |
| | 2.0-0.2 | 96 | .208 | 103 | .382 |
| | | 91 | .193 | 101 | .387 |
| | 0.2-2.0 | 108 | .205 | 174 | .430 |
| | | 112 | .214 | 181 | .454 |
| 77 | 2.0-20.0 | 130 | .213 | 218 | .446 |
| | | 138 | .220 | 221 | .417 |
| | 20.0-2.0 | 180 | .203 | 170 | .436 |
| | | 178 | .199 | 174 | .456 |
| | 2.0-0.2 | 131 | .208 | 138 | .433 |
| | | 131 | .209 | 135 | .416 |
| | 0.2-2.0 | 209 | .223 | 352 | .430 |
| | | 212 | .237 | 350 | .423 |
| | 2.0-20.0 | 281 | .255 | 486 | .403 |
| | | 282 | .256 | 486 | .402 |
| 0 | 20.0-2.0 | 391 | .257 | 326 | .516 |
| | | 380 | .230 | 323 | .543 |
| | 2.0-0.2 | 266 | .249 | 242 | .477 |
| | | 288 | .254 | 230 | .459 |

TABLE 58

CUMULATIVE DAMAGE TESTS

T-276
P/P in HTPB(humidified)

| Temp. °F | Head Speed in/min | σ @ Change | ϵ @ Change | σ Max. | ϵ @ σ Max. |
|-------------|----------------------|-------------------|---------------------|---------------|----------------------------|
| 150 | 0.2 - 2.0 | 60 | .147 | 120 | .422 |
| | | 77 | .214 | 122 | .404 |
| | 2.0 - 20.0 | 83 | .196 | 142 | .480 |
| | | 84 | .198 | 143 | .450 |
| | 20.0 - 2.0 | 104 | .219 | 103 | .375 |
| | | 108 | .221 | 109 | .388 |
| | 2.0 - 0.2 | 84 | .202 | 97 | .420 |
| | | 85 | .207 | 93 | .374 |
| | | | | | |
| | | | | | |
| 77 | 0.2 - 2.0 | 96 | .210 | 166 | .486 |
| | | 97 | .209 | 166 | .467 |
| | 2.0 - 20.0 | 120 | .213 | 211 | .456 |
| | | 119 | .204 | 214 | .503 |
| | 20.0 - 2.0 | 157 | .193 | 165 | .498 |
| | | 155 | .190 | 160 | .490 |
| | 2.0 - 0.2 | 116 | .205 | 132 | .502 |
| | | 109 | .196 | 125 | .465 |
| | | | | | |
| | | | | | |
| 0 | 0.2 - 2.0 | 201 | .231 | 357 | .492 |
| | | 195 | .235 | 349 | .506 |
| | 2.0 - 20.0 | 261 | .255 | 462 | .435 |
| | | 267 | .256 | 481 | .506 |
| | 20.0 - 2.0 | 368 | .189 | 313 | .566 |
| | | 347 | .257 | 297 | .569 |
| | 2.0 - 0.2 | 253 | .248 | 237 | .524 |
| | | 258 | .252 | 243 | .553 |
| | | | | | |
| | | | | | |

TABLE 59

CUMULATIVE DAMAGE TESTS

T-275
KM/P in HTPB(humidified)

| Temp. °F | Head Speed in/min | σ @ Change | ϵ @ Change | τ Max. | ϵ @ τ Max. |
|-------------|----------------------|-------------------|---------------------|-------------|--------------------------|
| 150 | 0.2 - 2.0 | 65 | .144 | 129 | .407 |
| | | 117 | .215 | 127 | .366 |
| | 2.0 - 20.0 | 95 | .210 | 153 | .427 |
| | | 93 | .203 | 150 | .407 |
| | 20.0 - 2.0 | 118 | .234 | 126 | .4 |
| | | 118 | .223 | 119 | .400 |
| | 2.0 - 0.2 | 86 | .208 | 92 | .369 |
| | | 91 | .209 | 99 | .400 |
| | 0.2 - 2.0 | 105 | .211 | 146 | .247 |
| | | 101 | .205 | 175 | .462 |
| 77 | 2.0 - 20.0 | 139 | .209 | 204 | .302 |
| | | 128 | .206 | 229 | .476 |
| | 20.0 - 2.0 | 166 | .189 | 163 | .462 |
| | | 163 | .194 | 153 | .394 |
| | 2.0 - 0.2 | 122 | .198 | 132 | .423 |
| | | 124 | .209 | 116 | .336 |
| 0 | 0.2 - 2.0 | 211 | .223 | 358 | .426 |
| | | 214 | .237 | 369 | .455 |
| | 2.0 - 20.0 | 273 | .254 | 479 | .459 |
| | | 273 | .254 | 486 | .451 |
| | 20.0 - 2.0 | 370 | .251 | 317 | .541 |
| | | 377 | .256 | 323 | .551 |
| | 2.0 - 0.2 | 258 | .221 | 239 | .472 |
| | | 271 | .251 | 235 | .493 |

Analysis of Soft Cure in CTPB Propellants

As has previously been pointed out, the source of the soft cure is not readily identifiable. Therefore, a series of experiments were performed and mixes manufactured to elucidate the source of the soft cure and provide a means through which improved mechanical properties could be obtained.

Among the possibilities for soft cure are the following:

- 1) Surface impurities on the surface of these particular lots of oxidizer which destroy cure agent or inhibit cure.
- 2) High water content of raw materials
- 3) A change in the functional group assay on polymer or cure agent
- 4) Since the oxidizer blends have been optimized for lower propellant viscosity, a higher cure agent to polymer ratio might be required to achieve improved mechanical properties.

In order to determine whether the amount of moisture on the oxidizer and the raw materials had increased markedly, a water analysis was performed on each of the pertinent raw materials. The results of these analyses indicated no significant change from those analyses performed earlier in the program.

A functional group assay was performed on CTPB polymer and the two curing agents used in the CTPB propellants. No change was noted in these assays.

The fact that the CTPB propellants made with the optimum PEPCON blend were considerably softer than those made with the optimum Kerr McGee blend tends to indicate that there exists an impurity on the PEPCON AP surface which tends to destroy curing agent or retard cure rate. A series of atomic absorption spectroscopy measurements were made on both the PEPCON and Kerr McGee oxidizer in order to determine if measurable differences in surface impurities could be detected. No differences of significance were detected.

In order to determine whether the inherently lower viscosity propellants provided thorough utilization of the optimum blends requiring a higher curing agent to polymer ratio to achieve good mechanical properties, a series of five-gallon mixes were manufactured. Table 60 contains a listing of the oxidizer size fractions utilized in this series of mixes. The standard TP-H7036 blend of oxidizer is listed as well as those blends of Kerr McGee and PEPCON determined to be the optimum blends earlier in this program.

A series of mixes were manufactured with the standard blends of Kerr McGee oxidizer and the optimum blend of Kerr McGee oxidizer and the curing agent to polymer ratio was varied in order to assess whether a different curing agent to polymer ratio should be required for the optimum blend. These data as well as the mechanical properties determined from each of the mixes are shown in Table 61. Initially, two five-gallon mixes were made; one with the optimum Kerr McGee blend and one with the standard Kerr McGee blend at a curing agent to polymer ratio of 0.8/1.0. Note that at identical polymer to curing agent ratios the standard Kerr McGee blend exhibits superior mechanical properties.

The curing agent to polymer ratio was increased to .85/1.0 and the two mixes (optimum Kerr McGee and standard Kerr McGee) were manufactured. The resulting properties are shown in Table 61. The maximum stress obtained in these two mixes is excellent. It appears that the strain capability has tended to level off and may have gone through a maximum whereas the modulus has increased beyond the desired level. Another mix was manufactured with the optimum Kerr McGee blend at a curing agent to polymer ratio of .90/1 and the suspicion that strain capability had leveled off was confirmed. Based on these data it appeared that the probable optimum curing agent to polymer ratio for the optimum Kerr McGee blend was .91/1. All of these mixes were manufactured in the five-gallon vertical mixer.

Table 62 contains a similar data matrix for the optimum and standard PEPCON blends. Note in this case that the strain at maximum stress tends to optimize at a curing agent to polymer ratio of approximately .85/1.0 and thereafter decreases. Based upon these data, the optimum curing agent to polymer ratio for the optimum PEPCON blend appeared to be approximately .84/1. The fact that a higher curing agent to polymer ratio is required to obtain equivalent mechanical properties with PEPCON AP when compared with those obtained with the Kerr McGee AP indicates that there does exist an impurity in the PEPCON oxidizer that we have been unable to detect and which results in an interaction with the curing agent thus requiring a higher concentration of curing agent to achieve equivalent properties.

The requirement for a higher curing agent/polymer ratio for PEPCON AP propellants might possibly also be explained by the fact that the optimum PEPCON blend has a total of special coarse and unground oxidizer of approximately 55% whereas the optimum Kerr McGee blend has a total sum of 47% special coarse and unground oxidizer. This greater amount of "as received" (non-ground) material will serve as a source for added curing agent requirements.

There has existed over the years some differences in mechanical properties for several propellants dependent upon whether the mix was manufactured in a horizontal or vertical mixer. A final series of mixes were manufactured at the selected curing agent to polymer ratios for both the

optimum Kerr McGee and optimum PEPCON blends to determine whether this mixer difference was real. Table 63 contains the data for two standard Kerr McGee blends mixes, one made in a five-gallon vertical mixer and the other in a 4 1/2 gallon horizontal mixer. Note the higher degree of cure obtained from the horizontal mixer. The optimum Kerr McGee blends were manufactured in the one-gallon mixer at the same curing agent to polymer ratio and a similar result was obtained.

Table 64 illustrates similar data for the optimum PEPCON blends manufactured in nominal five-gallon mixes at a constant curing agent to polymer ratio of .84/1. Note the excellent mechanical properties obtained from the horizontal mixer when compared with the vertical mixer.

The best explanation available for the improved properties noted in propellant manufactured in the horizontal mixer is that there is less propellant exposed to a humid atmosphere during a propellant scrape down and this lessening of exposure provides for more active curing agent and a resulting higher degree of cure.

TABLE 60

OXIDIZER FRACTION IN OPTIMUM BLENDS

| | <u>Standard</u> <u>TP-H7036 Blend</u> | <u>Optimum</u> <u>Kerr McGee</u> | <u>Optimum</u> <u>PEPCON</u> |
|------------|--|-------------------------------------|---------------------------------|
| 400 Micron | 30.60 | 21.10 | 30.94 |
| 200 Micron | 19.04 | 27.20 | 23.80 |
| 20 Micron | <u>18.36</u> | <u>19.70</u> | <u>13.26</u> |
| | 68.00 | 68.00 | 68.00 |

TABLE 61

MECHANICAL PROPERTIES FOR KERR MCGEE BLENDS IN TP-H7036

| | <u>Opt. KM</u> | <u>Std. KM</u> | <u>Opt. KM</u> | <u>Std. KM</u> | <u>Opt. KM</u> |
|---------------------------------|----------------|----------------|----------------|----------------|----------------|
| Cure Ratio (cure agent/polymer) | .8/1.0 | .8/1.0 | .85/1.0 | .85/1.0 | .90/1 |
| Modulus (psi) | 730 | 668 | 1314 | 1000 | 1332 |
| Ultimate Strain (in/in) | .299 | .299 | .287 | .334 | .284 |
| Strain at Max. Stress (in/in) | .266 | .282 | .265 | .300 | .267 |
| Max. Stress (psi) | 97.4 | 131 | 207 | 178 | 231 |

TABLE 62

MECHANICAL PROPERTIES FOR PEPCON BLENDS IN TP-H7036

| | <u>Opt. PEPCON</u> | <u>Std. PEPCON</u> | <u>Opt. PEPCON</u> | <u>Std. PEPCON</u> | <u>Opt. PEPCON</u> |
|---------------------------------|--------------------|--------------------|--------------------|--------------------|--------------------|
| Cure Ratio (cure agent/polymer) | .8/1.0 | .8/1.0 | .85/1.0 | .85/1.0 | .9/1.0 |
| Modulus (psi) | 404 | 624 | 1002 | 910 | 1393 |
| Ultimate Strain (in/in) | .325 | .327 | .304 | .300 | .290 |
| Strain at Max. Stress (in/in) | .259 | .273 | .281 | .265 | .267 |
| Max. Stress (psi) | 55.3 | 107 | 166 | 147 | 199 |

UNCLASSIFIED

TABLE 63

MIXER COMPARISON FOR KERR MCGEE BLENDS IN TP-H7036

| Mixer Type | Std. KM | Std. KM | Opt. KM | Opt. KM |
|--|----------------|----------------------|----------------|------------------|
| | 5-Gal Vertical | 4 1/2 Gal Horizontal | 1-Gal Vertical | 1 Gal Horizontal |
| Cure Ratio (cure agent/ polymer) | .81/1 | .81/1 | .81/1 | .81/1 |
| Modulus (psi) | 542 | 869 | 743 | 907 |
| Strain at Max. Stress (in/in) | .319 | .281 | .321 | .293 |
| Max. Stress (psi) | 105 | 138 | 116 | 147 |
| End of Mix Viscosity (Kp) at 140° F | 7.2 | 10. | -- | -- |

TABLE 64

MIXER COMPARISON FOR PEPCON BLENDS IN TP-H7036

| | <u>Std. PEPCON</u> | <u>Opt. PEPCON</u> | <u>Opt. PEPCON</u> |
|---------------------------------------|--------------------|--------------------|----------------------|
| Mixer Type | 1 Gal Horizontal | 5 Gal Vertical | 4 1/2 Gal Horizontal |
| Cure Ratio (cure agent/ polymer) | .84/1 | .84/1 | .84/1 |
| Modulus (psi) | 807 | 306 | 739 |
| Strain at Max. Stress (in/in) | .298 | .328 | .310 |
| Max. Stress (psi) | 131 | 67 | 126 |
| End of Mix Viscosity (Kp) at 140°F | -- | 9.6 | 10.0 |

EVALUATION OF AMMONIUM PERCHLORATE OBTAINED FROM THE DONALDSON CLASSIFIER

As it is pointed out in later sections of this report, the Donaldson Classifier was only successful in obtaining sharp fractional cuts of ammonium perchlorate on particle size distributions between 5 and 50 microns. More than 50 separate fractions were obtained and seven of these fractions varying in particle size from 14 to 48 microns, which were evaluated in conjunction with unground (190 micron) and special coarse (422 micron) oxidizer in TP-H7036 formulation. This evaluation also provided a means through which the theory generated within this program could be tested. In other words, with special coarse and unground oxidizer from Kerr-McGee, it had been previously determined that a weight median diameter of approximately 210 microns was required in a trimodal distribution in order to obtain desired burn rate for this particular propellant. Therefore, trimodal blends containing seven separate trimodal blends containing each of the seven size fractions in conjunction with special coarse and unground oxidizer were formulated so that the weight median diameter of the blend would be approximately 210. Those seven oxidizer ratios are shown in Table 65. The formulation, TP-H7036, is listed in Table 66. One pint mixes were manufactured for each of the seven oxidizer ratios. The weight median diameters for each of the blends are shown on Table 65, and the strand burn rates determined at 1000 psi are likewise shown. With exception of Mix No. 6, the trimodal containing 32% special coarse, 33% 190 micron, and 35% 40.3 micron, the burn rates are in the range predicted and exhibit excellent reproducibility. No ready explanation is available for the high burn rates of Mix No. 6.

TABLE 65

THEORY TEST DATA FOR VARIOUS SIZE FRACTIONS OF OXIDIZER

| Mix No. | Oxidizer Ratios | | | | | | |
|----------------|-----------------|----------|----------|----------|----------|----------|----------|
| | <u>1</u> | <u>2</u> | <u>3</u> | <u>4</u> | <u>5</u> | <u>6</u> | <u>7</u> |
| 422 micron | 31 | 31 | 30 | 31 | 31 | 32 | 30 |
| 190 micron | 40 | 40 | 41 | 39 | 37 | 33 | 37 |
| 14.0 micron | 29 | -- | -- | -- | -- | -- | -- |
| 16.0 micron | -- | 29 | -- | -- | -- | -- | -- |
| 22.4 micron | -- | -- | 29 | -- | -- | -- | -- |
| 24.5 micron | -- | -- | -- | 30 | -- | -- | -- |
| 32.0 micron | -- | -- | -- | -- | 32 | -- | -- |
| 40.3 micron | -- | -- | -- | -- | -- | 35 | -- |
| 47.7 micron | -- | -- | -- | -- | -- | -- | 33 |
| WMD | 210.9 | 211.4 | 209.1 | 212.3 | 211.5 | 211.9 | 212.6 |
| rb at 1000 psi | 0.339 | 0.347 | 0.337 | 0.340 | 0.350 | 0.386 | 0.344 |

TABLE 66

PROPELLANT FORMULATION

| <u>Material</u> | <u>Percentage</u> |
|-----------------------------------|-------------------|
| Ammonium Perchlorate (422 micron) | ---- |
| Ammonium Perchlorate (190 micron) | ---- |
| Ammonium Perchlorate (varied) | ---- |
| CTPB Polymer (HC-434) | 10.550 |
| MAPC | 0.290 |
| ERLA-0510 | 0.070 |
| Iron Linoleate | 0.100 |
| Diethyl Adipate | 1.000 |
| Aluminum | 20.000 |

A Donaldson Classifier, Model B, S/N 18-12003, was leased from the Donaldson Company, Inc., Majac Division, Minneapolis, Minnesota, 55431, and installed in an operating bay of an explosives processing building. This building is air conditioned to hold 77°F and 40 to 45% RH (when operating properly) all year around. The operating controls for the classifier were located in a remote area separated from the equipment itself by a distance of 45 feet (horizontally) and four 12-inch-thick reinforced concrete walls. Electrical connections were made through conduit with explosion-proof seal-offs. This layout was satisfactory for processing hazardous materials such as ammonium perchlorate or aluminum powder.

A detailed description of the classifier, together with the procedures used, is included in Appendix D. This appendix also contains a discussion of the analytical method used to evaluate the performance of the classifier for each run made, complete with an example calculation. Appendix E contains the chronological tabulation of data for the eighty classification runs made or attempted, complete with the particle size distribution plots and grade efficiency curves (an indicator of classifier performance) for each run.

Four runs were made using ground table salt (NaCl) under the direction of a representative of the Donaldson Company to check out the equipment and to familiarize Thiokol personnel with its operation and maintenance. Live classification experiments were started shortly thereafter using nominal 90 micron ammonium perchlorate (AP). Some 570 lbs. of this material were processed before a decision was made to substitute nominal 50 micron AP for the coarser material. More than 400 lbs. of nominal 50 micron materials were processed satisfactorily, resulting in some 247 lbs. of center-cut product from which excess coarse and fines tailings had been removed. High speed grind (HSG) AP was processed next, and more than 475 lbs. of material were collected as product fractions (there are always losses, and the Vibra-Screw feeder used was not readily amenable to accounting for weights of material fed to the classifier. Just under 608 lbs. of center-cut product were obtained from this work. Almost 120 lbs. of fluid energy milled AP, in the range of 1.7 to 2.5 microns weight mean diameter (WMD), were run through the classifier in a series of generally unsuccessful attempts to split out a submicron (WMD) fines fraction. Some 40 lbs. of a SWECO Vibro-Energy Mill ground dry powder were processed with comparative ease, resulting in the only submicron (WMD) product produced in the classification effort.

Following completion of the AP work, a rather extensive cleaning operation was undergone to ensure complete removal of all oxidizer residues and to remove the rust and corrosion products produced by the extensive chemical attack on the equipment by the AP. A means of providing a nearly pure nitrogen gas atmosphere inside the classifier was then devised, and a series of experimental runs made using various grades of aluminum powder as feed materi-

al. Due to the relatively high cost of charging the nitrogen storage tank and the short time (about four hours) available for operation per tank charge, limited experimentation was done with the aluminum, and much smaller quantities than desired were run. Approximately 80 lbs. of a nominal 6 micron irregular aluminum powder were run resulting in about 21.5 lbs. of a center-cut product. Nearly 200 lbs. of a nominal 30 micron irregular aluminum were processed, but the first half was lost due to an inadvertent operator error. About 28 lbs. of center-cut product were ultimately produced. Some 40 lbs. of a nominal 90 micron irregular aluminum were processed, but no further work was done because of the low fines yield and because of peculiar particle size results. Some 275 lbs. of M-3 grade spherical aluminum were then processed in an effort to produce nominal micron or submicron aluminum powder for experimental use. This work is also discussed in detail below.

90 Micron AP Runs

Eleven runs were made to study process variables and their effects using a nominal 90 micron (WMP) lot of AP. Parts of two drums of material were used, and each drum was blended prior to use to ensure homogeneity. The classification runs invariably resulted in fines fractions containing materials finer than in the original feed material, and the coarse fractions usually were smaller in particle size than the feed. This indicated that a significant degree of attrition was occurring inside the classifier. This, coupled with the fact that the yield of fines was generally very low, ultimately led to abandonment of this material as a suitable feed material. The product fraction data from the runs are summarized in Table 67. Runs DC-8 and DC-12 through DC-15 were made at conditions generally identical to those of the earlier runs the feed came from. These were originally intended to determine if additional fines product could be gleaned from the feed by repassing it through the classifier. It is more likely that repassing the coarse fraction resulted in grinding by attrition, thereby producing a fines fraction very similar to that obtained from the first pass.

After all the classification runs were completed, all the accumulated fine and coarse product fractions (less the particle size samples) were put back in the blender and blended. As shown in Figure 102, the particle size of the final blend differs considerable from those of the two drums of original feed material. This is felt to be conclusive proof that particle size reduction was occurring to a significant degree. Even so, valuable experience was gained in the operation of the equipment and in anticipating the results obtained. Figure 103 illustrates some of this knowledge. As the feed rate increases, for a given set of machine conditions, the actual cut point decreases as does the percentage of product collected as fines. It appears, in fact, that the percentage of fines (total fined efficiency, or E_{tf}) reaches a minimum. Run DC-6 compared

Distribution Curves

- Drum No. 1 When Opened; 126 μ WMD
- Drum No. 2 When Opened; 126 μ WMD
- △ Blended composite from both drums, after classification and rebinding; 87 μ WMD

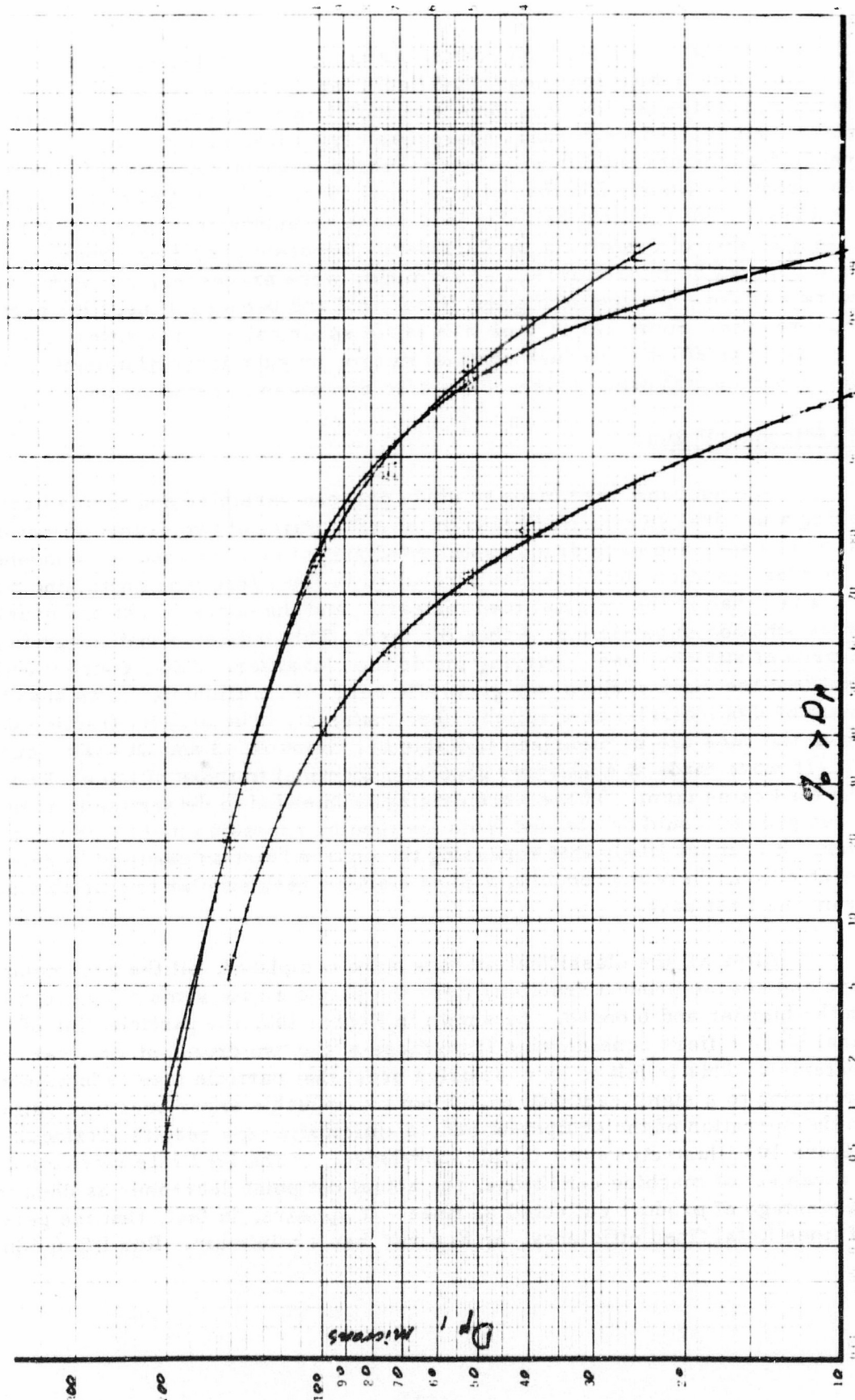


Figure 102. Lot 4087 90 Micron AP Particle Size

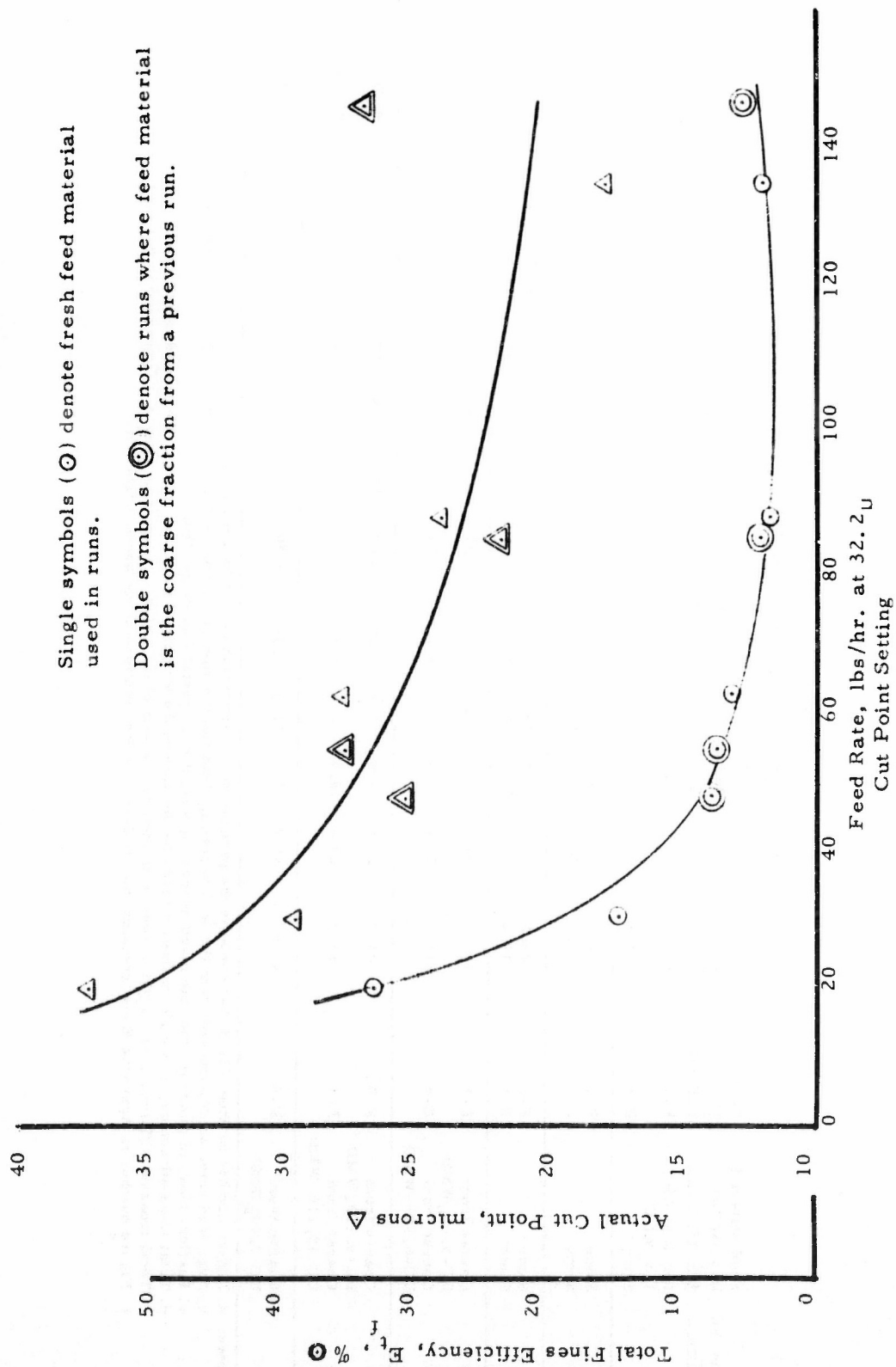


Figure 103. Effects of Feed Rate on 90 Micron AP Runs

TABLE 67
SUMMARY OF WORK WITH NOMINAL 90 MICRON AP (U)

| Run No. DC- | Feed Material Description and WMD | Figure No. of Feed Distribution ^a | Feed Rate ^b lbs/hr | | | Fines Product Size ^c | | | Fines Product Wt., lbs | E ^d f | Coarse Product Size ^c | | | Coarse Product Weight, lbs. | E ^e t | Figure No. of Product Distributions ^f |
|----------------|--|--|----------------------------------|------|------|---------------------------------|-------|-------|------------------------------|---------------------|----------------------------------|-------|-------|--------------------------------|---------------------|---|
| | | | 20% | 50% | 80% | 20% | 50% | 80% | | | 20% | 50% | 80% | | | |
| 5 | Lot 4087 AP, 113 _U WMD | E-1 | 135.5 | 67 | 25.5 | 13.1 | 2.64 | 3.90 | 121 | 96 | 68.8 | 65.11 | 96.10 | E-1 | | |
| 6 | Same | E-1 | 124.6 | 39.3 | 18.9 | 11.1 | 4.76 | 7.64 | 137 | 105 | 74.5 | 57.54 | 92.36 | E-3 | | |
| 9 | Same | E-1 | 87.3 | 29.8 | 16.3 | 10.5 | 2.20 | 3.36 | 135 | 110 | 76 | 63.27 | 96.64 | E-9 | | |
| 10 | Same | E-1 | 61.3 | 28.5 | 17.1 | 11.9 | 3.80 | 6.20 | 147 | 118 | 80 | 57.51 | 93.80 | E-11 | | |
| 7 | Same | E-1 | 29.5 | 37 | 17.1 | 10.7 | 10.21 | 17.31 | 105 | 79 | 55 | 48.77 | 82.69 | E-5 | | |
| 11 | Same | E-1 | 19.2 | 47 | 27.2 | 15.5 | 19.09 | 33.13 | 103 | 72 | 48 | 38.53 | 66.87 | E-13 | | |
| 12 | Coarse from DC-5, 96 _U WMD | E-1 | 146.2 | 56 | 25.2 | 14.3 | 3.39 | 5.35 | 153 | 121 | 85 | 59.95 | 94.65 | E-15 | | |
| 13 | Coarse from DC-6, 105 _U WMD | E-3 | 141.6 | 29.8 | 17.3 | 11.8 | 4.16 | 7.19 | 87 | 76 | 64 | 53.67 | 92.81 | E-17 | | |
| 14 | Coarse from DC-9, 110 _U WMD | E-9 | 84.2 | 27.6 | 17.6 | 12.4 | 2.29 | 4.08 | 127 | 98 | 67 | 53.85 | 95.92 | E-19 | | |
| 15 | Coarse from DC-10, 118 _U WMD | E-11 | 53.9 | 29.6 | 18.5 | 12.8 | 3.51 | 7.37 | 128 | 99 | 67 | 44.10 | 92.63 | E-21 | | |
| 8 | Coarse from DC-7, 79 _U WMD | E-5 | 47.0 | 31.8 | 18.7 | 11.9 | 2.84 | 7.70 | 97 | 72 | 53 | 34.04 | 92.30 | E-7 | | |

Notes: a. Figure number in Appendix E that contains the particle size distribution of this feed material.
b. Avg. feed rate, as determined from the feed operating time and the sum of the coarse and fines fraction product weights.
c. Particle size, in microns, that the noted percent by weight of material was larger than.
d. Total fines efficiency, or weight of fines divided by the sum of the weights of fines and coarse. Expressed in per cent.
e. Total (coarse) efficiency, or weight of coarse divided by the sum of the weights of fines and coarse. Expressed in per cent.
f. Figure number in Appendix E that contains the particle size distributions of the product fractions.

to DC-5 (as well as DC-13 compared to DC-12) shows the effect of increasing the air flow through the classifier while holding rotor speed and feed rate constant. As expected, the cut point increased, however, a greater increase in cut point was obtained by dropping the feed rate (DC-11). It is apparent that the advertised maximum cut point of 50 microns applies when the rotor speed is minimum, the feed rate is very low, and (probably) the feed material density is low.

50 Micron AP Runs

Nine runs or series of runs were made to process a lot of nominal 50 micron AP as a substitute for the 90 micron AP. As can be seen from Figure 104, which depicts the particle size distributions of original feed material, the coarse tailings, the fines tailings, and the center-cut product material from runs DC-19 and DC-20, a significant degree of attrition occurred with this material as it did with the 90 micron AP. Two "production" series of classification runs were subsequently made to produce center-cut product distributions and associated fines and coarse tailings. The two series differed only in the machine settings used for the coarse (second) separation. Runs DC-26 through DC-30 used 200 cfm of air flow while runs DC-63 through DC-65 used 150 cfm. The 200 cfm condition is difficult to attain and maintain and is excessively noisy. In addition, there is no latitude in air flow control to compensate for increasing pressure drop across the fines filter when 200 cfm is used. Dropping the air flow decreased the resulting cut point from 51.6 microns to 28.6 microns, although the particle size distributions of the products do not appear to be greatly different (see Figures 105 and 106). The product fraction data from all the runs are summarized in Table 68. Figure 107 depicts the effect of feed rate of 50 micron AP on the actual cut point and on total fines efficiency, holding rotor speed and air flow constant. The results are similar to those for the 90 micron material.

High Speed Grind AP Runs

Twelve runs and series of runs were made to classify HSG feed material at various cut point sizes. The HSG normally produces a ground AP distribution with a WMD in the range of 12 to 16 microns by MSA. Grind No. H11602 was made using a ISH Mikro-Pulverizer at 9400 rpm hammer speed and 0.013 HB screen to produce feed material for the Donaldson. Lot 3918 AP was used, and the ground material analyzed 16.2 microns WMD. A series of test runs was made first to determine the effect of feed rate on the cut point size, then production fractionation efforts were started. Runs DC-54 through DC-59 were made to split off the fines tailings, using a machine cut point setting of 25 microns to split out the coarse tailings. The feed rate for the coarse fractionation was higher than desired, caused by the greater fluidity of the material with fines removed, so the operation, runs DC-60 and DC-61, was halted before all the feed stock was used. The remaining feed stock, some 42 lbs. was

TABLE 68
SUMMARY OF WORK WITH NOMINAL 50 MICRON AP (U)

| Run No. DC- | Feed Material Description & WMD | Figure No. of Feed Distribution | Feed Rate | | | Fines Product Size | | | Fines Product | | | Coarse Product Size | | | Coarse Product | | | Figure No. of Product Distributions |
|----------------|--|---------------------------------------|----------------|--------------|-------------|--------------------|-----------------|----------------|---------------|------------|--------------|---------------------|----------------|--------------|----------------|-----|--|---|
| | | | lbs./hr. | 20% | 50% | 80% | Weight, lbs. | E _f | 20% | 50% | 80% | Weight, lbs. | E _t | 20% | 50% | 80% | | |
| 17 | Lot 4351 AP, 6 _U WMD | E-23 | 52.0 | 13.2 | 8.3 | 4.4 | 2.80 | 7.17 | 61 | 44.4 | 26.6 | 36.23 | 92.83 | E-25 | | | | |
| 16 | Same | E-23 | 35.5 | 13.6 | 8.5 | 4.8 | 3.38 | 9.22 | 63 | 46.2 | 29 | 33.29 | 90.78 | E-23 | | | | |
| 18 | Same | E-23 | 16.3 | 14.9 | 9.4 | 5.05 | 7.40 | 21.61 | 52 | 36 | 23 | 26.85 | 78.39 | E-27 | | | | |
| 19 | Same | E-23 | 16.0 | 10.6 | 6.6 | 3.83 | 4.68 | 12.07 | 49.6 | 35.3 | 21.6 | 34.09 | 87.93 | E-29 | | | | |
| 20 | Coarse from DC-19, 35.3 _U WMD | E-29 | 13.7 | 23.3 | 14.9 | 7.6 | 22.99 | 70.85 | 45.8 | 35.8 | 26.4 | 9.46 | 29.15 | E-31 | | | | |
| 21-25 | Lot 4351 AP, 6 _U WMD | E-23 | 16.19 | 10.2 | 6.4 | 3.53 | 25.06 | 12.39 | 64 | 44 | 26.7 | 177.27 | 87.61 | E-33 | | | | |
| 39-41 26-30 | Same Coarse from DC-21-25, 4 _U WMD | E-23 E-33 | 16.45 13.63 | 10.9 27.1 | 7.1 17.1 | 4.26 8.6 | 14.36 157.00 | 11.64 90.65 | 55.3 44.8 | 39 32.6 | 23.8 18.6 | 108.99 16.19 | 88.36 9.35 | E-50 E-35 | | | | |
| 63-65 | Coarse from DC-39-41, 3 _U WMD | E-50 | 11.61 | 24.3 | 16.8 | 9.5 | 60.70 | 57.05 | 48.3 | 37.0 | 27.0 | 45.70 | 42.95 | E-81 | | | | |

Notes: a. See notes at end of Table 67 for explanation of column headings.

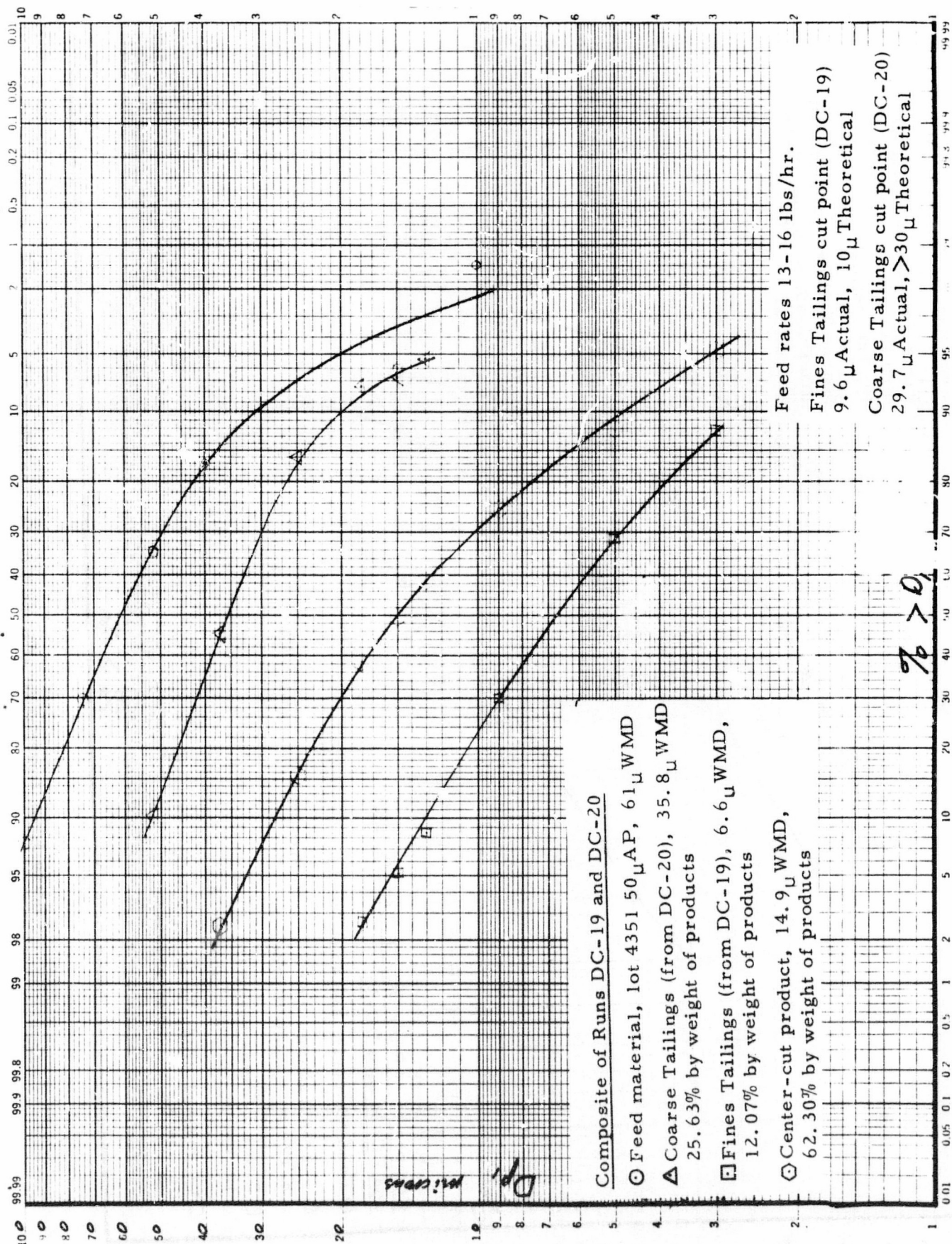


Figure 104. Composite of Runs DC-19 and DC-20

Feed Rates 13-16 lbs./hr.

Fines Tailings cut point (DC-21 thru DC-25) 11.2_U Actual, 10_U Theoretical

Coarse Tailings cut point (DC-26 thru DC-30) 51.6_U uncalibrated theoretical

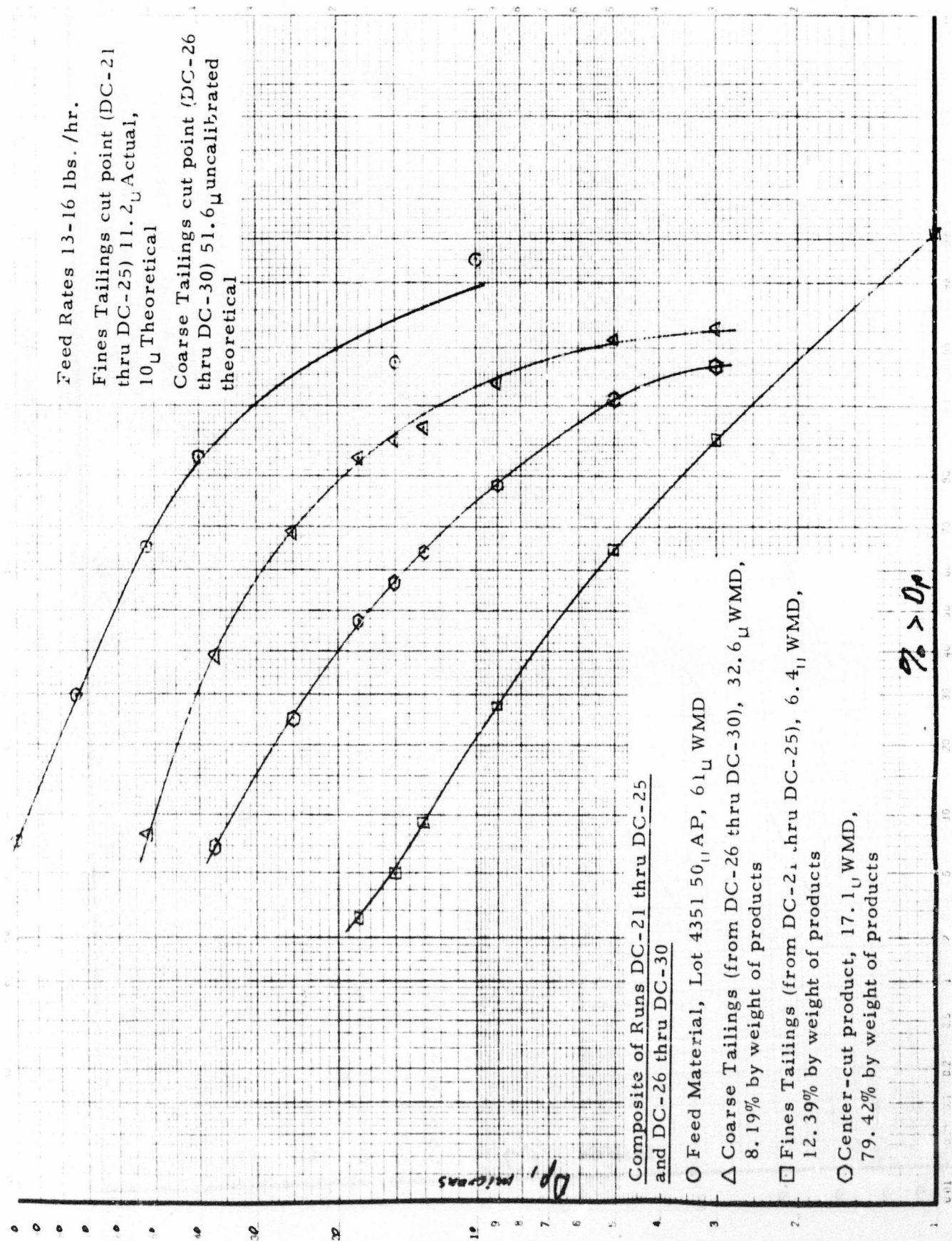


Figure 105. Composite of Runs DC-21 through DC-30

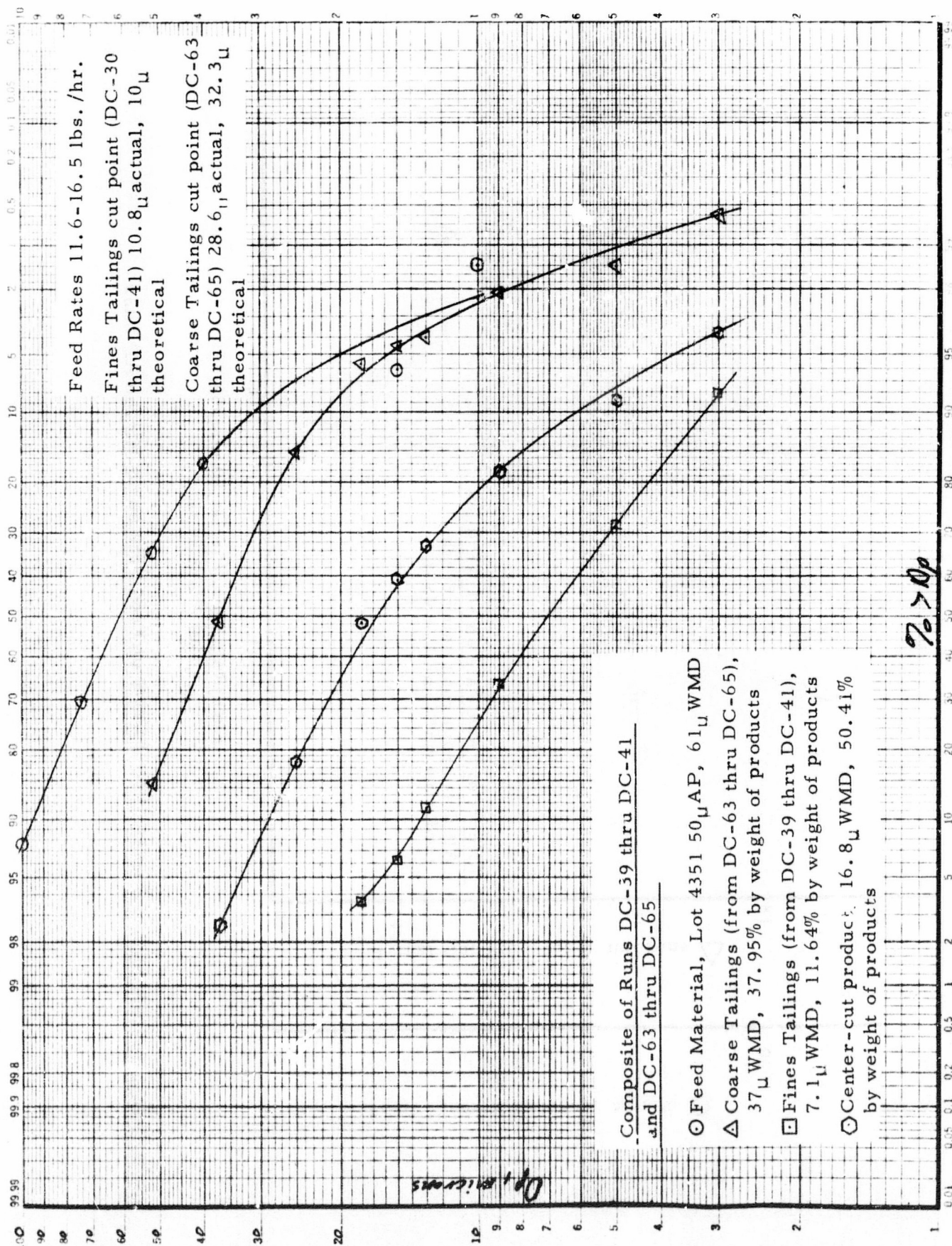


Figure 106. Composite of Runs DC-39 through -41 & DC-63 through DC-65

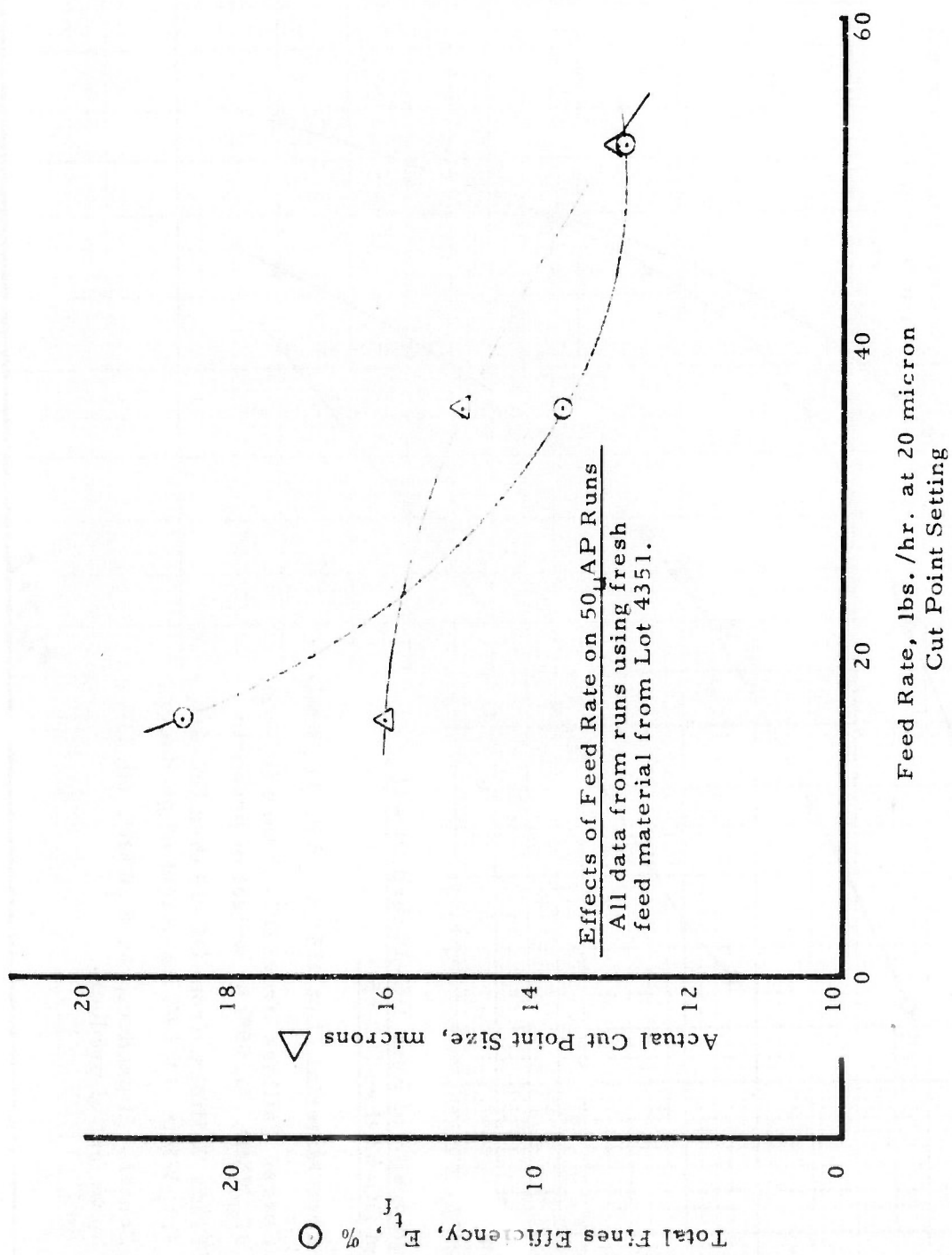


Figure 107. Effects of Feed Rate on 50 Micron AP Runs

then run through at the same machine cut point setting but at a much lower feed rate. Dropping the feed rate increased the actual cut point size slightly and increased the total fines efficiency significantly, as expected. The distributions of the fines tailings and of the center-cut product are nearly identical, as shown in Figures 108 and 109, while the coarse tailings produced at the lower feed rate contain a smaller percentage of the finer sized particles.

Changes in feed rate of HSG materials to the classifier produced at least one unexpected result, as shown in Figure 110, depicting the preliminary run data taken at a 10 micron machine cut point setting. The actual cut point size increased with increasing feed rate, contrary to the expectations from our conversations with the vendor and from our experiences with other materials. Figure 111, depicting data from runs at a machine cut point setting of 25 microns, show relationships more in conformation with expected results. A similar plot of run data from 5 micron cut point setting runs showed no particular relationship, so has not been included. Table 69 summarizes the product information from these runs.

Fluid Energy Milled AP Runs

Fourteen runs were made using various particle sizes of AP, ground on fluid energy mills, ranging from nominal 1.7 microns WMD up to around 2.6 microns WMD. The intent was to classify the material at the lowest cut point possible, thereby producing a fines fraction with a WMD smaller than one micron. The results, summarized in Table 70, indicate inadequate separation, although in at least one attempt (DC-66) the fines fraction was very nearly one micron WMD. The primary problems appeared to be in feeding the material to the classifier and then collecting the fines product in usable form. As explained below, the feeding problem was partially solved, but the collection problem was felt to be unsolvable with the existing equipment setup.

With the exception of Runs DC-36 and DC-37, the fluid energy mill ground AP had been packaged, when ground, with 30% by weight sorbents (fused silica gel pellets) to lower the surface moisture content and improve storage life. Just prior to classification efforts, the desiccant pellets were screened out of the AP with a 10-mesh sieve. The resulting material was a dry, reasonable free-flowing powder with a tendency to cake and pack into lumps. The Vibra-Screw Feeder tended to pack the material in the delivery tube, and the resulting lumps were too big and too hard to go through the classifier inlet orifice. A number of attempts were made to devise delumping mechanisms to break up the material before it reached the orifice, but none were very successful. One holdover from these efforts that was left on the classifier thereafter was a jet of compressed air discharging from the rear of the feed funnel into the inlet orifice. This high velocity jet tended to break down loose agglomerates and helped keep the feed funnel cleaned out. Prior to use of this air jet, feed material fell to the bottom of the funnel before being sucked into the inlet orifice. Impact against the funnel caused a coating

TABLE 69
SUMMARY OF WORK WITH HIGH SPEED GRIND (HSG) AP (U)

| Run No. DC- | Feed Material Description and WMD | Figure No. of Feed Distribution | Feed Rate lbs./hr. | Fines Product Size | | | Fines Product Weight, lbs. | E t | Coarse Product Size | | | Coarse Product Weight, lbs. | E t | Figure No. of Product Distributions |
|----------------|---|---------------------------------------|-----------------------|--------------------|------|------|-------------------------------|--------|---------------------|------|------|--------------------------------|--------|---|
| | | | | 20% | 50% | 80% | | | 20% | 50% | 80% | | | |
| 43 | Grind No. M11602, 16.2 _u | E-52 | 42.75 | 10.3 | 6.6 | 3.8 | 5.49 | 38.50 | 41.2 | 25.5 | 15.2 | 8.77 | 61.50 | E-54 |
| 42 | WMD Same | E-52 | 37.08 | 10.2 | 6.6 | 3.8 | 5.68 | 36.76 | 38.5 | 24.4 | 1.5 | 9.77 | 63.24 | E-52 |
| 44 | Same | E-52 | 24.47 | 9.6 | 6.6 | 4.1 | 9.46 | 38.66 | 36.5 | 21.4 | 13.2 | 15.01 | 61.34 | E-56 |
| 45 | Same | E-52 | 14.60 | 8.1 | 5.1 | 2.57 | 12.82 | 43.92 | --- | 9.2 | 2.82 | 16.37 | 56.08 | E-58 |
| 46 | Same | E-52 | 22.56 | 6.8 | 4.2 | 2.35 | 6.61 | 29.30 | --- | 12.9 | 6.8 | 15.95 | 70.70 | E-60 |
| 47 | Same | E-52 | 13.88 | 6.6 | 4.14 | 2.27 | 8.00 | 28.82 | --- | 14.7 | 7.9 | 19.76 | 71.18 | E-62 |
| 49 | Same | E-52 | 34.65 | 16.2 | 10.5 | 6.0 | 6.80 | 58.87 | 45.6 | 31.0 | 20.8 | 4.75 | 41.13 | E-66 |
| 48 | Same | E-52 | 27.70 | 17.7 | 10.6 | 5.5 | 8.52 | 61.52 | 41.5 | 25.5 | 20.0 | 5.33 | 38.48 | E-64 |
| 50 | Same | E-52 | 18.40 | 16.3 | 9.6 | 4.82 | 11.60 | 63.04 | 44.2 | 30.8 | 21.0 | 6.80 | 36.96 | E-68 |
| 54-59 | Same | E-52 | 20.34 | 4.8 | 3.06 | 1.69 | 81.58 | 27.25 | --- | 12.9 | 5.1 | 217.82 | 72.75 | E-75 |
| 60-61 | Coarse from DC-54-59, 12.9 _u WMD | | 65.08 | 17.7 | 12.9 | 8.9 | 82.72 | 47.66 | 44.2 | 29.6 | 22.3 | 90.84 | 52.34 | E-77 |
| 62 | Same | | 29.23 | 19.0 | 13.3 | 9.2 | 25.00 | 59.66 | 41.0 | 29.6 | 21.0 | 16.90 | 40.34 | E-79 |

Note: a. See Notes at end of Table 67 for explanation of column headings.

TABLE 70
SUMMARY^a OF WORK WITH FLUID ENERGY MILLED AP (U)

| Run No. DC- | Feed Material Description and WMD | Figure No. of Feed Distribution | Feed Rate lbs./hr. | Fines Product Size | | | Fines Product Weight, lbs. | E t f | Coarse Product Size | | | Coarse Product Weight, lbs | E t | Figure No. of Product Distributions |
|-----------------|--|---------------------------------------|-----------------------|--------------------|------|------|-------------------------------|-------------|---------------------|------|------|-------------------------------|--------|---|
| | | | | 20% | 50% | 80% | | | 20% | 50% | 80% | | | |
| 31 ^b | EFEM-73, 1.80 _u WMD | E-37 | N/A | 2.50 | 1.84 | 1.24 | N/A | N/A | 2.54 | 1.90 | 1.27 | N/A | N/A | E-37 |
| 32 ^c | Same | E-37 | N/A | 2.61 | 1.96 | 1.33 | 1.94 | 51.87 | 3.33 | 2.43 | 1.62 | 1.80 | 48.13 | E-38 |
| 33 ^c | EFEM-73, with 0.2% Silanox 101, 1.80 _u WMD | E-37 | N/A | 2.62 | 1.90 | 1.32 | 2.92 | 26.94 | 3.70 | 2.84 | 2.10 | 7.92 | 73.06 | E-40 |
| 34 | Same | E-37 | 5.45 | 2.38 | 1.88 | 1.47 | 6.26 | 40.57 | --- | 2.90 | 1.59 | 9.17 | 59.43 | E-42 |
| 35 ^d | EFEM-71, with 0.2% Silanox 101, 2.12 _u WMD | E-43 | 6.25 | N/A | N/A | N/A | 4.07 | 15.32 | N/A | N/A | N/A | 22.49 | 84.68 | E-43 |
| 36 | Freshly ground EFEM-74, 1.81 _u WMD | E-44 | N/A | 2.44 | 1.77 | 1.18 | 1.00 | 34.60 | 2.87 | 2.16 | 1.43 | 1.89 | 65.40 | E-44 |
| 37 | Freshly ground EFEM-75, with 0.2% Cab-O-Sil, 1.73 _u WMD | E-46 | N/A | 1.96 | 1.47 | 1.07 | 0.76 | 10.84 | 3.01 | 2.10 | 1.38 | 6.25 | 89.16 | E-46 |
| 38 | Same | E-46 | 8.05 | 2.07 | 1.54 | 1.16 | 1.36 | 12.67 | 3.01 | 2.26 | 1.68 | 9.37 | 87.33 | E-48 |
| 53 ^e | EFEM-78, with 0.5% Silanox 101, 1.99 _u WMD | E-74 | 7.53 | N/A | N/A | N/A | 0.31 | 13.43 | 3.27 | 2.44 | 1.71 | 2.00 | 86.58 | E-74 |
| 67 | Blended mix of EFEM-78 (67%) with fines from DC-43(33%), with 0.2% Silanox, WMD unknown | N/A | 15.17 | 3.10 | 2.51 | 1.91 | 0.74 | 6.10 | 6.6 | 3.94 | 2.55 | 11.40 | 93.90 | E-85 |

Table 70 continued
Summary of Work with Fluid Energy Milled AP

| Run No. DC- | Feed Material Description and WMD | Figure No. of Feed Distribution | Feed Rate lbs./hr. | Fines Product Size | | | Fines Product Weight, lbs. | E t f | Coarse Product Size | | | Coarse Product Weight, lbs. | E t | Figure No. of Product Distributions |
|----------------|--|---------------------------------------|-----------------------|--------------------|------|------|-------------------------------|-------------|---------------------|------|------|--------------------------------|--------|---|
| | | | | 20% | 50% | 80% | | | 20% | 50% | 80% | | | |
| 60 | FEM-338, with 0.2% Silanox 101, 2.58% WMD | E-83 | 2.34 | 1.67 | 1.07 | 0.61 | 0.18 | 2.43 | 3.73 | 2.61 | 1.65 | 7.23 | 97.57 | E-83 |
| 70 | Same | E-83 | 5.42 | 3.00 | 2.31 | 1.65 | 6.34 | 39.01 | 3.77 | 2.53 | 1.33 | 9.91 | 60.99 | E-91 |
| 71 | Coarse from DC-70, 2.53% WMD | E-91 | 22.26 | 4.70 | 3.39 | 2.24 | 8.64 | 93.20 | 6.35 | 4.30 | 2.91 | 0.63 | 6.80 | E-93 |
| 68 | Blended mix of FEM-338 (67%) with coarse from DC-43 (33%), with 0.2% Silanox 101, WMD unknown | N/A | 4.32 | 2.69 | 2.19 | 1.60 | 1.10 | 9.91 | 14.2 | 5.45 | 3.18 | 10.00 | 90.09 | E-87 |

Notes: a. See Notes at end of Table 67 for explanation of column headings.
b. Run DC-31 halted almost immediately because of feeding problems. No weight data obtained.
c. Feed rate was intermittent during entire run due to efforts to screen or otherwise disperse the lumpy feed material.
d. Sampler appear to have been mislabelled as fines came out larger in size than coarse.
e. The DC-53 fines sample compacted in the MSA tube every time an analysis attempt was made, hence no data. Compaction apparently caused by the Silanox 101 anti-caking agent.

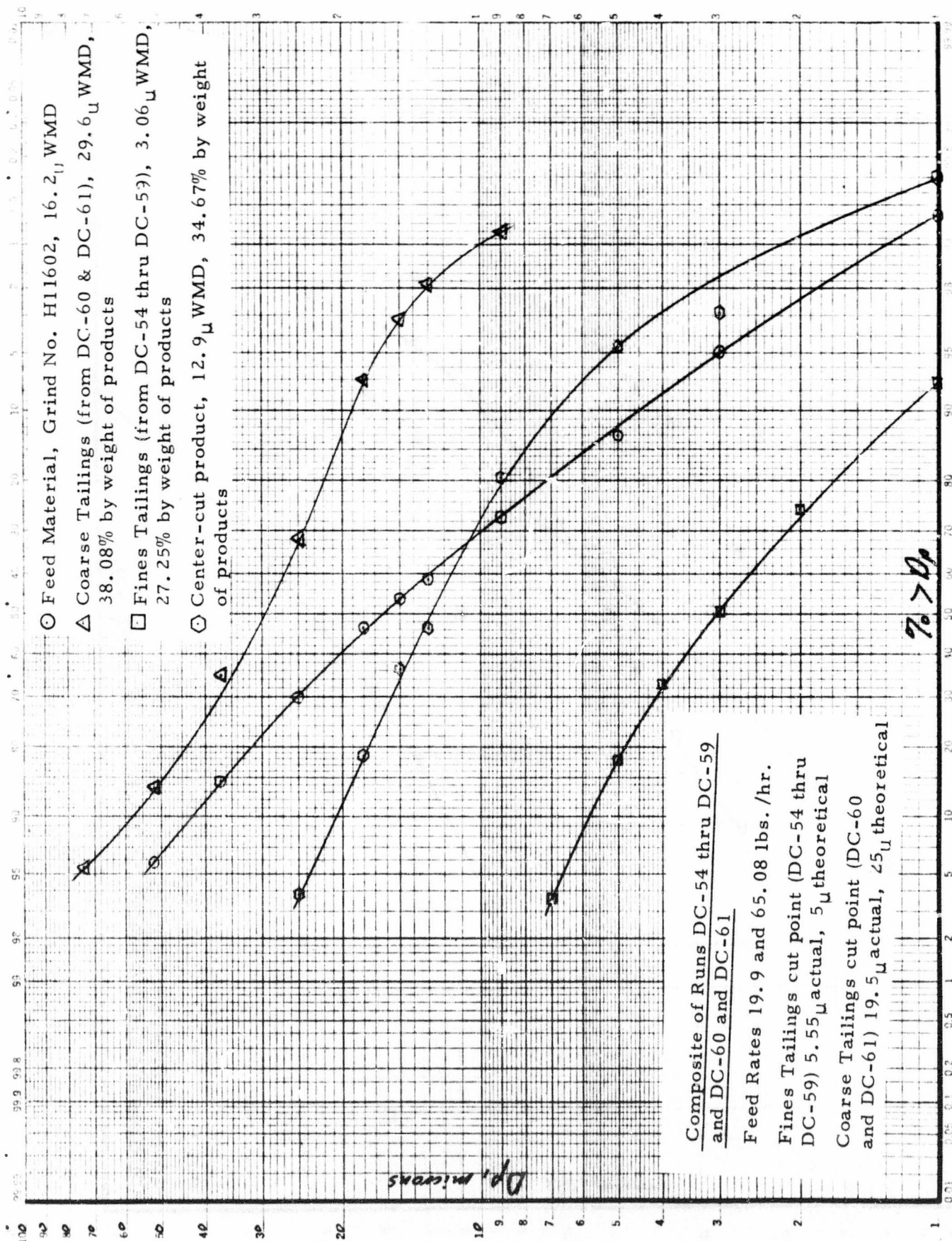


Figure 108. Composite of Runs DC-54 through DC-59 & DC-60 and DC-61

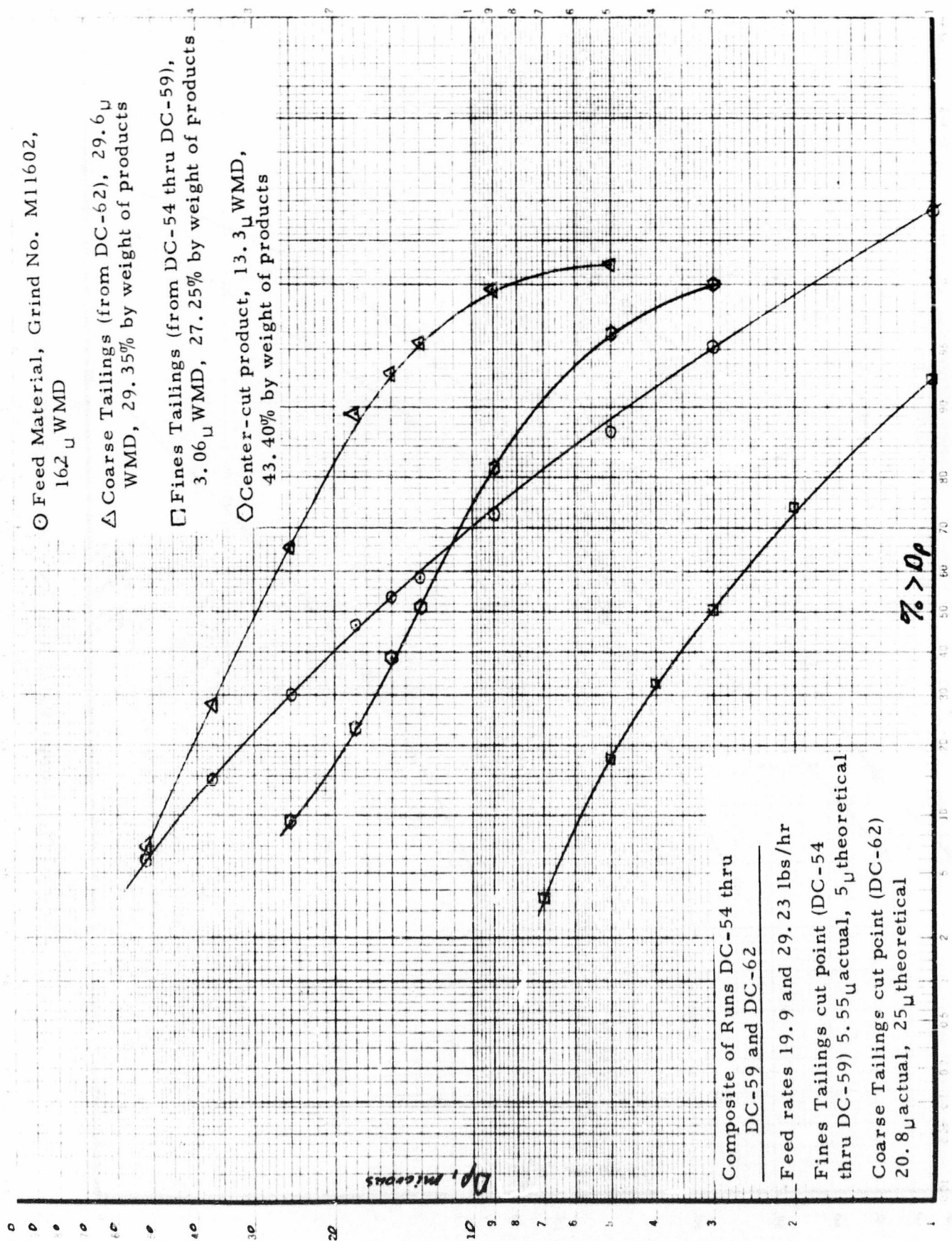


Figure 109. Composite of Runs DC-54 through DC-59 and DC-62

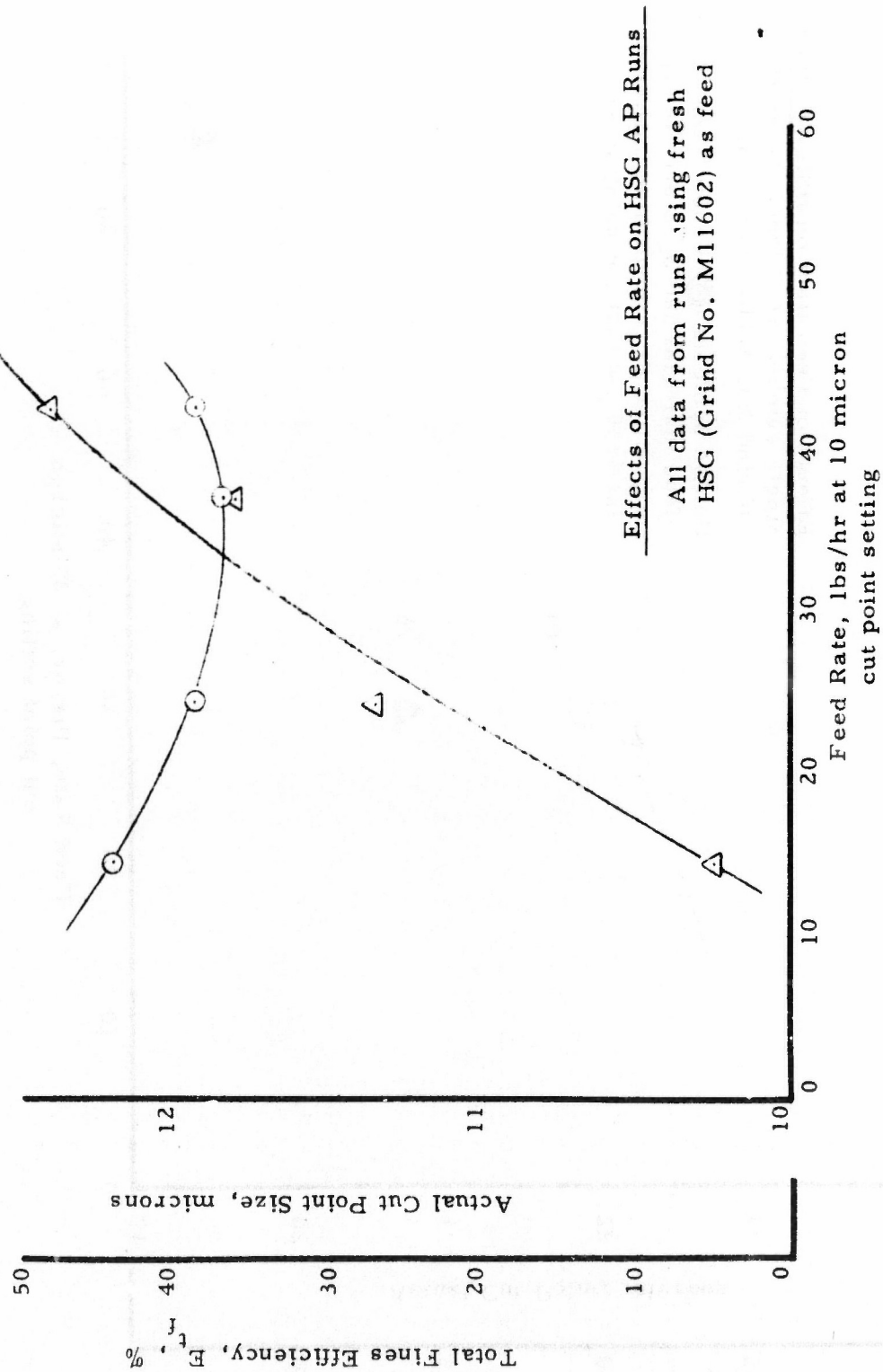


Figure 110. Effects of Feed Rate on HSG AP Runs

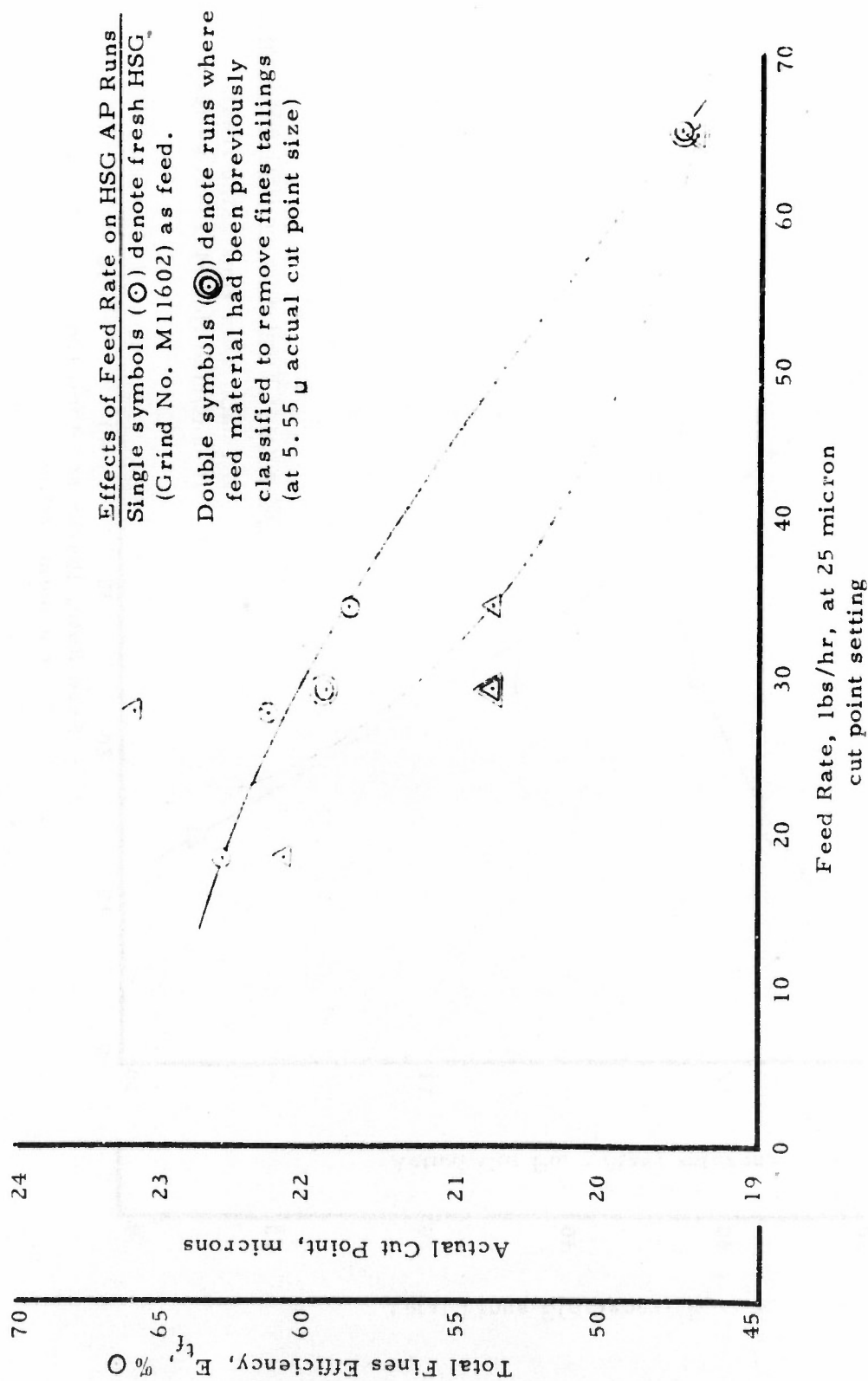


Figure 111. Effects of Feed Rate on HSG AP Runs

to build up that would increase in thickness until the funnel was nearly choked off. The jet entrained the particles before they could contact the bottom and stick.

The only suitable correction to the feed problem was the addition of an anticaking agent to the material as soon as the Sorbead desiccant was removed. Silanox 101, a product of the Cabot Corporation, was the primary material used, although Cab-O-Sil was substituted on occasion. Silanox or Cab-O-Sil was blended into the UFAP using a lab model Patterson-Kelley twin-shell blender with intensifier bar. The resulting material was a dusty, free-flowing material with little or no tendency to lump. The general level of anticaking agent used was 0.2% by weight of the AP, although as much as 0.5% by weight was tried. It was found that with the anticaking agent in the AP, a smooth feed rate could be established with little or no lumping problems. Without the anticaking agents, feeding of fluid energy milled AP to the classifier was virtually impossible. Feeding freshly ground AP, with or without anticaking agents, was also practically impossible, most probably due to the excess surface moisture on the particle surfaces; storage with Sorbead desiccant apparently removes this excess surface moisture. Unfortunately, the pressure of the Silanox or Cab-O-Sil interferes with the MSA particle size analysis, usually resulting in compaction of the column of solids in the analysis tube. Run DC-53 used 0.5% Silanox as anticaking agent in the feed. Five or more analysis attempts were made to measure the fines particle size distribution from this run, but every attempt failed due to column compaction. Control Lab personnel report that Silanox has invariably caused problems of particle size analysis when used. It is possible that the analysis problems could contribute to the general failure of the classifier to produce a submicron fines fraction.

The collection problem is partly caused by the properties of uncoated UFAP itself and partly by the collection equipment itself. In every run made using fluid energy mill (FEM) ground AP, a heavy buildup of AP occurred on the walls of the fines fraction conveying line and on the inner surfaces of the fines fraction cyclone collector. This buildup was usually soft, but difficult to remove except by either scraping or dissolving with water. A relatively high percentage of fines also went through the cyclone and was carried on to the fines filter, from which it could not be recovered. Loss of fines material by any of these conditions resulted in two effects noticeable in the data: the total fines efficiency (E_{t_f}) was reduced

and the smaller particle sizes were removed from the collected product fraction. Decreasing the total fines efficiency tends to lower the calculated cut point size somewhat. Loss of the smaller particles from the fines would greatly increase the WMD of the material and would generally increase the calculate cut point size. If, instead of a cyclone followed by a total-capture, air cleaning filter, a self-cleaning bag or cartridge filter had been available for the fines fraction collector, it is quite possible that a sub-micron WMD fines fraction might have been produced.

Conversations with the Donaldson Company indicated reservations on their part that the equipment could ever be successful in splitting out a submicron WMD fines fraction from the nominal 1.7 micron feed. They suggested trying a somewhat coarser feed material. This was partially successful, as evidenced by Run DC-66, in which nominal 2.6 micron WMD feed material was used. However, DC-66 was made using an air flow of only, 100 cfm instead of 150 cfm. This approach was subsequently abandoned because of excessive noise and difficulty in controlling the air flow. The 1.7 micron WMD may have been a result of the reduced air flow rather than the feed material particle size. Attempts to blend in a coarser grade of material into either 1.7 or 2.6 micron WMD feed, however, were totally disappointing, as demonstrated by Runs DC-67 and DC-68, respectively. In both cases, both the cut point sizes calculated from the data as well as the fines fraction WMD increased drastically.

SWECO Mill Grind AP Runs

A twenty-gallon SWECO mill grind was made using 0.4% n-phenethyl aziridine as grinding aid/coating agent. The target particle size for the grind, VMA-101, was 0.7 microns WMD. For unexplained reasons, the slurry samples indicated the grind achieved only a 0.94 micron WMD size at 162 hours, at which time a 0.6 micron WMD value had been expected. The slurry was discharged and oven-dried to a powder which was subsequently fed to the classifier in three experimental runs. The dry powder analysed 1.15 microns WMD when removed from the oven. In contrast to the fluid energy milled material, the coated SWECO product did not tend to lump up in the feeder or to buildup on the cyclone walls. The fines filter, however, did clog fairly rapidly.

Table 71 summarizes the product results for the runs. As can be seen, the fines fraction WMD was, in every case, smaller than that of the feed material, and for Run DC-69, was well under one micron. This indicates the equipment is capable of separating materials in this particle size range if properly fed and the fines properly collected. Grade efficiency curves were determined for the three runs, but the values were all well above 50%, so no actual cut points or sharpness indices could be determined. Again, a bag or cartridge-type self-cleaning filter for a fines collector might have provided a better and more meaningful result.

TABLE 71
SUMMARY^a OF WORK WITH SWECO GROUND DRY POWDER

| Run No. DC- | Feed Material Description and WMD | Figure No. of Feed Distribution | Feed Rate lbs./hr. | Fines Product Size | | | Fines Product Weight, lbs. | E t f | Coarse Product Size | | | Coarse Product Weight, lbs. | E t | Figure No. of Product Distributions |
|----------------|---|---------------------------------------|-----------------------|--------------------|------|------|-------------------------------|-------------|---------------------|------|------|--------------------------------|--------|---|
| | | | | 20% | 50% | 80% | | | 20% | 50% | 80% | | | |
| 52 | VMA-101, 1.15 _u WMD | E-70 | 15.2 | 1.64 | 1.00 | 0.65 | 0.16 | 3.52 | 3.37 | 1.74 | 0.89 | 4.39 | 96.48 | E-73 |
| 51 | Same | E-70 | 2.3 | 1.90 | 1.14 | 0.73 | 0.17 | 12.69 | 3.10 | 1.71 | 0.85 | 1.17 | 87.31 | E-70 |
| 69 | Same | E-70 | 26.22 | 1.43 | 0.89 | 0.57 | 1.56 | 4.52 | 2.29 | 1.26 | 0.66 | 32.96 | 95.48 | E-89 |

Notes: a. See Notes at end of Table 67 for explanation of column headings.

Aluminum Powder Runs

Four sizes of aluminum powder were to be processed through the classifier: nominal WMD sizes of 6, 30, 60, and 90 microns. Of these, only the 6 and 30 micron materials are in common use at this plant, and only spherical 6 micron material is on hand. Consequently, quantities of nominal 6, 60, and 90 micron irregular (not spherical) aluminum powders were procured. Through an error, a super coarse grade with a WMD around 180 microns was ordered in lieu of the 60 micron material, so only three grades were available for actual use.

Because of the extreme hazard of dust cloud explosion with aluminum powder, a system was devised to operate that portion of the classification system in contact with the aluminum powder under a virtually complete nitrogen blanket. Nitrogen was supplied to the main gas inlet to the classifier from a large tube trailer capable of holding around 35,000 standard cubic feet of gas at 2000 psig. Reducer valves were used to step down the pressure before entering the velocity breaker drum at the classifier inlet. Standard nitrogen gas cylinders were used to supply the coarse ejector requirements as well as the fluidizing jet in the back of the feed funnel. It is estimated, from the values supplied by the equipment vendor, that the atmosphere inside the classifier was maintained at less than 1% oxygen by volume, or well under the lower combustion limits of 9+ % oxygen in nitrogen. Careful and complete electrical grounding and rigidly controlled safety precautions minimized the potential hazard even more.

Because the tank supply of nitrogen was limited (to about four hours of operation) and the cost of recharging the tank was high (ca. \$400 - \$500 per fill), the quantities of materials classified were greatly reduced, and no experimental runs were made to optimize feed rates. Production fractionation runs were made immediately, in attempts, where possible, to obtain center-cut products. Table 72 summarizes the product results. Runs DC-72 and DC-73 were made, using nominal 6 micron aluminum (actual size was 9.5 microns WMD), to cut out fines tailings at a machine cut point of 5 microns and coarse tailings at 13 microns. Since the cut point of the fines separation run was 5.4 microns, it is possible the feed rate could have been increased some. The second pass cut point of 10.65 microns, however, indicates the feed rate for it was probably too high. The Syntron feeder was used for all the aluminum powder runs, and it is much more sensitive to particle size distribution than the Vibra-Screw unit. Runs DC-72 and DC-73 were run using the exact same vibration levels; the feed rate difference is entirely due to the absence of fines in the material handled in Run DC-73. The results are shown in Figure 112.

TABLE 72
SUMMARY^a OF WORK WITH ALUMINUM POWDERS (U)

| Run No. DC- | Feed Material Description and WMD | Figure No. of Feed Distribution | Feed Rate lbs./hr. | Fines Product Size | | | Fines Product Weight, lbs. | E t f | Coarse Product Size | | | Coarse Product Weight, lbs. | E t | Figure No. of Product Distributions |
|-----------------|--|---------------------------------------|-----------------------|--------------------|------|------|-------------------------------|-------------|---------------------|------|------|--------------------------------|--------|---|
| | | | | 20% | 50% | 80% | | | 20% | 50% | 80% | | | |
| 72 | Lot 4445 Al Powder, 9.5 _u WMD | E-95 | 53.58 | 6.0 | 4.46 | 3.03 | 13.90 | 17.49 | 15.3 | 11.2 | 6.8 | 65.58 | 82.51 | E-95 |
| 73 | Coarse from DC-72, 11.2 _u WMD | E-95 | 102.17 | 10.7 | 9.1 | 7.3 | 21.54 | 33.29 | 18.4 | 14.2 | 10.3 | 43.17 | 66.71 | E-97 |
| 74 ^b | Lot 3432 Al Powder, 36.4 _u WMD | E-99 | N/A | N/A | N/A | N/A | N/A | N/A | N/A | N/A | N/A | N/A | N/A | N/A |
| 75 | Same | E-99 | 170.95 | 22.8 | 11.6 | 7.9 | 7.20 | 7.22 | 45.2 | 30.3 | 14.7 | 92.52 | 92.78 | E-99 |
| 76 | Coarse from DC-75, 30.3 _u WMD | E-99 | 159.10 | 37.4 | 23.6 | 15.2 | 27.76 | 30.35 | 52.0 | 39.5 | 28.2 | 63.72 | 69.65 | E-101 |
| 77 ^c | Lot 4443 Al Powder, 107 _u WMD | E-103 | 119.36 | N/A | N/A | N/A | 1.27 | 3.17 | N/A | N/A | N/A | 38.85 | 96.83 | E-103 |
| 78 | Lot 3916 Al Powder, 5.70 _u WMD | E-105 | 19.24 | 2.66 | 1.62 | ---- | 0.43 | 2.23 | 9.20 | 5.68 | 3.03 | 18.81 | 97.77 | E-105 |
| 79 | Same | E-105 | 62.73 | 2.24 | 1.40 | ---- | 0.90 | 1.64 | 7.9 | 5.12 | 3.09 | 53.99 | 98.36 | E-107 |
| 80 | Same | E-105 | 100.4 | 3.00 | 1.62 | 1.06 | 0.35 | 0.71 | 9.9 | 5.40 | 2.43 | 49.00 | 99.29 | E-109 |
| 81 | Same | E-105 | 83.54 | 2.49 | 1.49 | 1.10 | 0.39 | 0.78 | 10.7 | 6.50 | 3.40 | 49.43 | 99.22 | E-111 |
| 82 | Same | E-105 | 44.99 | 2.53 | 1.65 | 1.13 | 0.68 | 0.69 | 8.4 | 5.86 | 3.27 | 98.49 | 99.31 | E-113 |

Notes: a. See Notes at end of Table 67 for explanation of column headings.
b. Part way through DC-74, the coarse fraction eductor was shut off; machine clogged and run terminated. No data at all.
c. Samples appear to have been mislabelled as fines came out larger in size than coarse.

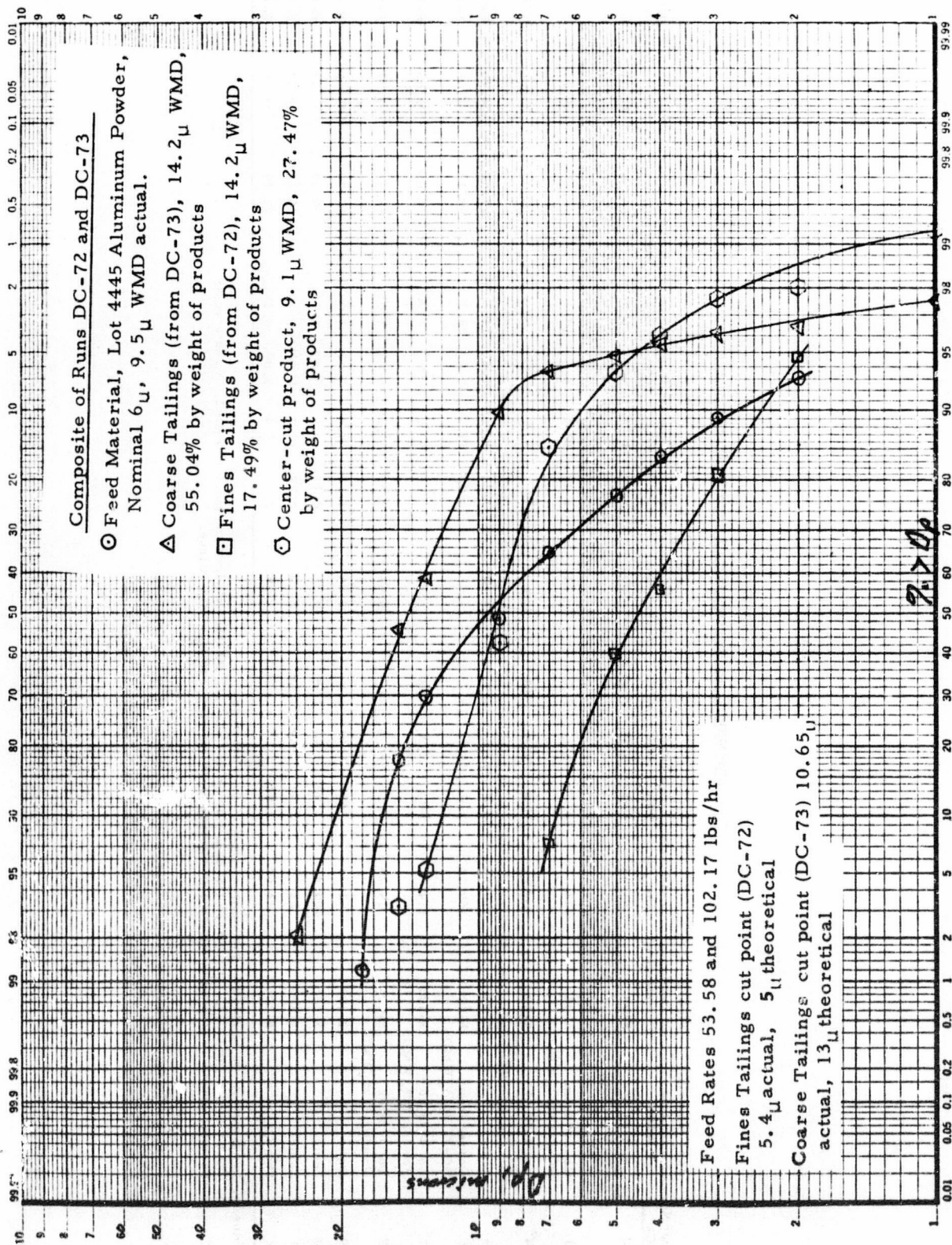


Figure 112. Composite of Runs DC-72 and DC-73

Run DC-74 was made in an effort to make a first cut at 15 microns using nominal 30 micron feed material (actual size was 36.4 microns WMD). Sometime midway in the run, the coarse ejector nitrogen supply bottle emptied, and during changeover to the manifolded second cylinder, the ejector flow was inadvertently shut off for several minutes. The feeder continued to feed more aluminum powder in until the classifier jammed. Unfortunately, the classifier pressure drop set pointer had not been properly adjusted, so the equipment did not automatically shut off at this point. The rotor ceased turning while the blower continued to pull nitrogen and aluminum through the system. The malfunction was discovered when the rotor speed indicator showed no evidence of motion. Apparently, the rotor drive developed enough "slip" in the variable speed belt and sheaves to continue running with the rotor locked tight. After cleanup and reassembly of the unit, extensive checkout operations were completed to ensure that there was no permanent damage incurred and that the equipment still functioned properly.

Runs DC-75 and DC-76 were then successfully completed to cut the nominal 30 micron material at 15 microns and at 28 microns as had been originally planned. Actual cut points of 8.2 microns and 23.1 microns, respectively, indicate that both passes were run at higher than optimum feed rates. Nevertheless, the operations went smoothly and easily, and approximately 28 lbs. of center-cut product were obtained. The results are shown in Figure 113.

Run DC-77 was made to see if any usable results could be obtained feeding the nominal 90 micron aluminum (actual particle size 107 microns WMD), even though experience with the 90 micron AP indicated poor prospects for success. Some 40 lbs. of feed material were processed, yielding only 1.27 lbs. of fines. Either the samples were inadvertently mislabelled (unlikely), the material removed for analysis was not representative (quite possible), or the classifier merely shuffled the distributions around in a crazy way (also possible), because the fines came out generally larger in size than the coarse fraction. No attempt was made to analyze the results, and continued work with this feed material was abandoned.

Since the aluminum powder passed through the classifier without building up or otherwise being lost, and its higher density ensured high efficiency collection in the cyclone, it was felt that good separations might be obtained at the lowest possible cut point of the equipment. Runs DC-78 and DC-79 were made with this goal in mind, using an in-house lot of type M-3 spherical aluminum. Weight median diameters of the fines fractions were 1.62 and 1.40 microns. Runs DC-80, DC-81, and DC-82 were made to see if higher feed rates and/or lower nitrogen gas flows would reduce the fines fraction WMD. As can be seen from Table 72 only DC-81 came

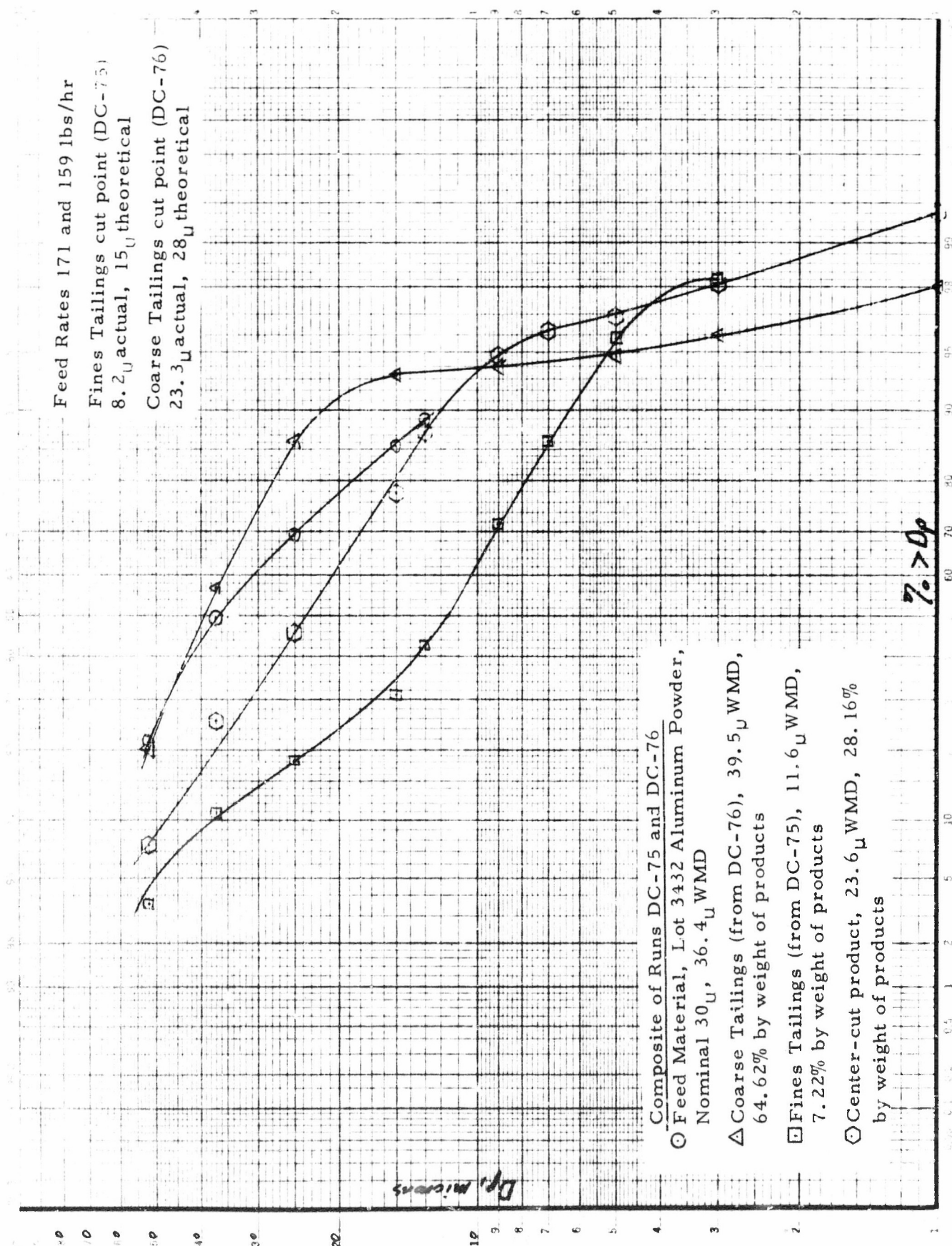


Figure 113. Composite of Runs DC-75 and DC-76

close to the 1.40 microns WMD that DC-79 gave, but it was still larger. It would appear that finer particle size fines can not be produced with the equipment, although additional work might have yielded different results.

It should be noted that if a facility were set-up to classify aluminum powder on a production (or even a pilot plant) basis, several features could be added to minimize the operating costs. One approach would be to use a closed-circuit gas loop to recycle the nitrogen, adding only enough make-up to maintain some fixed, maximum allowable oxygen content. A large cooler would be required to remove the heat added to the gas by the exhaust blower/compressor, and the recycled and cooled gas would have to be piped to both the classifier inlet and to the by-pass valve inlet. A second approach would be to use an inert gas generator, burning nitrogen gas or other fuel, with the necessary dehumidifiers and, preferably, CO₂ absorption columns. With a closed-circuit gas system with coolers, the gas supply costs would be quite reasonable for the inert gas generator system; the initial capital costs would, however, be high.

CONCLUSIONS

1. A total chemical assay of the 400 micron and 200 micron ammonium perchlorate obtained from each vendor, Kerr McGee and Pacific Engineering Company, revealed the following differences:

- 1) There exists an order of magnitude more chloride ion in PEPCON AP (Pacific Engineering Co.) than in Kerr-McGee AP. The source is not known and projections of interference with ballistic or mechanical property behavior would be minimal.
- 2) The higher sulfated ash content (metal oxides, etc.) of PEPCON AP follows the historical trend. Slight increases in burn rate or decreases in thermal stability might result from this difference in ash content.
- 3) The high chlorate content of PEPCON AP is of concern in that thermal stability will be degraded. Data elsewhere in this section illustrate these thermal stability differences.
- 4) The perchlorate assay of the AP from each vendor is similar. Running a material balance indicates that the PEPCON AP should be less pure. The fact that free perchloric acid (an impurity) will analyze as perchlorate casts doubt upon the validity of a perchlorate assay as a means of ascertaining purity.

2. Differential scanning calorimetric measurements, as well as isothermal thermogravimetric analyses, confirmed the decreased thermal stability of the PEPCON ammonium perchlorate.

3. A ROTAP screen analysis on each lot of ammonium perchlorate shows a slightly lower particle size (WMD) for PEPCON oxidizer when compared with similar Kerr McGee samples.

4. The MSA technique for particle size distribution was modified in order that the distribution of large sized oxidizer could be determined. The modification involved changing both the feed and settling liquids to higher viscosity materials.

5. Examination of the MSA distribution curves for 200 and 400 micron AP from each vendor revealed the following differences:

- 1) The weight median diameter of PEPCON (200 micron) is lower than that for Kerr McGee, whereas the opposite trend is apparent for 400 micron oxidizer.

- 2) PEPCON unground AP (200 micron) exhibits a more broad distribution than does Kerr McGee unground oxidizer, whereas the Kerr McGee special coarse AP (400 micron) has a more broad distribution than a similar sample of PEPCON AP.
6. Kryston absorption (BET) measurements on each lot of AP received from the vendors indicated the following:
- 1) Generally, the 200 micron AP exhibits a higher surface area than does the 400 micron material, but the differences are less than theoretical based upon a spherical particle.
 - 2) The reproducibility in surface area between two lots of Kerr McGee special coarse oxidizer (400 micron) was extremely poor with one sample exhibiting nearly twice the surface area as the other.
7. Assays on CTPB and HTPB binder ingredients as well as the aluminum to be used in propellant studies were within normal specification limits.
8. TP-H7036, an 88% total solids (20% aluminum); CTPB propellant was selected as the baseline propellant from which judgements of mechanical property improvements and improved reproducibility could be made.
9. Viscosity response plots, prepared for trimodal mixtures of Kerr McGee AP (400 micron, 200 micron, and 20 micron) and for PEPCON AP, clearly indicate the areas of formulation interest where minimum viscosity can be obtained.
10. A series of parameters which describe the particle size distribution for trimodal mixtures of either Kerr McGee or PEPCON AP were calculated from the MSA distribution and the measured surface area. Following burn rate determination on a series of mixes of TP-H7036 containing different trimodal blends and plotting these burn rate data versus values of each "distribution describing parameter", it was determined that weight median diameter was the parameter which would best correlate the burn rate data.
11. The design burn rate for TP-H7036 is 0.303 in/sec at 1000 psi. The value of weight median diameter for a Kerr McGee trimodal blend required to meet this burn rate is 210 microns. This means that any trimodal mixture of the Kerr McGee AP lots studied which exhibits a WMD of 210 microns will provide a burn rate of 0.303 in/sec in TP-H7036 propellant.

Similar studies of trimodal blends of PEPCON AP indicate the value of weight median diameter required to meet design burn rate in TP-H7036 is 254 microns.

12. There exist an infinite number of Kerr McGee trimodal blends and a like number of PEPCON trimodal blends which will exhibit the design burn rate in TP-H7036 propellant. The optimum Kerr McGee blend is that single blend which will provide the design burn rate and at the same time exhibit the lowest viscosity. Similarly the optimum PEPCON blend can be so defined. A series of Kerr McGee and PEPCON mixes were manufactured at several points along the constant burn rate lines (.303 in/sec at 1000 psi) and the resultant burn rates and viscosities measured. Excellent agreement was obtained between the burn rates measured and that which was predicted (0.303 in/sec at 1000 psi). Viscosity data were plotted versus composition and the optimum Kerr McGee blend was selected as that composition which exhibited minimum viscosity. For an all Kerr McGee blend the optimum composition was 21.10 parts of 400 micron, 27.20 parts of 200 micron, and 19.70 parts of 20 micron to make up the total of 68% AP in TP-H7036 propellant. For PEPCON AP, the optimum blend was determined to be 30.94 parts of 400 micron, 23.80 parts of 200 micron and 13.26 parts of 20 micron.
13. Replicate five gallon mixes of TP-H7036 and an HTPB analog of TP-H7036 were manufactured with each of the selected optimum blends. Mix reproducibility was excellent. The viscosities obtained for the CTPB mixes containing the optimum blends were 30% lower than the normal trimodal production blends.
14. A ballistic evaluation of the optimum blends in TP-H7036 was conducted in TX-3 motor (3 lb. C.P.). The burn rates in motors were 8% higher for the PEPCON blend and 15% higher for the Kerr McGee blend than those burn rates measured in strands.
15. A comprehensive mechanical property characterization of the CTPB and HTPB propellants containing the optimum blends of Kerr McGee and PEPCON AP was performed. The mechanical properties of the HTPB propellants were excellent. The CTPB propellants did not reach a high enough degree of cure and the resultant data was rendered somewhat meaningless.
16. The optimum oxidizer blends provided slightly lower viscosities in propellant. The mechanical property data indicate that blend optimization also results in a modest improvement in propellant physical properties.
17. The substitution of HTPB binder for CTPB binder provides a dramatic improvement in propellant physical properties.
18. The propellants containing HTPB binder appeared to be substantially less sensitive to moisture during processing than those containing CTPB binder.
19. The mix-to-mix reproducibility was excellent both from the standpoint of propellant response properties (relaxation modulus, characteristic relaxation times, etc.) and ultimate properties (failure boundaries, strain endurance).

20. The CTPB propellants, with only one exception, failed when the sum of the principal stresses reached a critical level. Such failure behavior suggests failure due to void formation (in the vicinity of perchlorate particles) followed by growth and interconnection of the voids to cause catastrophic failure.

21. The HTPB propellants failed when the maximum principal stress reached a critical level. Such behavior is suggestive of failure due to flaw initiation in the binder matrix followed by binder crack propagation leading to catastrophic failure. If void formation around the oxidizer takes place, it does not appear to be the origin of the mechanistic chain of events leading to failure.

22. Both CTPB and HTPB propellants exhibited strain behavior which was in accordance with the maximum principal strain theory of failure, as have all other propellants tested at the Huntsville Division.

23. Among the possible explanations for the soft cure in the CTPB propellants are the following:

- 1) Surface impurities on the surface of these particular lots of oxidizer which destroy cure agent or inhibit cure.
- 2) High water content of raw materials
- 3) A change in the functional group assay on polymer or cure agent.
- 4) Since the oxidizer blends have been optimized for lower propellant viscosity, a higher cure agent to polymer ratio might be required to achieve improved mechanical properties.

A water analysis was performed on all ingredients and had not changed from prior analysis. No significant change in functional group analysis on the curing agent and polymer could be detected.

A series of five gallon mixes were then manufactured with increased cure agent to polymer ratios. The mechanical properties measured indicated improved properties with slightly increased cure agent/polymer ratios; however, the PEPCON blend required more cure agent to achieve equivalent properties. This indicates that there does exist on the surface of the PEPCON AP an impurity which does interact with the cure reaction resulting in soft cures.

A final series of mixes indicated a significant difference in mechanical properties depending upon whether horizontal or vertical mixes are utilized.

24. Normal characterization of new lots of ammonium perchlorate for a production program normally involves the manufacture and testing of several five gallon characterization mixes at considerable expense. This program has provided as its end result the first step toward devising a significantly lower cost, yet reliable means through which new oxidizer lots can be characterized without the aforementioned expense. Laboratory characterization tests have been devised through which minimum viscosity at design burn rate can be determined for any given lot of ammonium perchlorate.

25. The Donaldson Classifier appears to be quite effective in making predictable fractionations with good sharpness of separation generally over the advertised cut point range of 0.5 to 50 microns. However, due to the limitations of the fines collection system and the properties of the feed material, it becomes less effective and less efficient as the cut point for AP or aluminum powder approaches 0.5 to 1.0 microns. Cut points over about 30 microns cannot be accurately predicted for these same materials because of a lack of calibration data for any gas flow rates but the nominal 150 actual cfm.

26. A more efficient and effective fines collection device is needed for the Donaldson Classifier when the unit is used with ammonium perchlorate in the lower cut point sizes (i. e., 1-2 microns or smaller). Since the pleated paper cartridge filter used as an air cleaning device downstream from the cyclone appeared to be 100% effective, it would appear that Donaldson's Company's own QUIK-CHANGETM self-cleaning cartridge dust filter would be a natural choice since it also used a pleated paper cartridge filter element.

27. Stainless steel should be used as the material of construction for all material-contacting parts of any Donaldson Classifier procured for AP service. The leased unit was pulled from the production line on an expedited basis in order to meet program schedules, so no effort was made to satisfy corrosion-resistance requirements. As a result, the carbon steel components rusted considerably when washed down, even though efforts were made to remove the water as rapidly and as completely as possible.

28. Over the range of cut points of about 5 microns to about 30 microns, with due regard to effects of feed rate, the Donaldson Classifier can be used to effectively narrow the particle size distribution of either AP or aluminum powder feed materials, while maintaining a comparable weight mean diameter, by fractionating out fines tailings in a first pass and coarse tailings in a second pass.

29. Without additional experimental work, using a classifier with a suitable fines collector as noted in item 26 above, it must be concluded that a submicron AP material cannot be produced by classifying some larger particle size, relatively inexpensive feed stock (i. e., fluid energy milled UFAP) with the Donaldson Classifier.

30. Regardless of the fines collector type and/or arrangement, the effective handling and classification of fluid energy milled UFAP requires that at least 0.2% of some anticaking agent (e. g., Silanox 101) be blended with the AP. This may, however, prevent meaningful particle size analysis of the fines fraction. Possibly a larger particle size feed material would be of aid (e. g., 4-6 microns WMD, such as produced on the Mikro-Atomizer) in minimizing the need for the anticaking agent.

31. Based on the runs made with SWECO-ground UFAP, the Donaldson Classifier is capable of splitting out a fines fraction with a WMD smaller than one micron but only if the feed material has the proper physical properties. Unfortunately, uncoated UFAP, such as fluid energy-milled AP, does not have these proper characteristics.

RECOMMENDED PROCEDURE FOR CHARACTERIZING AP

As a result of this program, a recommended procedure for characterizing new lots of ammonium perchlorate, no matter what size or shape they might be, has been made available. The recommended procedure is listed in Table 73. Although the number of steps required to determine the optimum blend is greater in number than those required for characterization by large scale mixes and testing of ballistic test motors, the costs involved are significantly less. It is recommended that this procedure be utilized in addition to the standard characterization technique for at least six separate lots of ammonium perchlorate in order that greater assurance and confidence can be placed in this particular technique.

TABLE 73

RECOMMENDED PROCEDURE FOR CHARACTERIZING

A NEW LOT OF AMMONIUM PERCHLORATE

(For Trimodal Oxidizer Blends)

1. Chemical Assay
2. Physical Characterization
 - A) MSA particle size distribution
 - B) Krypton (BET) surface area measurement
3. Calculate all "distribution describing parameters" for seven separate oxidizer blends
4. Manufacture seven pint mixes (incorporate new lot of AP) of separate oxidizer blends
 - A) Oxidizer blend varied within realms of processibility
5. Determine strand burning rate at 1000 psi
6. Plot the burn rate for each of the seven mixes versus the values of each "distribution describing parameter" for these seven formulations.
7. Select that parameter which gives the best linear correlation with burn rate as the one of choice.
8. Determine from the plot in (7) that value of the parameter which will result in design burn rate.
9. Manufacture seven pint mixes with seven separate oxidizer blends which all exhibit the value of "distribution describing parameter" corresponding to design burn rate.
 - A) Measure end of mix viscosity
 - B) Ascertain constancy of burn rate
10. Select that oxidizer blend which exhibits lowest end of mix viscosity as the optimum blend for the particular lots of oxidizer in question.

GLOSSARY

| | |
|-------------------|--|
| AP | Ammonium Perchlorate |
| CTPB | Carboxyl Terminated Polybutadiene |
| HTPB | Hydroxyl Terminated Polybutadiene |
| KM | Kerr-McGee Corporation |
| PEPCO | Pacific Engineering Company |
| TCP | Tricalcium Phosphate |
| DSC | Differential Scanning Calorimeter |
| TGA | Thermo Gravimetric Analyzer |
| WMD | Weight Median Diameter |
| MSA | Mine Safety Appliance Company |
| BET | Nitrogen Adsorption Surface Measurement |
| HC-434 | Carboxyl Terminated Polybutadiene, Thiokol Polymer |
| M ² /g | Meters Square Per Gram |
| ROTAP | Automatic Sieving Screens |
| TCC | Thiokol Chemical Corporation (Now Thiokol Corporation) |
| DOA | Diocetyl Adipate, Plasticizer |
| Kps | Kilopoise |
| μ | Micron |
| APD | Average Diameter for i th Particle Size |

interval, d_i

$$d_i = \left[\left(d_j^2 + d_{j+1}^2 + 1 \right) \left(d_j + d_{j+1} + 1 \right) \right]^{\frac{1/3}{4}}$$

where d_j = diameter for jth percentage point of distribution
d_j + 1 = diameter for jth + 1 percentage point distribution

SSA

Specific Surface Area ($m^2/8$), S_w

$$S_w = \frac{6}{p} \sum \frac{W_i}{d_i} = \frac{6}{pd_{32}}$$

where: m^2 = meters squared
 g = grams
 p = true density of particles
 W_i = weight fraction of particles in i^{th} interval
 $d_{32} = \frac{\sum f_i d_i^3}{\sum f_i d_i^2}$
 f_i = number of particles in i^{th} interval
 d_i = see APD

WMD

Weight Median Diameter, d_{43}

$$d_{43} = \sum d_i W_i = \frac{\sum f_i d_i^4}{\sum f_i d_i^3}$$

where: f_i = number of particles in i^{th} interval
 f_i (relative) = $\frac{W_i}{d_i^3}$
 W_i = weight fraction of particles in i^{th} interval
 d_i = see APD

AMD

Arithmetic Mean, d_{10}

$$d_{10} = \frac{1}{n} \sum d_i f_i$$

where: n = total number of particles = $\sum f_i$
 d_i = see APD
 f_i = number of particles in i^{th} interval
 f_i (relative) = $\frac{W_i}{d_i^3}$
 W_i = weight fraction of particles in i^{th} interval

MSD

Mean Surface Diameter, d_{20}

$$d_{20} = \left(\frac{\sum f_i d_i^2}{n} \right)$$

where: f_i = number of particles in i^{th} interval
 f_i (relative) = $\frac{W_i}{d_i^3}$
 d_i = see APD
 n = total number of particles = $\sum f_i$

LMD

Linear Mean Diameter, d_{21}

$$d_{21} = \frac{\sum f_i d_i^2}{\sum f_i d_i}$$

where: f_i = number of particles in i^{th} interval

$$f_i \text{ (relative)} = \frac{W_i}{d_i^3}$$

d_i = see APD

MWD

Mean Weight Diameter, d_{30}

$$d_{30} = \left(\frac{\sum f_i d_i^3}{n} \right)^{1/3}$$

where: n = total number of particles = $\sum f_i$

f_i = number of particles in i^{th} interval

d_i = see APD

MVD

Mean Volume Diameter, d_{31}

$$d_{31} = \left(\frac{\sum f_i d_i^3}{\sum f_i d_i} \right)^{1/2}$$

where: f_i = number of particles in i^{th} interval

$$f_i \text{ (relative)} = \frac{W_i}{d_i^3}$$

d_i = see APD

SMD

Surface Mean Diameter, d_{32}

$$d_{32} = \frac{\sum f_i d_i^3}{\sum f_i d_i^2}$$

where: f_i = number of particles in i^{th} interval

$$f_i \text{ (relative)} = \frac{W_i}{d_i^3}$$

d_i = see APD

W_i = weight fraction of particles in i^{th} interval

HMD

Harmonic Mean, d_{HA}

$$d_{HA} = \left(\frac{1}{n} \sum \frac{f_i}{d_i} \right)^{-1}$$

where: n = total number of particles $= \sum f_i$
 f_i = number of particles in i^{th} interval

$$f_i \text{ (relative)} = \frac{W_i}{d_i^3}$$

W_i = weight fraction of particles in i^{th} interval
 d_i = see APD

APDF

Average Particle Diameter Factor

R_b

Burning Rate (inches/second)

EOM

End of Mix

T-

Five Gallon Mixer

R. H.

Relative Humidity

TX-

Thiokol Experimental Test Motor

C. P.

Cylindrically Perforated

JANNAF

Joint Army Navy NASA Air Force

psi

Pounds per Square Inch

in/in

Inches per Inch

M. S.

Maximum Stress

in/min

Inches per Minute

σ

Maximum Stress

ϵ

Strain at Maximum Stress

T

Temperature of Test ($^{\circ}$ A)

Er

Relaxation Modulus

Eg

Glassy Modulus

Ee

Equilibrium Modulus

| | |
|------------|--|
| t/T | Characteristic Relaxation Time |
| β | Slope of Straight Line Portion of Relaxation Modulus Curve |
| T_g | Glass Transition Temperature |
| α | Linear Coefficient of Thermal Expansion |
| cfm | Cubic feet per minute |
| rpm | Revolutions per minute |
| EFEM | Elkton Fluid Energy Mill |
| FEM | Fluid Energy Mill |
| HSG | High Speed Grind |
| UFAP | Ultra Fine Ammonium Perchlorate |
| D_c | Cut size for materials being classified |
| C_m | Density of material being classified |
| D_c | $0.614 D_c \sqrt{e_m}$ |
| Δp | Pressure differential |
| $G(x)$ | Grade efficiency for particle size x |
| W_c | Weight of coarse fraction product |
| W_f | Weight of fine fraction |
| $F_f(x)$ | Cumulative particle size distribution of fines fraction |
| $F_c(x)$ | Cumulative particle size distribution of coarse fraction |
| E_t | $W_c/W_{ct} W_f$ |
| D_p | Particle diameter for microns |

APPENDIX A

M-S-A ANALYSIS ON 200 AND 400 micron AP

The normal settling liquid used for the M-S-A test on fine AP (maximum particle = 100 micron) is chlorobenzene. This liquid is not suitable for coarser material as the settling times become prohibitively short above 100 micron and error is introduced due to a significant increase in the "Reynolds Number" of the system placing it outside the "Stokesian Regime".

The settling liquid selected for 200 and 400 micron AP was diethyl phthalate, which is technically suitable for this size material and produced reasonable settling times (see schedule). The only problem encountered was in sample transfer. The standard M-S-A chamber contains a 40 mesh screen in the bottom. This gives a 420 micron opening which is suitable for 200 micron AP but presents a problem with 400 micron AP. One approach was to remove the 40 mesh screen and seal the bottom of the chamber with aluminum foil. The chamber would be placed in the M-S-A tube and the foil diaphragm penetrated, releasing the sample into the feed liquid.

M-S-A SCHEDULE FOR AMMONIUM PERCHLORATE (77°F)

Settling liquid --ethyl phthalate
Feed liquid--n-butyl sebacate

| <u>Microns</u> | <u>Settling Time (Min:Sec)</u> |
|----------------|--------------------------------|
| 550 | :07 |
| 500 | :09 |
| 450 | :11 |
| 400 | :14 |
| 350 | :18 |
| 300 | :25 |
| 250 | :36 |
| 200 | :56 |
| 150 | 1:40 |
| 100 | 3:44 |
| 74 | 6:50 |
| 52 | 13:50 |
| 37 | |
| 25 | |
| 18 | |
| 15 | |
| 10 | |
| 5 | |

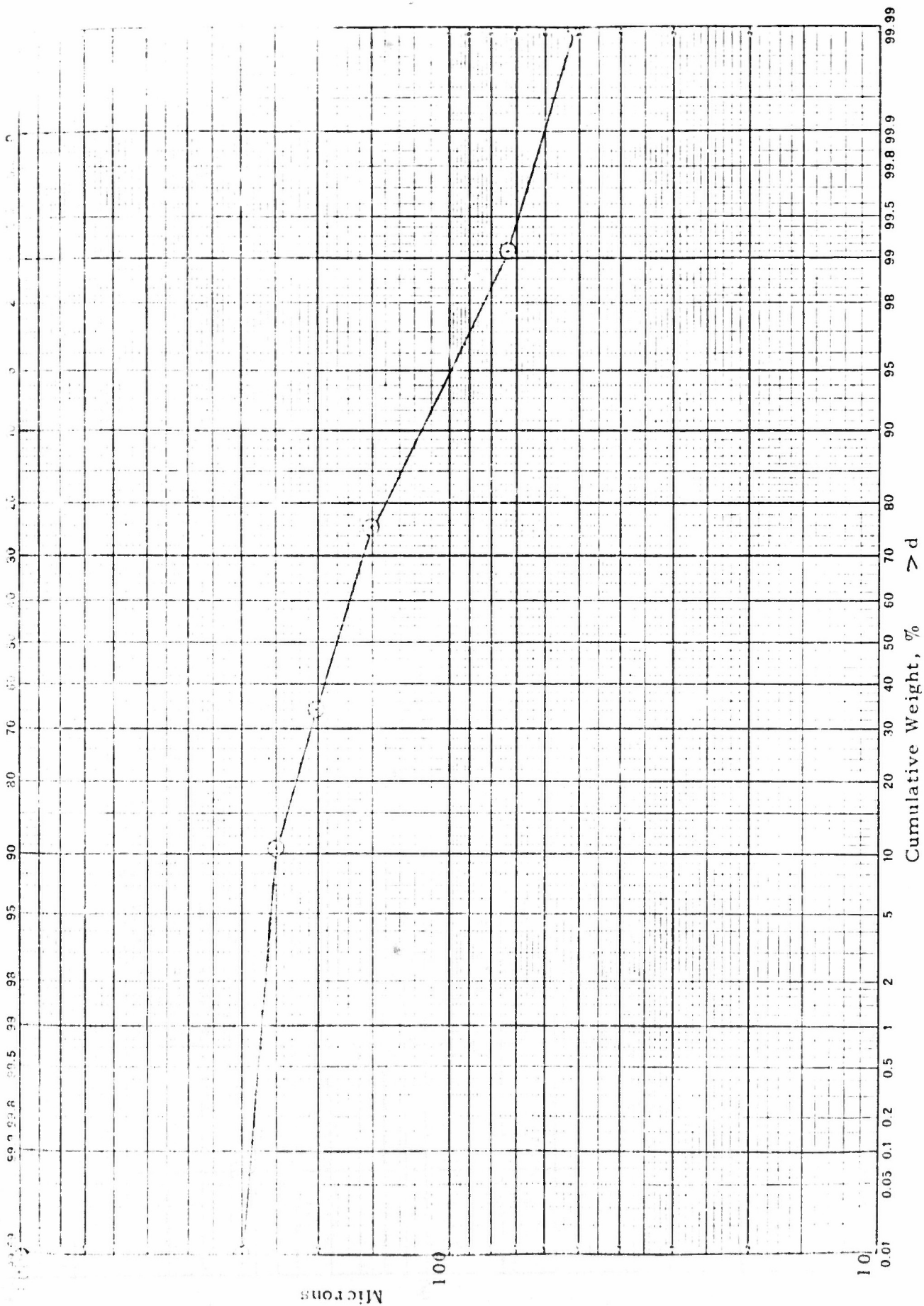
APPENDIX B

M-S-A DISTRIBUTION CURVES
on

Kerr-McGee and PEPCON Oxidizer Lots

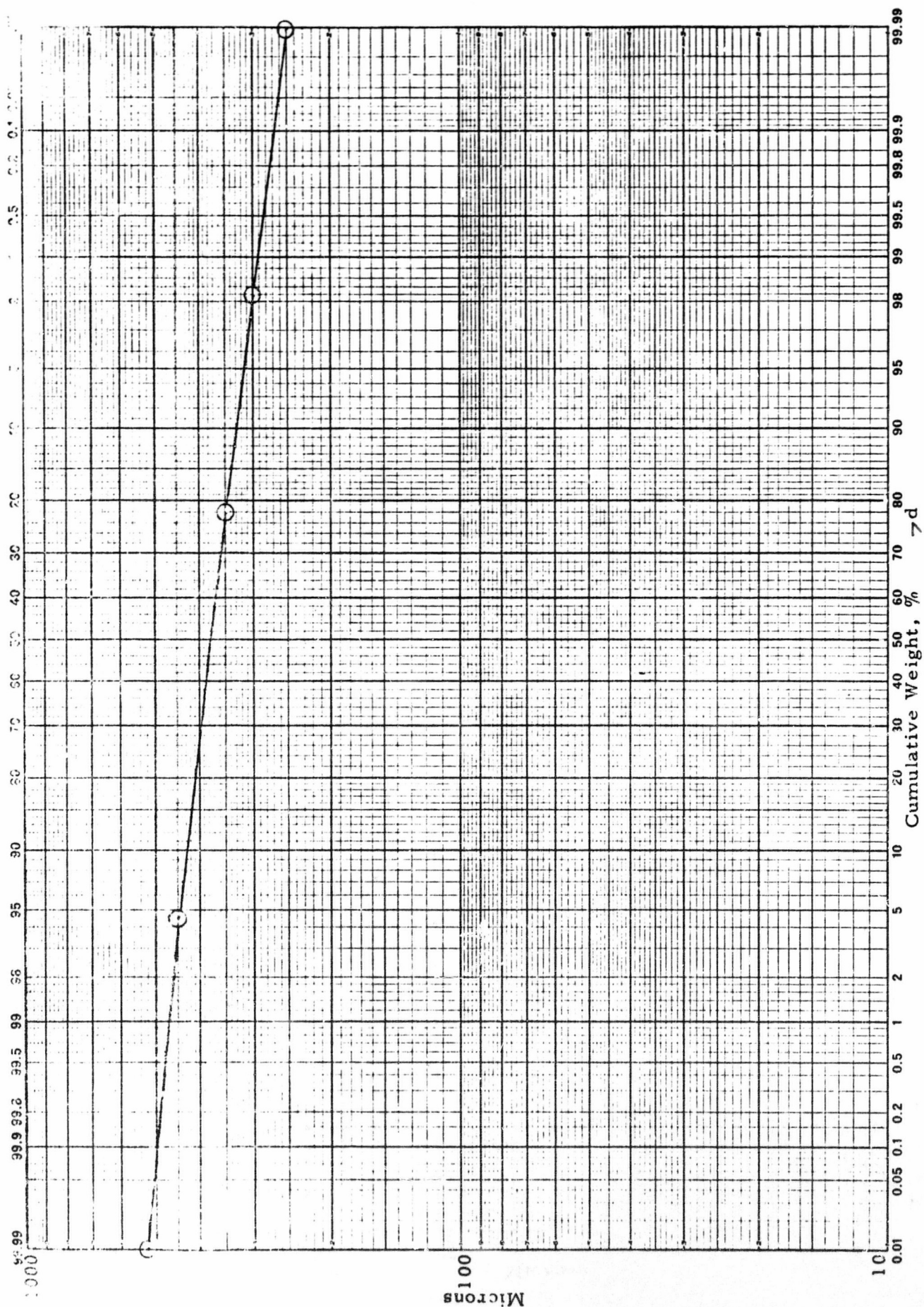
B-i.

Porter McGee, Lot 4089 M NISA

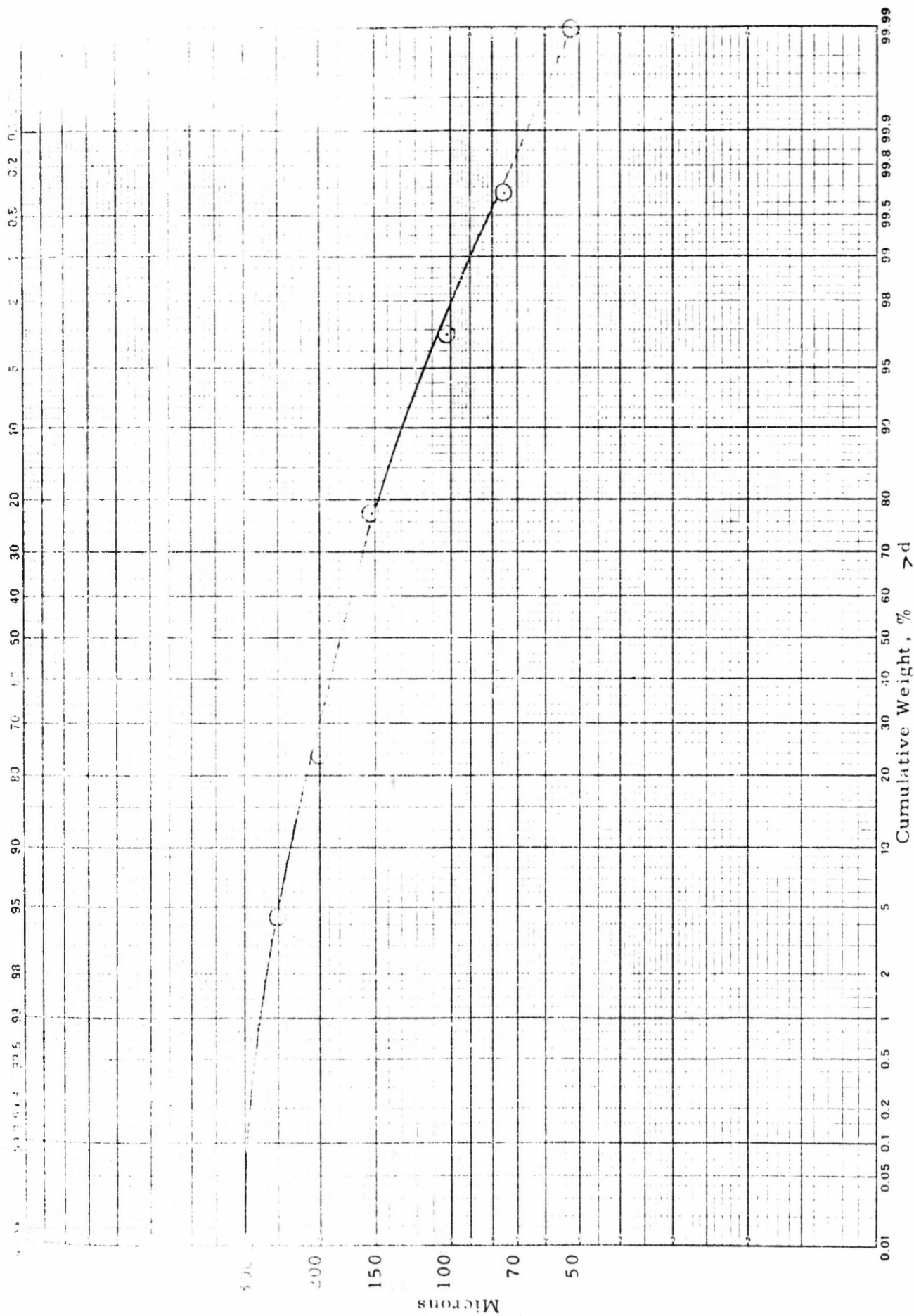


B-1

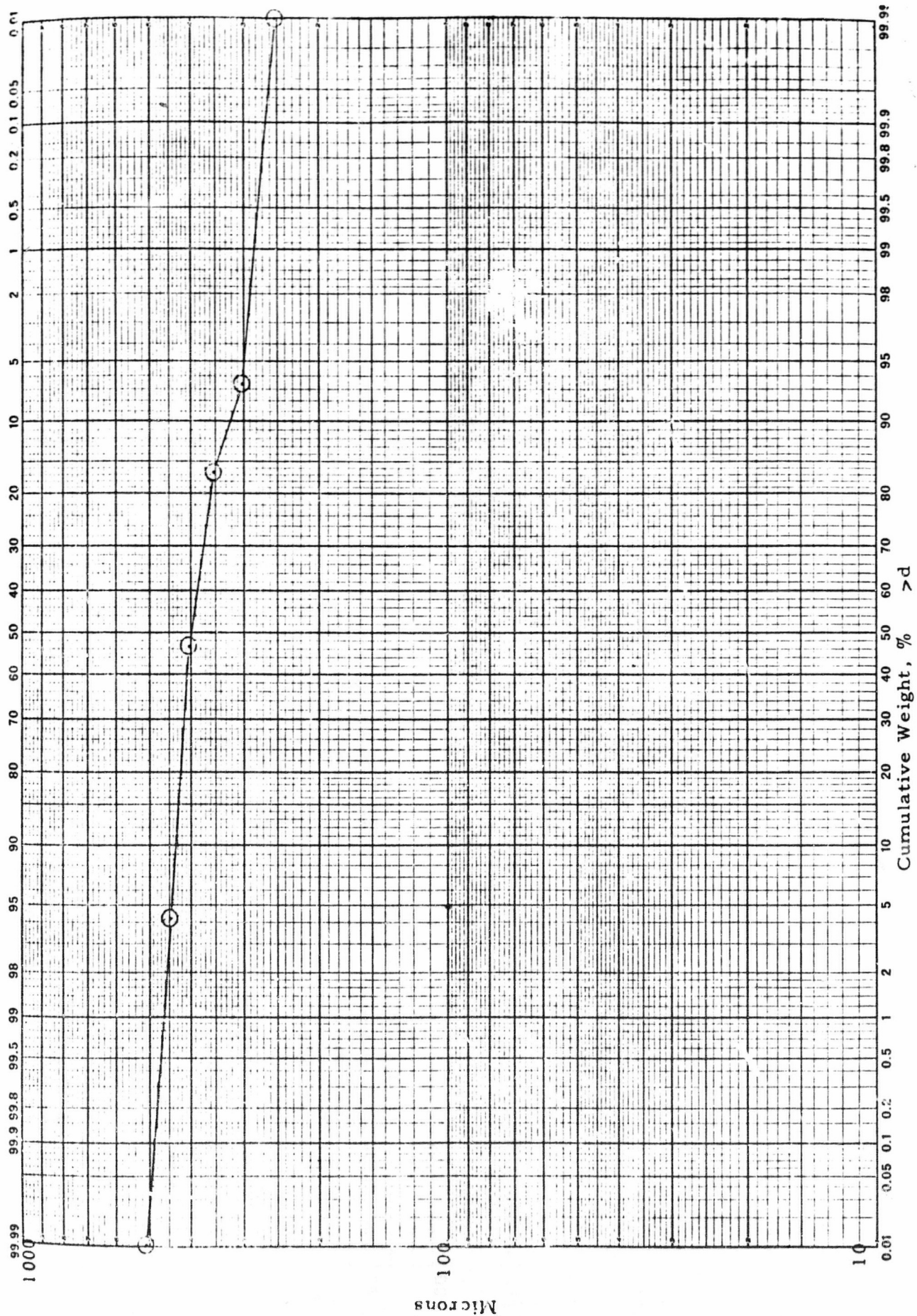
Kerr-McGee Lot 4093 M-MSA



B-2



PEPCON Lot 4104 M - MSA



Microns

B-4

UNGROUND AMMONIUM PERCHLORATE FRIABILITY TEST METHOD

DISCUSSION

A specially classified fraction of ammonium perchlorate is Rotapped with glass beads. The resulting weight of the original sample that was fractured and passed to the Rotap pan is determined. The percent friability is obtained by dividing the weight of ammonium perchlorate in the pan by the sample weight and converting to a percent.

TEST PROCEDURE

- Stack the 35, 70, and 100 MS Standard sieves in descending order of mesh, place the pan under the sieves.
- Place 100.0 grams of ammonium perchlorate, which has been passed through a sample splitter, on the 35 sieve.
- Rotap for 15 minutes.
- Transfer 25.0 grams of the material retained on the 100 sieve to another 100 sieve.
- Place 25 eight millimeter glass beads in with the sample.
- Place a 35 and 70 sieve under the 100 sieve.
- Place a tared pan under the stack.
- Rotap for 10 minutes.
- Disassemble the stack, brush any material adhering to the 35 or 70 sieve into the pan.
- Determine the weight of ammonium perchlorate in the pan.

$$\% \text{ Friability} = \frac{\text{Weight of ammonium perchlorate in pan} \times 100}{\text{Sample Weight}}$$

APPENDIX D

Contents:

1. Equipment Description and Operation
2. Procedure 00000-7320-401, Donaldson Classifier
3. Procedure 0000A-3179-401, Classification of Ammonium Perchlorate
4. Procedure 0000B-3179-401, Classification of Aluminum Powder
5. Evaluation of Classification Results
6. Particle Size Classification of Plastic Powders, Shaller, R. E.
and Lapple, C. E., 1971

Reproduced from
best available copy.



SECTION 1.
EQUIPMENT DESCRIPTION AND OPERATION

The Donaldson Classifier operates by the opposing forces of air drag operating predominantly on finer particles and centrifugal force acting predominantly on coarser particles. Air drag is controlled by regulating the flow of air into and through the classification section over the range of approximately 100 to 200 actual cubic feet per minute (acfm). Centrifugal force is controlled by regulating the rotational speed of the classifier rotor over the range of 420 to 4200 rpm. Most classification runs are made at 150 acfm, with the rotor speed being the primary cut point adjustment. Air flow is induced by a lobe-type blower operating at fixed speed and constant throughput, on the down-stream end of the classifier, and discharging to the atmosphere through noise-reducing silencers. Air enters the classifier through a prefilter, to remove dust or other contaminants, then passes through an orifice-type flow meter into the classifier. The air drags the fines fraction particles inward through the rotor and out of the classifier. The fines-laden air stream enters the fines collector, a high efficiency cyclone separator, where most of the fines fraction material is removed from the air stream. The air, with unremoved fines material, then passes through a pleated-paper filter to remove essentially all of the remaining particulate matter. The clean air then passes through a secondary pleated-element filter, for protection of the blower from abrasive particles, to a tee on the inlet silencer on the blower. The other side of the tee has a throttling control valve which regulates the flow of filter-cleaned ambient air into the blower to by-pass the classifier. Since the blower pulls air through the system, the classifier, and all components down-stream of it, operates under a slight vacuum.

Figure D-1 shows the installation of the Donaldson Classifier in Bay J, Building 7603. To the left is the motor-driven lobe blower, mounted inside a sound-damping box, with its associated mufflers and inlet filters. The central unit in the figure is the classifier itself, complete with coarse fraction collector (in right foreground) and fines fraction collector (partially hidden to left rear). To the right is the Vibra-Screw feeder, mounted on a movable dolly. Behind the feeder is the velocity breaker drum (wrapped in felt to damp out noise) used to supply low dew point air to the classifier from a system normally used with a fluid energy mill.

Feed material, supplied by an appropriate powder feeding device, is aspirated into the classifier by the reduced pressure inside the classifier. It is dispersed in the classification zone at the edge of the rotor where the classification air stream enters the outer edge of the rotor. Fines fraction material is swept inward toward the center of the rotor by the air stream. Coarse fraction particles are accelerated outward, by the rotation of the rotor, where they are collected by a volute opening and pulled into the coarse collection container by a small air stream induced by a venturi-type eductor. The eductor discharges back into the classification zone

so that any fine particle size material swept into the coarse collection container, by accident, will re-enter the classifier. Figure D-2 shows the feed inlet funnel to the classifier and the discharge end of the Vibra-Screw feeder. The short tube projecting inward from the right end of the bottom of the funnel is a fluidizing jet. It was provided to help fluidize and inject the feed material into the classifier.

(U) Figure D-3 shows the fines fraction container, removed from its operating position underneath the fines cyclone separator. The round plate to the right of the container is a life platform (operated by a pneumatic cylinder). The container is provided with four spring catches that engage the cover plate at the bottom of the cyclone. The catches pull the container against a sponge rubber sealing gasket in the under surface of the cover plate.

(U) The classifier rotor speed is controlled by a Reeves drive system having an electric-motor-type output speed adjustment. Rotor speed is sensed by an electromagnetic pickup reading a 30-tooth gear mounted on the drive shaft. The pickup signal is sent either to a transducer with a meter-type read-out or to an electronic counter. Rotor speed can be determined and adjusted remotely. The air flow through the classifier is regulated by adjusting the volume of by-pass air to the blower with the throttling valve. The valve is motor driven, so the air flow can be regulated remotely. Air flow level is determined from calibration curves, using pressure drop readings across the flow meter and across the classifier. The pressure drop meters are installed in the control panel, along with a meter indicating the pressure drop across the (pleated element) fines filter, indicating how dirty the filter is.

Figure D-4 shows the control module for the classifier, installed in a room remote from the classifier installation itself. A detailed explanation of the controls and instruments is given in the operating procedure for the classifier, No. 00000-7320-401.

(U) The operating procedures for the classifier itself, and for classification of ammonium perchlorate, are attached, and include detailed information on the controls, equipment layout and operation, and the method of adjusting the cut point for the operation. An explanation of the cut point is given later in this report.

(U) Although a Syntron vibratory feeder is supplied with the classifier, we selected a Vibra-Screw feeder for controlling the rate of feed since we have the broadest experience with it. The Vibra-Screw feeder is shown in Figure D-5. The Syntron feeder was used in a number of runs where small quantities of feed material were involved and where the completely self-emptying feature was desired. It was used with all the aluminum powder work. It should be noted that neither feeder is very satisfactory with extremely small particle size powder, particularly material that readily cakes or bridges in a bin.

Entering air to the classifier is ambient bay air, held to 40-45% relative humidity and 77°F. It was felt that such conditions would be undesirable for the smaller sizes of AP, so the normal inlet opening was piped up to an air supply system used for the fluid energy mills operated in the next bay in Building 7603. This system consists of an oil-free compressor/aftercooler/receiver supplying 125 psig air to a Kemp Oriad regenerating drier. The outlet air from the drier is at about 110 psig and 80-100°F, with a dew point in the range of -40°F or lower (on expansion to atmospheric pressure, the dew point is even lower). This air was piped, through control valves, to a final expansion tank, denoted a velocity-breaker, where it was reduced to atmospheric pressure just before being aspirated into the inlet filter of the classifier. The velocity-breaker drum is shown in Figure D-5. In order to keep from oversupplying the classifier, a flue back-pressure regulator was installed in an outlet from the drum. The inlet air control valve was manually regulated to maintain a very slight overpressure (e.g. a fraction of an inch of water column) above atmospheric pressure in the drum. This condition was indicated by a slight motion of the regulator damper flap in the partly open state. The regulator, with its control weight, is shown in Figure D-5 on the right side of the drum.

For the classification of aluminum powder, it was decided that the same inlet gas system would be used to supply pure nitrogen gas to the classifier to maintain an inert (essentially oxygen-free) atmosphere. This would prevent an explosion of the dispersed cloud of aluminum in the classifier, in the event a spark or other ignition source was generated, by preventing combustion of the aluminum with the oxygen in air. Nitrogen was supplied from a high pressure tube trailer having a capacity of about 40,000 cubic feet of gas (at atmospheric pressure) when charged to 2000 psig. The high pressure gas was throttled across some thirty feet of 1/2-inch flexible hose (stainless-steel-braided) and a high pressure needle valve. As noted in Figure D-6, this system provided up to four hours of operating time at a utilization rate of 150 cfm. The data for this figure came from runs DC-72 through DC-77. At this utilization rate, the effective cut-off point was about 200 psig in the tube trailer. Since the fluidizing jet in the classifier feed funnel was also operating on nitrogen, the actual oxygen level inside the classifier was maintained well below the nominal 9% minimum volume required for combustion.

The actual cut point of a classification operation is a function not only of the rotor speed and air flow, but also of the feed material density, the feed rate, and, of course, the particle size distribution of the feed material. In general, the cut point decreases as the rotor speed increases, as the air flow decreases, and as the feed rate increases. The feed material must, of course, contain material both above and below the cut point. The limits of rotor speed and air flow are explained more fully above and in the procedures, as is the effect of feed material density. The feed rate can be increased to a point where the classification zone becomes choked; at that point, the

classifier will become plugged and will malfunction. Conversely, the feed rate can be reduced essentially to zero; doing so may increase the sharpness of the classification, but the production rate may become uneconomically small.

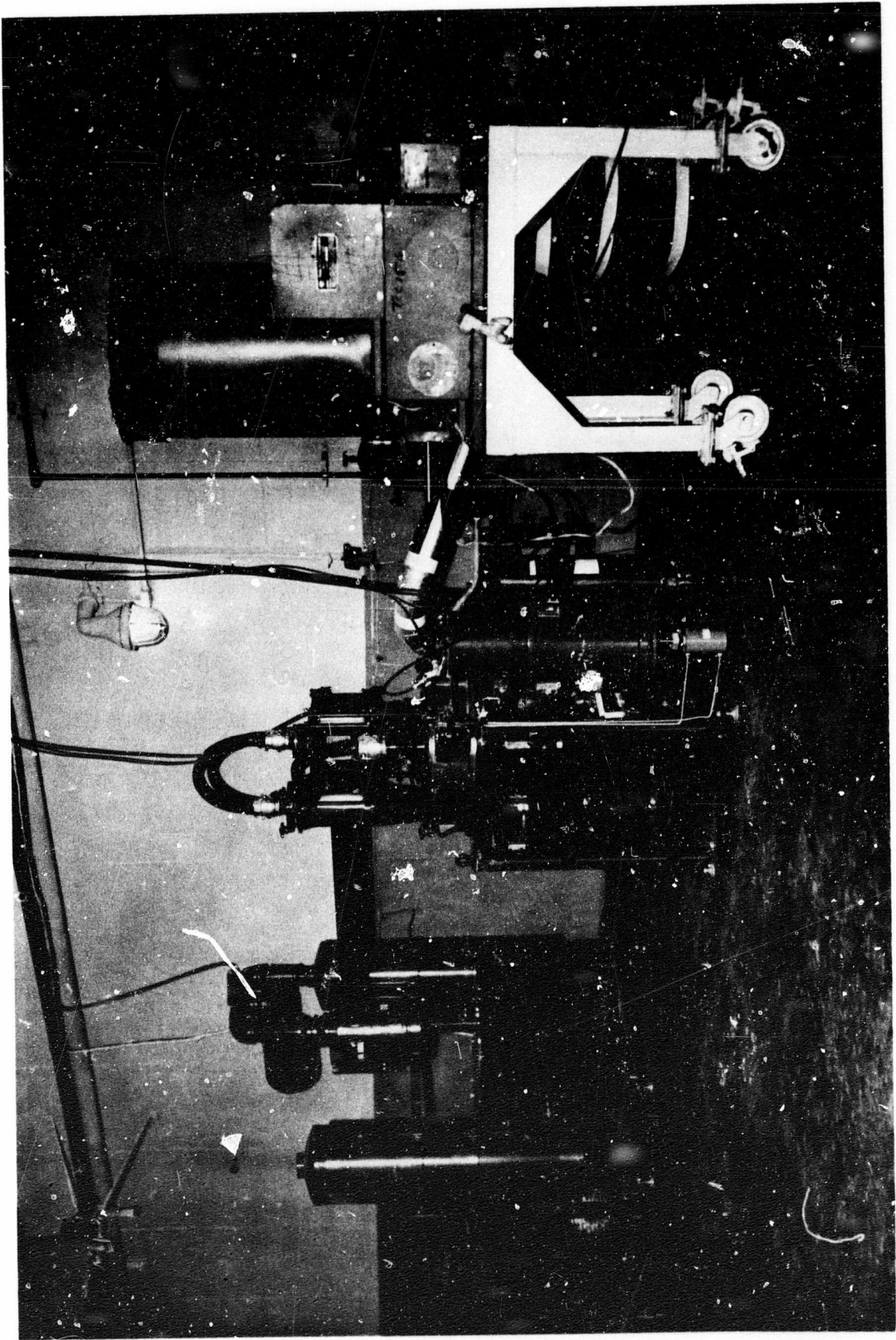


Figure D-1. Donaldson Classifier Installation

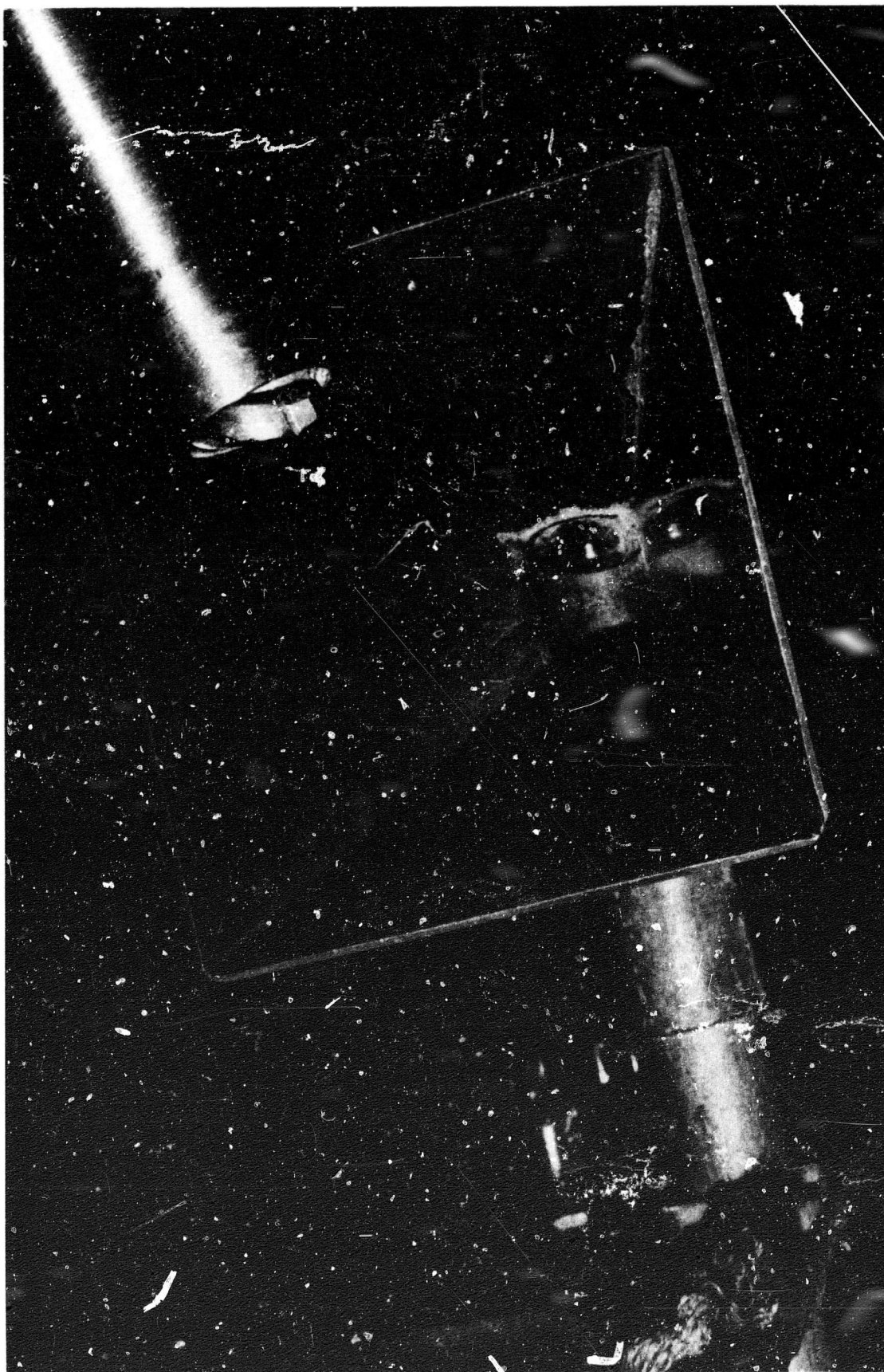


Figure D-2. Feed Inlet Funnel, with Vibra-Screw Feeder Tube

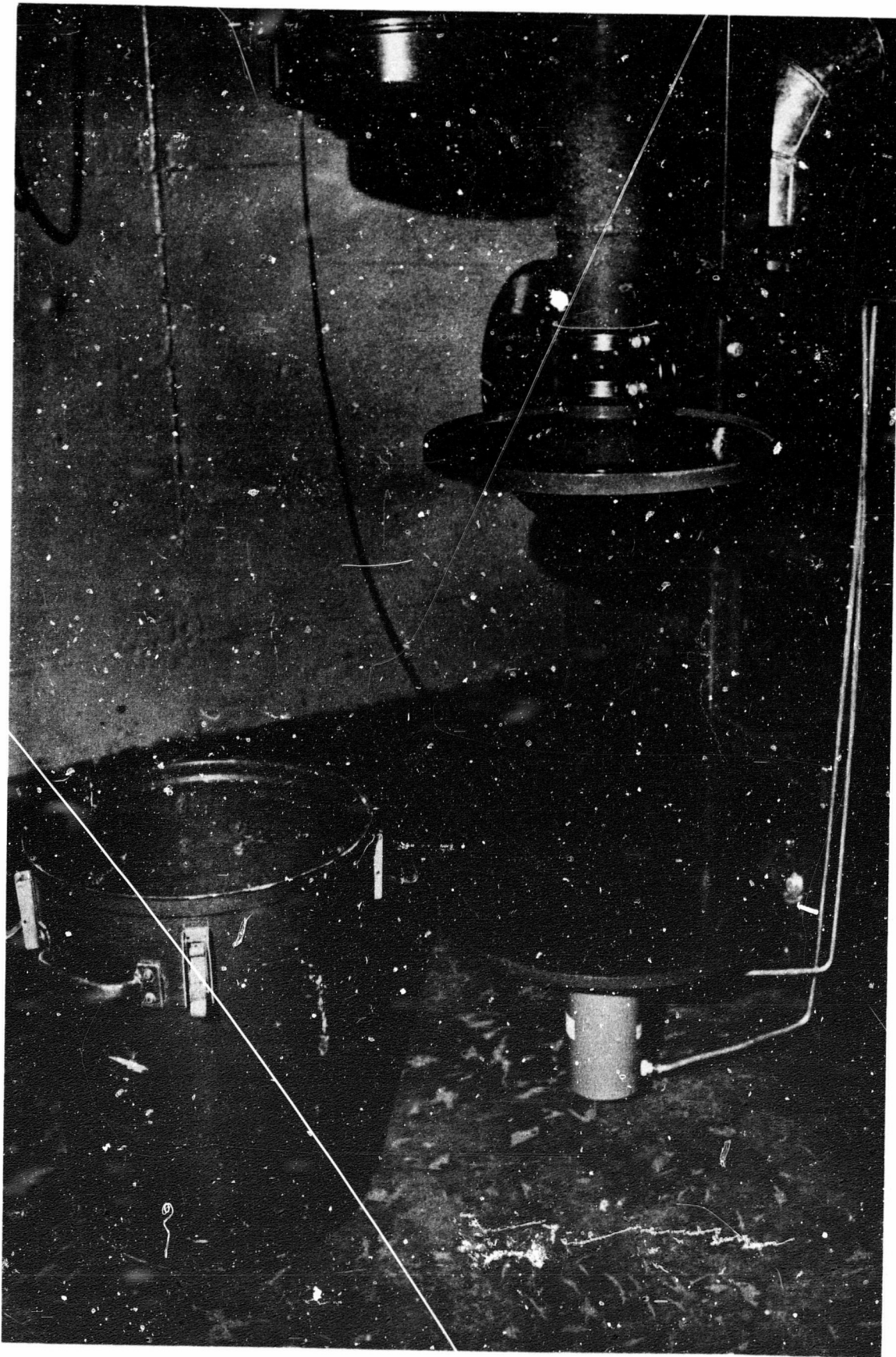


Figure D-3. Fines Fraction Container, Shown Removed from Classifier



Figure D-4. Classifier Control Module

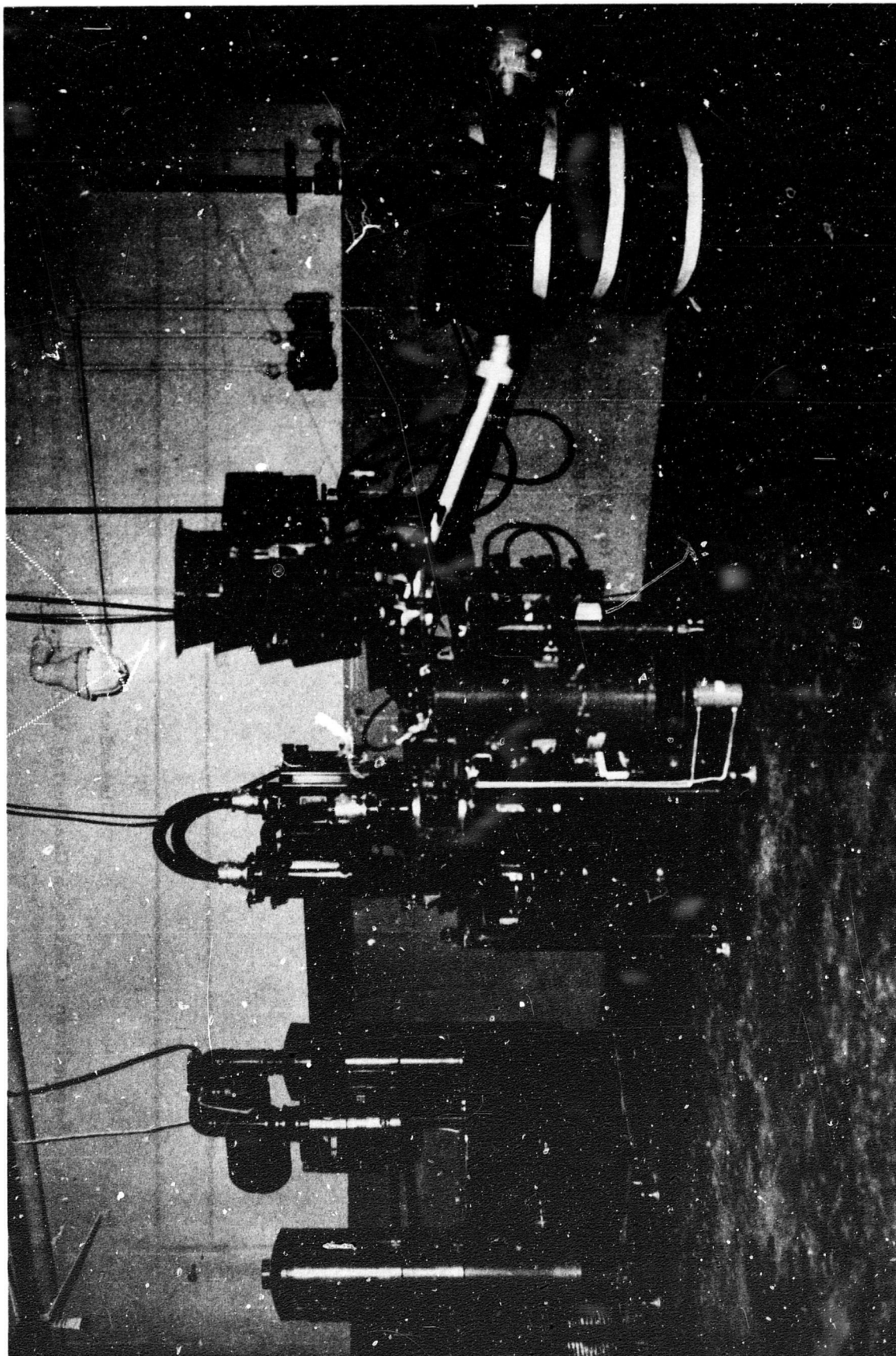


Figure D-5. Donaldson Classifier Set-Up Using Syntron Vibratory Feeder

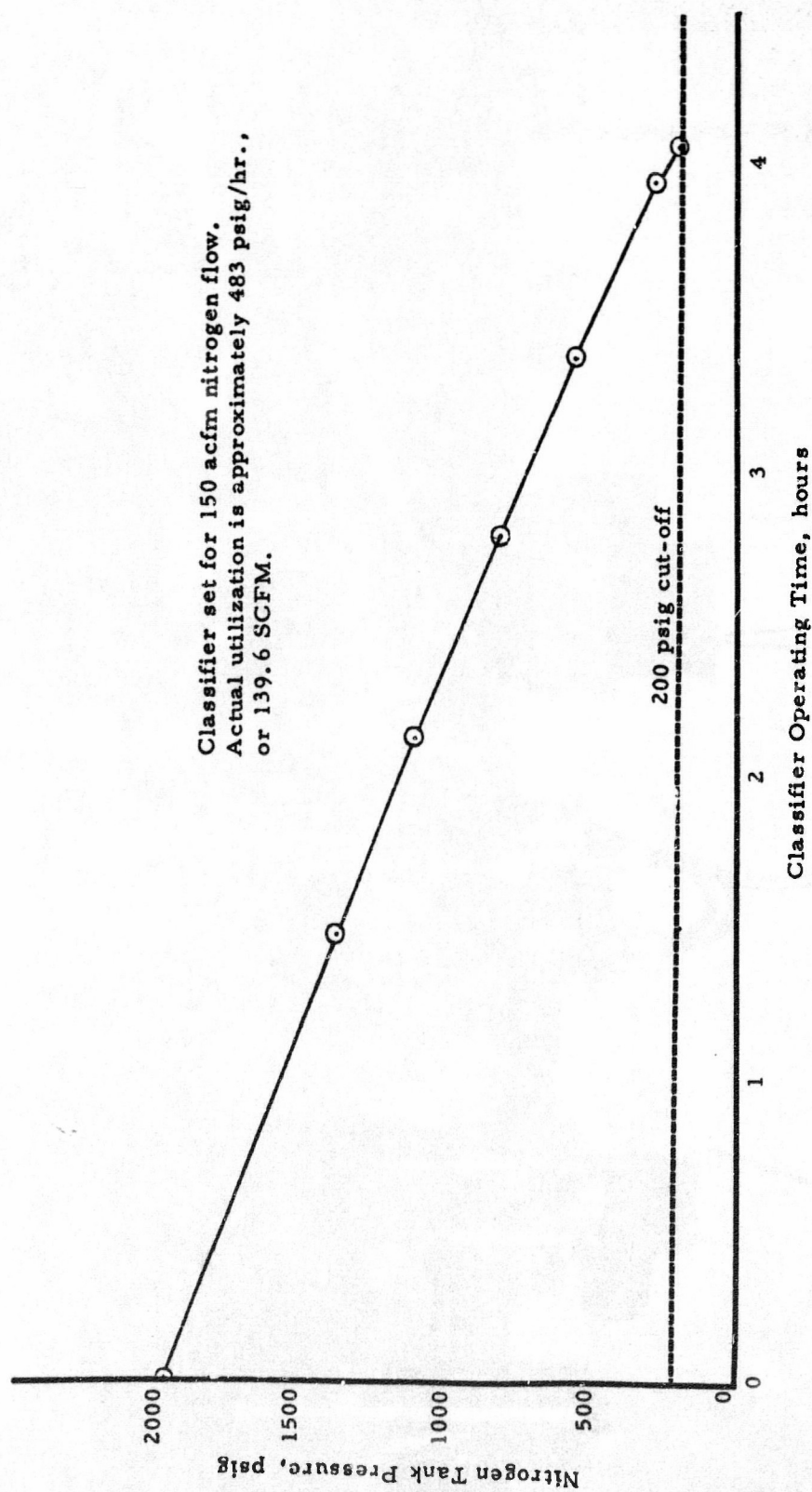


Figure D-6. Expenditure of Nitrogen Gas During Aluminum Powder Classification Runs

SECTION 2.

| OFFICIAL APPROVED APPROVED ✓ APPROVED OTC NO. 9297 DATE 5/17/73 | Thiokol / HUNTSVILLE DIVISION Huntsville, Alabama <small>A DIVISION OF THYROL CHEMICAL CORPORATION</small> <h1 style="margin: 10px 0;">OPERATION PROCEDURE</h1> | PROCEDURE NO. 00000-7320-401 SUPERCEDES NO. N/A | DATE 5/9/73 PAGE 1 of 13 | | | | | | | | | | | | | | | |
|--|---|--|-----------------------------------|------|----------|--|--|--|--|--|--|--|--|--|--|--|--|--|
| | | <table border="1" style="width: 100%; border-collapse: collapse;"> <tr> <th style="width: 50%;">REVISION</th> <th style="width: 50%;">DATE</th> <th style="width: 50%;">APPROVED</th> </tr> <tr><td> </td><td> </td><td> </td></tr> <tr><td> </td><td> </td><td> </td></tr> <tr><td> </td><td> </td><td> </td></tr> <tr><td> </td><td> </td><td> </td></tr> </table> | REVISION | DATE | APPROVED | | | | | | | | | | | | | |
| REVISION | DATE | APPROVED | | | | | | | | | | | | | | | | |
| | | | | | | | | | | | | | | | | | | |
| | | | | | | | | | | | | | | | | | | |
| | | | | | | | | | | | | | | | | | | |
| | | | | | | | | | | | | | | | | | | |

DONALDSON CLASSIFIER

A. GENERAL DESCRIPTION

The Donaldson Classifier is designed to disperse, then classify fine particles into coarse and fine fractions. The basic components include a feeder, the classifier, a blower package, fine and coarse fraction product collection equipment and a control panel package. The blower package provides the primary air flow for conveying feed through the classification zone and to carry the fines fraction to its collection point. The feeder meters material into an aspirated conveying air stream which carries the particles into the dispersion and classification zones. Coarse particles are pushed outward by centrifugal force, then pulled into the coarse collector by a low volume air sweep produced by a compressed air eductor. The fine particles are drawn inward to the center of the classification rotor by drag force, and conveyed to the fines collector cyclone. The air stream, from which most of the fines fraction material has been separated, is pulled through two cartridge filter type air cleaners (in series) then into the blower package. The inlet air or gas stream to the classifier also passes through a cartridge-filter type cleaner to prevent contamination of the product. The desired cut point is selected by adjustment of the rotor speed, the air flow through the classifier, and, to some extent, the rate of feed. To be effective, the feed material must, of course, contain material both larger and smaller than the cut point size.

A block diagram of the Donaldson Classifier system is given as Figure 1. The control panel layout is shown in Figure 2. The classifier is described as follows:

Donaldson Classifier Model B

Serial No. 18-12003

Nominal feed rate range 20 to 400 lbs. /hr.

Nominal cut point range 0.5 to 50 microns

Rotor speed range 420 to 4200 rpm

Rotor drive 2 Hp 1730 rpm electric motor input to Reeves

Drive equipped with electrically operated output speed controls

Blower drive 15 Hp 1765 rpm electric motor

Classifier air flow 150 acfm nominal, 100 to 200 acfm range by calibration chart

Classifier air flow control by electrically operated valve regulating flow of by-pass air to blower package

Capacity of collection containers 1.0 cubic foot each

B. SAFETY REGULATIONS

1. When operating with hazardous materials, classification must be carried out remotely, with safety chains installed per Figure 3. The warning light (on the access road) must also be operated.
2. Aluminum powder represents an extreme dust explosion hazard. Such hazard may, however, be eliminated by proper inert atmosphere controlled to maintain the oxygen level below the minimum level for combustion (nominally 9% oxygen, the remainder being nitrogen).
3. Check the electrical grounding of all components of the classifier system per procedure "Electrical Grounding" prior to any operation.
4. All feed material should be screened through a 10 or 20 mesh screen prior to charging to the feeder.
5. All feed and product fraction materials must be handled to minimize spills and/or dusting, and spills are to be cleaned up immediately.
6. Operating personnel must wear an approved dust respirator and goggles, as well as conductive-sole safety shoes or conductive "Leg Stats," when handling materials and/or exposed to dust from the classifier. All persons concerned with the operation must, in addition, wear flame-resistant protective clothing (coveralls or lab jackets).
7. The posted limits of Bay J are 300 lbs. of Class 2 or 300 lbs. of Class 7 material. During operation of the classifier, however, the quantity is to be limited to the capacity of the feeder hopper plus the collection containers. Extra feed material, as well as accumulated product materials, must be stored in Bays H or I, or other areas as approved. All other raw materials must be removed from Bay J prior to operation.

C. ASSEMBLY AND CHECKOUT

NOTE: Disassembly and reassembly of the classifier itself is beyond the scope of this procedure. It must be carried out only under the direct supervision of the Process Engineer or a properly trained alternate designated by him.

1. Inspect all parts to see that they are clean, dry and in operating condition (free from nicks, dents, warpage, etc., and all fittings are properly secured).
2. Check the coarse and fine fraction collection containers for evidence of damage, and repair any defects before proceeding. Reinstall on the equipment.

73 May 09

3. Remove the feed funnel/conveying tube assembly and check for contamination. Remove any present, then reinstall and secure with the cam-lock clamp.
4. Check the primary cartridge-filter air cleaner down stream from the fines fraction collector and replace if severely contaminated. It may also be necessary to clean the filters installed on the manometer taps on this air cleaner.
5. Check secondary cartridge-filter air cleaner only if primary unit needs replacing. Replace it if badly contaminated.
6. Check the cartridge-filter air cleaner on the classifier inlet and replace it if badly contaminated.
7. Apply power to the control panel, and push the "Emergency Stop" button (10) to reset the automatic controls.
8. Check the compressed air supply to the classifier and ensure the filter and drier have both been bled down, the regulator is set for 50 psi, and compressed air is applied to the unit.
9. Start the classifier rotor by depressing the "Start" button (1). Observe the tachometer (or counter) while running the rotor speed up and down through its range by pressing the "fast" (2) or "slow" (3) buttons as needed. Bring the rotor speed back to about 500 rpm. Listen for any unusual sounds from the classifier during the speed traversing. Shut off immediately if any peculiarities are noted.
10. Set "mode switch" (4) to "hand" position, then start the blower drive by pressing the blower "start" button (5). Operate blower bypass controls to increase classifier air flow, by pressing "open" (6) or "close" (7) buttons as needed, to run the Air Flow meter reading up to about 15 in. H₂O, then back down at least to 5 in. H₂O. Observe pressure drop across classifier while doing so. Limit adjustment needle (11) on classifier pressure drop meter should be set to 10 in.Hg or higher during this operation. Also observe fines filter pressure drop for excessive reading (e.g. 30 in. H₂O or higher) indicating the filter is clogged.
11. Open the ejector valve on the coarse fraction collector, and ensure air is flowing through it.

73 May 09

12. Close the ejector valve, then push the "slow" (3) and "close" (7) buttons simultaneously until the rotor speed drops to 420 rpm and the air flow meter reads 5 in. H_2O or less. At that time, push both the blower and classifier "stop" buttons (8) and (9).
13. Recheck the collection containers and the collector housings for contamination, and remove any present.
14. If all operations proceeded satisfactorily, the equipment is now ready for classification operations.

D. CLASSIFICATION OPERATIONS

1. Based on the particle size distribution of the feed material and the requirements of the work to be accomplished, select a cut point (or cut points) to be used. Calculate the conversion factor to be applied to Figure 4 to compensate for the material density, then determine the required rotor speed.

NOTE: If two or more cut points are to be used (e. g. removal of both the coarse and fine ends of some feed material), select the lowest cut point for the first pass, then proceed to the next larger cut point, etc.

2. Check out the classifier as in Part C, above.
3. Screen the feed material as required, and charge it to the feeder (normally the Vibra-Screw feeder will be used). Consult the feeder charts and adjust the feeder controls for the desired feed rate.
4. Start the classifier rotor by pushing the "start" button (1).
5. Set the rotor speed to that determined in Step 1, above, by pressing the "fast" (2) or "slow" (3) buttons, as needed, to bring the tachometer meter or counter reading to that desired.

NOTE: If the electronic counter is used, with the time function set at 1.0 seconds, the digital reading will be exactly one-half the true rpm of the rotor. This is because a 30 tooth gear is used as the generator rather than a 60 tooth gear.

6. Set the mode switch (4) to "hand" position.
7. Start the blower by pressing the blower "start" button (5).
8. Set the lower limit set pointer (12) on the air flow meter to about 10 inches H_2O , and the upper set pointer (13) to about 15 inches H_2O . Set the mode switch (4) to "auto."

NOTE: The meter will now increase the air flow automatically until the actual pressure drop across the flow meter is between the set pointer limits. Any changes that occur due to external causes will be automatically corrected for by the meter.

9. Consult Figure 5 or Table I to determine the balance between air flow pressure drop (Δp) and classifier Δp for 150 acfm (or whatever air flow is desired). Increase or decrease the air flow Δp as required, by adjusting the set pointers, until the proper balance is obtained. Set the upper set pointer about 1.0 inch H_2O above the lower set pointer.

10. Set the upper limit set pointer (11) on the classifier Δp meter about 1.0 inch Hg above the stable meter reading.

NOTE: If actual meter reading of classifier Δp exceeds the set pointer adjustment, or if the fines collector Δp exceeds 50 inches H_2O , or if the "Emergency Stop" button (10) is pushed while the machine is running, all the classifier functions will be immediately shut off. The feeder, however, will not be shut off automatically. It is therefore imperative that an operator remain at the controls at all times to shut down the feeder in the event the classifier is automatically shut off by its own instruments.

11. When the air flow adjustment has been completed, open the ejector valve for the coarse collector.
12. If hazardous materials are to be classified, set up the necessary safety chains and barricades and turn on the warning light per Figure 3. Retire to the control station and operate the classifier remotely.
13. Start the feeder. When material is flowing into the feed inlet, readjust the air flow set pointers (but not the upper limit set pointer on the classifier Δp meter) as in Steps 9 and 10, above, to compensate for changes in the air flow conditions.

NOTE: As soon as feed material enters the classifier, the classifier Δp will drop to some lower level, indicating less actual cfm of air are now passing through the classifier. This necessitates readjustment of the air flow to maintain the balance for 150 acfm (or the desired air flow) through the classifier. When the feeder is turned off, the change will tend to reverse itself, however, readjustment is not needed then.

14. Operate the classifier and feeder for the required period of time.

73 May 09

NOTE: The operating time must be the shorter of the following:

- a. The available feed material runs out.
 - b. One or both of the collection containers become filled up.
 - c. The fines filter becomes clogged as indicated by Δp and/or automatic shut down.
 - d. Some other malfunction or problem occurs.
15. Turn off the feeder.
 16. After the classifier has run two minutes to clear itself, turn off the coarse collector ejector valve.
 17. Turn the mode switch (4) to "hand," then simultaneously press the "close" (7) and "slow" (3) buttons.
 18. When the rotor speed has reached 420 rpm, release the "slow" button. When the air flow meter reading reaches 5 inches H_2O , release the "close" button.
 19. Push both "stop" buttons, (8) and (9), to shut off the classifier.
 20. Empty the product collection containers and prepare for the next operation.

E. OPERATION OF COLLECTION CONTAINERS

To remove containers:

1. Undo the four catches around the top of the collection container and swing the hooks down against the container wall.
2. Pull the lift control valve handle to lower the lift and the container.

NOTE: If the container is empty, it may not release from the seal gasket when the lift is dropped. In this event, push down lightly on the container handles to break it away from the gasket.

3. Remove the container and weigh, discharge, cleanup, etc.

To reinstall containers:

4. Clean container with water and rags, if needed, or with dry brushes. If classification at the same conditions is to continue, cleaning may not be required.

73 May 09

5. Place the container on the lift, and, holding two opposing catch hooks, lift the container and engage the hooks over the cover plate. Position the two remaining hooks over the plate. Center the container and secure two opposing catches, then the remaining two. Inspect the container to ensure proper contact and sealing against the gasket.

NOTE: Do not, under any circumstance, raise the container into place with the lift. If the container is not perfectly aligned with the cover, the lift will crush the plastic container and destroy it.

6. Push the control valve handle in to raise the lift to support the container in place.

F. CLEANUP OF EQUIPMENT

The classifier and components can be cleaned up with soft bristle brushes, vacuum sweep, and rags, if permissible for the material being classified. It may also be washed with water from a hose, providing certain precautions are taken. If washed with water, the unit can be turned on and allowed to dry itself out after reassembly. See NOTE at beginning of Part C.

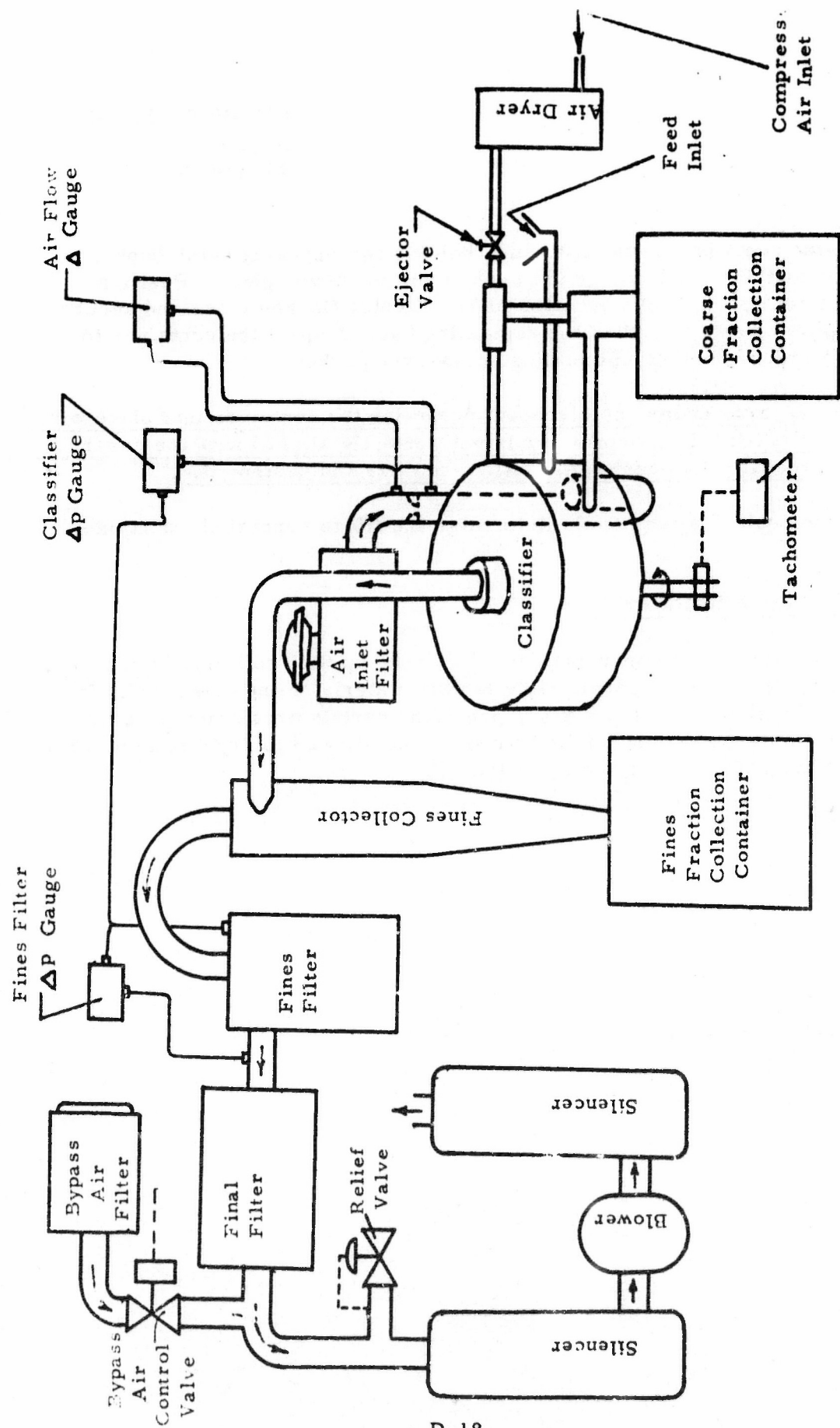


Figure 1. Donaldson Classifier System

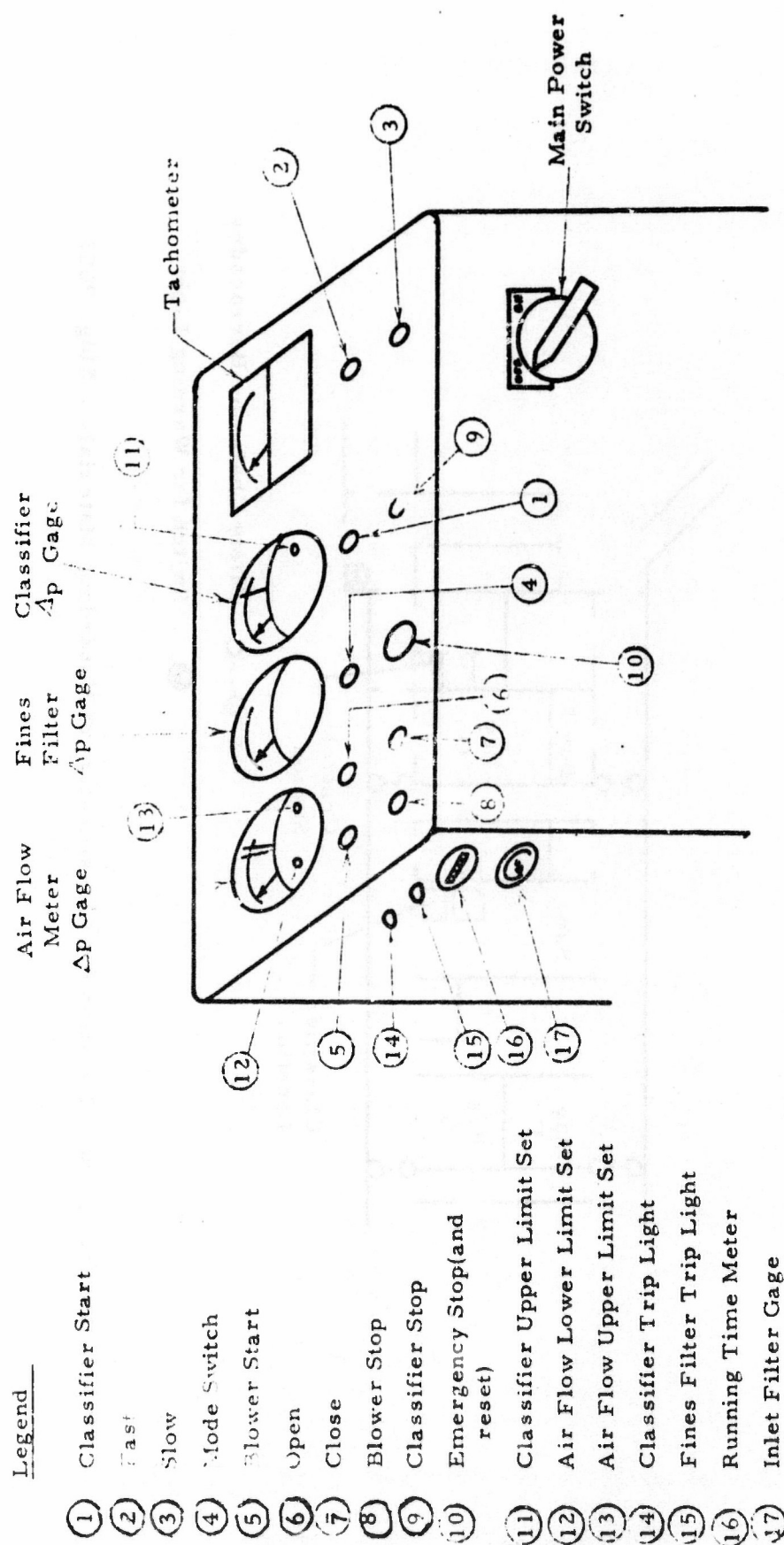


Figure 2. Control Panel Layout

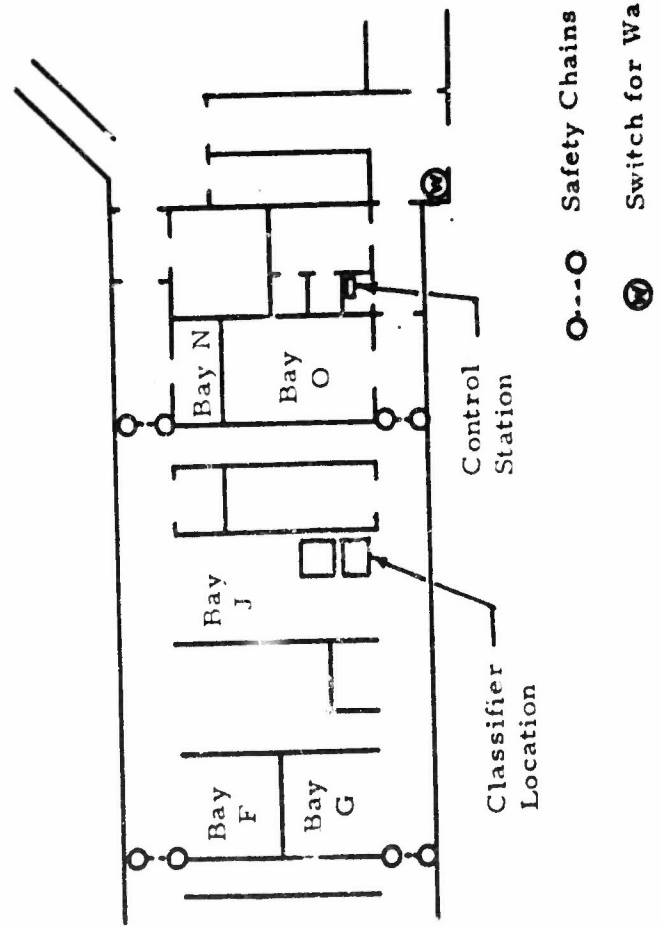


Figure 3. Safety Chain Location for Classification of Hazardous Materials - Bldg. 7603

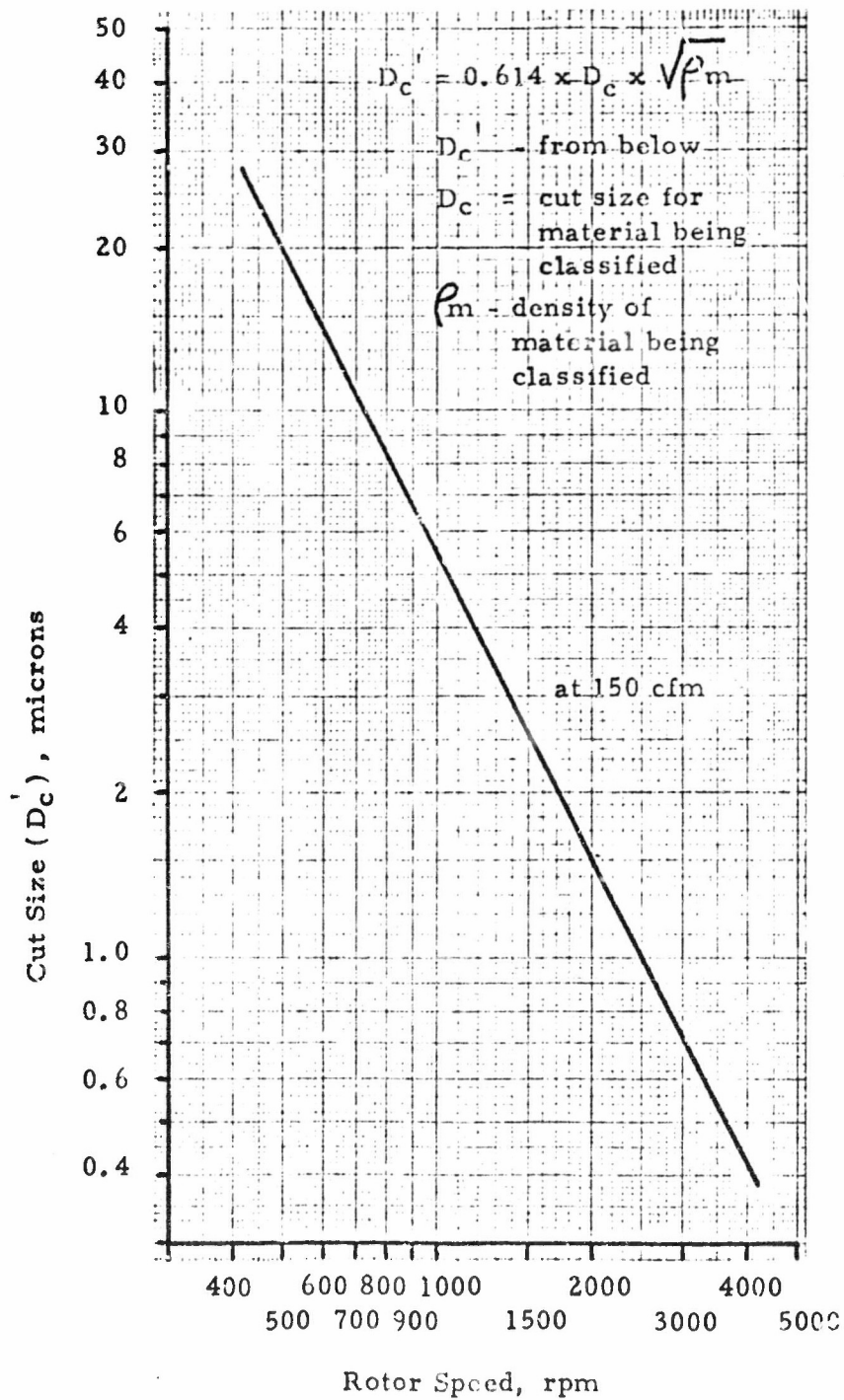


Figure 4 - Cut Point Size Versus Rotor Speed

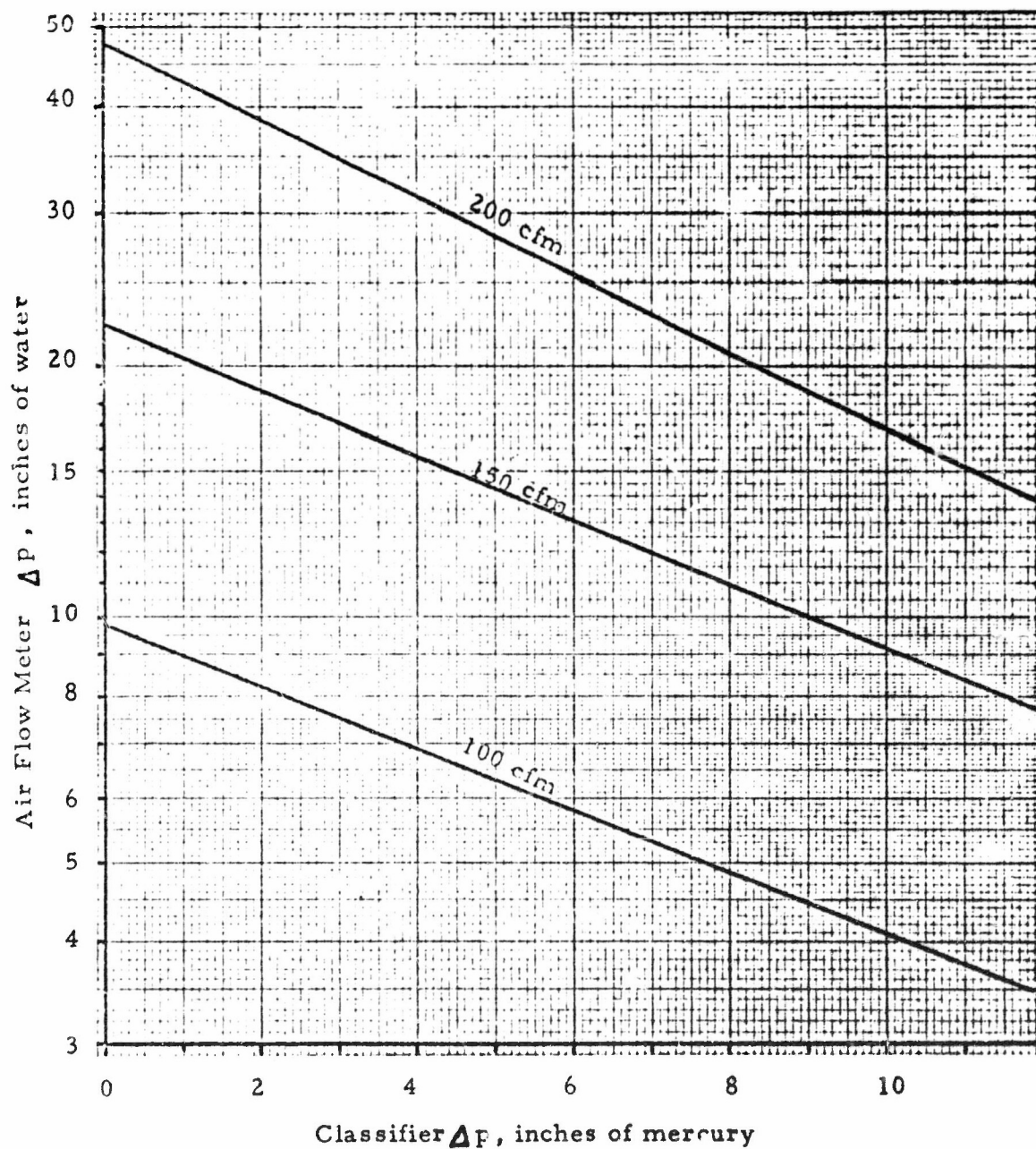
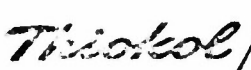


Figure 5 - Air Flow Balance Conditions

TABLE I
PRESSURE DROP BALANCE POINTS FOR 150 CFM
THROUGH CLASSIFIER

| <u>Classifier Δp, in. Hg</u> | <u>Flow Meter Δp, in. Water</u> | <u>Classifier Δp, in. Hg</u> | <u>Flow Meter Δp, in. Water</u> |
|---|--|---|--|
| 0 | 22.4 | 7.5 | 11.5 |
| 0.5 | 21.4 | 8 | 11.0 |
| 1 | 20.5 | 8.5 | 10.5 |
| 1.5 | 19.6 | 9 | 10.0 |
| 2 | 18.7 | 9.5 | 9.6 |
| 2.5 | 17.9 | 10 | 9.2 |
| 3 | 17.1 | 10.5 | 8.8 |
| 3.5 | 16.4 | 11 | 8.4 |
| 4 | 15.7 | 11.5 | 8.0 |
| 4.5 | 15.0 | 12 | 7.7 |
| 5 | 14.3 | 12.5 | 7.3 |
| 5.5 | 13.7 | 13 | 7.0 |
| 6 | 13.1 | 13.5 | 6.7 |
| 6.5 | 12.5 | 14 | 6.4 |
| 7 | 12.0 | | |

SECTION 3.

| | | | | |
|----------------------------------|--|---------------------------------|-------------------|----------|
| ORIGINATOR <i>S. L. Vance</i> |  HUNTSVILLE DIVISION Huntsville, Alabama A DIVISION OF THIOKOL CHEMICAL CORPORATION OPERATION PROCEDURE | PROCEDURE NO. 0000A-3179-401 | DATE 73 May 16 | |
| APPROVED <i>[Signature]</i> | | SUPERCEDES NO. | PAGE 1 of 2 | |
| APPROVED <i>[Signature]</i> | | REVISION | DATE | APPROVED |
| APPROVED | | | | |
| OTC NO. 9300 | | DATE 5/17/73 | | |

CLASSIFICATION OF AMMONIUM PERCHLORATEI. GENERAL

This procedure specifies the operations for classification of ammonium perchlorate using the Donaldson Classifier. Equipment operation shall be generally per procedure "Donaldson Classifier", 00000-7320-404, with changes or precautions specified below. Ammonium perchlorate is a white crystalline oxidizer with good stability. It generally presents only a fire hazard, but as the particle size goes down, particularly below 10 to 20 microns, it becomes progressively more hazardous from an explosion standpoint. When contaminated with fuels, it can be caused to explode quite readily. Unless contaminated with more than 1% fuel and of sufficiently small size to readily disperse in a dust cloud, it represents a minimal dust explosion hazard.

II. SAFETY

1. Classification of ammonium perchlorate shall be considered a hazardous operation and must be performed remotely.
2. Safety chains or barricades must be placed as shown in Figure 1, and the warning light (on the access road) operated, to prevent entry to the area during classifier operations.
3. Check electrical grounding of all components of the classifier system, and specifically install a ground strap from the feeder to the classifier, per procedure "Electrical Grounding" prior to any operation.
4. Operating personnel shall wear conductive-sole safety shoes (or regular safety shoes and conductive "Leg-Stats"), flame resistant coveralls or lab coats, and goggles. When handling fine particle size, dusty materials, approved dust respirators must be worn.
5. No other materials may be stored in the Classifier Bay (Bay J) during classification operations with ammonium perchlorate.
6. All feed and product fraction materials must be handled to minimize spills and/or dusting, and any spills must be cleaned up immediately.
7. All feed material must be screened through a 10 or 20 mesh screen prior to charging to the feeder hopper. A conductive plastic dust cover

shall be installed over the feeder hopper as soon as the hopper is charged. All operations must be halted immediately if any evidence is noted that foreign objects have penetrated the dust cover.

8. The quantity of ammonium perchlorate in the classifier bay during operations must be limited to the capacity of the feeder hopper. Extra feed material and accumulated product materials must be stored in Bays I or H, or in other approved areas.

III. OPERATIONS

1. Assemble and check out the equipment per procedure "Donaldson Classifier".
2. Use of low dew point air from the fluid energy mill system is required for processing ammonium perchlorate smaller than 20 microns, but is optional for larger materials. If used, remove the dust cap from the inlet air filter and connect the five inch ducting from the velocity breaker drum.
3. Select a cut point to be used, based on project requirements and the feed material particle size distribution. Determine the rotor speed to be used from Figure 2 (derived for ammonium perchlorate; specific gravity of 1.95).
4. If the low humidity air supply is not used, proceed with classification operations as specified in procedure "Donaldson Classifier", adhering to all applicable safety regulations.
5. If the low humidity air supply is to be used, open the air supply valve just above the velocity breaker drum immediately after turning on the classifier blower. Adjust the supply valve as needed to maintain an excess of supply air over that called for by the classifier. An excess is indicated by opening of the flapper valve on the velocity breaker drum. The supply valve should be readjusted, as needed, after the classifier air flow controls have been balanced for the desired classifier air flow. All other operations will be as specified in procedure "Donaldson Classifier", except for closing the air supply valve (to the velocity breaker drum) immediately after shutting off the classifier at the end of a run.

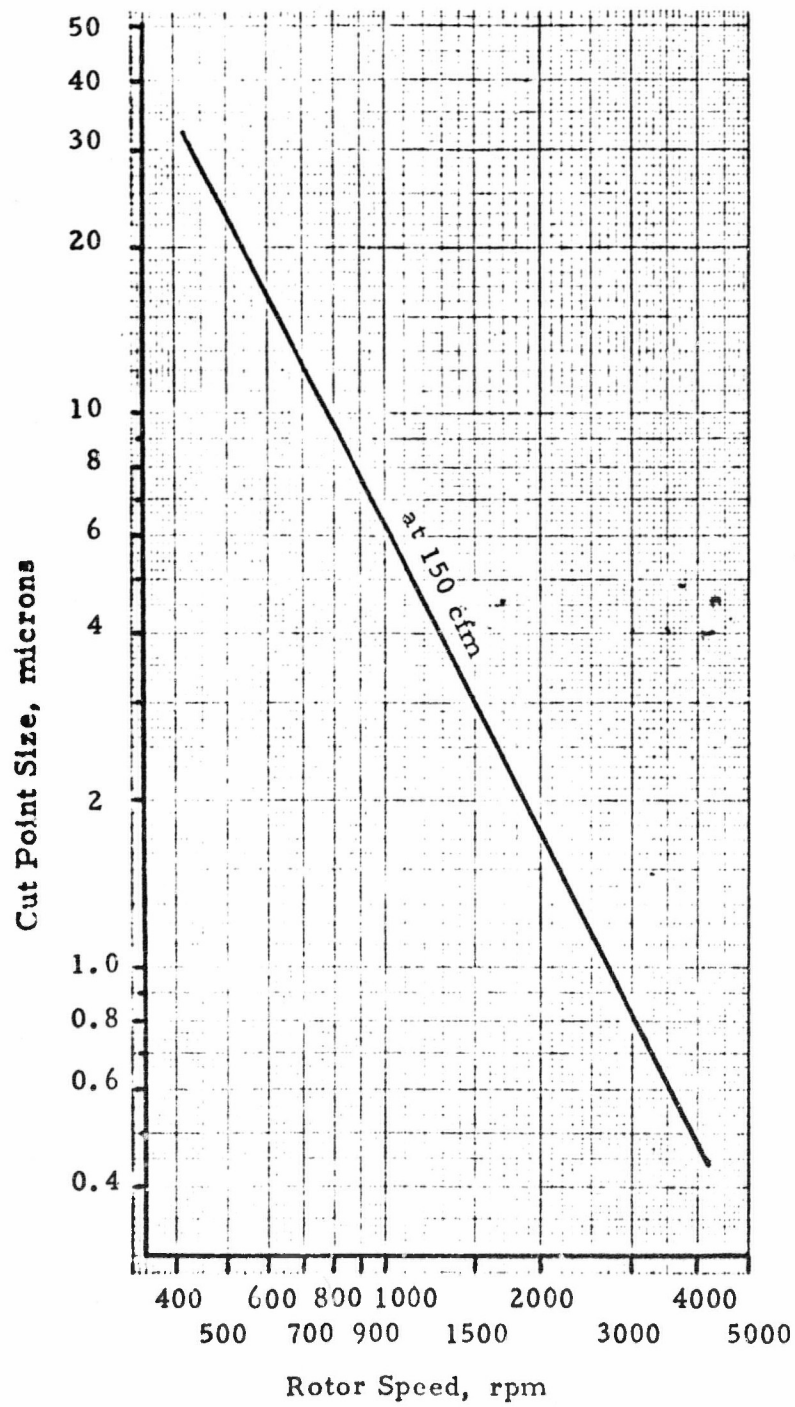


Figure 2. Cut Point Curve for Classification of AP

| | | | | | | | |
|---|--|---|--|--|--|-------------------------------------|--|
| ORIGINAL FOR APPROVED APPROVED APPROVED OTC NO. 9343 DATE 73 Jun 105 | | Thiokol / HUNTSVILLE DIVISION Huntsville, Alabama A DIVISION OF THIOKOL CHEMICAL CORPORATION OPERATION PROCEDURE | | PROCEDURE NO. 0000B-3179-401 SUPERCEDES NO. N/A REVISION DATE APPROVED | | DATE 73 Jun 28 PAGE 1 of 5 | |
|---|--|---|--|--|--|-------------------------------------|--|

CLASSIFICATION OF ALUMINUM POWDER

I. GENERAL

This procedure specifies the operations for classification of aluminum powder using the Donaldson Classifier. Equipment operation shall be generally per procedure "Donaldson Classifier", 00000-7320-401, with changes or precautions specified below. Aluminum powder is a grey metal powder that dusts up quite readily. It is essentially non-toxic; however, breathing of the dust should be avoided. Aluminum powder burns rapidly when ignited in the air, and if ignited in dust cloud form in the air, a violent explosion will result. Ignition from a static electrical discharge probably is the greatest hazard. The fire and explosion hazard can be, for all practical purposes, completely eliminated by exclusion of oxygen or oxidizing materials. Therefore, aluminum powder will be classified only in an inert atmosphere of gaseous nitrogen, as detailed in this procedure.

II. SAFETY

1. The classifier must be completely washed down, prior to use with aluminum powder, to remove all traces of oxidizer left from previous operations.
2. All oxidizer must be completely removed from the classifier bay when aluminum powder is to be processed.
3. No operations shall be permitted, within two operating bays of the classifier, that generate oxidizer dust.
4. Operating personnel shall wear conductive-sole safety shoes (or regular safety shoes and conductive "Leg-Stats"), flame-resistant coveralls or lab coats, and goggles. When handling fine particle size, dusty materials, approved dust respirators must be worn. While the classifier is in operation, all persons within two operating bays of the classifier must wear hearing protective devices (ear plugs or ear muffs, as desired) to prevent hearing damage.
5. The electrical grounding of all components of the classifier system must be checked prior to operations. Of specific importance is an effective electrical bond, per procedure "Electrical Grounding", between the feeder outlet and the classifier inlet.

73 Jun 28

6. All feed and product fraction materials must be handled to minimize spills and or dusting, and any spills must be cleaned up immediately. Spills should be carefully and gently swept up, and any residues wiped up with damp rags. Waste aluminum powder and contaminated residues must be placed in waste containers positioned outside the operating building, and the containers disposed of per procedure "Disposal of Hazardous Waste".
7. Aluminum powder is to be transferred, from shipment drums, direct to conductive plastic bags for handling, weighup, etc. Aluminum scoops shall be used, and the transferring person must contact the drum at all times with a bare hand. Insulating gloves must not be worn as these would electrically isolate the scoop and its aluminum powder content. The shipping drum and the conductive plastic bag must be grounded per procedure "Electrical Grounding" to a common ground.
8. Personnel operating the equipment and/or handling aluminum powder must avoid any actions which might generate sparks. In addition, general purpose electrical equipment must not be operated within two operating bays of the classifier.
9. Aluminum powder storage drums must be resealed as soon as transfer operations are complete. Aluminum powder, except that being transferred or that already in the feeder or the classifier, must be stored in sealed metal drums at all times. The drum lids must be mechanically clamped in place except during transfer operations.
10. Aluminum powder transfer and weighup operations must be confined to Bay J (the classifier bay) of 7603.
11. Only the drum of powder being processed, and the product fraction storage drums associated with it, may be kept in the classifier bay during classifier operations.
12. Nitrogen gas storage tanks must be constantly monitored to ensure an adequate supply of nitrogen is available. The supply valve adjustment to the velocity breaker drum must be constantly monitored to ensure that only nitrogen gas is being supplied to the classifier. The feeder must be shut off immediately in the event of any interruption in the supply of nitrogen. An oxygen analyzer will be used to remotely monitor the discharge gas stream from the classifier.

73 Jun 28

III. OPERATIONS

1. Assemble and check out the equipment per procedure "Donaldson Classifier".
2. Select a cut point to be used, based on project requirements and the distribution of the feed material to be used. Determine the rotor speed to be used from Figure 1 (derived for aluminum powder, specific gravity 2.702).
3. Check the pressure gages on the nitrogen supply tank and the supply bottles to ensure sufficient nitrogen is available for the classification operation. If necessary, obtain fresh supplies as needed.
4. Weigh out and charge the necessary quantity of aluminum powder to the hopper of the feeder, then place a dust cover, of conductive plastic film, over the hopper.
5. Recheck to assure the required electrical grounding bonds are in place between the feeder outlet and the classifier inlet funnel.
6. Start the classifier rotor and adjust it to the required rotational speed.
7. Open the nitrogen supply valve to pass nitrogen gas from the storage tank into the velocity breaker drum.
8. Start the blower and adjust the air control valve to produce the required N₂ flow (150 cfm assumed), and readjust the nitrogen supply valve, as needed, to maintain the flapper valve in the open position.
9. Open the ejector valve on the coarse collection container to supply nitrogen gas, from the cylinder bottles, to the coarse collector and to the feed inlet line. Recheck the regulator on the cylinder to ensure the setting is 50 psig output pressure.
10. Check and rebalance the air flow valve and the main nitrogen supply valve to produce the desired gas flow.
11. Operate the feeder for the required period of time to feed aluminum powder to the classifier.
12. Turn off the feeder, then, after one or two minutes, turn off the ejector valve.
13. After one or two minutes delay, shut down the classifier per procedure "Donaldson Classifier".

14. Immediately turn off the nitrogen supply valve to the velocity breaker drum (to conserve nitrogen).
15. Rap down the cyclone, coarse collector head, and both collection containers, using a wooden brush handle. Wait at least five minutes, to allow the dust to settle, before opening the containers.
16. Remove one container at a time, placing a drum lid (or other container) under the collector to catch any material that might subsequently fall. Weigh the container, sample the contents for particle size, then immediately transfer the material to the appropriate product drum. Replace the container before removing the other container.
17. After the product fractions have been removed, set up the next operation, or else clean up the equipment per the following steps.
18. The classifier is to be cleaned by disassembly and removal of the component parts for washing with water, brushes, soap, and rags, as needed, followed by drying with compressed dry air. Washing is to be done to discharge the wastes, outside the building, to the industrial drain.
19. Stationary, non-removable components of the classifier system are to be washed in-place, after all the removable parts are out of the way. Any aluminum wastes flushed out at this time are to be immediately swept and flushed down the nearest industrial drain. The floors are to be mopped to near-dryness to ensure no aluminum remains.

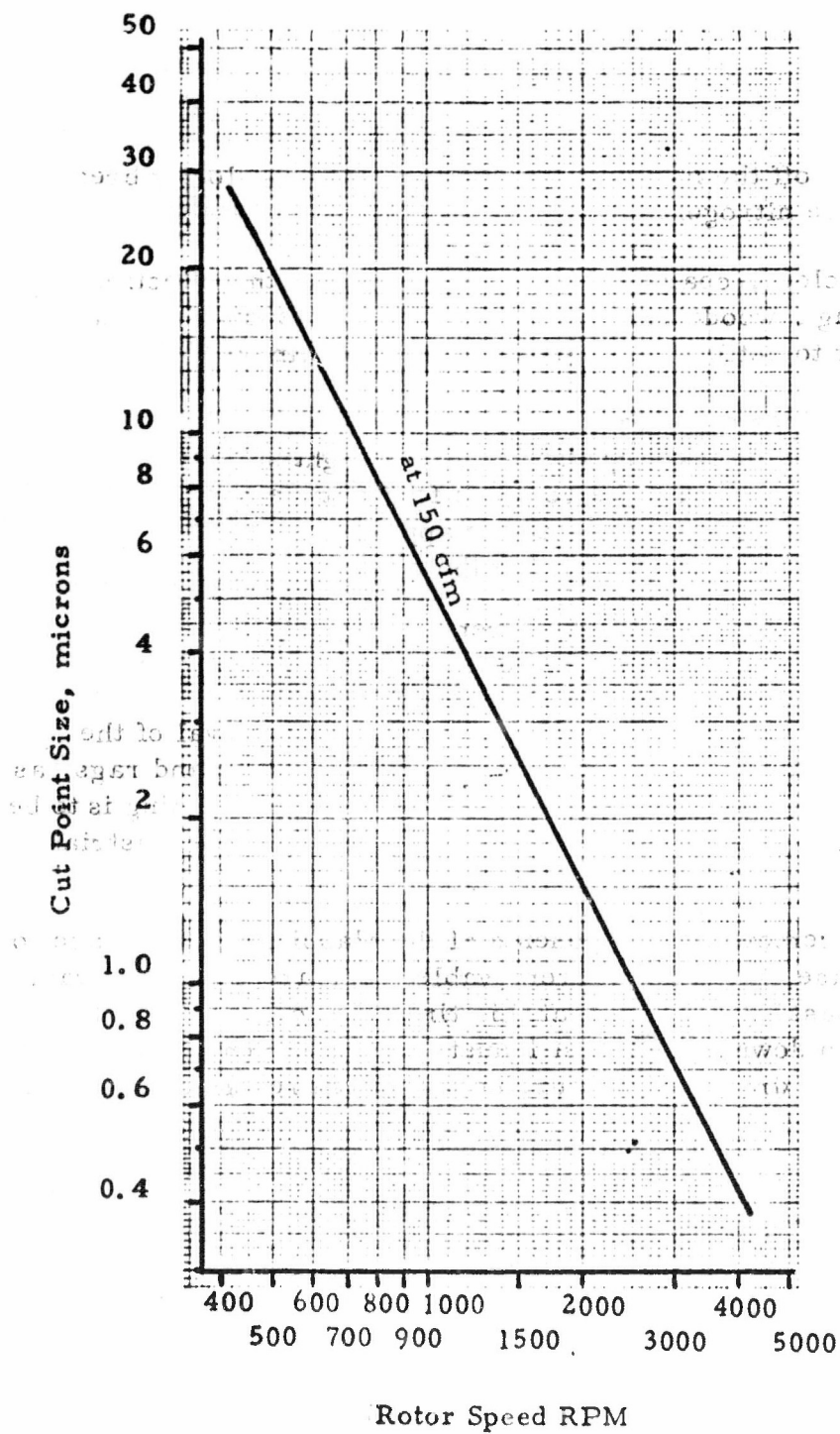


Figure 1. Cut Point Curve for Classification of Aluminum Powder

SECTION 5

EVALUATION OF CLASSIFICATION RESULTS

Evaluation of classifier performance has been the subject of discussion, efforts, and argument for years, and many methods have been proposed and reduced to practice. The developer and manufacturer of the Donaldson classifier recommends the use of the "grade efficiency concept"; for which special analytical techniques have been derived and tested. The grade efficiency of a classifier is defined as the percentage or fraction of material of a given particle size that is collected in the coarse fraction, based on the total material of that size collected. For a given classifier, set for a given cut point adjustment, the grade efficiency will be a continuous function running from zero for, some particle size, up to a hundred percent, for some larger particle size. In between, the continuous function predicts the probability that a particle of any particular particle size will go either to the coarse fraction or to the fines fraction. (An illustrated example is given later in this report.) A report on the technique and its application is available from The Donaldson Company.* The technique presented in that reference is generally the one used in this program to analyze the performance of the Donaldson Classifier.

The mathematical expression used to compute grade efficiency values for experimental classifier runs is:

$$1/G(x) = 1 + \left(\frac{1}{E_t} - 1 \right) \left[\frac{d F_f(x)}{d F_c(x)} \right] \quad (\text{Equation 1})$$

where $G(x)$ = grade efficiency for particle size x

$$E_t = W_c / (W_c + W_f)$$

$F_f(x)$ = cumulative particle size distribution of fines fraction

$F_c(x)$ = cumulative particle size distribution of coarse fraction

x = particle size of material

W_f = weight of fine fraction product

W_c = weight of coarse fraction product

Particle Size Classification of Plastic Powders, Schaller, Robin E., and Lapple, Charles E., presented at 162nd National Meeting of A.C.S., Sept. 12-17, 1971. A copy of this report is included in this appendix as Section 6.

Similar equations exist using the cumulative particle size distribution of the feed material with either the coarse or the fines fraction; however, grinding occurred during classification of the coarser materials, so the product fractions were felt to be the only valid data source. As an illustration of the grade efficiency analysis, refer to Figures A-7, A-8, and A-9, representing run DC-7, made with 90 micron feed material.

Figure A-7 gives the particle size distribution data for the feed material and for the coarse and fines product fractions. As can be noted, the coarse fraction is smaller in particle size than the feed material, indicating particle size reduction has occurred during classification. Figure A-8 is a plot of the fines fraction cumulative percentage versus that of the coarse fraction for specific sizes (e.g. for 52 microns, F_f is 10.6 and F_c is 83.6). A smooth curve has been drawn through the points, and the slope of the curve determined at intervals from orthogonals (the lines perpendicular to the curve) located by mirror image techniques. The size is then used to calculate the grade efficiency for that particle size. Tabulated data for DC-7 is given in Table A-I. Figure A-9 is the grade efficiency values plotted against their associated particle sizes. The cut point for the system is the equiprobable point, where $G(x)$ is 50%, or, is the particle size that has a 50% probability of going into the coarse fraction (or, conversely, a 50% probability of going into the fines fraction). For DC-7, the cut point is 29.5 microns, quite close to the value predicted by calibration curves for the classifier (32.3 microns). Figure A-9 indicates that a 20 micron particle has a 33% probability that it will go the coarse fraction, or, in a more practical way, 33% of the 20 micron particles will appear in the coarse fraction while 67% will appear in the fines fraction. The sharpness index, or particle size at 75% probability divided by the particle size at 25% probability, measures the spread or overlap of "misplaced" material. For DC-7, the value of 2.38 indicates a relatively poor separation, particularly compared to other runs and to the equipment specifications.

Based on the way the equipment works, and the manner in which the operating variables affect the product fractions, some intuitive comments about the relationship of the sharpness index to the feed rate can be made. As the feed rate is decreased, holding the classifier variables constant, the sharpness index should decrease to a minimum. Decreasing the feed rate more should not affect the sharpness index. Likewise, there should be a feed rate below which the cut point no longer changes (increases). This can most readily be understood by noting what happens to the classification process as the feed rate increases.

Although centrifugal force and gas drag forces are the two primary factors that affect the movement of a particle in the classification zone, particle-to-particle interactions play an increasing role as feed rate is increased. As the mass concentration of particles in the classification zone increases, there is a greater tendency for large particles to push smaller ones along, dragging material into the coarse fraction collector that theoretically shouldn't move in that direction. This "hindrance"

that the similarity to "hindered" settling) to the motion of smaller particles should predominantly affect the (relatively) coarser of the particles that should move into the fines fraction conveying stream. The (relatively) finer particles should have a greater tendency to be swept around the large obstacles and, therefore, be less "hindered" in their motion. This is the reason why the cut point size decreases with increasing feed rate. Because increasing the feed rate misplaces more material into the coarse fraction, it stands to reason that the sharpness index should increase accordingly.

(11) It should be strongly noted that the grade efficiency method of classifier analysis is accurate and appropriate only when the input data is precise and accurate and truly representative of the materials and operations involved. Samples submitted for particle size analysis that are not representative of the bulk materials involved can throw the entire approach into complete error. This can occur, for instance, in the fines fraction collection container because of the high velocity swirling induced by the cyclone; such swirling can result in classification by particle size within the collected material. The same is true if accurate recovery data on the product fractions is not obtained. Due to the large number of samples involved, and the relatively new analysis methods required on some of the materials, it is quite possible that some of the experimental run results reported herein may be of limited accuracy.

TABLE I

GRADE EFFICIENCY CALCULATIONS FOR DC-7 (U)

$$W_c = 48.77 \text{ lbs.}$$

$$W_f = 10.21 \text{ lbs.}$$

$$E_t = \frac{48.77}{48.77 + 10.21} = 0.8269 \text{ or } 82.69\% \text{ of product collected as coarse}$$

$$E_{t_f} = \frac{10.21}{48.77 + 10.21} = 0.1731 \text{ or } 17.31\% \text{ of product collected as fines}$$

| <u>D_p, microns</u> | <u>F_c, %</u> | <u>F_f, %</u> | $\frac{dF_f}{dF_c}$ | $\frac{1}{G(x)}$ | <u>G(x)</u> |
|-------------------------------|-------------------------|-------------------------|---------------------|------------------|-------------|
| 150 | 2.3 | ---- | | | |
| 100 | 2.6 | ---- | | | |
| 74 | 56.5 | 2.0 | 0.271 | 1.057 | 0.946 |
| 52 | 83.6 | 10.6 | 0.467 | 1.098 | 0.911 |
| 40 | 92.4 | 18.0 | 1.630 | 1.341 | 0.746 |
| 25 | 96.7 | 33.0 | 6.800 | 2.423 | 0.413 |
| 15 | 100.0 | 58.5 | 13.333 | 3.791 | 0.264 |
| 10 | ---- | 85.2 | | | |

F_c and F_f are the cumulative percentages of coarse and fine fraction material larger than the noted particle size (D_p).

G(x), or grade efficiency, is expressed above in fractional value; thus, a 40 micron particle has a 74.6% probability of going into the coarse fraction.

Run DC-7 29.5 lbs/hr. 10.21

Drum No. 1

79 μ WMD

17.1 μ WMD

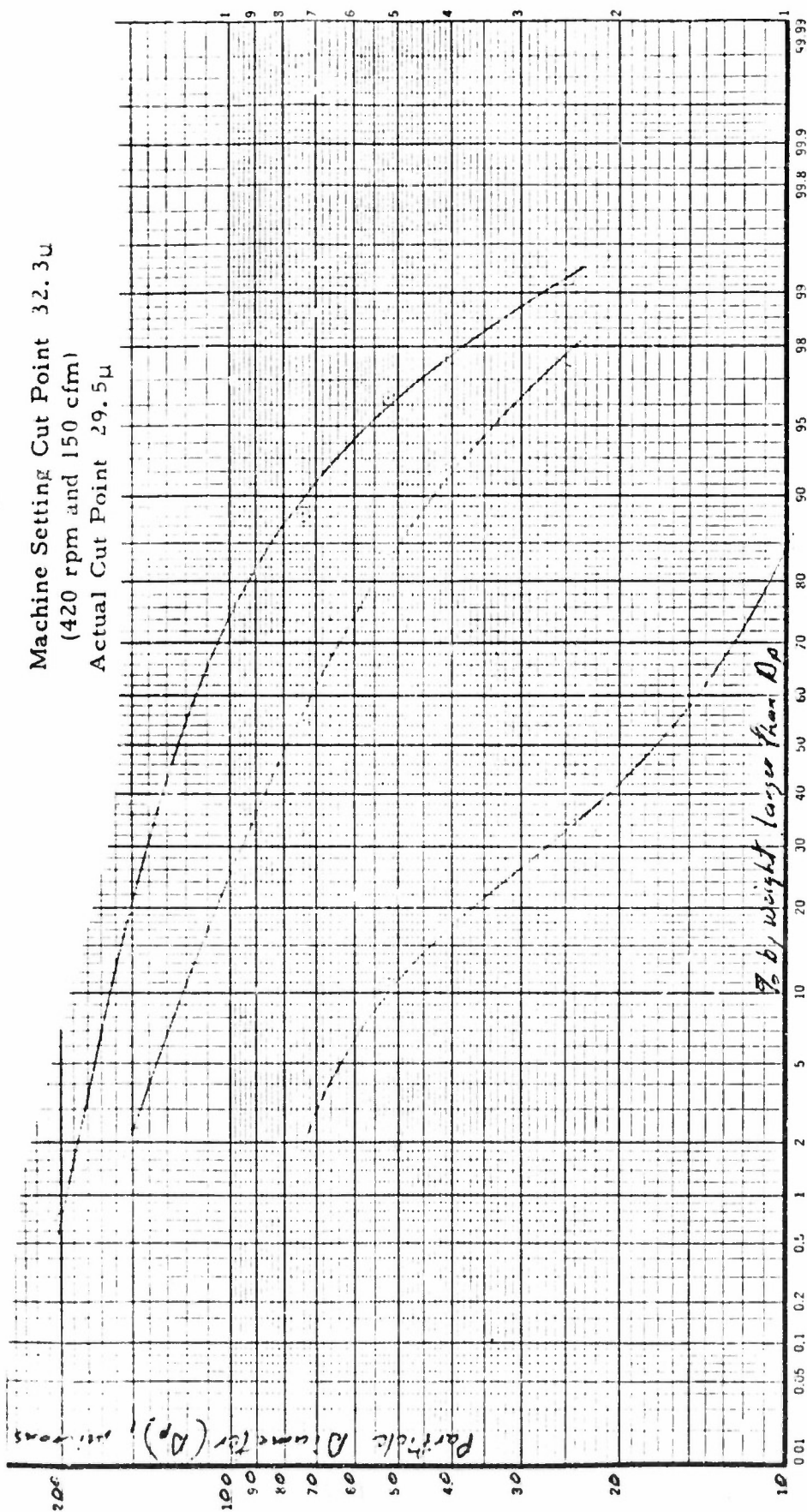
48.77 lbs. or 82.69%

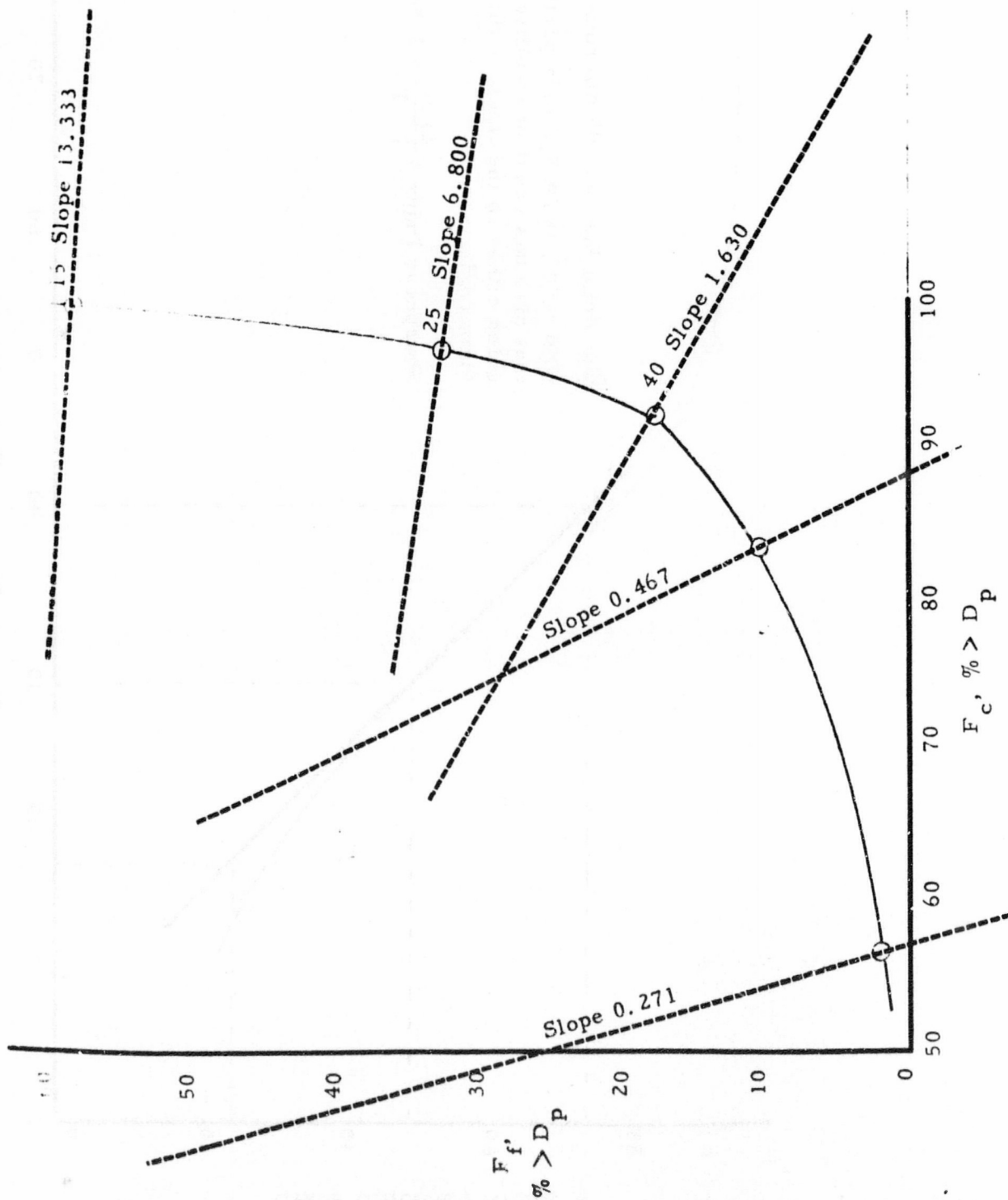
10.21 lbs. or 17.31%

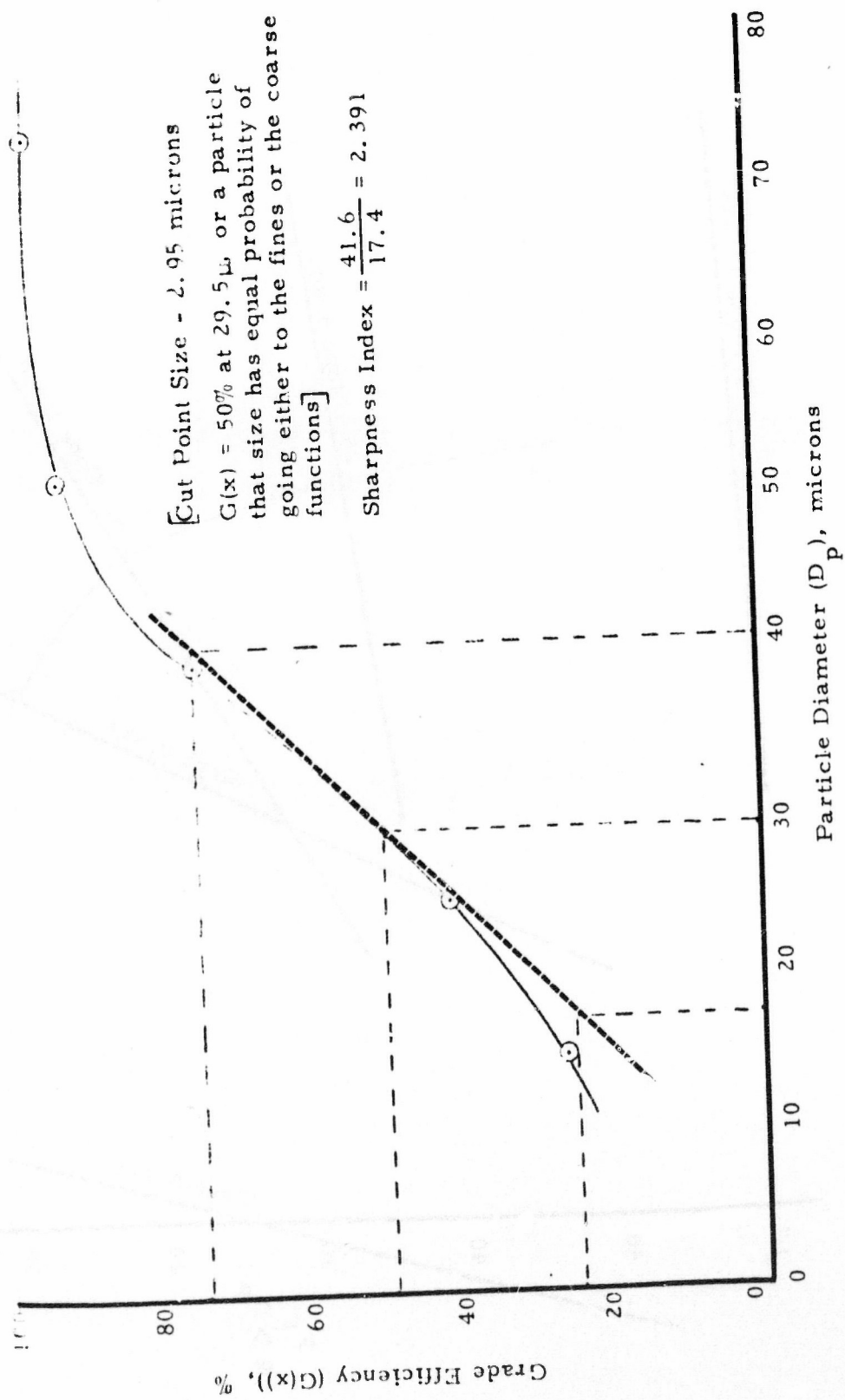
Machine Setting Cut Point 32.3 μ

(420 rpm and 150 cfm)

Actual Cut Point 29.5 μ







donaldson



Donaldson Company, Inc.
1400 West 94th Street
Minneapolis, Minnesota 55431

SECTION 6.

PARTICLE SIZE CLASSIFICATION OF
PLASTIC POWDERS

Robin E. Schaller
Senior Project Engineer
Donaldson Company, Inc.
Minneapolis, Minnesota 55431

and

Charles E. Lapple
Senior Scientist
Stanford Research Institute
Menlo Park, California 94025

Presented at the 162nd National Meeting
of the American Chemical Society
Washington, D.C., September 12-17, 1971,
Division of Organic Coatings and
Plastics Chemistry

PARTICLE SIZE CLASSIFICATION OF PLASTIC POWDERS

Robin E. Schaller

Charles E. Lapple

INTRODUCTION

One of the most important characteristics of any powder is the size distribution of individual particles making up the powder. Powder handling properties, electrostatic charging characteristics, optical properties and specific surface area are just a few factors influenced by particle size.

Particle size is similarly important in the field of plastic powder coating. Many problems such as orange peel, pin holing and deposition efficiency can be affected by particle size. One author has even indicated a potential health hazard with powder coating systems related to inhalation of particles in the size range below 10 microns. (Reference 1). There are surely other examples that could be cited as well. It appears certain that as powder coating techniques develop and are exploited to their maximum potential, further research into the effects of particle size will play a significant role. This appears especially true for particles below 50 microns.

Particle size classifiers can be effectively used to "tailor" a powder to a desired particle size at reasonable cost. A classifier is defined as a device capable of separating a bulk feed into two (or more) fractions according to some characteristic variable of the powder. The essential requirement is that the particles to be separated have some singular distinguishing property. This property is usually expressed in terms of an equivalent particle size. The screen is perhaps the best known type of classifier and is used primarily for separating particles coarser than 100 microns. For dry classification below 100 microns, and in particular below 50 microns, centrifugal air classifiers are most commonly used.

A recently developed centrifugal air classifier has made possible precision particle size separation for both research and production requirements in the fine particle

size range. This new design has been used to classify plastic powders as well as a wide variety of other materials. Before discussing centrifugal air classifier equipment, it is appropriate to briefly review how such a device works and how one evaluates what it does.

CLASSIFIER OPERATION AND PERFORMANCE MEASUREMENT

Centrifugal classification is a rather complex process involving the motion of solid particles in a fluid flow field. The basic theoretical principles can be described by a math model using equations of particle dynamics and fluid mechanics. This has been done adequately in existing literature. (See for example, Reference 8). In this presentation a more illustrative approach is taken, with emphasis on practical aspects wherever possible. An idealized case - the motion of discrete particles - is examined first. This is then followed by a discussion of "real" effects and their significance on performance.

Idealized Case

Centrifugal classifiers normally are designed to make use of a vortical flow of fluid, and can be categorized as either rotary or cyclonic. The cyclonic type causes a vortex flow within stationary walls using guide vanes or tangential fluid inlets. Figure 1 illustrates an idealized case in which a rotor is used. One typical flow streamline is shown by the solid line, representing fluid which enters at the rotor periphery, spirals inwardly and finally exits through a central outlet. This is known technically as a "vortex-sink" flow. The fluid velocity can be vectorially resolved into radial (V_R) and tangential (V_θ) components as shown. The radial velocity at any radial position, R , can be expressed by:

$$V_R = \frac{Q}{2 \pi H R} \quad (1)$$

The tangential velocity component at any radial position, R , can be expressed by:

$$V_{\theta} = K R^n \quad (2)$$

Two tangential velocity profiles theoretically are possible. A fluid rotating as a solid body (forced vortex) tends to maintain a constant angular velocity and in this case the exponent $n = 1.0$ and $K = 2 \pi \omega$. In the completely nonviscous case, the fluid tends to retain constant angular momentum (free vortex) and $n = -1.0$. The actual tangential velocity profile obtained normally will be some combination of these as shown graphically in Figure 2.

An arbitrary particle introduced into this flow field will be acted upon by an outwardly directed centrifugal force and an inwardly directed drag force. The centrifugal force is proportional to the cube of the particle diameter and square of the particle tangential velocity component. The latter can be assumed equal to the local fluid tangential velocity. The drag force is directly proportional to both particle diameter and relative radial velocity between the fluid and particle.

The dashed lines of Figure 1 illustrate the paths of three sizes of particles. Large particles, dominated by centrifugal forces, follow a trajectory to the periphery of the rotor where they are collected as the coarse fraction. Small particles, having large drag per unit mass, follow the fluid to the central outlet and are collected as the fine fraction. At some critical particle diameter, when drag and centrifugal forces are equal, particles will have equal probability of entering either the coarse or fine fraction. This is known as the "cut size", $D_{50\%}$, and can be estimated from the following equation.

$$D_{50\%} = \frac{3 \delta}{\pi D_o \omega} \sqrt{\frac{\mu Q}{\pi H \rho_p}} \quad (3)$$

The constant δ is dependent on the flow pattern existing within the rotor and as a rule must be determined experimentally. Several observations can be made from inspection of Equation 3.

- Decreasing particle density increases cut size;
- Increasing fluid flow rate increases cut size;
- Increasing rotor speed decreases cut size.

The first observation means that with a given classifier, it is more difficult to separate low density powders such as plastics at low cut sizes than a higher density powder such as aluminum oxide. The latter two observations have significance in that they indicate how equipment operating parameters affect cut size.

Since a powder is made up of individual particles widely varying in size, it is best described statistically with a particle size distribution curve. A commonly used form is the cumulative particle size distribution. This represents the cumulative percent of a powder sample less than a corresponding particle diameter D (usually on a weight basis). A more comprehensive discussion of particle size analysis is presented by Lapple. (Reference 3).

Figure 3 typifies the results of a single classification in terms of cumulative size distribution curves of the feed, coarse and fine fractions. In the ideal case, there is a sharply defined "boundary" between coarse and fine fractions as illustrated by the dashed curves. There would be no particles larger than $D_{50\%}$ in the fine fraction and no particles smaller than $D_{50\%}$ in the coarse fraction. The cumulative percent by weight less than $D_{50\%}$ in the feed analysis is therefore identically equal to the total fine fraction weight yield, $(1 - N_o) 100$.

Real Effects

Discussion to this point has been limited to spherical particles of like density, each behaving in a discrete manner within a well defined, uniform centrifugal flow field. As might be expected, this desirable situation is not actually realized in practice. For example, powder feed rates normally encountered result in relatively high particle concentration. Not only does this tend to change the fluid flow pattern

as compared to unladen gas flow, but more importantly, causes particle interference to occur along respective trajectories. Interference can take the form of agglomeration in the case of small particles, effectively forming larger particles, or bouncing in the case of large particles. Agglomeration can cause fine particles to be carried to the coarse fraction either because of adhesion of fine particles to coarser particles or to one another. Since fine particles have an increased surface area to mass ratio, their behavior is governed by Van der Waal's forces and other surface forces. (Reference 3). As a result, particle dispersion becomes increasingly difficult as particle size decreases, particularly for particle diameters below 10 microns. For this reason, the lowest cut size possible with most production classifiers has been approximately five microns.

Fluid flow patterns existing within a classifier also differ from the theoretical and ordinarily are of a complex nature. Turbulence, boundary layer development and secondary flows often are of such magnitude that the actual classification process will deviate significantly from the ideal case.

Figure 3 includes classification results typical of those obtained in actual practice. As contrasted with the ideal case, there always is an overlapping of sizes due to the above effects. Particles smaller than the cut size are found in the coarse fraction and vice versa. The degree of overlap is characterized by the term "sharpness" of cut. For example, a separation with a high degree of overlap is considered to be poorly classified in terms of sharpness.

Performance Measurement

Since classification, like everything else in the real world, is imperfect, a method is needed to measure performance. There basically are three parameters that should be considered when evaluating a given classifier.

- Cut size;
- Sharpness of cut;
- Output rate of classified fractions.

Cut size is essential since this is the particle size at which classification actually takes place, while sharpness represents how effectively it was done. Feed rate is also important because it is directly related to finished product cost. With most conventional classifier designs, sharp separations in the region of lower cut sizes can only be achieved at the expense of reduced fraction output capacity.

Many attempts have been made to express performance by a single number, usually termed classifier "efficiency". One of the more common expressions in current use was introduced in 1932 by the Newtons (Reference 6).

$$\eta_N = 100 \frac{\text{Weight of classified material in either fraction}}{\text{Weight of classifiable material in the feed}} \quad (4)$$

This and similar classifier "efficiencies" are actually inadequate measures of performance and can be misleading. For example, single number efficiencies often are influenced by the size distribution of the particular feed powder used. As a result, it is possible for a poor separation to have an unrealistically high efficiency value. These problems are more fully discussed in Reference 7.

A better approach to performance measurement is the concept of "grade efficiency" recommended by Richards in England (Reference 7) and Wessel in Germany (Reference 10). Grade efficiency is defined as that portion of feed for particle size D entering the coarse fraction.

$$\eta(D) = 100 \frac{\text{Weight of size D entering coarse fraction}}{\text{Sum of weights of size D in fine and coarse fractions}} \quad (5)$$

It can be shown that the equivalent mathematical expression for this definition is:

$$\eta(D) = 100 \frac{N_o \frac{dF_C(D)}{dD}}{N_o \frac{dF_C(D)}{dD} + (1 - N_o) \frac{dF_F(D)}{dD}} \quad (6)$$

Grade efficiency therefore can be calculated from the cumulative size distribution curves of the coarse and fine fractions. A simple geometric method for doing this has been suggested by Eder. (Reference 2).

A distinguishing characteristic of grade efficiency as contrasted with all single number efficiencies is that it can be drawn graphically as shown in Figure 3. An ideal curve consists of a straight vertical line at the cut size $D_{50\%}$. This means 100 percent of all particles in the feed larger than $D_{50\%}$ have entered the coarse fraction, with none below this size. For an actual classification the curve is not vertical, indicating the extent to which particles found in one fraction should be in the opposite fraction. From its definition, cut size corresponds to the 50% value on the grade efficiency curve.

The slope of the grade efficiency curve at $D_{50\%}$ gives a measure of the "spread" of misplaced material or sharpness of cut. A common sharpness index based on this notion is:

$$\phi = D_{75\%} / D_{25\%} \quad (7)$$

For perfect classification, ϕ has a value of unity, while values above three or four are considered poor. There are other sharpness indices in use with no one universal standard adopted. However, the index defined by Equation 7 is presently one of the most widely accepted. (Reference 10).

The above discussion has shown that centrifugal air classifiers separate particles on the basis of differences in aerodynamic characteristics which are in turn expressed in terms of equivalent particle size. Similarly, most techniques for determining particle size do not measure size directly. Instead, some other property is measured and then interpreted as size through a theoretical or empirical relationship. (Reference 3). If the intrinsic effectiveness of a given classifier is to be determined, the measurement techniques used should evaluate the same particle properties as those operative in the unit itself. The use of techniques that measure other properties could give an unrealistically poor assessment of performance, and be subject to a variety of interpretation.

COMMERCIAL CLASSIFICATION EQUIPMENT

Experience with powders has shown that in order to achieve sharp classification, several conditions should be satisfied.

- Particles must be introduced to the classification zone uniformly and discretely - this means that they must be fully dispersed;
- There must exist a uniform separating action in all portions of the equipment where classification takes place;
- Once classification has occurred, the powder fractions must be removed as quickly as possible to prevent interference and reagglomeration.

The first condition probably is the most important and certainly the most difficult to accomplish. Problems concerning poor performance usually can be traced to ineffective dispersion of particles to be classified. This therefore is a prime consideration in equipment selection.

Conventional Centrifugal Air Classifiers

Figure 6 shows typical performance data for a number of conventional centrifugal air classifiers. This data is reasonably representative of the best performance possible with existing equipment. (Reference 4, 5 and 9). The comparative data given in the table of Figure 6 corresponds to approximately the lower limit of cut size in each case with particle densities of 2.7 gm/cu cm. There is a wide variety of equipment available ranging in solids feed rate capacity from tons per hour to grams per hour. The largest units commonly are used in closed-circuit grinding systems and have a useful cut size range on the order of 20 to 70 microns. There are a number of smaller production classifiers that are applicable for cut sizes under 10 microns, with a lower limit of approximately 5 microns. These units have a solids feed rate capacity on the order of pounds per hour. A few miniature units, termed "laboratory" classifiers, are capable of separations as low as one micron with feed rates of only grams per hour. Although the latter are included in Figure 6, their usefulness normally is limited to particle size analysis. Direct comparison with production machines is unrealistic because of the great differences in feed rate capacities.

Recent Development

The centrifugal air classifier shown in Figure 4 is a recent joint development by Donaldson Company, Inc. and Stanford Research Institute. This design is aimed at providing sharp classification on a production scale in the particle size region near one micron. It incorporates a unique rotor system to provide effective dispersion of fine particles.

Figure 5 schematically shows the general operation of this design. Feed particles are subjected to a high degree of dispersion just prior to being classified so that reagglomeration is minimized. Elutriating air enters the rotor radially around its outer edge, carrying with it dispersed fine particles as it spirals inward to the central fine

fraction outlet. Coarse particles and any remaining agglomerates of fine particles are continuously dispersed as they move around the rotor periphery to the coarse fraction outlet. Desired cut size is selected by adjustment of airflow rate, rotor speed or both.

Plastic powders can be classified with this design down to approximately one micron. Actually, using feed powders such as aluminum oxide having somewhat higher densities than plastics, sharp classification down to 0.5 micron has been accomplished. Figure 6 illustrates that this represents an increased range of cut sizes compared to more conventional production equipment.

Typical Materials Classified into Size Ranges

If a classification process is carried out in several steps at various cut sizes, the original feed powder will be separated into a number of closely sized fractions. The "closeness" of the particle diameters in the resultant fractions will depend on how sharply a particular unit can classify and how sensitive its corresponding machine settings are. Closely sized powders are commonly used in research work. For example, toxicologists use closely sized fractions of coal dust in the respirable range (less than 10 microns particle diameter) for inhalation studies so that standards can be set for allowable coal mine concentrations. Figure 7A shows a scanning electron micrograph of a closely sized coal dust sample, with the corresponding feed shown at left. The objective of this particular classification was to obtain a powder of nearly monosized particles. Two passes through the machine removed both undersize and oversize particles. This is a good example of what can be accomplished with precision classification. As a matter of interest, the density of coal is comparable to that of plastics.

A multiple classification of a plastic powder is shown in Figure 7B. The feed in this case was separated into three fractions, each consisting of a different particle size range. This was accomplished by setting the classifier to cut at different particle sizes for two successive machine passes. A number of special problems arise when classifying plastic powders, each tending to make separation more difficult. Particle

density problems have already been reviewed. Another significant factor is particle electrostatic charge. This can have the effect of reducing sharpness of cut unless proper dispersion is provided. Temperature problems also can occur with plastics, causing a fusing together of individual particles. The latter is most likely to happen when large relative velocities exist between fluid, particles and equipment.

Figure 7C shows photomicrographs of a specular hematite (iron ore) feed classified into four size ranges by making three machine passes at different cut sizes. The lowest cut size represented by these samples is in the submicron range, with a corresponding particle density of 5.07 gm/cu cm. The practical examples given in Figure 7 illustrate how a feed powder can be "tailored" effectively to a given particle size specification using centrifugal air classification. This is true despite the fact that parent material composition, finished product requirements and associated classification problems are somewhat different in each case.

Costs of Classification

One of the most important considerations for a potential user of classified powders pertains to costs. Although one would ideally like to obtain high performance at low cost, these two factors unfortunately are inversely related. Powder classification cost usually is affected by at least one of the following parameters.

- Solids feed rate to the classifier;
- Particle size distribution of the feed powder;
- Finished product requirements.

Solids feed rate is the most important of these factors since it is inversely proportional to machine operating time. This is another way of saying that increased feed rates result in reduced cost per pound. It should be pointed out that feed rate can be influenced by the latter two factors to varying degrees. For example, bulk density and specific surface area of the feed powder affect its flowability and dispersibility and therefore the ease with which it may be fed to the classifier. Each of these is in turn a function of particle size distribution. Moreover, if decreased cut sizes

are required for a given finished product, it often is necessary to decrease the corresponding solids feed rate.

Other requirements imposed on the finished product can be equally significant to its cost. Quite often, such as in the production of closely sized fractions, several passes through the classifier are necessary. This will naturally decrease the "effective" solids feed rate to produce the product.

Feed powder particle size distribution can play an important role in costs since this determines the amount of usable material available. For example, suppose a feed powder analysis contained 10 percent by weight less than three microns and that from this feed a finished product containing only particles up to three microns is to be processed. This means that 10 pounds of feed must be processed for each pound of finished product.

It is apparent from the above discussion that classification costs will vary widely from one application to the next. With low capacity operations (as with a pilot-plant classifier), classification costs will reflect primarily labor charges. For continuous classification in the one micron range with such units, classification costs may run as high as \$5.00 per pound of powder fed to the classifier. Because of the controlling influence of startup and shutdown, costs could run even higher when only small batches are processed. For large plant-scale machines and larger cut sizes, costs may be a few cents per pound of feed powder.

The purpose of this paper is to suggest possible advantages in the use of particle size classification for plastic powders. Factors involving the operation and performance of centrifugal air classifiers are described. The performance characteristics of commercial classification equipment, including a design recently developed by Donaldson Company, Inc. are also presented. Sharp classification of plastic powders on a production scale in the particle size range near one micron is now possible with the new machine concept. This represents an improvement in the state-of-the-art, and should serve both research and production requirements in the field of powder coating.

SYMBOLS

| | |
|------------|--|
| D | = Particle diameter, (microns) |
| D_o | = Rotor diameter, (ft) |
| $D_{25\%}$ | = Particle size corresponding to the 25 percent value on the grade efficiency curve, (microns) |
| $D_{50\%}$ | = Classification cut size, (microns) |
| $D_{75\%}$ | = Particle size corresponding to the 75 percent value on the grade efficiency curve, (microns) |
| $F_C(D)$ | = Cumulative percent of coarse fraction less than particle size D |
| $F_F(D)$ | = Cumulative percent of fine fraction less than particle size D |
| H | = Rotor width, (ft) |
| K | = Constant |
| N_o | = Yield of coarse fraction expressed as a decimal proportion of feed |
| n | = Fluid tangential velocity exponent |
| Q | = Volumetric airflow rate, (cfm) |
| R | = Radial coordinate on rotor, (ft) |
| V_R | = Fluid radial velocity component, (ft/sec) |
| V_θ | = Fluid tangential velocity component, (ft/sec) |
| V | = Fluid total velocity vector, (ft/sec) |
| δ | = Constant in cut size equation |
| $\eta(D)$ | = Grade efficiency, (percent) |
| η_N | = Newton classifier efficiency, (percent) |
| μ | = Fluid viscosity, (poise) |
| ρ_p | = True particle density, (gm/cu cm) |
| ϕ | = Sharpness index |
| ω | = Rotor rotational speed, (rpm) |

REFERENCES

1. Barracough, R.N.J., "Health Hazards of Wet and Dry Coating Systems", Paper V-20, Proceedings of the International Symposium on Powder Coatings, London, 13-15 February 1968.
2. Eder, Th., "Problems of Resolution in Separation", Aufbereitungs Technik, No. 4, 1961, p. 140.
3. Lapple, C.E., "Particle Size Analysis and Analyzers" Chem. Eng., Vol. 75, No. 11, May 20, 1968, p. 149.
4. Lauer, O., "Limit and Accuracy of Separation of the Spiral Air Separator with Circulating Air Separation Compartment Walls", Aufbereitungs Technik, No. 4, 1965.
5. Lauer, O., "A New Centrifugal Force Laboratory Air Classifier with a Wide Separating Range", Chemie-Ing.-Technik, Vol. 41, April 1969.
6. Newton, H.W., and Newton W. H., "A Study of Classification Calculation", Rock Products, Vol. 35, 1932.
7. Richards, J.C., "The Efficiency of Classifiers", BCURA Monthly Bulletin, Vol. 30, No. 4, April-May 1966, p. 113.
8. Rumpf, H., and Leschonski, K., "Principles and New Methods of Air Classification" Chemie-Ing.-Technik, Vol. 39, 1967, p. 1231.
9. Schaller, R.E., and Dunbar, R.M., Private Communication.
10. Wessel, J., "Fundamentals of Screening and Air Separation: Part I. Theoretical Representation and the Handling of Sizing", Aufbereitungs-Technik, No. 2, 1967, p. 53.

Figure 1. Idealized Classification Within a Centrifugal Classifier

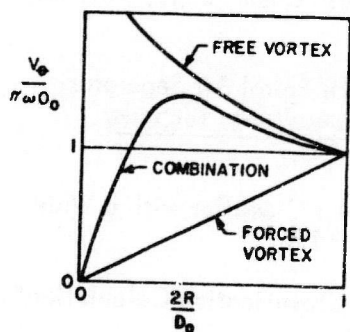
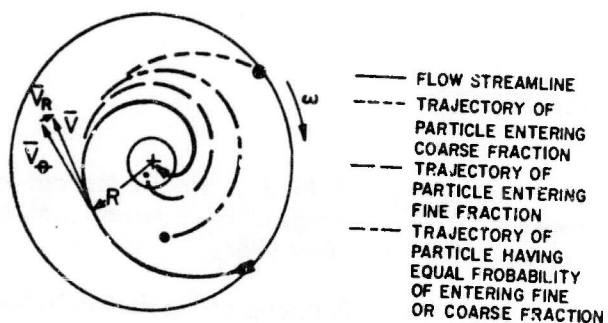


Figure 2. Fluid Tangential Velocity Profiles

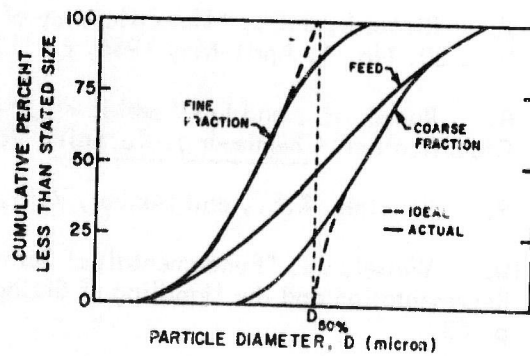
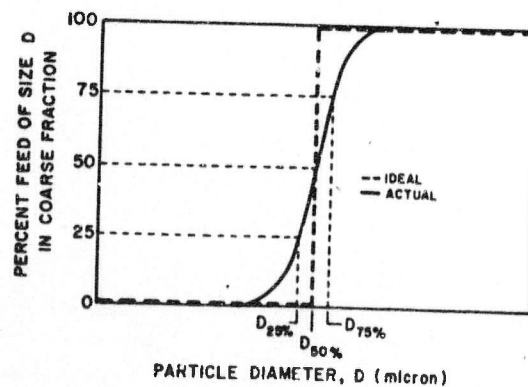


Figure 3. Graphical Presentation of Classification Results



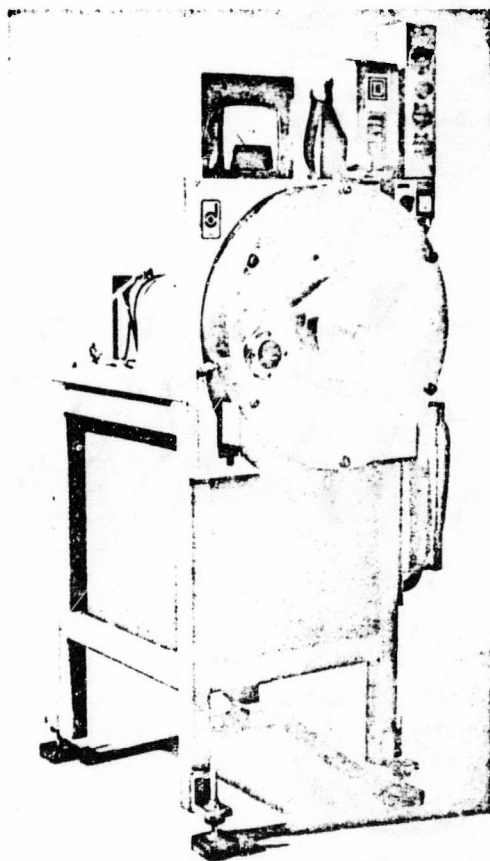


Figure 4. Donaldson Classifier

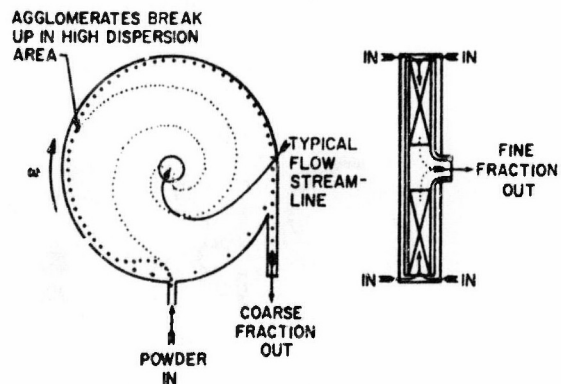


Figure 5. Schematic Diagram of Donaldson Classifier

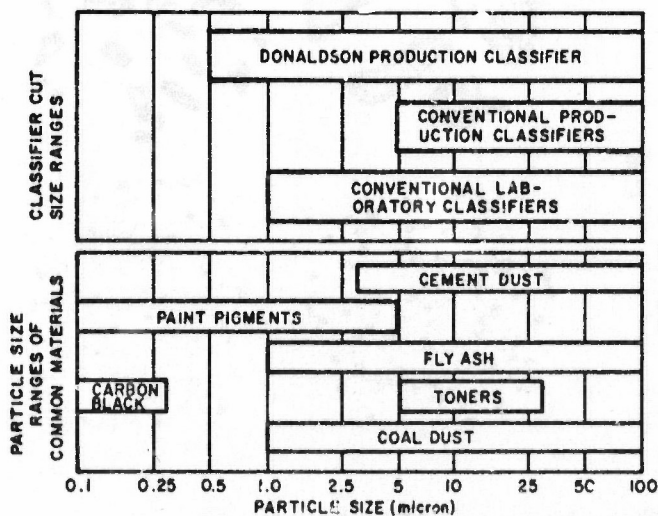


Figure 6. Typical Performance Data for Centrifugal Air Classifiers



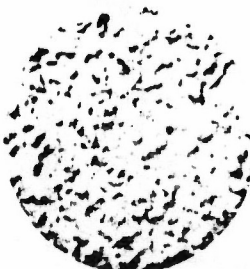
2μ



A. Coal: Feed Above;
Closely Sized
Fraction at Right



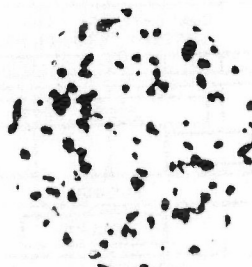
20μ



B. Plastic: Feed Above;
Multiple Classified
Fractions at Right



2μ



C. Hematite: Feed Above;
Multiple Classified
Fractions at Right

Figure 7. Photomicrographs of Classified Powders

APPENDIX E

TABULATED DATA FROM DONALDSON CLASSIFIER RUNS

PARTICLE SIZE DISTRIBUTION AND GRADE EFFICIENCY
CURVES FOR CLASSIFIER RUNS

Reproduced from
best available copy.



TABLE E-1
OPERATING DATA ON DONALDSON CLASSIFIER RUNS

| Run No., DC- | Date | Feed Material | Feed Rate, lbs./hr. | Classifier Settings, Rotor Speed/ Air Flow | Theoretical Cut Point Size, microne | Total Product Weight, lbs. | E _T | Actual Cut Point Size, microne | Sharpness Index |
|-----------------|------------|---|------------------------|--|---|---|----------------|--------------------------------------|-----------------------|
| 1 | 4/30/73 | Ground NaCl | 37 | 500/150 | 22 | 6.22 | 70.1 | N/A | N/A |
| 2 | 5/1/73 | Ground NaCl | 67.5 | 500/150 | 22 | 22.52 | 71.5 | N/A | N/A |
| 3 | 5/1/73 | Ground NaCl | 89.3 | 500/150 | 22 | 22.33 | 70.4 | N/A | N/A |
| 4 | 5/15/73 | Ground NaCl | 70.2 | 2000/150 | 1.5 | 27.31 | 99.5 | N/A | N/A |
| 5 | 5/18/73 | 90 μ AP | 135.5 | 420/150 | 32.3 | 67.75 | 96.1 | 18.0 | 1.935 |
| 6 | 5/18/73 | 90 μ AP | 124.6 | 420/200 | unknown | 62.30 | 92.4 | 30.1 | 1.858 |
| 7 | 5/21/73 | 90 μ AP | 29.5 | 420/150 | 32.3 | 58.98 | 82.7 | 29.5 | 2.391 |
| 8 | 5/21/73 | Coarse from DC-7 | 47.0 | 420/150 | 32.3 | 36.88 | 92.3 | 25.6 | 1.610 |
| 9 | 5/24/73 | 90 μ AP | 87.3 | 420/150 | 32.3 | 65.47 | 96.6 | 24.3 | 1.487 |
| 10 | 5/24/73 | 90 μ AP | 61.3 | 420/150 | 32.3 | 61.31 | 93.8 | 28.4 | 1.482 |
| 11 | 5/25/73 | 90 μ AP | 19.2 | 420/150 | 32.3 | 57.62 | 66.9 | 37.4 | 1.612 |
| 12 | 5/25/73 | Coarse from DC-5 | 146.2 | 420/150 | 32.3 | 63.34 | 94.6 | 27.2 | 1.904 |
| 13 | 5/29/73 | Coarse from DC-6 | 141.6 | 420/200 | unknown | 57.83 | 92.8 | 34.0 | 1.423 |
| 14 | 5/29/73 | Coarse from DC-9 | 84.2 | 420/150 | 32.3 | 56.14 | 95.9 | 22.0 | 2.063 |
| 15 | 5/29/73 | Coarse from DC-10 | 53.9 | 420/150 | 32.3 | 47.61 | 92.6 | 27.8 | 1.344 |
| 16 | 5/29/73 | 50 μ AP | 35.5 | 544/150 | 20.0 | 36.67 | 90.8 | 15.0 | 2.264 |
| 17 | 5/30/73 | 50 μ AP | 52.0 | 544/150 | 20.0 | 39.03 | 92.8 | 13.0 | 1.878 |
| 18 | 5/30/73 | 50 μ AP | 16.3 | 544/150 | 20.0 | 34.25 | 78.4 | 16.0 | 1.528 |
| 19 | 5/30/73 | 50 μ AP | 16.0 | 780/150 | 10.0 | 38.77 | 87.9 | 9.6 | 1.985 |
| 20 | 5/31/73 | Coarse from DC-19 | 13.7 | 420/200 | unknown | 32.45 | 29.2 | 29.7 | 1.428 |
| 21-25 | 6/4-5/73 | 50 μ AP (Lot 4351) | 16.19 | 780/150 | 10.0 | 202.33 | 87.61 | 11.2 | 1.511 |
| 26-30 | 6/6-7/73 | Coarse from DC-21-25 | 13.63 | 420/200 | unknown | 172.69 | 9.13 | 51.6 | 1.710 |
| 31 | 6/8/73 | 1.7 μ AP from EFEM-73 | 14.5 | 1380/150 | 2.0 | run cancelled due to feeding problems | | | |
| 32 | 6/8/73 | 1.7 μ AP from EFEM-73 | N/A | 1880/150 | 2.0 | 3.74 | 48.13 | 2.68 | 3.684 |
| 33 | 6/11/73 | 1.7 μ AP from EFEM-73, with 0.2% Silanox 101 | N/A | 2700/150 | 1.0 | 10.84 | 73.06 | 1.64 | 2.280 |
| 34 | 6/11/73 | 1.7 μ AP from EFEM-73, with 0.2% Silanox 101 | 5.45 | 2700/150 | 1.0 | 15.43 | 59.43 | could not be analyzed | |
| 35 | 6/12/73 | 1.7 μ AP from EFEM-74, with 0.2% Silanox 101 | 6.25 | 3900/150 | 0.5 | 26.56 | 84.68 | could not be analyzed | |
| 36 | 6/13/73 | Fresh ground 1.7 μ AP, EFEM-74 | N/A | 3900/150 | 0.5 | 3.55 | 53.24 | 0.62 | could not be analyzed |
| 37 | 6/13/73 | Fresh ground 1.7 μ AP, EFEM-75 | N/A | 3900/150 | 0.5 | 7.01 | 89.16 | could not be analyzed | |
| 38 | 6/13/73 | Fresh ground 1.7 μ AP, EFEM-75 with 0.2% Cab-O-Sil | 8.05 | 3900/150 | 0.5 | 10.73 | 87.32 | 0.75 | 7.882 |
| 39-41 | 6/18/73 | 50 μ AP (Lot 4351) | 16.45 | 780/150 | 10.0 | 123.35 | 88.36 | 10.8 | 1.790 |
| 42 | 6/19/73 | 16 μ AP (No. H11602) | 37.08 | 780/150 | 10.0 | 15.45 | 63.24 | 11.8 | 1.551 |
| 43 | 6/19/73 | 16 μ AP (No. H11602) | 42.75 | 780/150 | 10.0 | 17.25 | 61.50 | 12.4 | 1.661 |
| 44 | 6/19/73 | 16 μ AP (No. H11602) | 24.47 | 780/150 | 10.0 | 24.47 | 61.34 | 11.35 | 1.545 |
| 45 | 6/19/73 | 16 μ AP (No. H11602) | 14.60 | 780/150 | 10.0 | 29.19 | 56.08 | 10.25 | 1.758 |
| 46 | 6/19/73 | 16 μ AP (No. H11602) | 22.56 | 1140/150 | 5.0 | 22.56 | 70.70 | 6.9 | 1.956 |
| 47 | 6/19/73 | 16 μ AP (No. H11602) | 13.88 | 1140/150 | 5.0 | 27.76 | 71.18 | 7.35 | 2.095 |
| 48 | 6/19/73 | 16 μ AP (No. H11602) | 27.70 | 482/150 | 25.0 | 13.85 | 34.48 | 23.2 | 1.718 |
| 49 | 6/19/73 | 16 μ AP (No. H11602) | 34.65 | 482/150 | 25.0 | 11.55 | 41.13 | 20.8 | 1.494 |
| 50 | 6/19/73 | 16 μ AP (No. H11602) | 18.40 | 482/150 | 25.0 | 18.40 | 36.96 | 22.2 | 1.337 |
| 51 | 6/20/73 | VMA-101 | 2.3 | 3900/150 | 0.5 | 1.34 | 87.31 | could not be analyzed | |
| 52 | 6/20/73 | VMA-101 | 15.2 | 3900/150 | 0.5 | 4.55 | 96.48 | could not be analyzed | |
| 53 | 6/20/73 | 1.7 μ AP EFEM-78, with 0.5% Silanox 101 | 7.53 | 3900/150 | 0.5 | 2.31 | 86.58 | could not be analyzed | |
| 54-59 | 6/20-21/73 | 16 μ AP (No. H11602) | 20.34 | 1140/150 | 5.0 | 299.40 | 72.75 | 5.55 | 2.235 |
| 60-61 | 6/22/73 | Coarse from DC-54-59 | 65.08 | 482/150 | 25.0 | 173.56 | 52.34 | 19.5 | 1.254 |
| 62 | 6/22/73 | Coarse from DC-54-59 | 29.23 | 482/150 | 25.0 | 41.90 | 40.34 | 20.8 | 1.356 |
| 63-65 | 6/22-25/73 | Coarse from DC-39-41 | 11.61 | 420/150 | 32.3 | 106.40 | 42.95 | 28.6 | 1.405 |
| 66 | 6/25/73 | 2.6 μ AP (FEM-338) with 0.2% Silanox 101 | 2.34 | 4200/100 | unknown | 7.41 | 97.57 | could not be analyzed | |
| 67 | 6/26/73 | Blended mix of 1.7 μ AP (EFEM-78) with fines from DC-43, with 0.2% Silanox 101 | 15.17 | 4200/150 | 0.44 | 12.14 | 93.90 | could not be analyzed | |
| 68 | 6/26/73 | Blended mix of 2.6 μ AP (FEM-338) with coarse from DC-43, with 0.2% Silanox 101 | 4.32 | 4200/150 | 0.44 | 11.10 | 90.09 | 2.15 | 1.538 |
| 69 | 6/27/73 | VMA-101 | 26.22 | 4200/150 | 0.44 | 34.52 | 95.48 | could not be analyzed | |
| 70 | 6/27/73 | 2.6 μ AP (FEM-338) with 0.2% Silanox 101 | 5.42 | 2700/150 | 1.0 | 16.25 | 59.99 | 2.82 | 1.321 |
| 71 | 6/27/73 | Coarse from DC-70 | 22.26 | 1140/150 | 5.0 | 9.27 | 6.80 | could not be analyzed | |
| 72 | 7/11/73 | Lot 4445 Aluminium Powder | 53.58 | 1040/150 | 5.0 | 79.48 | 82.51 | 5.4 | 2.434 |
| 73 | 7/11/73 | Coarse from DC-72 | 102.17 | 630/150 | 13.0 | 64.71 | 66.71 | 11.65 | 1.290 |
| 74 | 7/12/73 | Lot 3432 Aluminium Powder | (?) | 590/150 | 15 | Classifier jammed and rotor stopped. Run cancelled. | | | |
| 75 | 7/12/73 | Lot 3432 Aluminium Powder | 170.95 | 590/150 | 15 | 99.72 | 92.78 | 8.2 | 2.554 |
| 76 | 7/12/73 | Coarse from DC-75 | 159.10 | 420/150 | 28 | 91.48 | 69.65 | 23.3 | 1.473 |
| 77 | 7/13/73 | Lot 4443 Aluminium Powder | 110.36 | 420/150 | 28 | 40.12 | 96.83 | could not be analyzed | |
| 78 | 7/19/73 | Lot 3916 Aluminium Powder | 19.74 | 4200/150 | 0.38 | 19.24 | 97.77 | 0.72 | 1.900 |
| 79 | 7/19/73 | Lot 3916 Aluminium Powder | 100.73 | 4200/150 | 0.38 | 54.89 | 98.36 | 0.54 | 7.231 |
| 80 | 7/26/73 | Lot 3916 Aluminium Powder | 100.4 | 4200/150 | 0.38 | 49.35 | 99.29 | could not be analyzed | |
| 81 | 7/26/73 | Lot 3916 Aluminium Powder | 100.54 | 4200/100 | unknown | 49.82 | 99.22 | 0.54 | 2.690 |
| 82 | 7/27/73 | Lot 3916 Aluminium Powder | 44.99 | 4200/100 | unknown | 99.17 | 99.31 | could not be analyzed | |

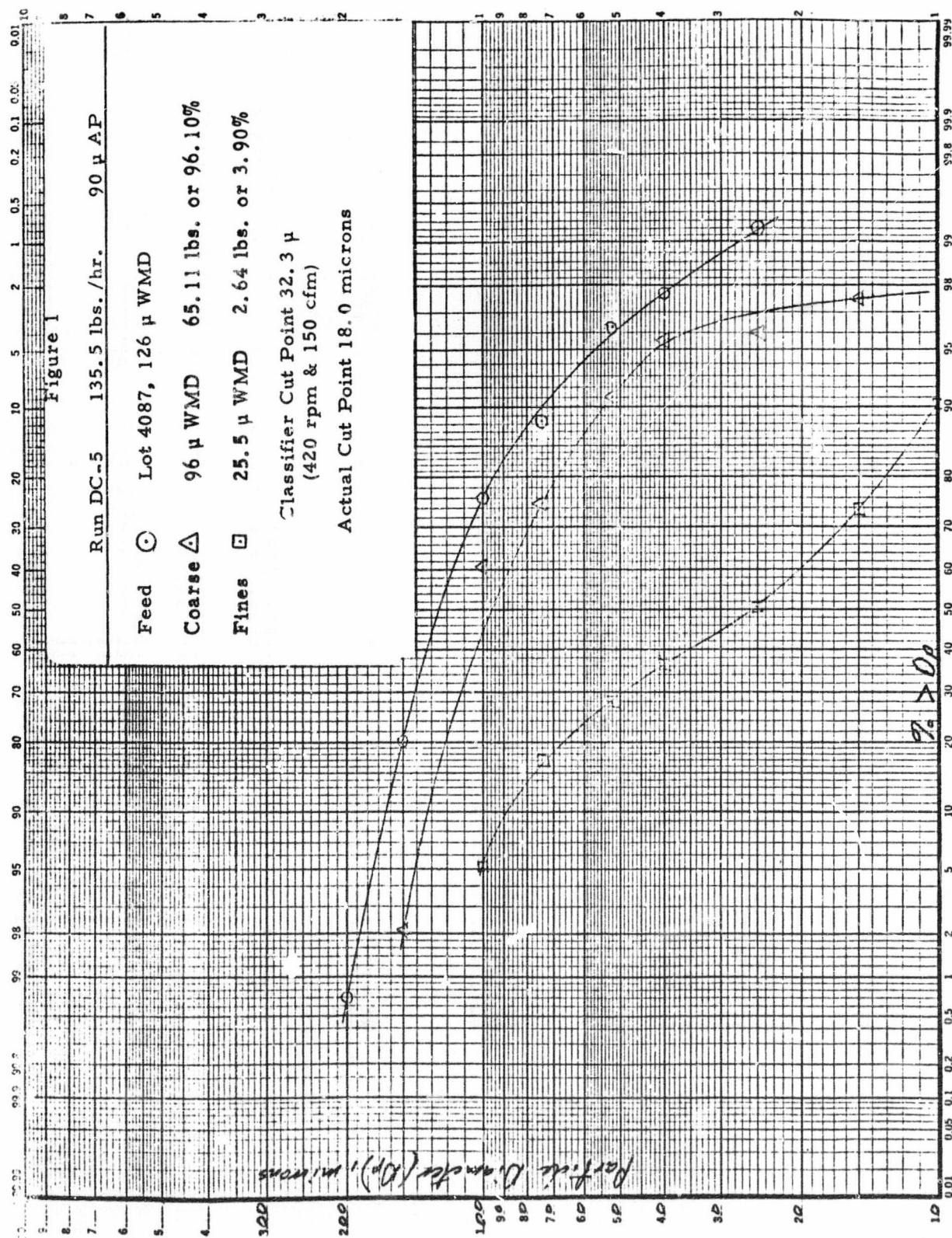
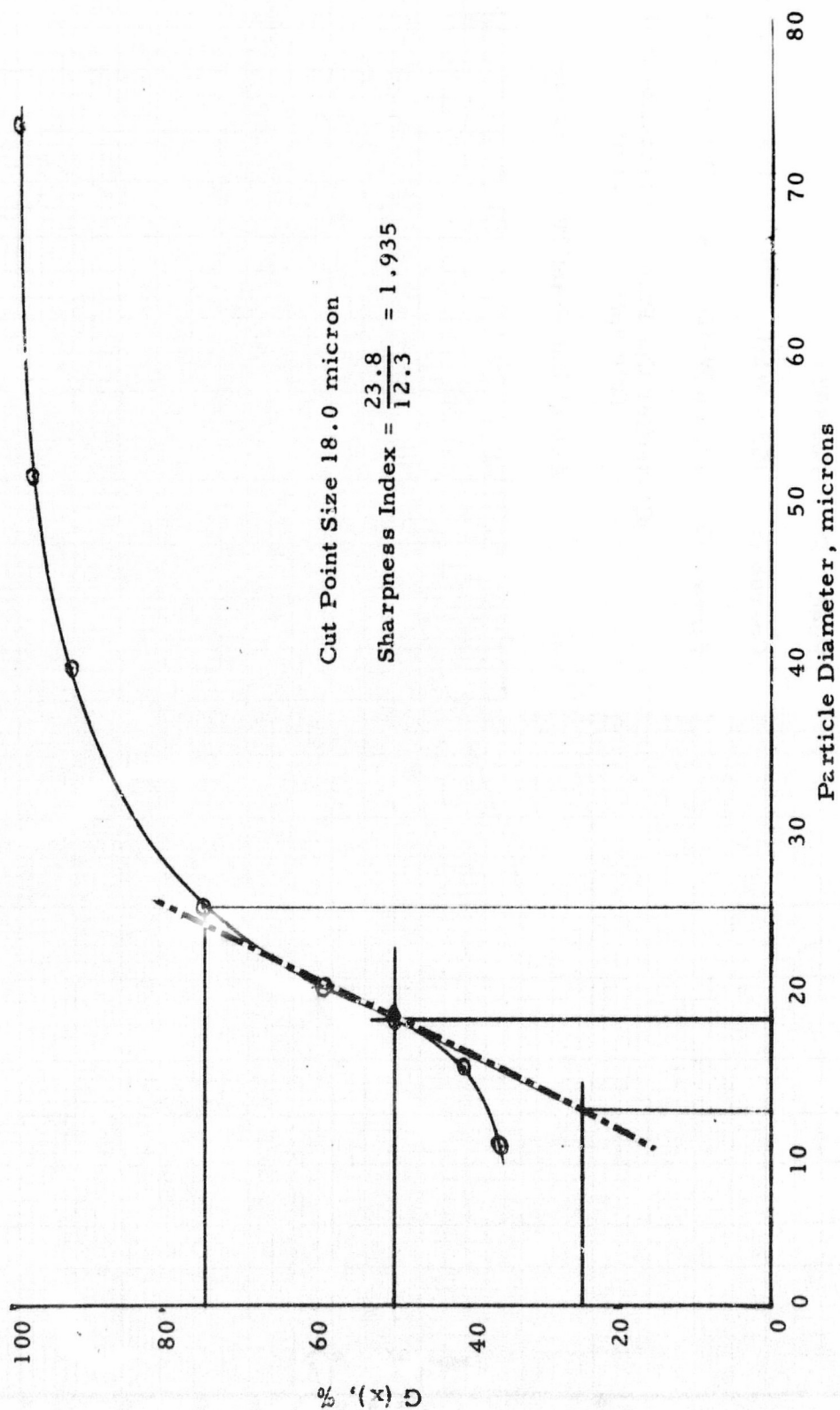


Figure 2
Grade Efficiency Curve for DC-5



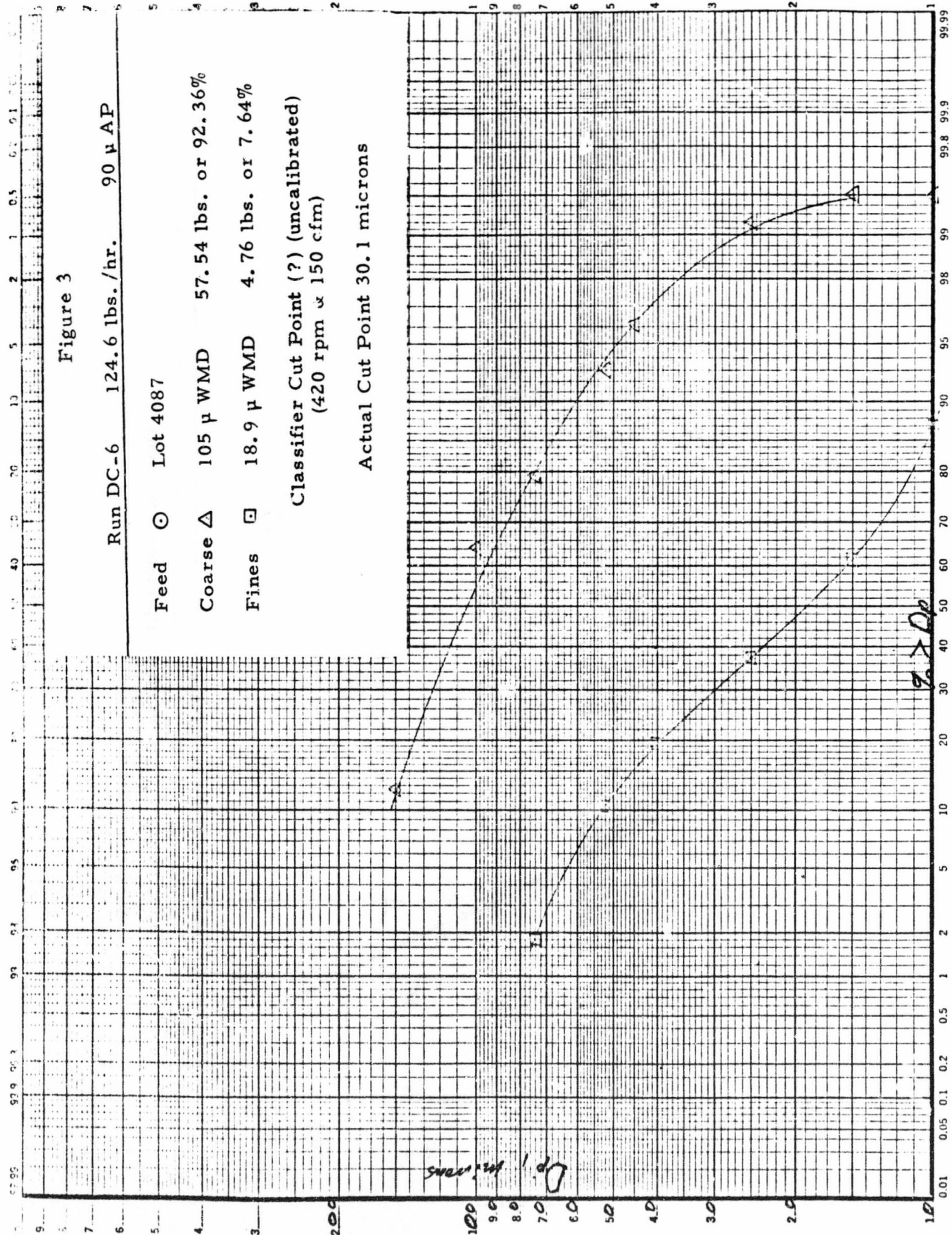


Figure 4

Grade Efficiency Curve For DC-6

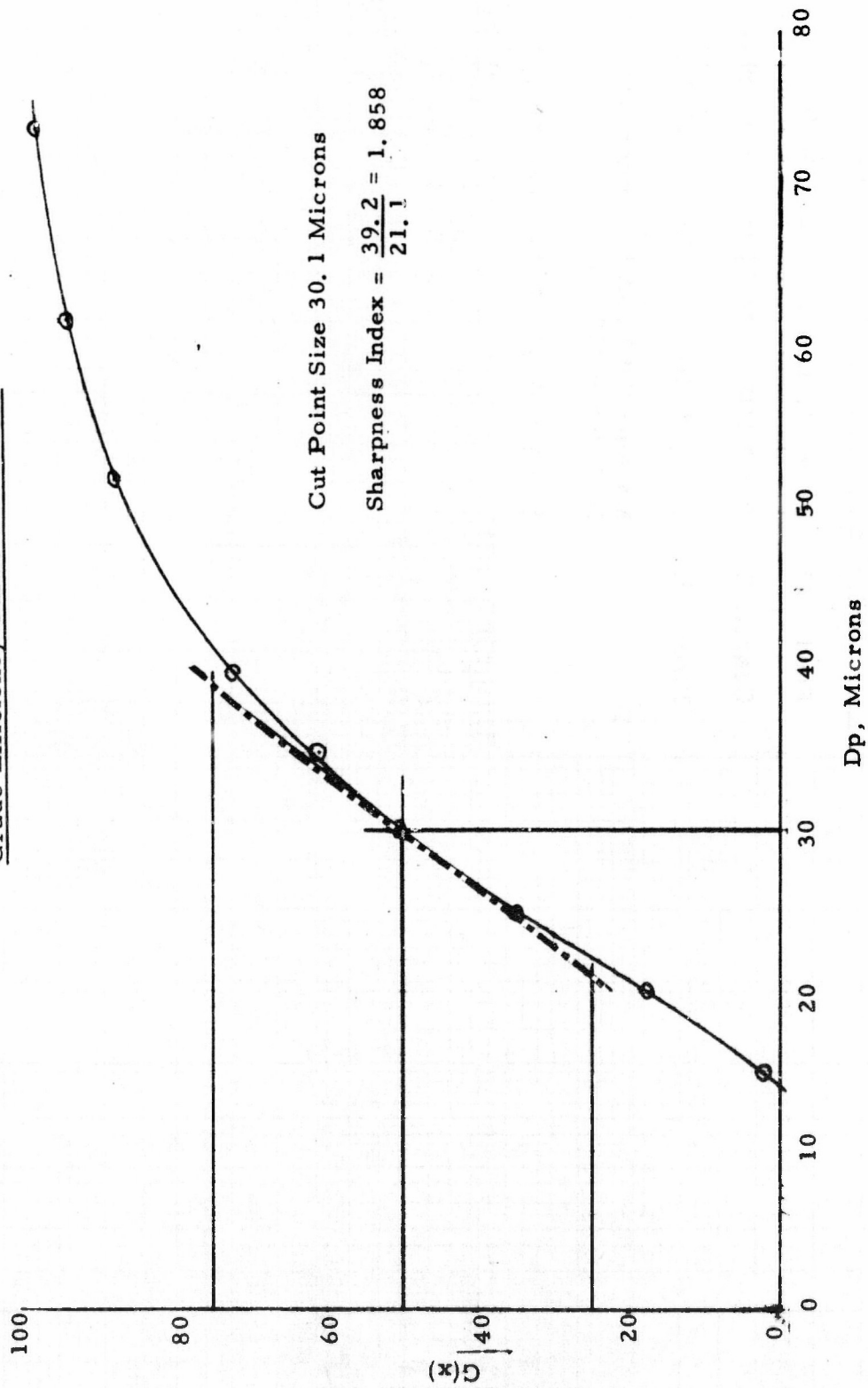
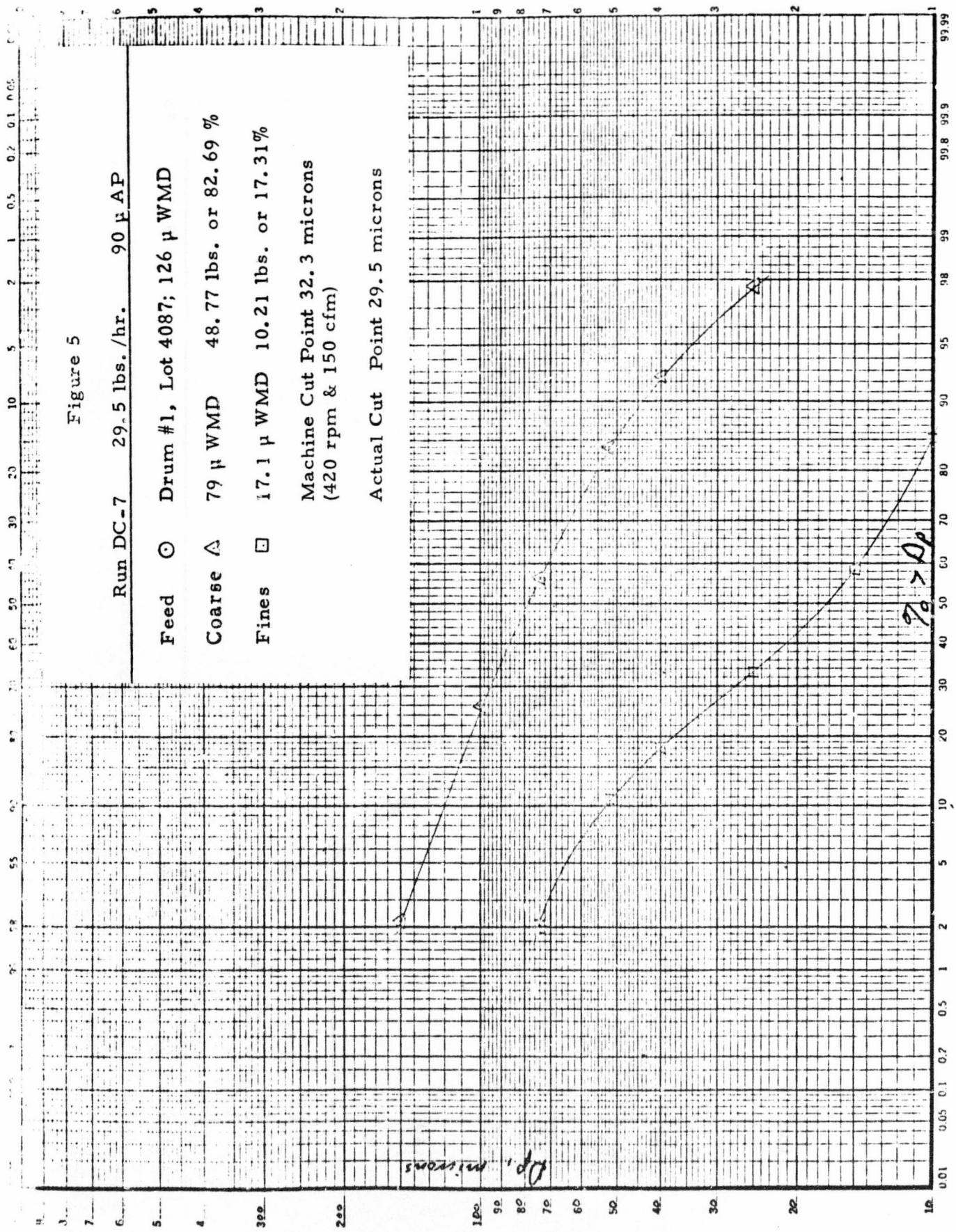


Figure 5

Run DC-7 29.5 lbs./hr. 90 μ AP

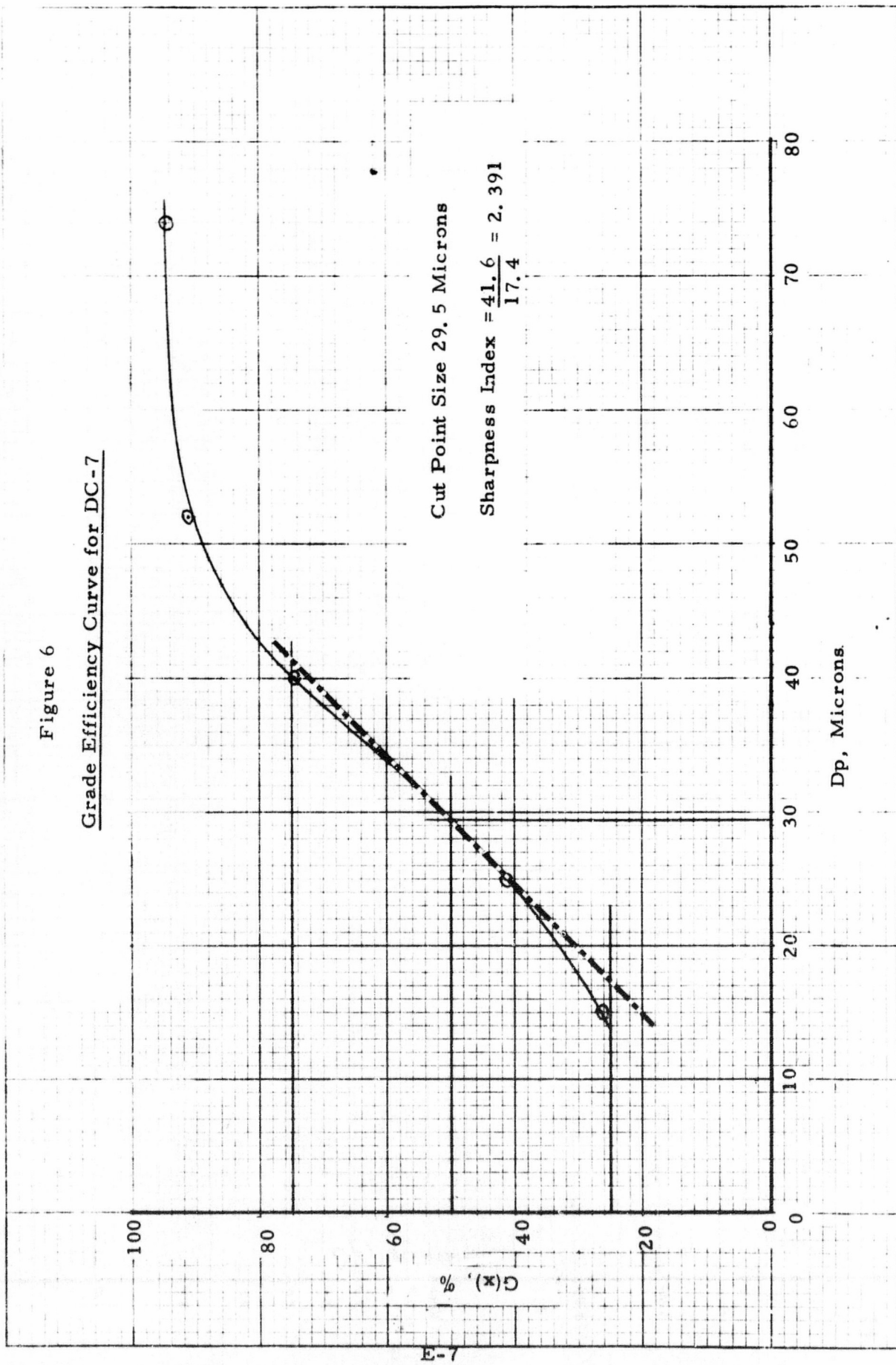
Feed \odot Drum #1, Lot 4087; 126 μ WMD
 Coarse \triangle 79 μ WMD 48.77 lbs. or 82.69 %
 Fines \square 17.1 μ WMD 10.21 lbs. or 17.31 %
 Machine Cut Point 32.3 microns
 (420 rpm & 150 cfm)
 Actual Cut Point 29.5 microns



10 X 10 TO THE INCH 46 C-200
 7 X 1 1/2 ALUMINUM
 1000000 5 45

Figure 6

Grade Efficiency Curve for DC-7



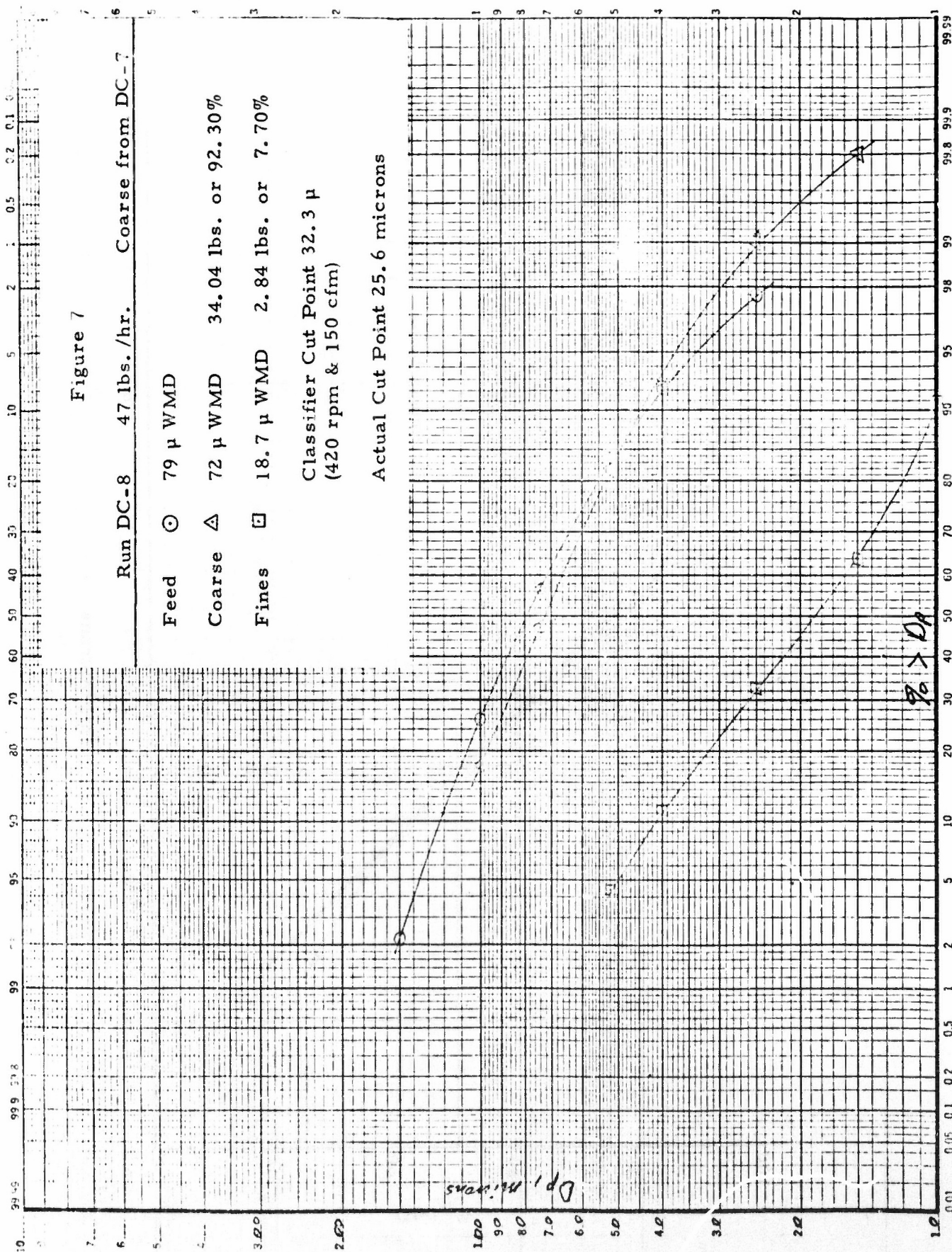
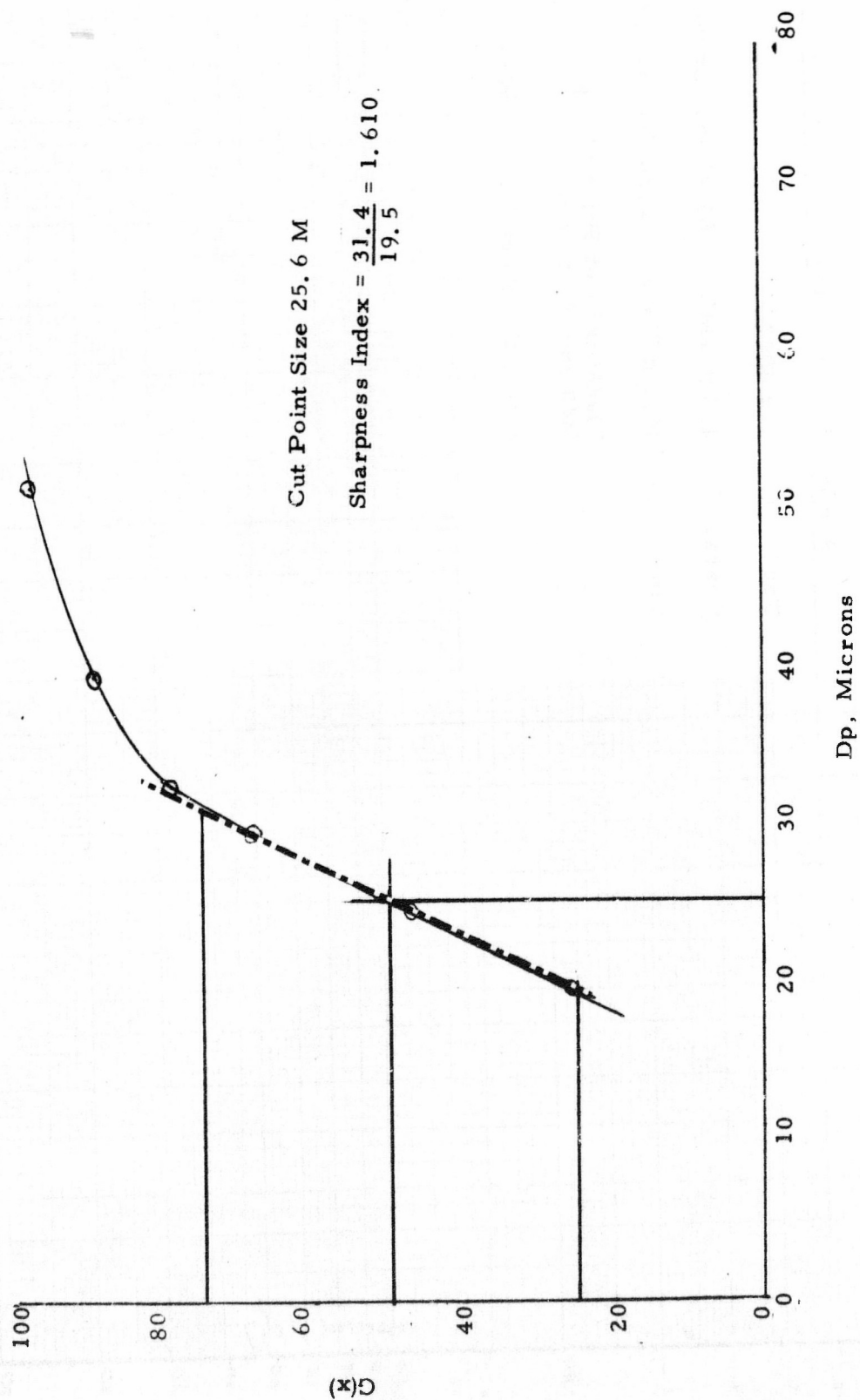


Figure 8

Grade Efficiency Curve for DC-8



10
9
8
7
6
5
4
3
2
1
0.1
0.05
0.01

Figure 9

Run DC-9 87.3 lbs./hr. 90 μ AP

Feed \odot Lot 4087

Coarse \triangle 110 μ WMD 63.27 lbs. or 96.64%

Fines \square 16.3 μ WMD 2.20 lbs. or 3.36%

Classifier Cut Point 32.3 μ
(420 rpm & 150 cfm)

Actual Cut Point 24.3 microns

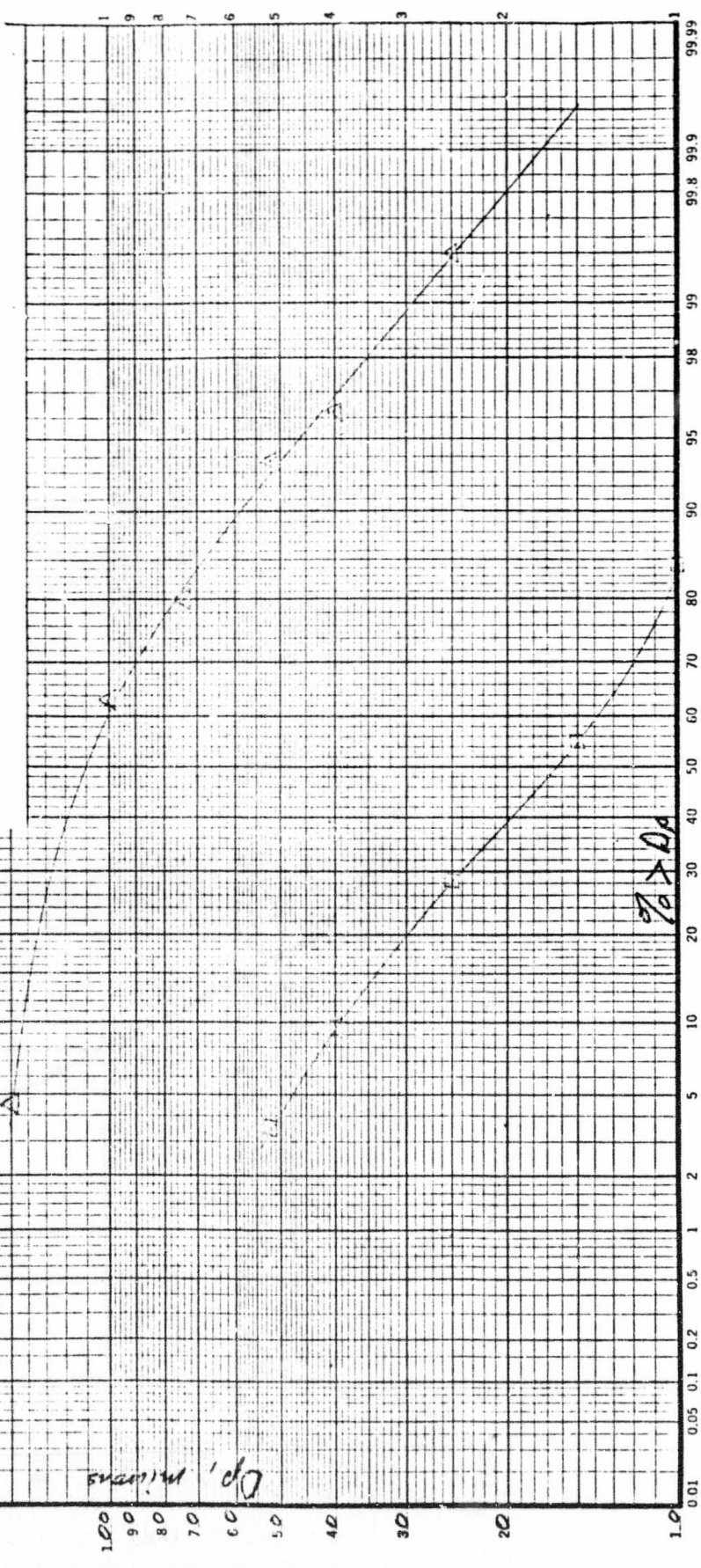


Figure 10
Grade Efficiency Curve for DC-9

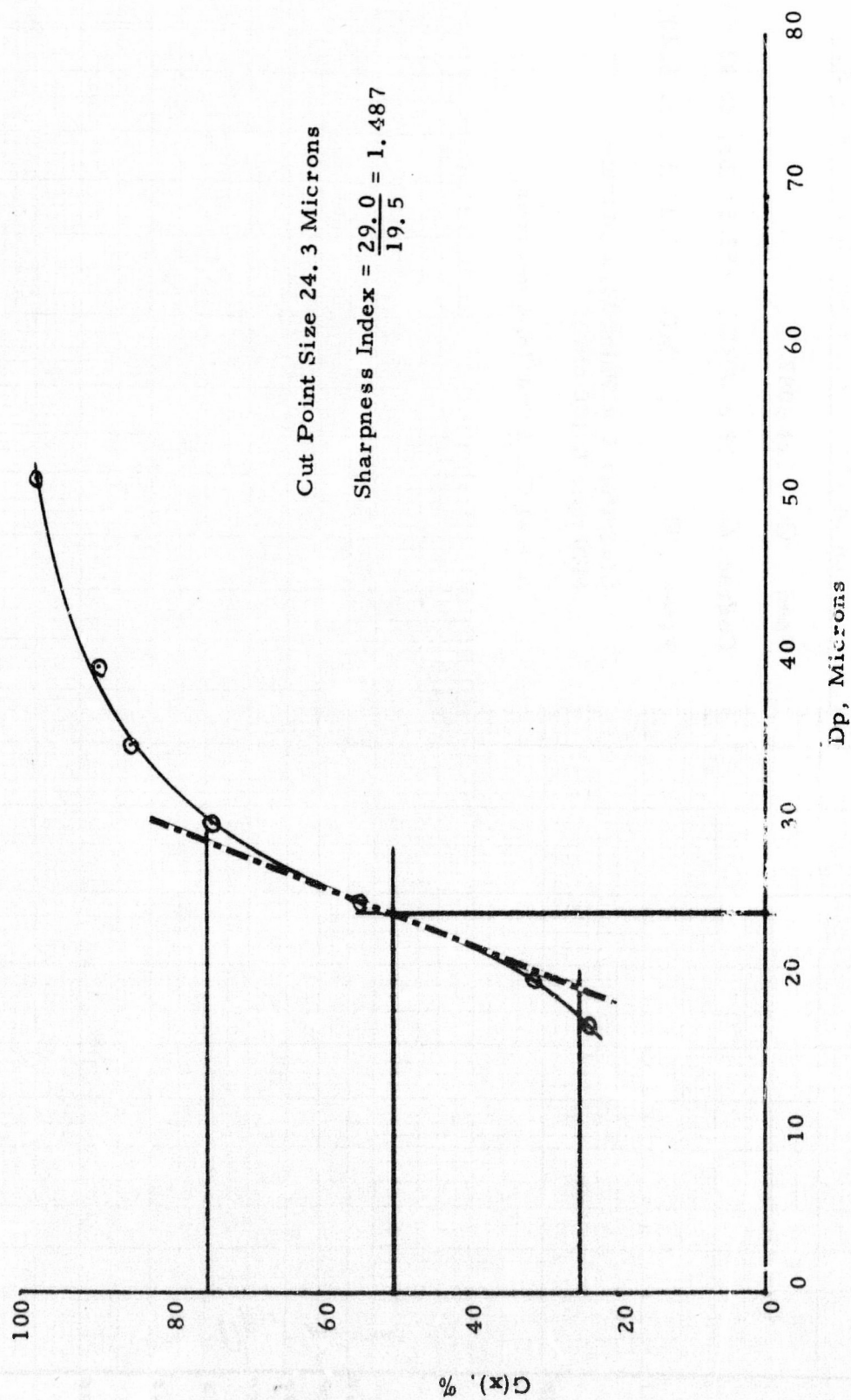


Figure 11

Run DC-10 61.3 lbs./hr. 90 μ AP

Feed \bigcirc Lot 4087

Coarse \triangle 118 μ WMD 57.51 lbs. or 93.80%

Fines \square 17.1 μ WMD 3.80 lbs. or 6.20%

Classifier Cut Point 32.3 microns
(420 rpm & 150 cfm)

Actual Cut Point 28.4 microns

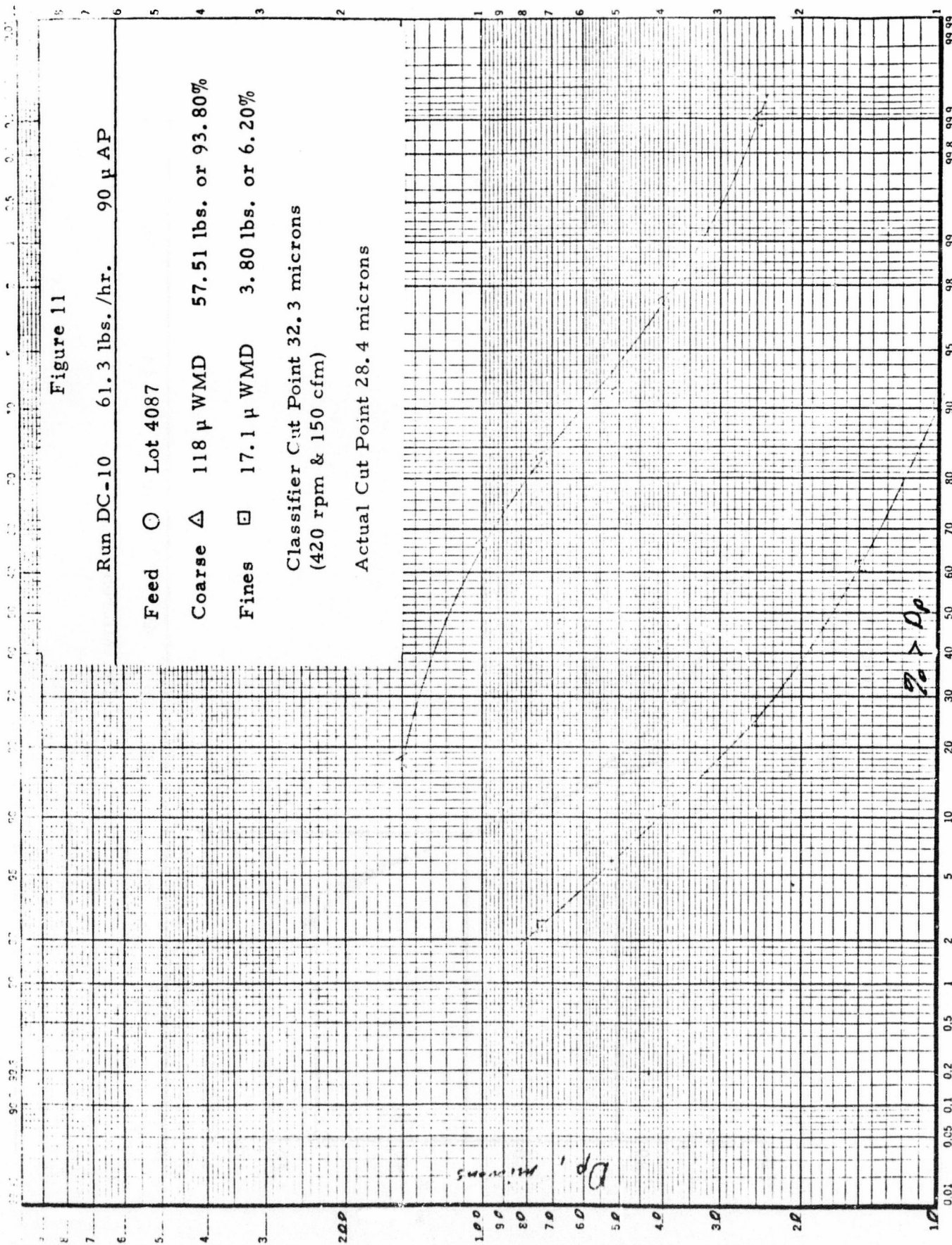


Figure 12
Grade Efficiency Curve for DC-10

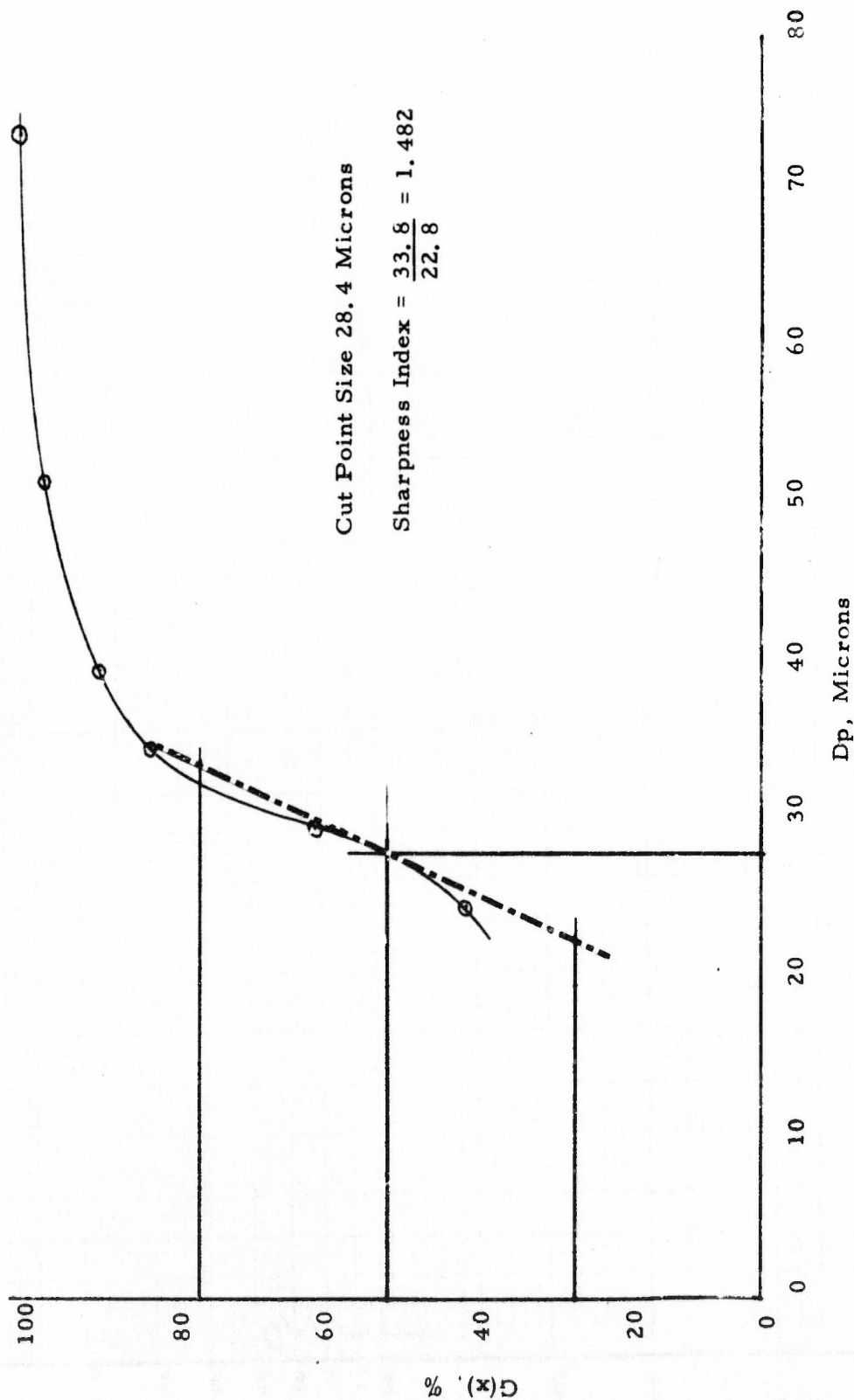


Figure 13

Run DC-11 19.2 lbs./hr. 90 μ AP

Feed \odot Lot 4087

Coarse Δ 72 μ WMD 38.53 lbs. or 66.87%

Fines \square 27.2 μ WMD 19.09 lbs. or 33.13%

Classifier Cut Point 32.3 microns
(420 rpm & 150 cfm)

Actual Cut Point 37.4 microns

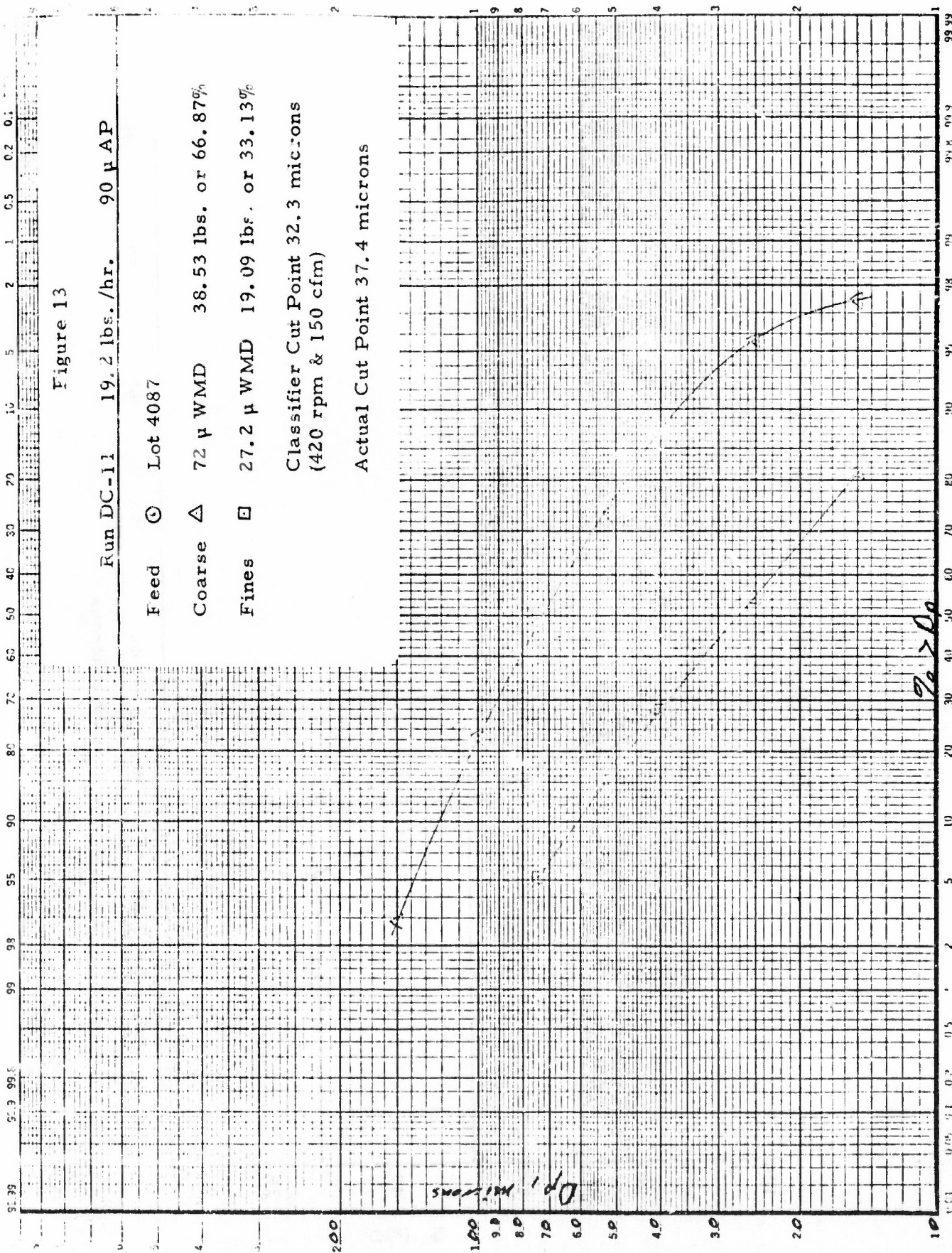
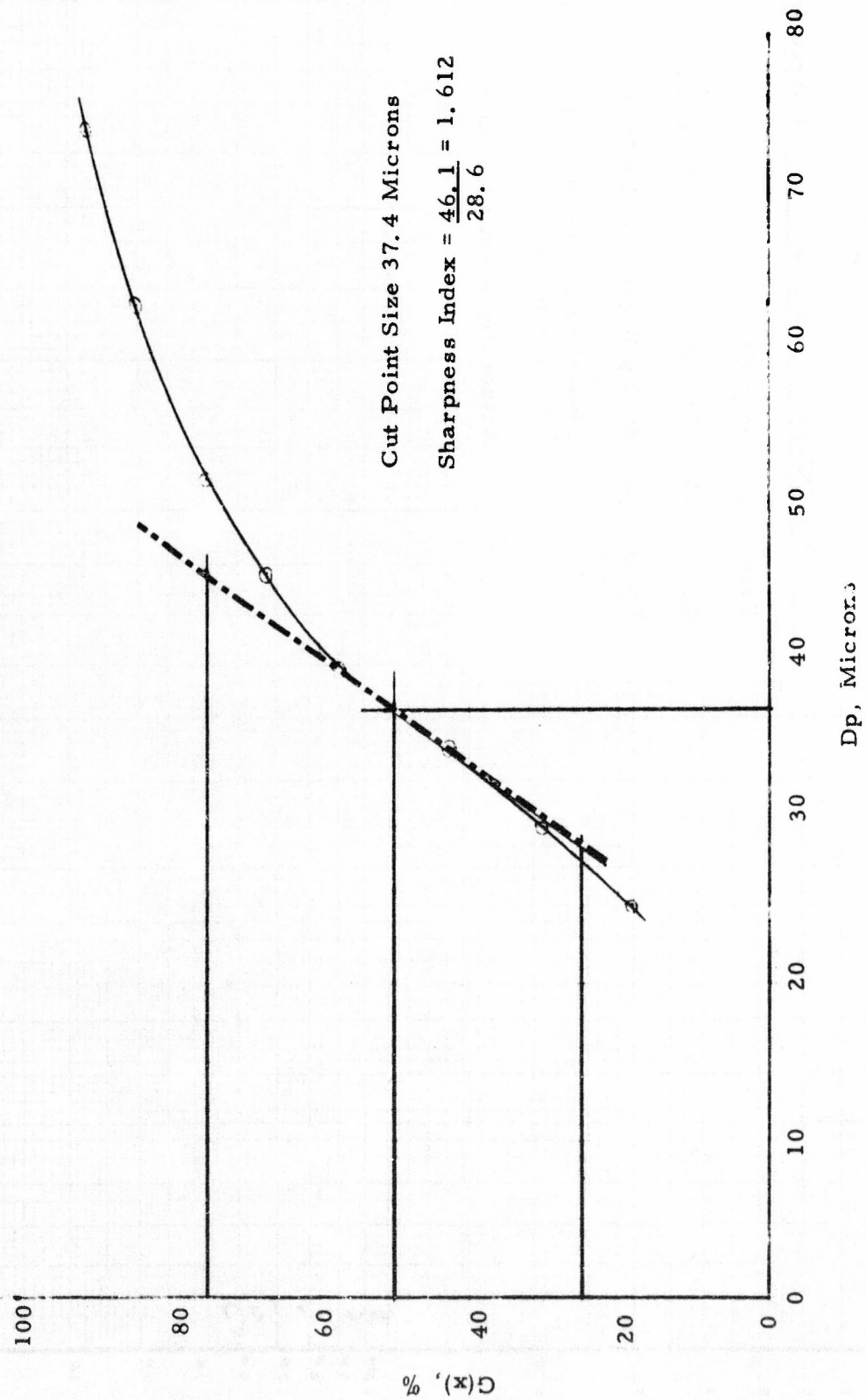


Figure 14
Grade Efficiency Curve for DC-11



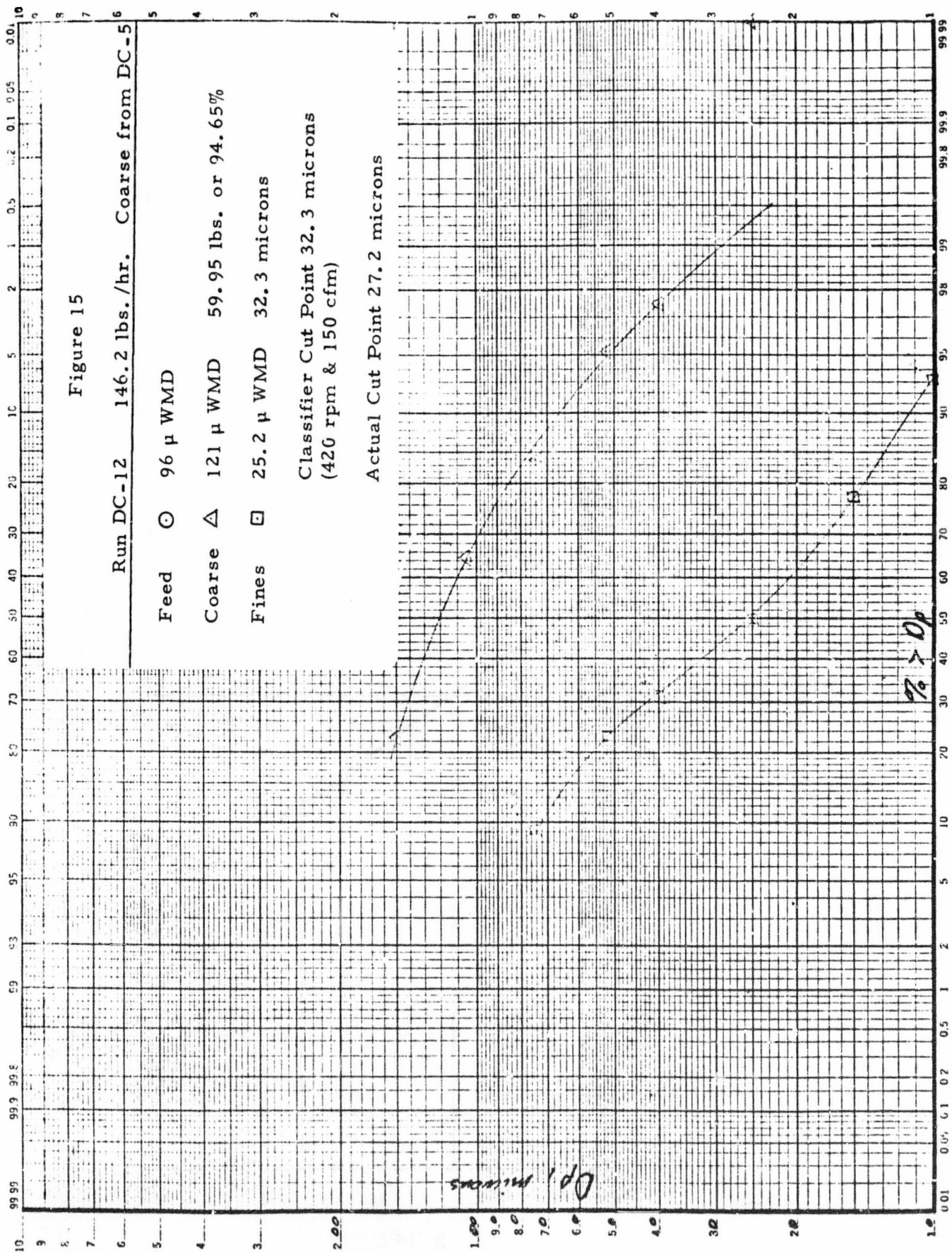


Figure 16

Grade Efficiency Curve for DC-12

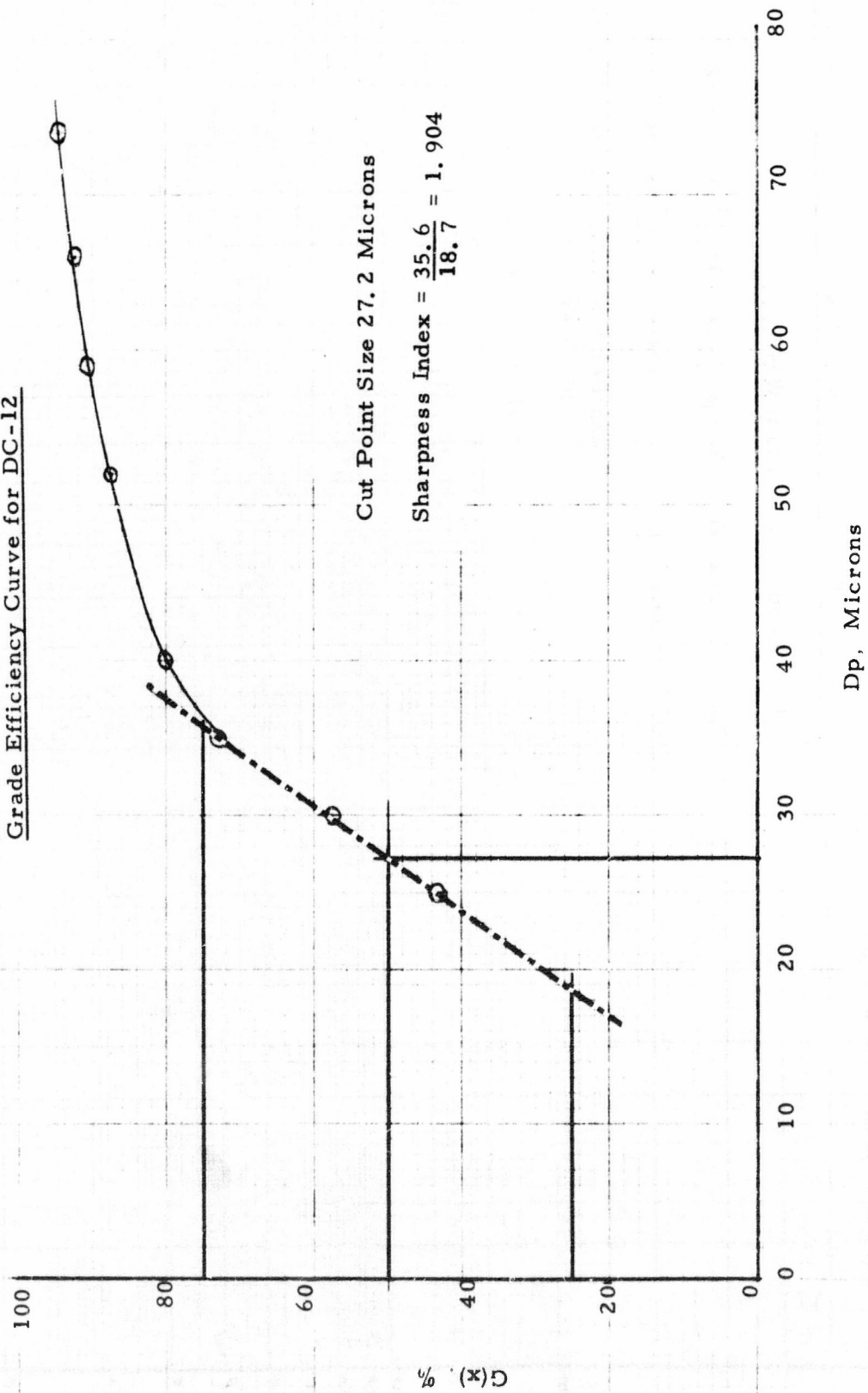


Figure 17

Run DC-13 141.6 lbs./hr. Coarse from DC-6

Feed \odot 105 μ WMD

Coarse Δ 76.0 μ WMD 53.67 lbs. or 92.81%

Fines \square 17.8 μ WMD 4.16 lbs. or 7.19%

Classifier Cut Point (?) (uncalibrated)
(420 rpm & 200 cfm)

Actual Cut Point 34.0 microns

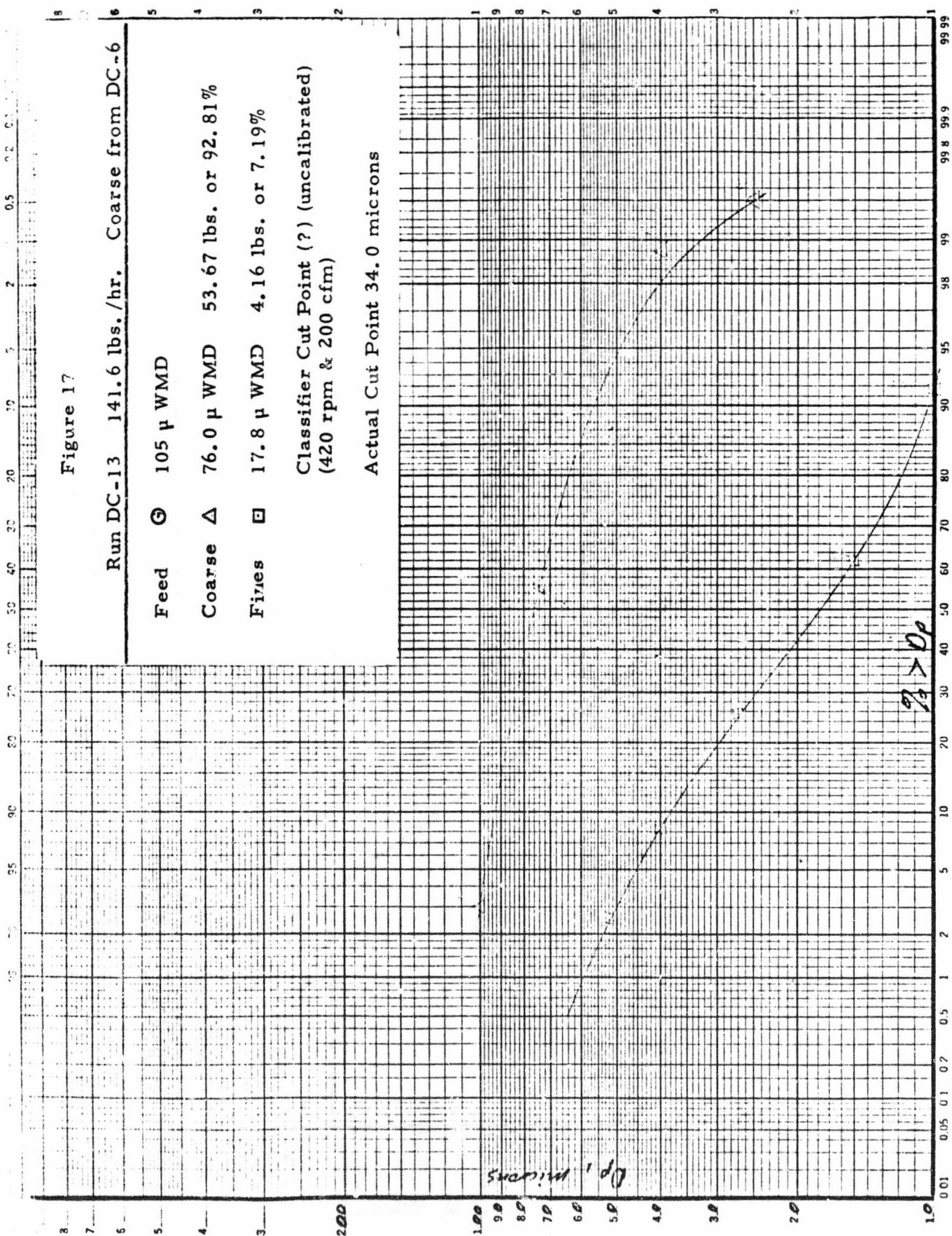


Figure 18

Grade Efficiency Curve for DC-13

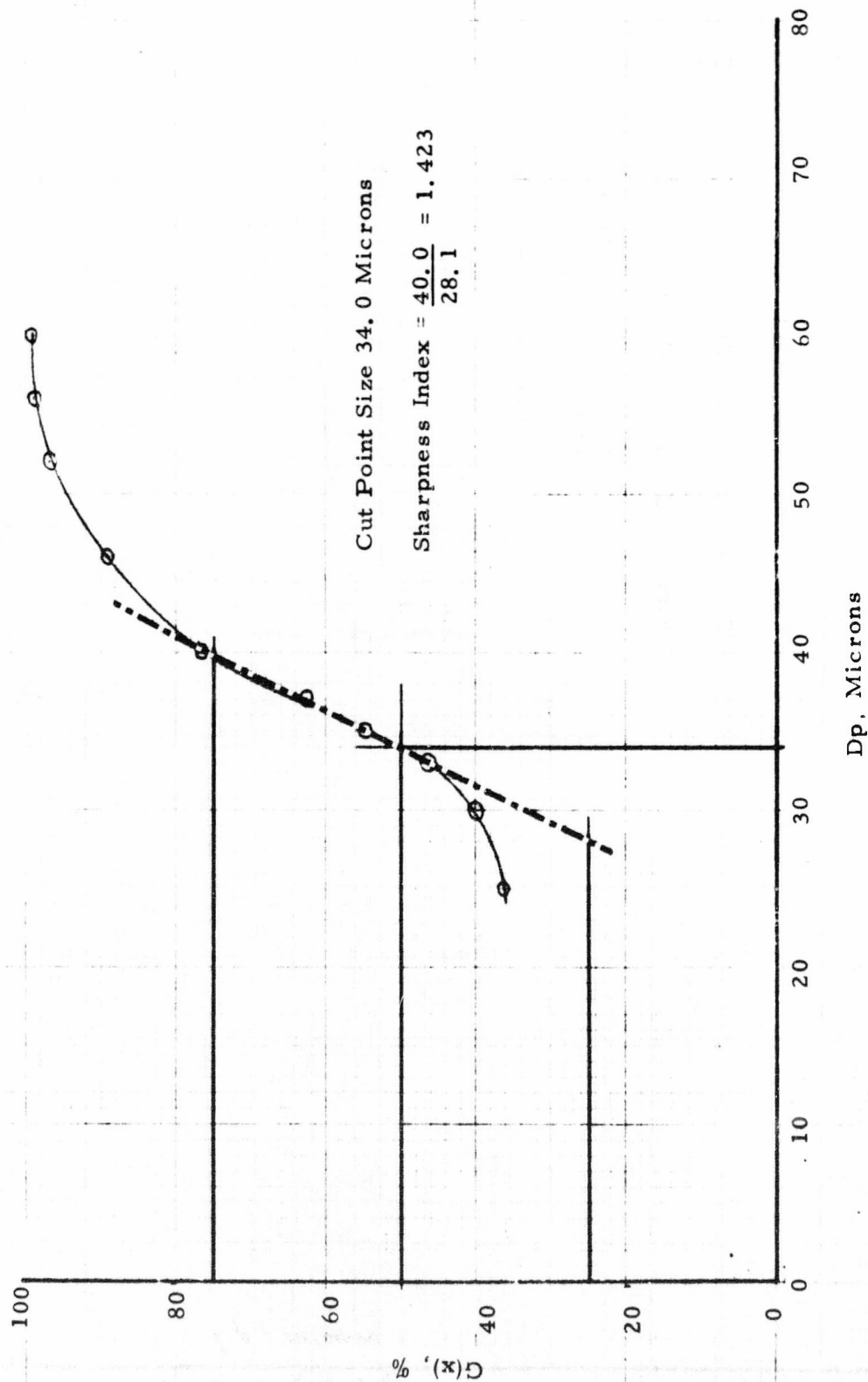


Figure 19

Run DC-14 84.2 lbs./hr. Coarse from DC-9

Feed ○ 110 μ WMD

Coarse △ 98 μ WMD 53.85 lbs. or 95.92%

Fines □ 17.6 μ WMD 2.29 lbs. or 4.08%

Classifier Cut Point 32.3 microns
(420 rpm & 150 cfm)

Actual Cut Point 22.0 microns

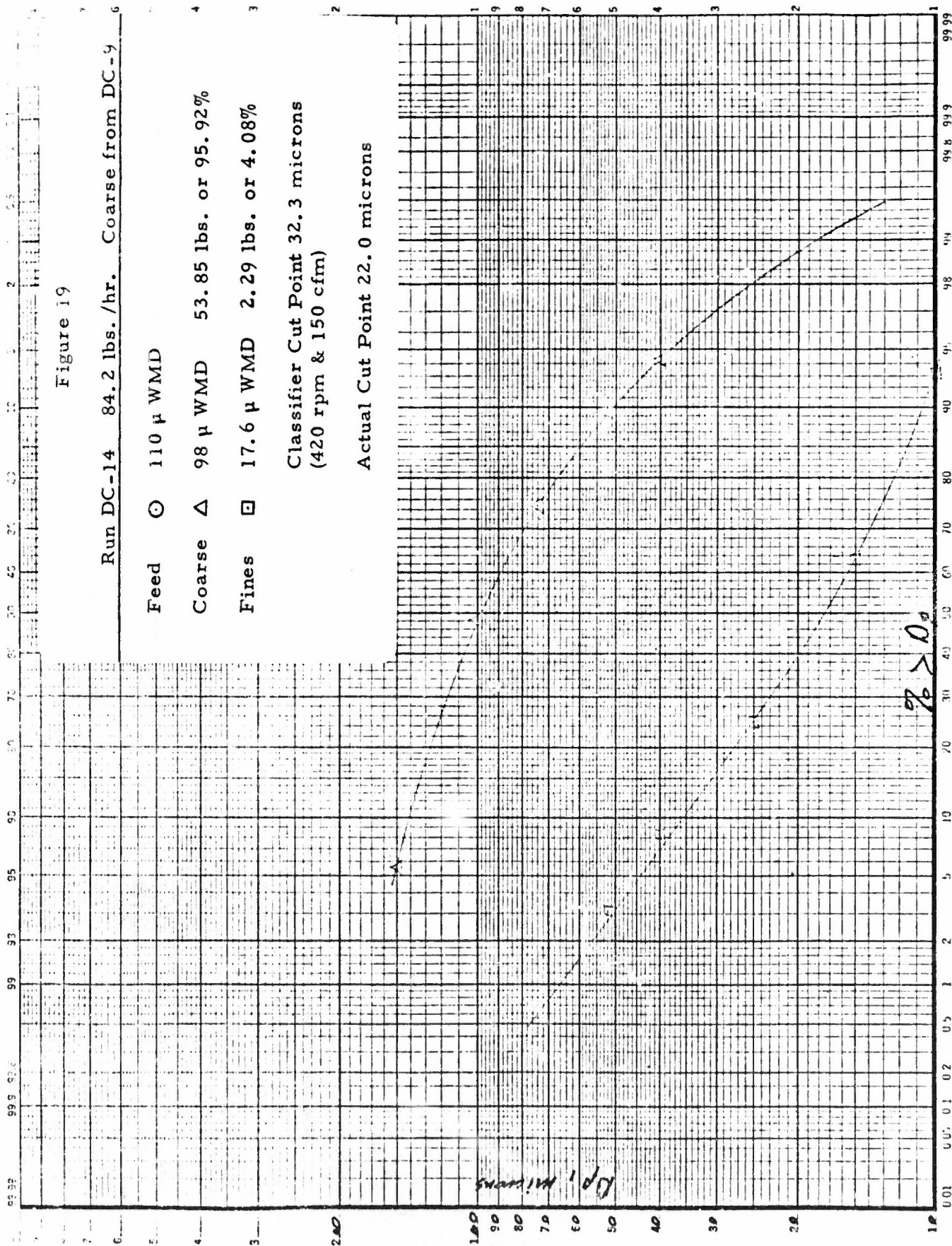
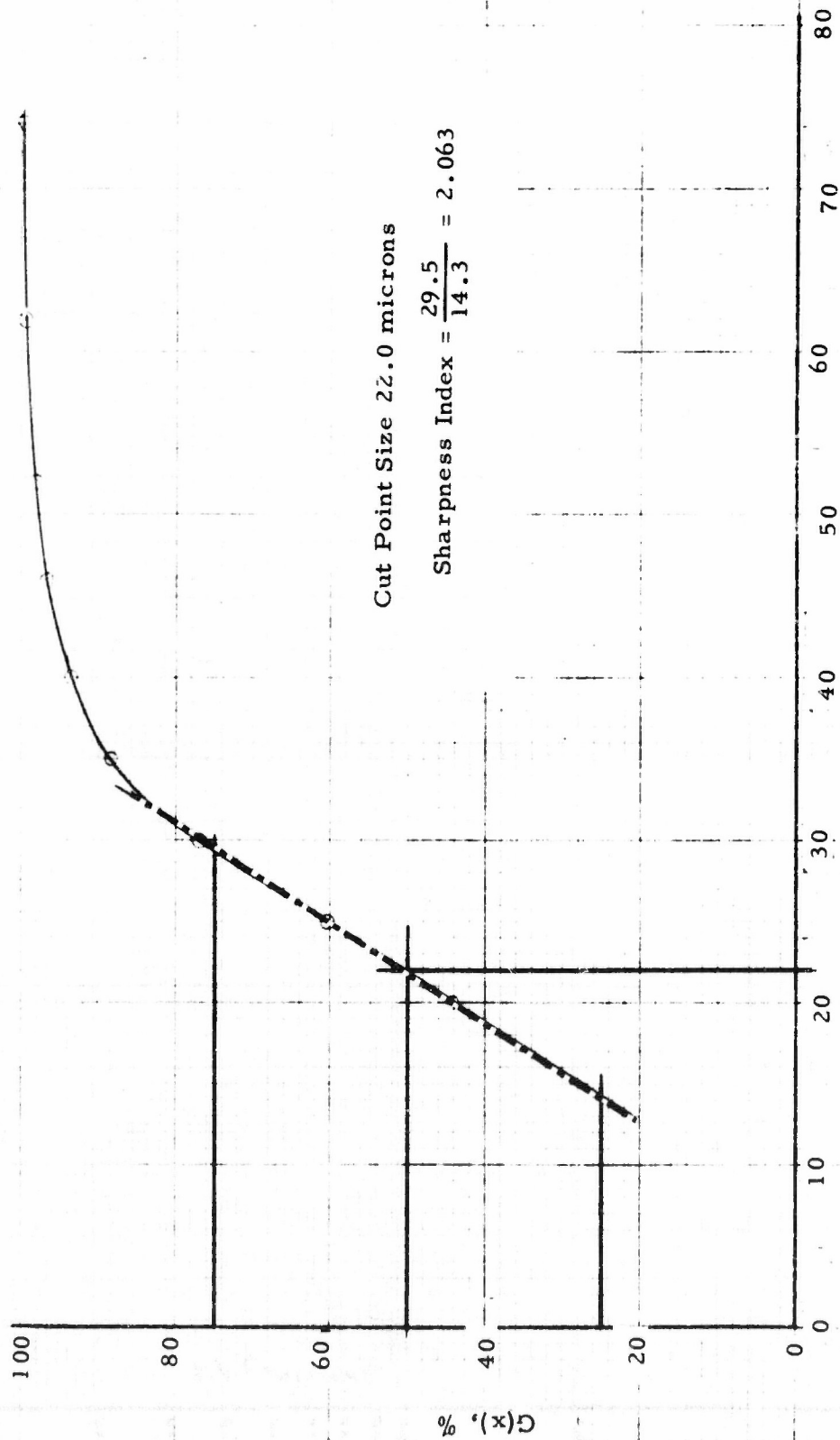


Figure 20
Grade Efficiency Curve for DC-14



Cut Point Size 22.0 microns
Sharpness Index = $\frac{29.5}{14.3} = 2.063$

Figure 21

Run DC-15 53.9 lbs./hr. Coarse from DC-10

Feed ○ 118 μ WMD

Coarse △ 99 μ WMD 44.10 lbs. or 92.63%

Fines □ 18.5 μ WMD 3.51 lbs. or 7.37%

Classifier Cut Point 32.3 microns
(420 rpm & 150 cfm)

Actual Cut Point 27.8 microns

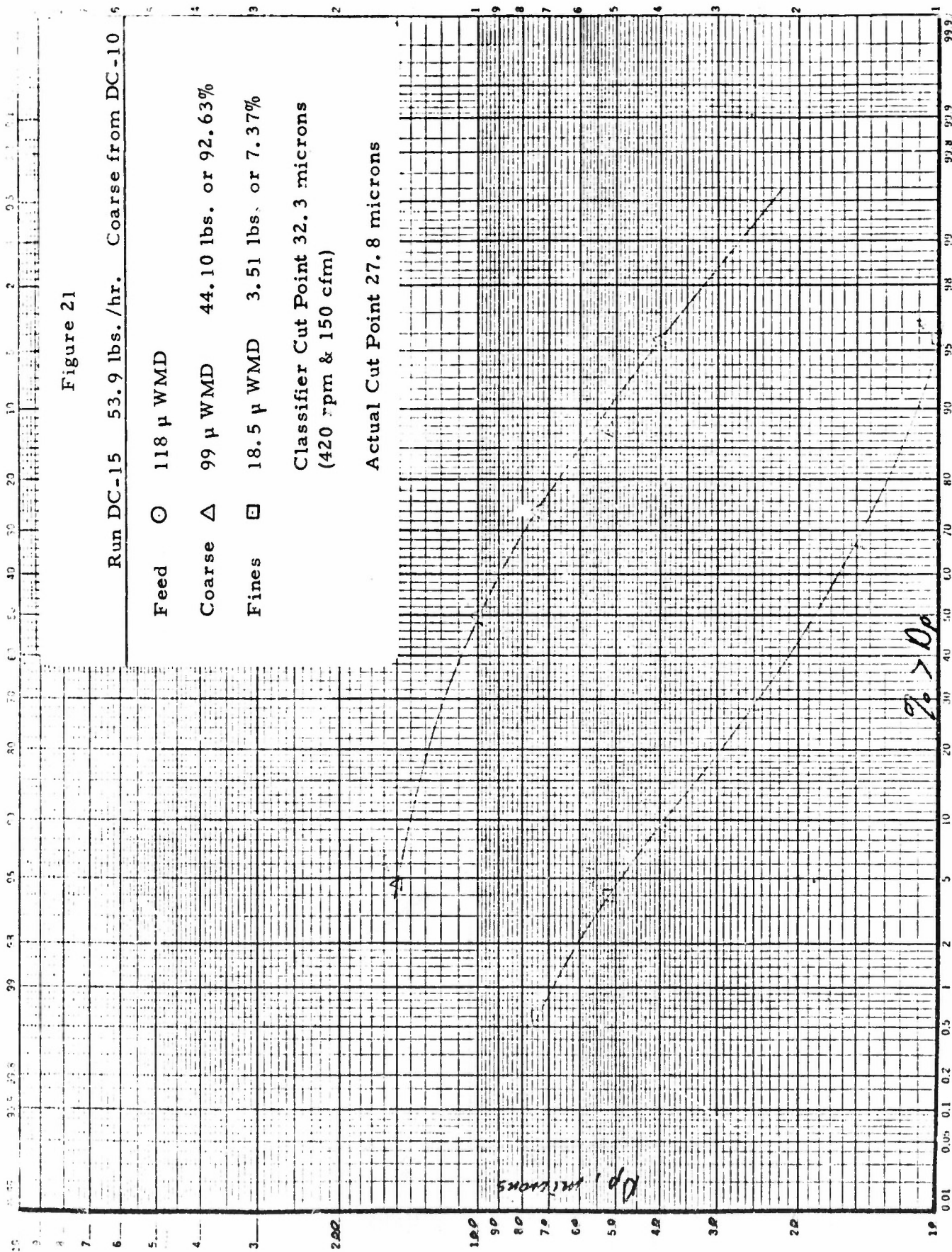
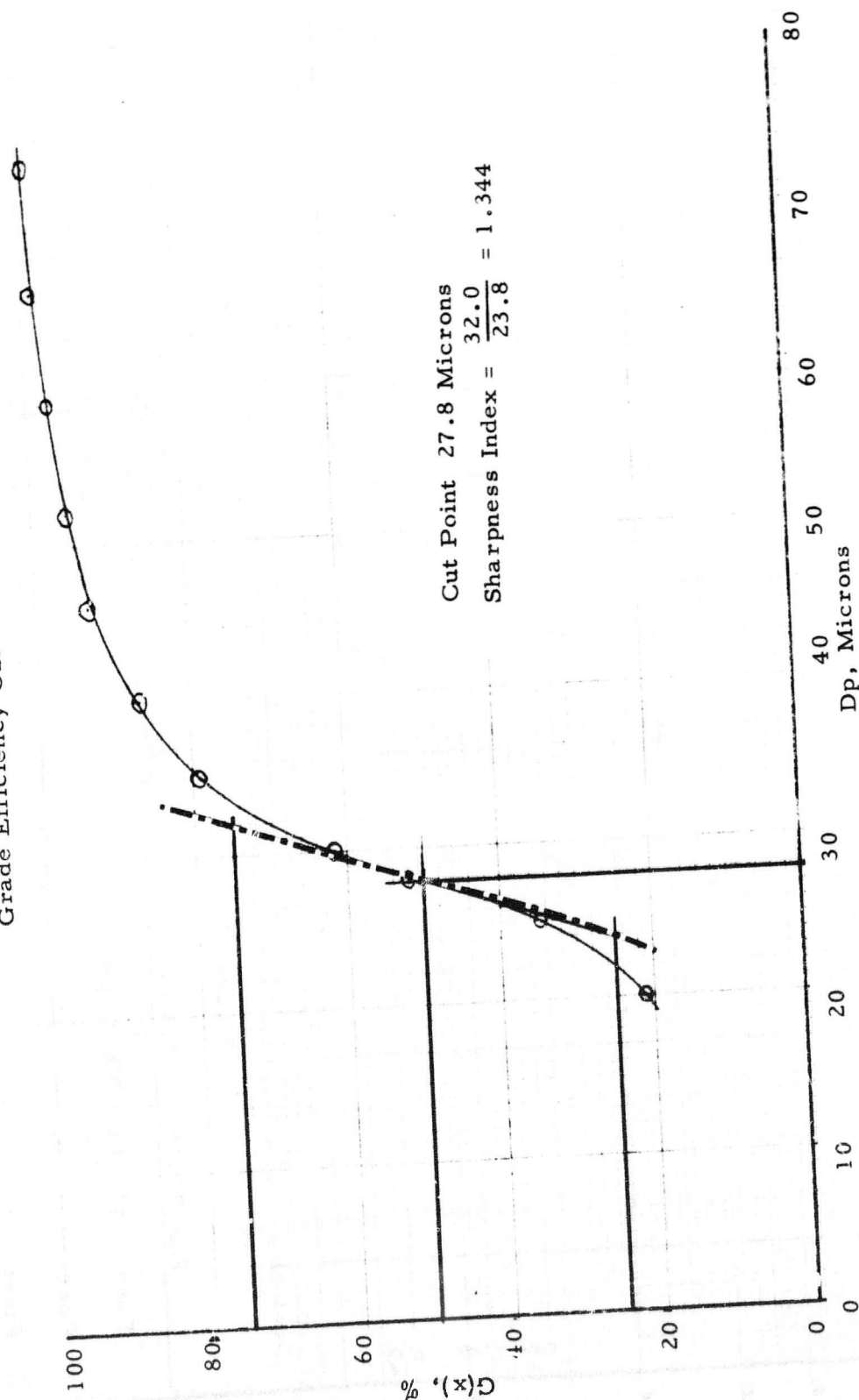


Figure 22
Grade Efficiency Curve for DC-15



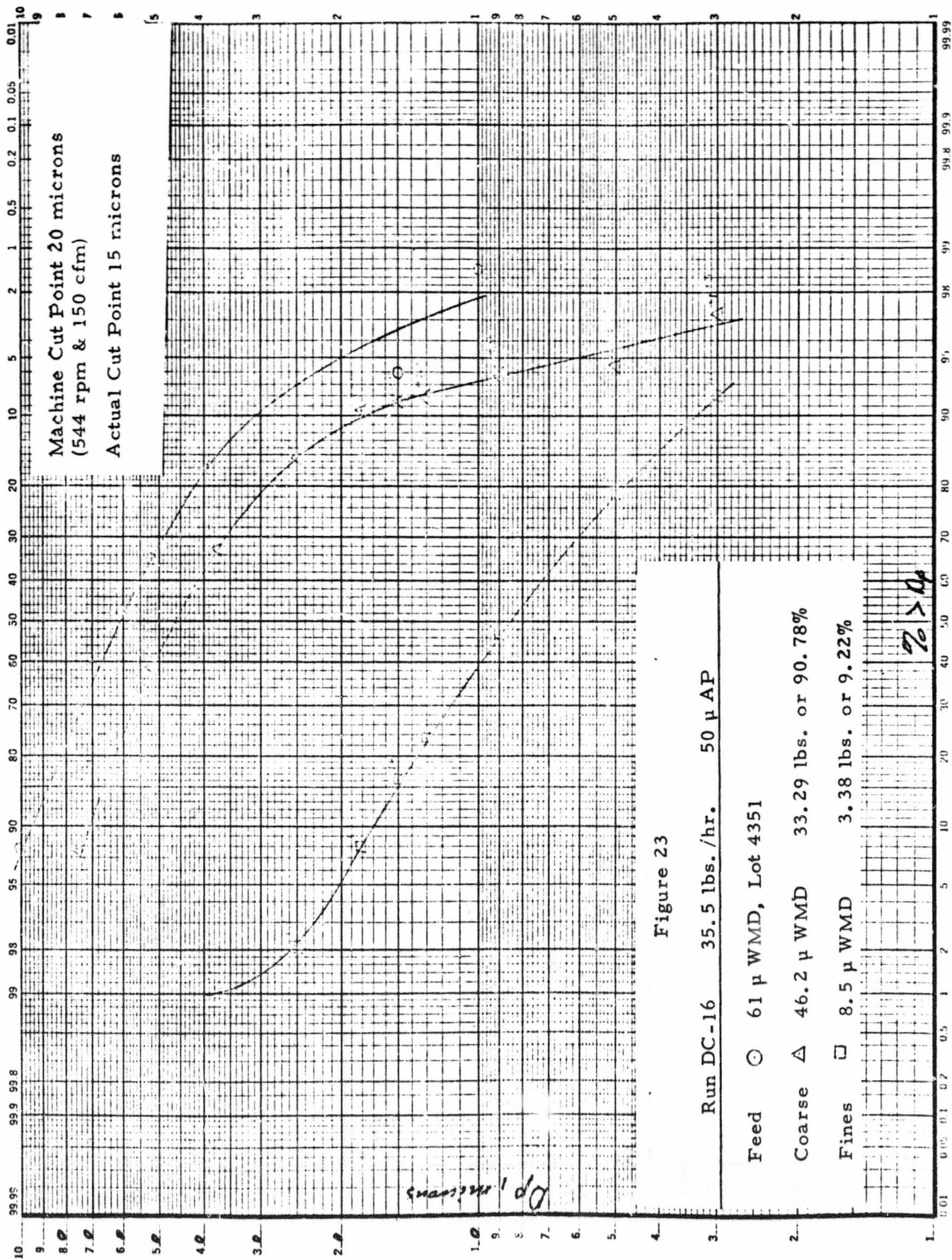
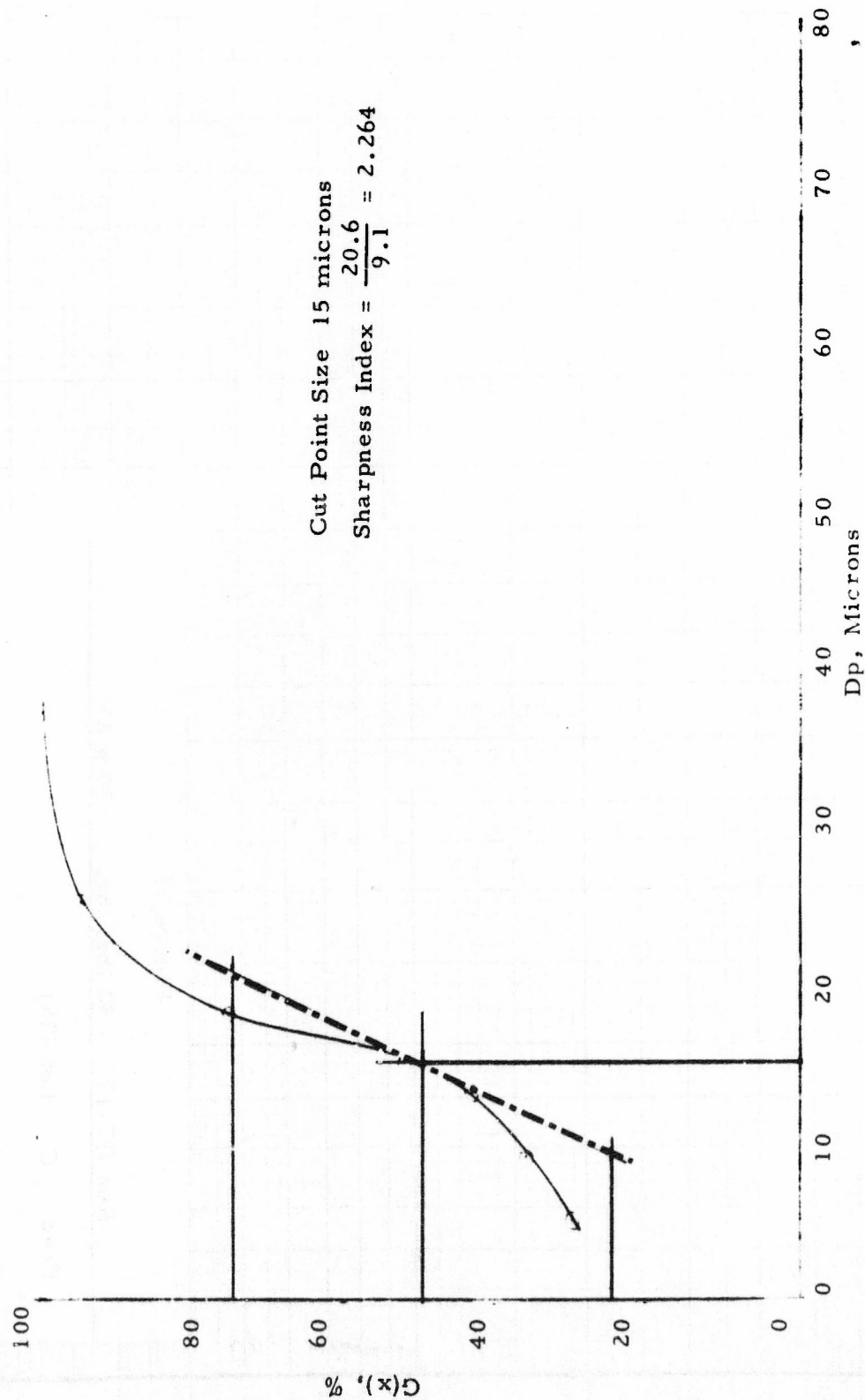


Figure 24
Grade Efficiency Curve for DC-16



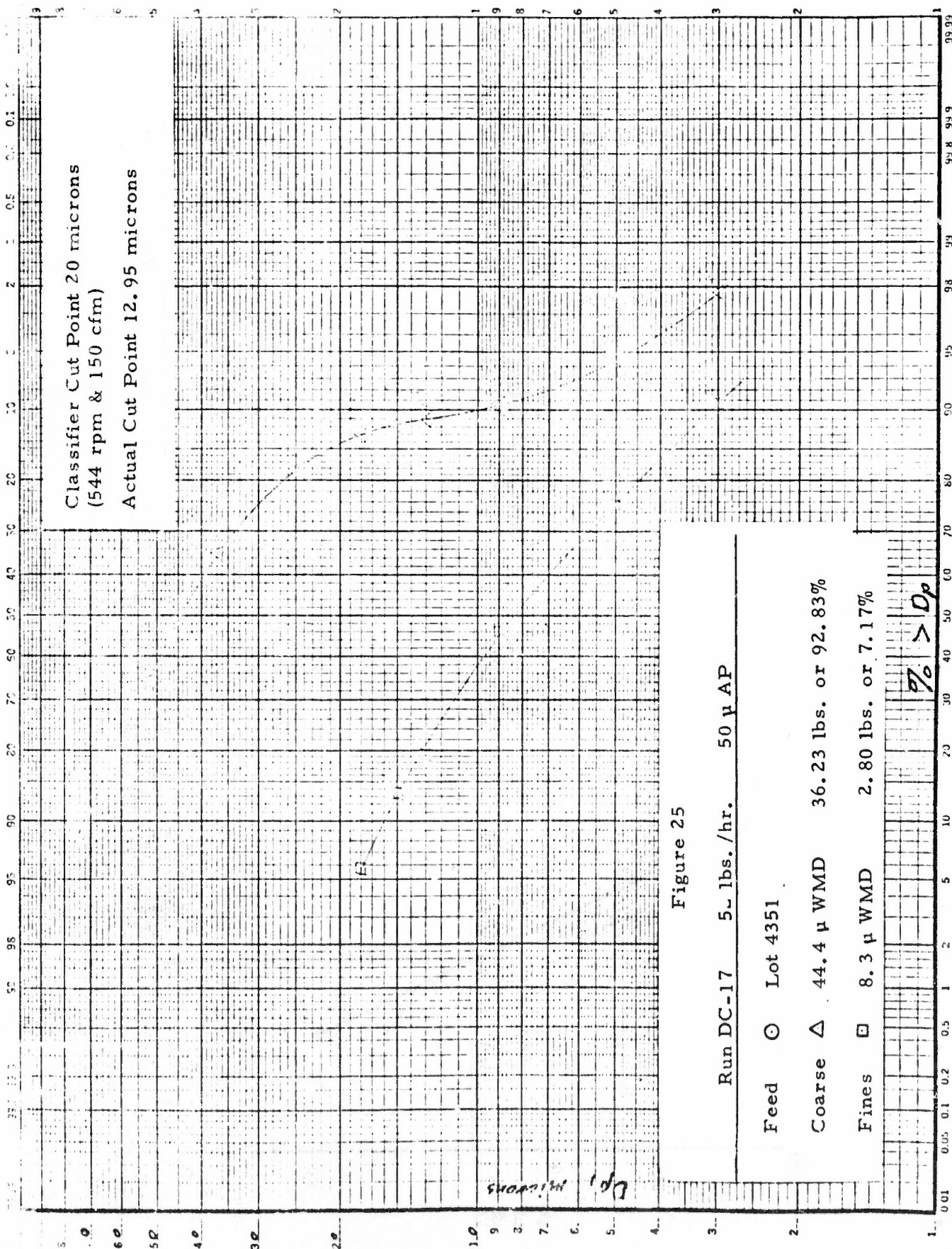


Figure 25

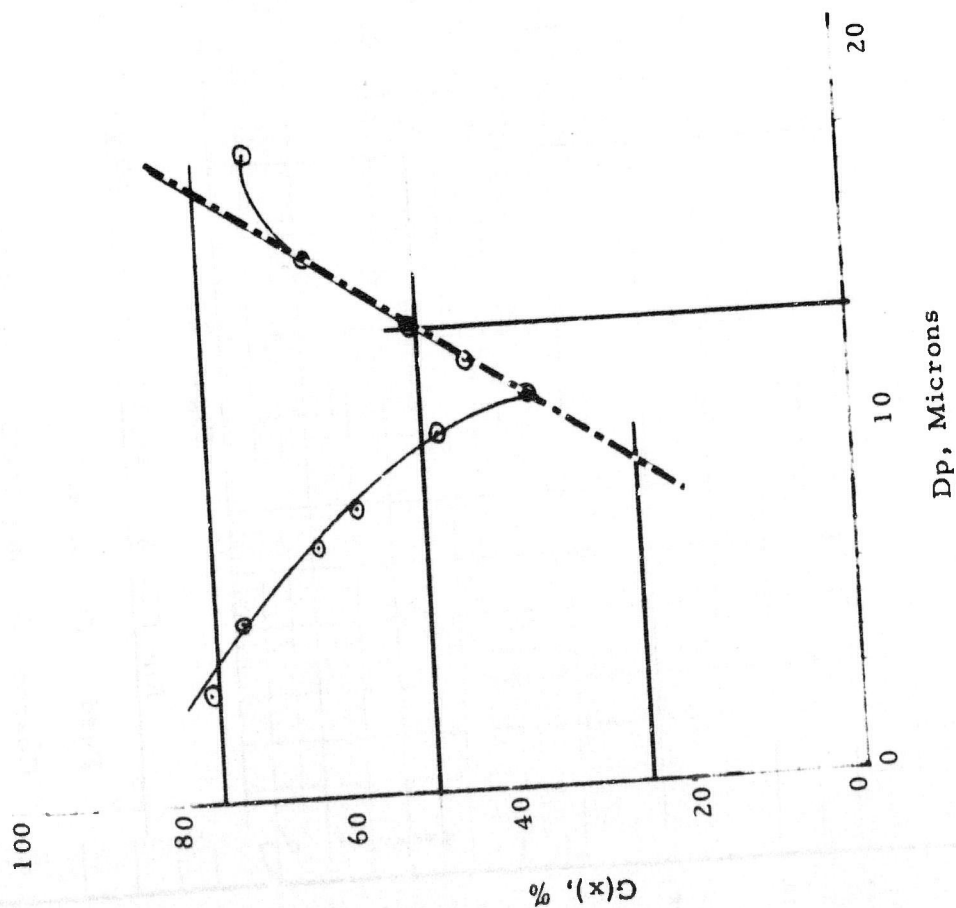
Run DC-17 5 lbs./hr. 50 μ AP

Feed \odot Lot 4351

Coarse \triangle 44.4 μ WMD 36.23 lbs. or 92.83%

Fines \square 8.3 μ WMD 2.80 lbs. or 7.17%

Figure 26
Grade Efficiency Curve for DC-17



Cut Point Size 12/95 Microns
Sharpness Index = $\frac{16.9}{9.0} = 1.878$

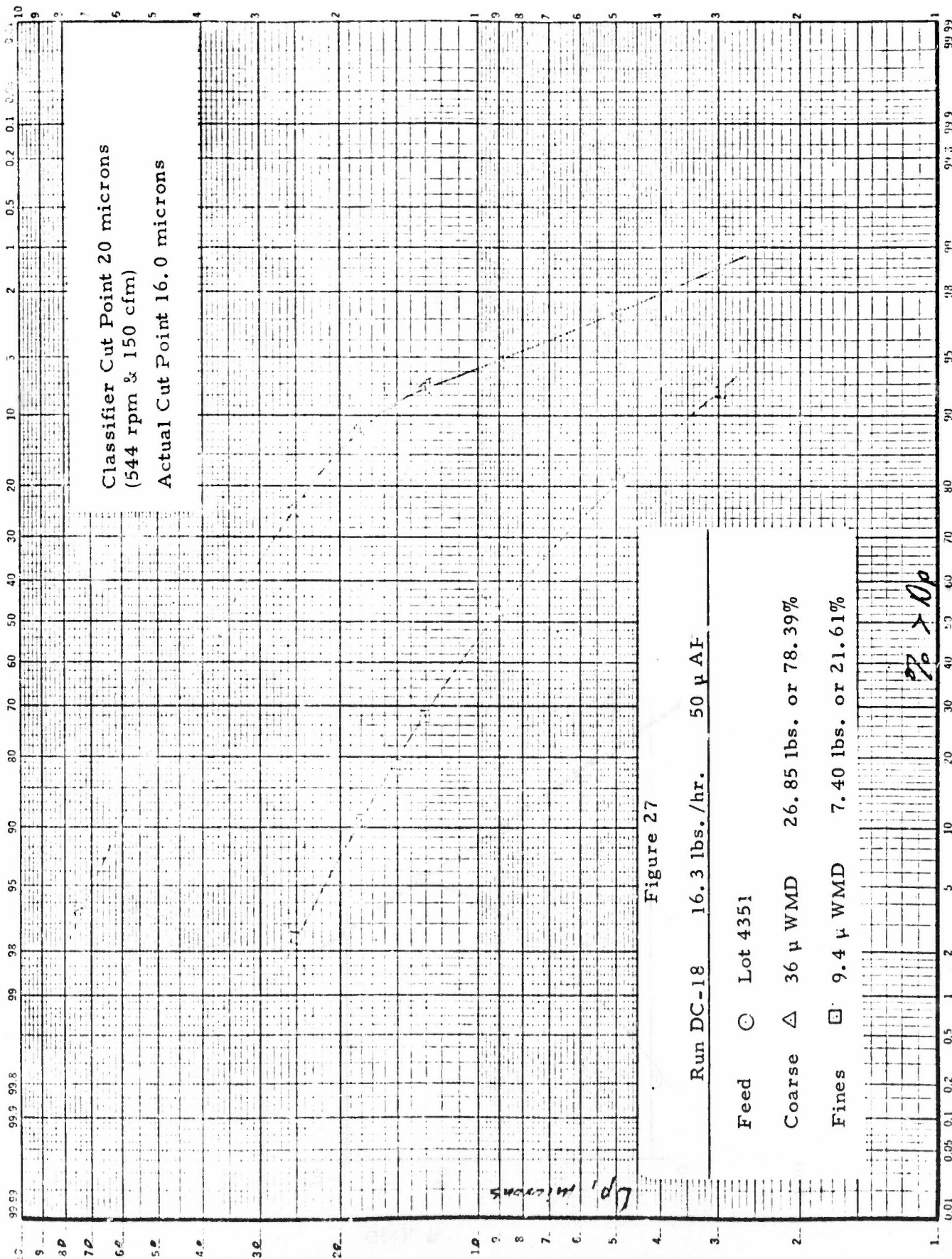
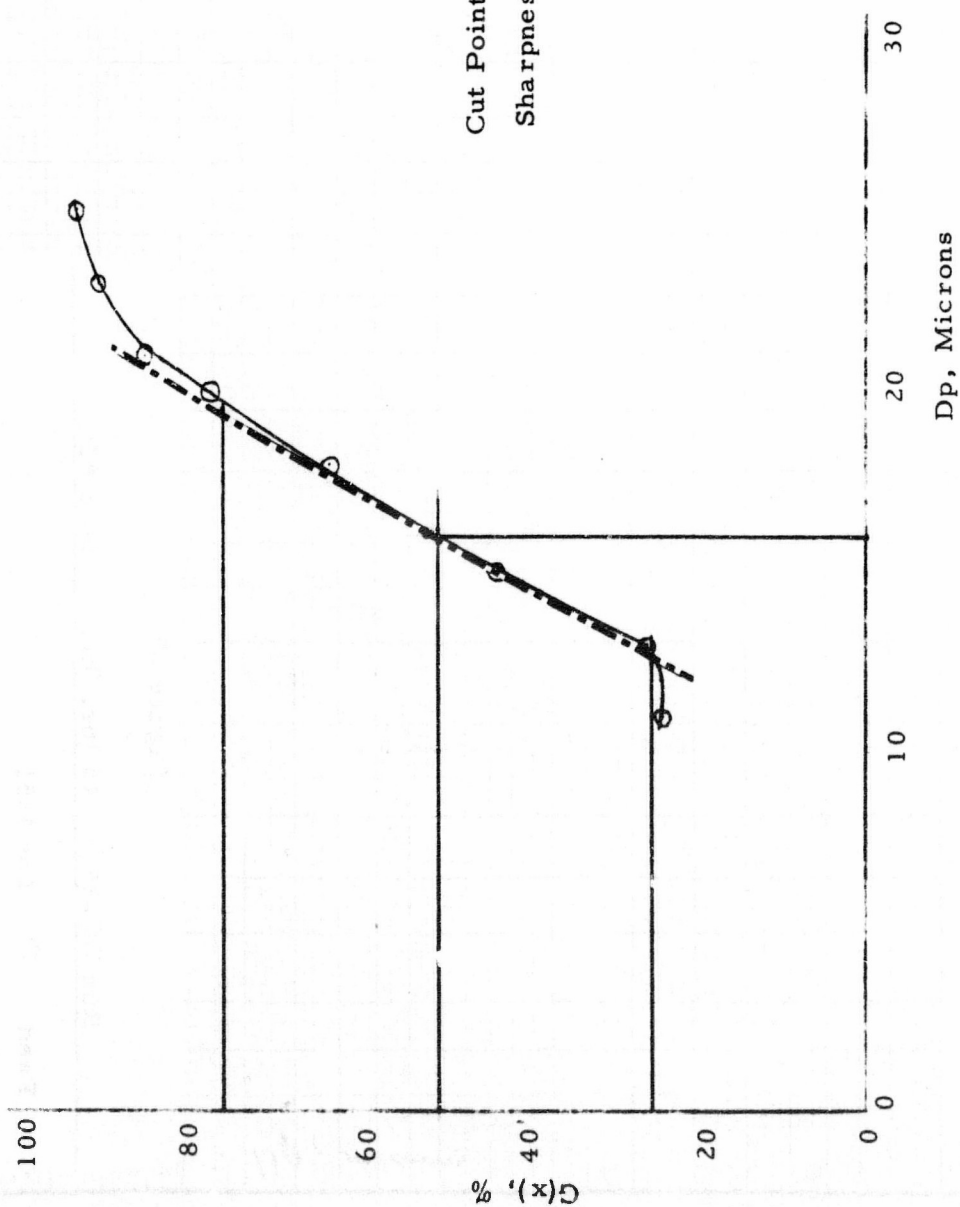


Figure 28
Grade Efficiency for DC-18



Cut Point 16.0 microns
 $\text{Sharpness Index} = \frac{19.4}{12.7} = 1.528$

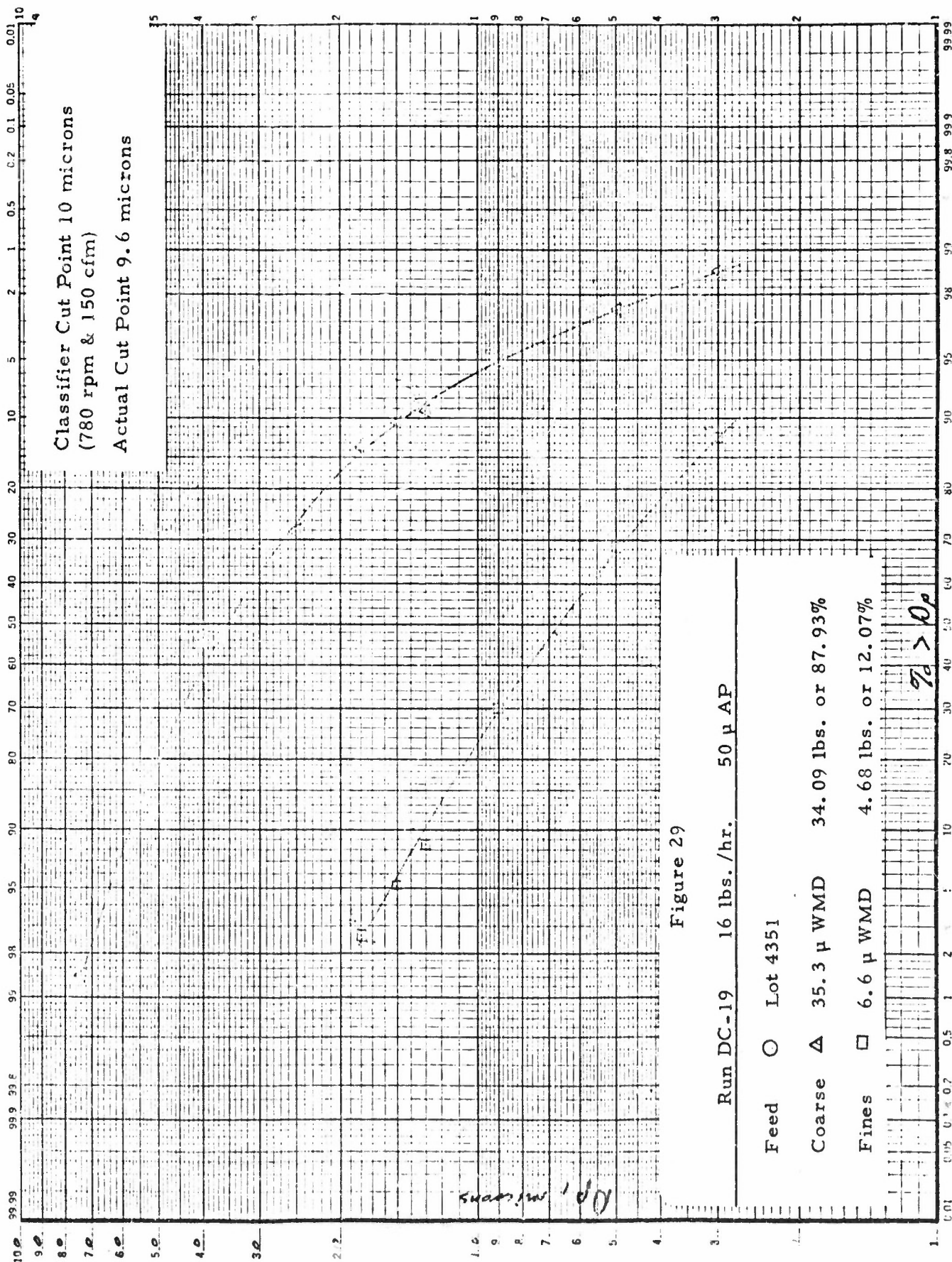
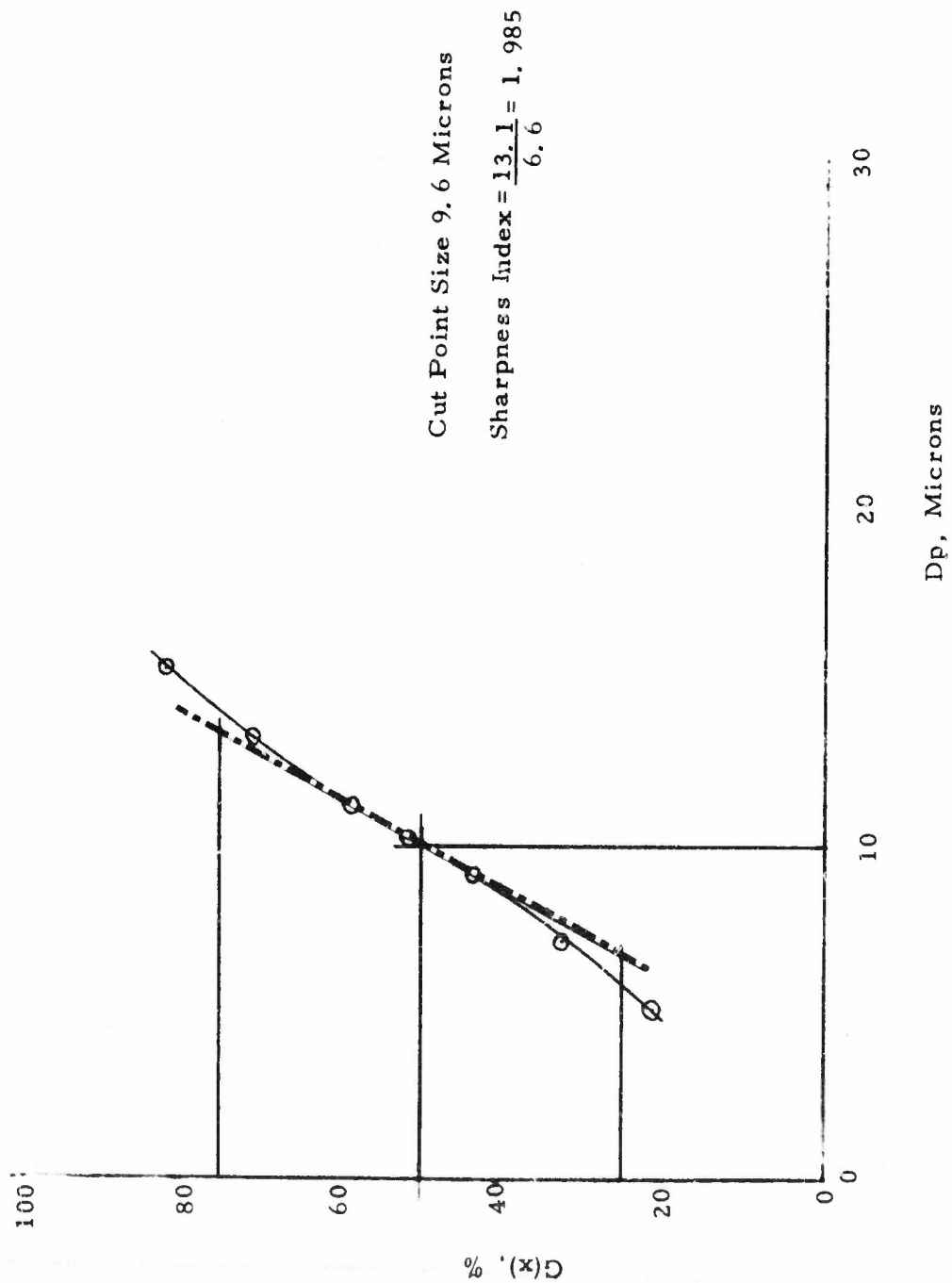


Figure 30
Grade Efficiency Curve for DC-19



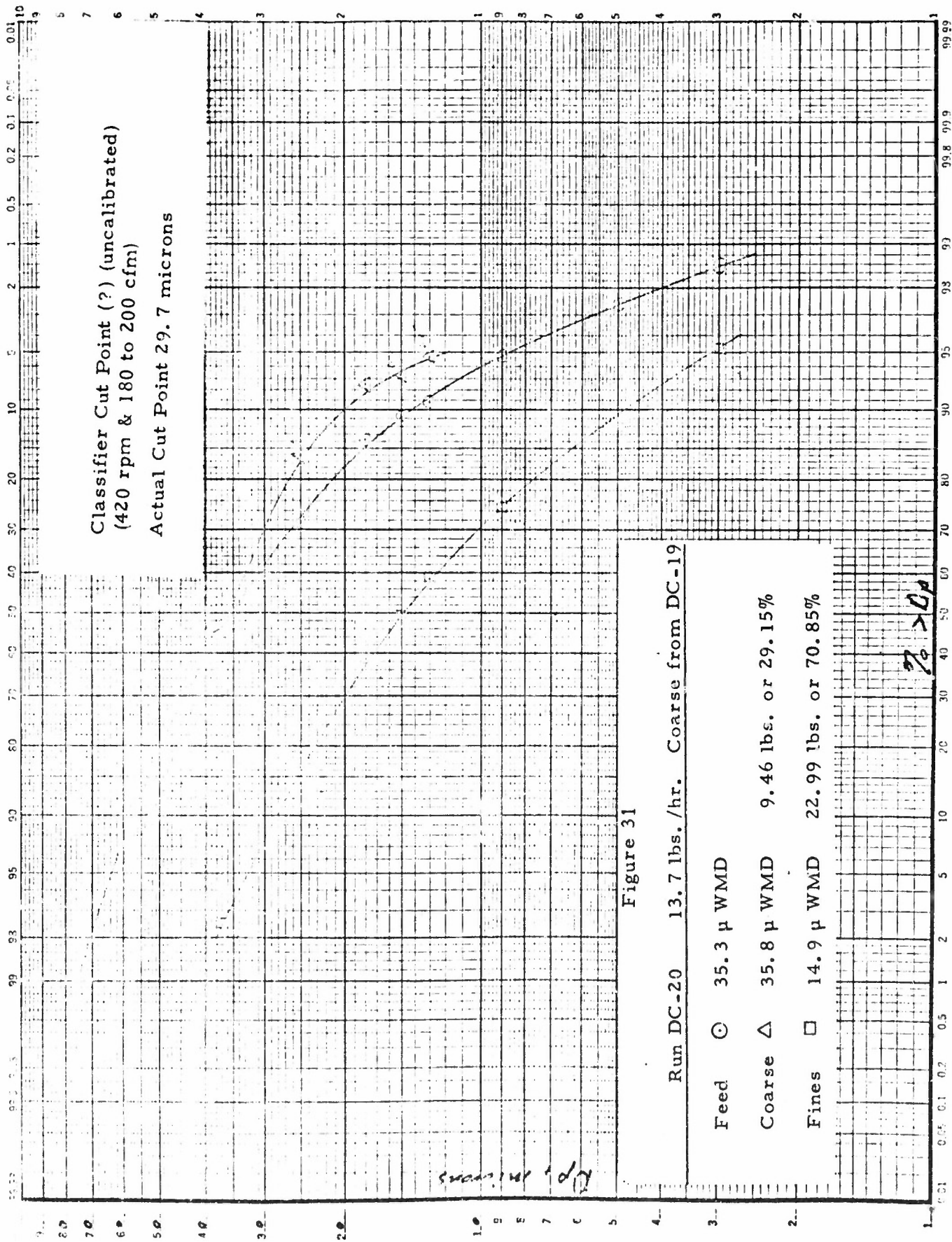
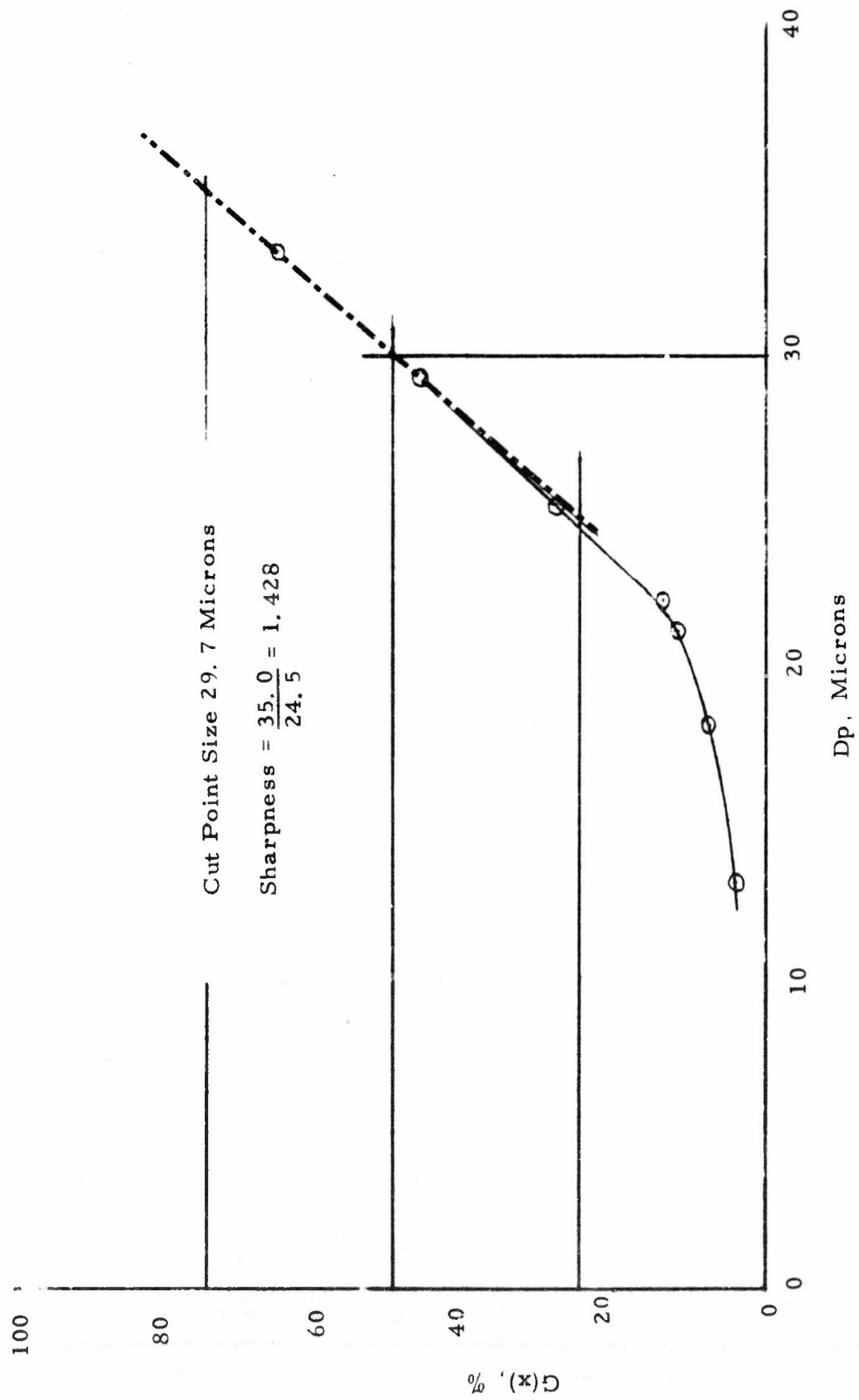


Figure 31

Figure 32

Grade Efficiency Curve for DC-20



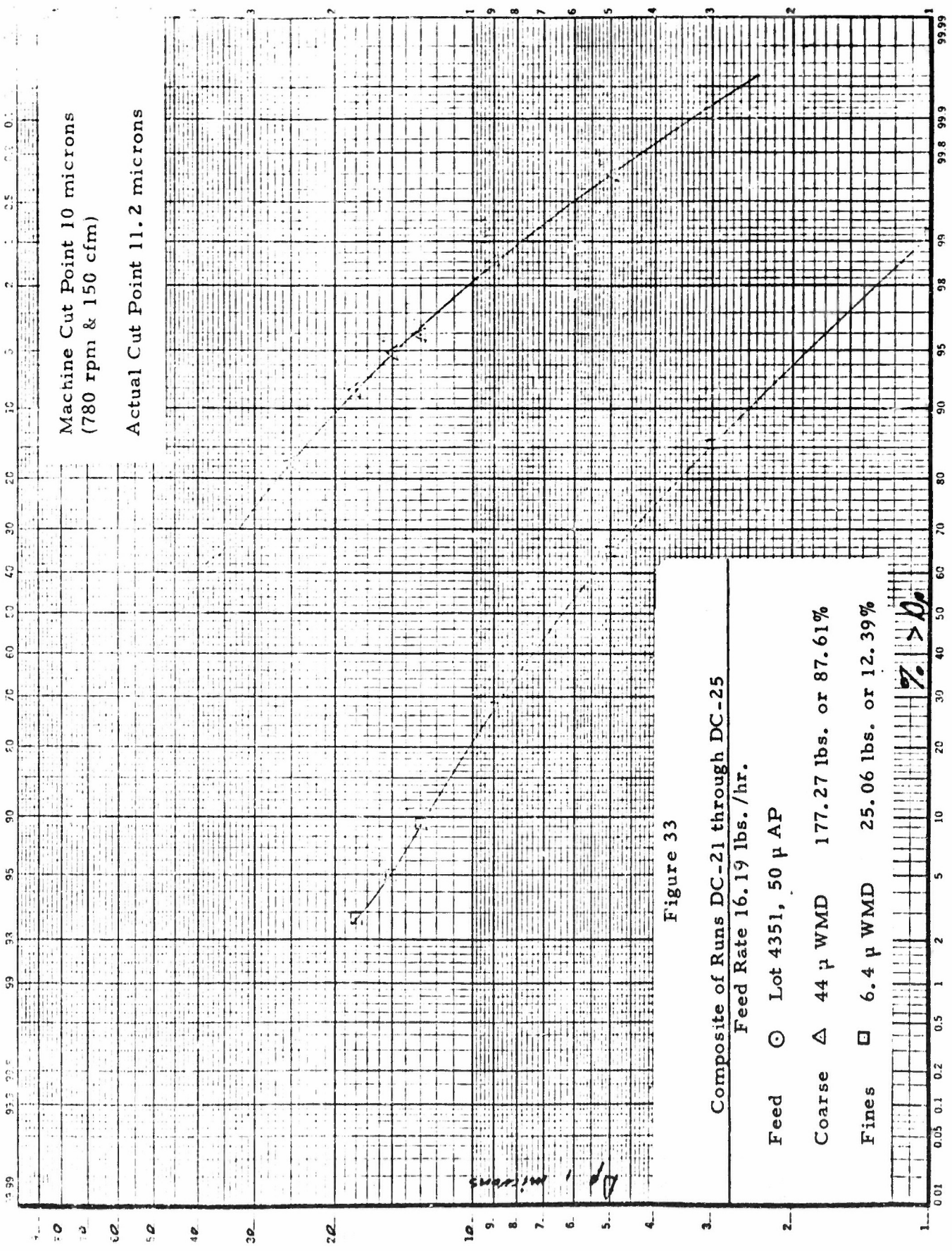


Figure 33

Composite of Runs DC-21 through DC-25

Feed Rate 16.19 lbs./hr.

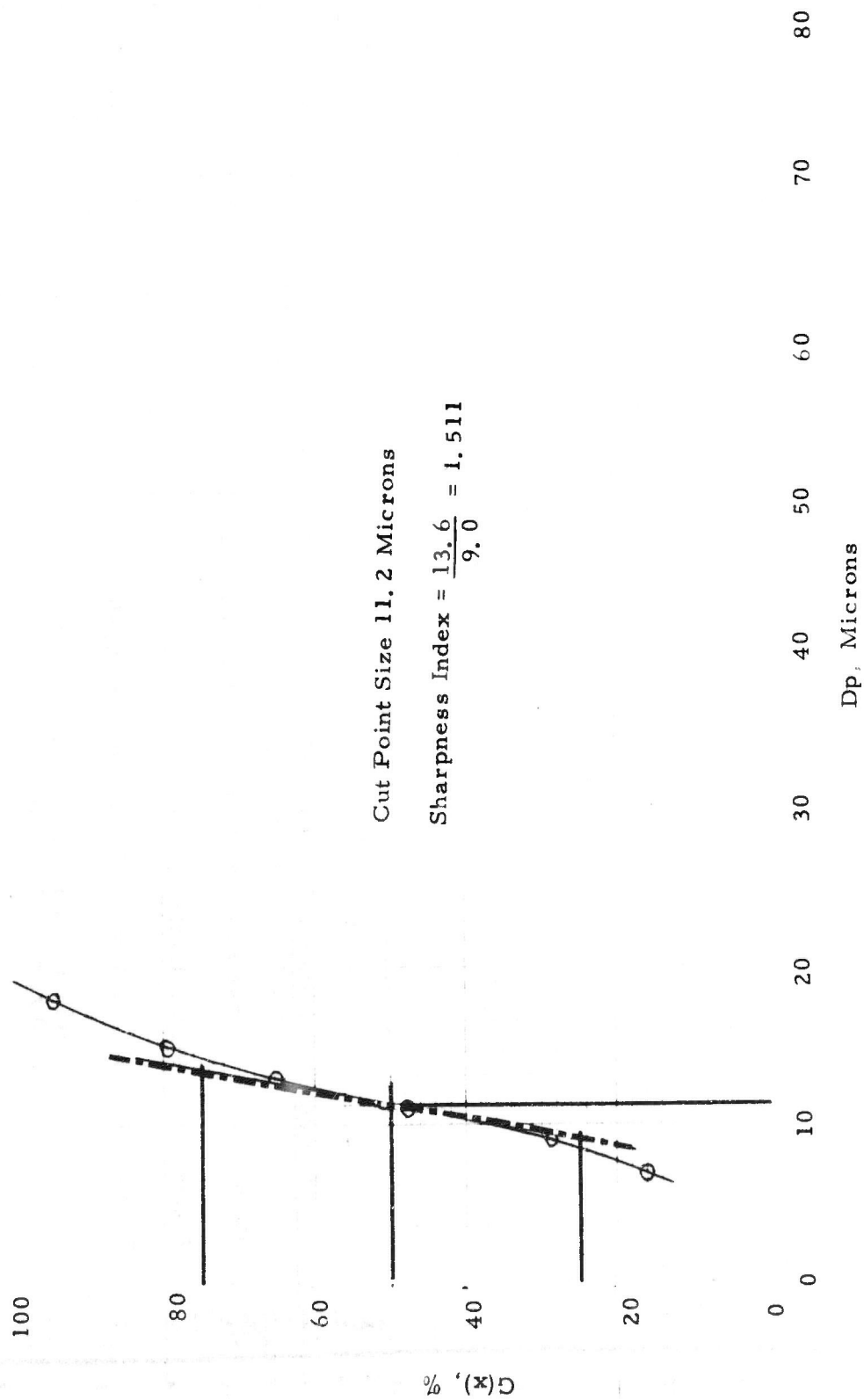
Feed ○ Lot 4351, 50 μ AP

Coarse △ 44 μ WMD 177.27 lbs. or 87.61%

Fines □ 6.4 μ WMD 25.06 lbs. or 12.39%

Figure 34

Grade Efficiency Curve for DC-21 thru -25



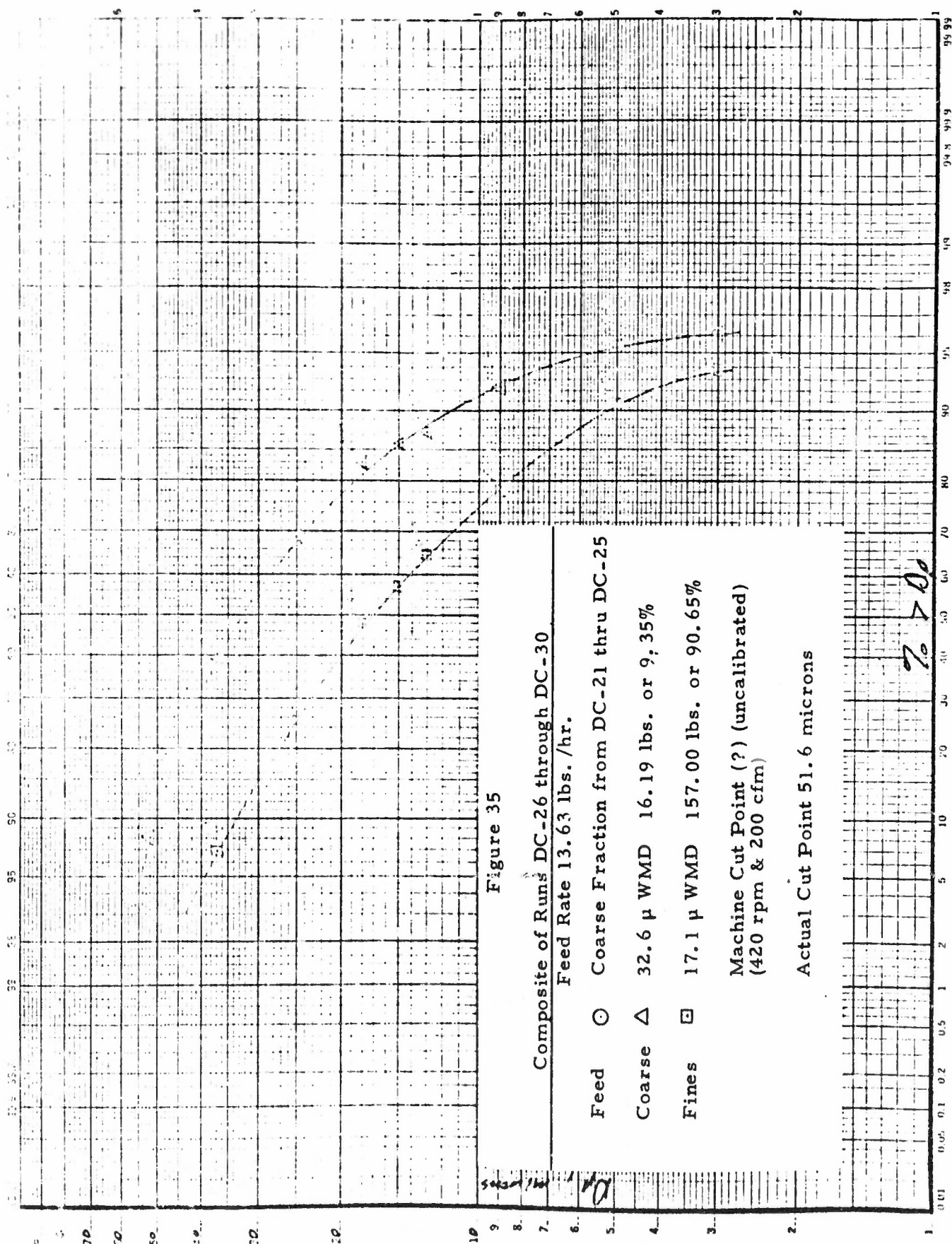
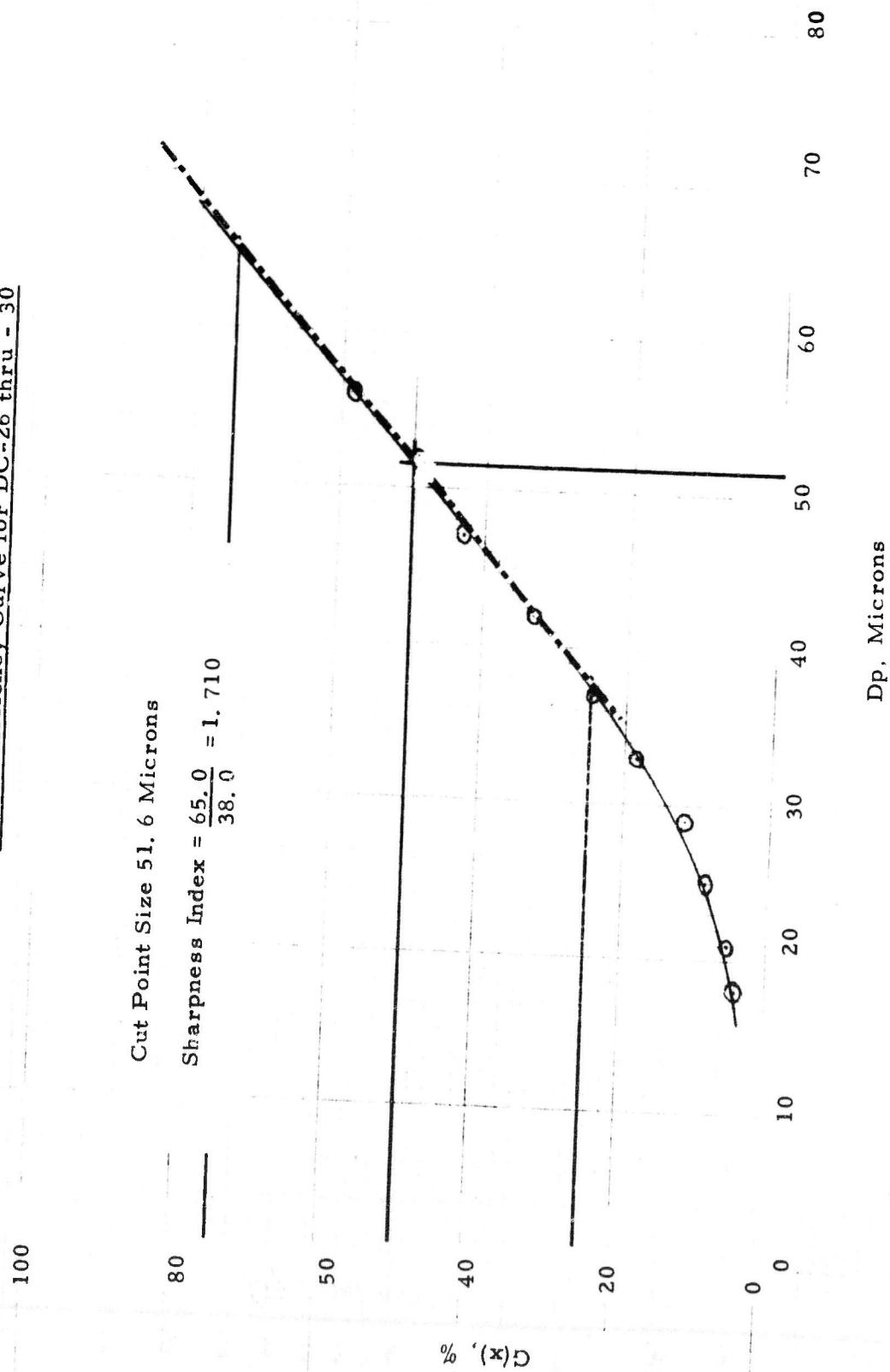


Figure 36

Grade Efficiency Curve for DC-26 thru - 30



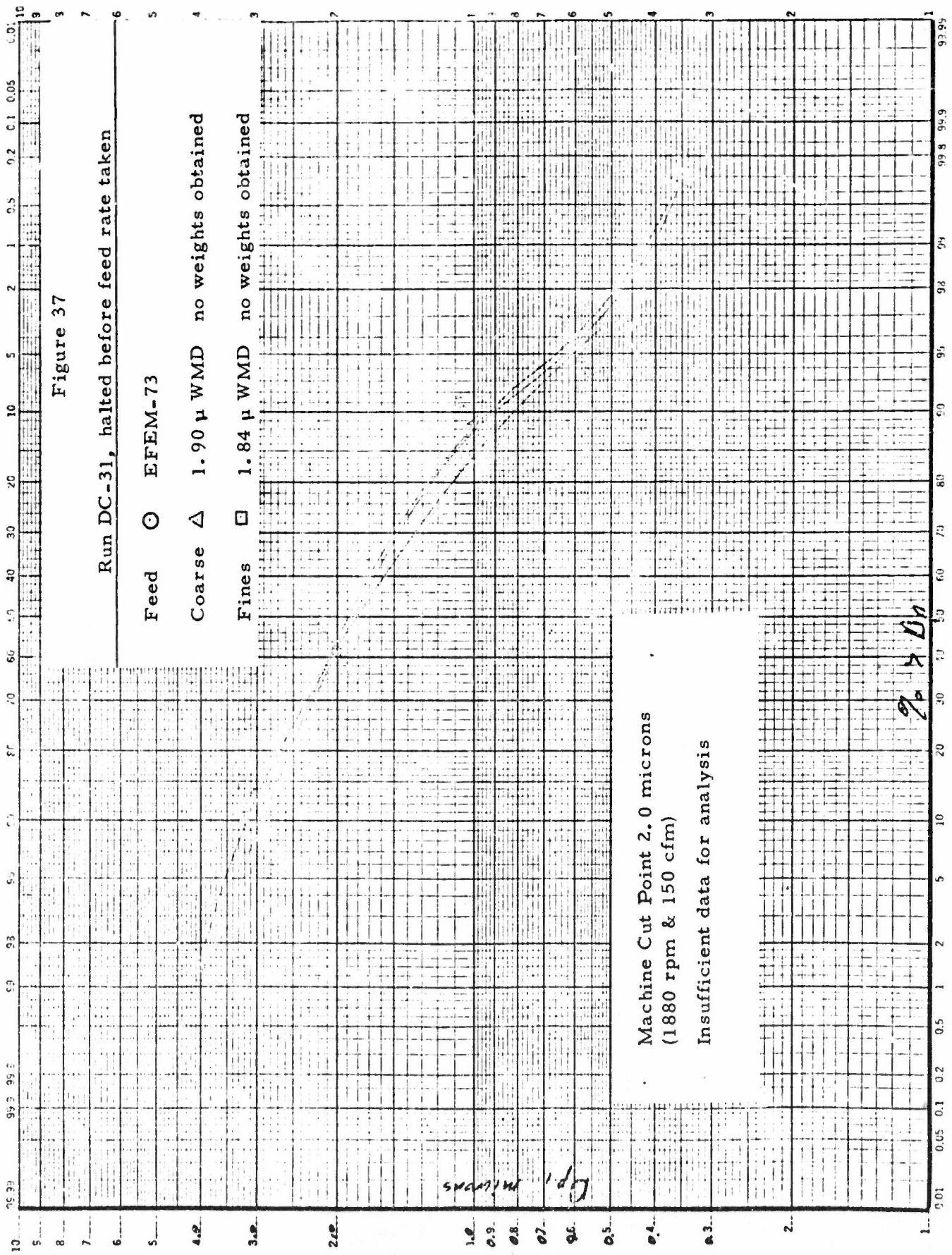


Figure 38

Run DC-32 at varying feed rate

Feed \odot EFEM-73, 1.80 μ WMD
 Coarse Δ 2.43 μ WMD 1.80 lbs. or 48.13%
 Fines \square 1.96 μ WMD 1.94 lbs. or 51.87%

Machine Cut Point 2.0 microns
 (1880 rpm & 150 cfm)
 Actual Cut Point 2.68 microns

Figure 39

Grade Efficiency Curve for DC-32

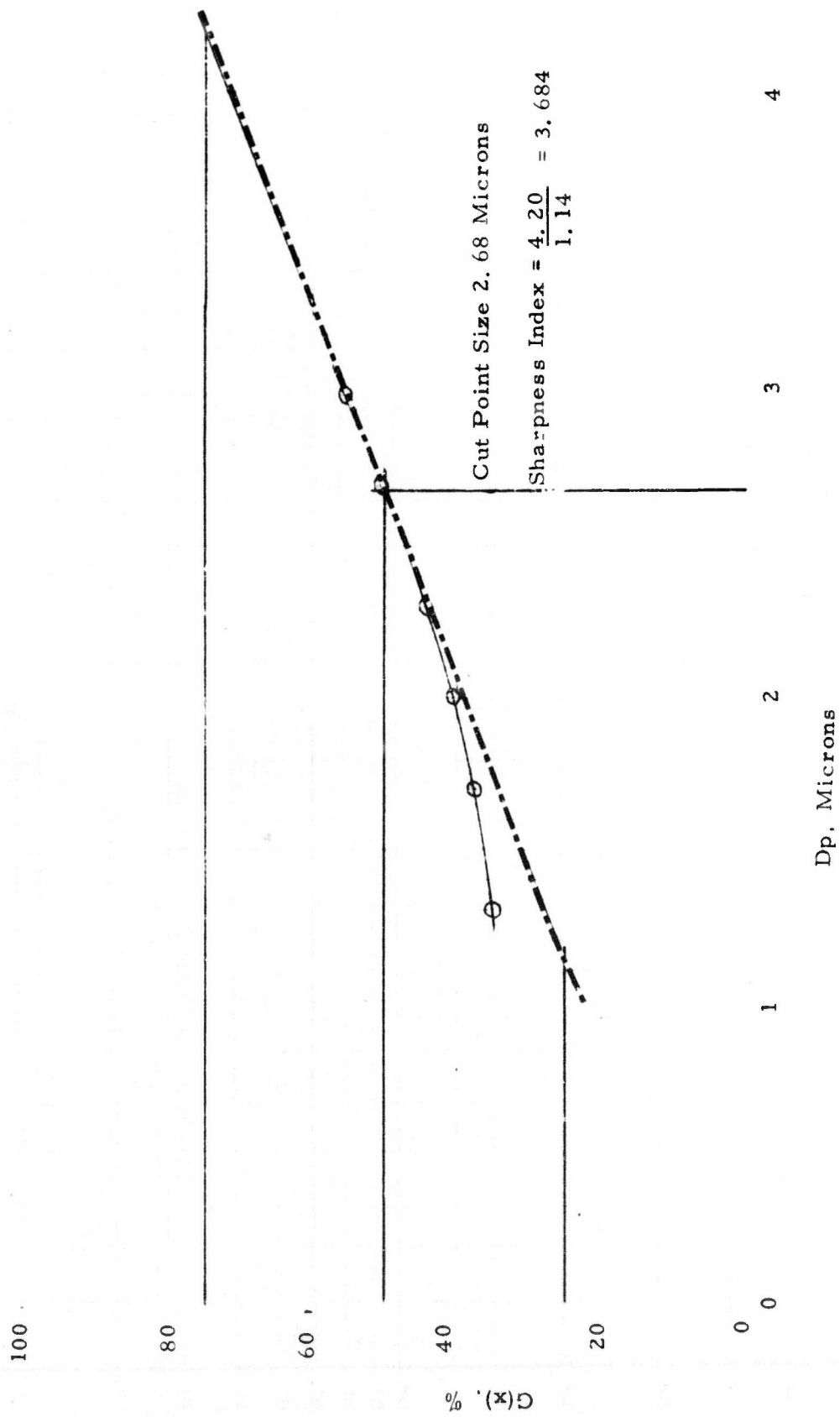


Figure 40

Run DC-33 at varying feed rate

Feed ○ EFEM-73 with 0.2% Silanox 101

Coarse △ 2.84 μ WMD 7.92 lbs. or 73.06%

Fines □ 1.90 μ WMD 2.92 lbs. or 26.94%

Classifier Cut Point 1.0 microns
(2700 rpm & 150 cfm)

Actual Cut Point 1.64 microns

90% > 0.2

Figure 41

Grade Efficiency Curve for DC-33

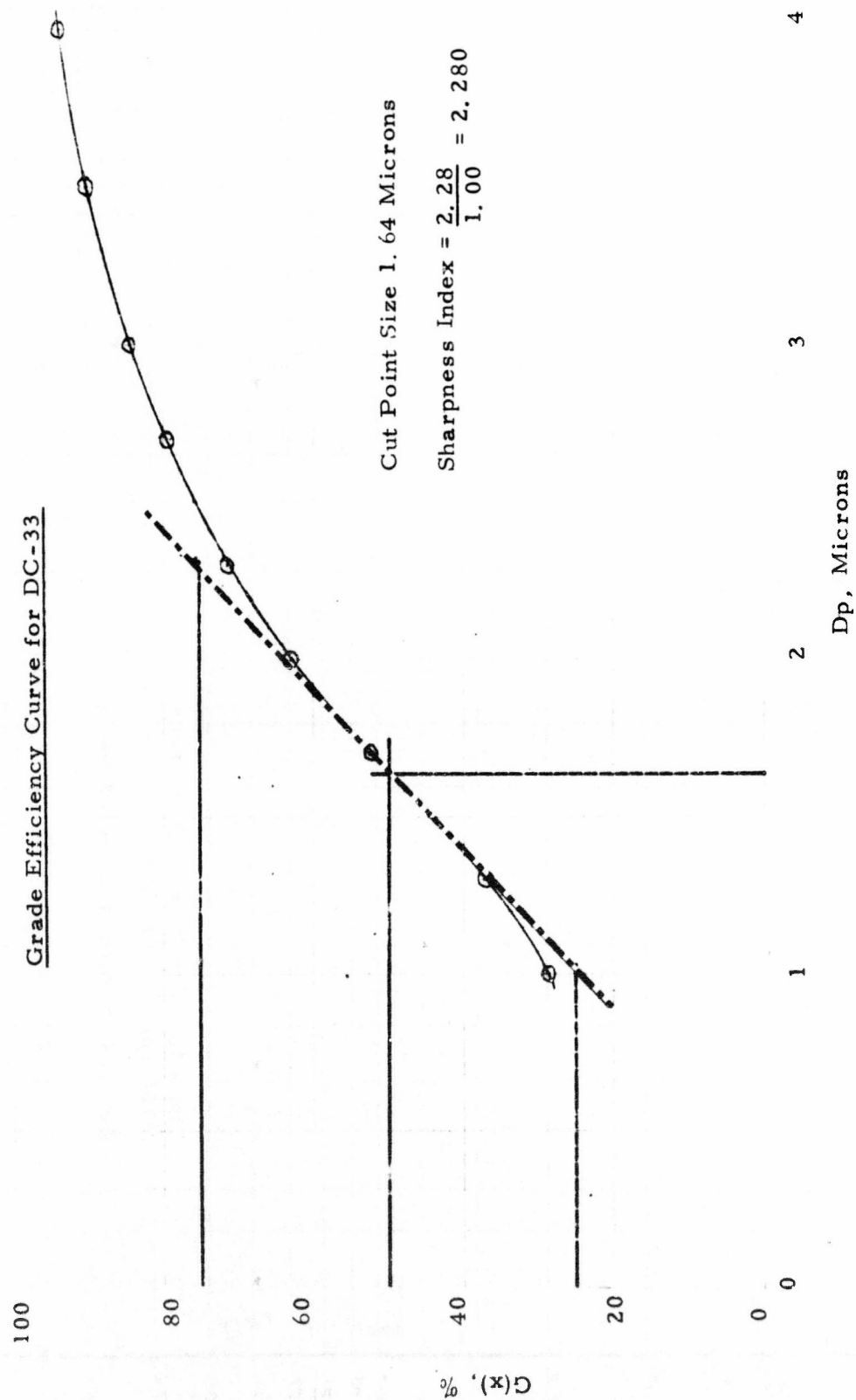


Figure 42

Run DC-34 5.5 lbs./hr. feed rate

Feed ○ EFEM-73 with 0.2% Silanox 101

Coarse △ 2.90 μ WMD 9.17 lbs. or 59.43%

Fines □ 1.88 μ WMD 6.26 lbs. or 40.57%

Machine Cut Point 1.0 microns
(2700 rpm & 150 cfm)

Data unsuitable for grade efficiency
analysis technique.

97.99

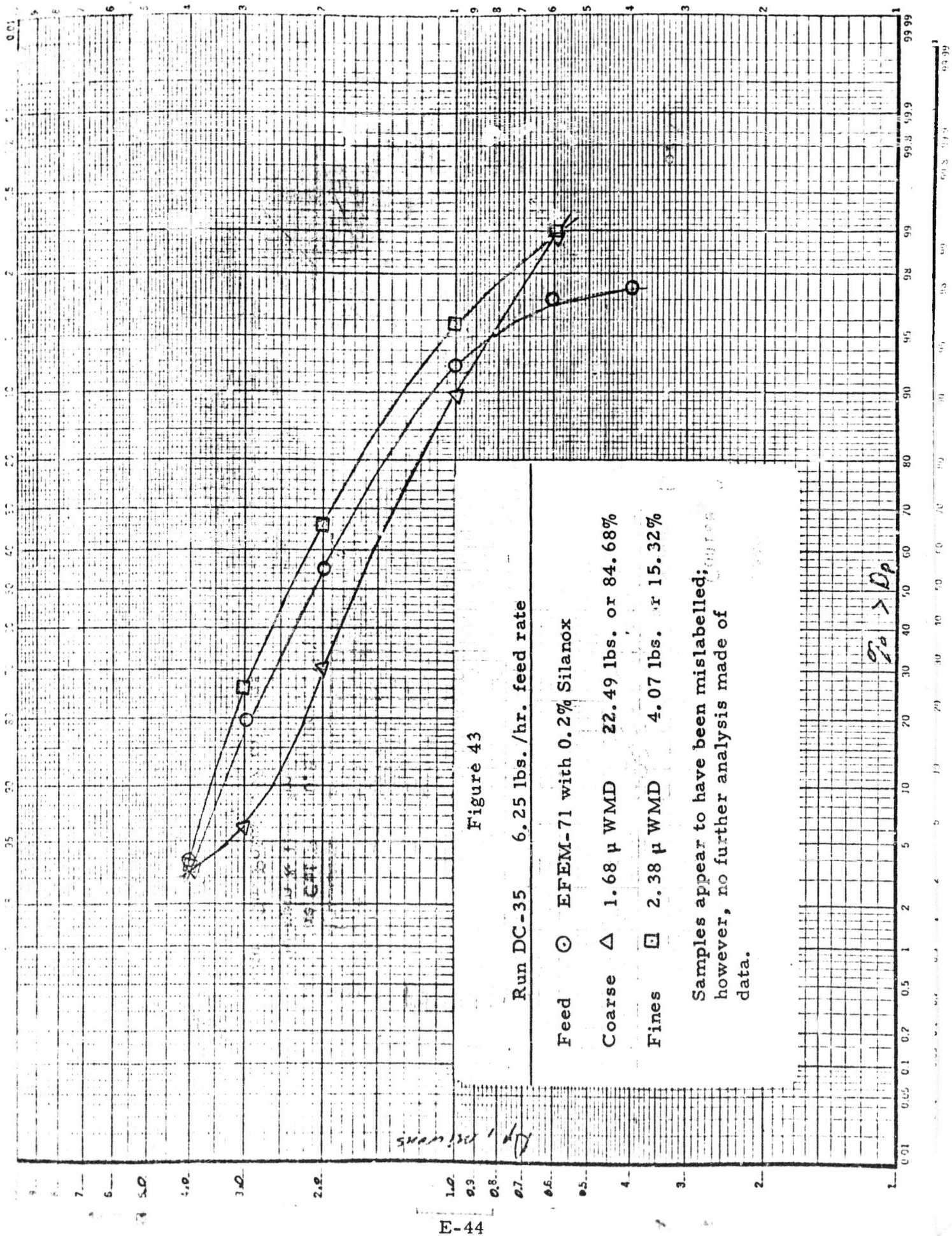


Figure 44

Run DC-36 at varying feed rate

Feed: ○ Freshly ground EFEM-74

Coarse: △ 2.16 μ WMD 1.89 lbs. or 65.40%

Fines: □ 1.77 μ WMD 1.00 lbs. or 34.60%

Machine Cut Point 0.5 microns
(3900 rpm & 150 cfm)

Actual Cut Point 0.62 microns

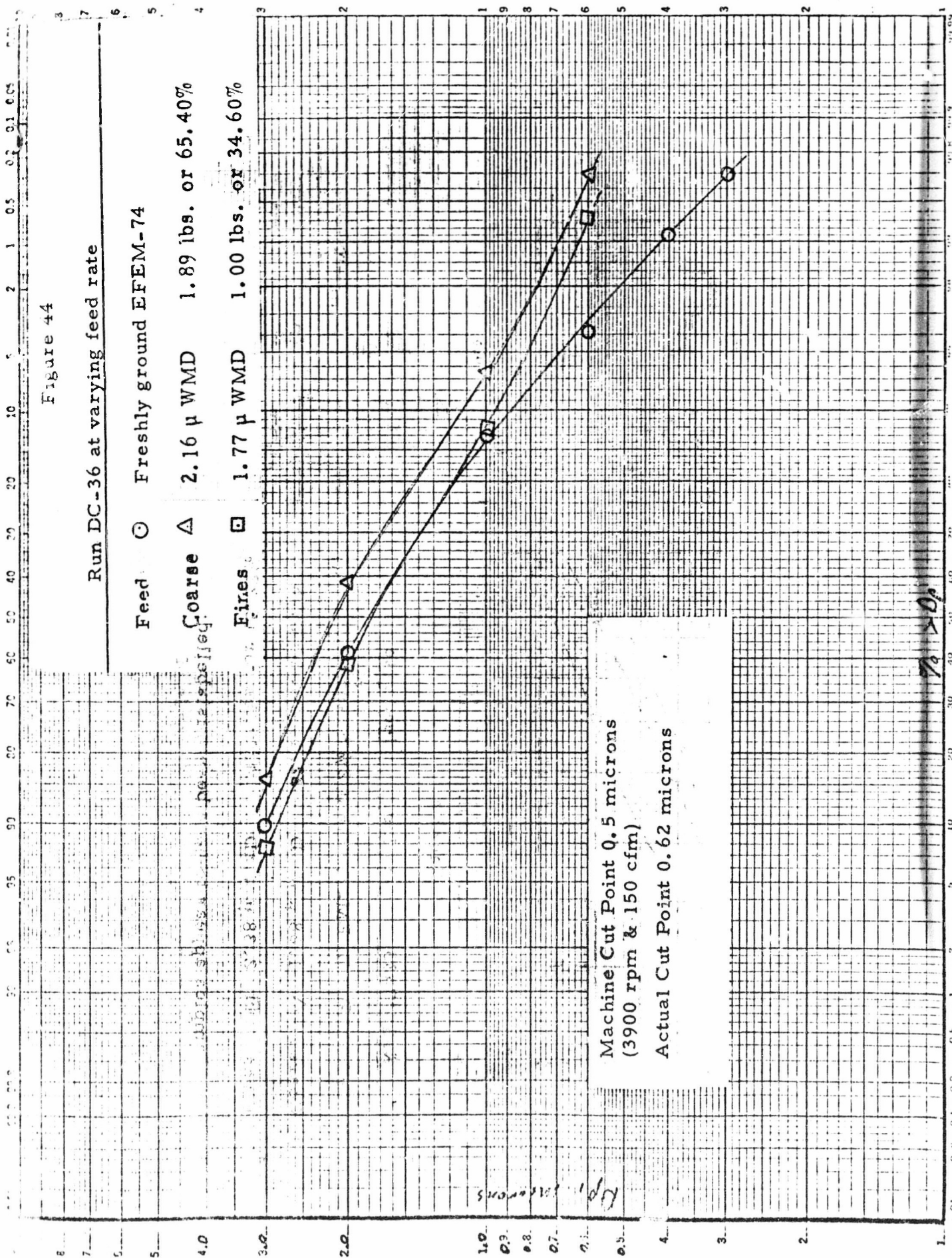
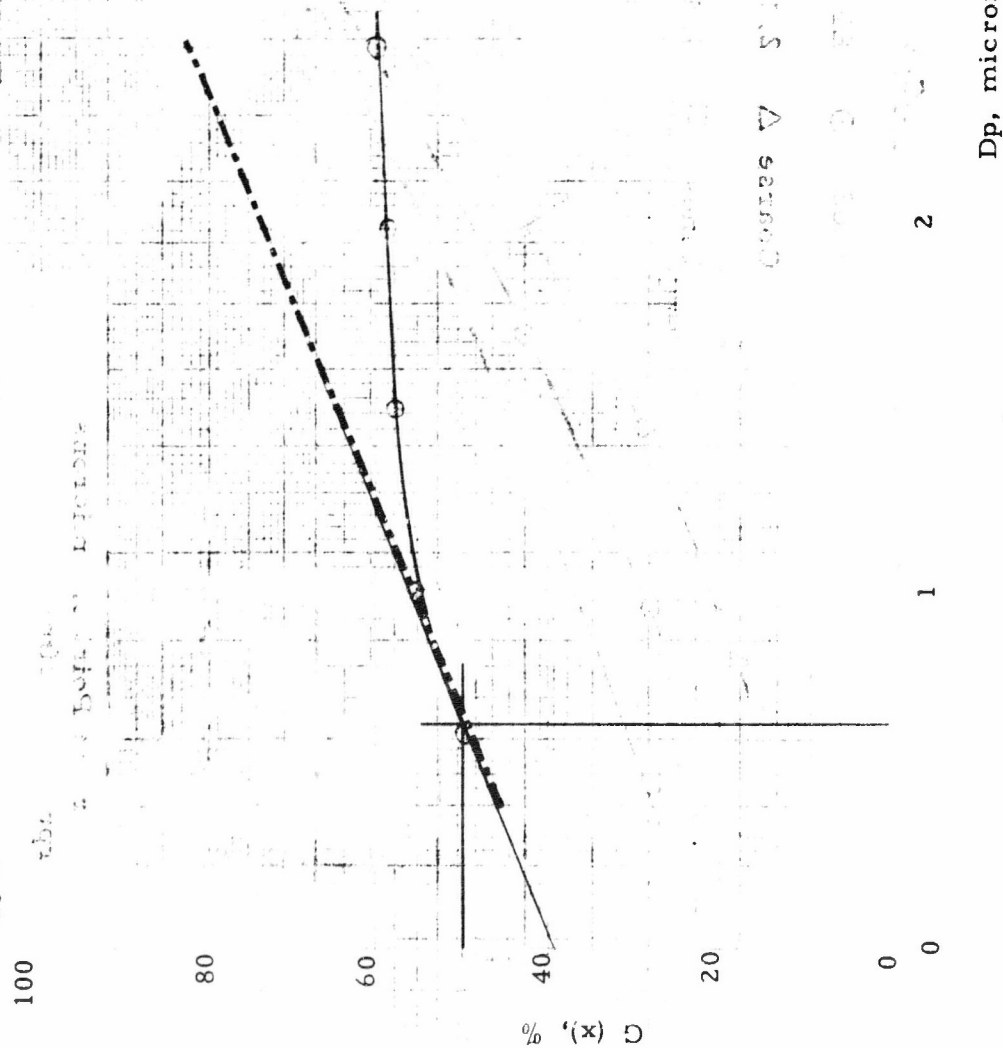


Figure 45

Grade Efficiency Curve for DC-36



Cut Point Size 0.62 microns
Sharpness Index not attainable by
prescribed technique.
Extrapolation would yield a meaningless,
negative value (-2.442)

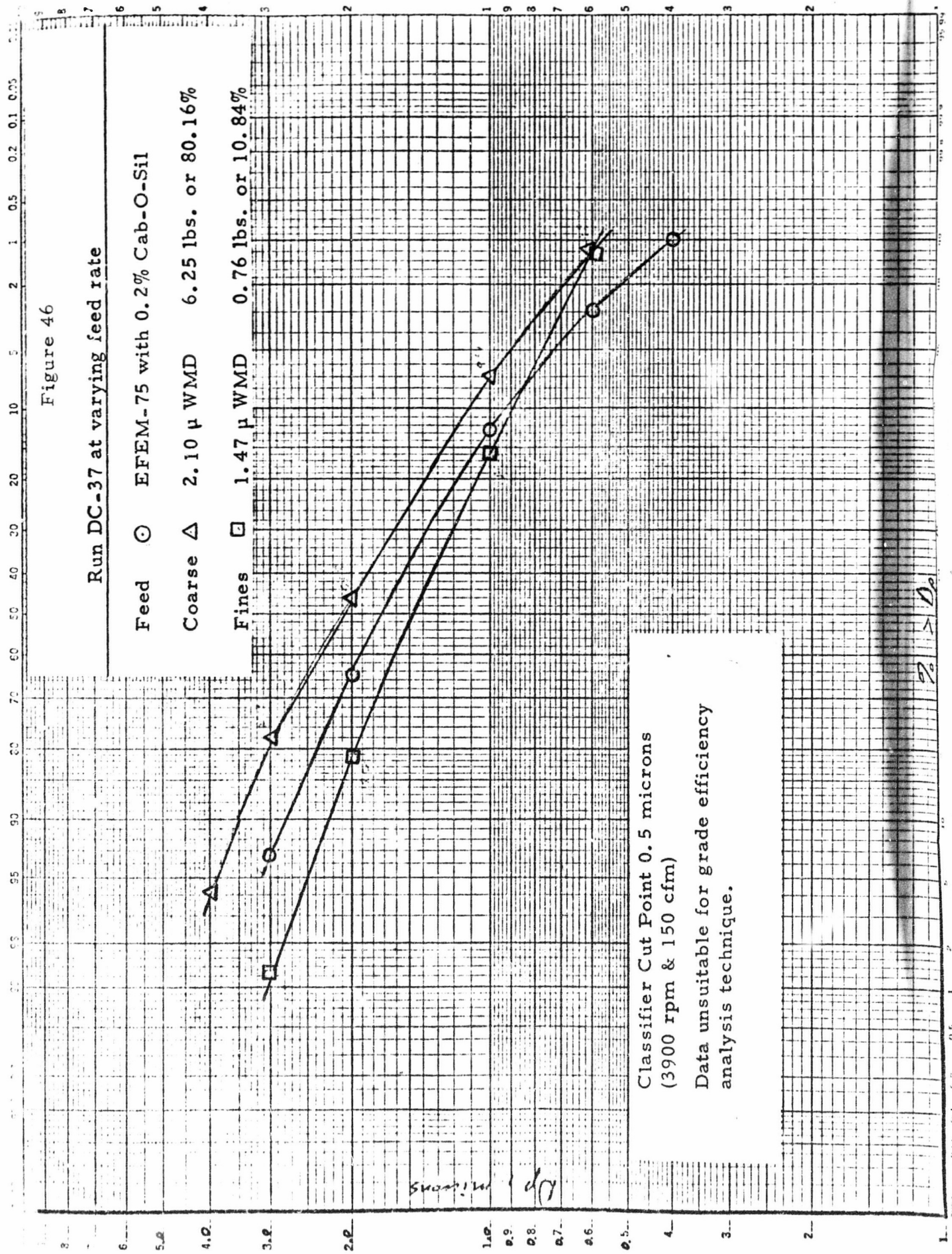


Figure 47

Grade Efficiency Curve for DC-37

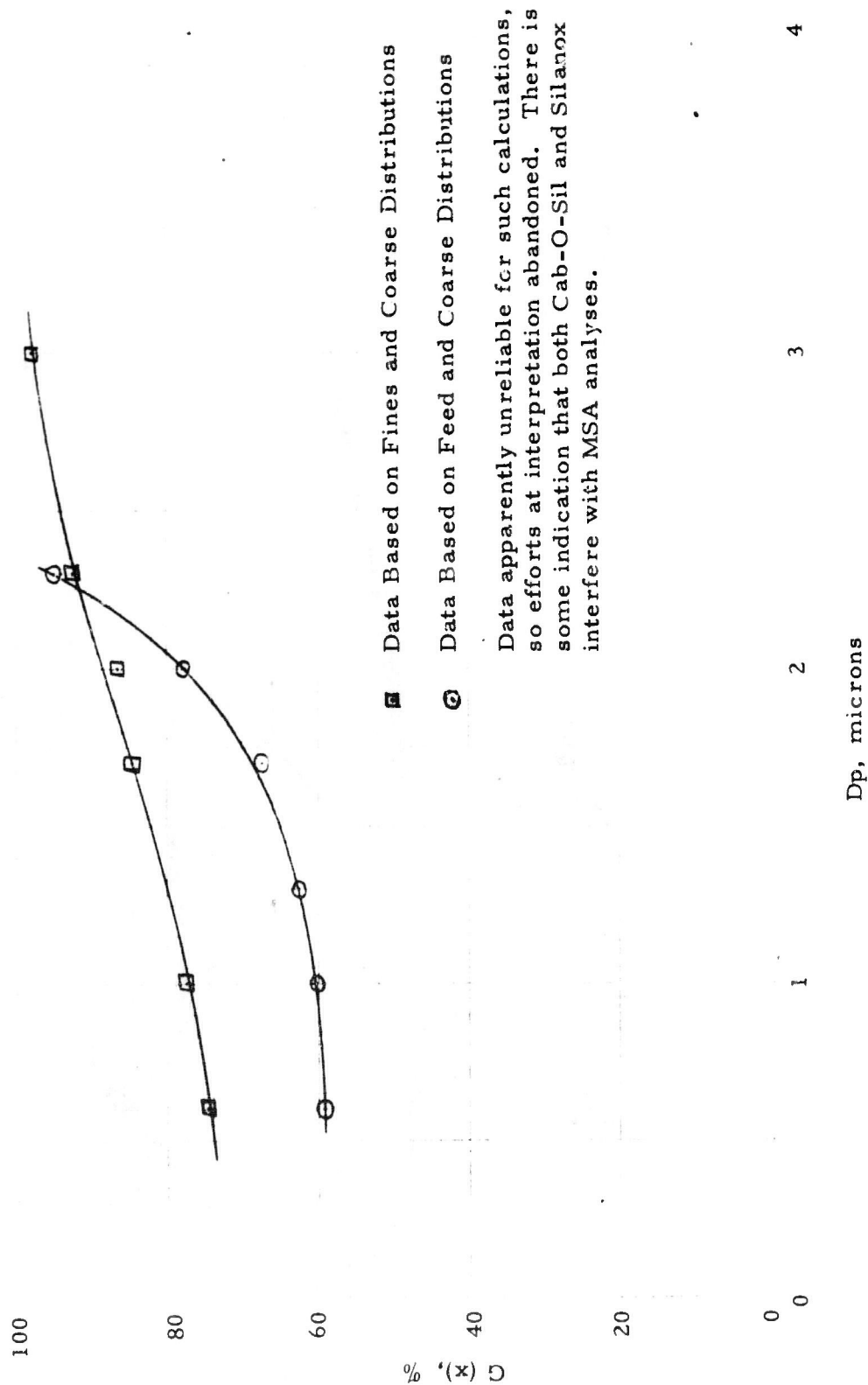


Figure 48

Run DC-38 8.05 lbs./hr. Norm. 1.7 μ

Feed \odot EFEM-75 with 0.2% Cab-O-Sil

Coarse Δ 2.26 μ WMD 9.37 lbs. or 87.33%

Fines \square 1.54 μ WMD 1.36 lbs. or 12.67%

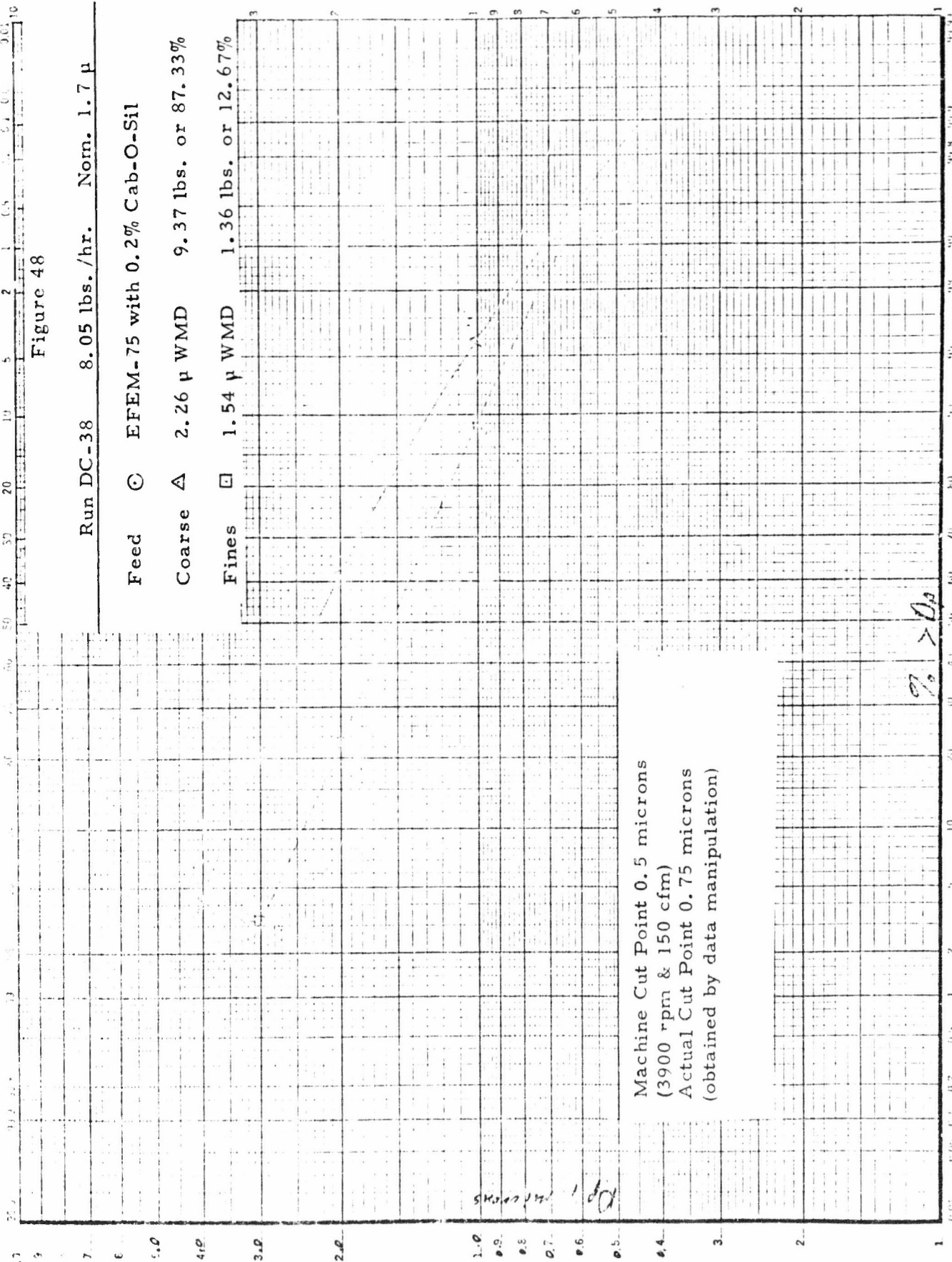
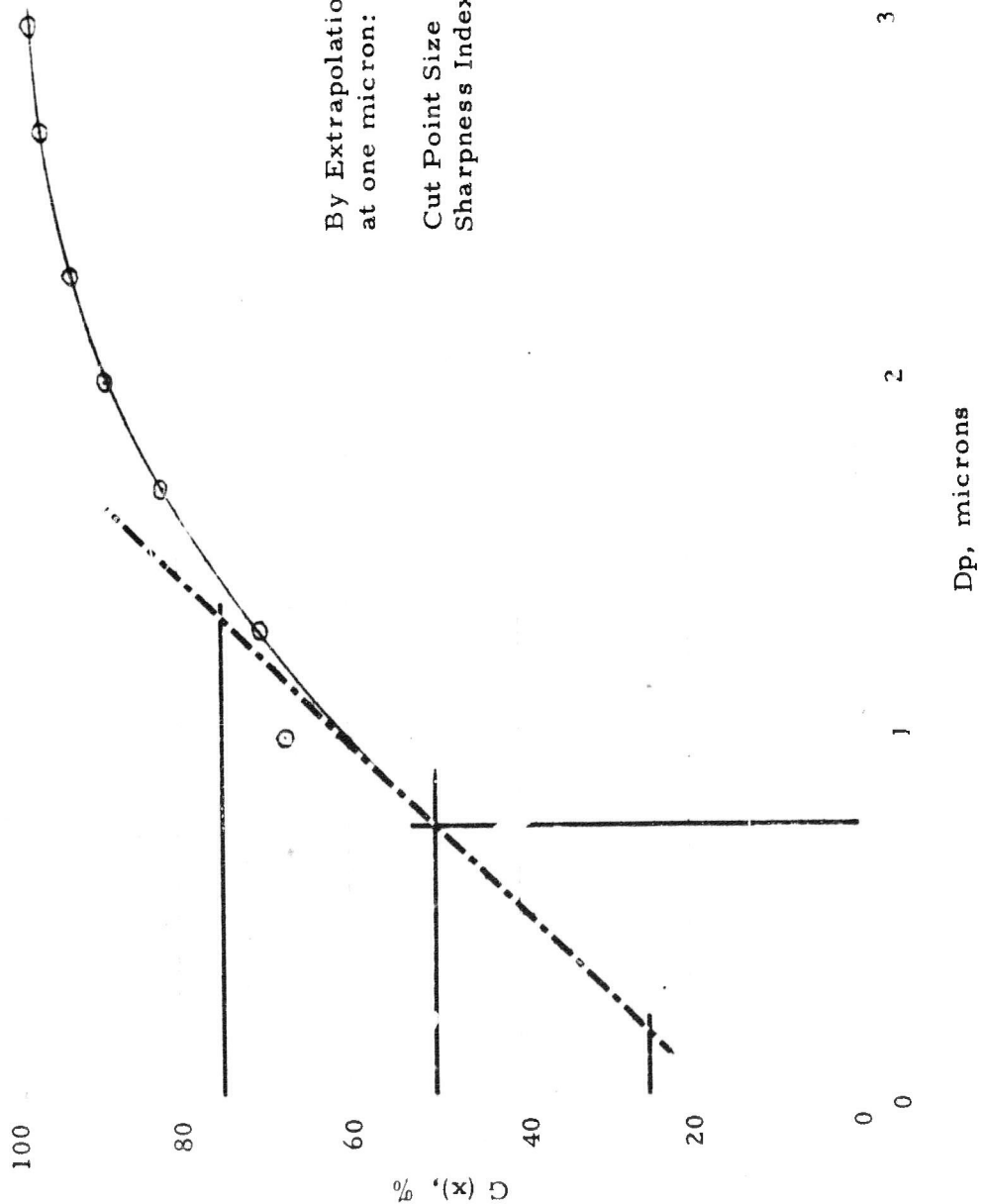


Figure 49

Grade Efficiency Curve for DC-38



By Extrapolation, ignoring the data point at one micron:

Cut Point Size 0.75 microns
 Sharpness Index = $\frac{1.34}{0.17} = 7.892$

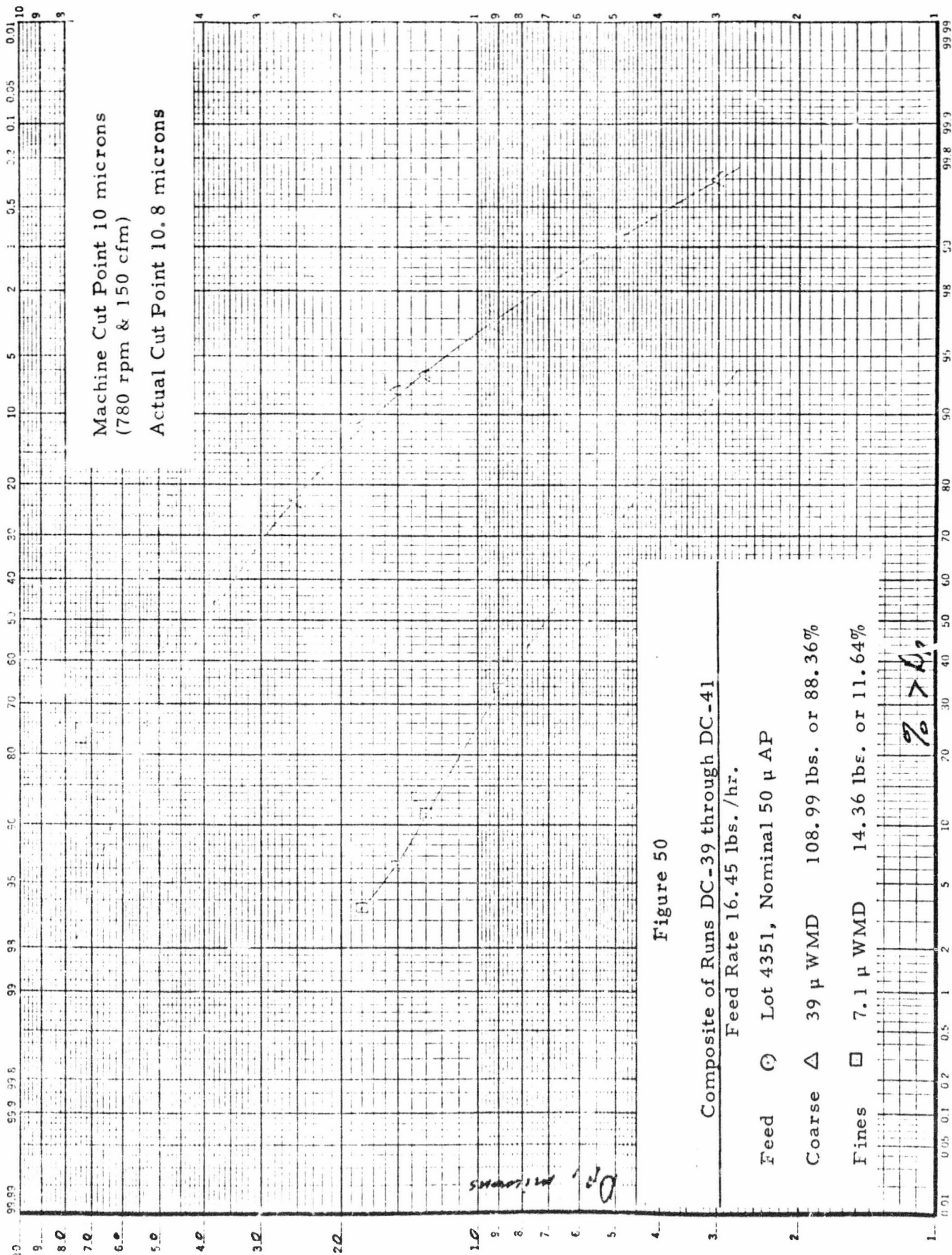
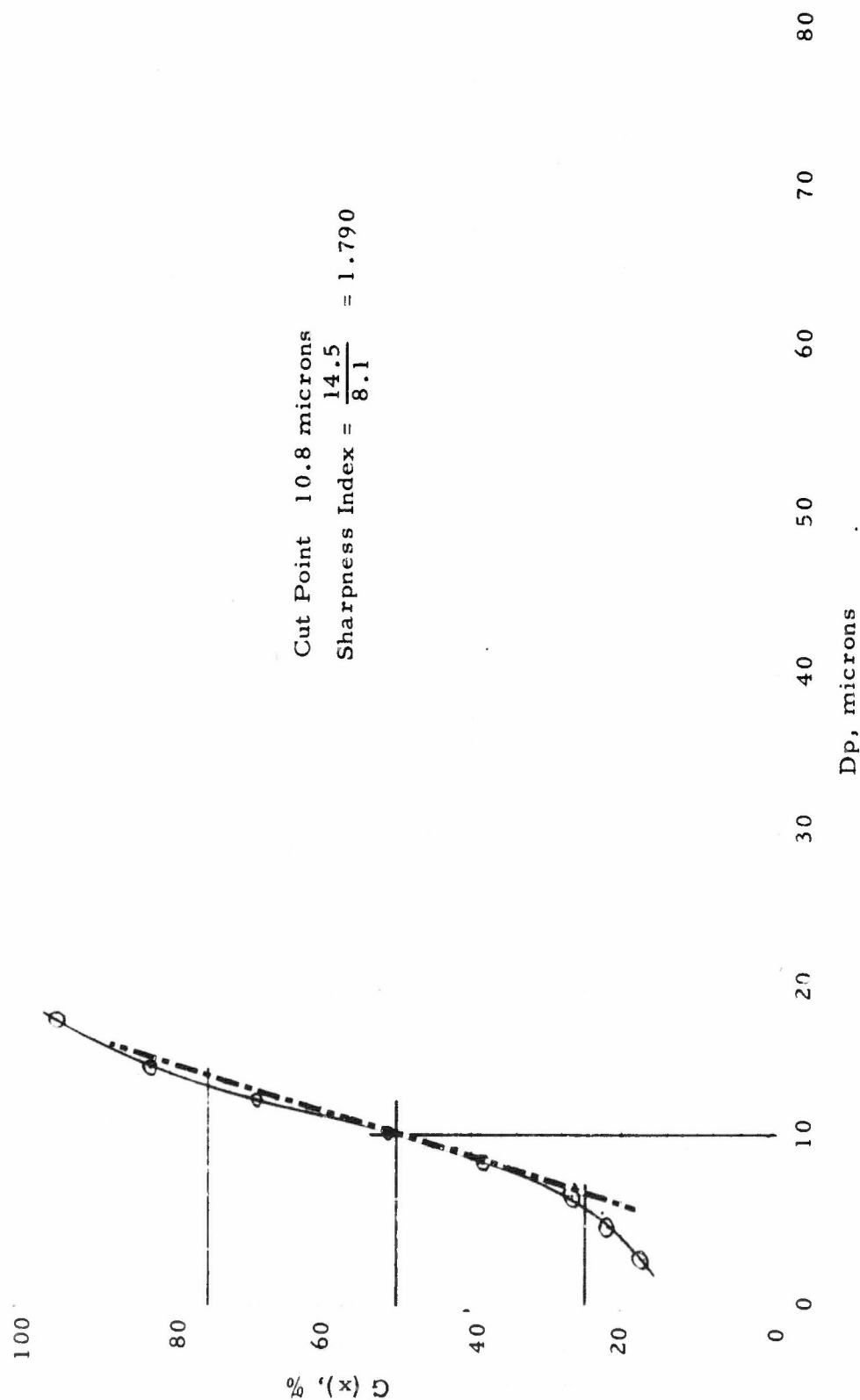


Figure 51

Grade Efficiency Curve for DC-39 through DC-41



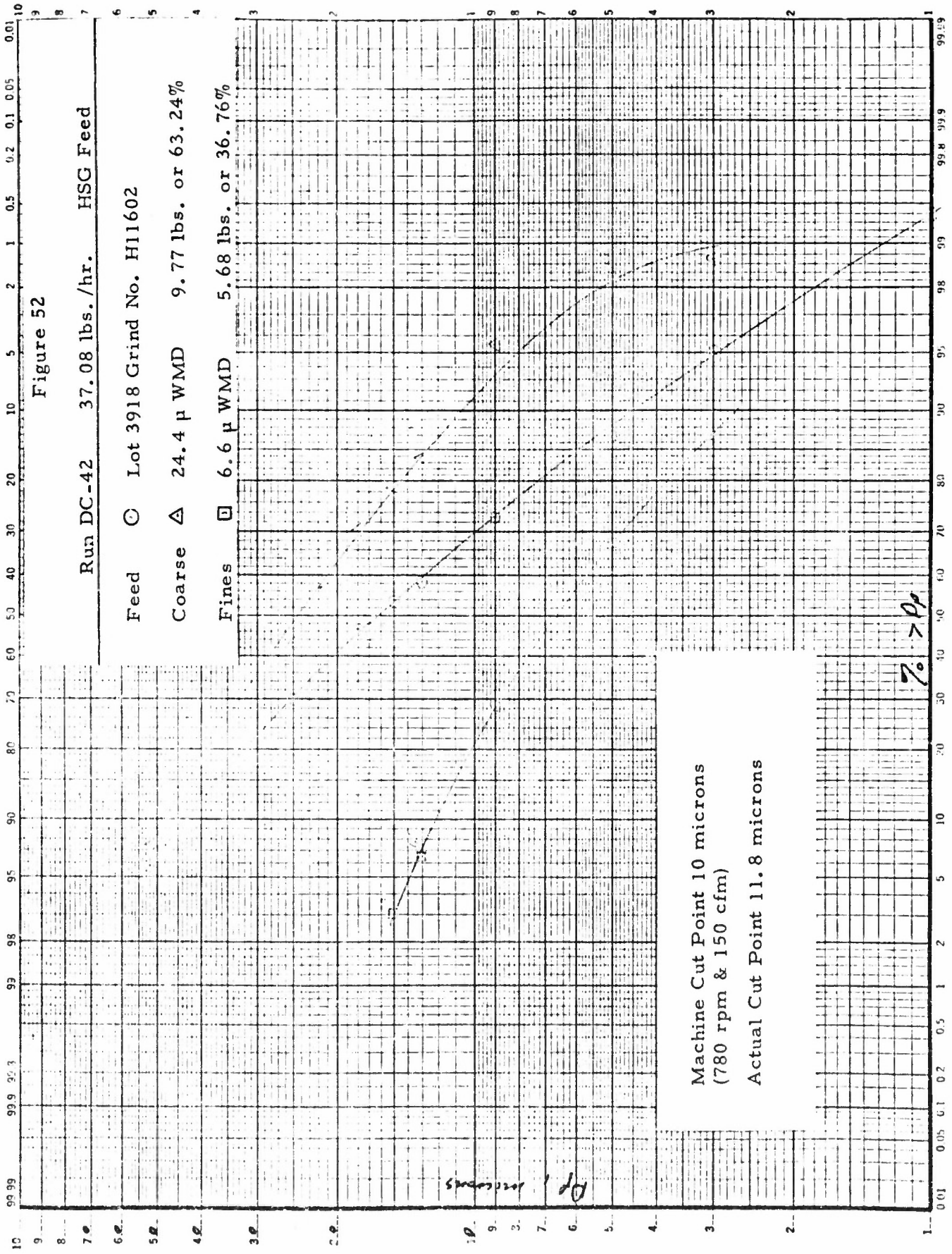


Figure 53

Grade Efficiency Curve for DC-42

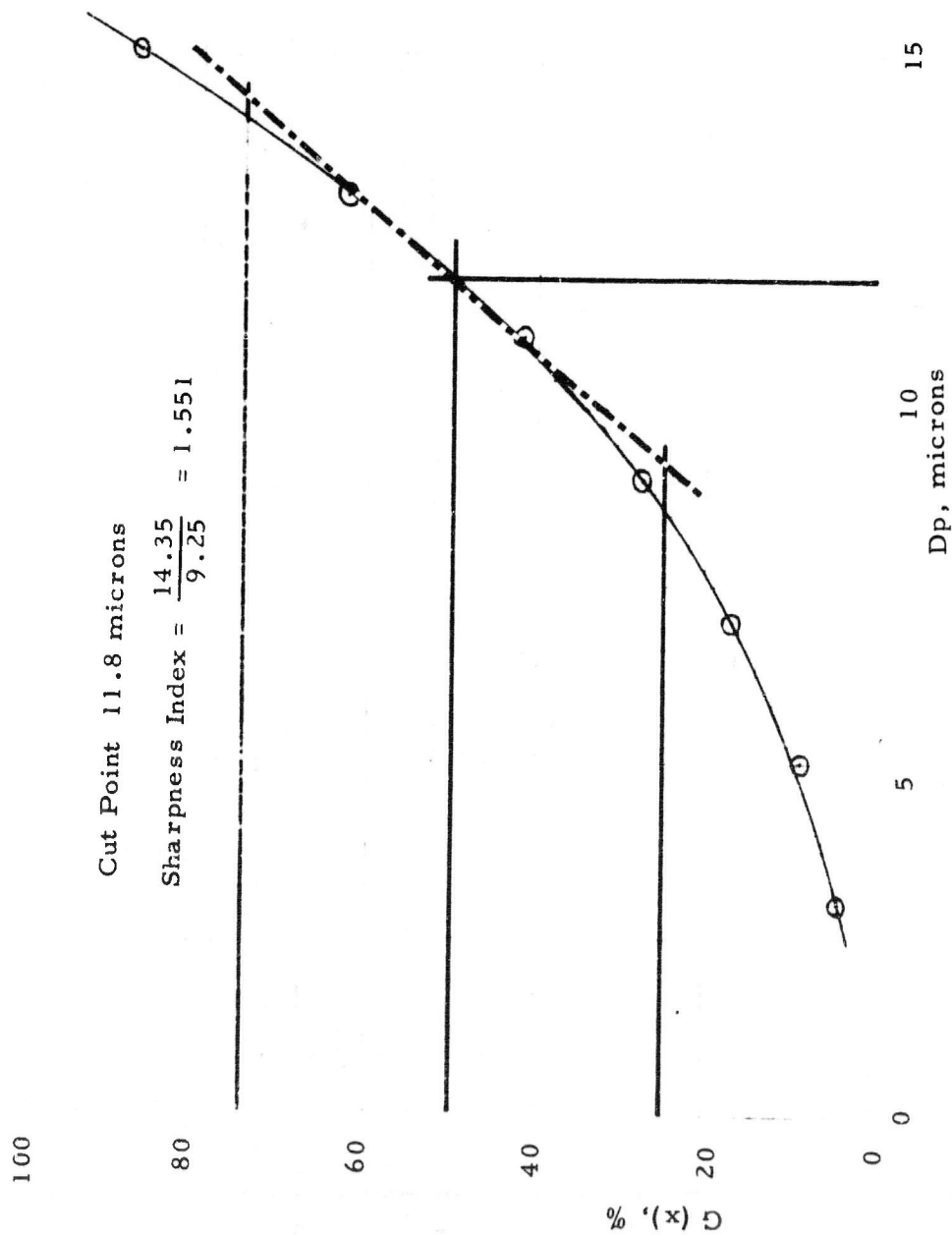


Figure 54

Run DC-43 42.75 lbs./hr. HSG Feed

Feed \odot Lot 3918 Grind No. H11602

Coarse Δ 25.5 μ WMD 8.77 lbs. or 61.50%

Fines \square 6.6 μ WMD 5.49 lbs. or 38.50%

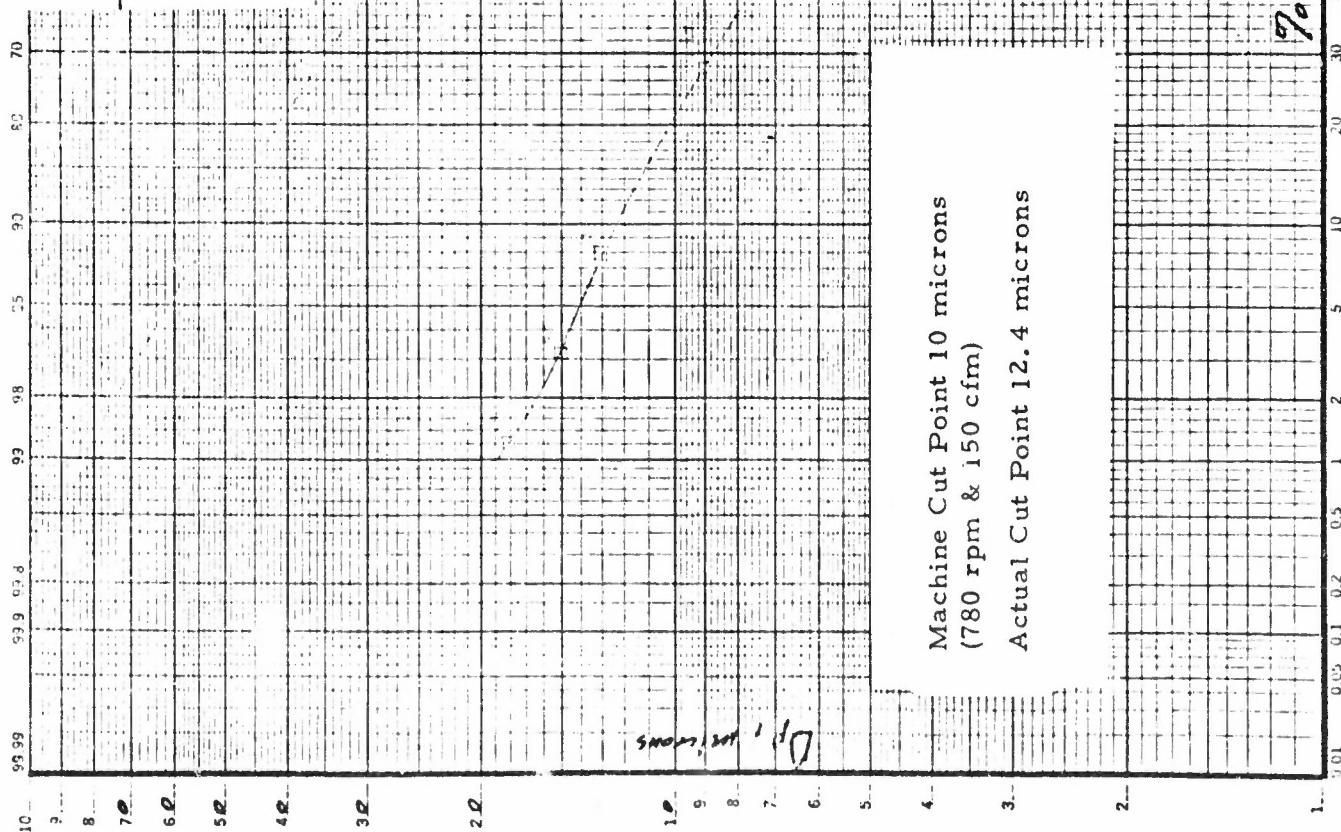


Figure 55

Grade Efficiency Curve for DC-43

Cut Point Size 12.4 microns

$$\text{Sharpness Index} = \frac{15.45}{9.30} = 1.661$$

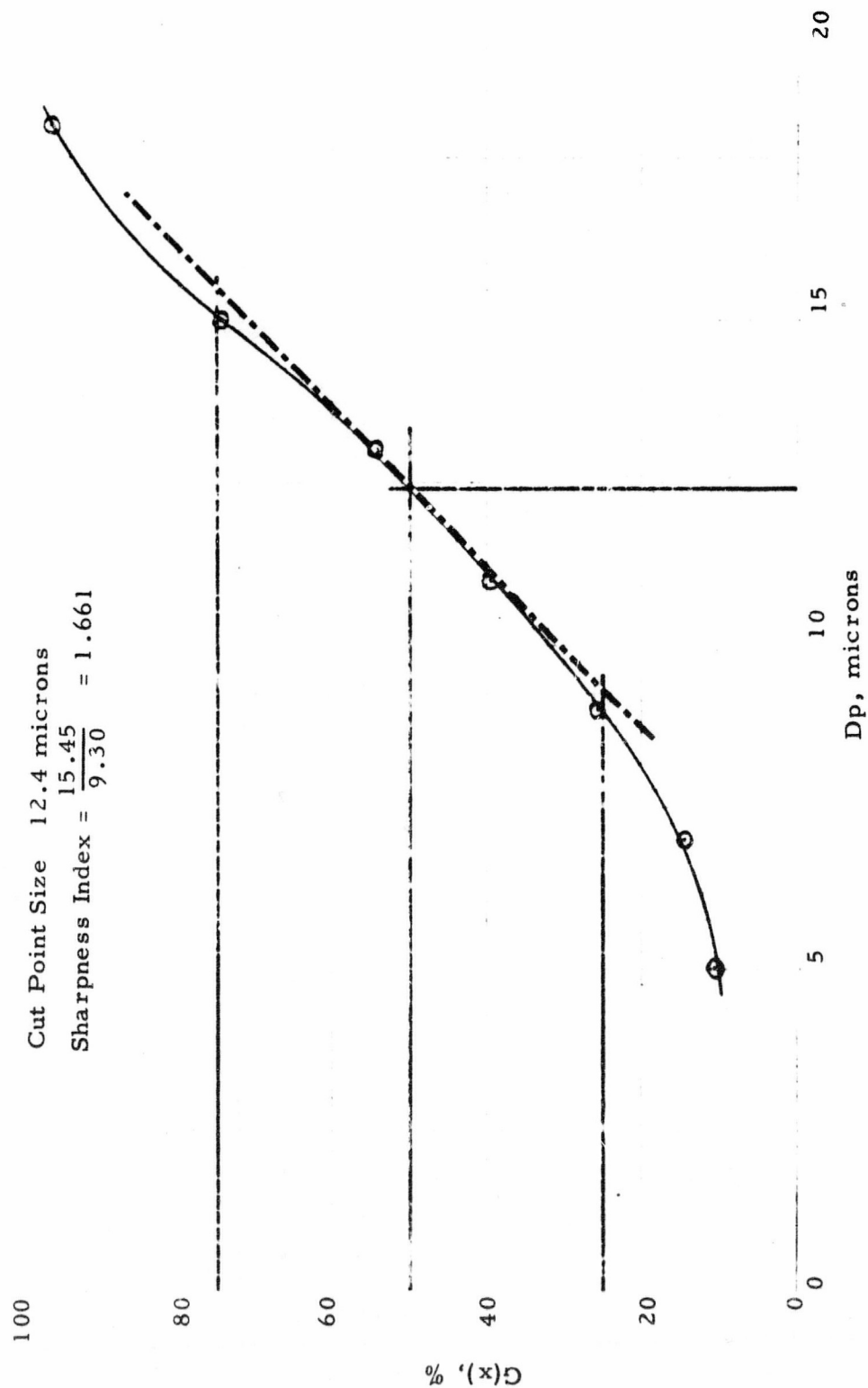


Figure 56

Run DC-44 24.47 lbs./hr. HSG Feed

Feed \odot Lot 3918 Grind No. H11602

Coarse Δ 21.4 μ WMD 15.01 lbs. or 61.34%

Fines \square 6.6 μ WMD 9.46 lbs. or 38.66%

Machine Cut Point 10 microns
(780 rpm & 150 cfm)

Actual Cut Point 11.35 microns

% > ϕ_p

Figure 57
Grade Efficiency Curve for DC-44

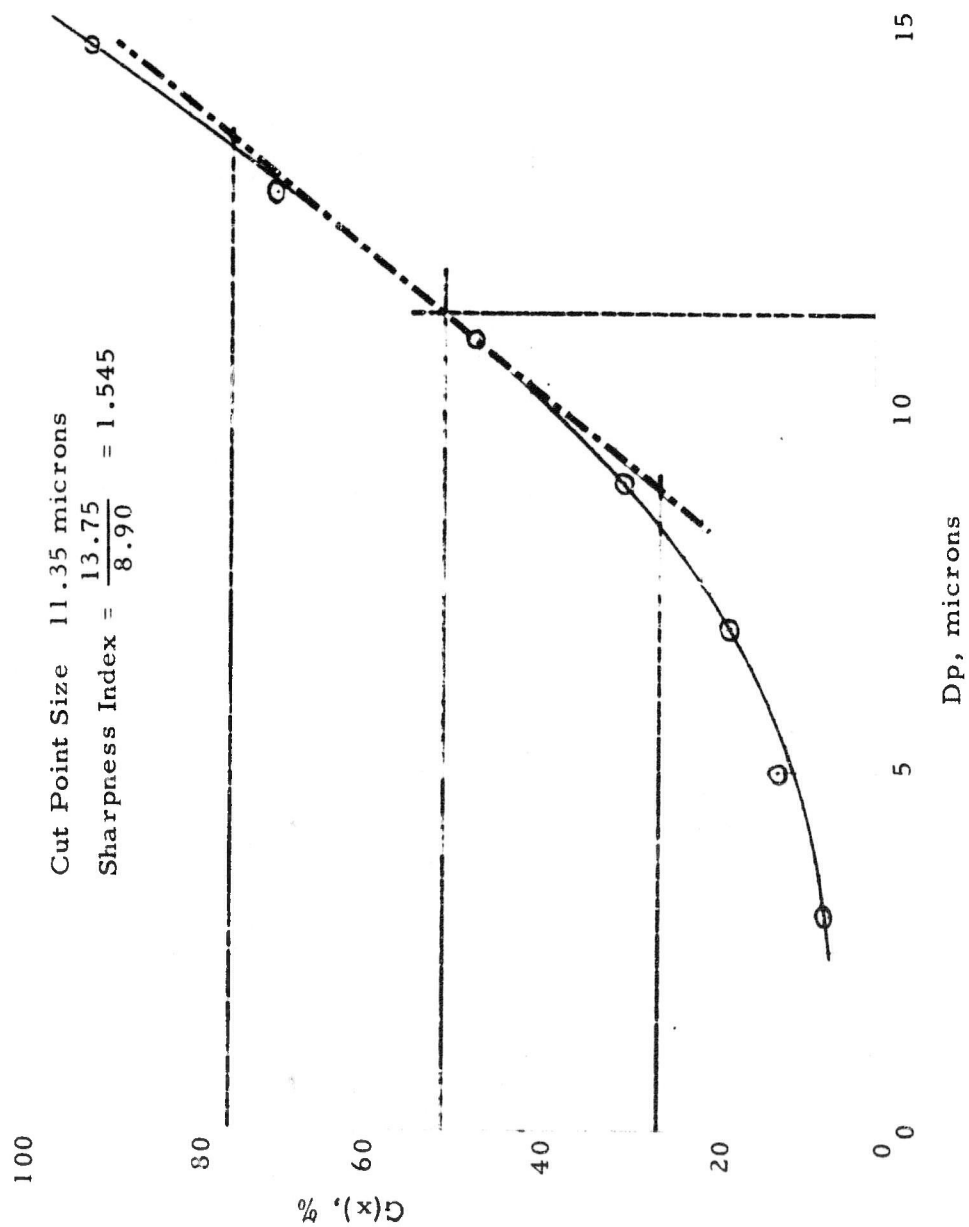


Figure 58

Run DC-45 14.6 lbs./hr. HSG Feed

Feed ○ Lot 3918 Grind No. H11602

Coarse △ 9.2 μ WMD 16.37 lbs. or 56.08%

Fines □ 5.1 μ WMD 12.82 lbs. or 43.92%

Machine Cut Point 10 microns
(780 rpm & 150 cfm)

Actual Cut Point 10.25 microns

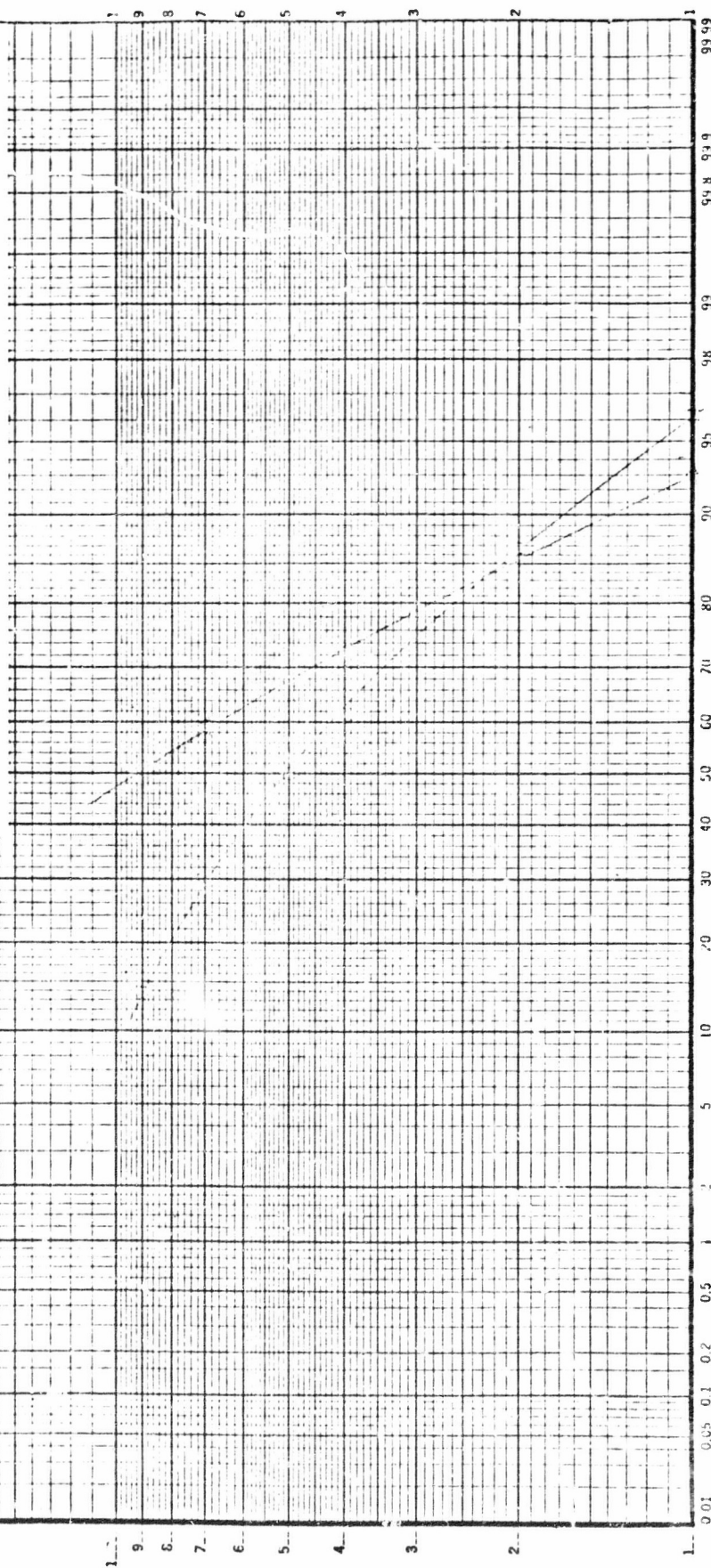


Figure 59

Grade Efficiency Curve for DC-45

100

80

60

40

20

0

0

$G(x), \%$

E-60

Cut Point Size 10.25 microns

Sharpness Index = $\frac{13.1}{7.45} = 1.758$

15

10

5

D_p , microns

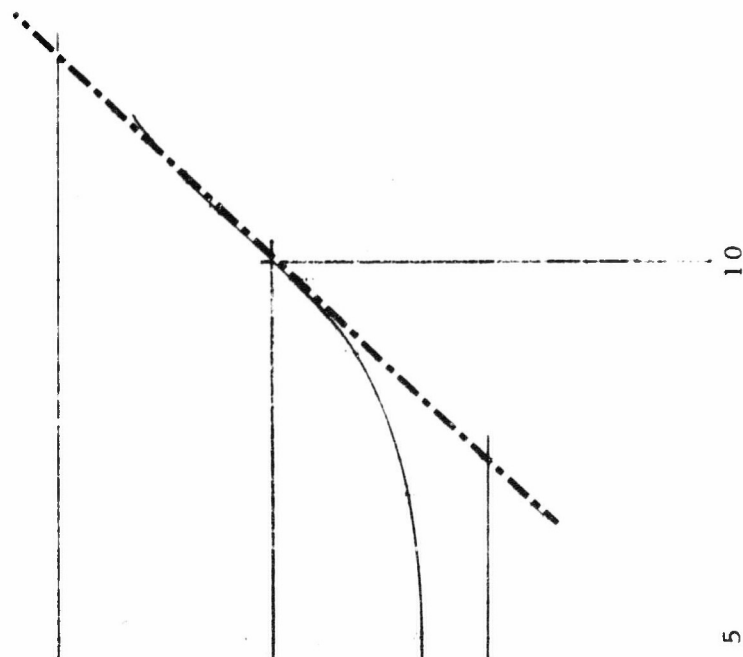


Figure 60

Run DC-46 22.5 lbs./hr. HSG Feed

Feed ○ Lot 3918 Grind No. H11602

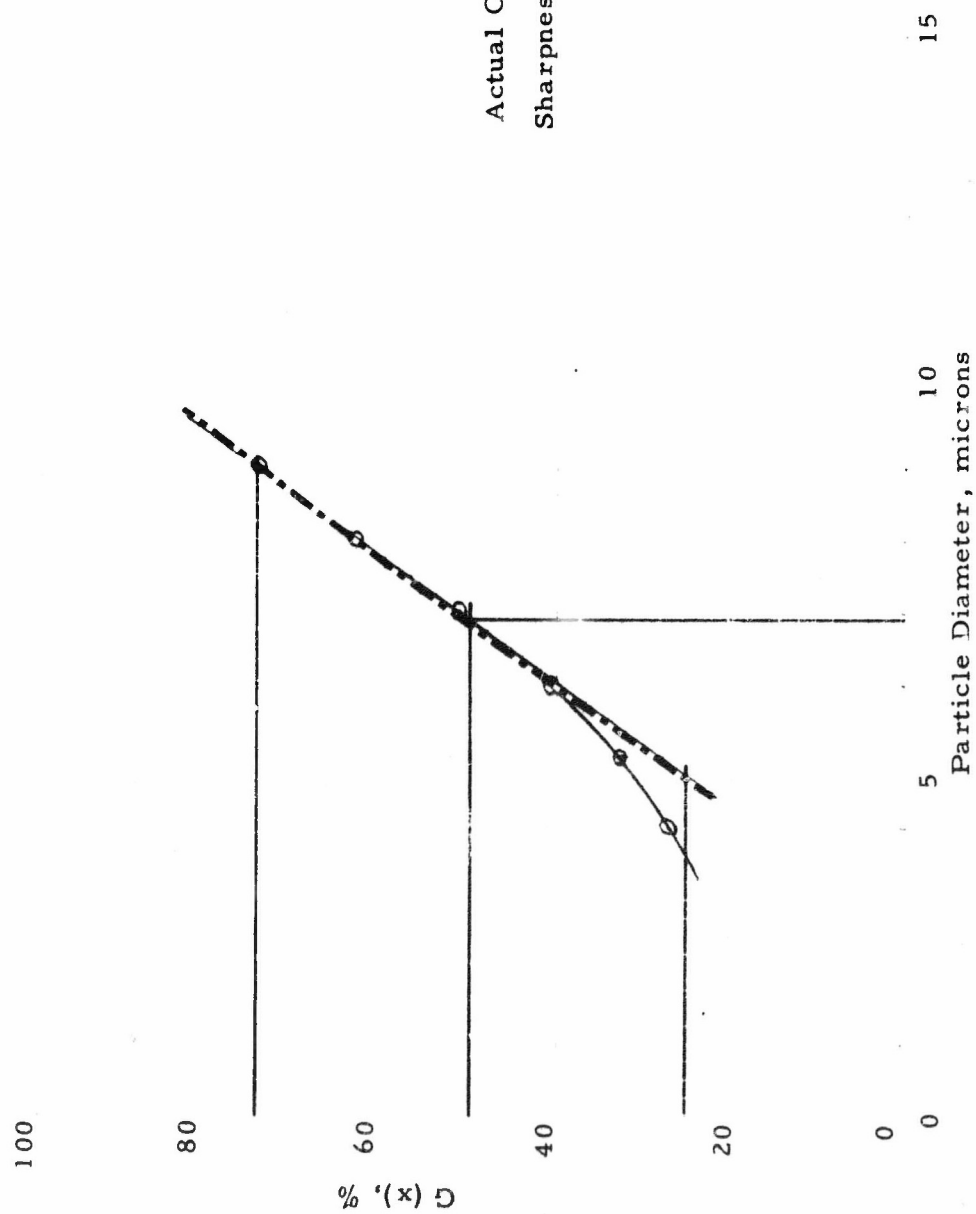
Coarse △ 12.9 μ WMD 15.95 lbs. or 70.70%

Fines □ 4.2 μ WMD 6.61 lbs. or 29.30%

Machine Cut Point 5 microns
(1140 rpm & 150 cfm)
Actual Cut Point 6.9 microns

Figure 61

Grade Efficiency Curve for DC-46



Actual Cut Point Size 6.9 microns
 Sharpness Index = $\frac{9.0}{4.6} = 1.956$

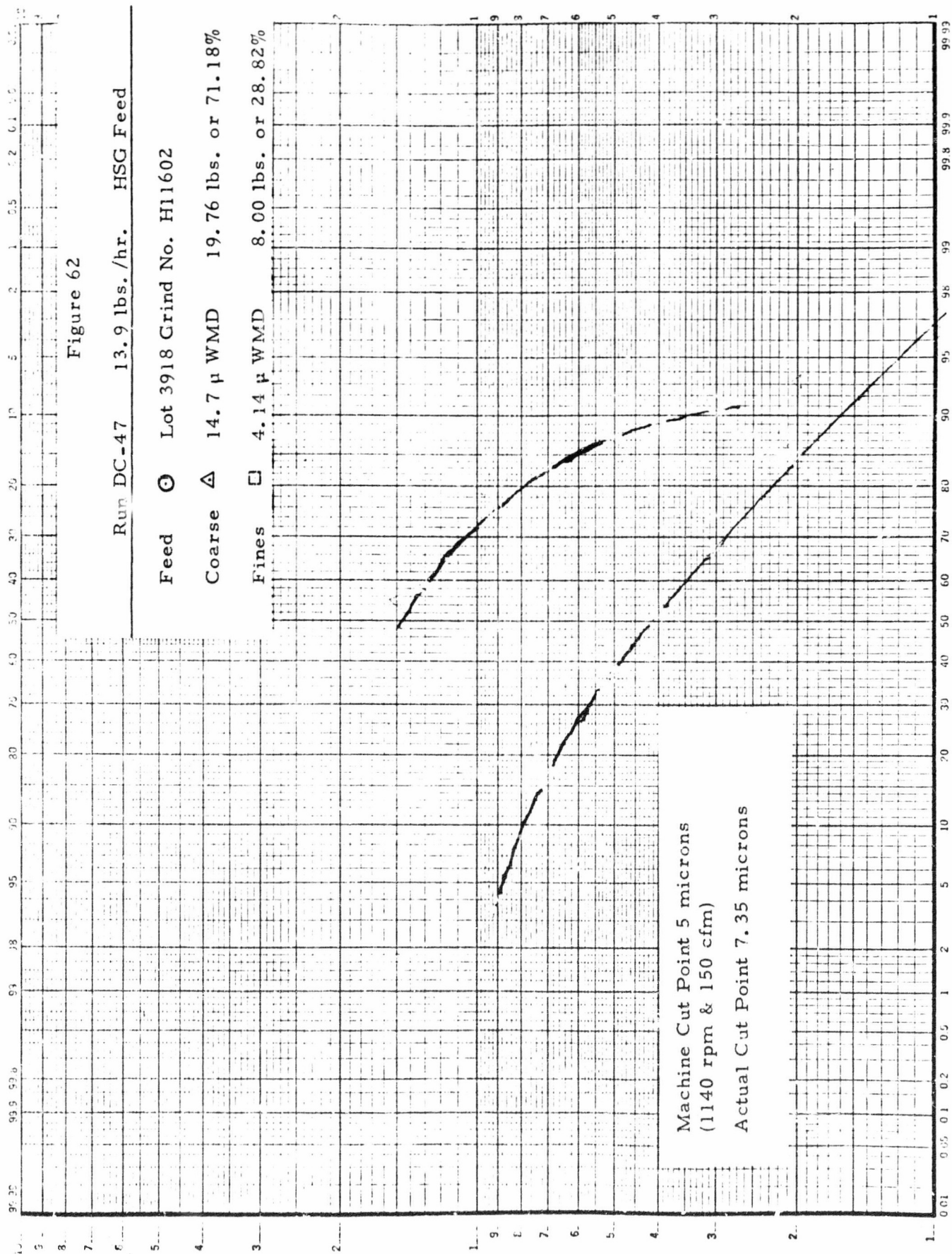
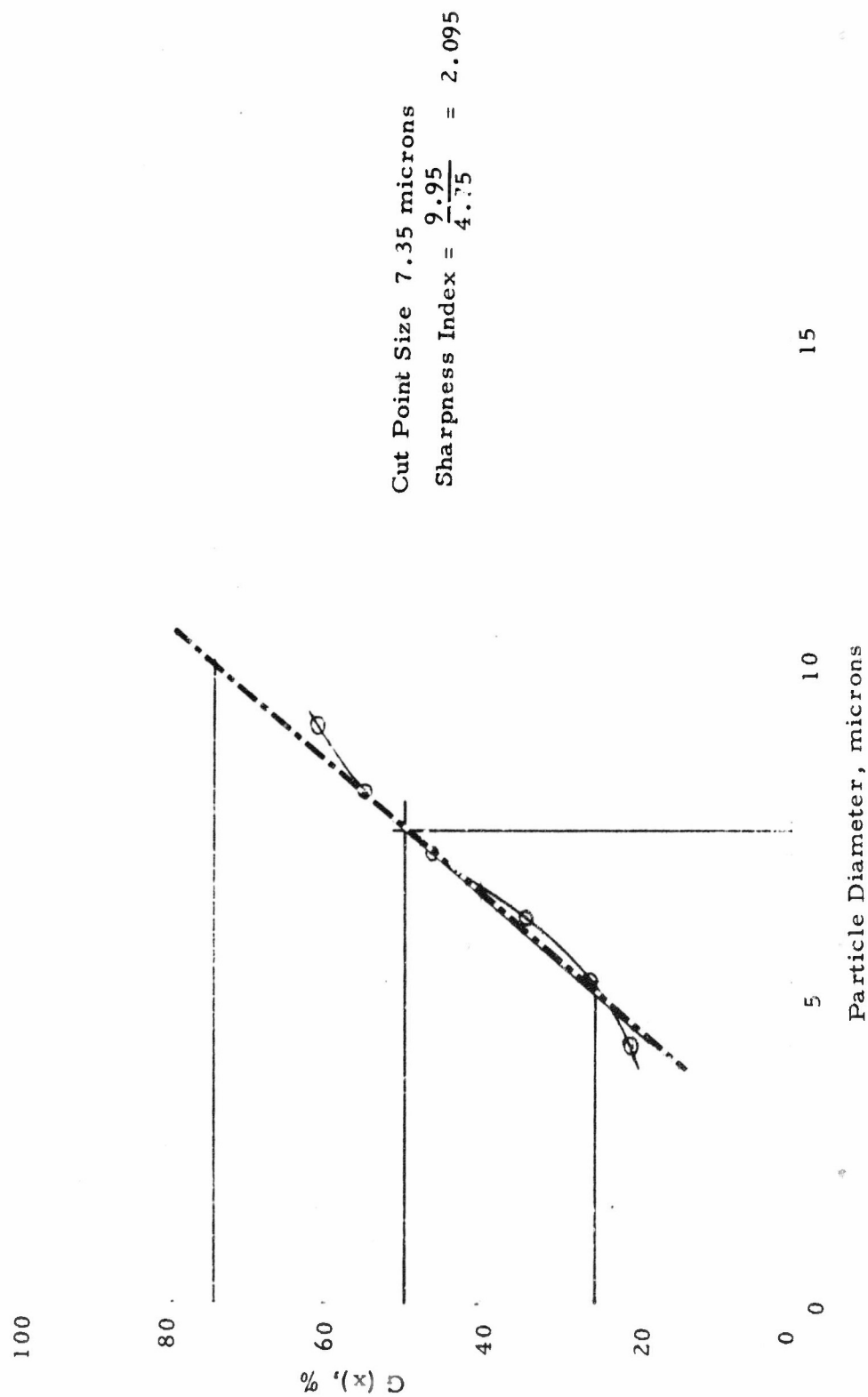


Figure 63

Grade Efficiency Curve for DC-47



Machine Cut Point 25 microns
(482 rpm & 150 cfm)
Actual Cut Point 23.2 microns

Figure 64

Run DC-48 27.7 lbs./hr. HSG Feed

Feed ○ Lot 3918 Grind H11602

Coarse △ 29.5 μ WMD 5.33 lbs. or 38.48%

Fines □ 10.6 μ WMD 8.52 lbs. or 61.52%

% > D_p

D_p Microns

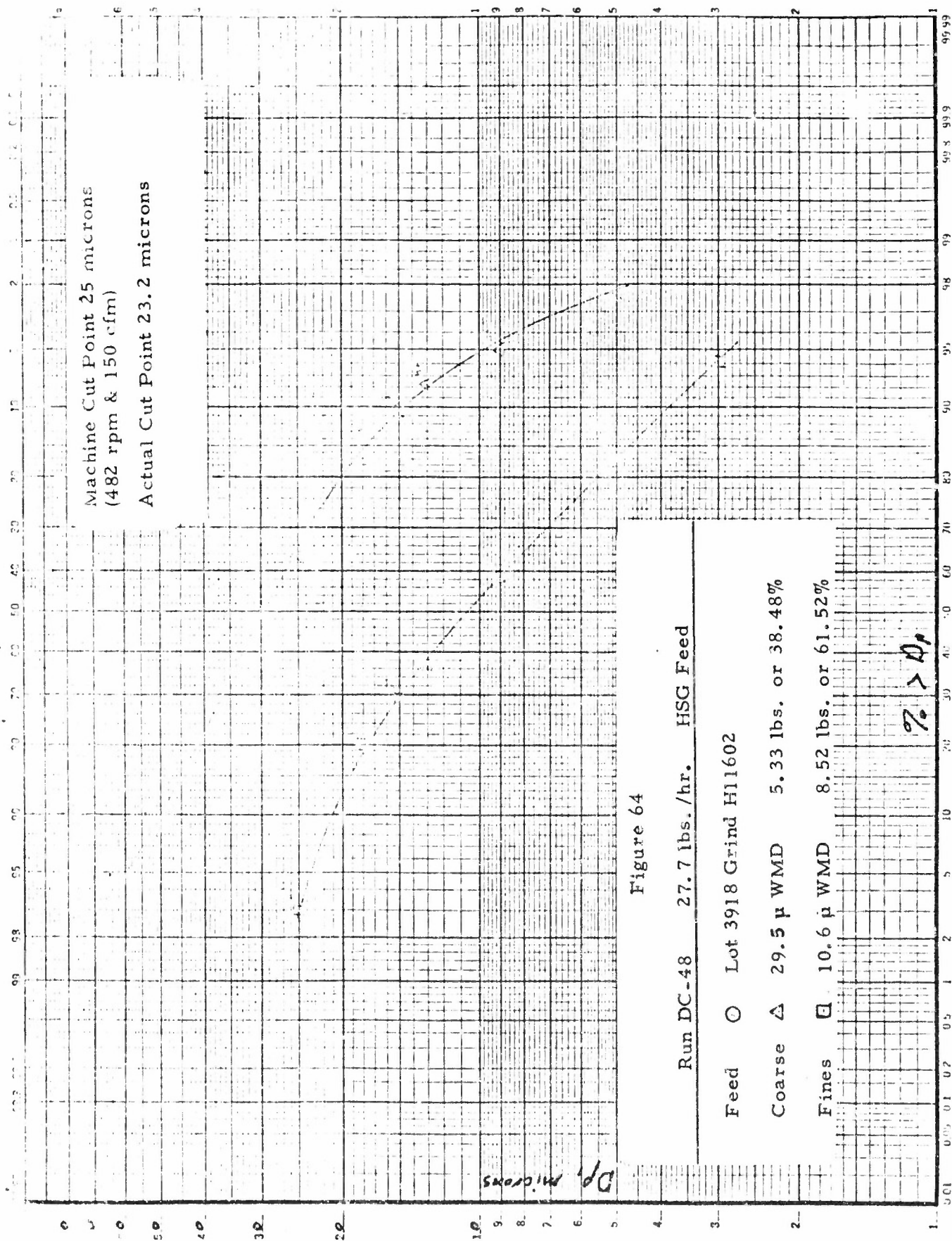
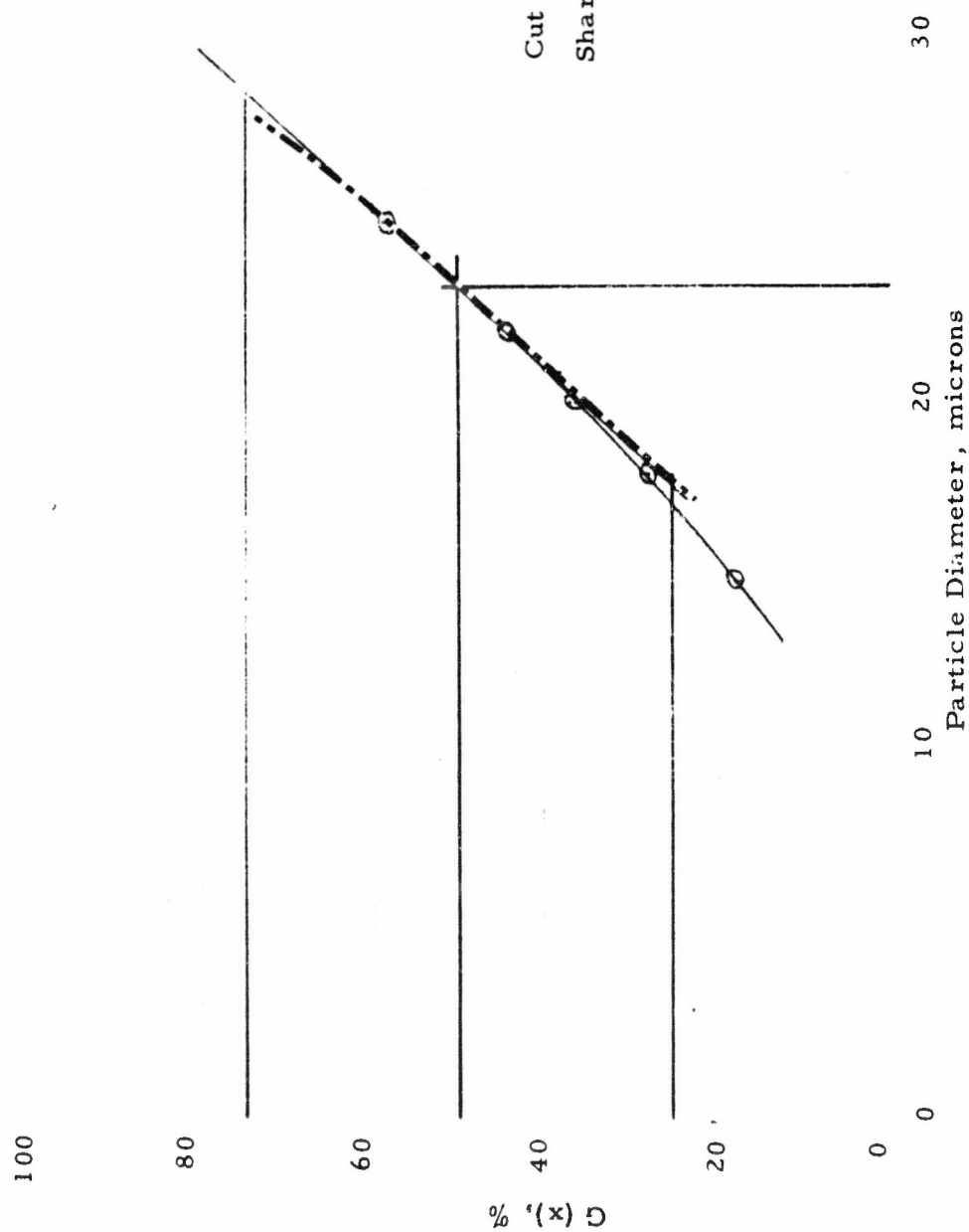


Figure 65
Grade Efficiency Curve for DC-48



Cut Point Size 23.2 microns
Sharpness Index = $\frac{28.7}{16.7} = 1.718$

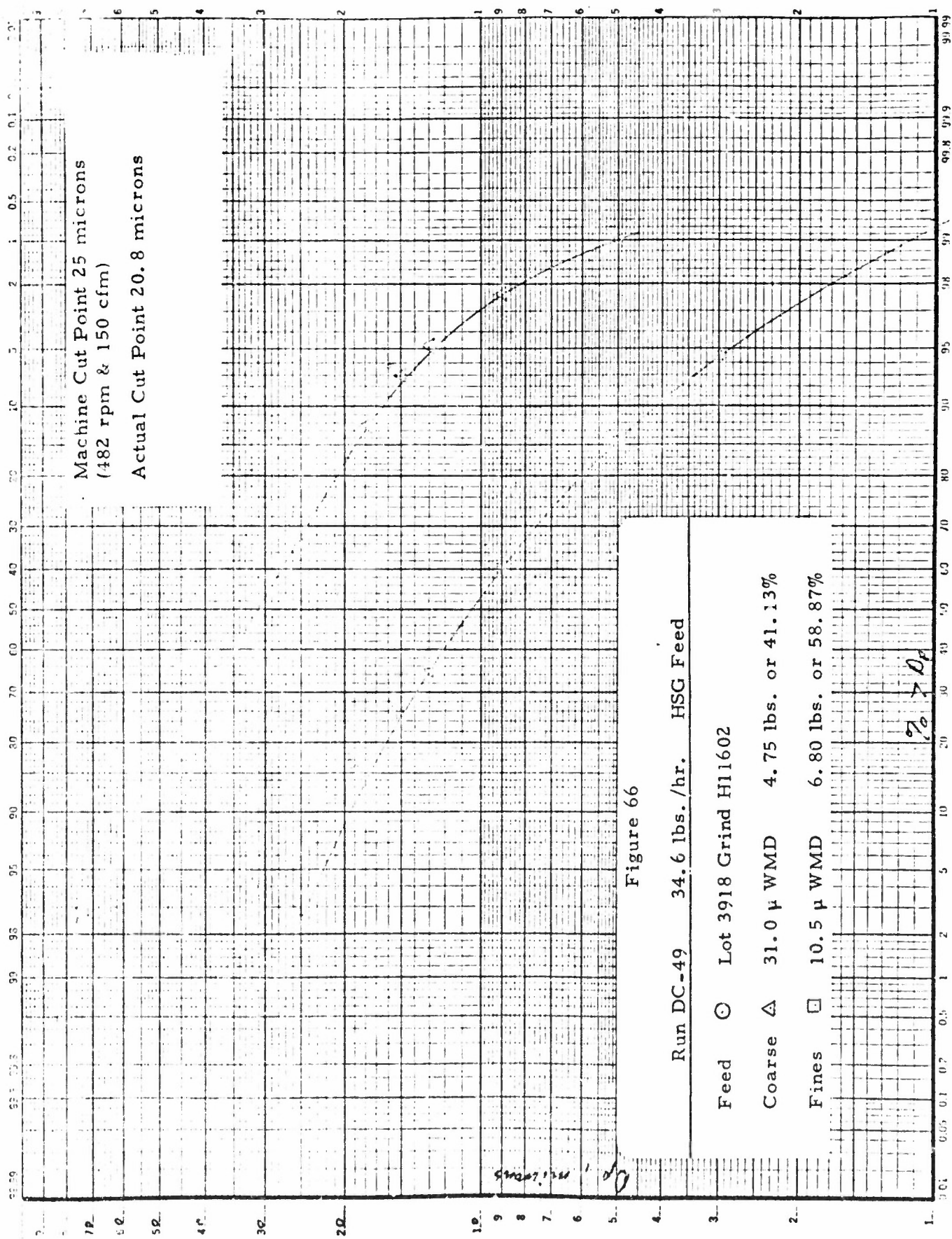
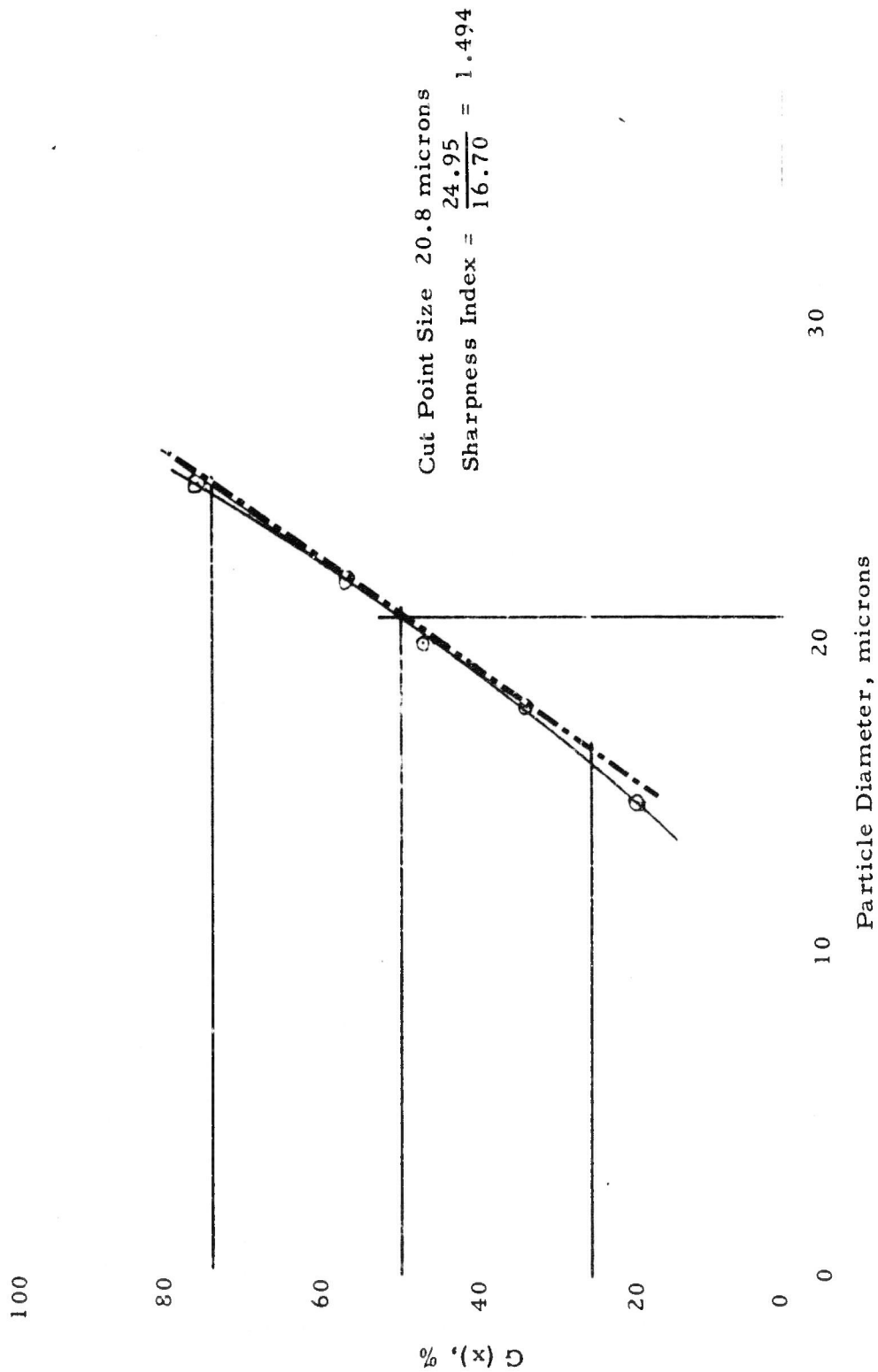


Figure 67
Grade Efficiency Curve for DC-49



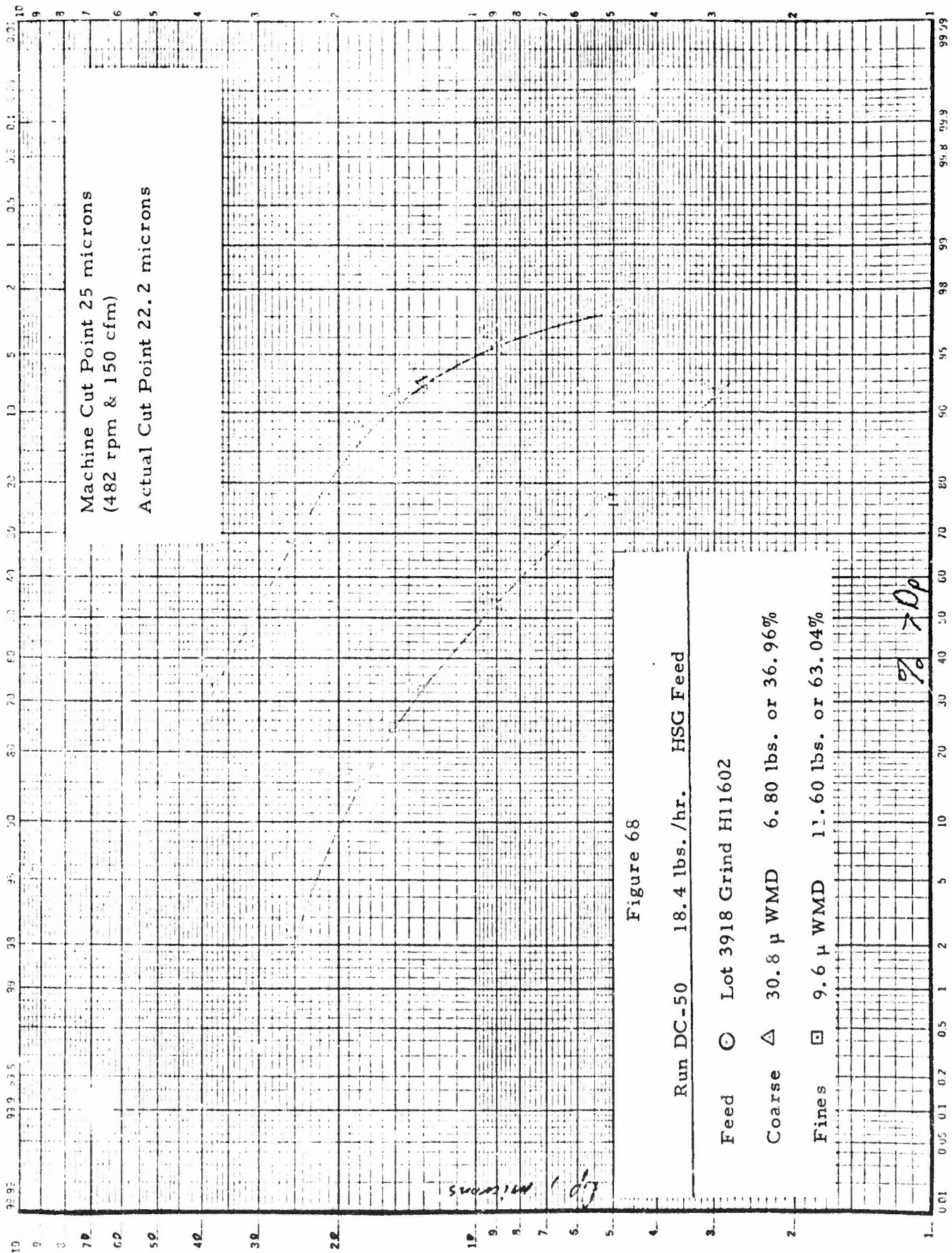


Figure 68

Run DC-50 18.4 lbs./hr. HSG Feed

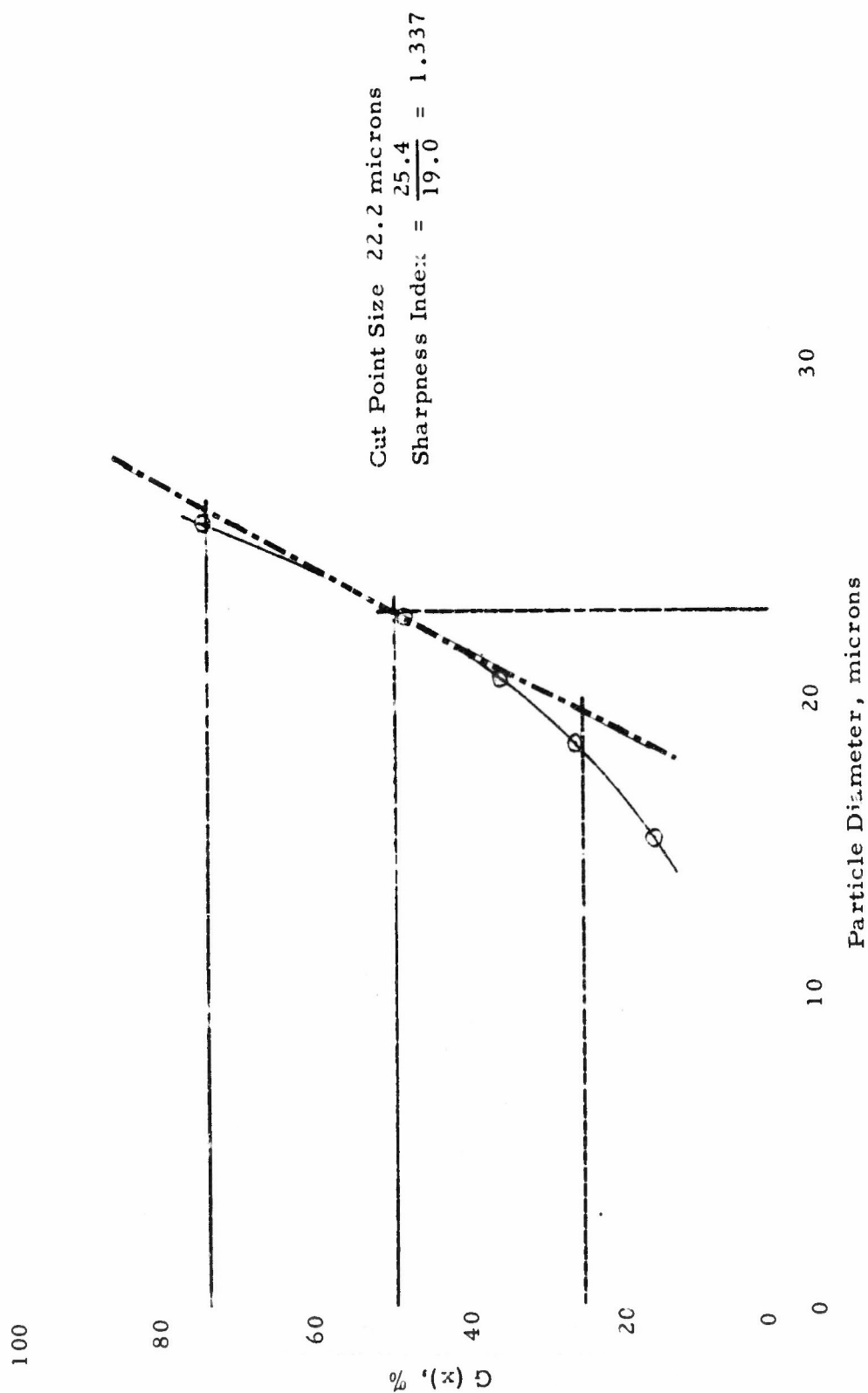
Feed ○ Lot 3918 Grind H11602

Coarse △ 30.8 μ WMD 6.80 lbs. or 36.96%

Fines □ 9.6 μ WMD 11.60 lbs. or 63.04%

Figure 69

Grade Efficiency Curve for DC-50



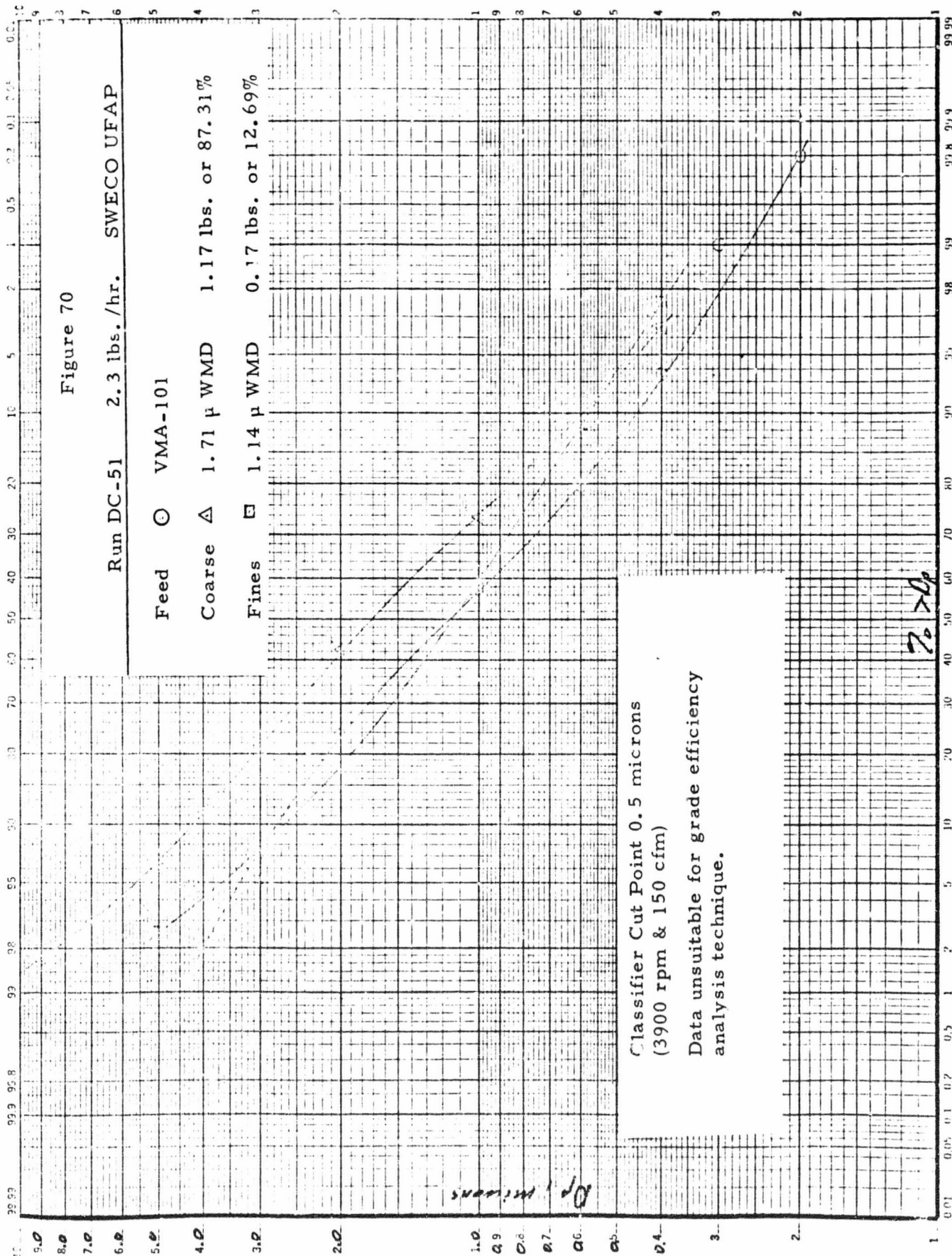
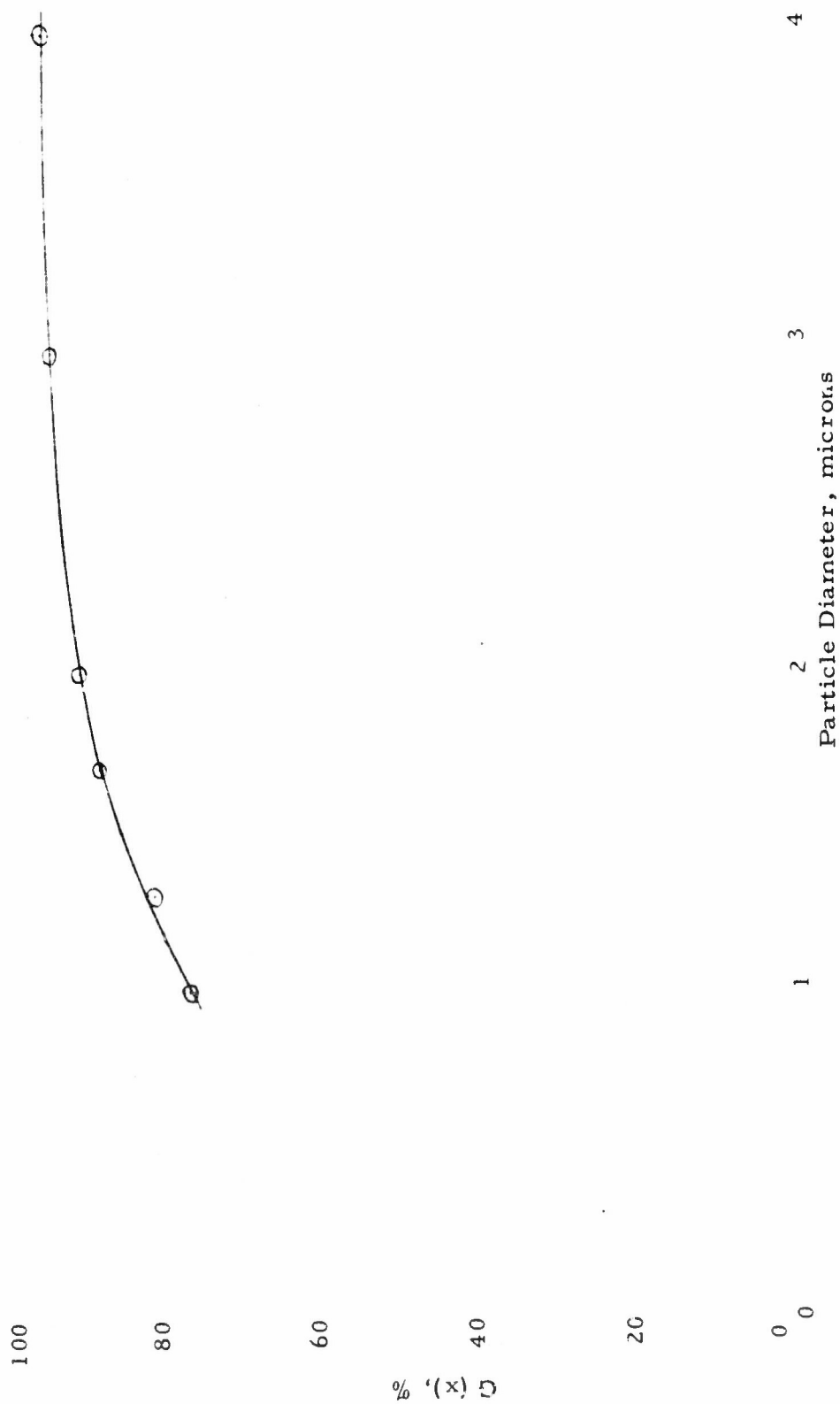


Figure 71
Grade Efficiency Curve for DC-51



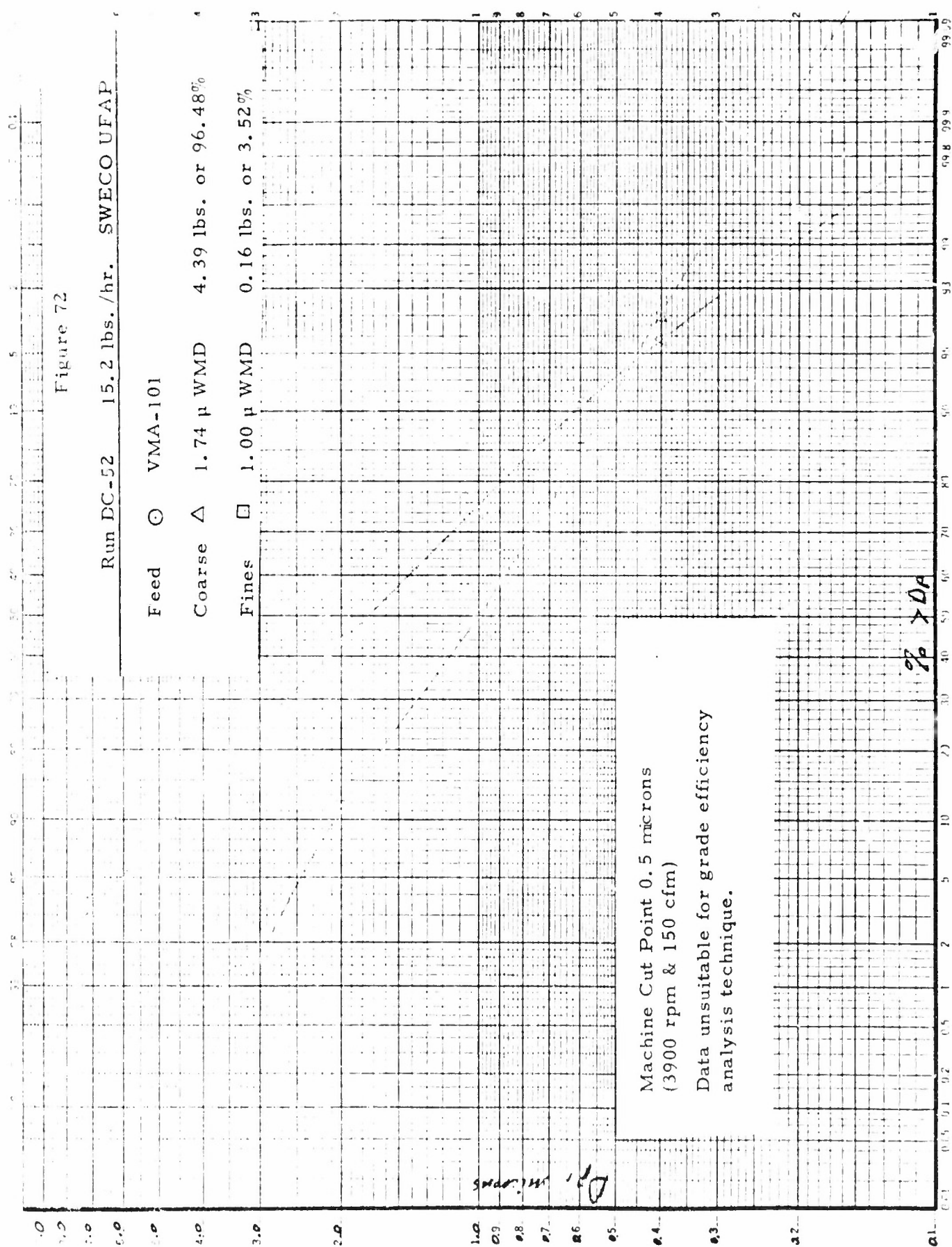


Figure 72

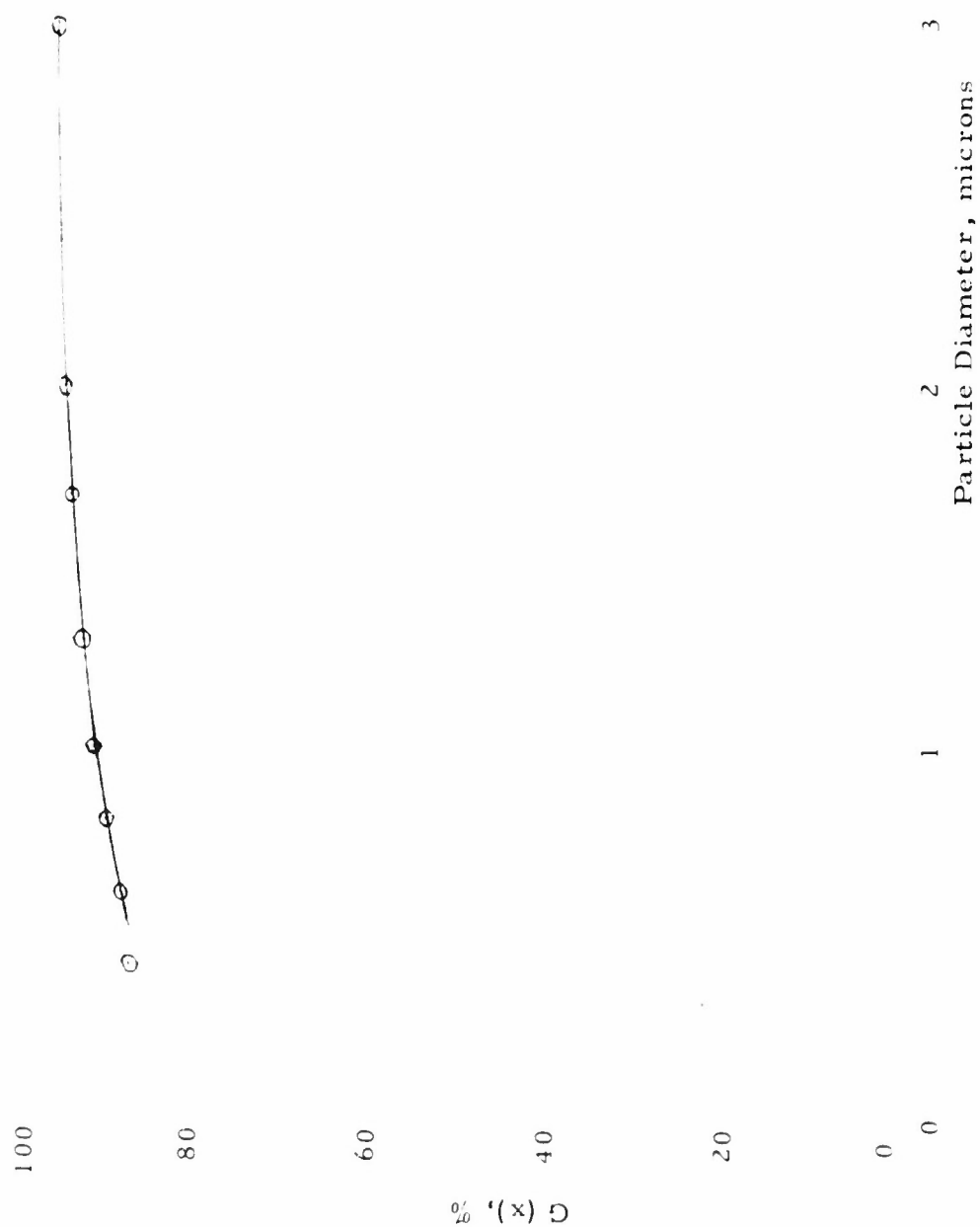
Run DC-52 15.2 lbs./hr. SWECO UFAP

Feed ○ VMA-101

Coarse △ 1.74 μ WMD 4.39 lbs. or 96.48%

Fines □ 1.00 μ WMD 0.16 lbs. or 3.52%

Figure 73
Grade Efficiency Curve for DC-52



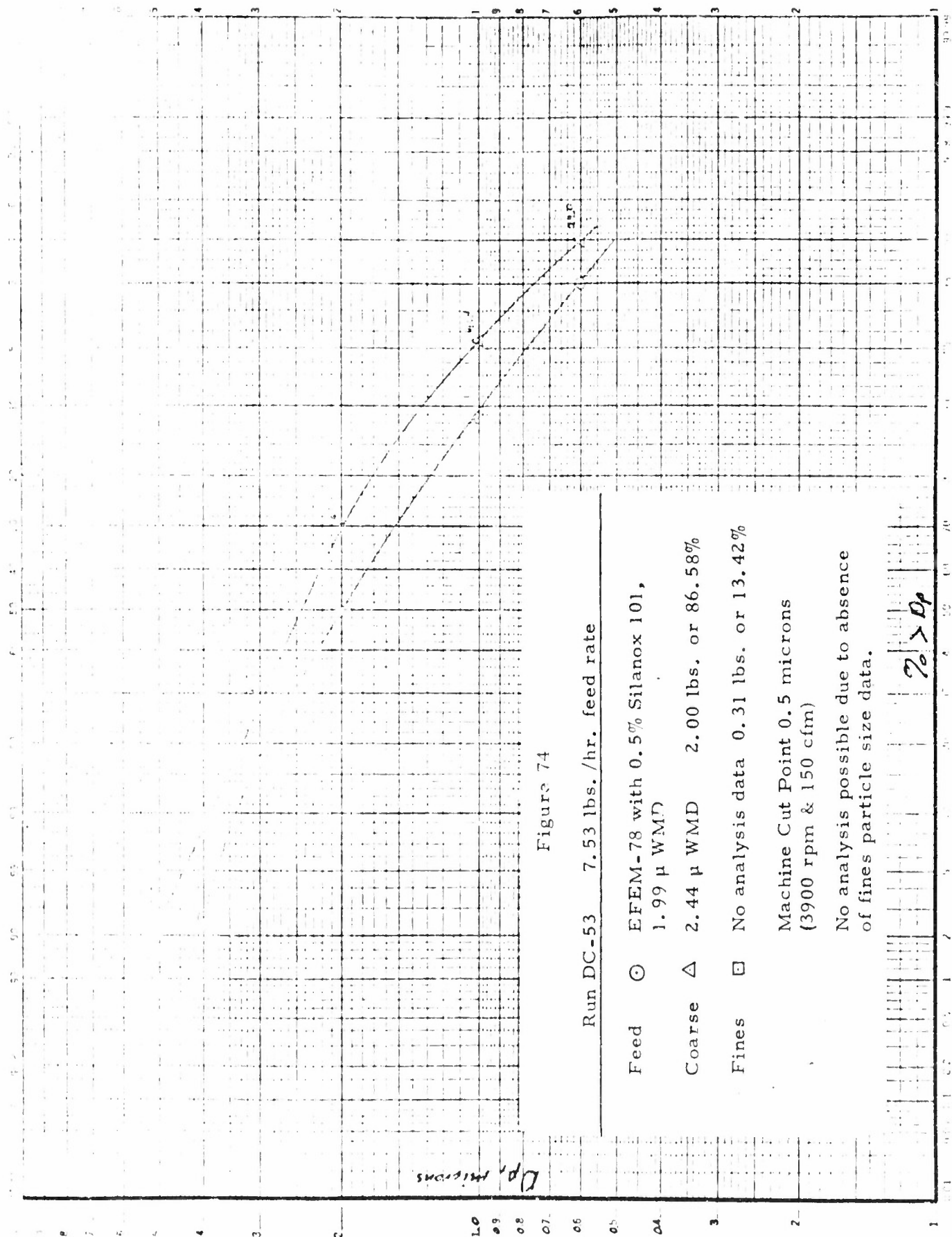


Figure 75

Composite of Runs DC-54 through DC-59

Feed Rate 19.9 lbs./hr.

Feed O HSG Grind No. H11602, 16.2 μ WMD

Coarse Δ 12.9 μ WMD 217.82 lbs. or 72.75%

Fines \square 3.06 μ WMD 81.58 lbs. or 27.25%

Machine Cut Point 5 microns
(1140 rpm & 150 cfm)

Actual Cut Point 5.55 microns

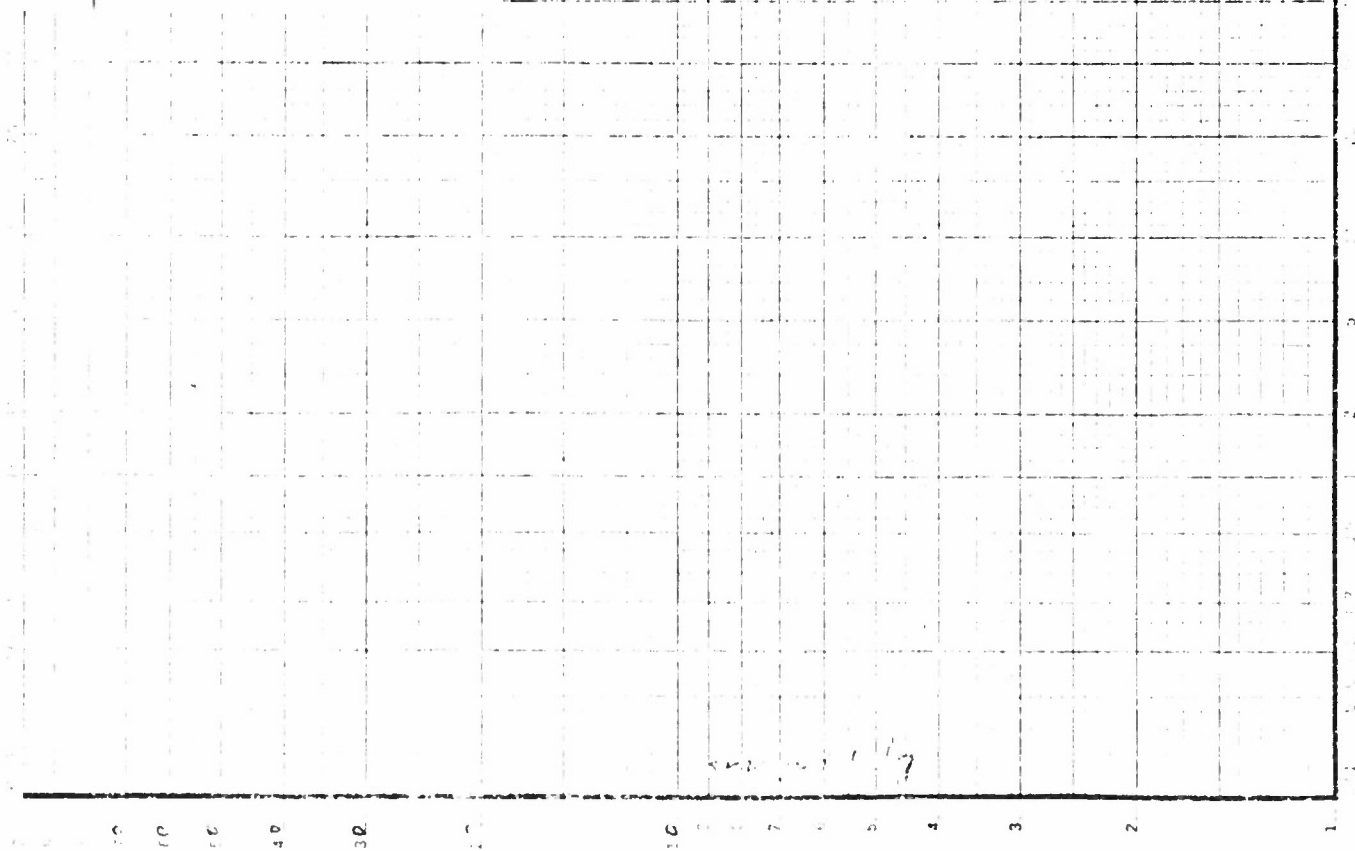
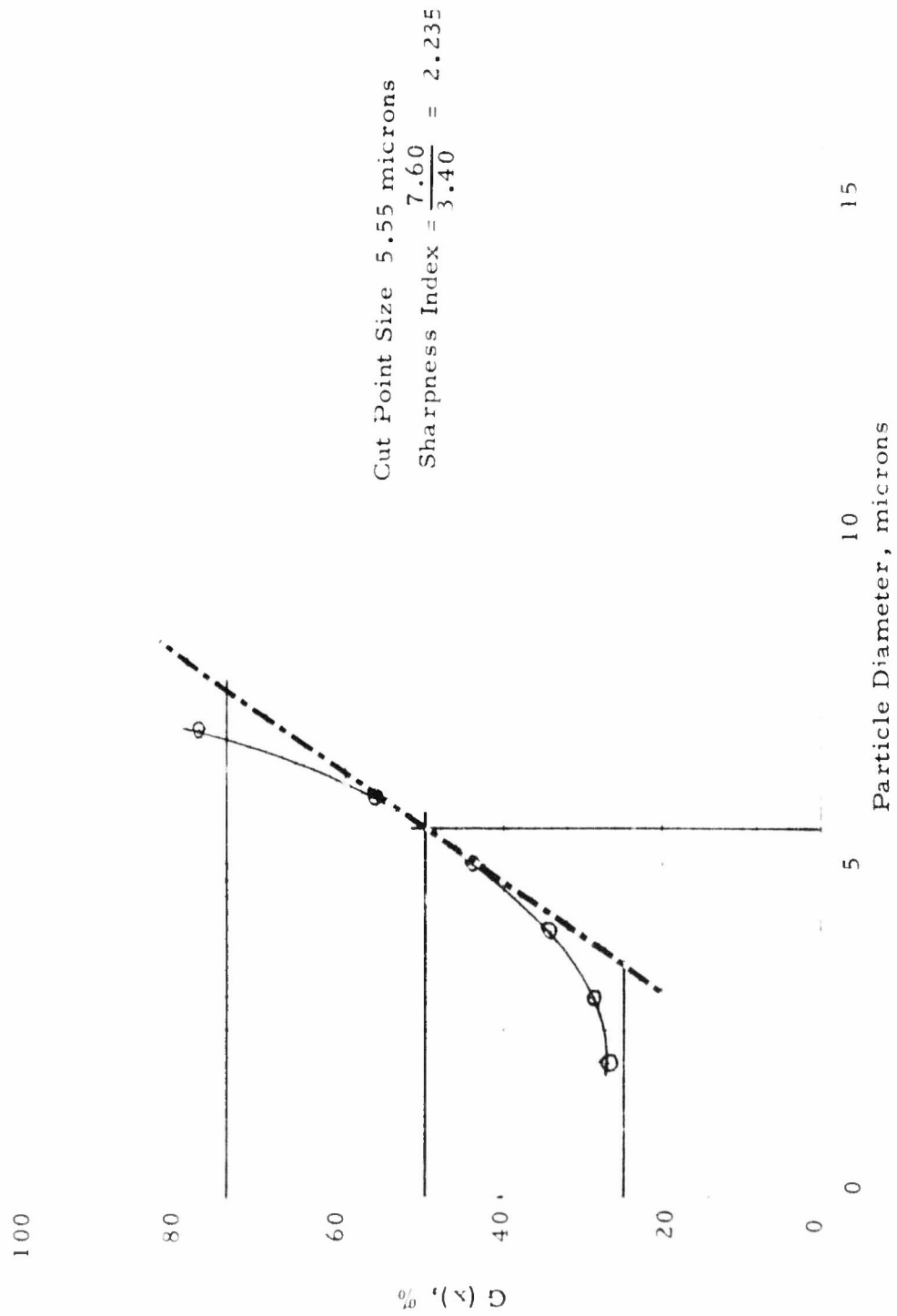


Figure 76
Grade Efficiency Curve on DC-54
through DC-59



Machine Cut Point 25 microns
6482 rpm & 150 cfm

Actual Cut Point 19.5 microns

Figure 77

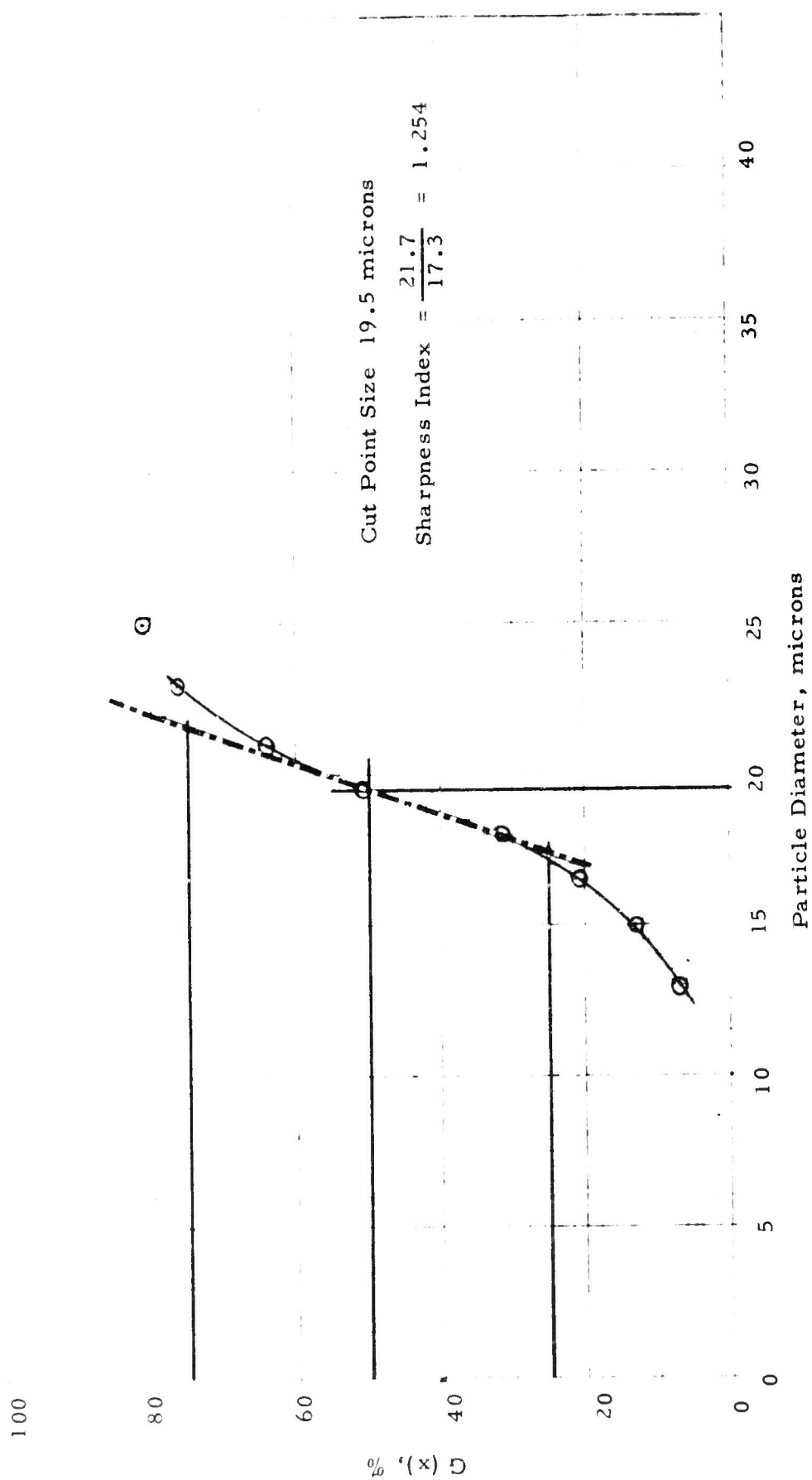
Composite of Runs DC-60 and DC-61
Feed Rate 65.08 lbs./hr.

Feed © Coarse Fraction from Runs DC-54
 thru DC-59

Coarse Δ 29.6 μ WMD 90.84 lbs. or 52.34%

Fines □ 12.9 μ WMD 82.72 lbs. or 47.66%

Figure 78
Grade Efficiency Curve for PC-60 and -61



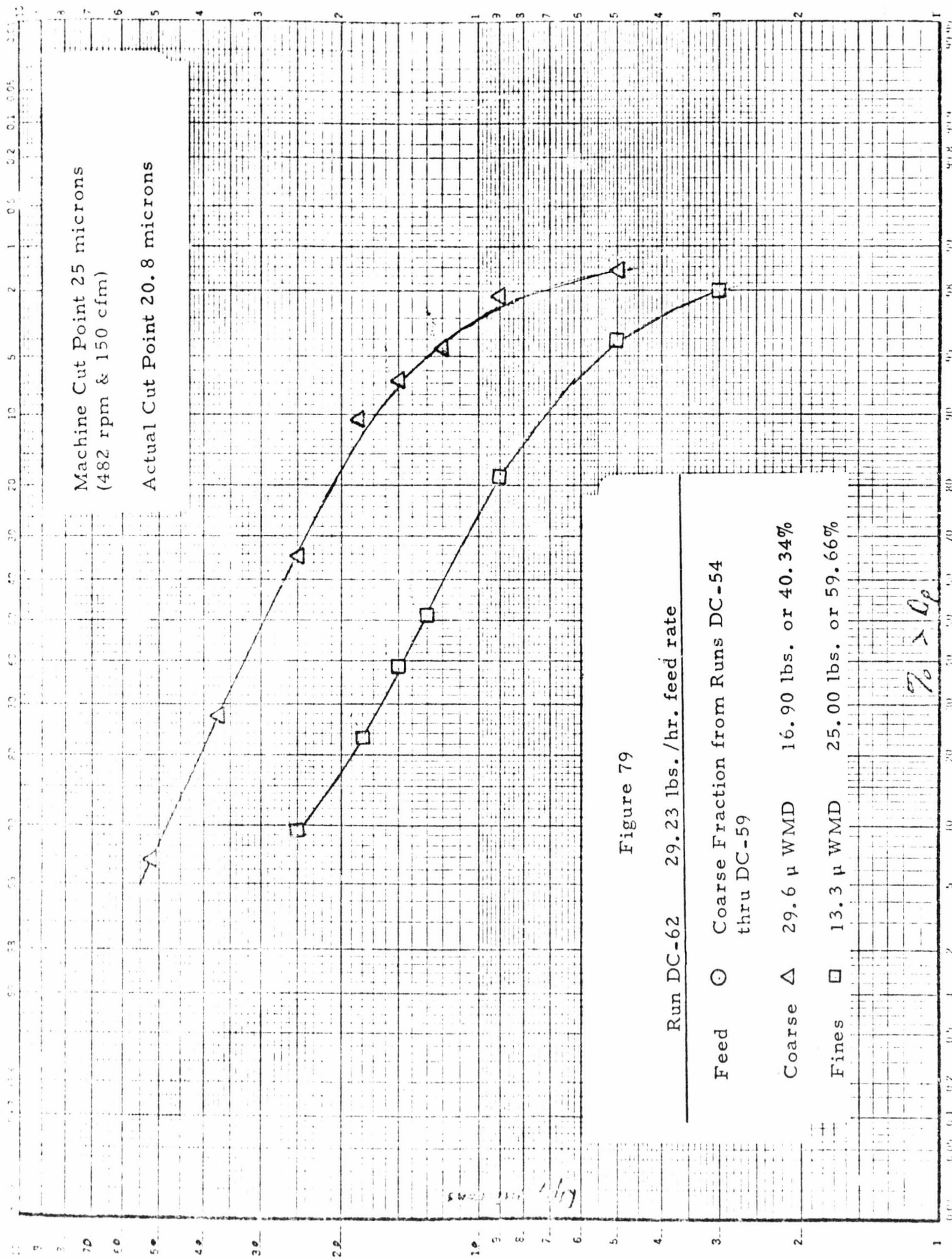


Figure 80
Grade Efficiency Curve for DC-62

100

80

60

40

20

0

$G(x), \%$

E-81

Cut Point Size 20.8 microns
Sharpness Index = $\frac{24.0}{17.7} = 1.356$

40

35

30

25

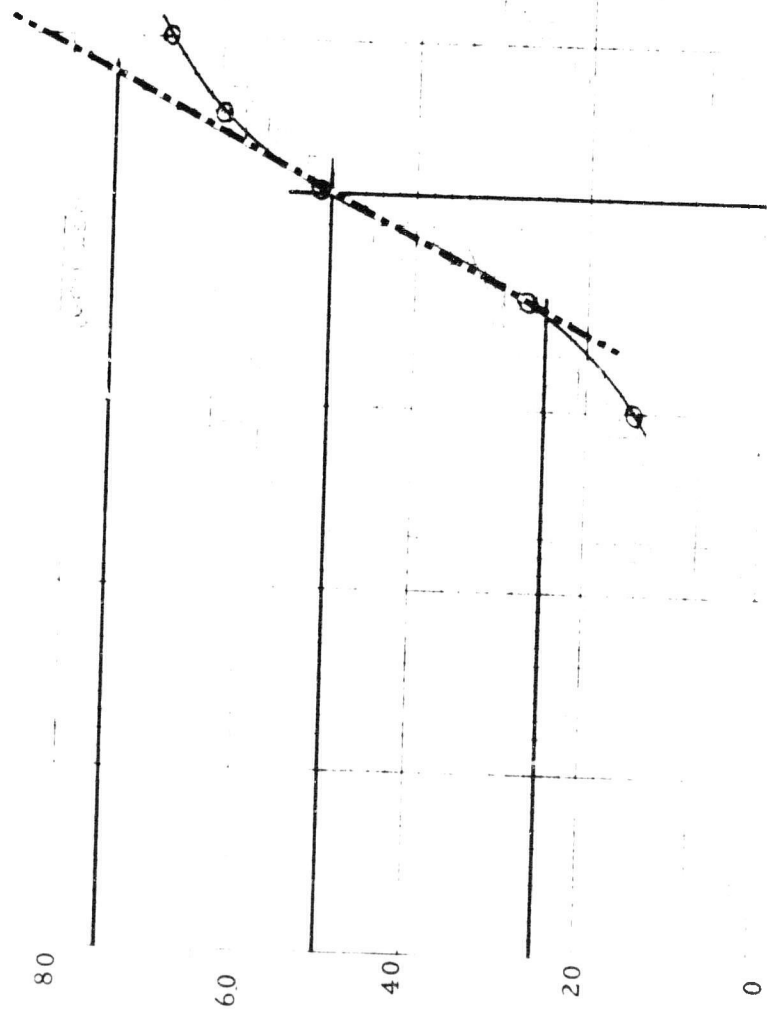
20

15

10

5

Particle Diameter, microns



Machine Cut Point 32.5 microns
(420 rpm @ 150 cfm)

Actual Cut Point 28.9 microns

Figure 81

Composite of Runs DC-63 thru DC-65

Feed Rate 11.61 lbs./hr.

Feed ○ Coarse Fraction from Runs DC-39
thru DC-41

Coarse △ 37 μ WMD 45.70 lbs. or 42.95%

Fines □ 16.8 μ WMD 60.70 lbs. or 57.05%

Figure 82
Grade Efficiency Curve for DC-63 through DC-65

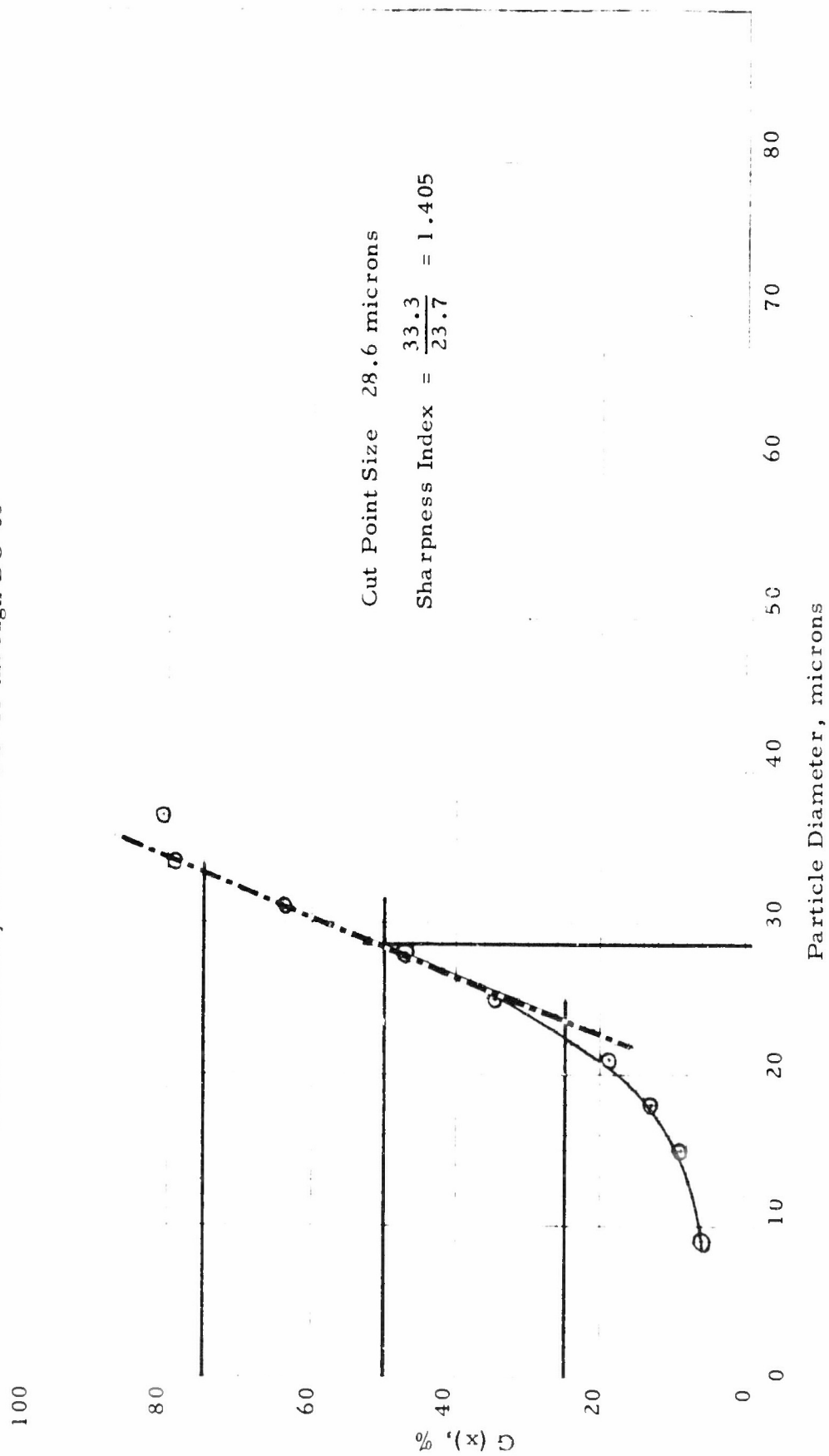


Figure 83

Run DC-66 2.34 lbs./hr. 2.5 μ AP

Feed C FEM-338 with 0.2% Silanox

Coarse Δ 2.61 μ WMD 7.23 lbs. or 97.57%

Fines \square 1.07 μ WMD 0.18 lbs. or 2.43%

Machine Cut Point \angle 0.44 microns
(4200 rpm & 100 cfm)
Data unsuitable for grade efficiency
analysis technique.

1.0
0.8
0.6
0.4
0.2
0.0

Figure 84
Grade Efficiency Curve for DC-66

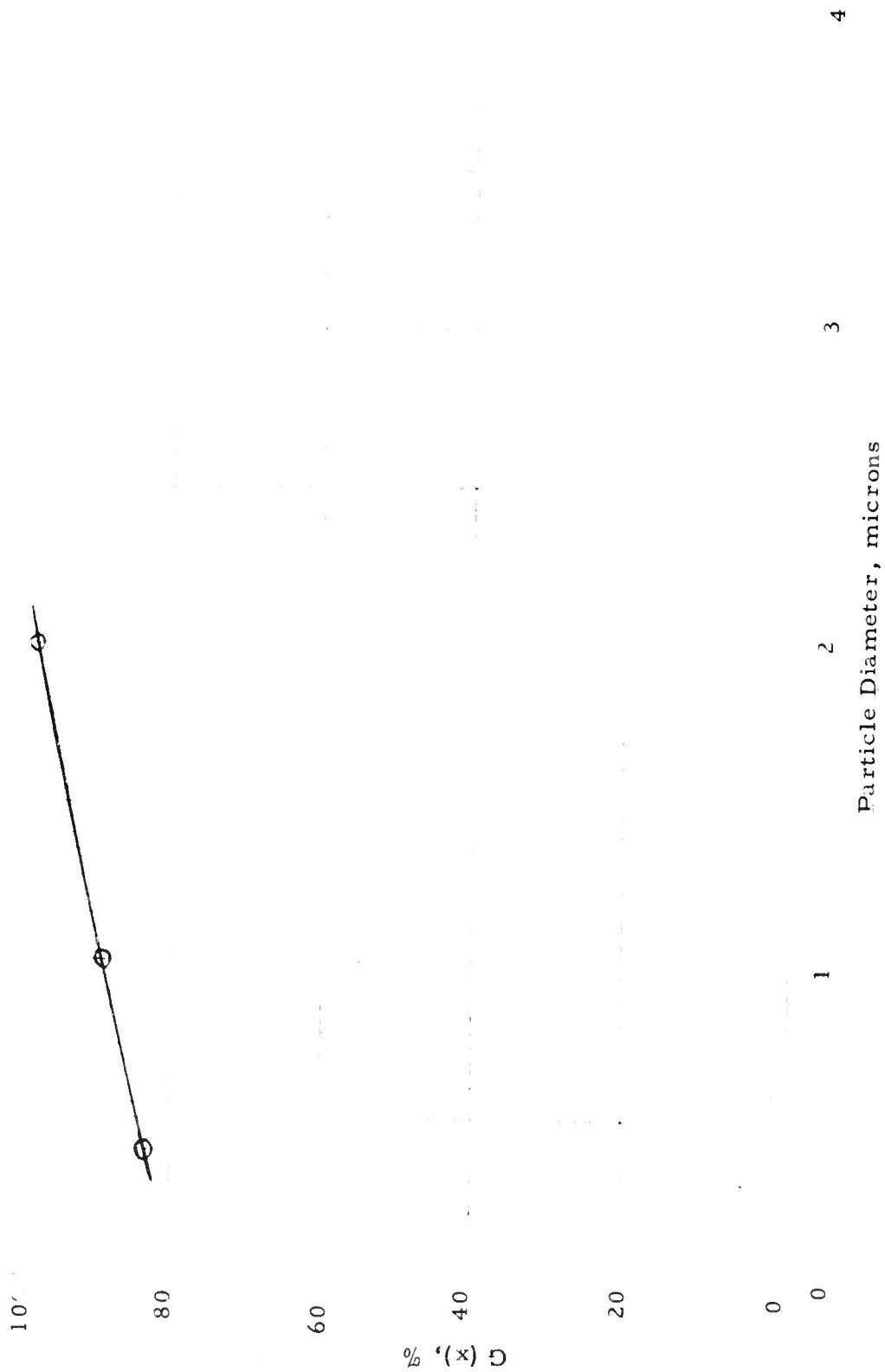


Figure 85

Run DC-67 15.17 lbs./hr. feed Rate

Feed C Blended mix of 2/3rds EFFA-100 and
1/3rd fines from DC-43, with 0.2%
Silanoc 101 added

Coarse Δ 3.94 μ WMD 11.40 lbs. or 93.90%

Fines \square 2.51 μ WMD 0.74 lbs. or 6.10%

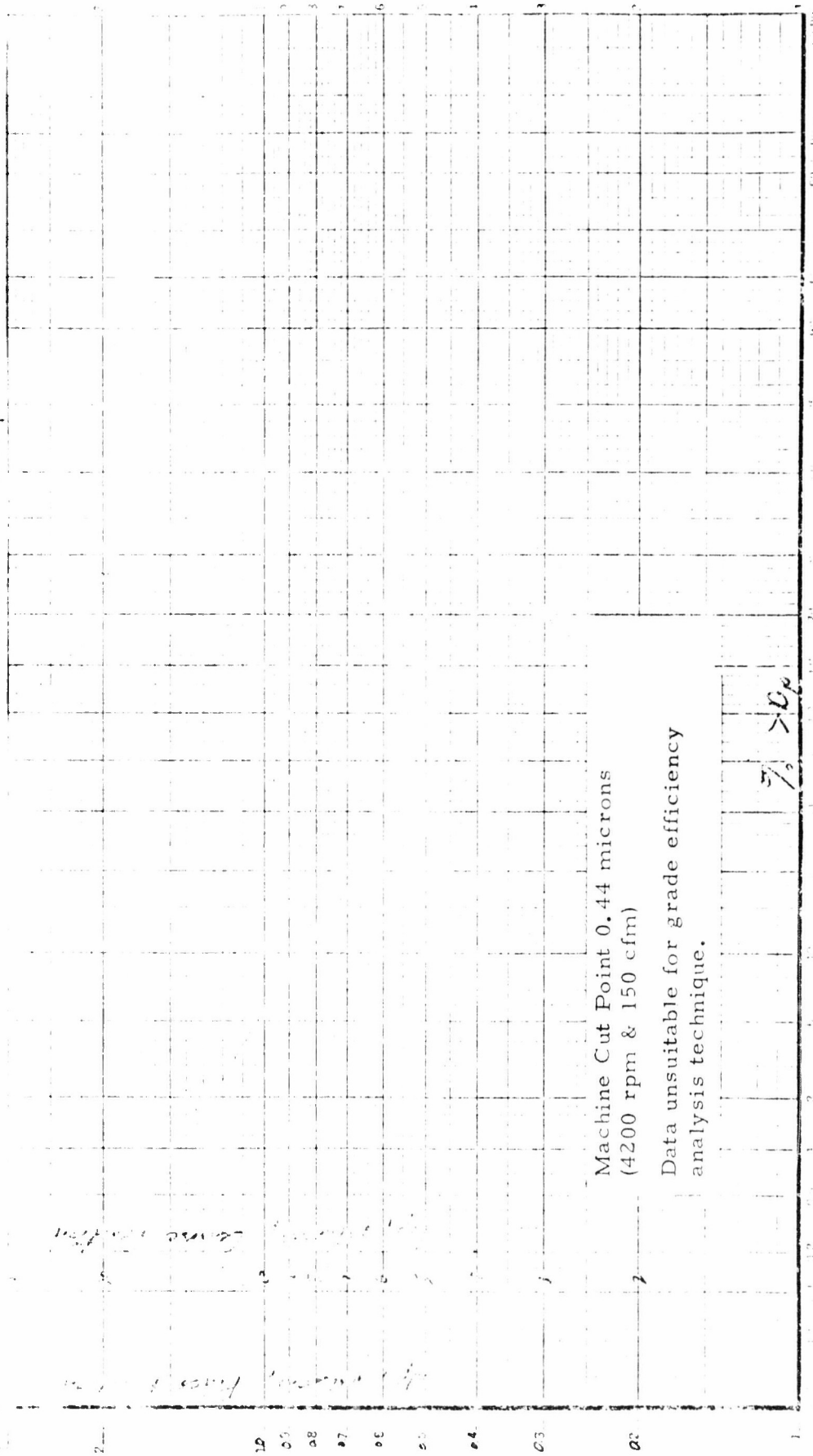


Figure 86

Grade Efficiency Curve for DC-67

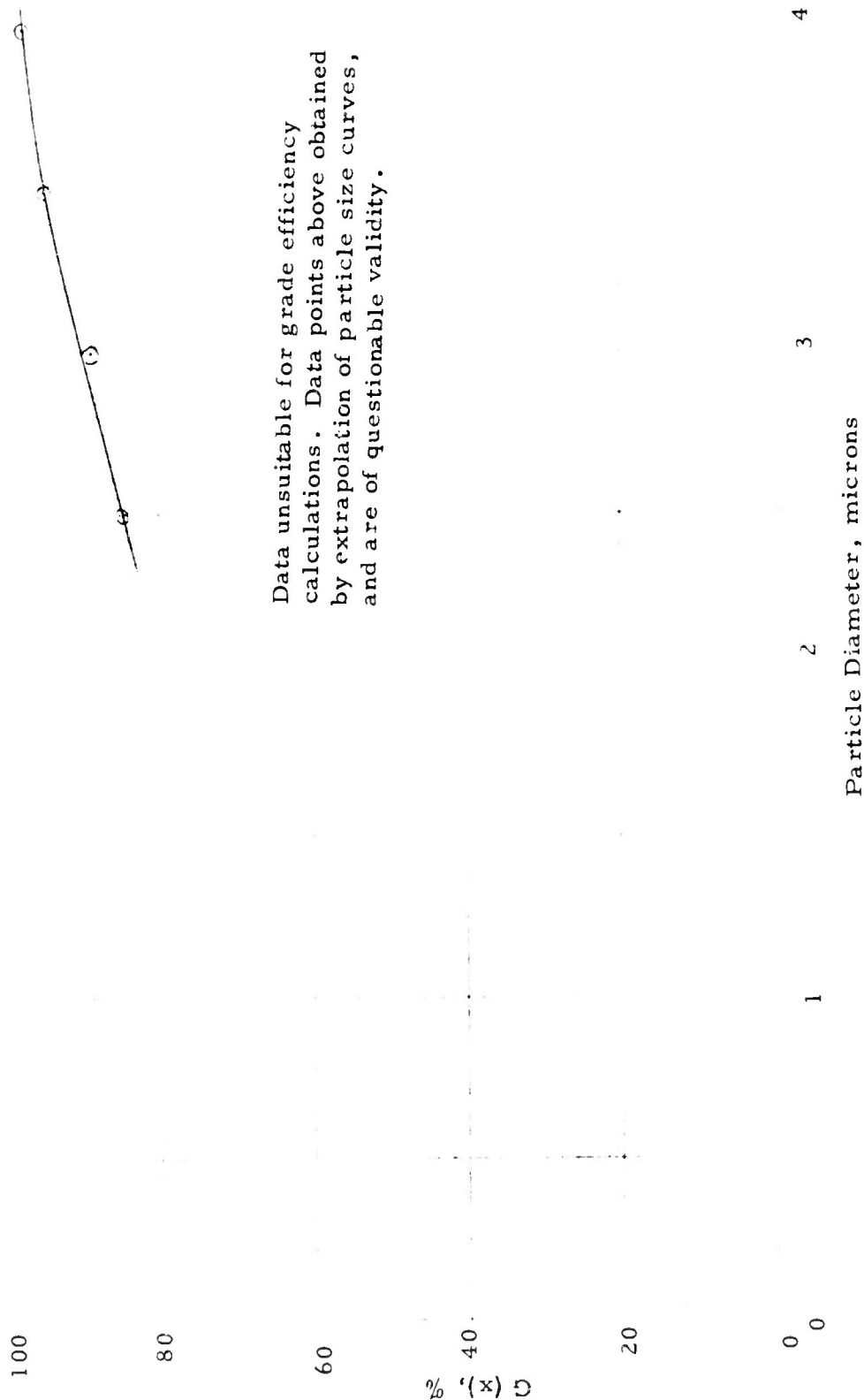


Figure 87

Run DC-68 4.32 lbs./hr. feed rate

Feed ○ Blended mix of 2/3rds FEM-338 and
1/3rd coarse from DC-43, with 0.2%
Silanox 101 added

Coarse △ 5.45 μ WMD 10.00 lbs. or 90.09%

Fines □ 2.19 μ WMD 1.10 lbs. or 9.91%

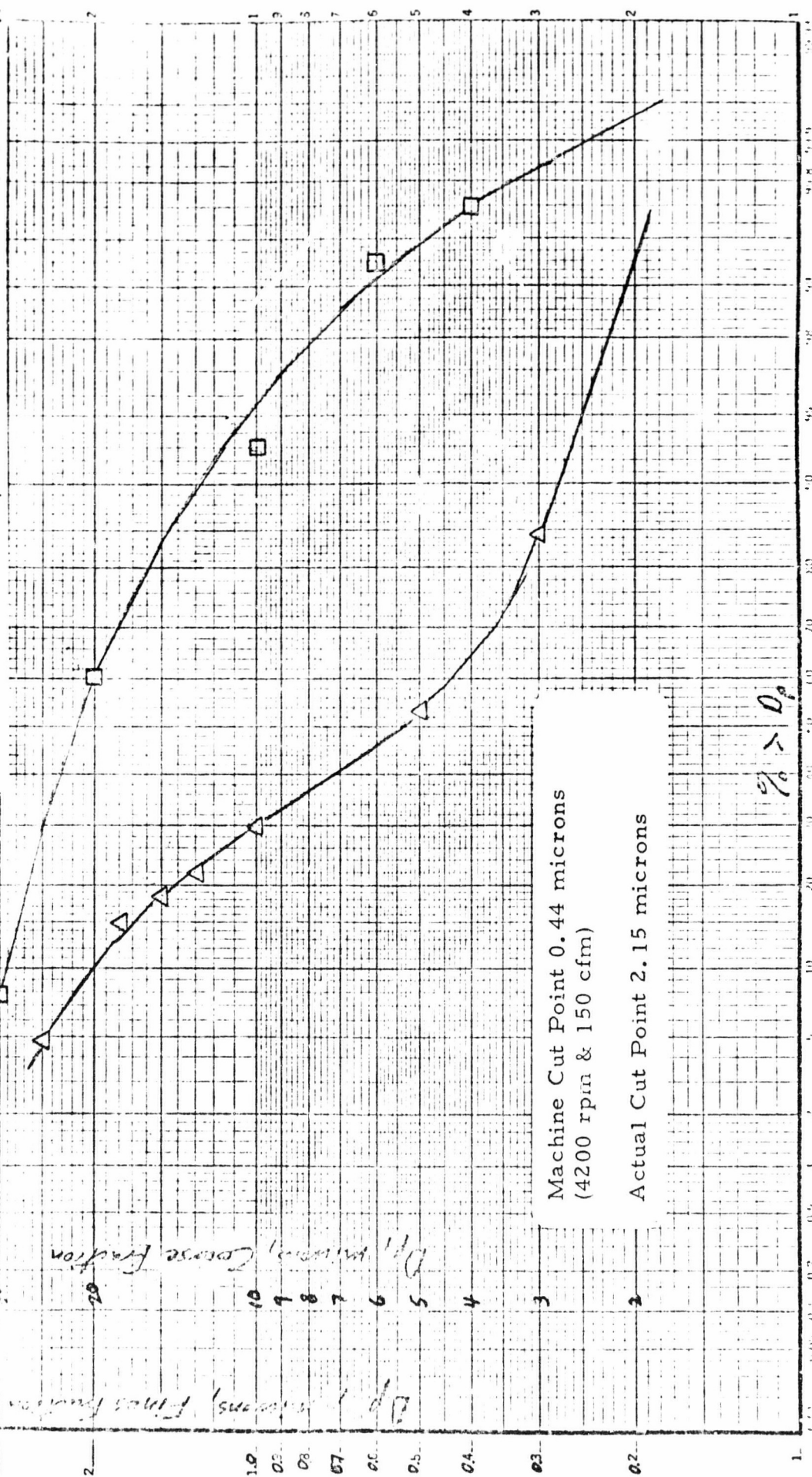


Figure 88
Grade Efficiency Curve for DC-68

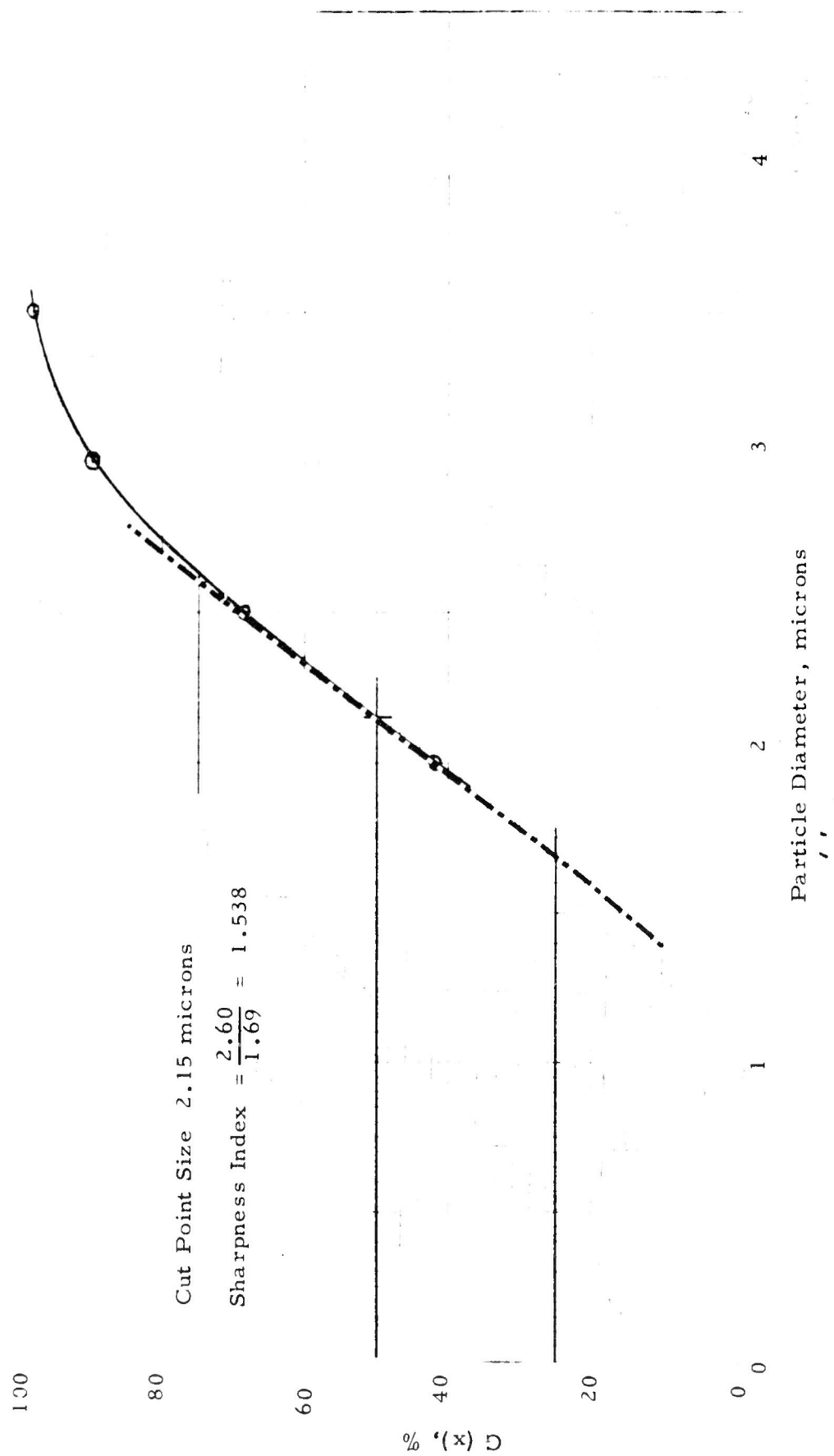


Figure 89

Run DC-69 26.22 lbs./hr. SWECO UFAP

Feed C VMA-101

Coarse Δ 1.26 μ WMD 32.96 lbs. or 95.48%

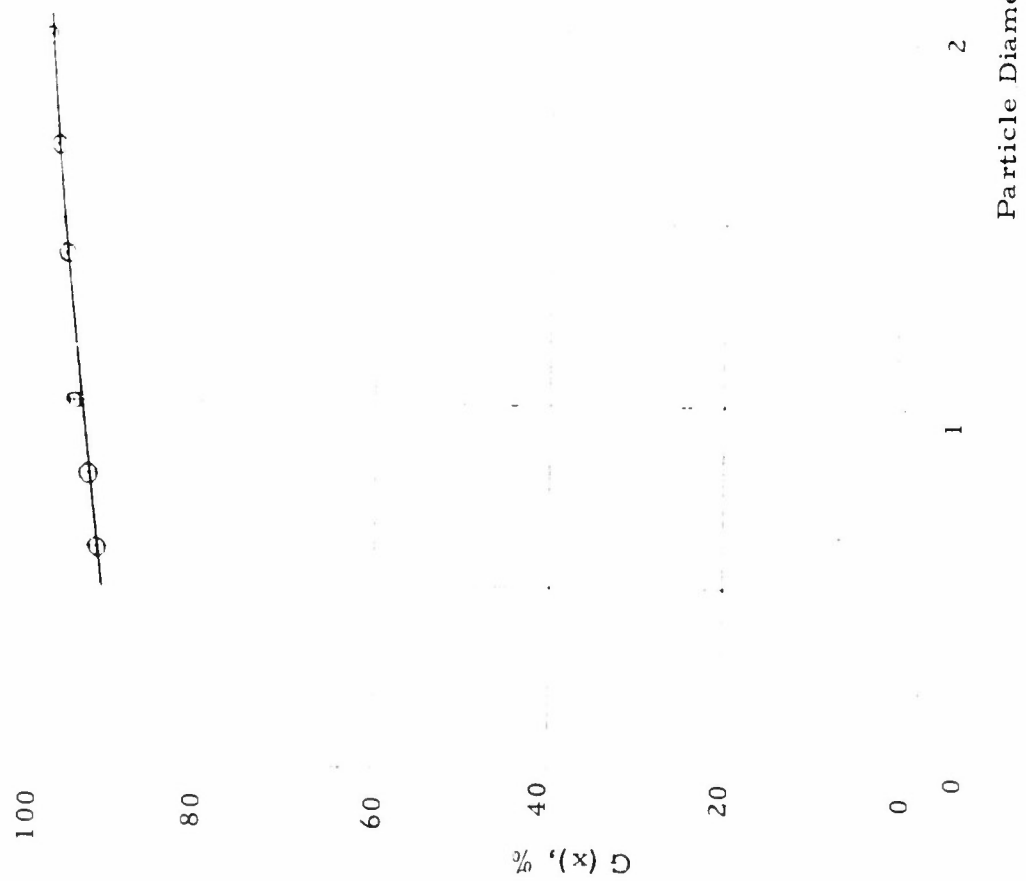
Fines Γ 0.89 μ WMD 1.56 lbs. or 4.52%

Machine Cut Point 0.44 microns
(4200 rpm & 150 cfm)

Data unsuitable for grade efficiency
analysis technique.

$\frac{7}{2} > D_p$

Figure 90
Grade Efficiency Curve for DC-69



Run DC-70 5.42 lbs./hr. 2.5 μ UFAP

Feed O FEM-338 with 0.2% Silanox

Coarse Δ 2.53 μ WMD 9.91 lbs. or 60.99%

Fines \square 2.31 μ WMD 6.34 lbs. or 39.01%

Machine Cut Point 1.0 microns
(2700 rpm & 150 cfm)

Actual Cut Point 2.82 microns

Figure 92
Grade Efficiency Curve for DC-70

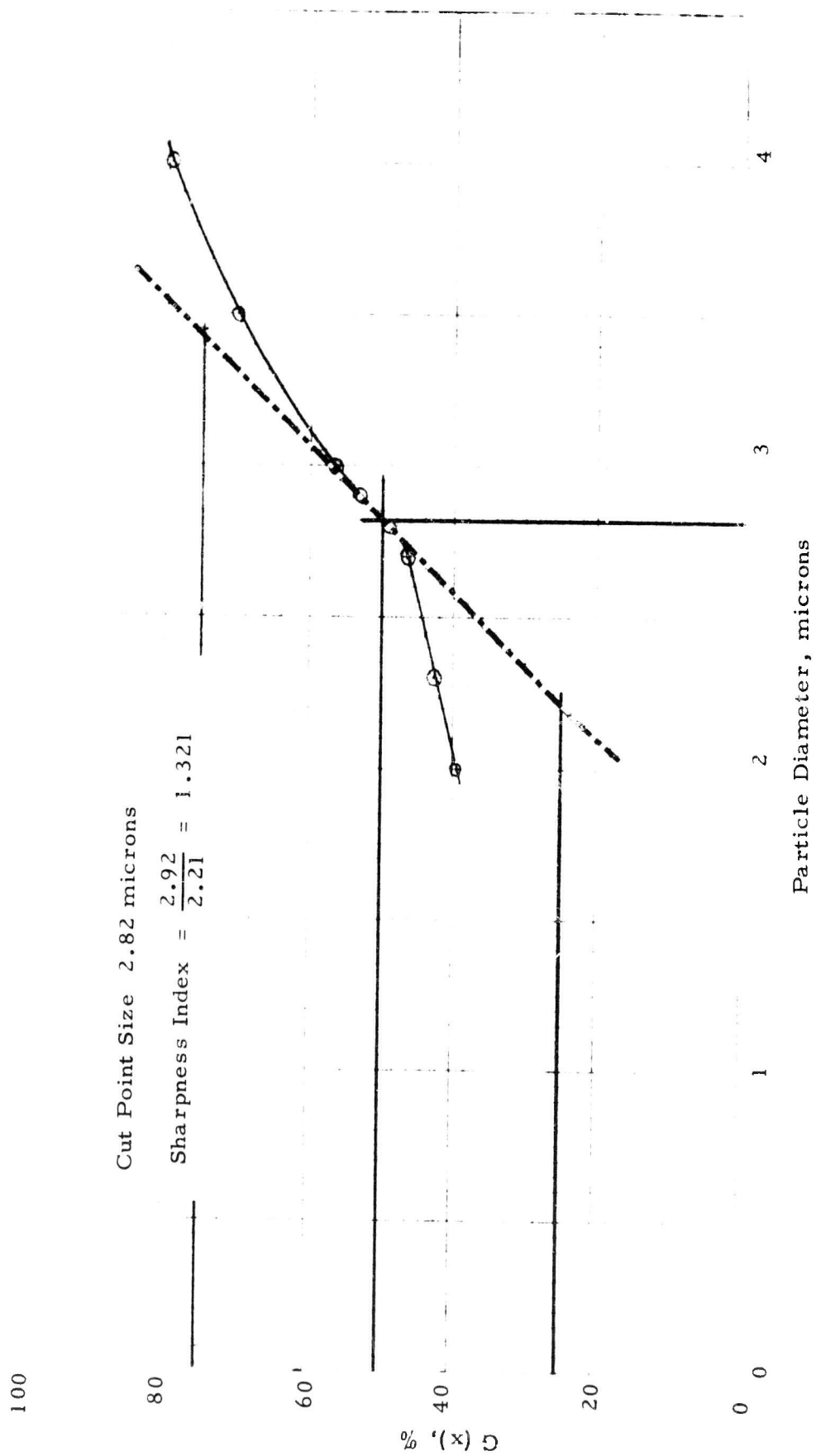


Figure 93

Run DC-71 22.26 lbs./hr. Coarse from DC-70

Feed ○ 2.53 μ WMD

Coarse △ 4.30 μ WMD 0.63 lbs. or 6.80%

Fines □ 3.39 μ WMD 8.64 lbs. or 93.20%

Machine Cut Point 5 microns
(1140 rpm & 150 cfm)

Data unsuitable for grade efficiency
analysis technique.

51
6a

Figure 94
Grade Efficiency Curve for DC-71

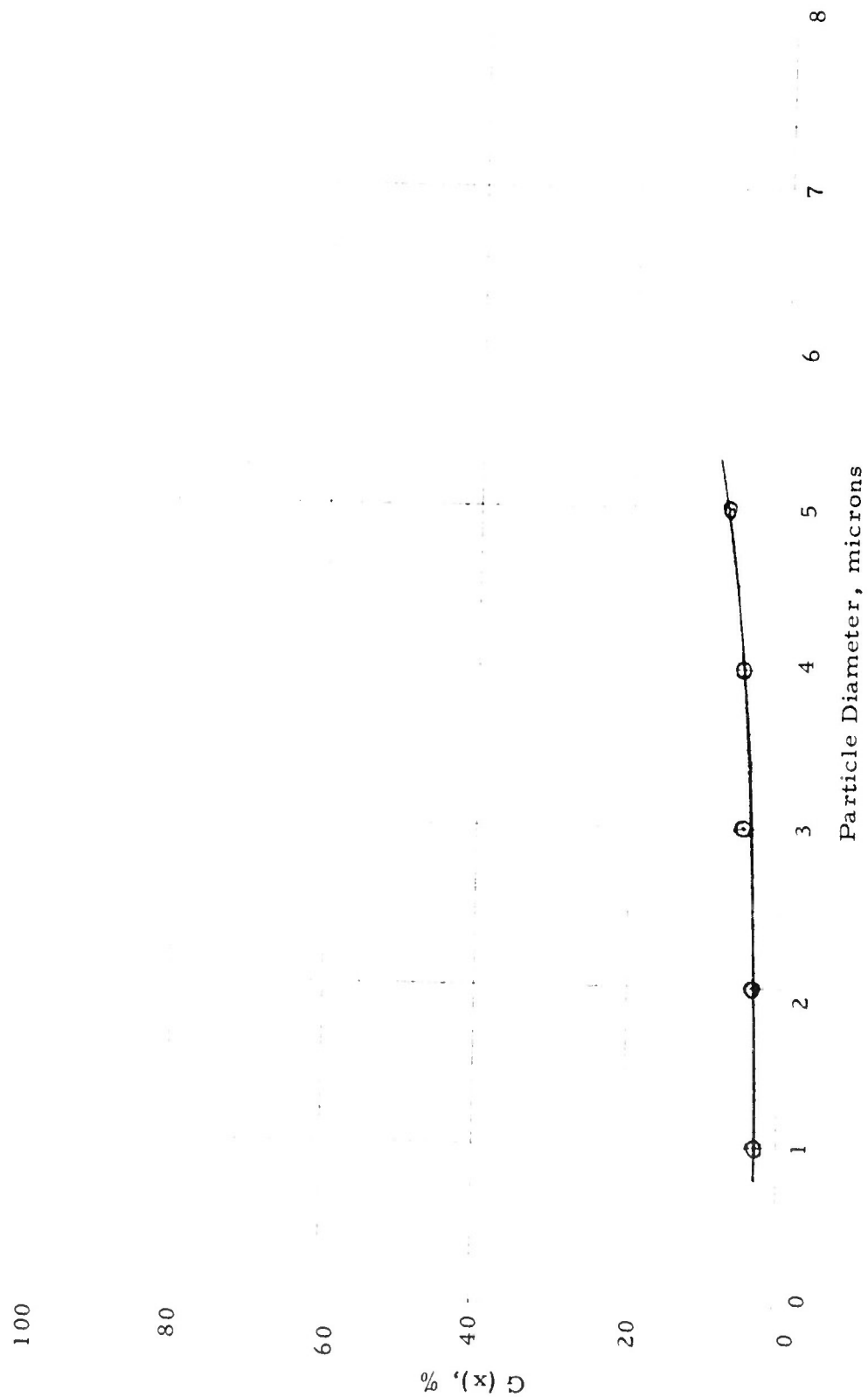


Figure 95

Run DC-72 53.58 lbs./hr. feed rate

Feed O Lot 4445 Aluminum Powder,
9.5 μ WMD (Nominal 6 μ)

Coarse Δ 11.2 μ WMD 65.58 lbs. or 82.51%

Fines \square 4.46 μ WMD 13.90 lbs. or 17.49%

Machine Cut Point 5 microns
(1040 rpm & 150 cfm)

Actual Cut Point 5.4 microns

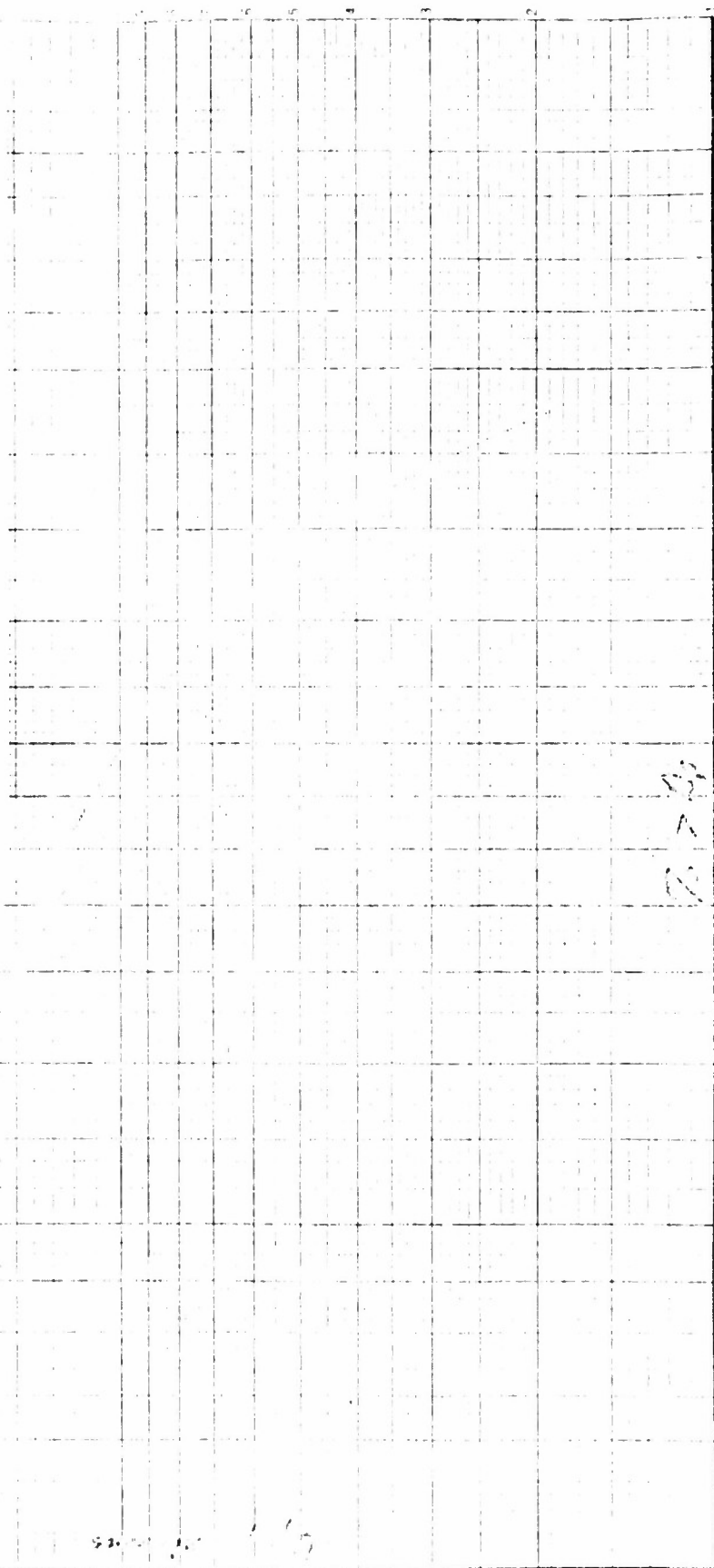


Figure 96

Grade Efficiency Curve for DC-72

Cut Point Size 5.4 microns
 Sharpness Index = $\frac{7.62}{3.13} = 2.434$

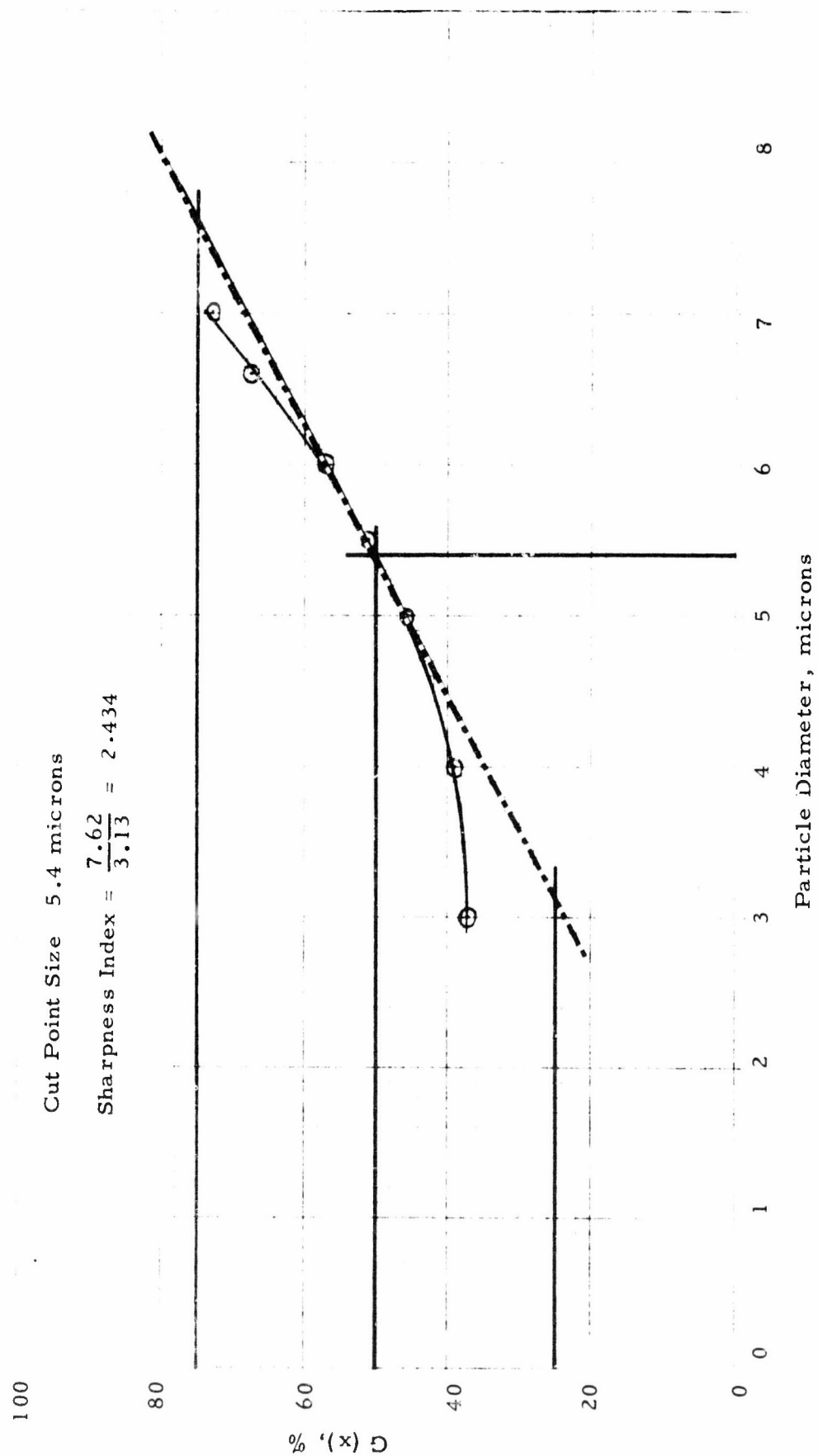


Figure 97

Run DC-73 102.17 lbs./hr. feed rate

Feed \bigcirc Coarse Fraction from DC-72

Coarse Δ 14.2 μ WMD 43.17 lbs. or 66.71%

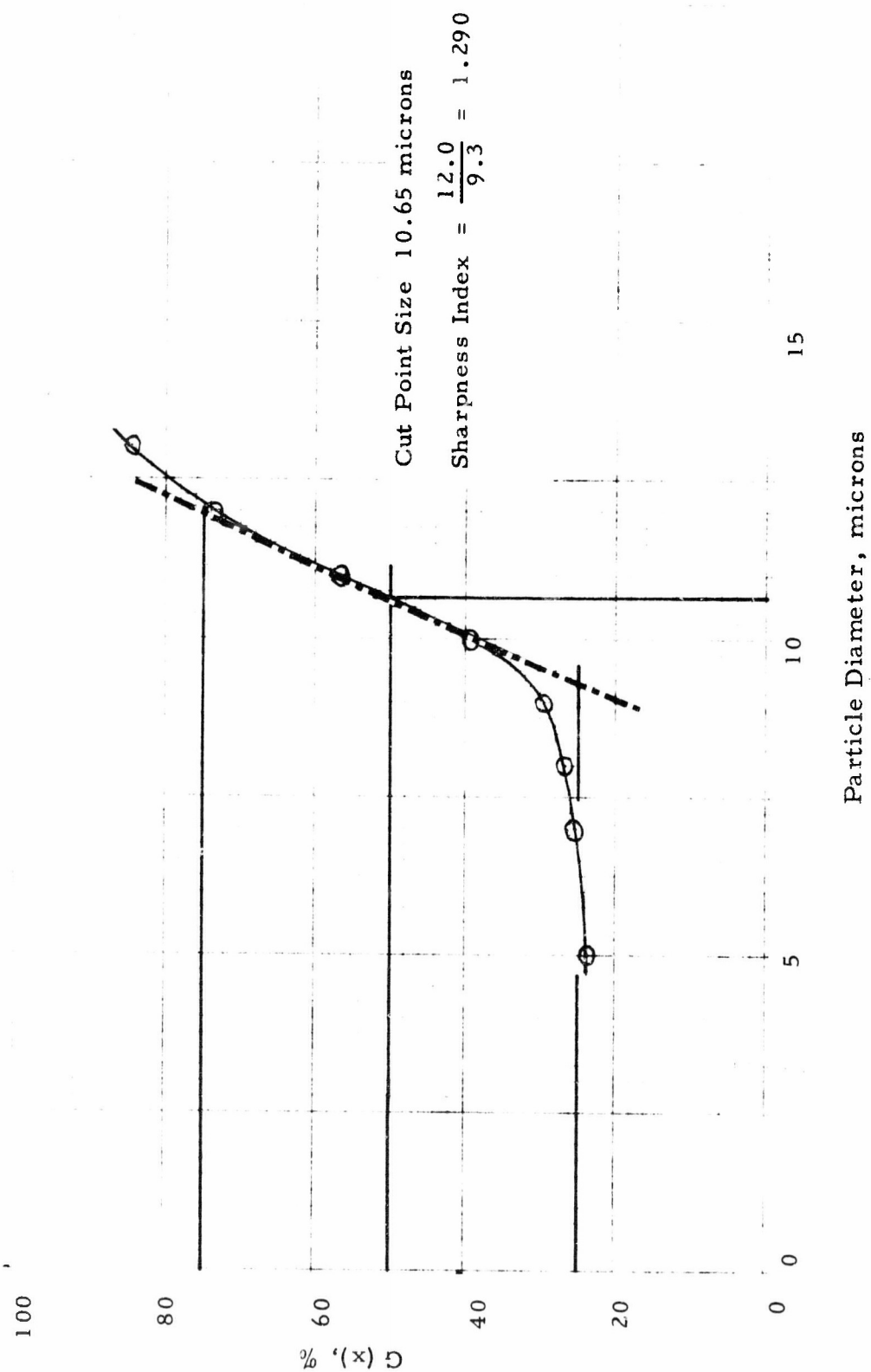
Fines \square 9.1 μ WMD 21.54 lbs. or 33.29%

Machine Cut Point 13 microns
(630 rpm & 150 cfm)

Actual Cut Point 10.65 microns

2% > 6 μ

Figure 98
Grade Efficiency Curve for DC-73



Machine Cut Point 15.0 microns
(590 rpm & 150 cfm)

Actual Cut Point 8.2 microns

Figure 99

Run DC-75 171 lbs./hr. feed rate

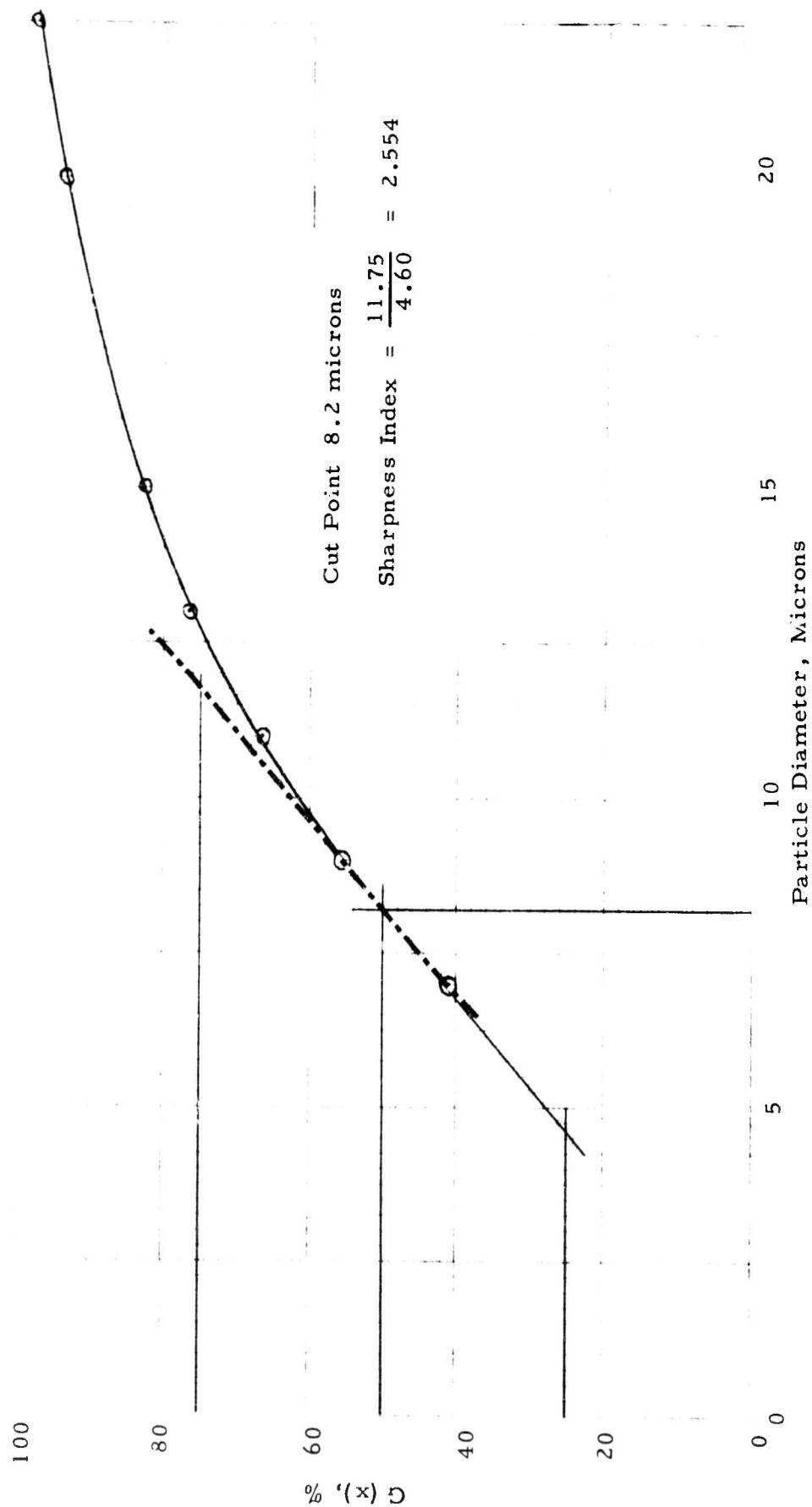
Feed C Lot 3432 Aluminum Powder, 36.4 μ WMD
(Nominal 30 μ)

Coarse Δ 30.3 μ WMD 92.52 lbs. or 92.78%

Fines \square 11.6 μ WMD 7.20 lbs. or 7.22%

7/8 1/16

Figure 100
Grade Efficiency Curve for DC-75



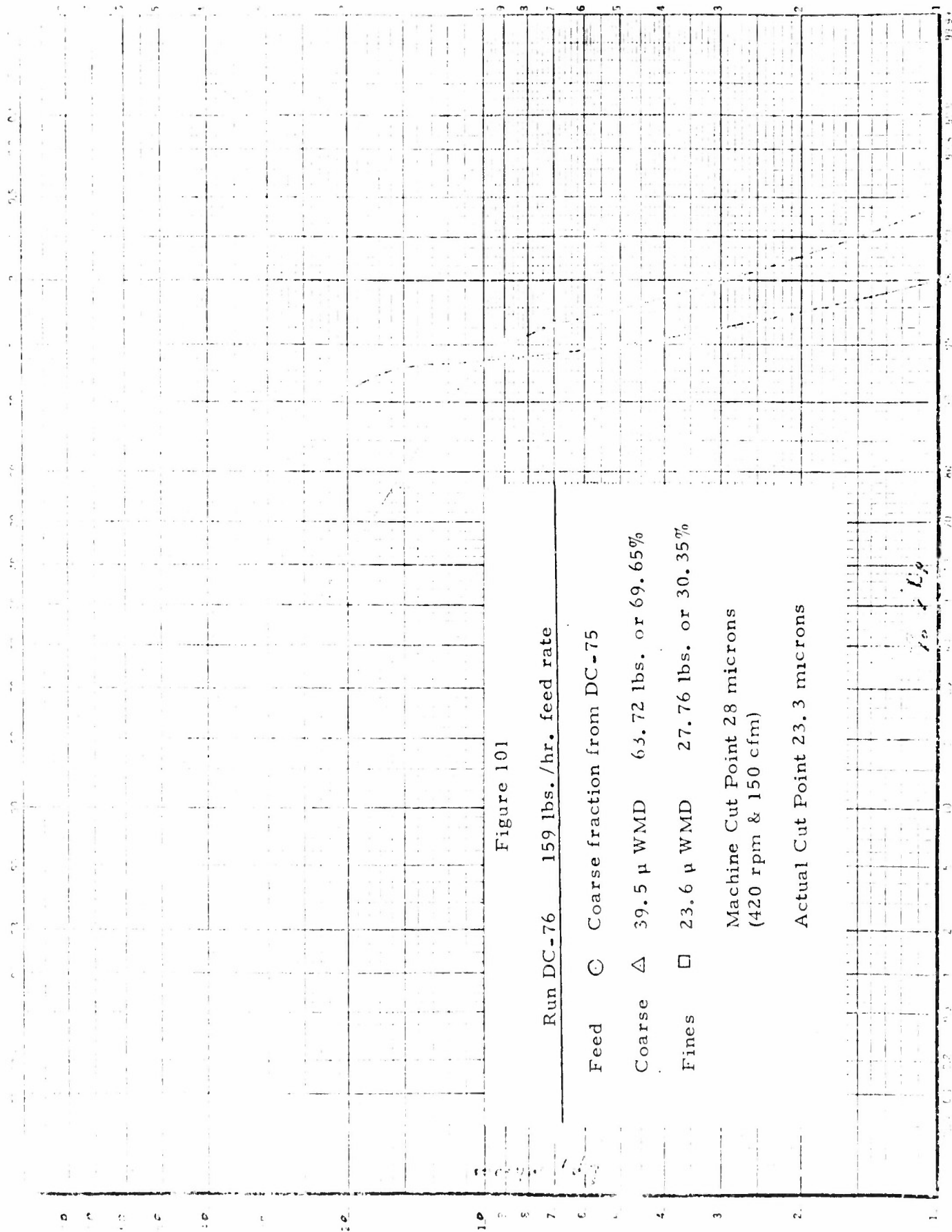


Figure 102
Grade Efficiency Curve for DC-76

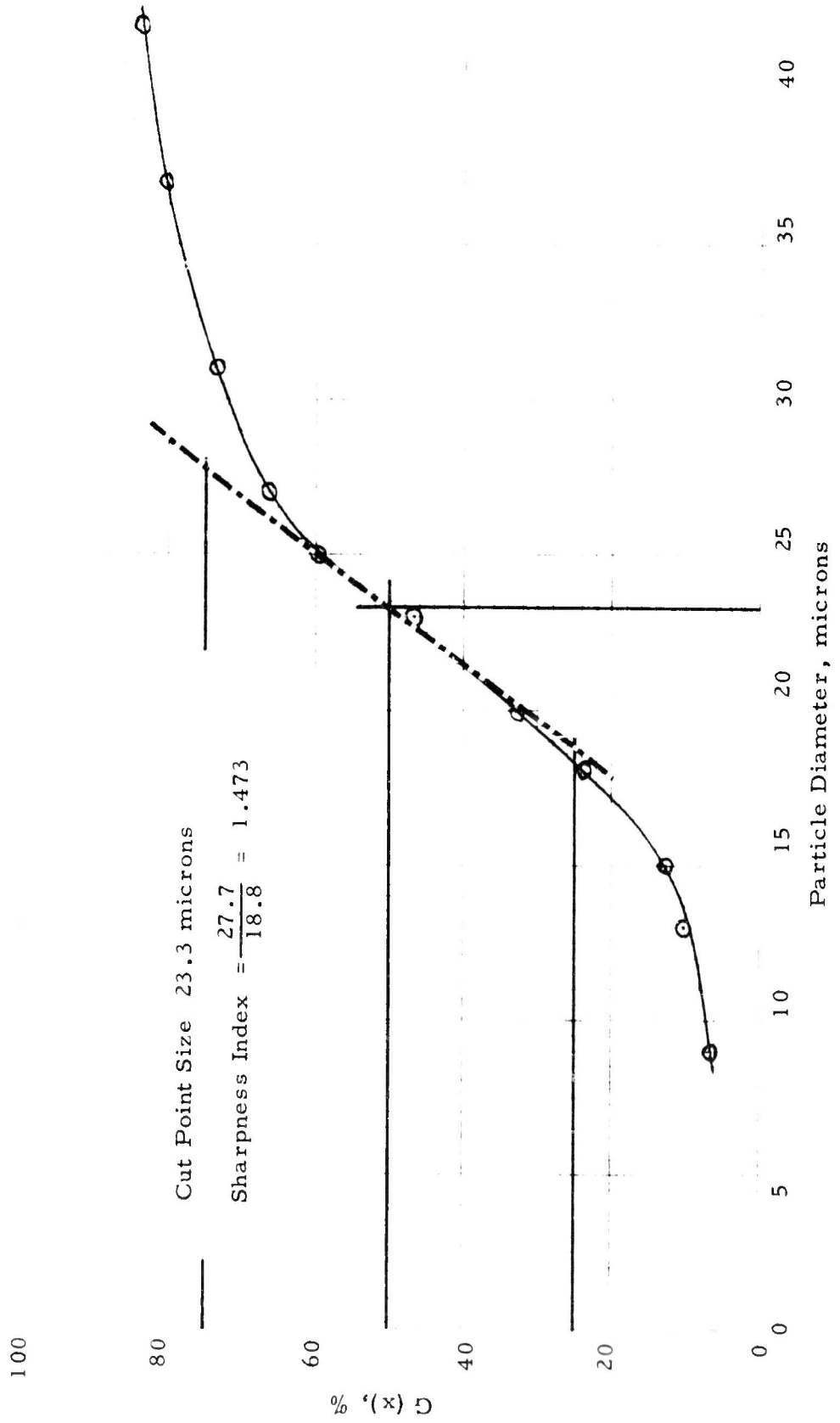


Figure 103

Run DC-77 119.36 lbs./hr. feed rate

Feed C Lot 4443 Aluminum Powder
107 μ WMD (Nominal 90 μ)

Coarse Δ 136 μ WMD 38.85 lbs. or 96.83%

Fines \square 195 μ WMD 1.27 lbs. or 3.17%

Machine Cut Point 28 microns
(420 rpm & 150 cfm)

Samples appear to be mislabelled.

72 > 100

Figure 104
Grade Efficiency Curve for DC-77*

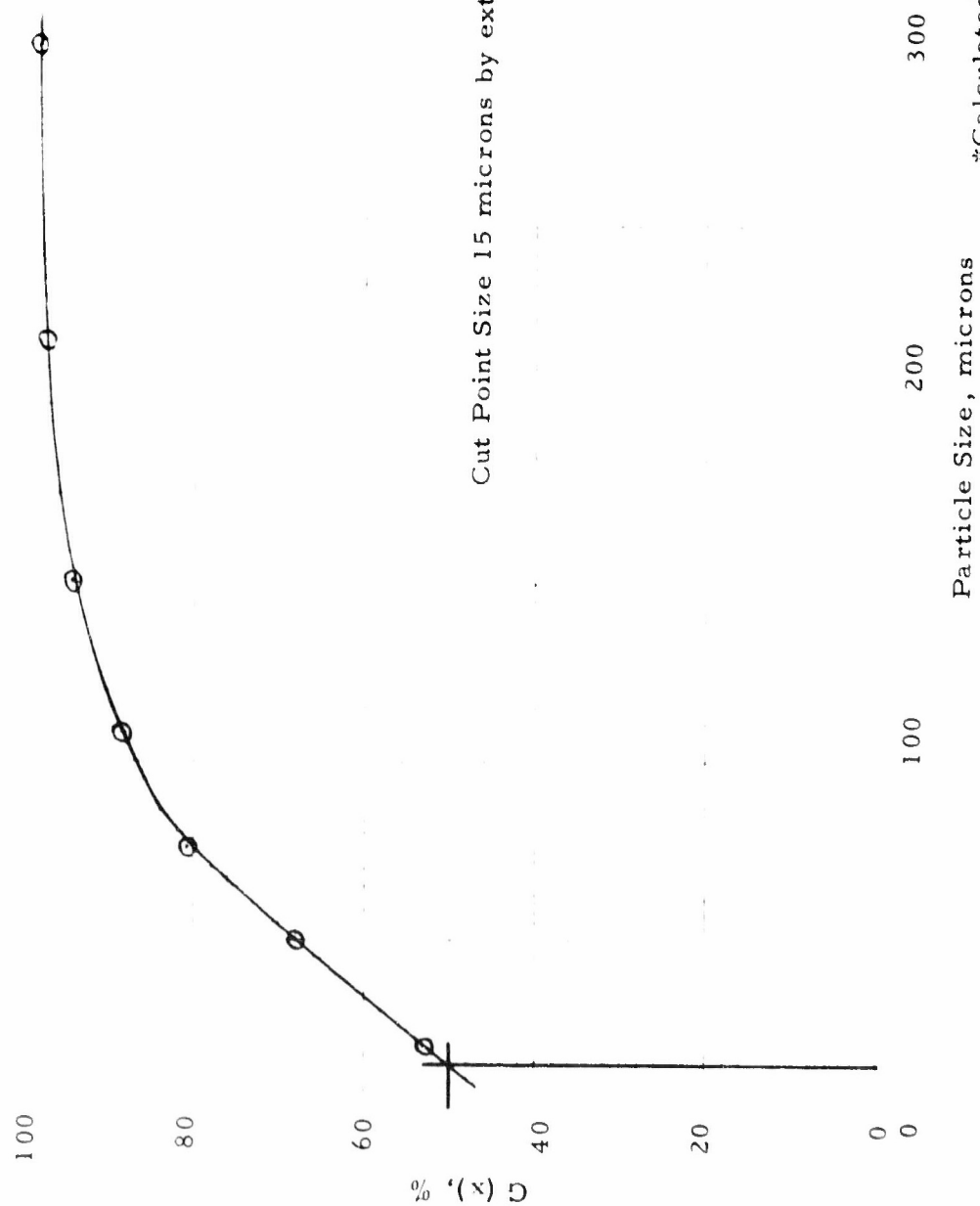


Figure 105

Run DC-78 19.24 lbs./hr. feed rate

Feed ○ Lot 3916 Type H-3 Aluminum Powder,
5.70 u WMD

Coarse △ 5.68 μ WMD 18.81 lbs. or 97.77%

Fines □ 1.62 μ WMD 0.43 lbs. or 2.23%

Machine Cut Point 0.38 microns
(4200 rpm & 150 cfm)

Actual Cut Point 0.72 microns by
extrapolation of data

microns

$\sigma_0 > D_0$

Figure 106
Grade Efficiency Curve for DC-78

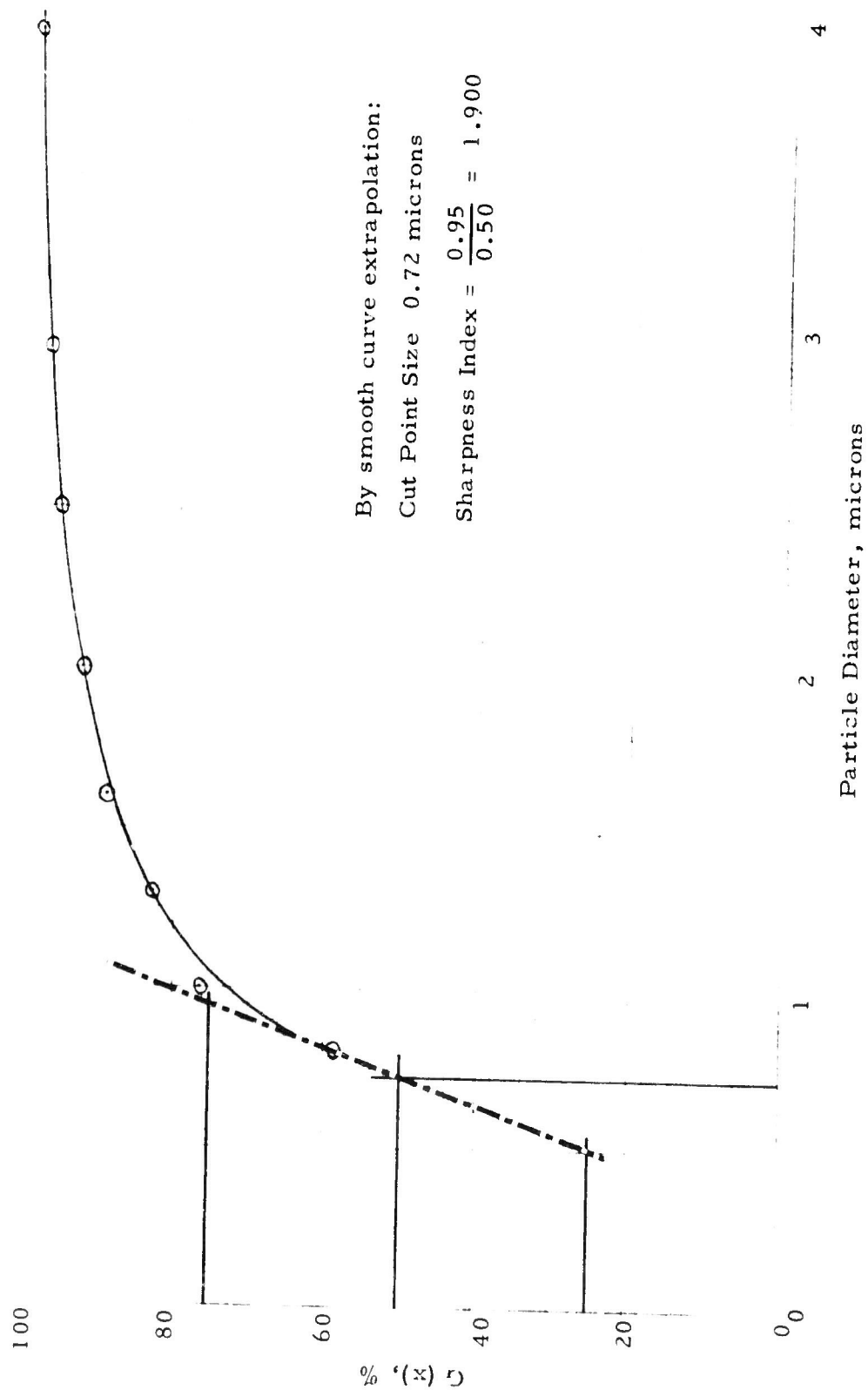


Figure 107

Run DC-79 62.73 lbs./hr. feed rate

Feed © Lot 3916 Type H-3 Aluminum Powder
5.70 u WMD

Coarse ▲ 5.12 u WMD 53.99 lbs. or 98.36%

Fines □ 1.40 u WMD 0.90 lbs. or 1.64%

Machine Cut Point 0.38 microns
(4200 rpm & 150 cfm)

Actual Cut Point 0.54 microns, by
extrapolation of data

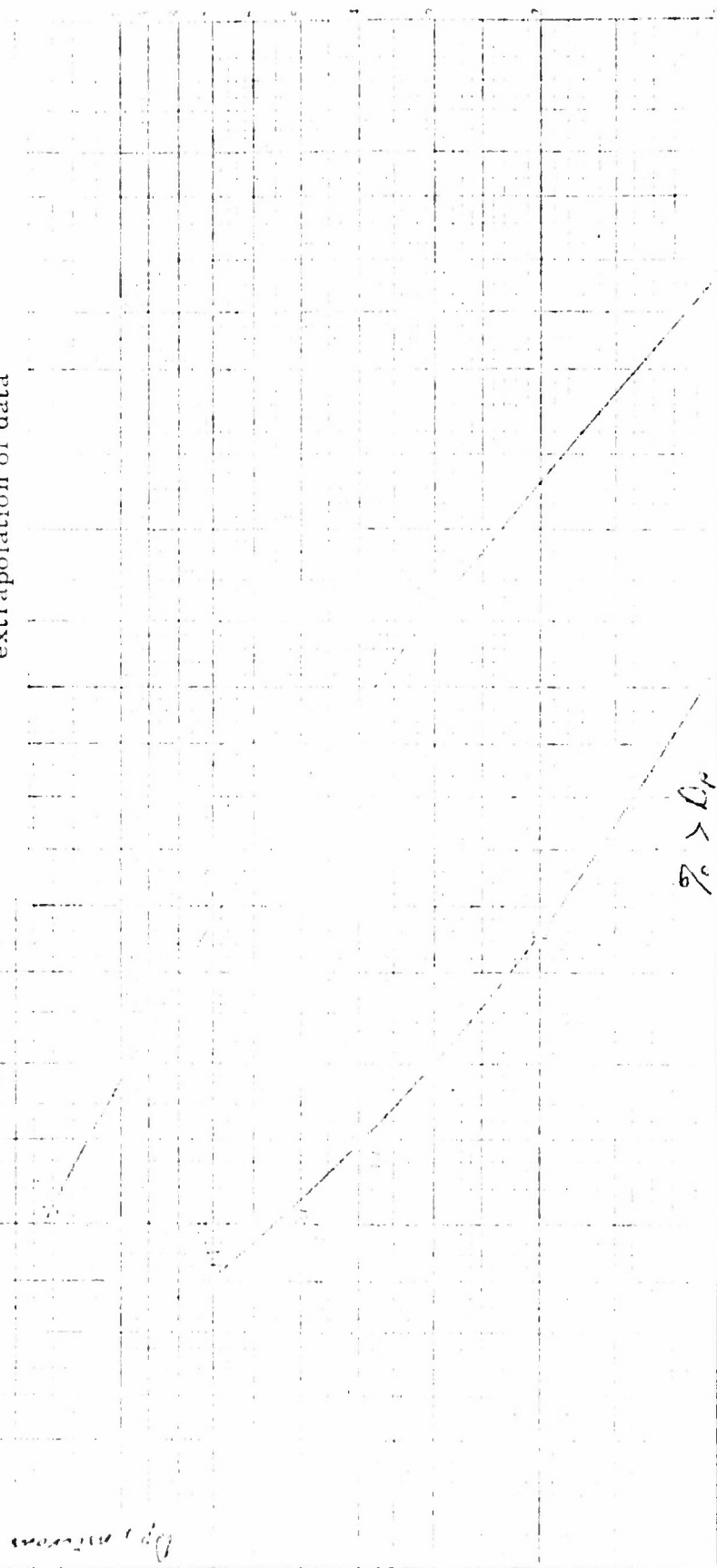


Figure 108

Grade Efficiency Curve for DC-79

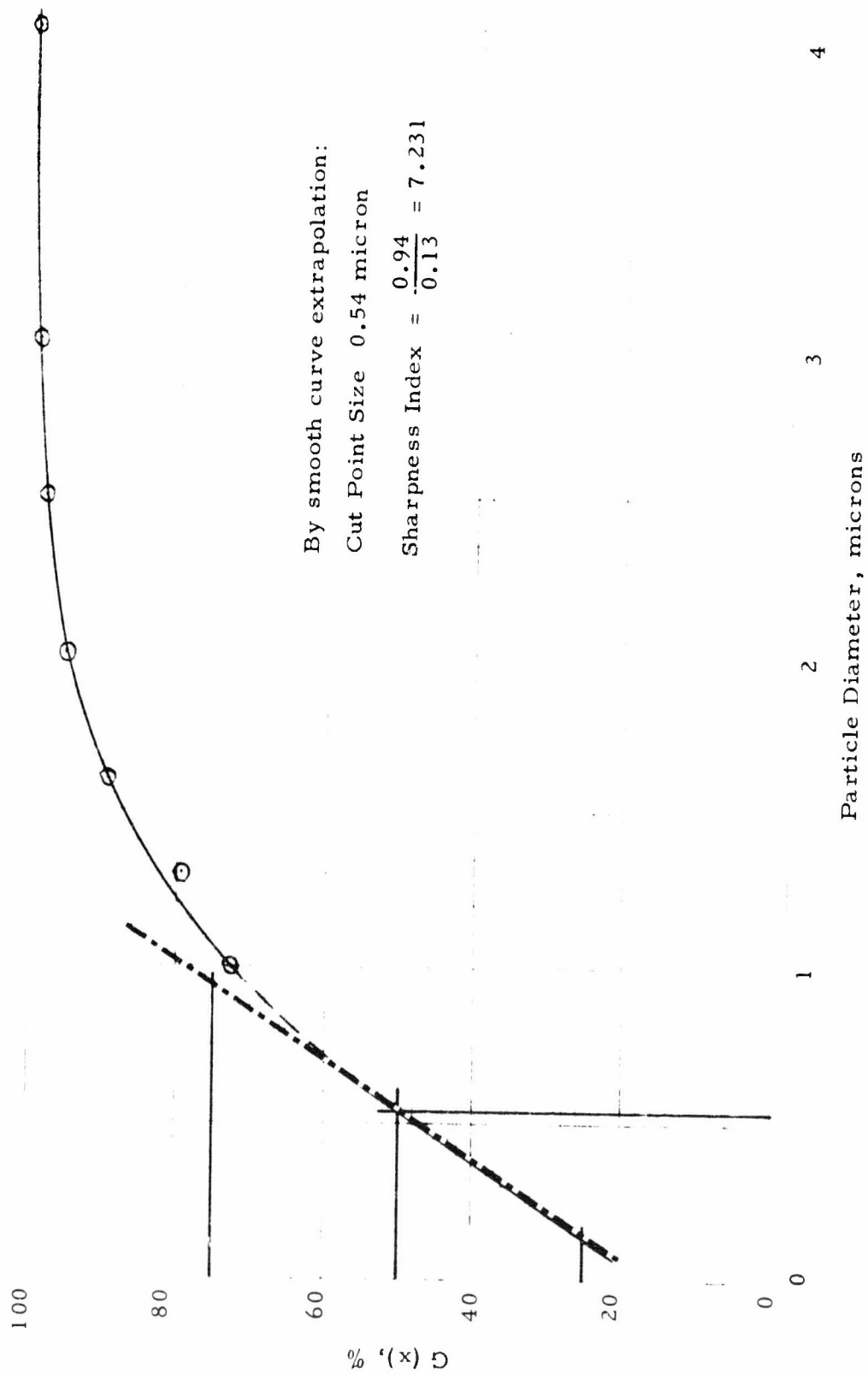


Figure 109

Run DC-80 100.4 lbs./hr. feed rate

Feed C Lot 3916 Type H-3 Aluminum Powder
5.70 μ WMD

Coarse Δ 5.4 μ WMD 49.00 lbs. or 99.29%

Fines \square 1.62 μ WMD 0.35 lbs. or 0.71%

Machine Cut Point 0.38 microns
(4200 rpm & 150 cfm)

Data unsuitable for grade efficiency
analysis technique.

5.70 μ WMD

7.2 μ WMD

Figure 110

Grade Efficiency Curve for DC-80

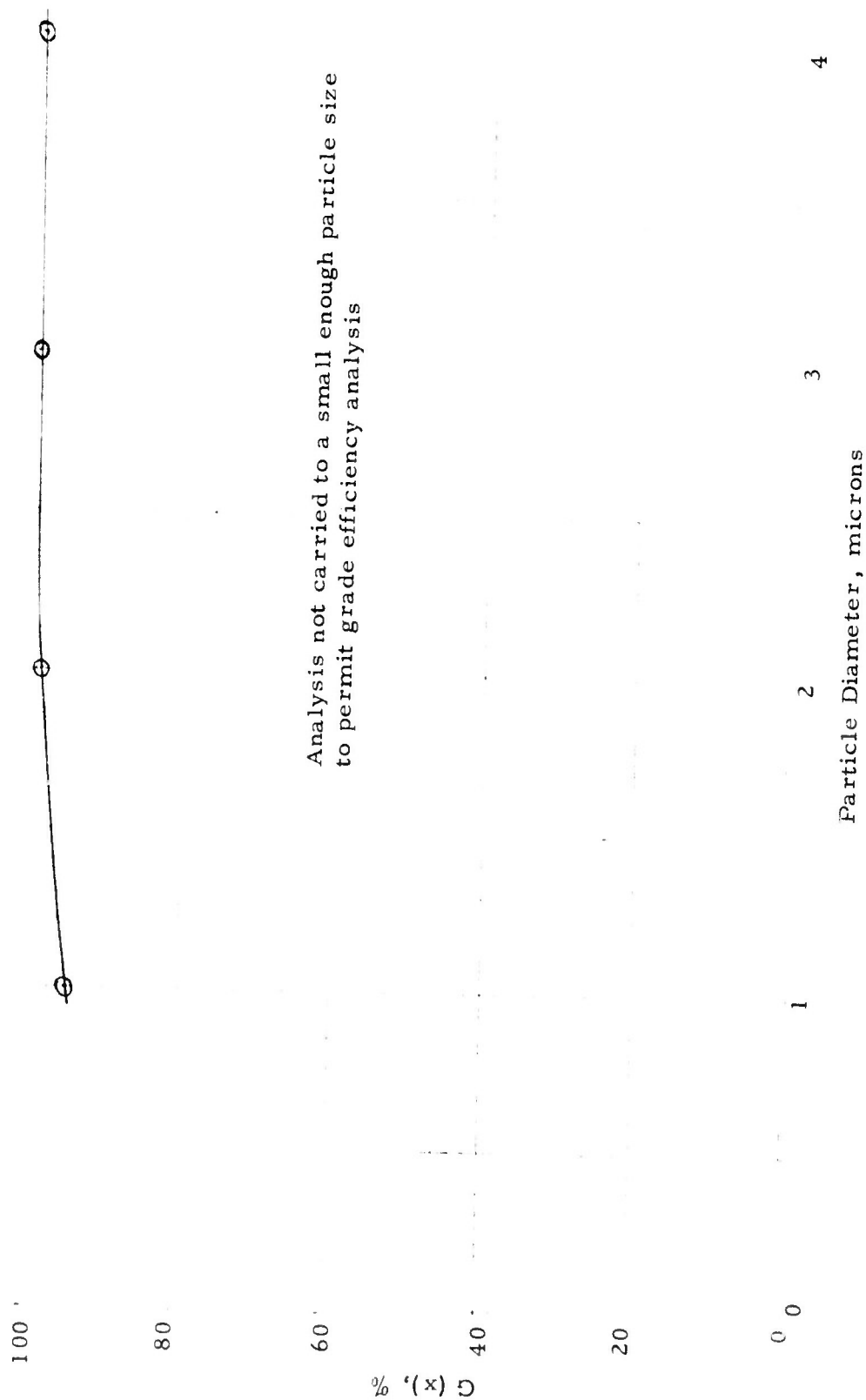


Figure 111

Run DC-81 83.54 lbs./hr. feed rate

Feed \odot Lot 3916 Type H-3 Aluminum Powder,
5.70 μ WMD

Coarse Δ 6.5 μ WMD 49.43 lbs. or 99.22%

Fines \square 1.49 μ WMD 0.39 lbs. or 0.78%

Machine Cut Point < 0.38 microns
(4200 rpm & 100 cfm)

Actual Cut Point 0.54 microns, by
extrapolation of data



Figure 112
Grade Efficiency Curve for DC-81

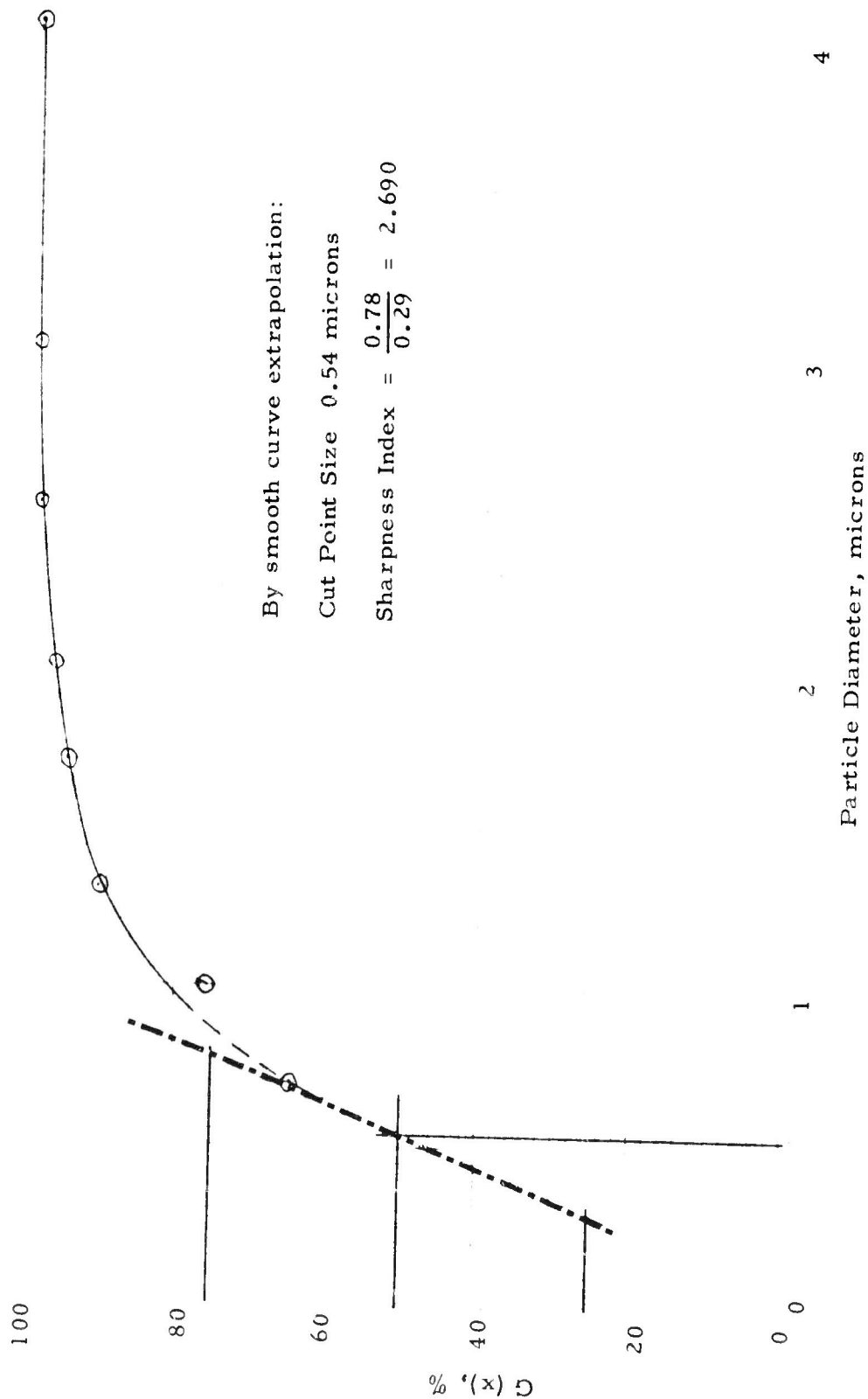


Figure 113

Run DC-82 44.90 lbs./hr. feed rate

Feed C Lot 3916 Type H-3 Aluminum Powder,
5.70 μ WMD

Coarse Δ 5.8 μ WMD, 98.49 lbs. or 99.31%

Fines \square 1.65 μ WMD, 0.68 lbs. or 0.69%

Machine Cut Point < 0.38 microns
(4200 rpm & 100 cfm)
Data unsuitable for grade efficiency
analysis technique

7-2-72

Figure 114
Grade Efficiency Curve for PC-82

